A417 Missing Link
TR010056

6.4 Environmental Statement
Appendix 9.3 Ground Investigation Factual Report
Part 3 of 5

Planning Act 2008

APFP Regulation 5(2)(a)
Infrastructure Planning (Applications: Prescribed Forms and Procedure) Regulations 2009

Volume 6

May 2021

Infrastructure Planning

Planning Act 2008

The Infrastructure Planning (Applications: Prescribed Forms and Procedure) Regulations 2009

A417 Missing Link

Development Consent Order 202[x]

6.4 Environmental Statement
Appendix 9.3 Ground Investigation Factual Report
Part 3 of 5

Regulation Number:	5(2)(a)
Planning Inspectorate Scheme Reference	TR010056
Application Document Reference	6.4
Author:	A417 Missing Link

Version	**Date**	**Status of Version**
C01	May 2021	Application Submission

EUROPEAN GEOPHYSICAL SERVICES LTD

Client:	**Geotechnical Engineering**	Log Type: ***Image***
Borehole:	**OH413**	

Location: **A417 Birdlip** Area: **Gloucestershire** Grid Ref: **394312.1E 214960.1N** Elevation: **270.65m**

Drilled Depth: (m)	**104.0**	Date:	**26.09.19**
Logged Depth: (m)	**101.0**	Recorded By:	**M. Kynaston**
Logging Datum:	**Ground Level**	Remarks:	
Logged Interval: (m)	**8.0 - 101.0**		
Fluid Level: (m)	**79.4**		

BOREHOLE RECORD		
Bit: (mm)	From: (m)	To: (m)

CASING RECORD			
Type	Size: (mm)	From: (m)	To: (m)
Steel	**150**	**0.0**	**9.0**

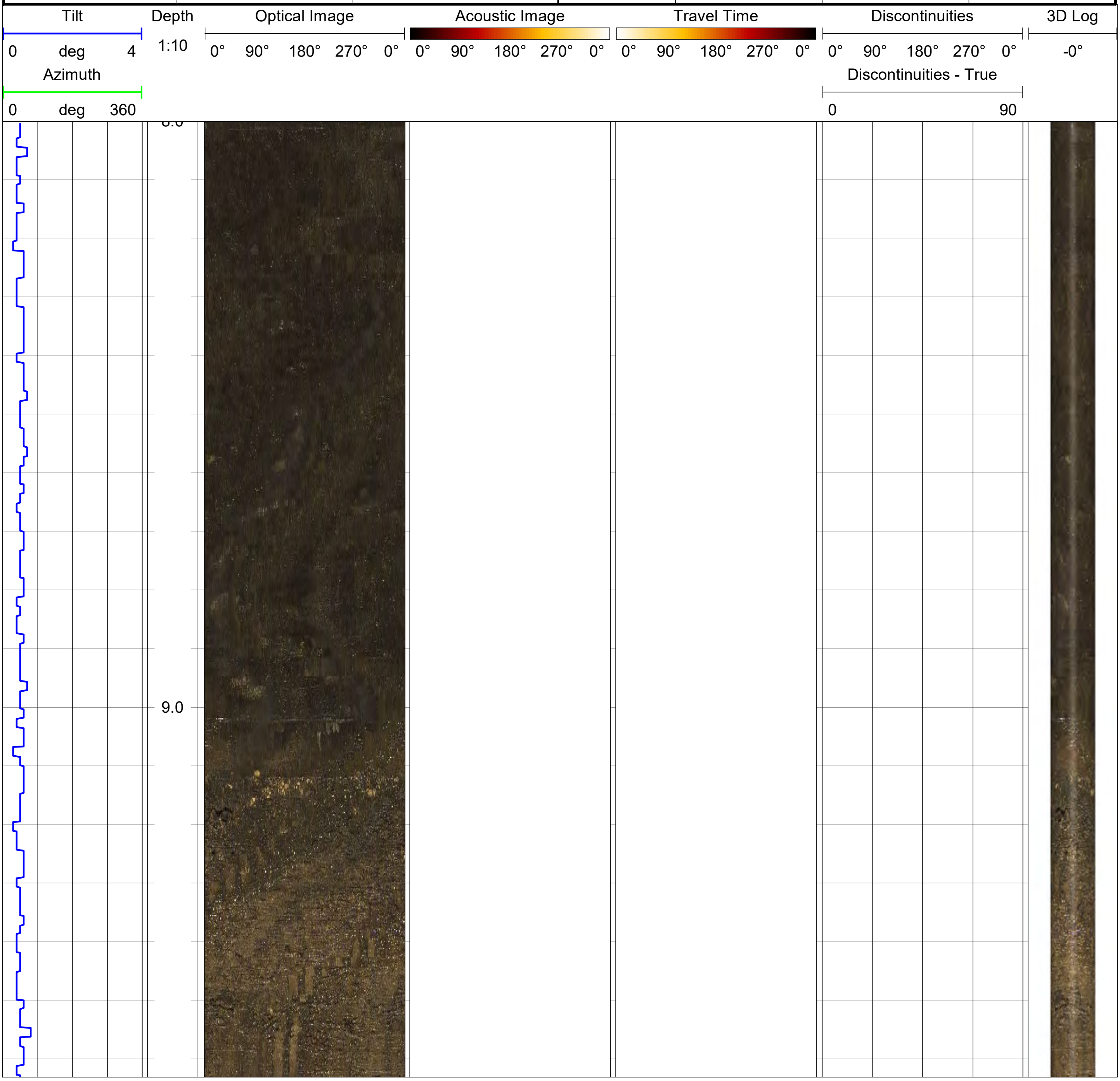

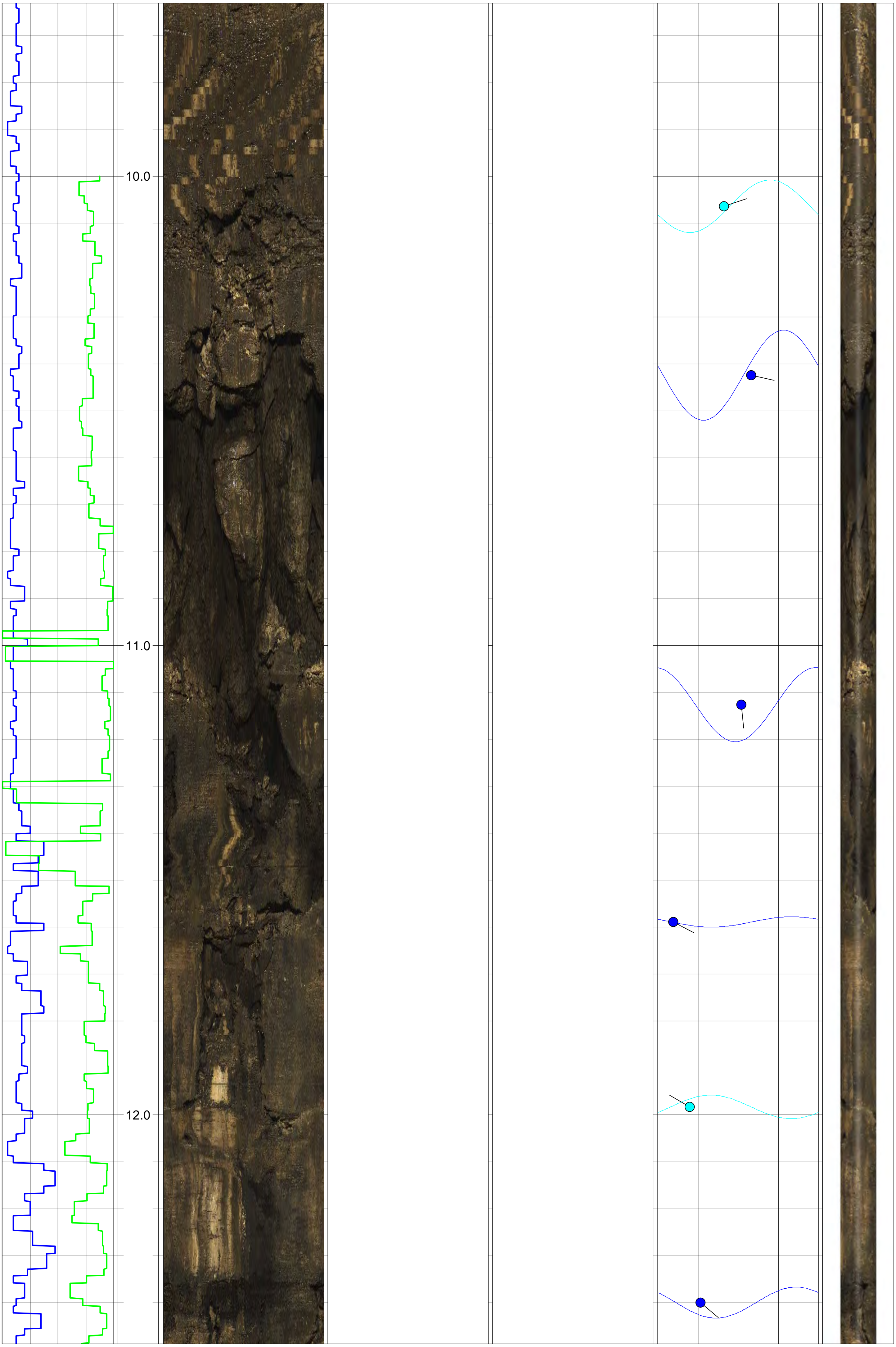
10.0
11.0
12.0

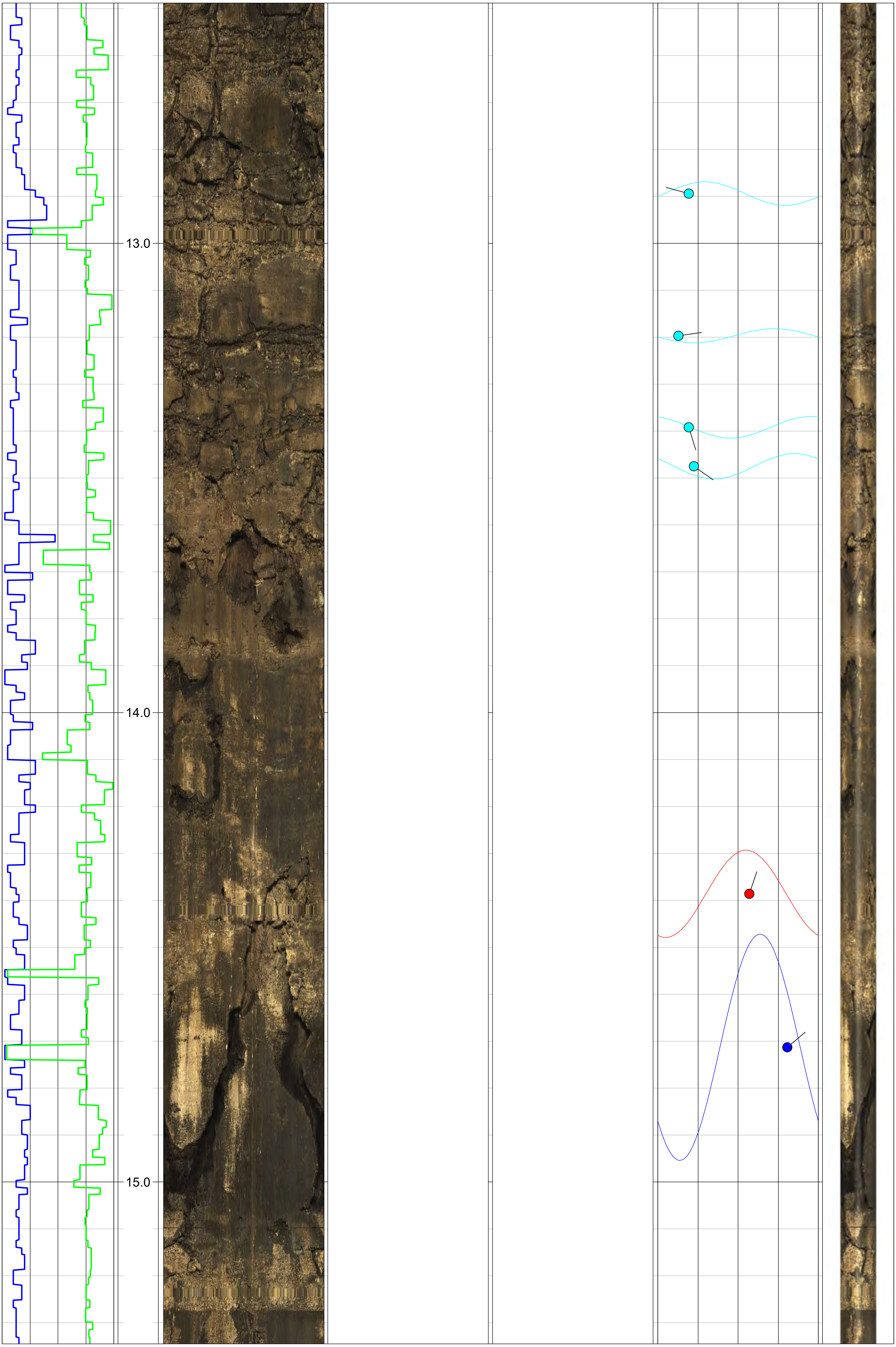
13.0
14.0
15.0

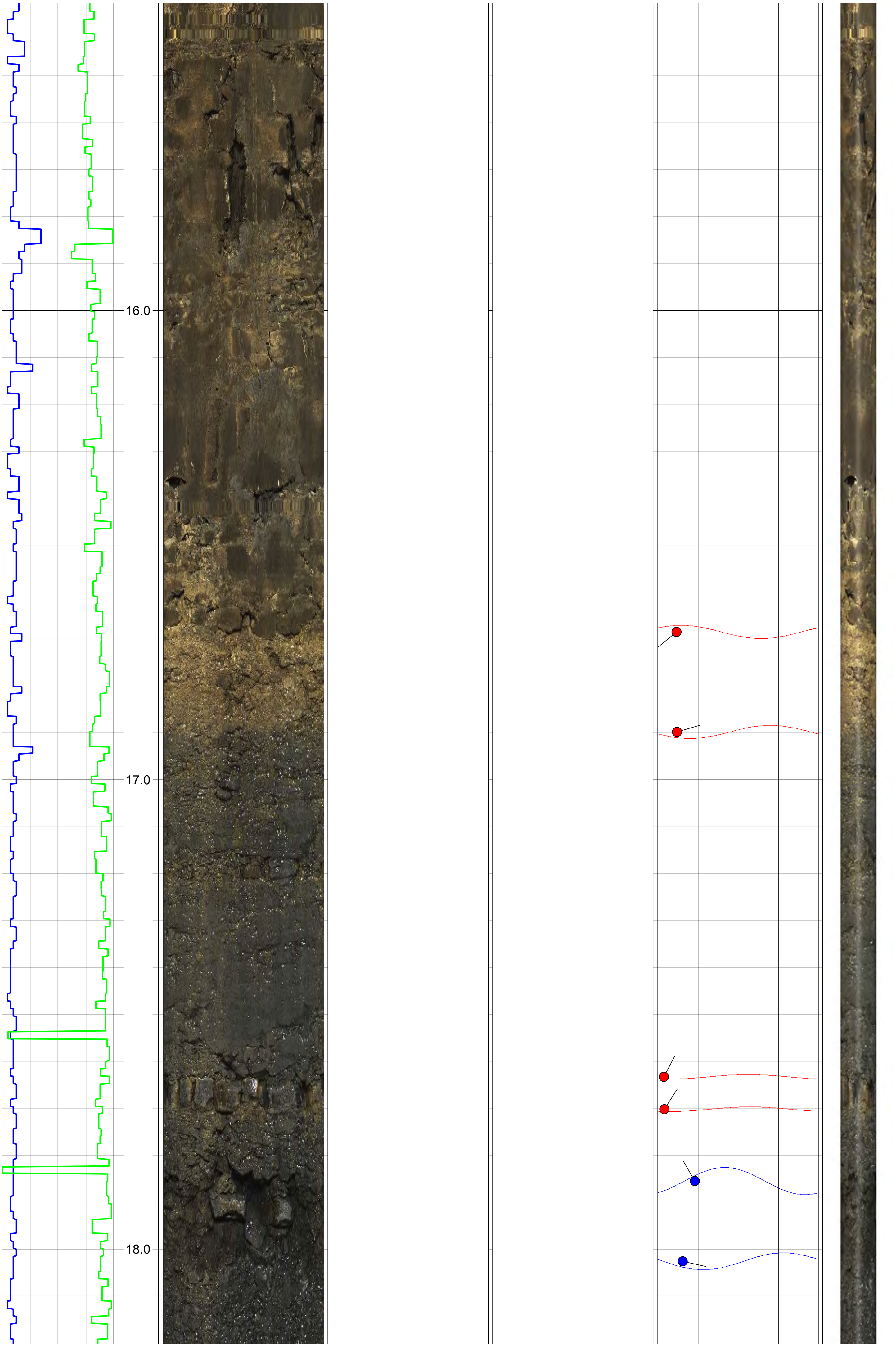
16.0
17.0
18.0

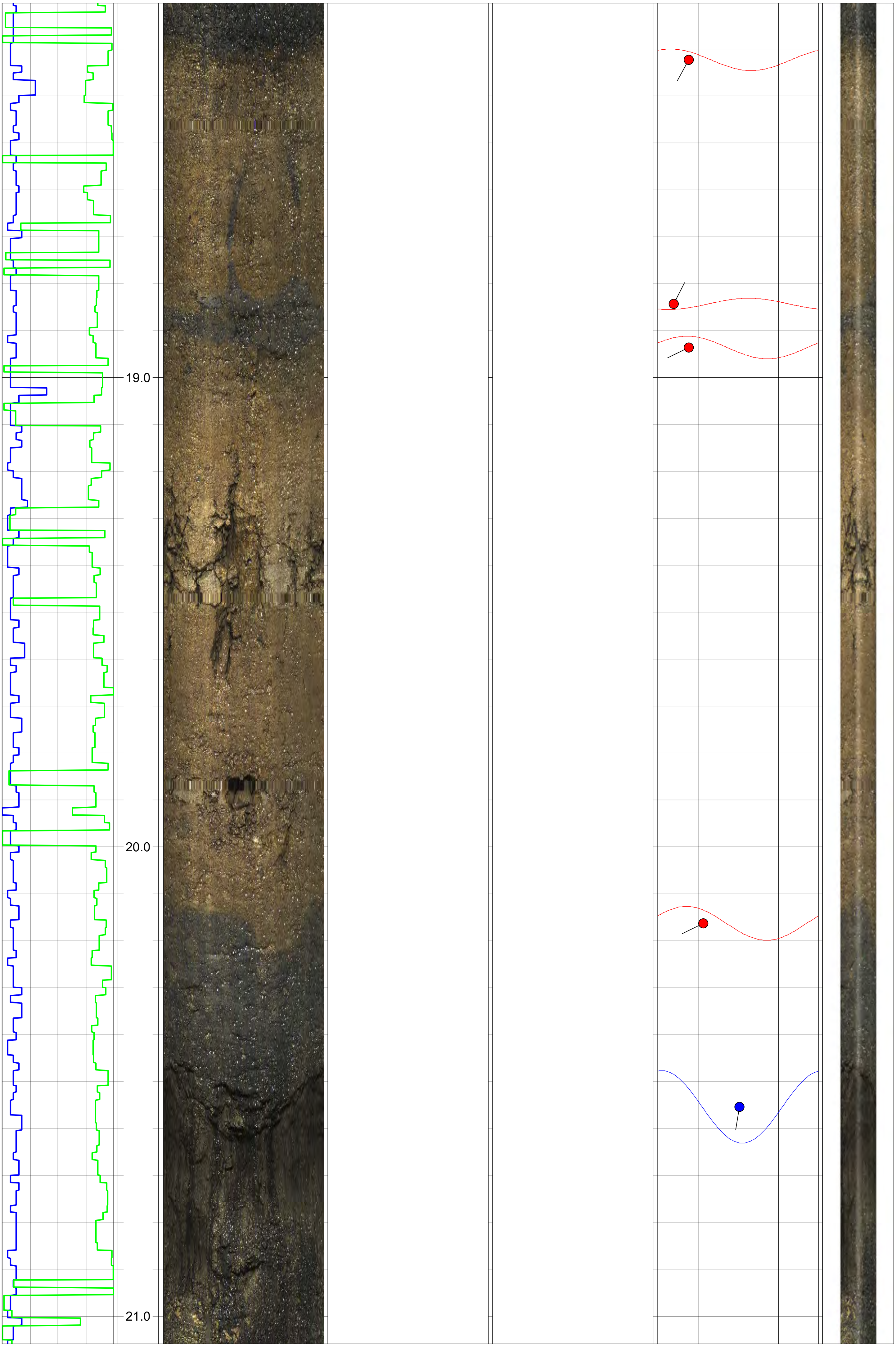
19.0
20.0
21.0

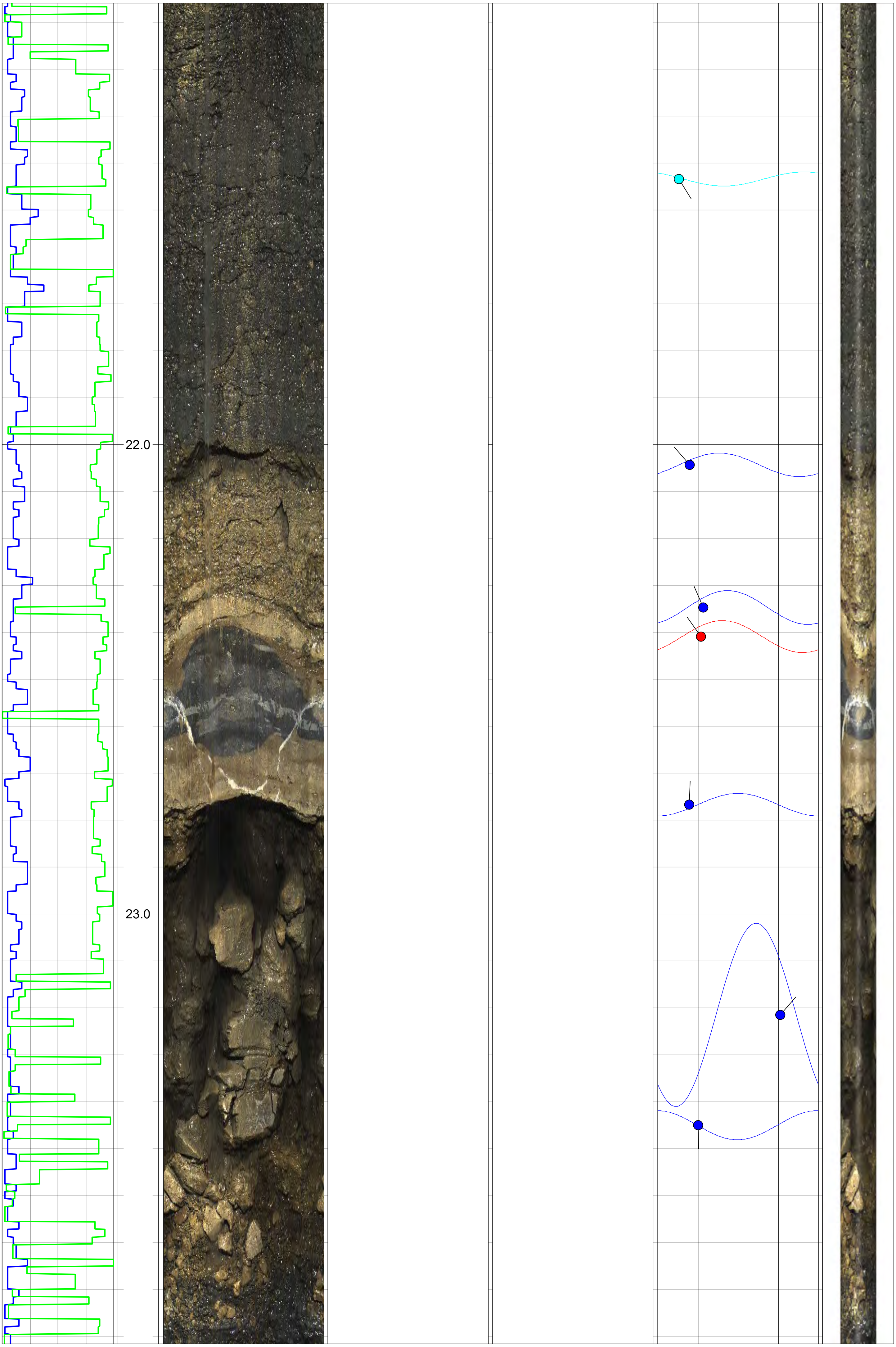
22.0
23.0

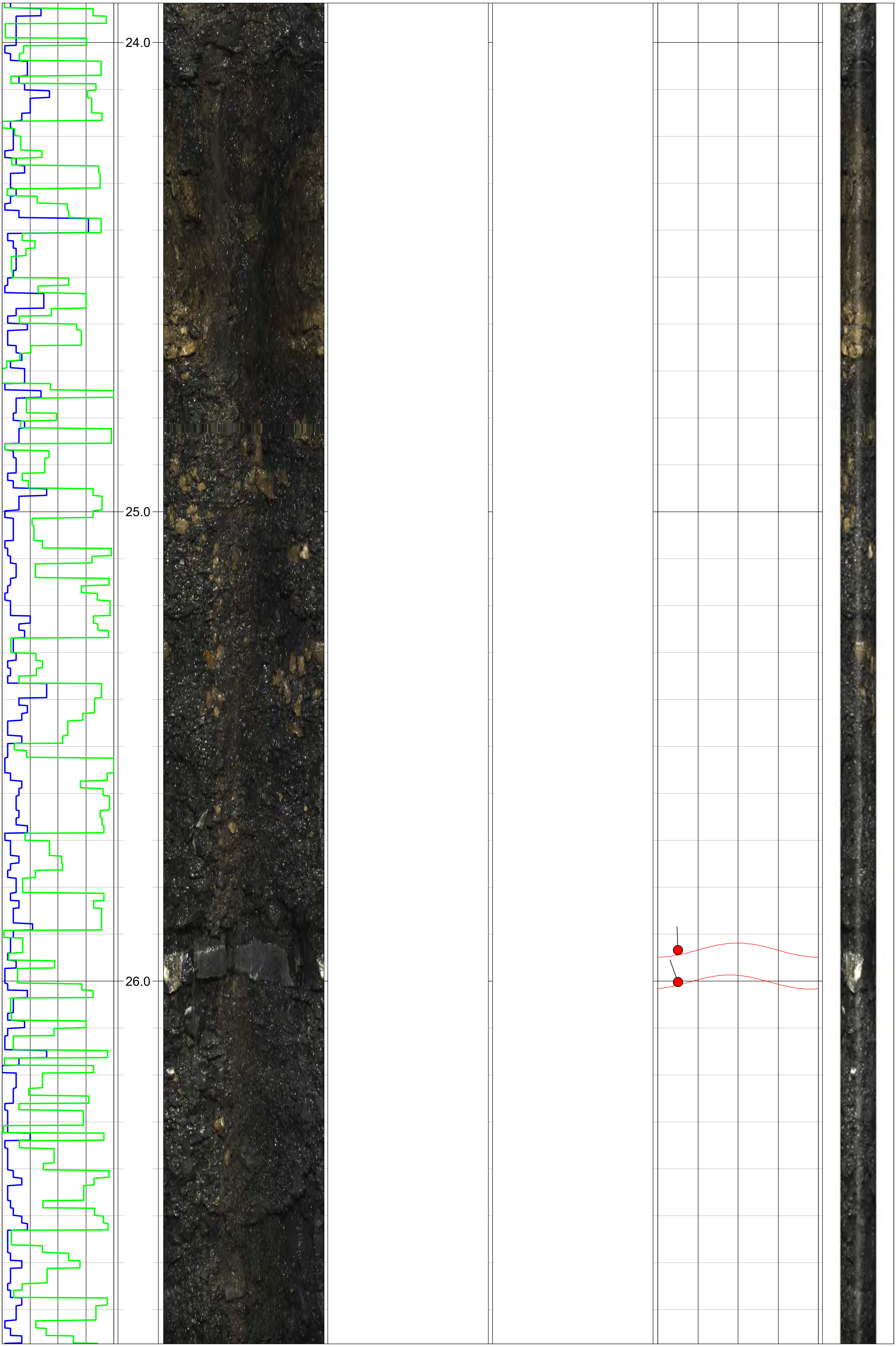
24.0
25.0
26.0

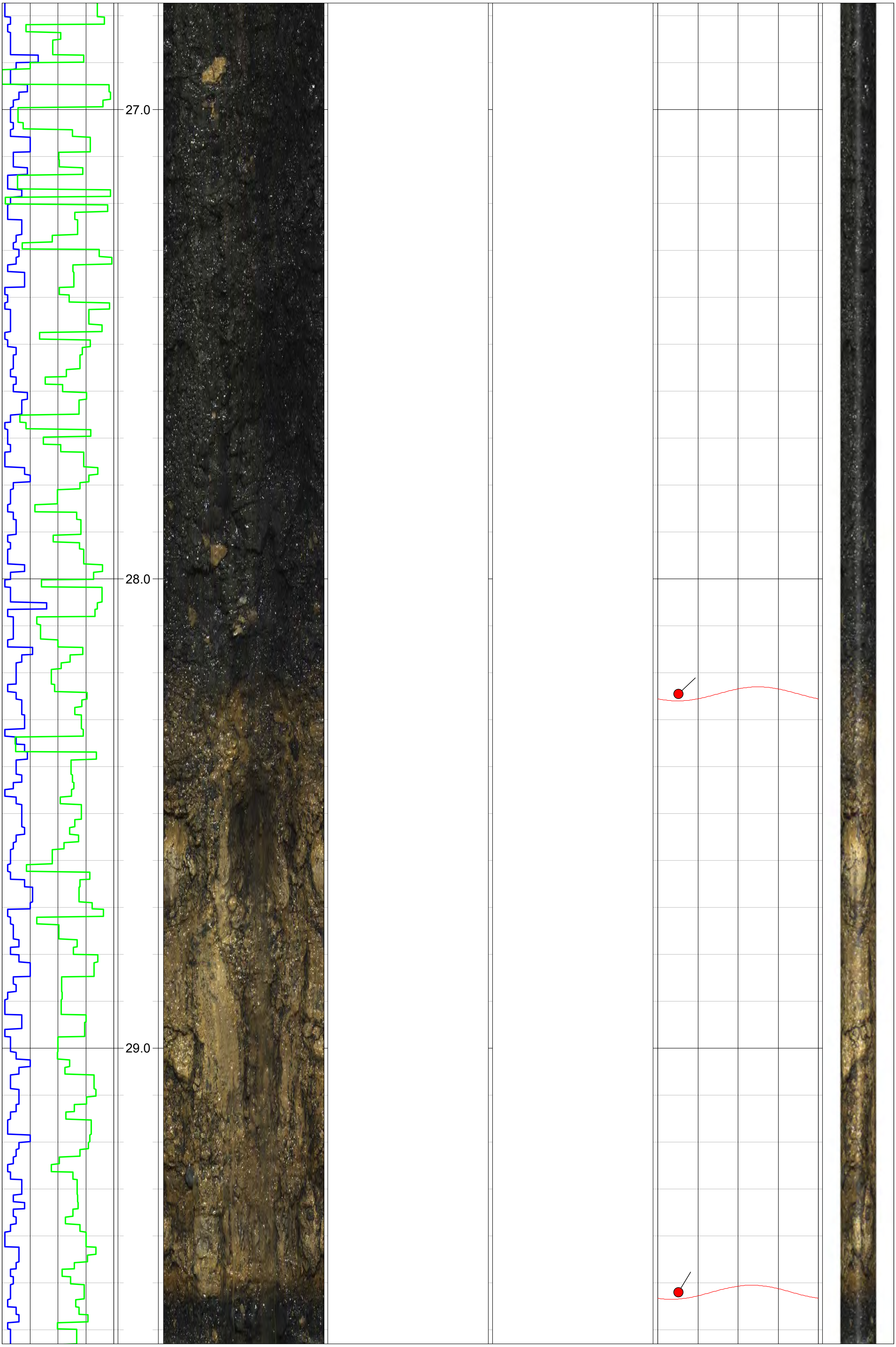
27.0
28.0
29.0

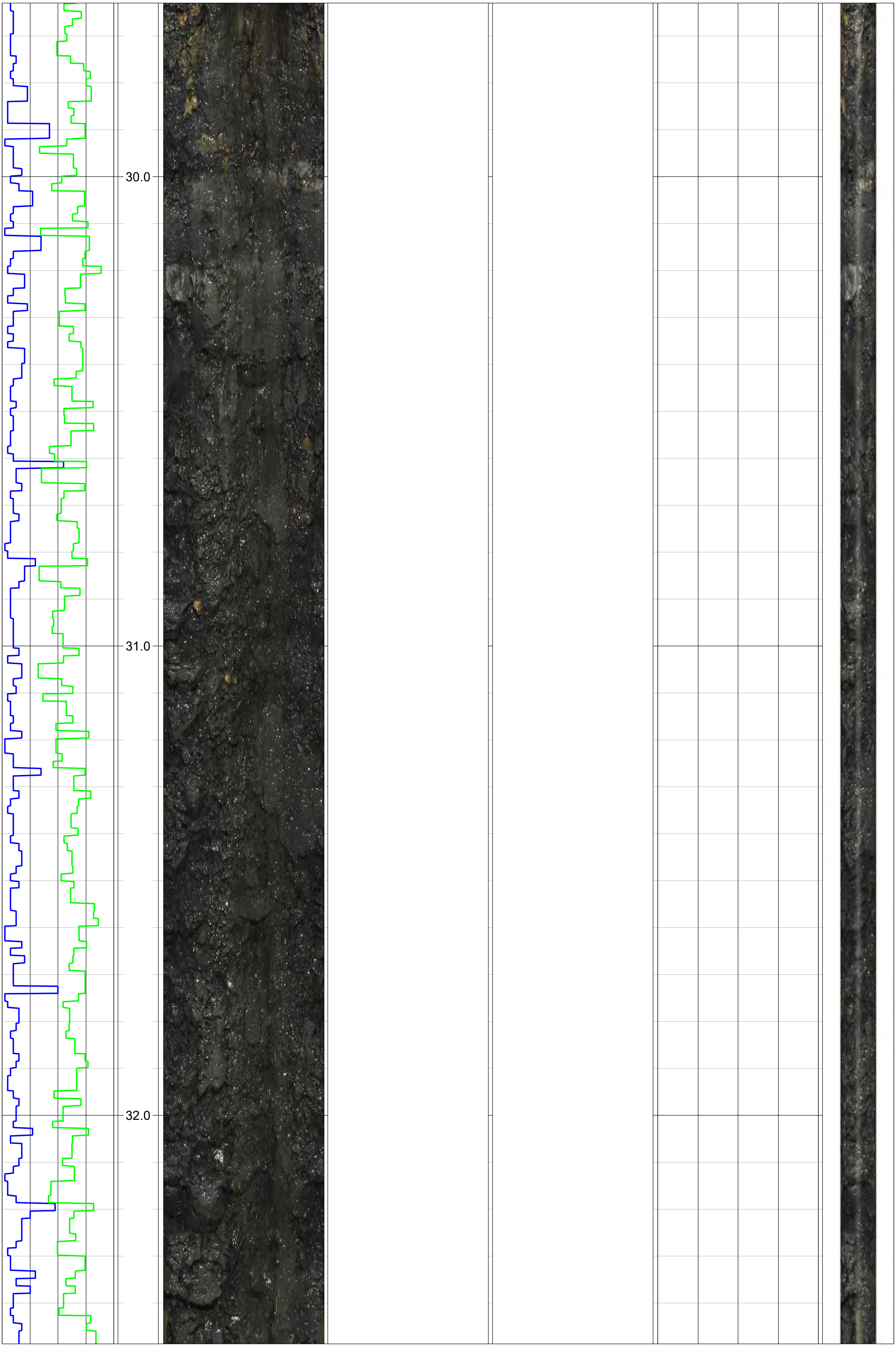
30.0
31.0
32.0

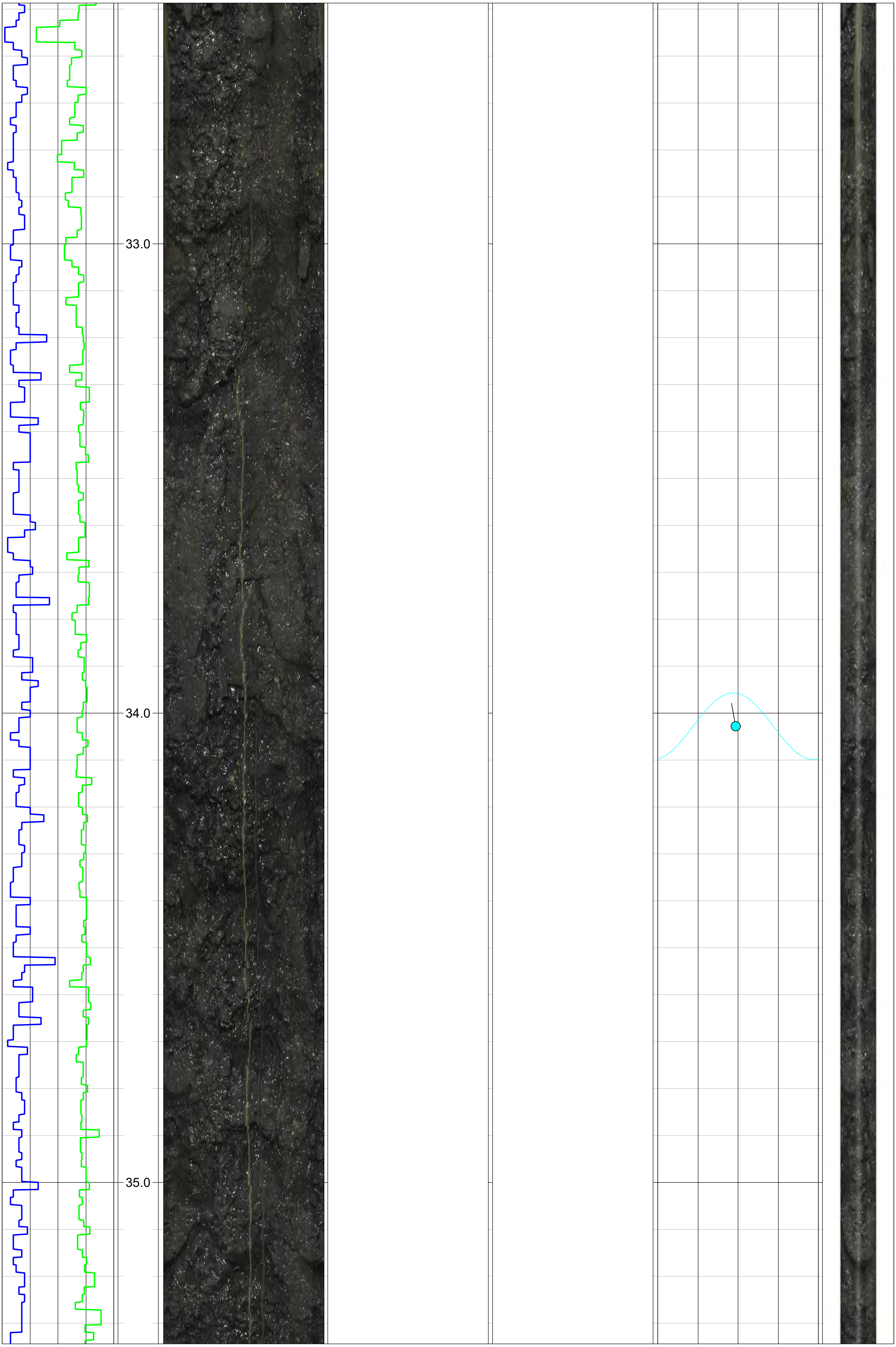
33.0
34.0
35.0

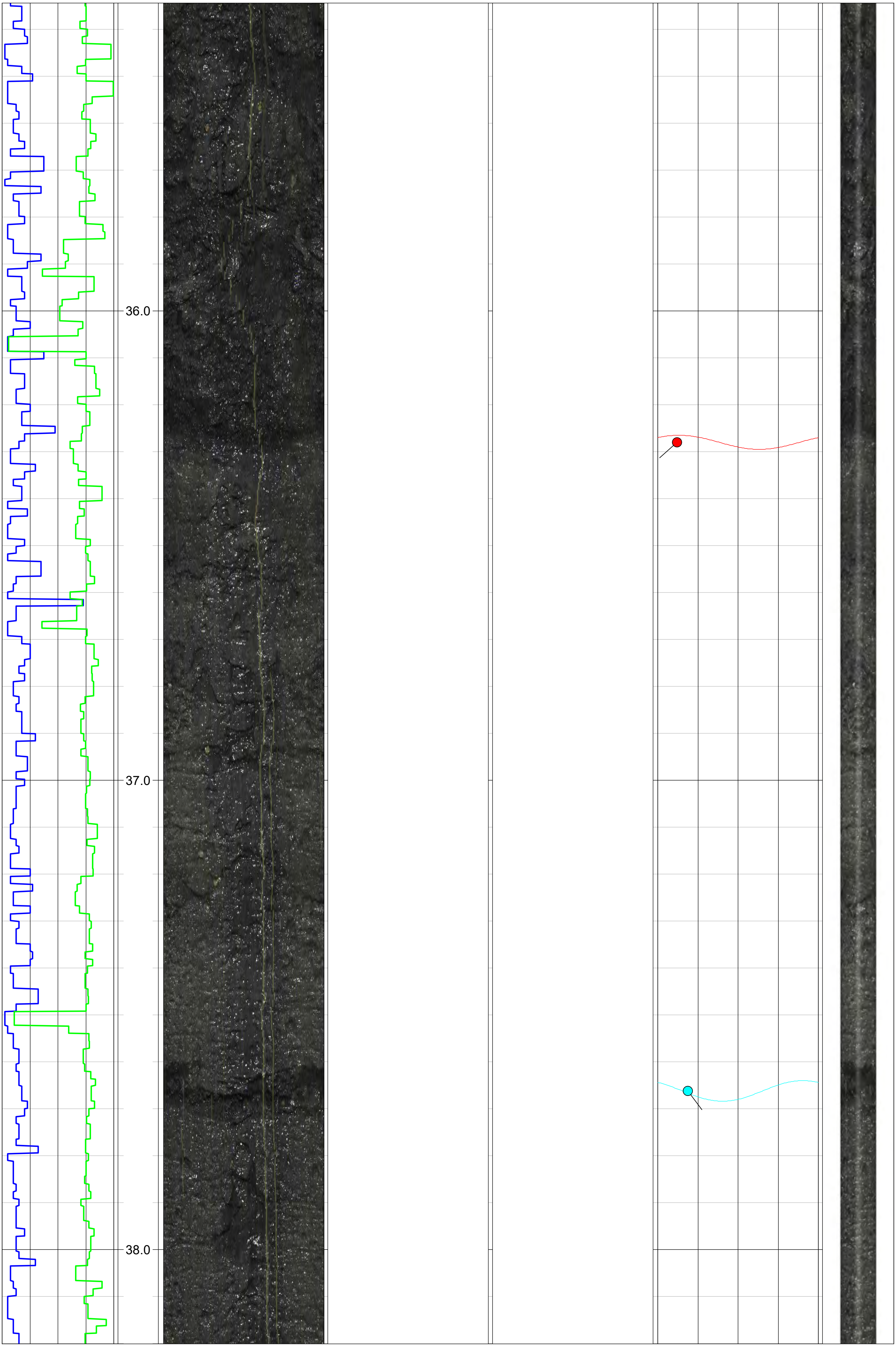
36.0
37.0
38.0

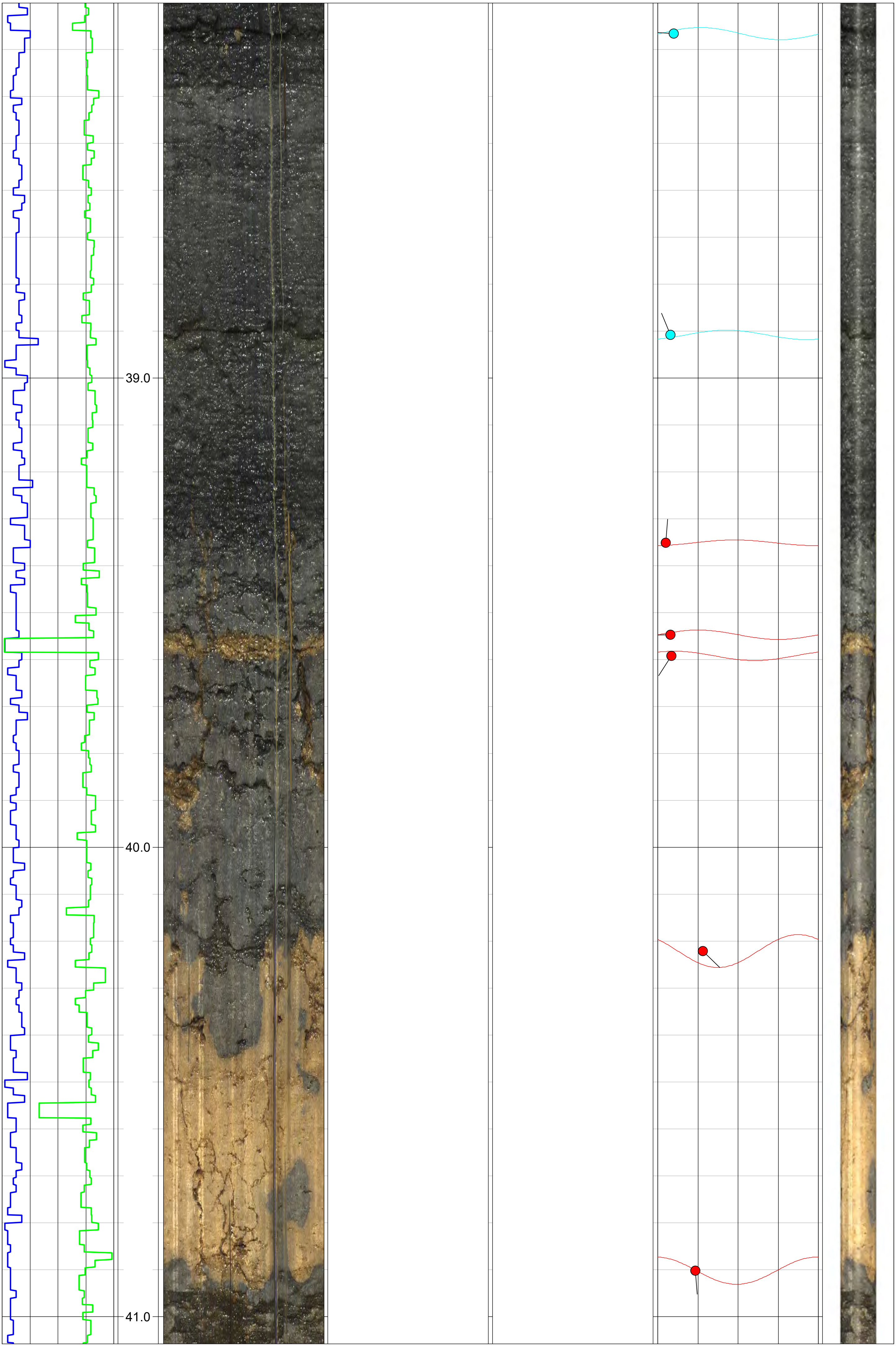
39.0
40.0
41.0

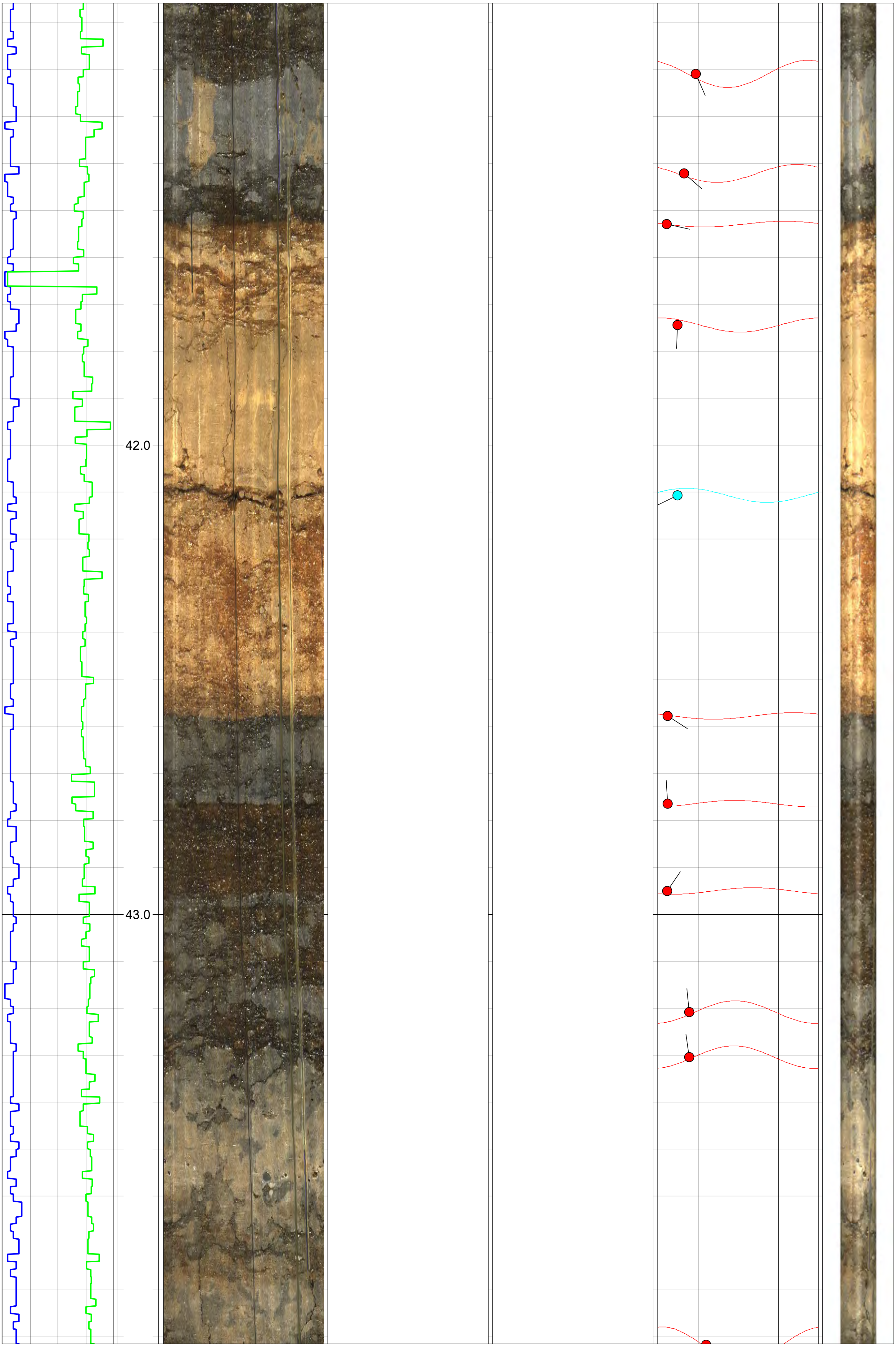

42.0
43.0

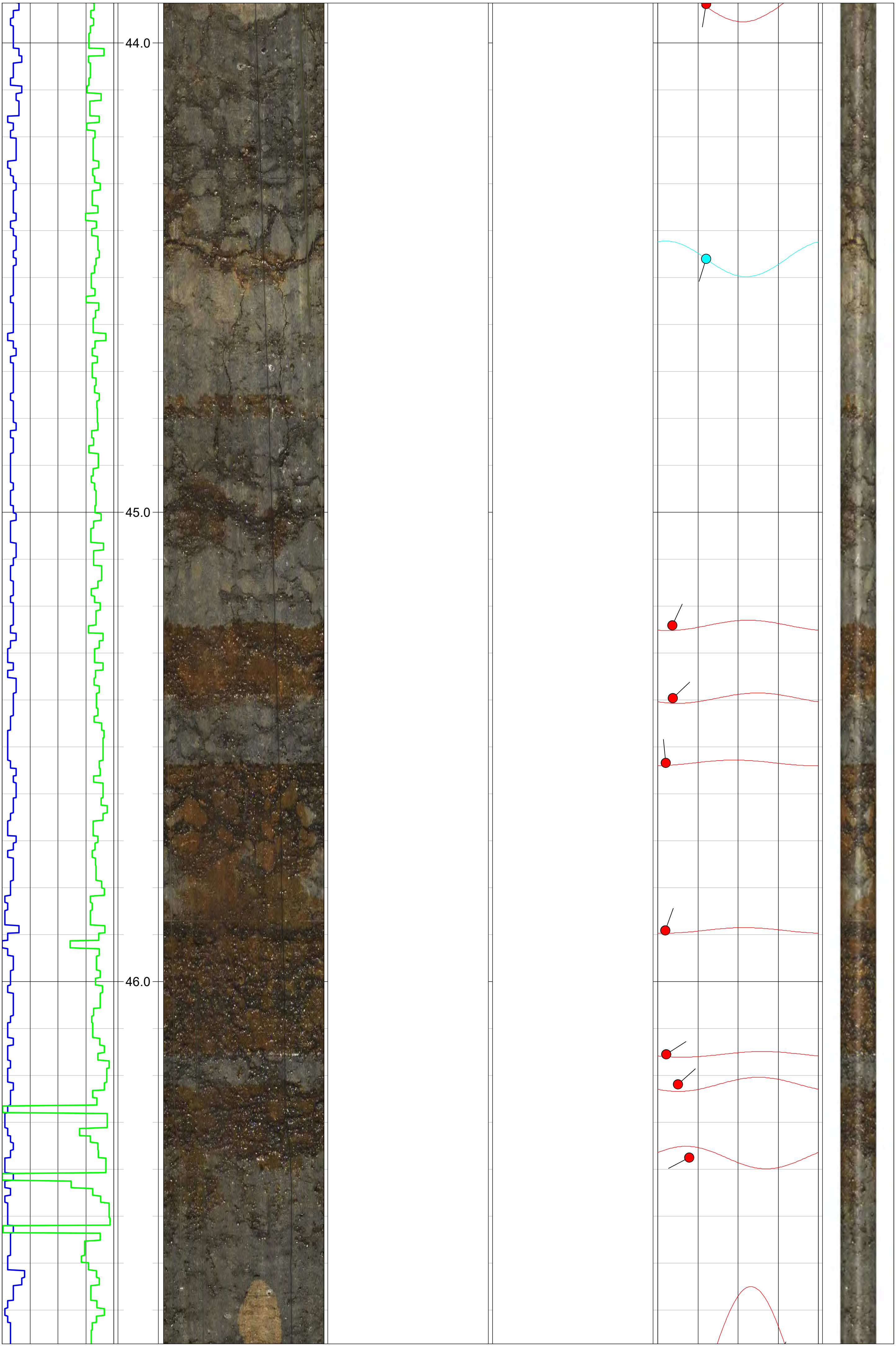
44.0
45.0
46.0

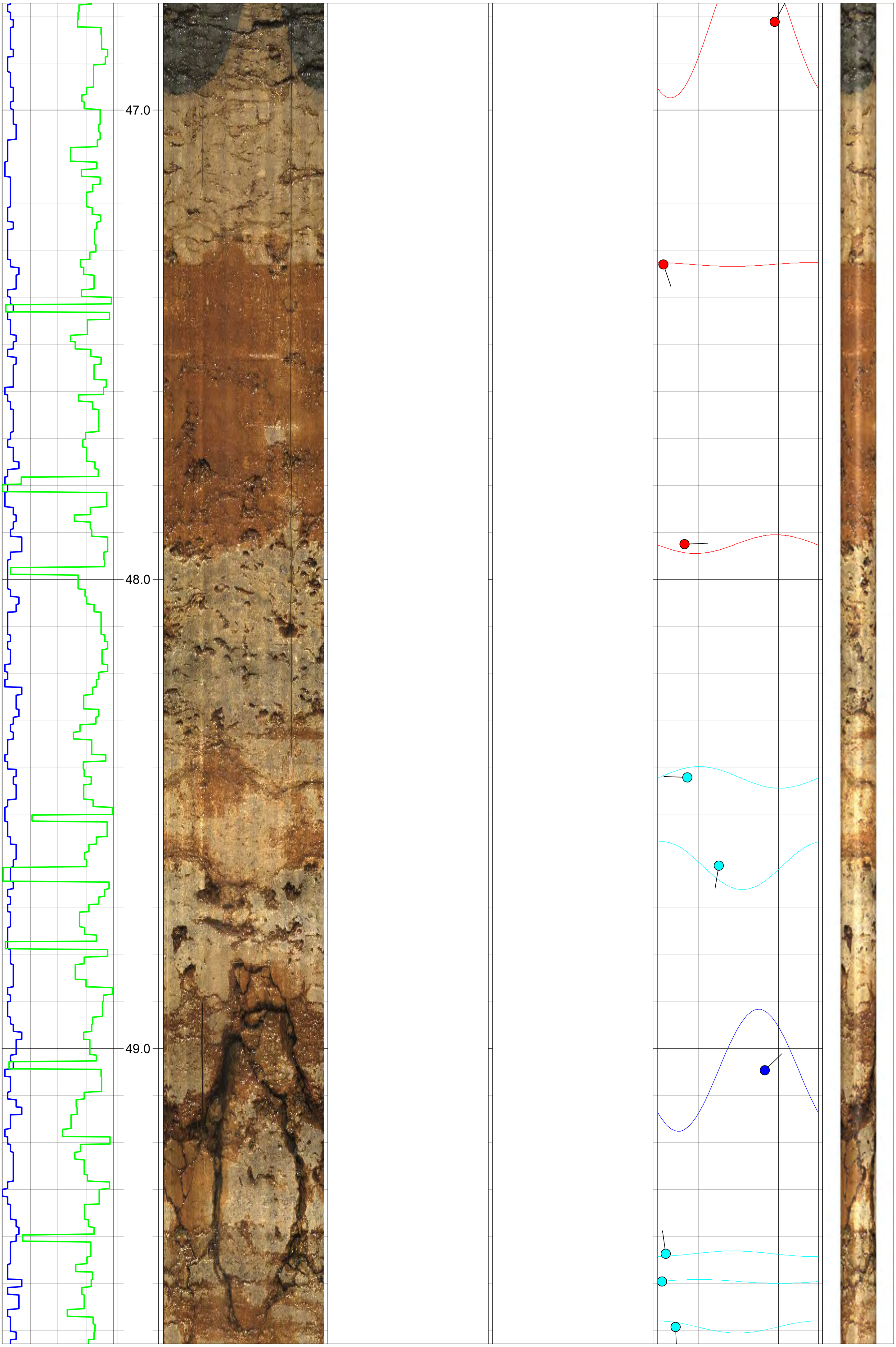
47.0
48.0
49.0

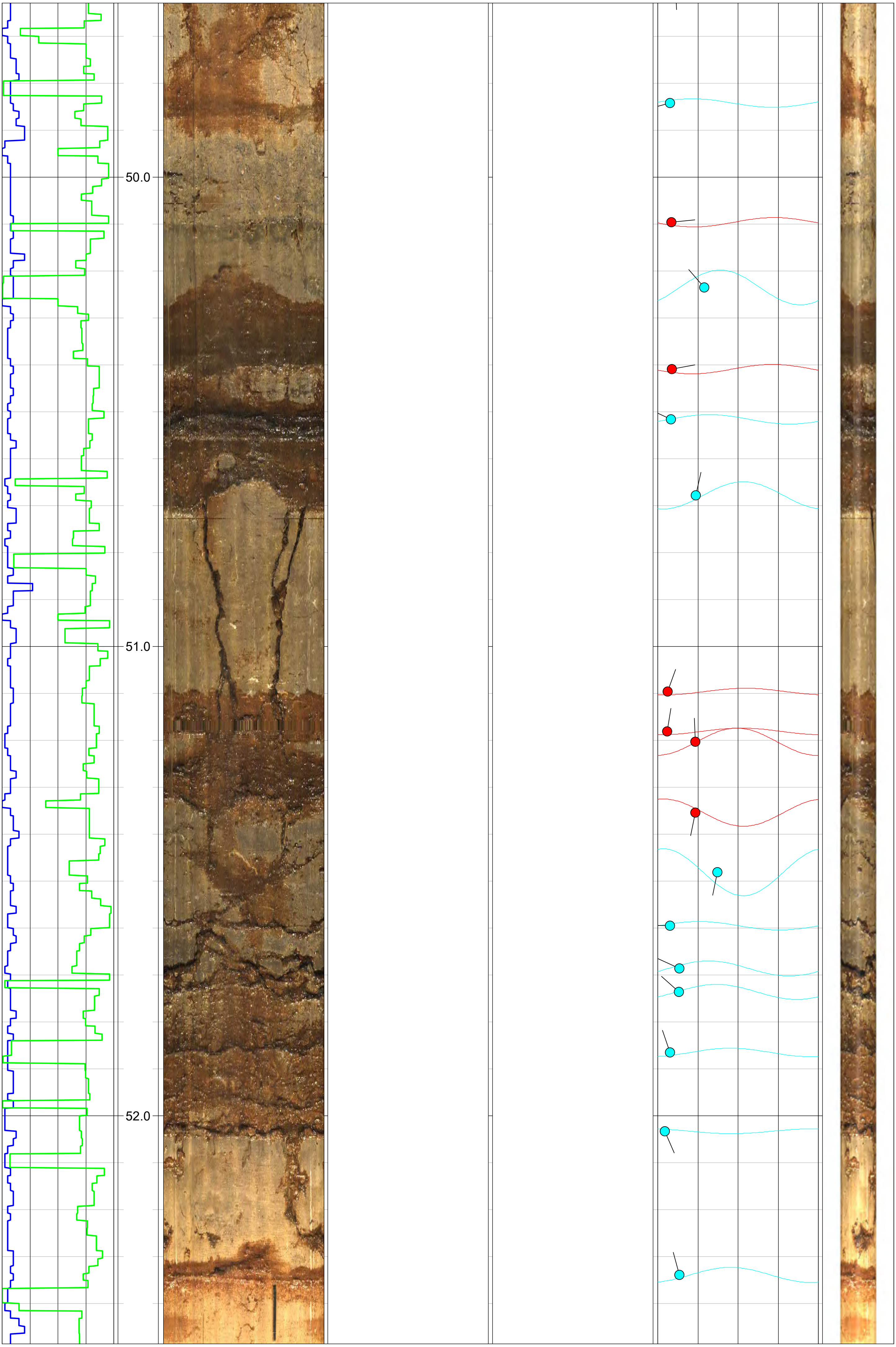
50.0
51.0
52.0

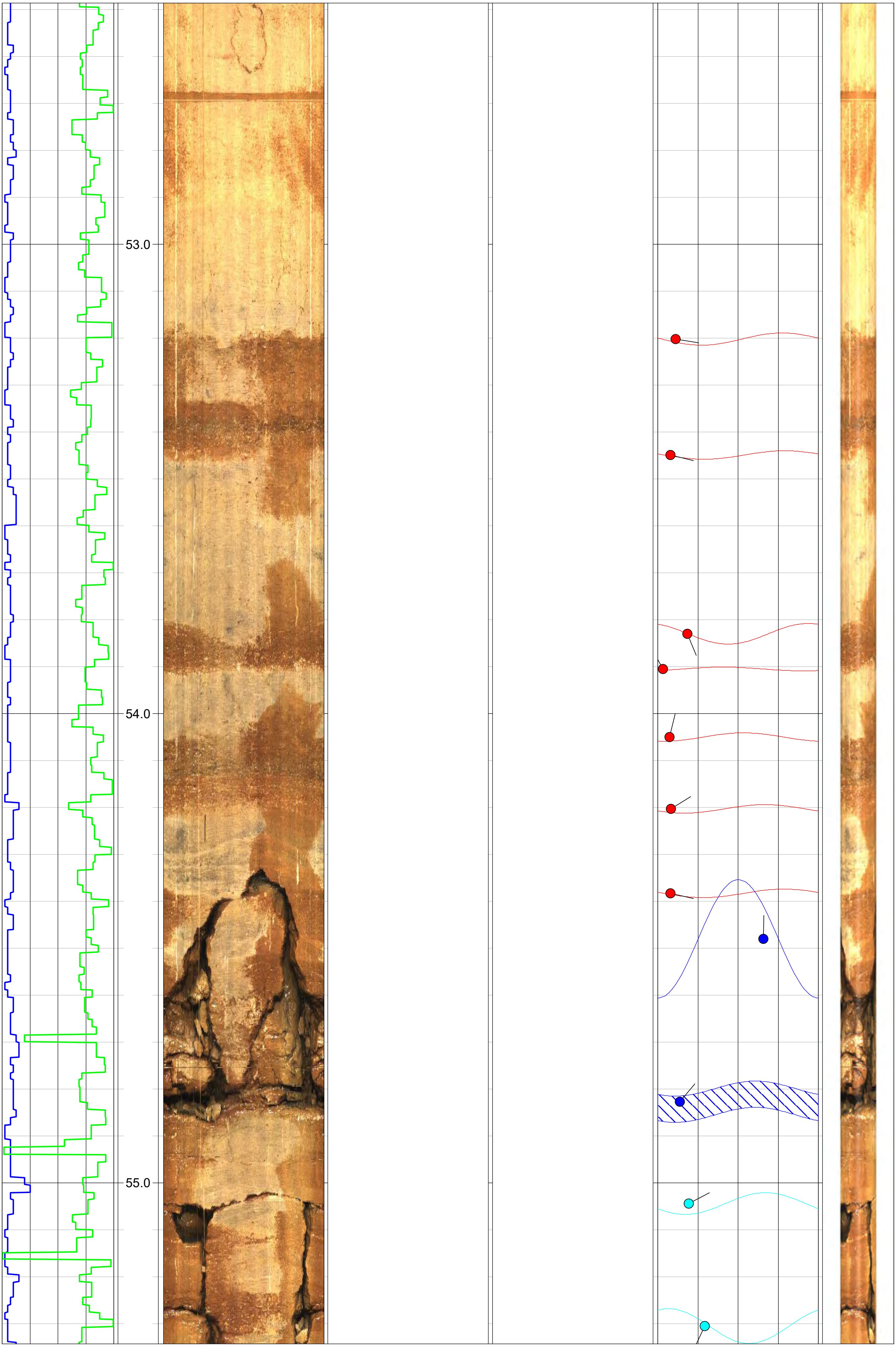
53.0
54.0
55.0

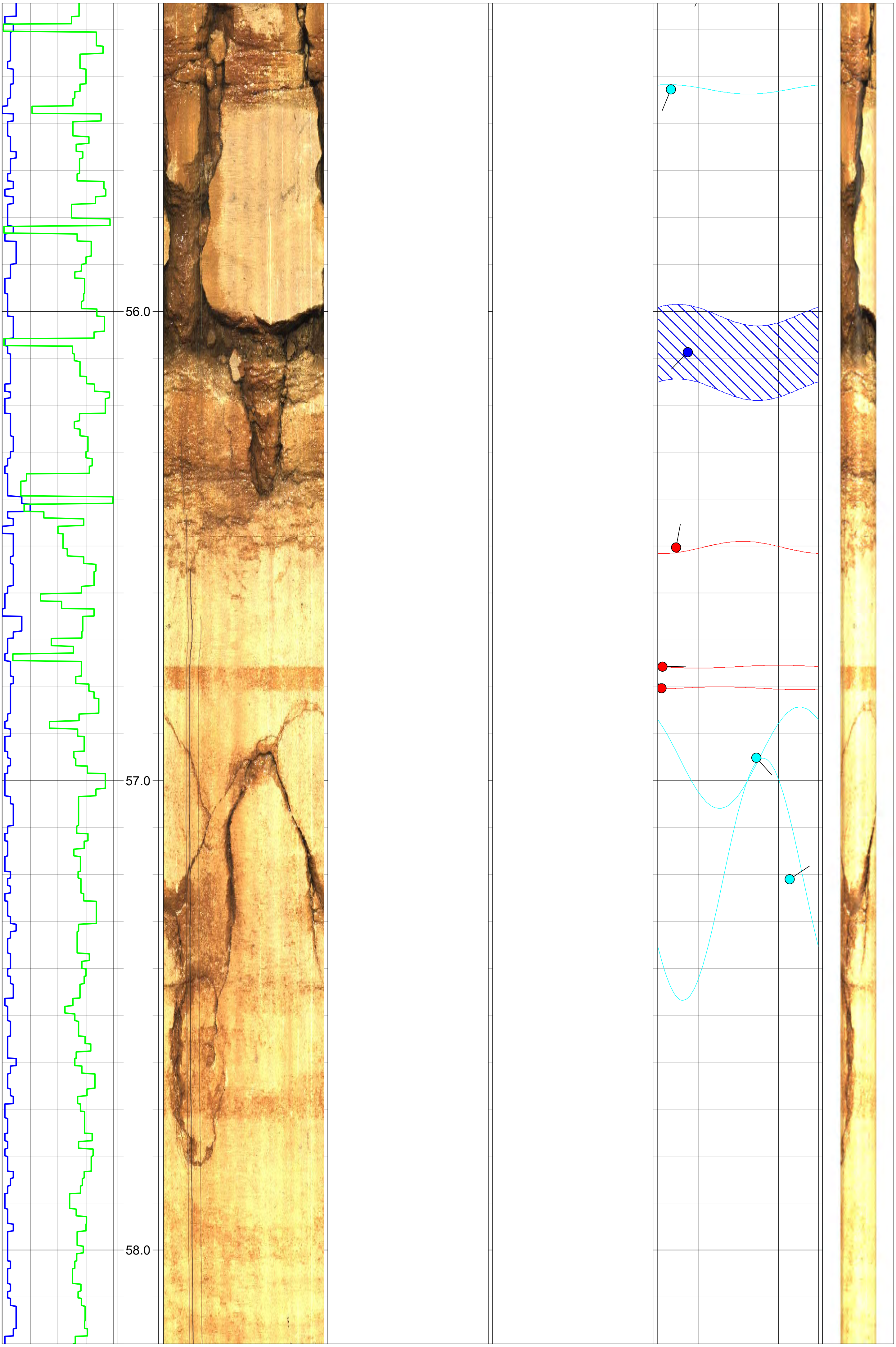
56.0
57.0
58.0

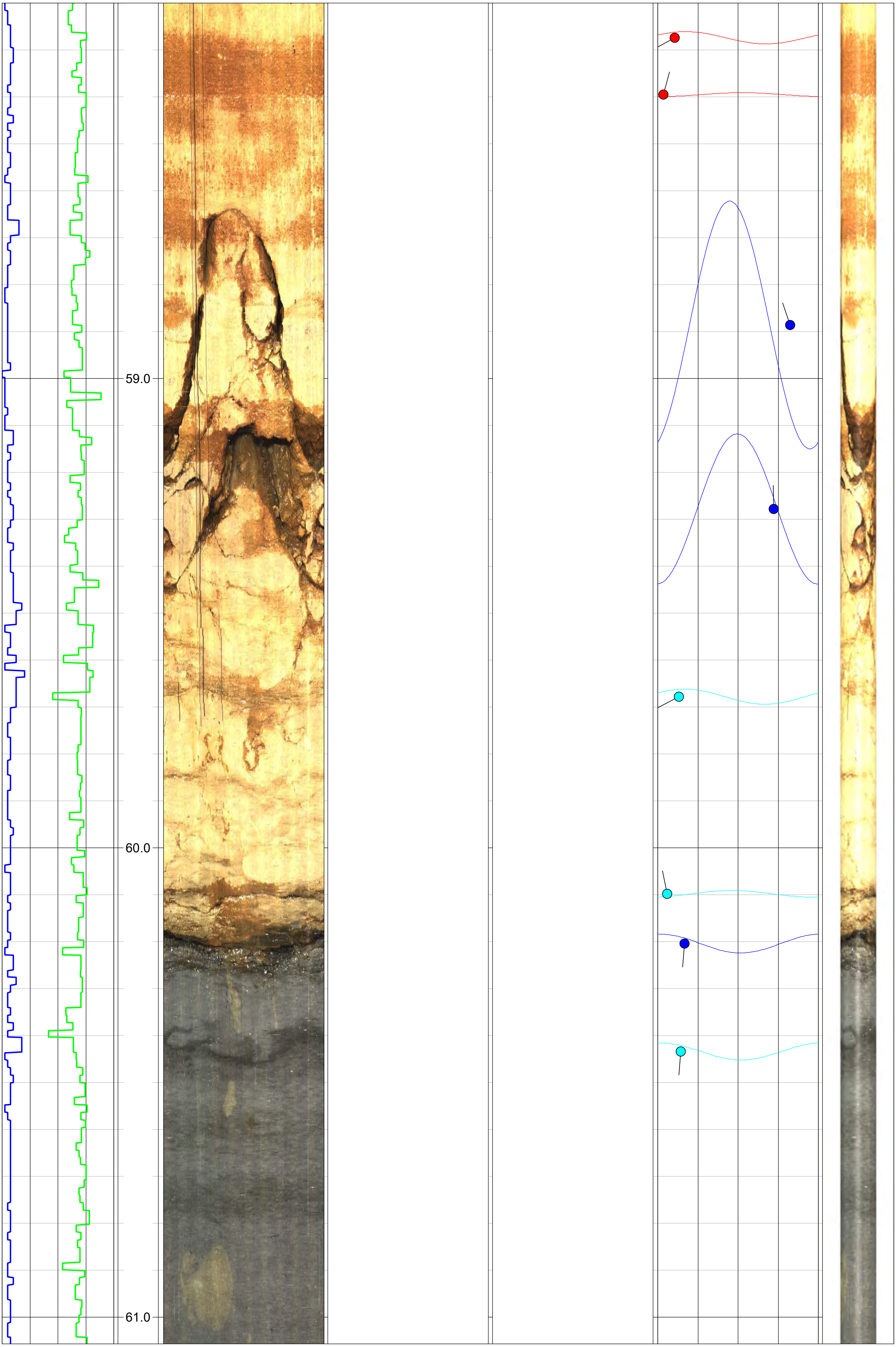
59.0
60.0
61.0

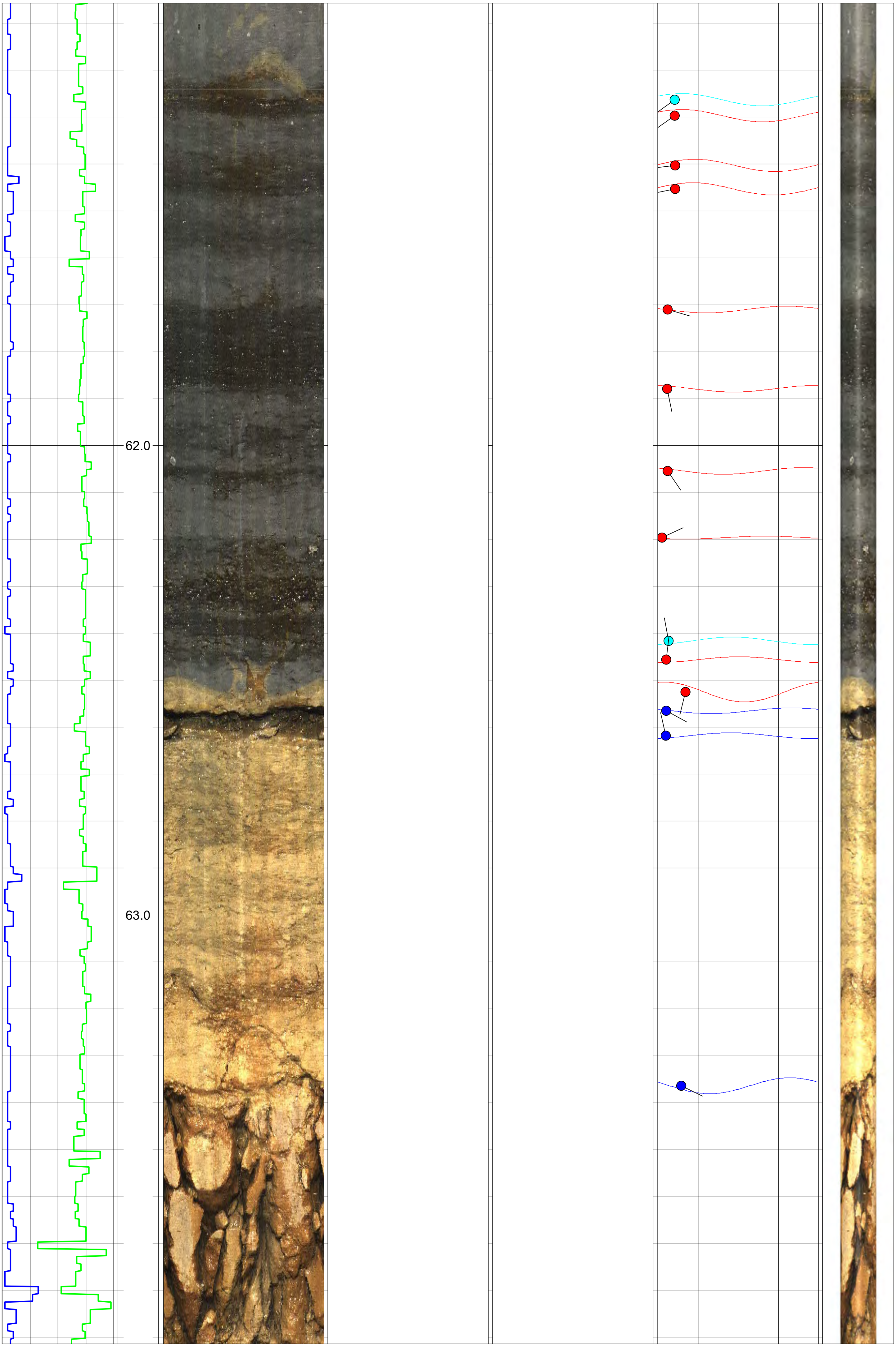
62.0
63.0

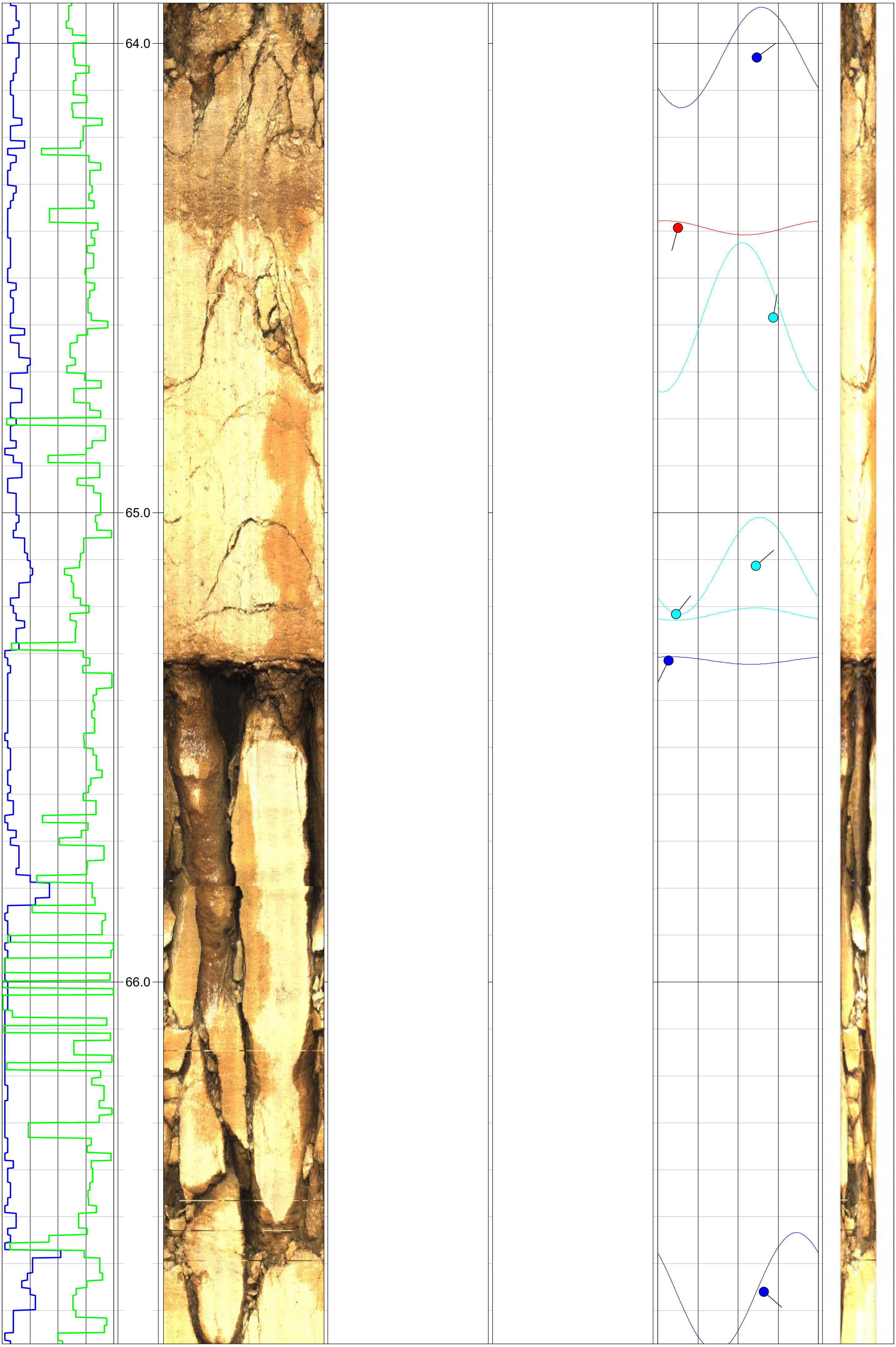
64.0
65.0
66.0

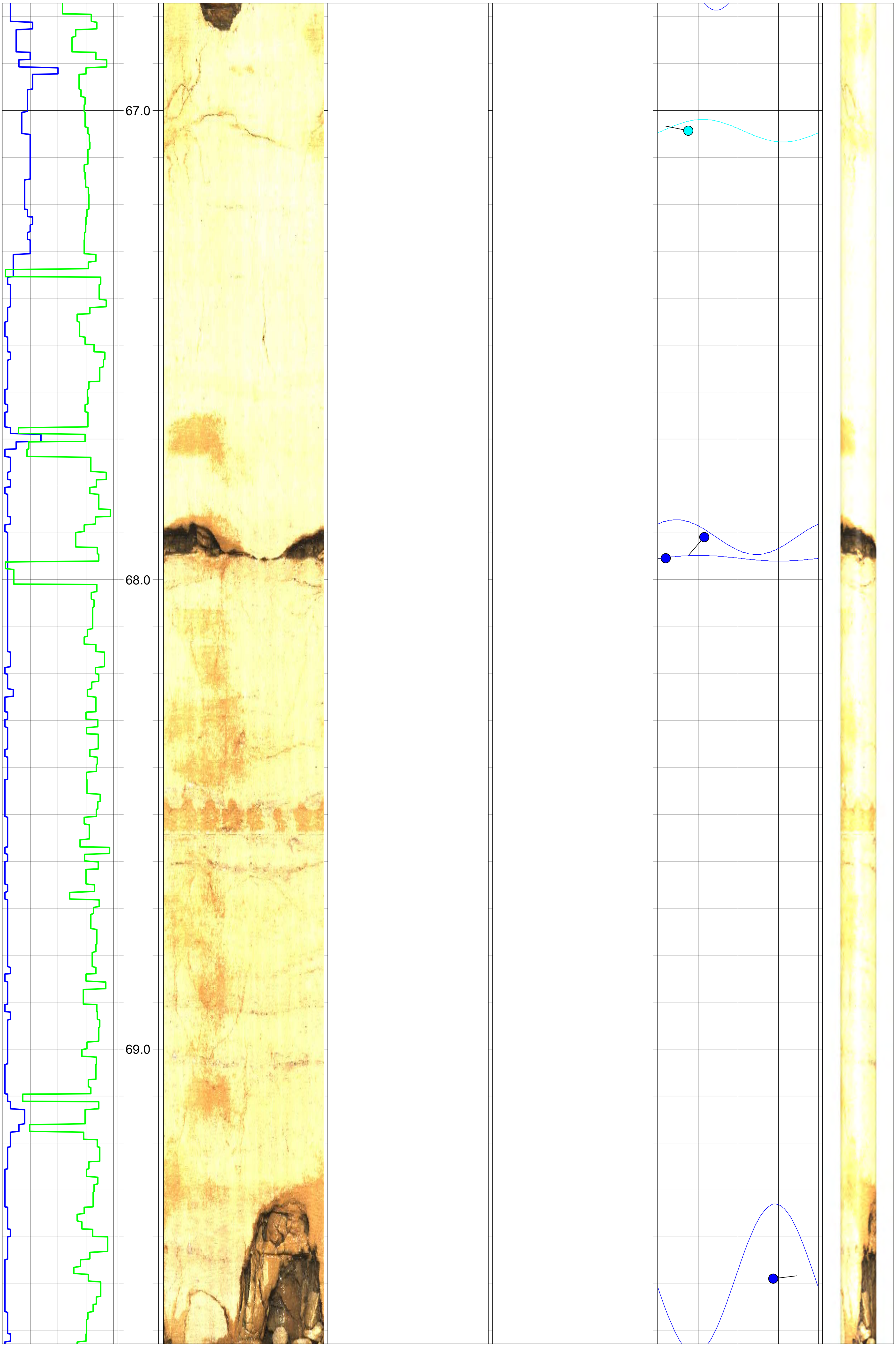
67.0
68.0
69.0

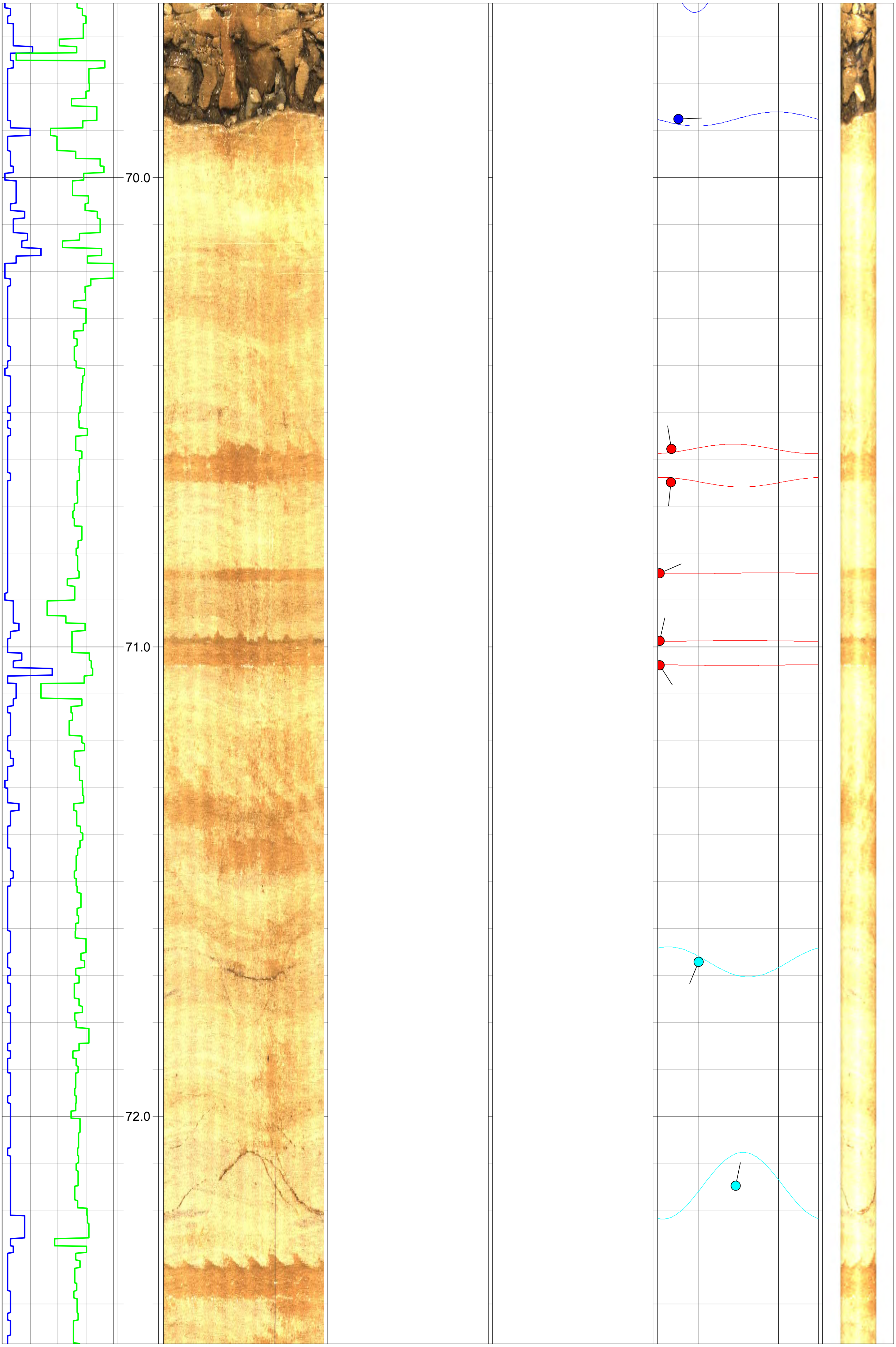
70.0
71.0
72.0

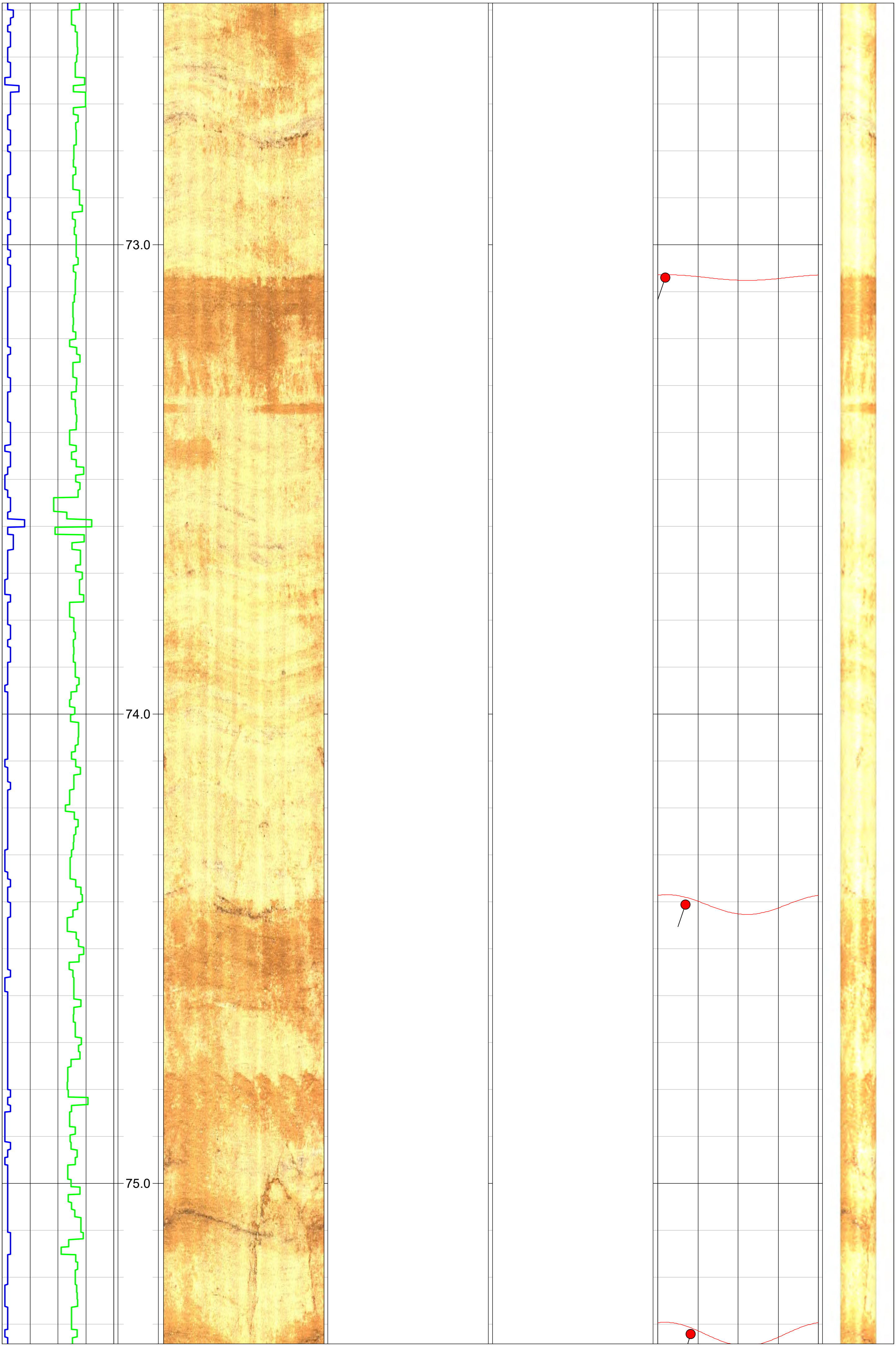
73.0
74.0
75.0

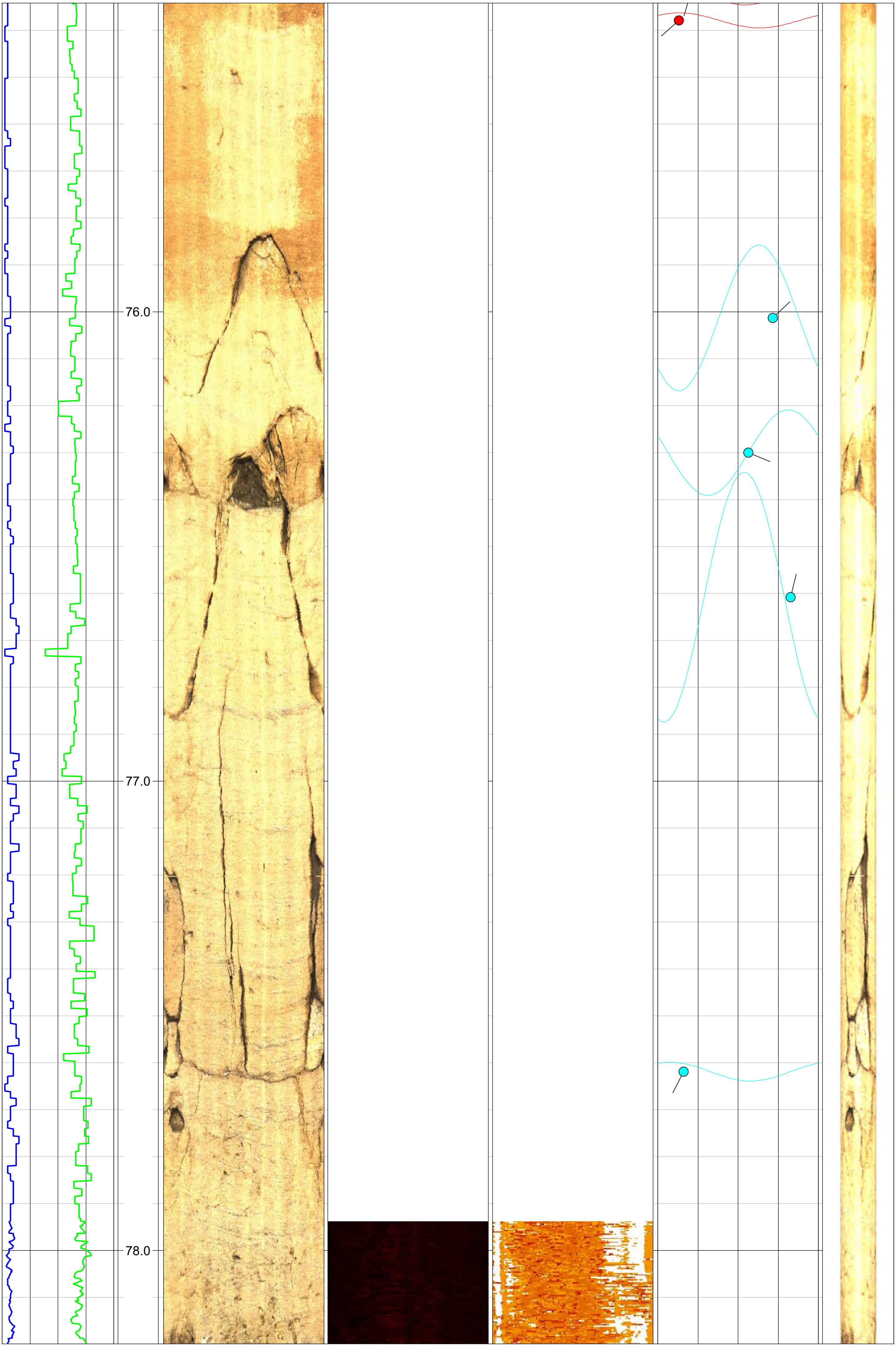
76.0
77.0
78.0

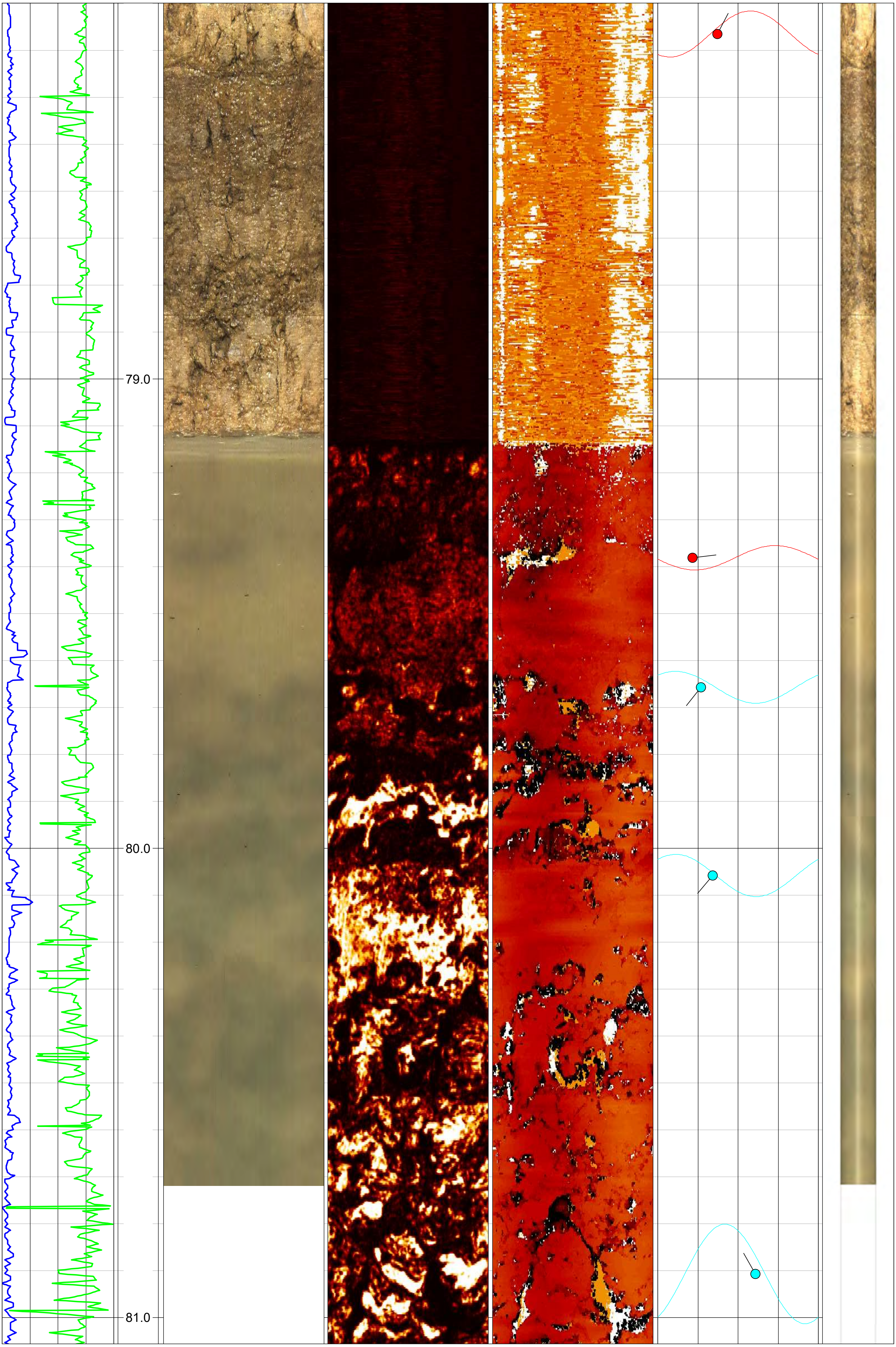
79.0
80.0
81.0

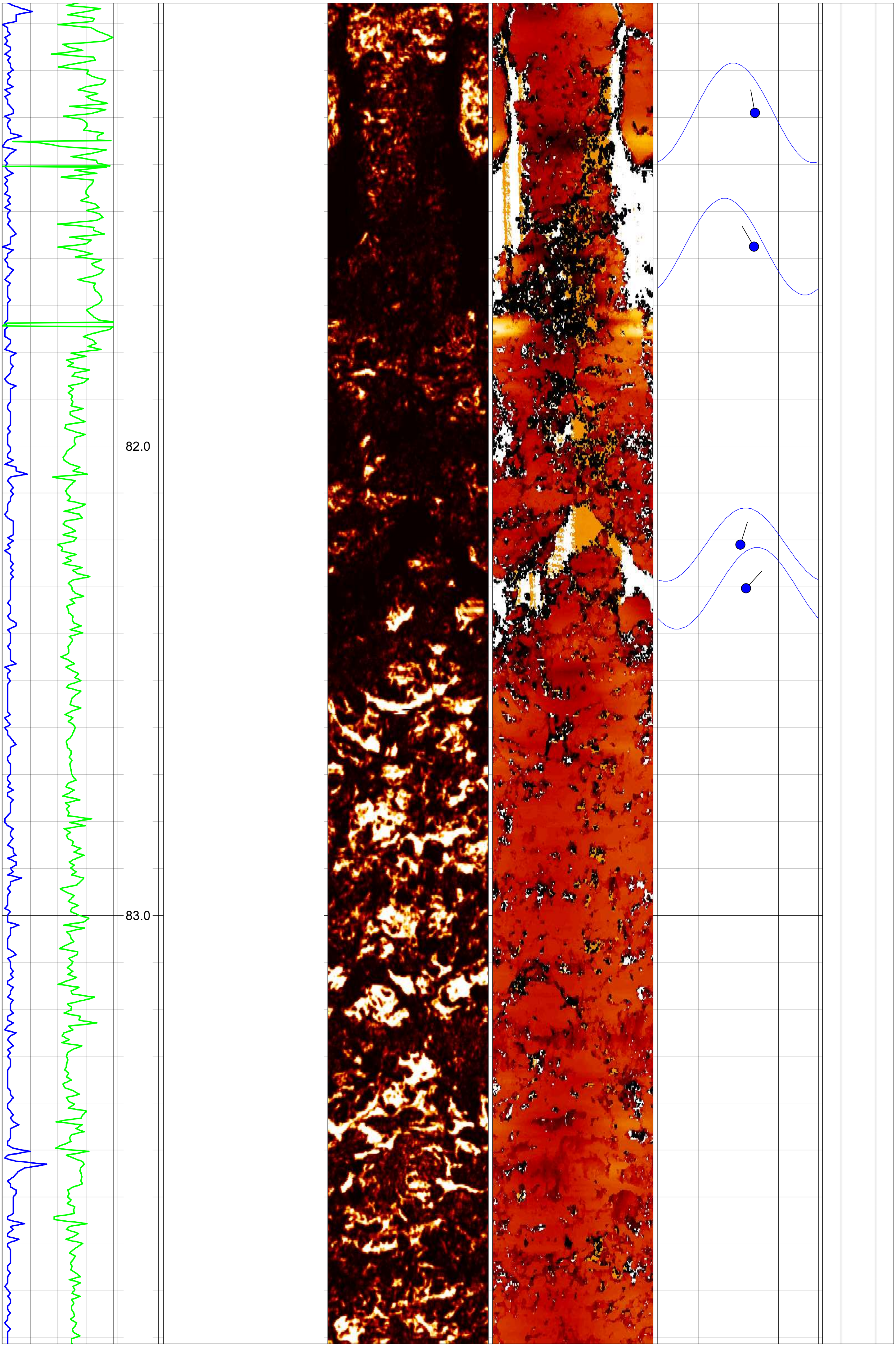
82.0
83.0

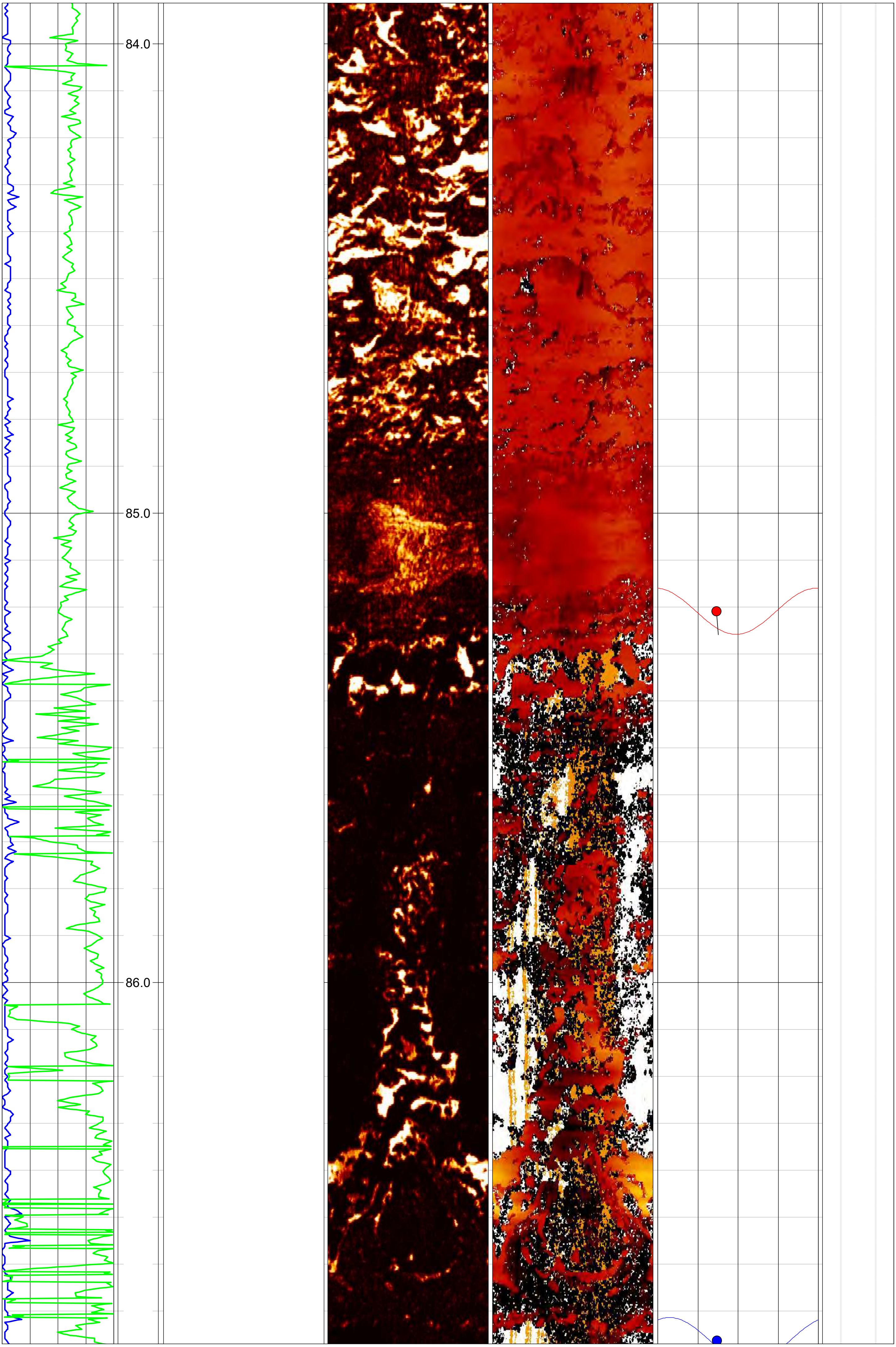
84.0
85.0
86.0

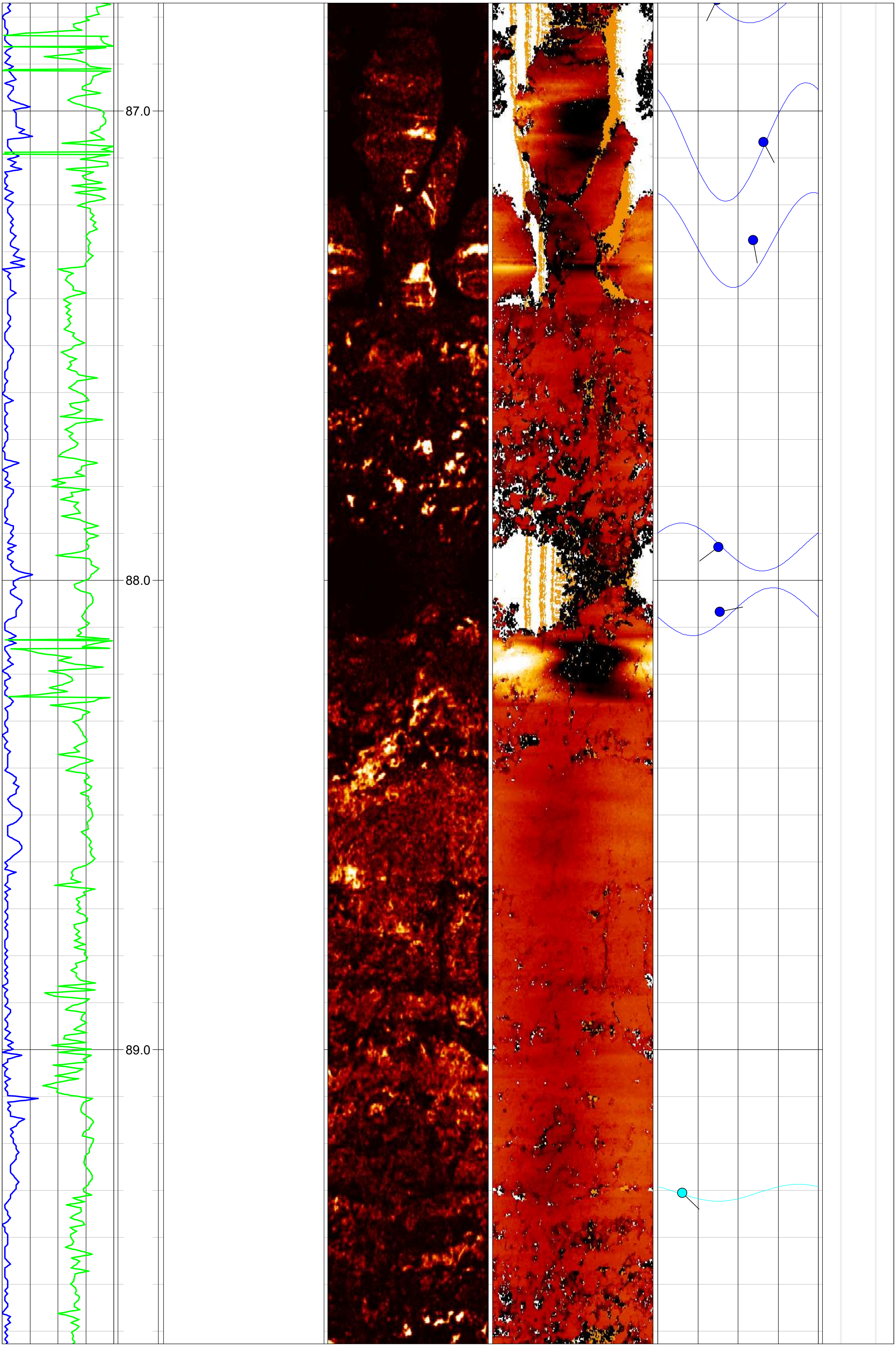

87.0
88.0
89.0

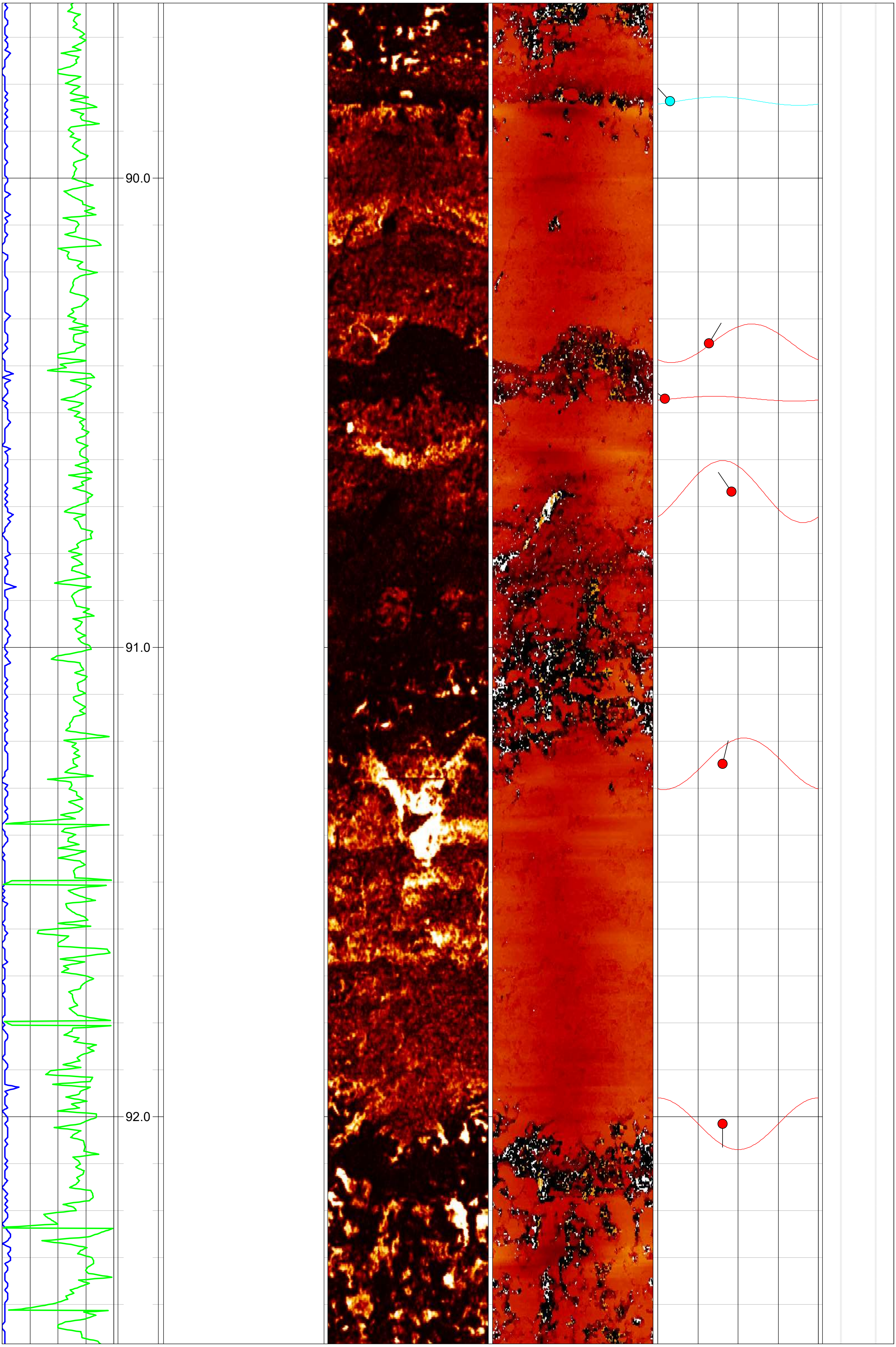
90.0
91.0
92.0

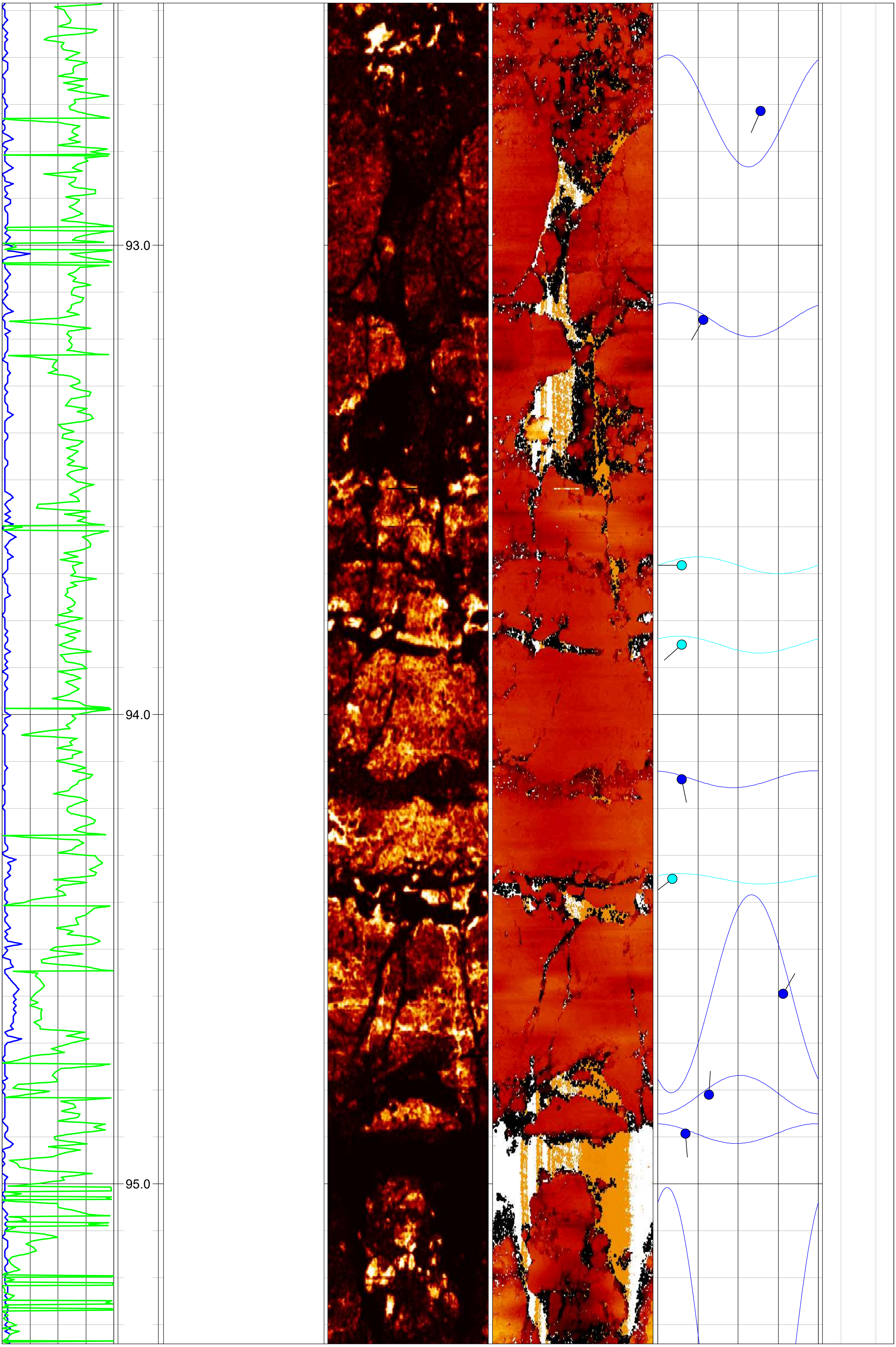

93.0
94.0
95.0

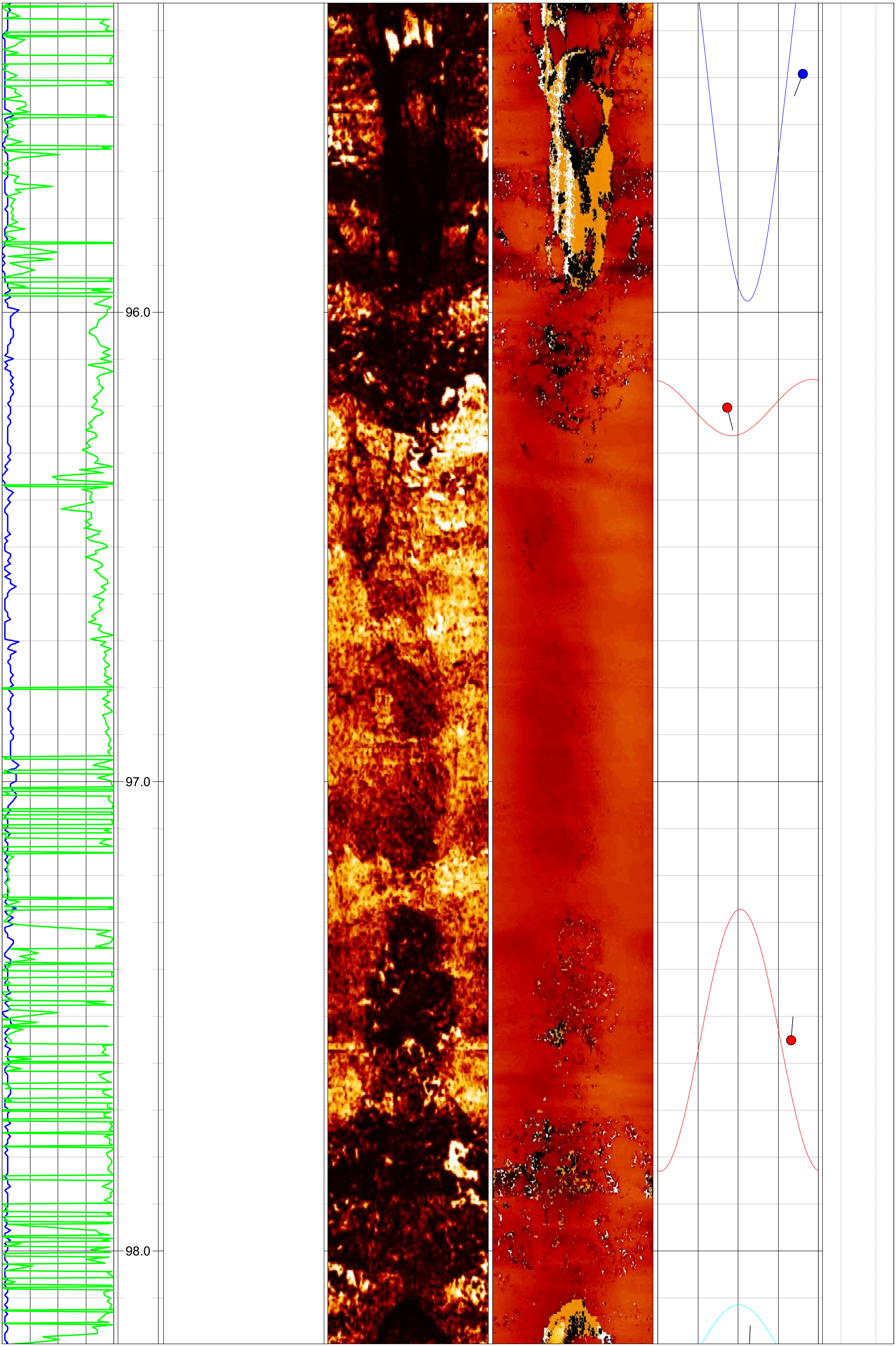
96.0
97.0
98.0

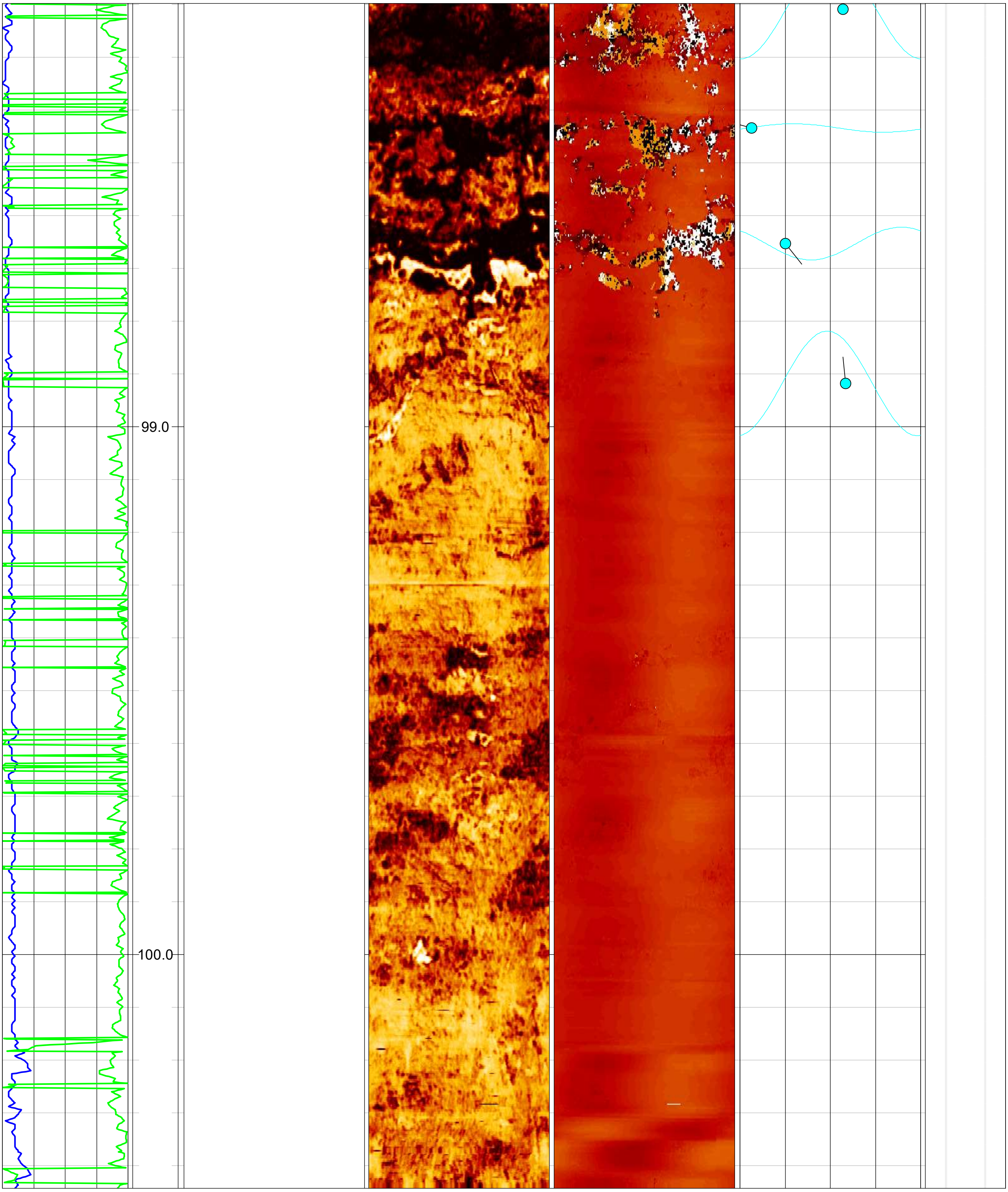
99.0
100.0

ROBERTSON GEO SERVICES
Unlocking Your GeoData

CO		COMPANY	Geotechnical Engineering
WELL		WELL ID	DSRC414
FLD		FIELD	Barrow Wake viewpoint
CTY		COUNTRY	England
STE		STATE	
FILING No		LOCATION	

SEC	TWP	RGE		OTHER SERVICES
PERMANENT DATUM	GL	ELEVATION		K.B.
LOG MEAS. FROM	GL	ABOVE PERM. DATUM		D.F.
DRILLING MEAS. FROM	GL			G.L.

DATE	01.10.19	TYPE FLUID IN HOLE	Water
RUN No		SALINITY	
TYPE LOG	Composite	DENSITY	
DEPTH-DRILLER	90	LEVEL	63.2
DEPTH-LOGGER	87.7	MAX. REC. TEMP.	
BTM LOGGED INTERVAL	87.7		
TOP LOGGED INTERVAL	0.00	CASING SHOE	
OPERATING RIG TIME			
RECORDED BY	JB		
WITNESSED BY	KO		

RUN	BOREHOLE RECORD			CASING RECORD			
NO.	BIT	FROM	TO	SIZE	WGT.	FROM	TO

Depth	Optical	Amplitude	Borehole Diameter	Density	Single-Point Resistance	Temperature	Azimuth
1:20	0° 90° 180° 270° 0°	0° 90° 180° 270° 0°	0 mm 300	0 gm/cc 4	0 OHM 200	0 DegC 20	0 Deg 360
			Natural Gamma	HRD	16" Resistivity	Absolute Cond	Inclination
			0 API 200	0 20000	0 OHMM 200	0 uS/cm 200	0 Deg 5
				BRD	64" Resistivity	Cond @ 25DegC	
				0 30000	0 OHMM 200	0 uS/cm 200	

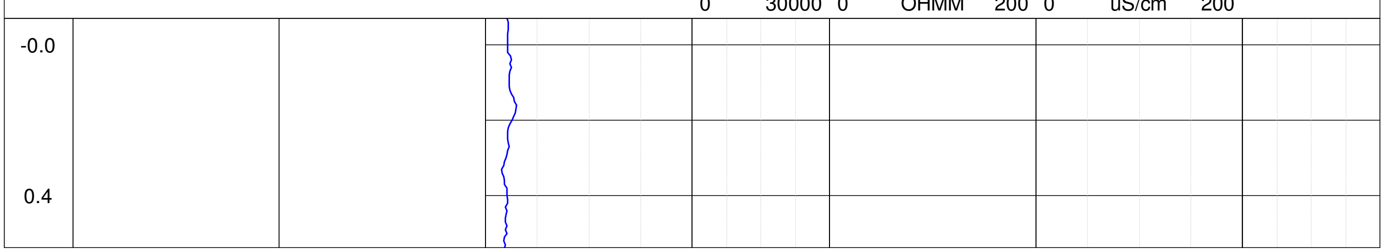

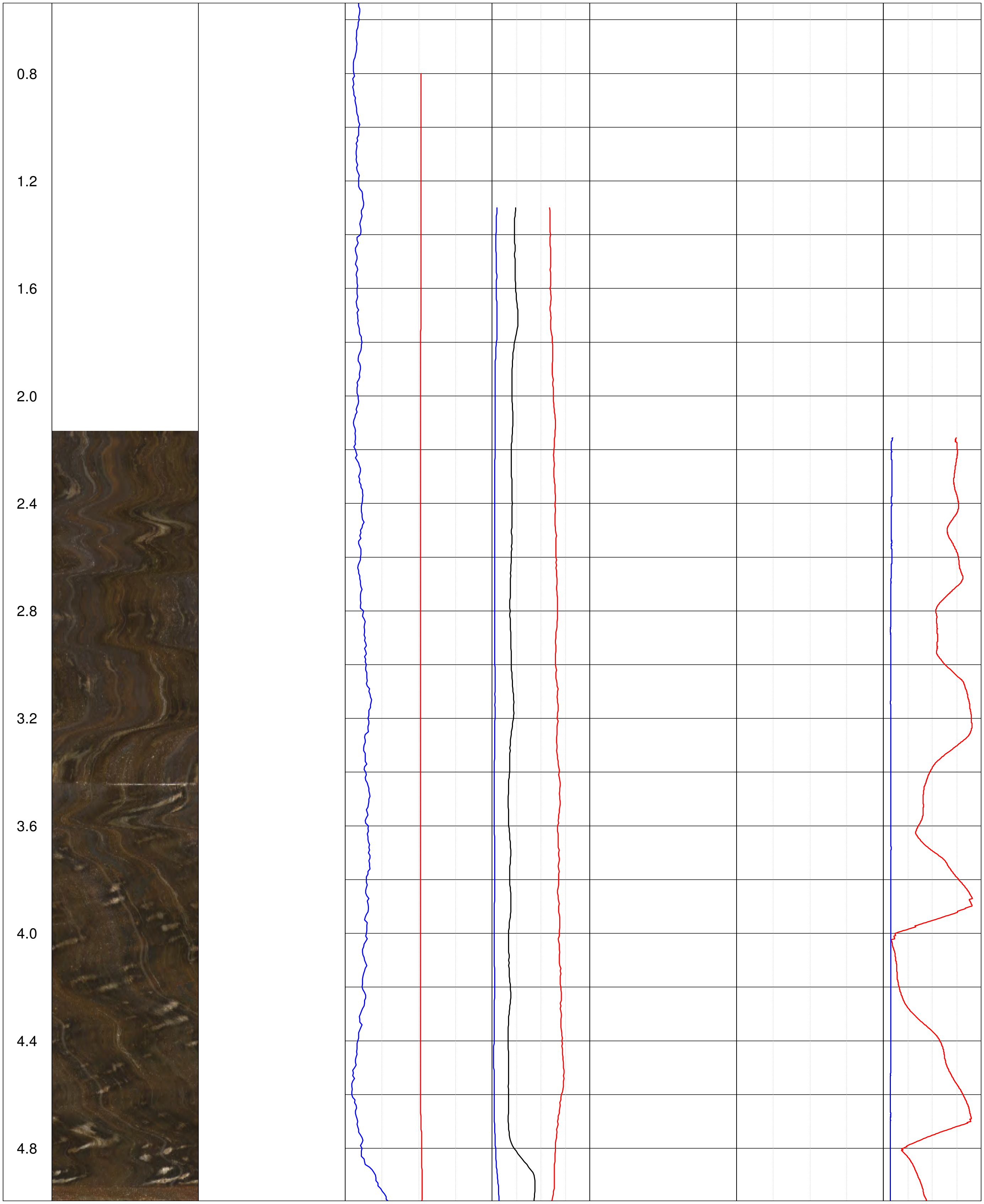
0.8
1.2
1.6
2.0
2.4
2.8
3.2
3.6
4.0
4.4
4.8

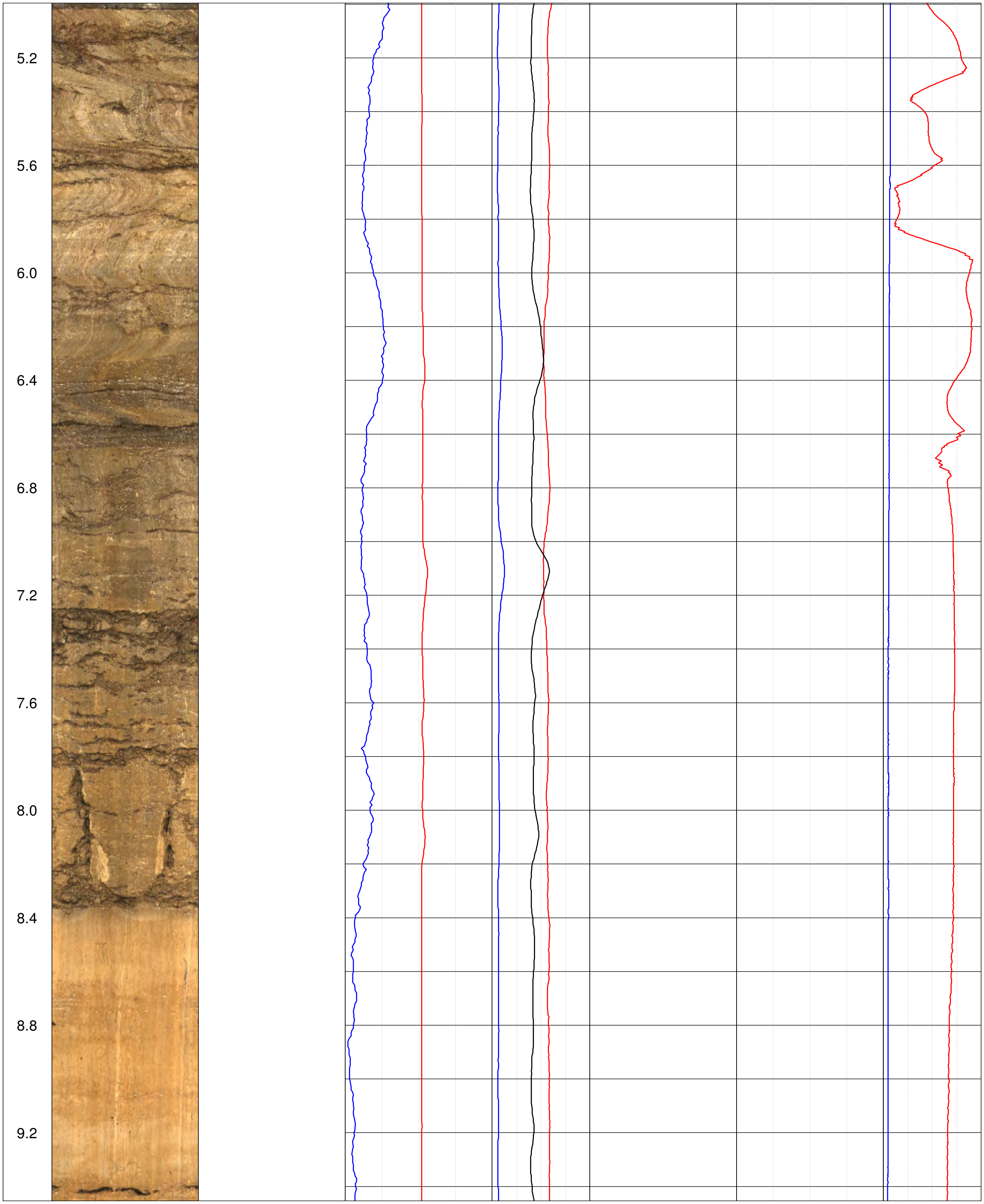
5.2
5.6
6.0
6.4
6.8
7.2
7.6
8.0
8.4
8.8
9.2

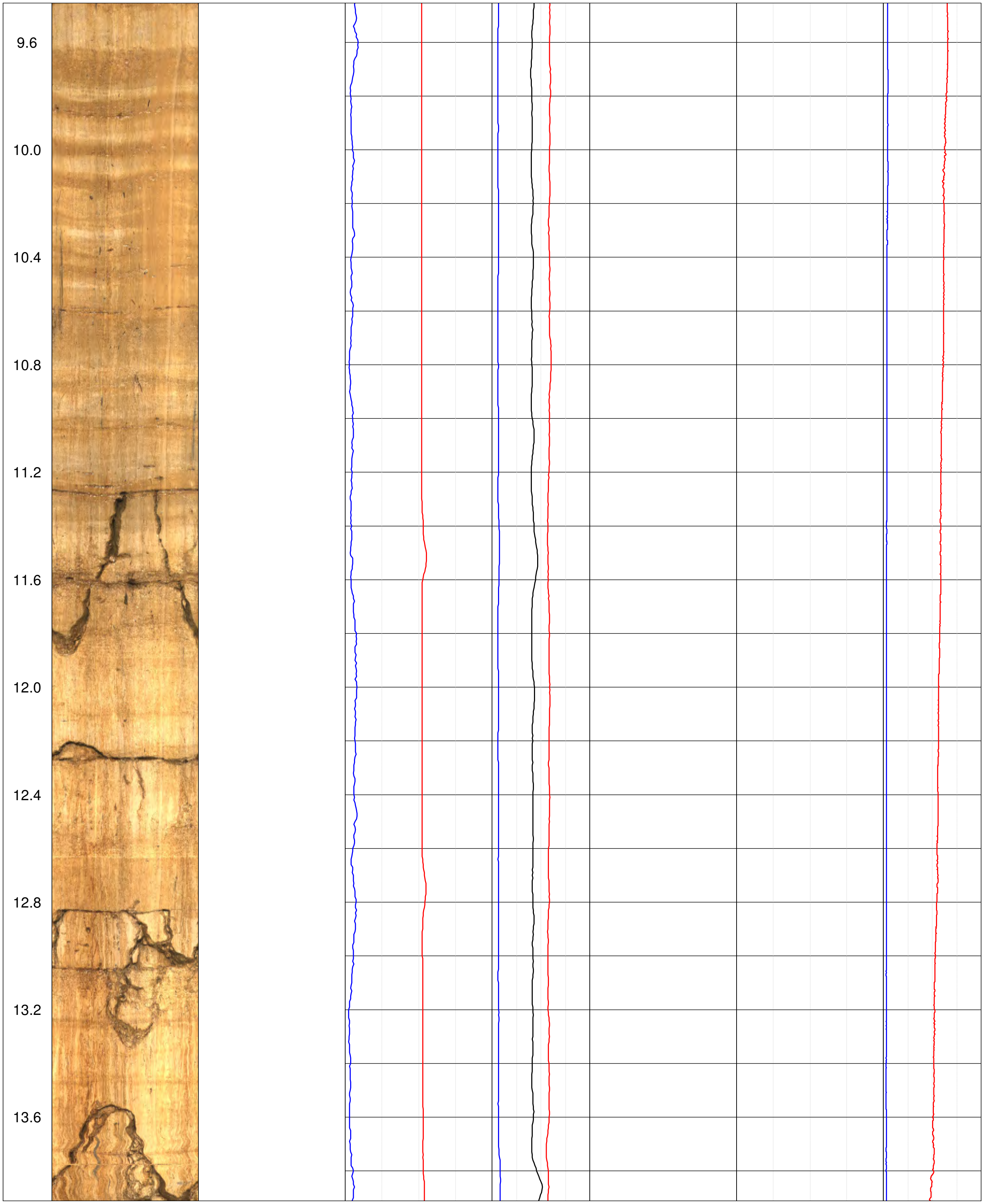
9.6
10.0
10.4
10.8
11.2
11.6
12.0
12.4
12.8
13.2
13.6

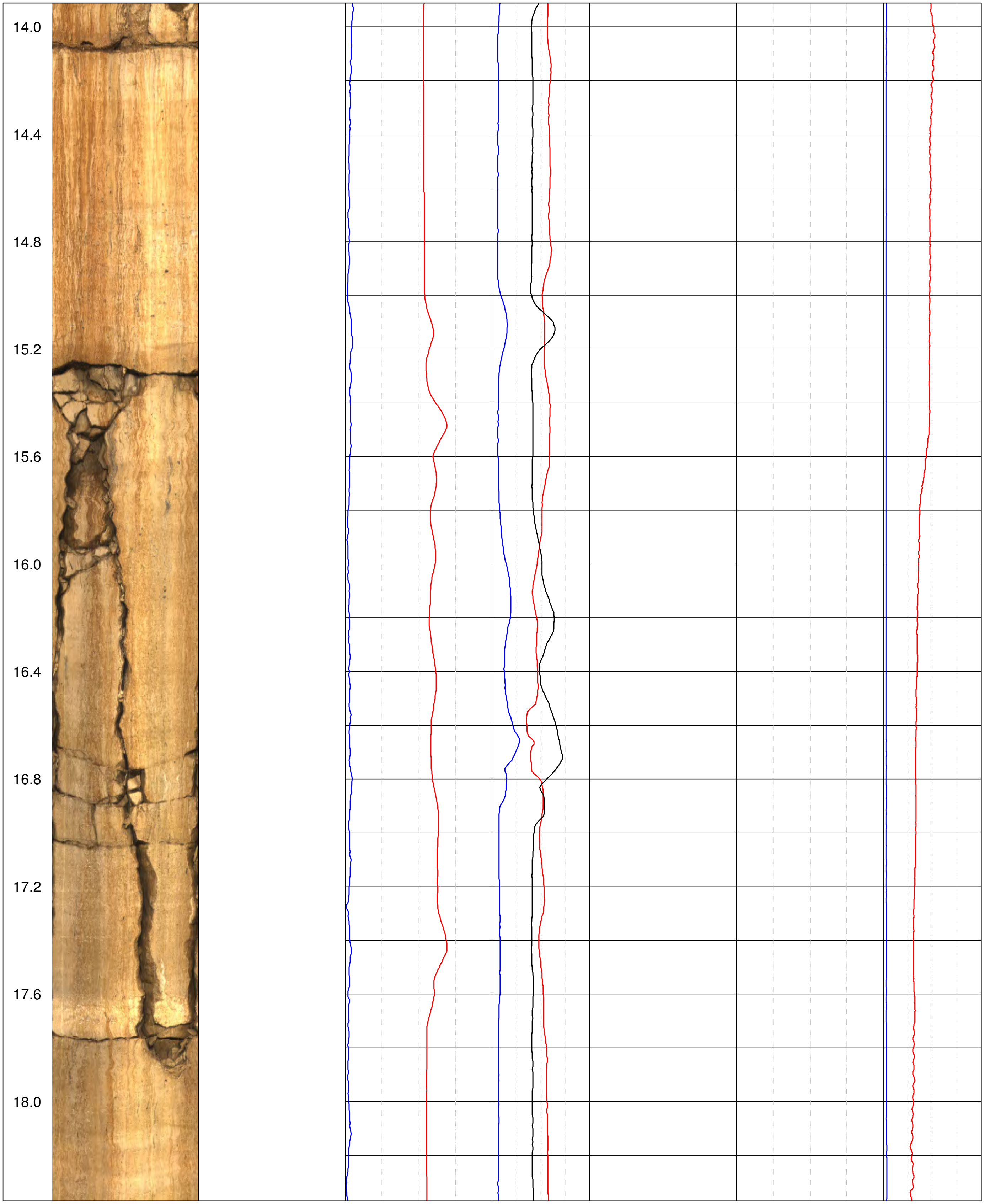
14.0
14.4
14.8
15.2
15.6
16.0
16.4
16.8
17.2
17.6
18.0

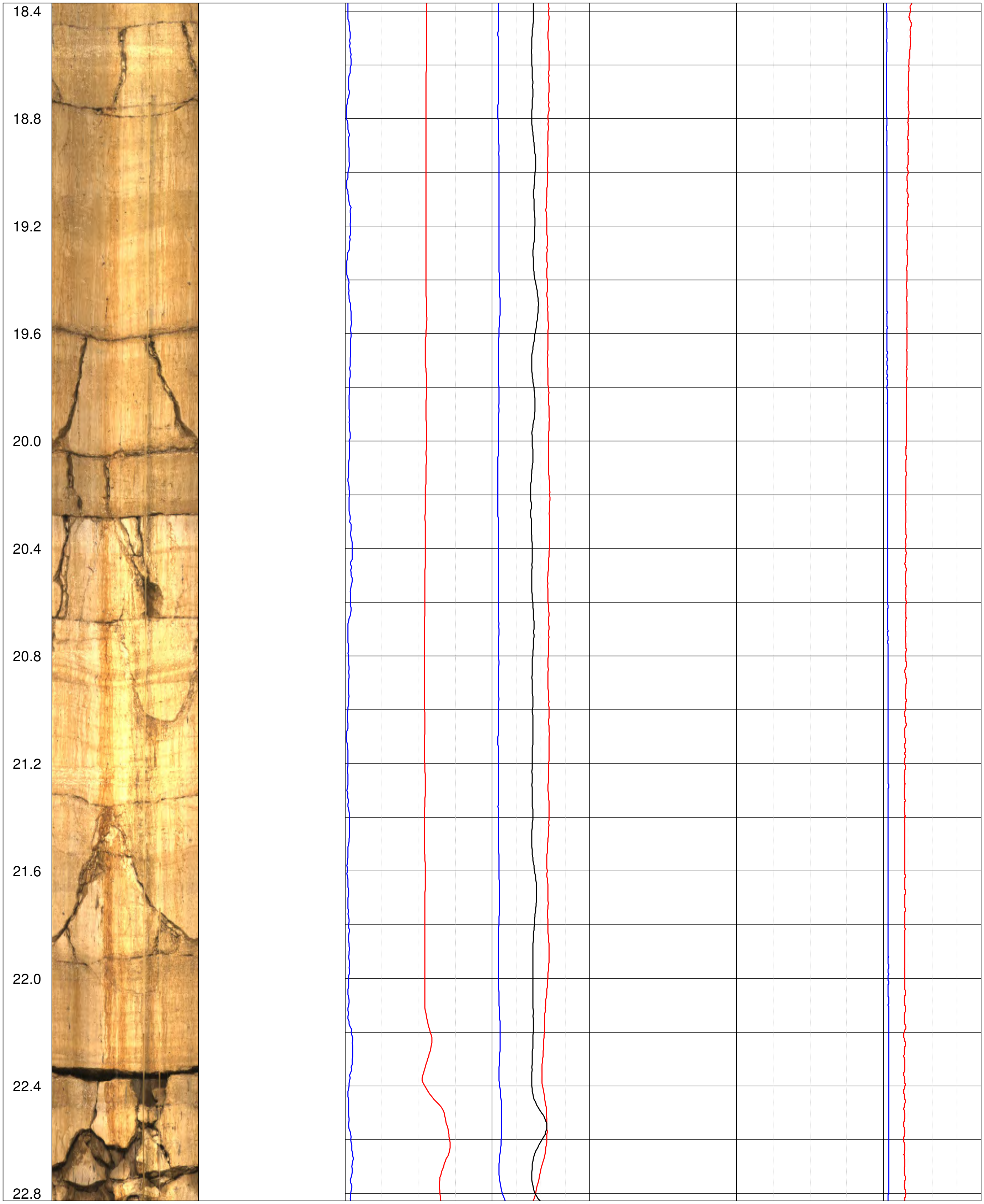
18.4
18.8
19.2
19.6
20.0
20.4
20.8
21.2
21.6
22.0
22.4
22.8

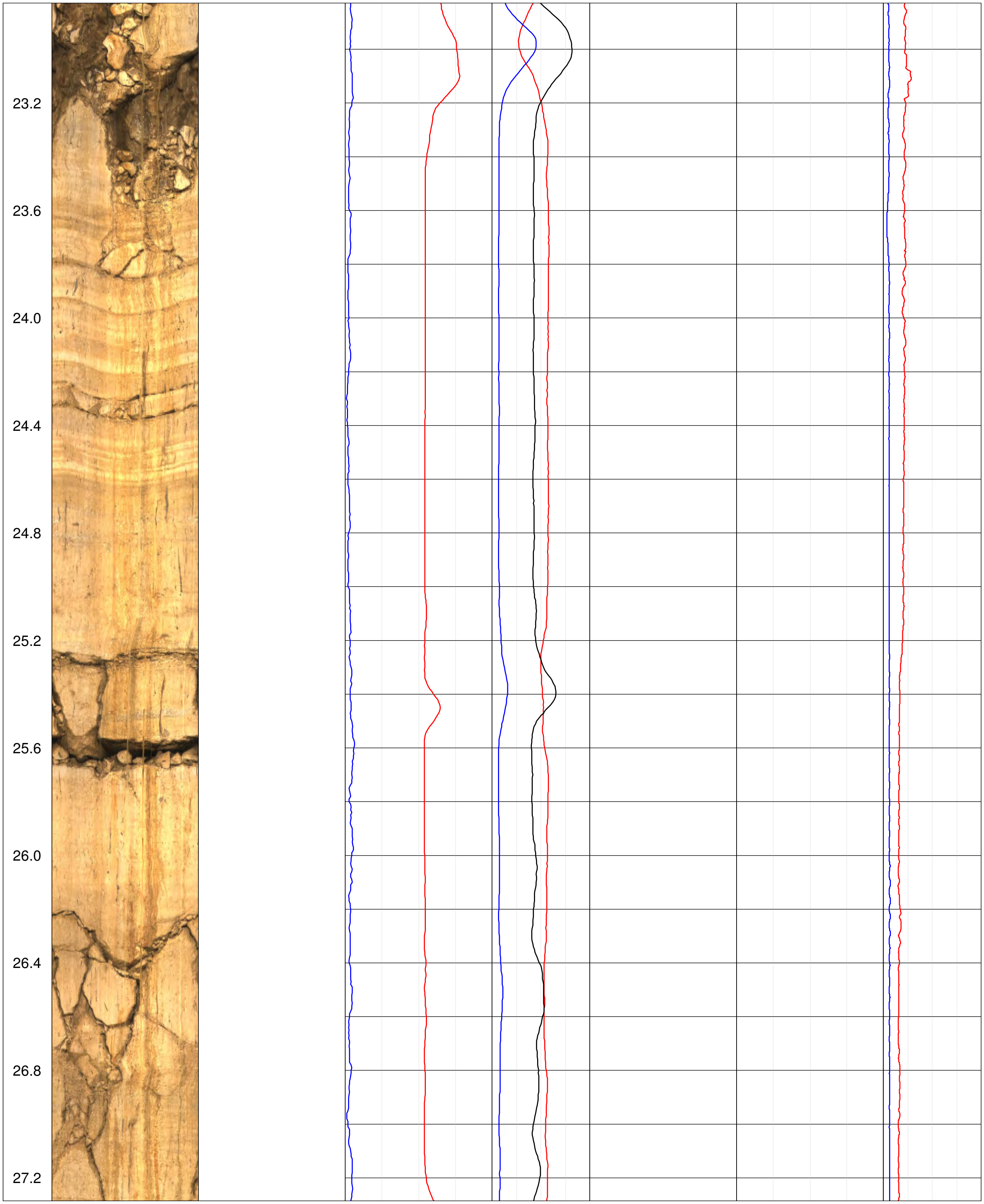
23.2
23.6
24.0
24.4
24.8
25.2
25.6
26.0
26.4
26.8
27.2

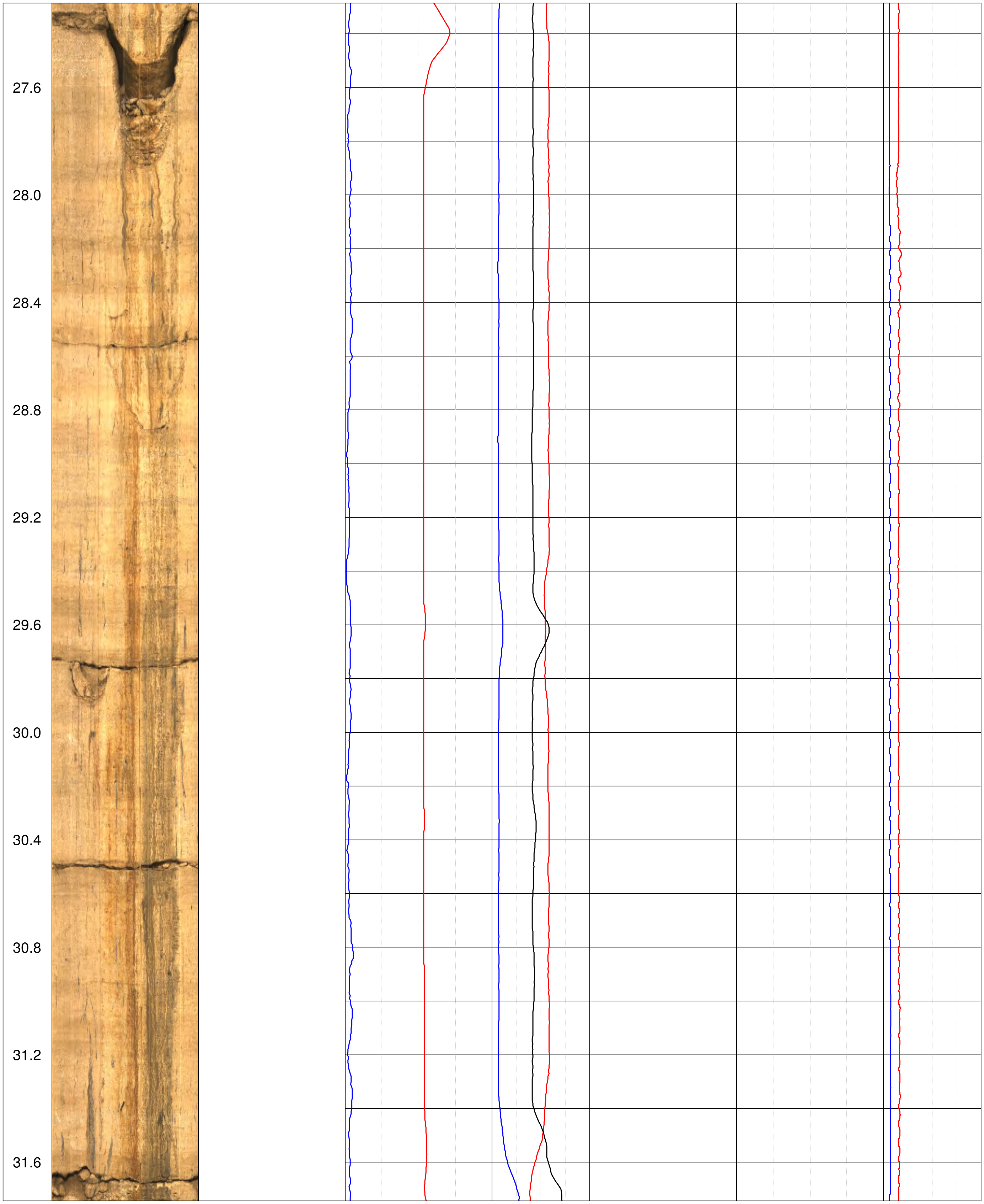
27.6
28.0
28.4
28.8
29.2
29.6
30.0
30.4
30.8
31.2
31.6

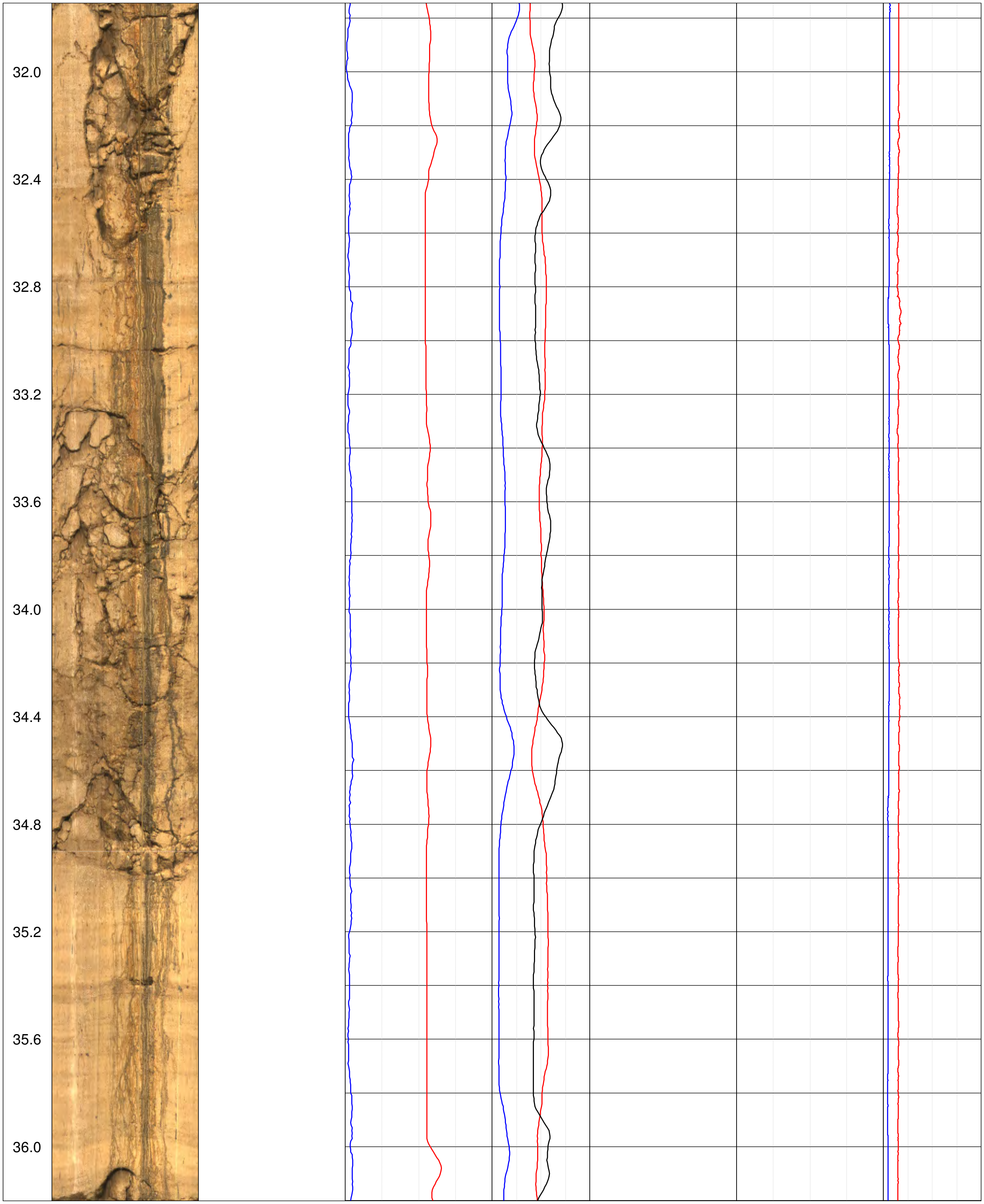
32.0
32.4
32.8
33.2
33.6
34.0
34.4
34.8
35.2
35.6
36.0

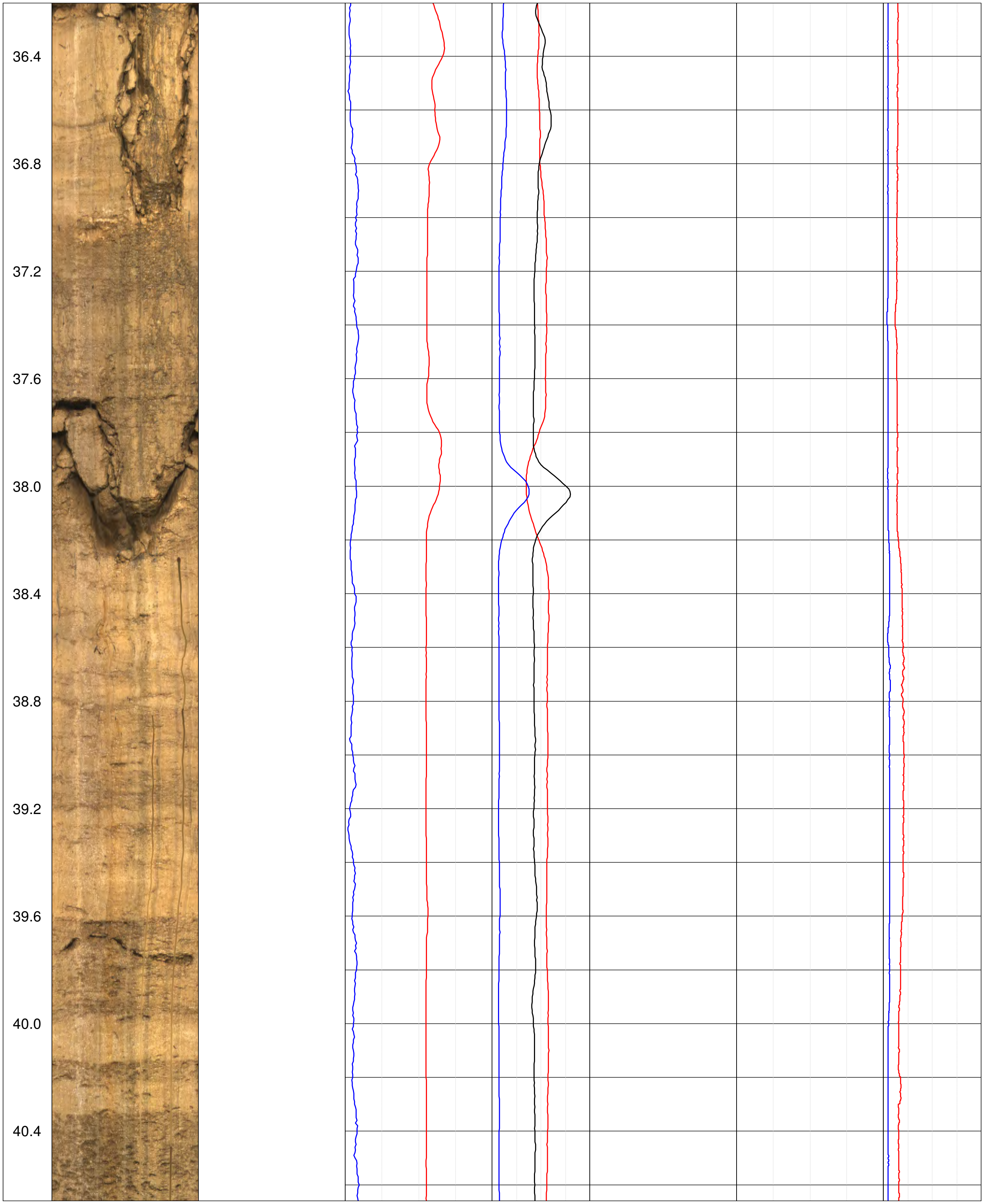
36.4
36.8
37.2
37.6
38.0
38.4
38.8
39.2
39.6
40.0
40.4

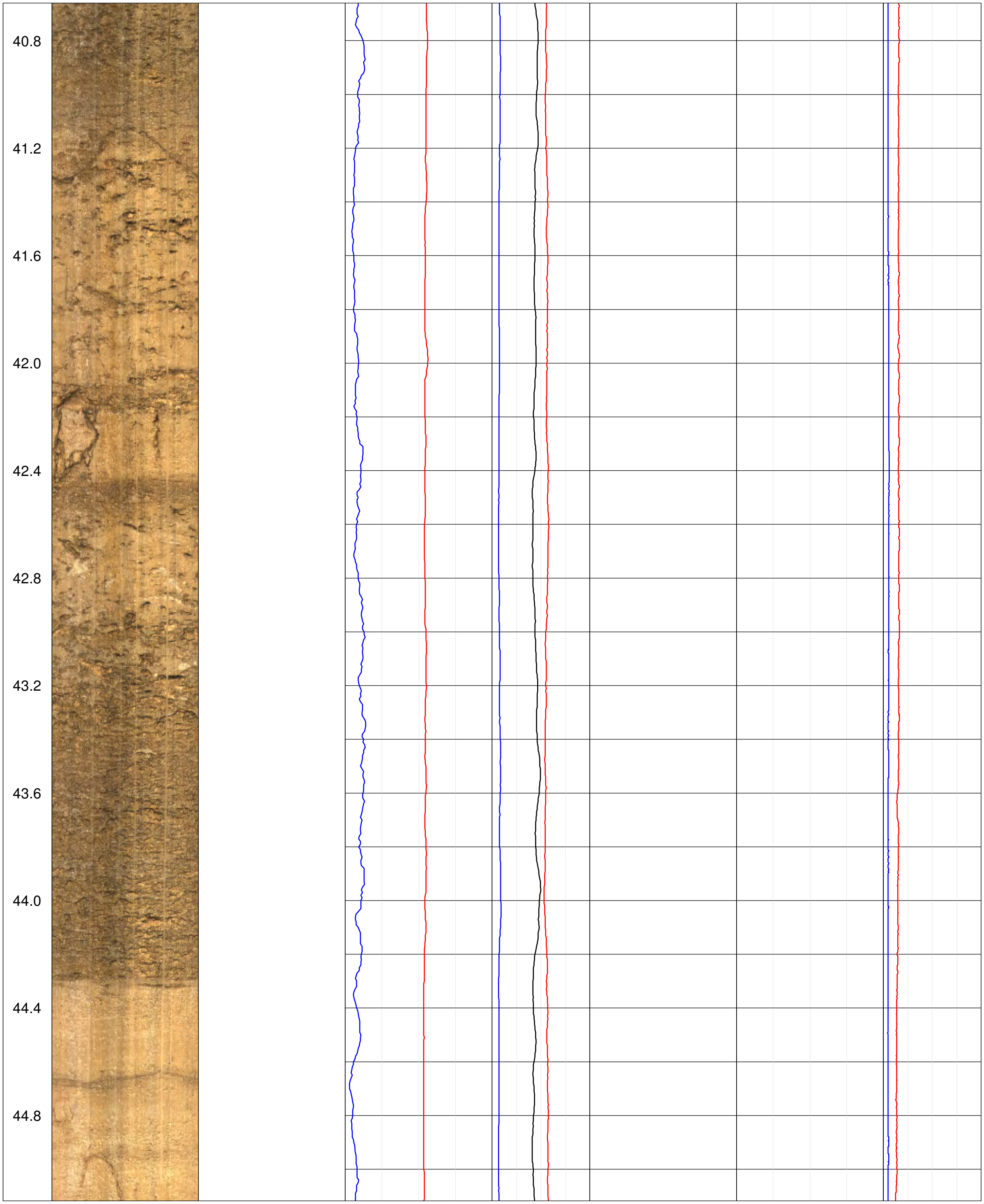
40.8
41.2
41.6
42.0
42.4
42.8
43.2
43.6
44.0
44.4
44.8

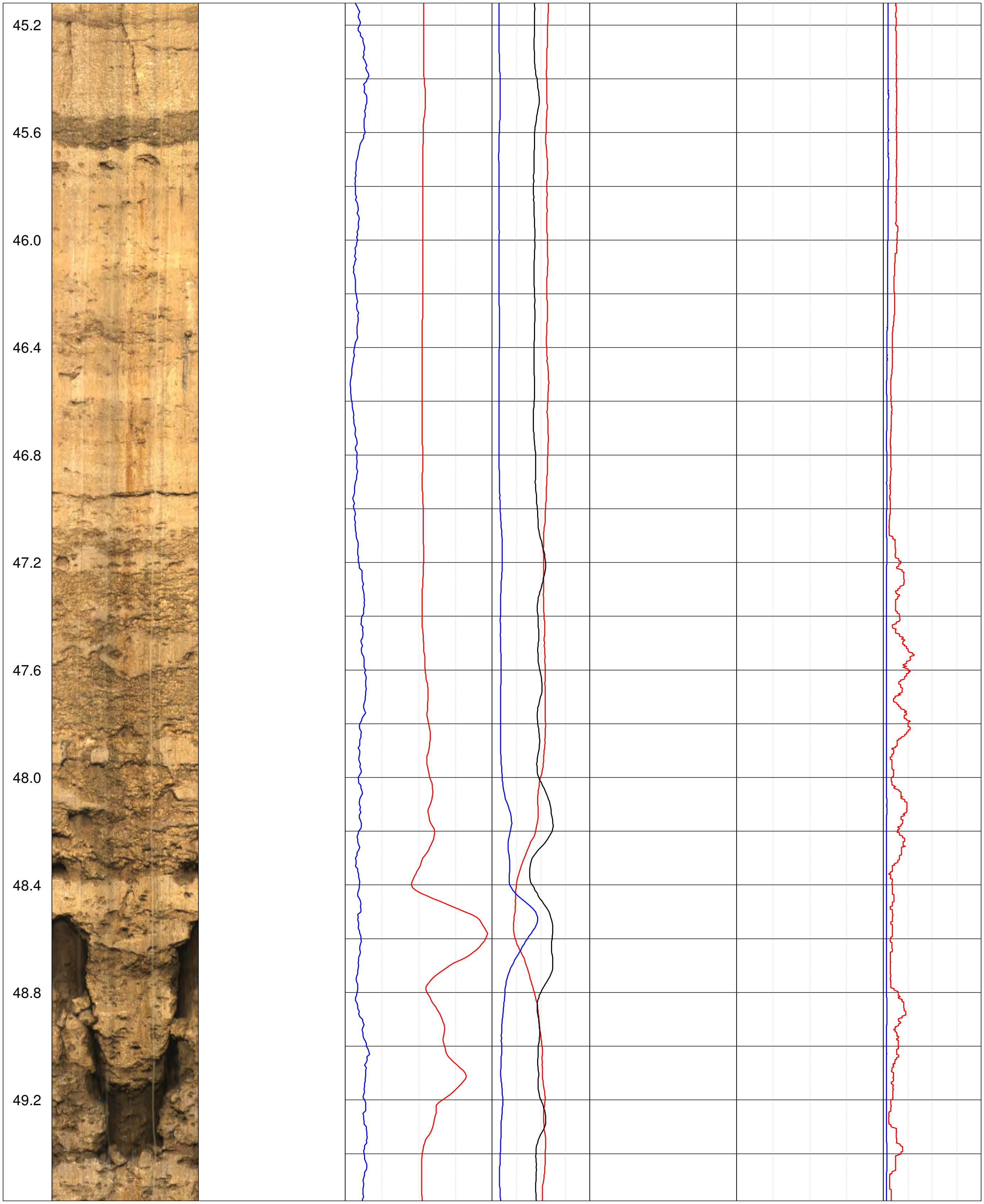
45.2
45.6
46.0
46.4
46.8
47.2
47.6
48.0
48.4
48.8
49.2

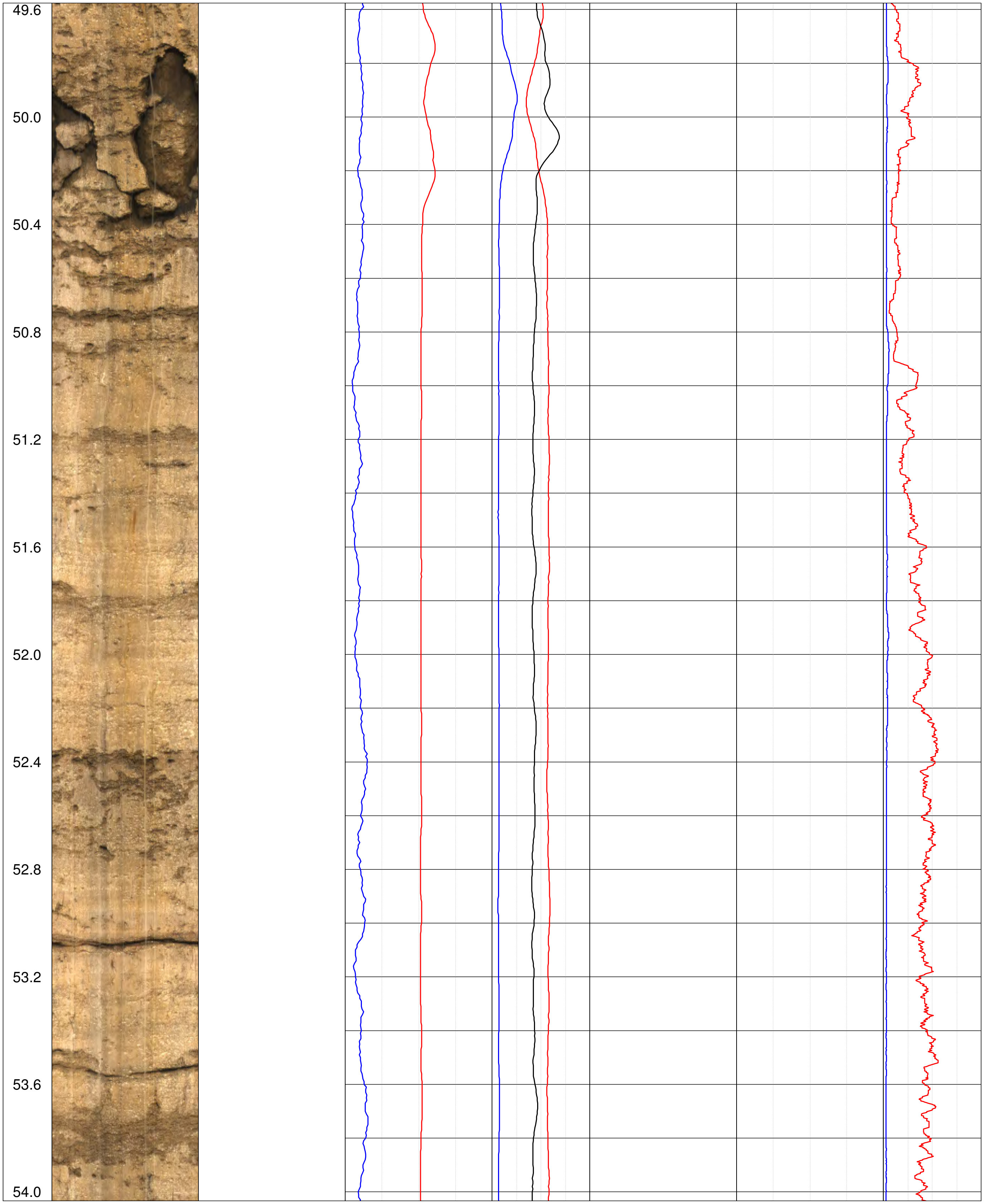
49.6
50.0
50.4
50.8
51.2
51.6
52.0
52.4
52.8
53.2
53.6
54.0

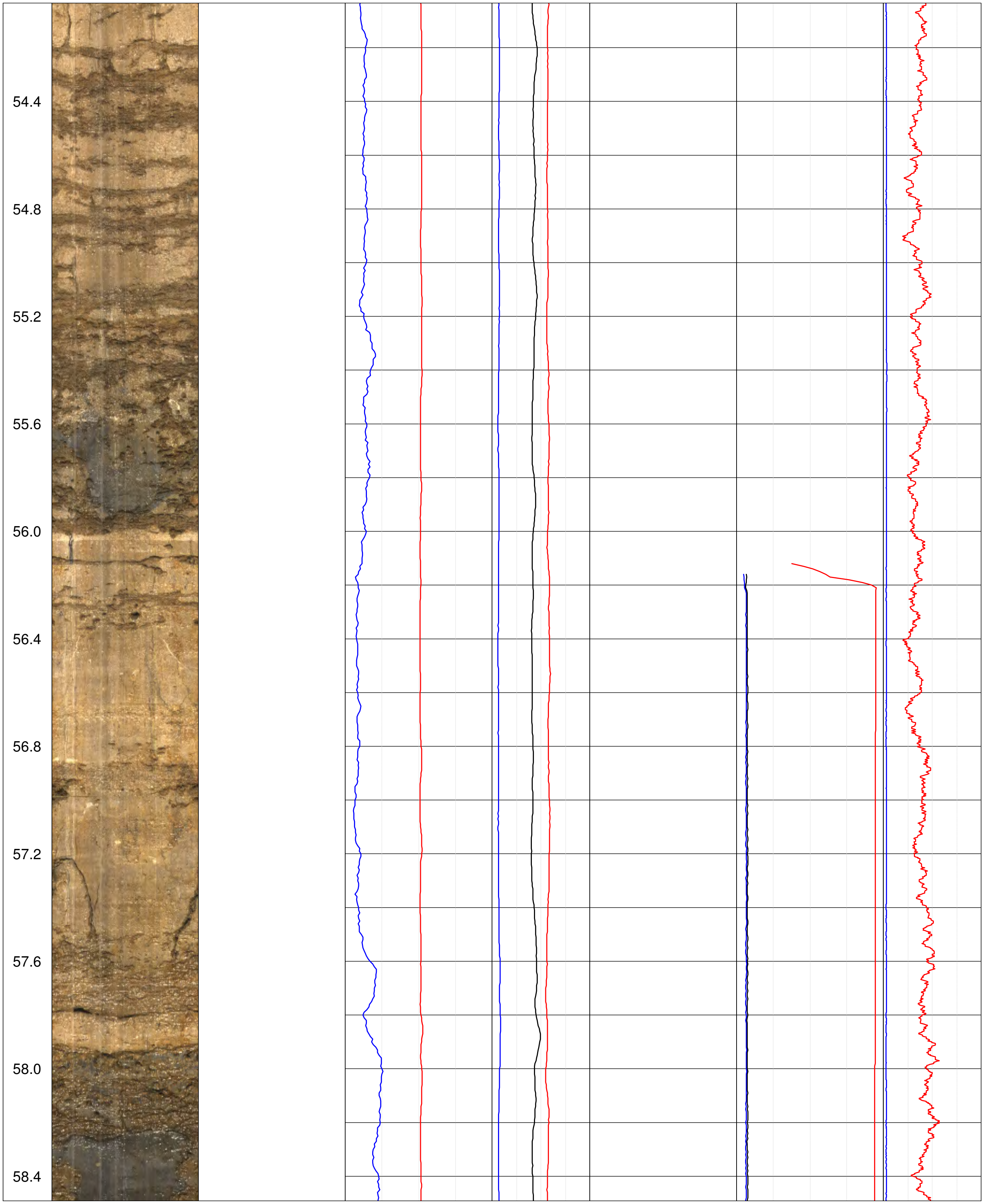
54.4
54.8
55.2
55.6
56.0
56.4
56.8
57.2
57.6
58.0
58.4

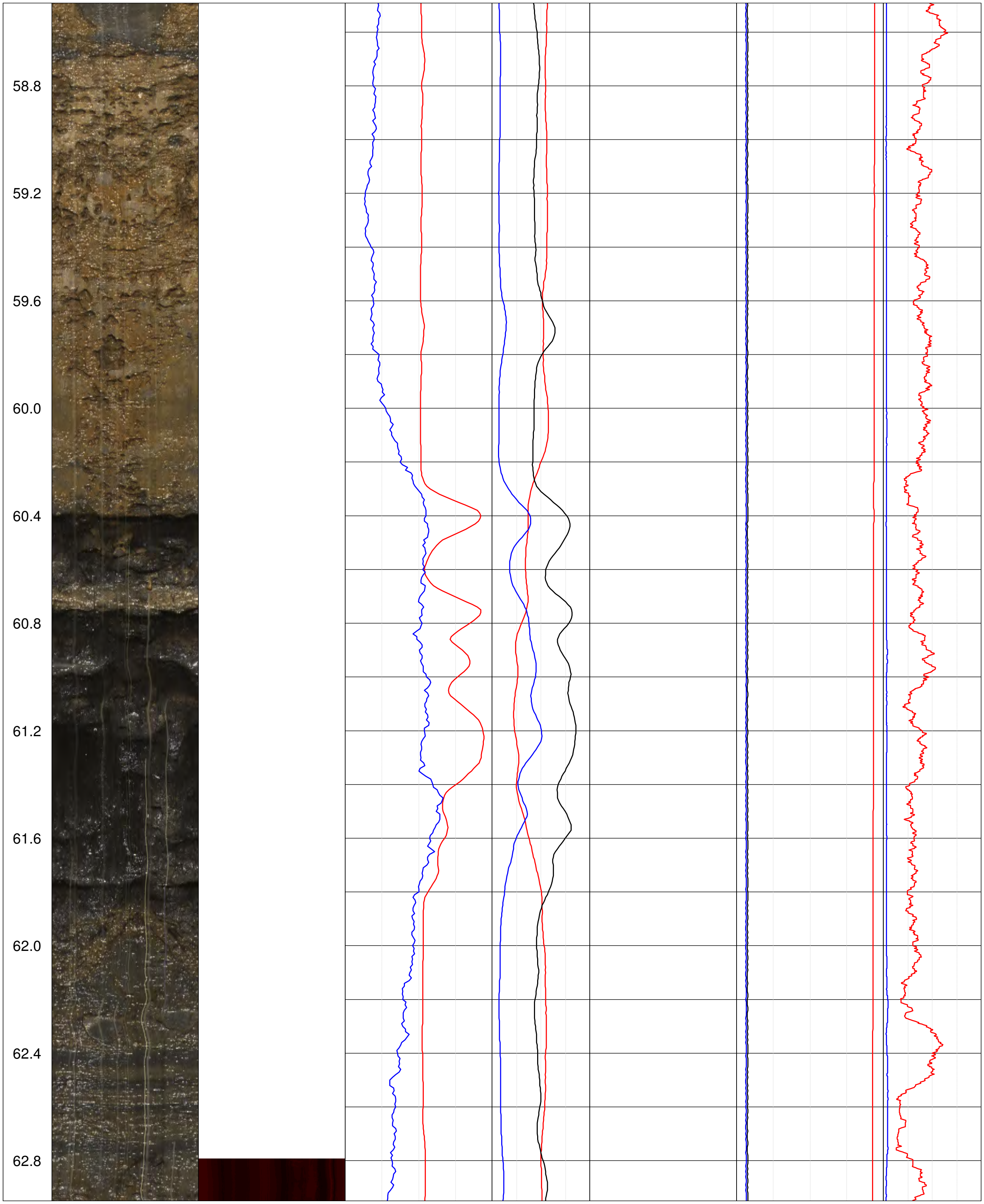
58.8
59.2
59.6
60.0
60.4
60.8
61.2
61.6
62.0
62.4
62.8

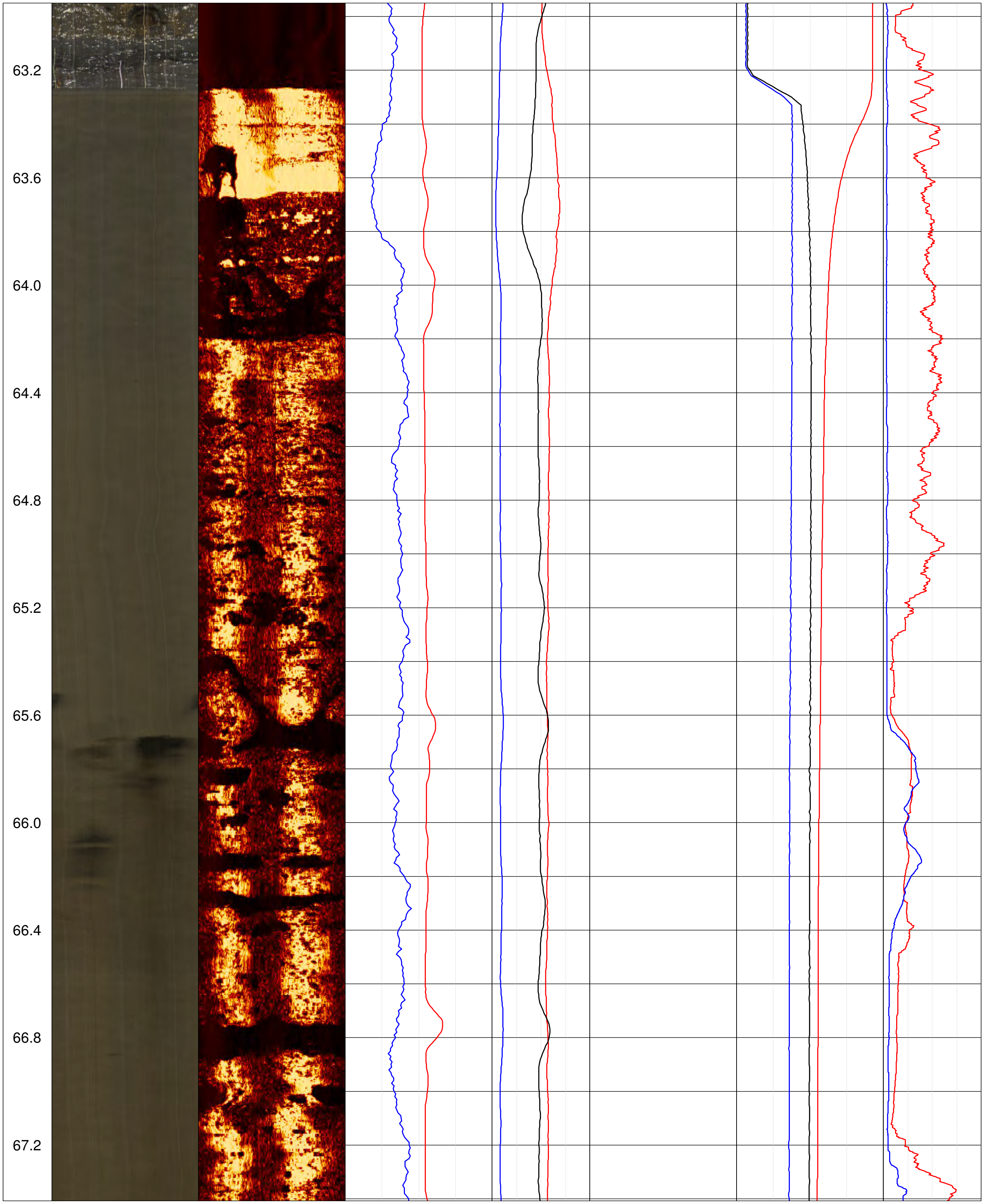
63.2
63.6
64.0
64.4
64.8
65.2
65.6
66.0
66.4
66.8
67.2

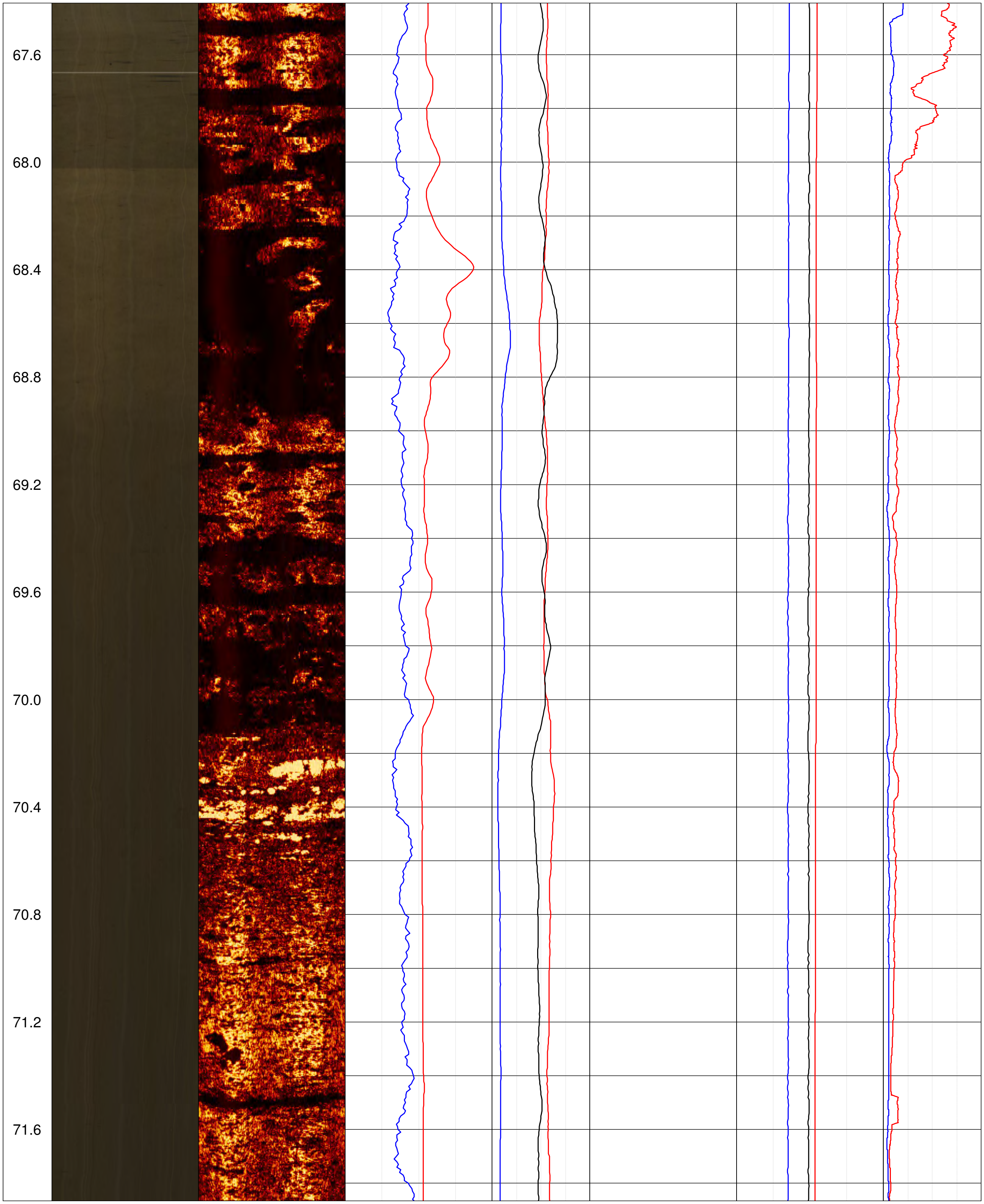
67.6
68.0
68.4
68.8
69.2
69.6
70.0
70.4
70.8
71.2
71.6

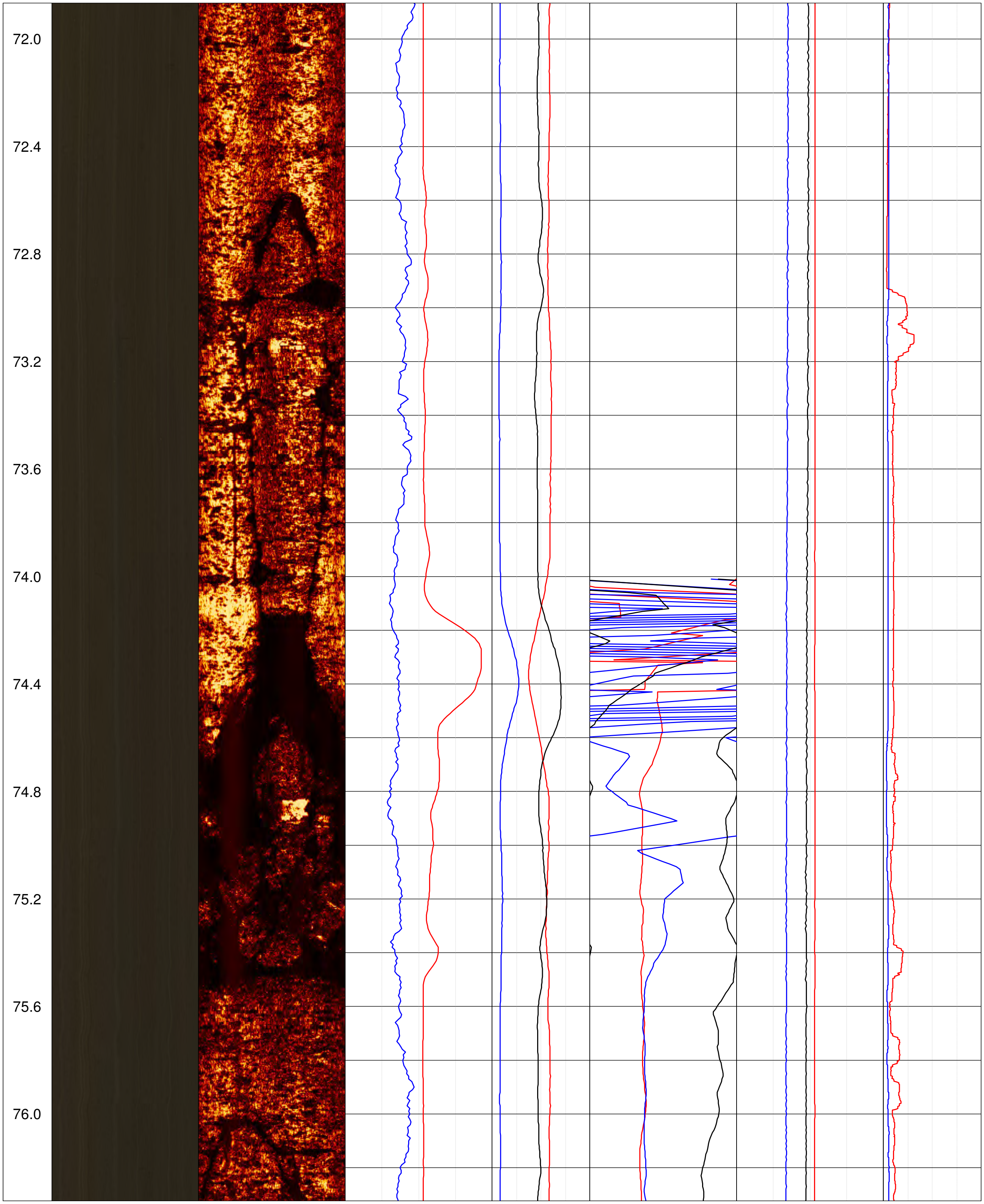
72.0
72.4
72.8
73.2
73.6
74.0
74.4
74.8
75.2
75.6
76.0

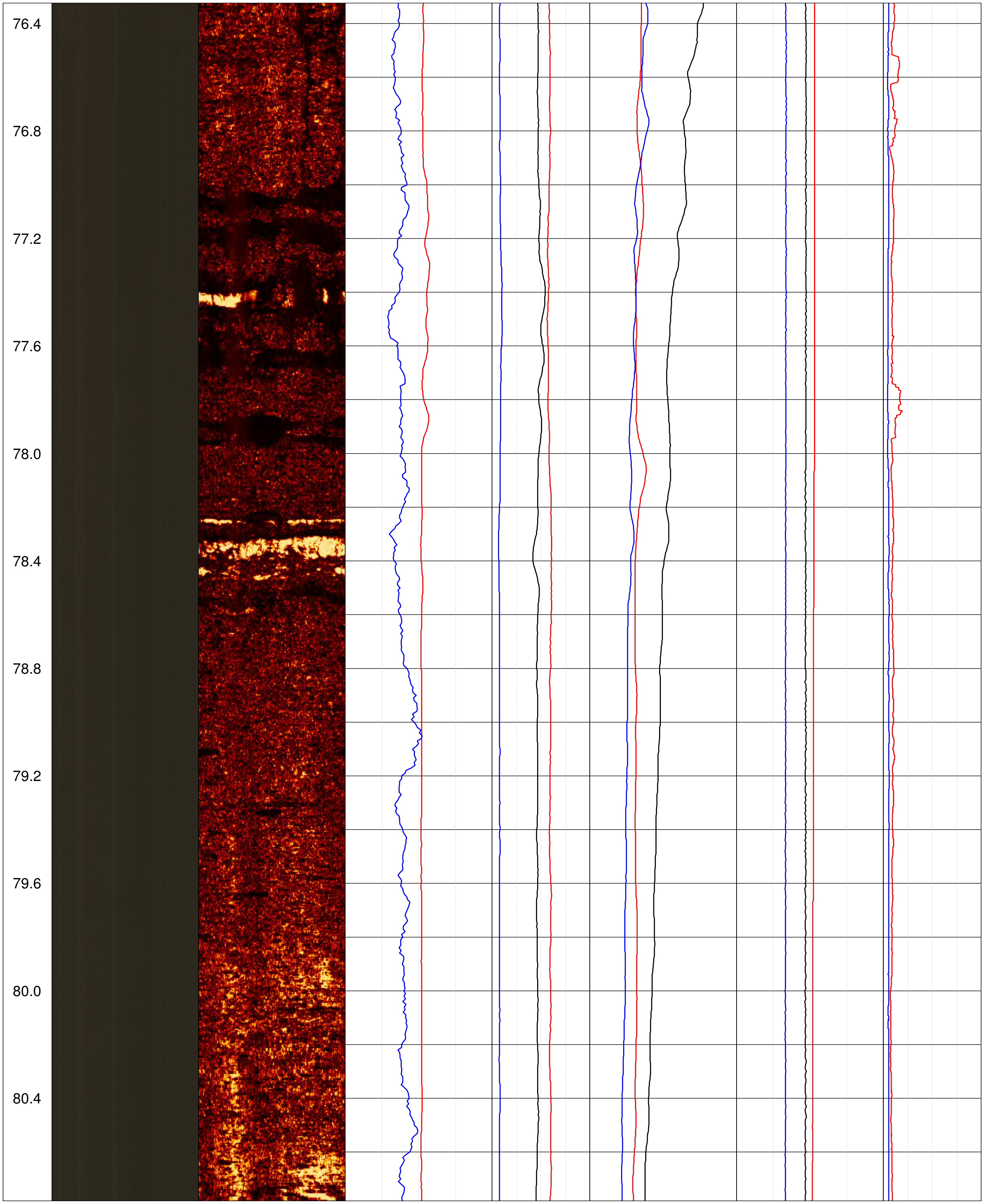
76.4
76.8
77.2
77.6
78.0
78.4
78.8
79.2
79.6
80.0
80.4

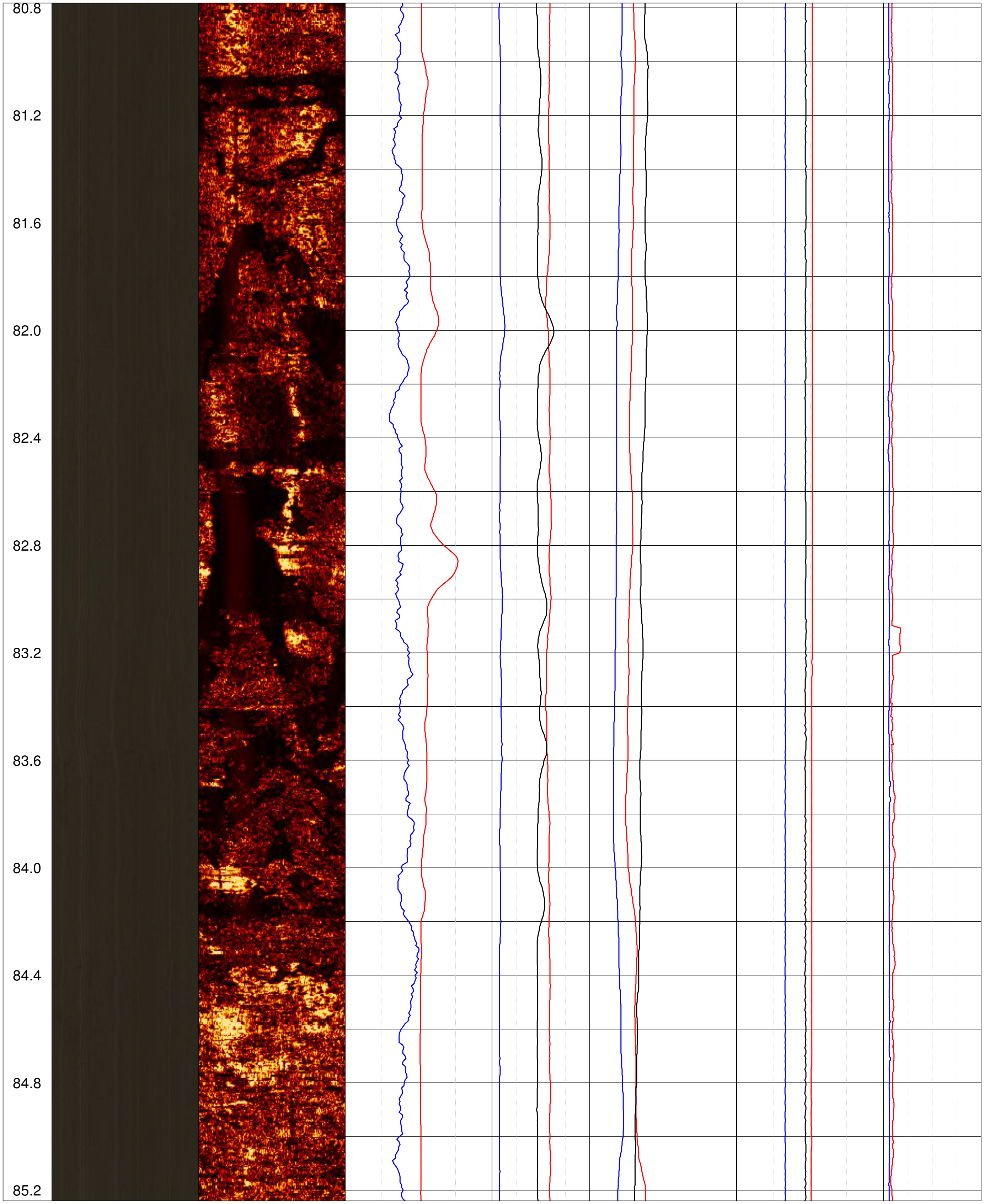
80.8
81.2
81.6
82.0
82.4
82.8
83.2
83.6
84.0
84.4
84.8
85.2

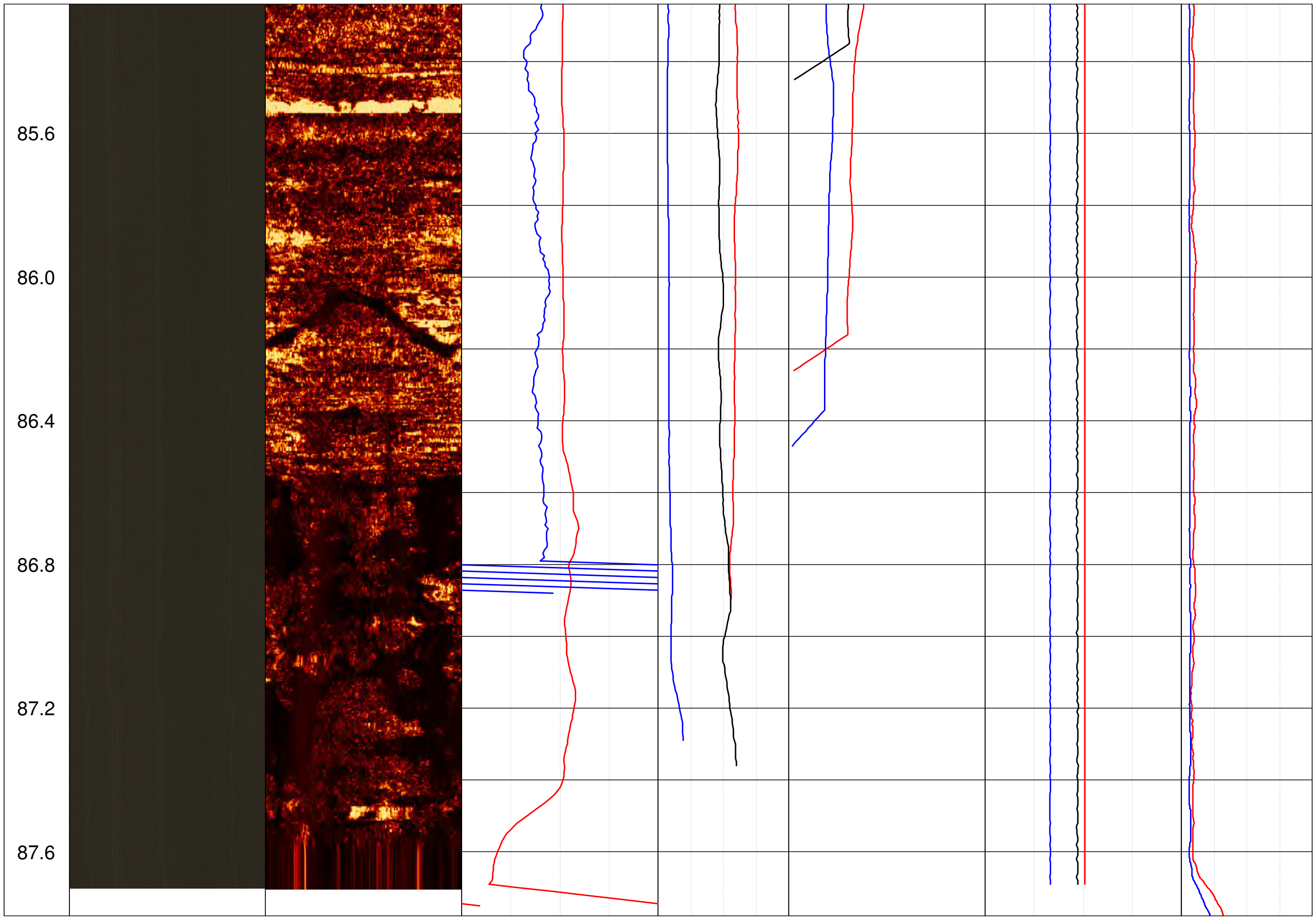
85.6
86.0
86.4
86.8
87.2
87.6

POINT OF WORK RISK ASSESSMENT

ROBERTSON GEO
Unlocking Your GeoData

PROJECT: BARROW WAKE VIEWPOINT
CLIENT: GEOTECHNICAL ENGINEERING
LOCATION: BIRDLIP
DATE: 01/10/19

PART 1 - STOP

BEFORE YOU START

	YES	NO	N/A
Have you had the site induction?	✓		
Are you at the correct location?	✓		
Do you have correct documents for the job?	✓		
Do you have the correct PPE?	✓		
Is all equipment tested and certified?	✓		
Have you read and understood the RAMS for the job?	✓		
Do you have the necessary qualifications and authorisation to carry out the work?	✓		
Have you got safe access to the area and adequate lighting for access and work in the area?	✓		
Have you got adequate space for safe work?	✓		
Have you displayed adequate barriers and warning signs in the work area?	✓		
Are you protected from moving parts or from being struck by vehicles?	✓		
Can you ensure protection to the environment (drip trays)?	✓		

If you have answered 'NO' to any of the above then take required action or report to the site manager

PART 2 - THINK

SAFETY ASSESSMENT – PLEASE TICK ANY HAZARDS THAT ARE PRESENT

✓	Slips, trips and falls		Confined space		Vibration
	Falls from height		Open excavation	✓	Radiation
	Falling/flying objects	✓	Manual handling		Poor lighting
	Asbestos		Dust		Temperature
	Heat/fire/explosion		Fumes		Adverse weather
	Asphyxiation or drowning		Noise		Risk to you from others
	Vehicle/mobile plant		Electricity		Risk to others from you
	Contact with sharp object		Residues		Other (please specify below)

If you answered 'OTHER' please specify below:

POINT OF WORK RISK ASSESSMENT

PART 3 - ACT

ADDITIONAL SAFETY ASSESSMENT

HAZARD (IDENTIFIED OVERLEAF):	CONTROL MEASURES/PRECAUTIONS:	REMAINING RISK: HIGH	MED	LOW
S.T.F's	GOOD HOUSEKEEPING	☐	☐	☑
MANUAL HANDLING	PROPER LIFTING TECHNIQUE	☐	☐	☑
RADIATION	TIME DISTANCE SHIELDING	☐	☐	☑
		☐	☐	☐
		☐	☐	☐

All engineers involved with the works please sign below if you have read and understand the risks involved with the work

NAME:	SIGNATURE:	DATE:
S BOYETT	[redacted]	01/10/19
K. OWEN	[redacted]	01.10.19

PART 4 - REVIEW

END OF JOB REVIEW - PLEASE TICK AS APPROPRIATE

	YES	NO
Are there any lessons for next time?	☐	☐
Has the work created any new hazards?	☐	☐

If you have answered 'YES' to either of the above please provide a brief note below:

POWRA approved by: [redacted]

Date: 01. 10.19

CERTIFICATE OF CONFORMITY

Certificate of Conformity

This is to certify that the following equipment conforms to the specification detailed below

ROBERTSON GEO®
Unlocking Your GeoData

Equipment type: High Resolution Optical Televiewer

RG Order No: ORD00000

Serial No: Hi-OPTV 11106

Comm. Type: Differential 4-Core/Coaxial

Quality Management System:
ISO 9001:2015
Certified by TÜV SÜD

Tested by: T Hamflett

Date: 16/07/19

Approved by:

[redacted]

Tim Hamflett | *Test Engineer*

Date: 16/07/19

TÜV SÜD ISO 9001
ISO 9001
Certified
Quality Management System
www.tuv-sud.com/ms-cert

Robertson Geologging Ltd.
Deganwy, Conwy, LL31 9PX,
United Kingdom
T: +44 (0) 1492 582 323
E: support@robertson-geo.com
www.robertson-geo.com

ROBERTSON GEO®
Unlocking Your GeoData

CERTIFICATE OF CONFORMITY

The probe detailed has been calibrated and then logged in the **ROBERTSON GEO** Test Borehole (Deganwy, UK). The resulting data falls within acceptable tolerances and meets all test criteria.

ROBERTSON GEO
Unlocking Your GeoData

Main Pass: 70-40m

Repeat Pass: 70-40m

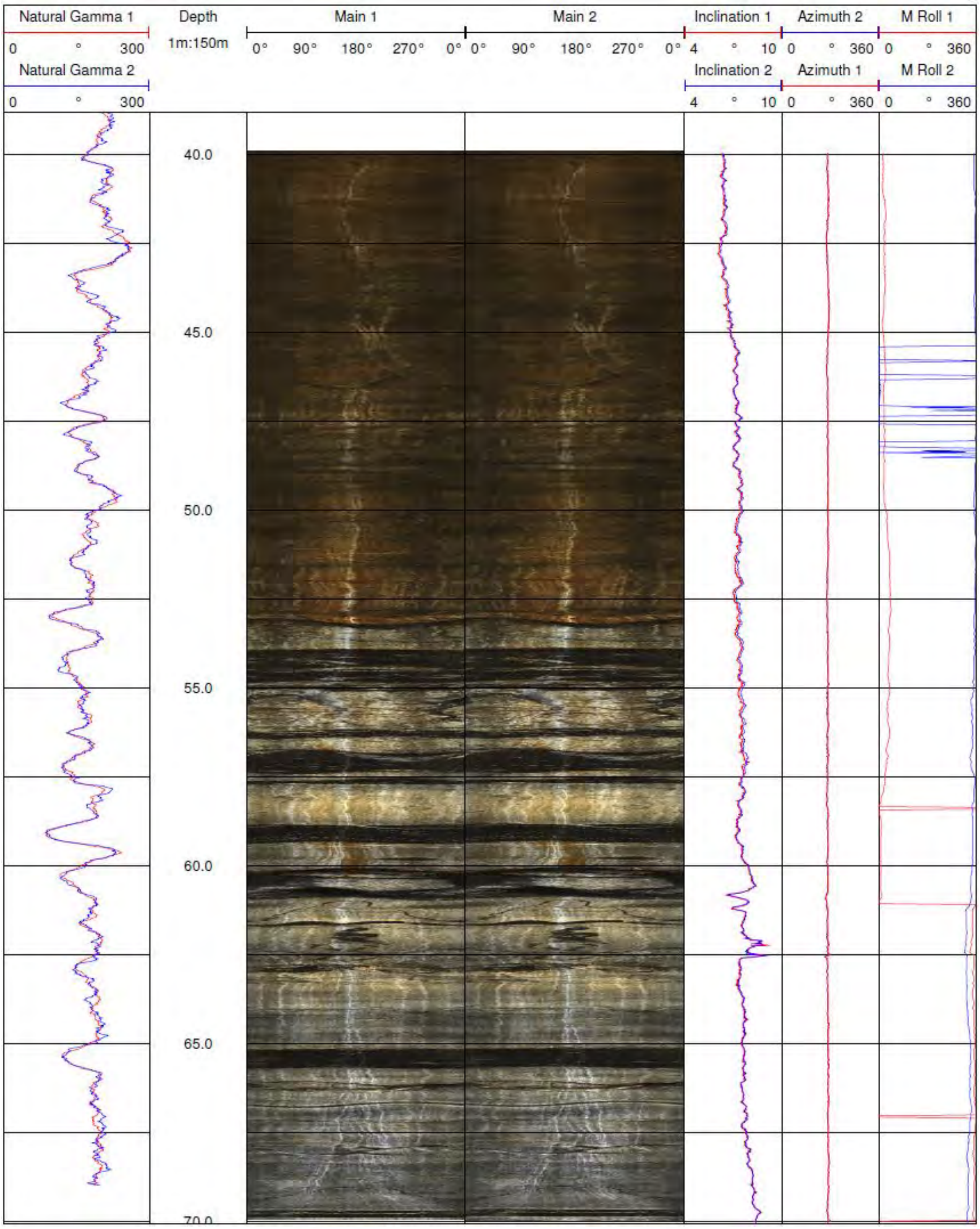

ISO 9001
Certified
Quality Management System
www.tuv-sud.com/ms-cert

Robertson Geologging Ltd.
Deganwy, Conwy, LL31 9PX,
United Kingdom
T: +44 (0) 1492 582 323
E: growlands@robertson-geo.com
www.robertson-geo.com

ROBERTSON GEO
Unlocking Your GeoData

CERTIFICATE OF CONFORMITY

Certificate of Conformity

This is to certify that the following equipment conforms to the specification detailed below

ROBERTSON GEO
Unlocking Your GeoData

Equipment type: High Resolution Acoustic Televiewer

RG Order No: ORD00000

Serial No: HiRAT 8237

Comm. Type: Standard 4-Core

Quality Management System:
ISO 9001:2015
Certified by TÜV SÜD

Tested by: T Hamflett

Date: 16/07/19

Approved by:

[redacted]

Tim Hamflett | *Test Engineer*

Date: 16/07/19

ISO 9001
Certified
Quality Management System
www.tuv-sud.com/ms-cert

Robertson Geologging Ltd.
Deganwy, Conwy, LL31 9PX,
United Kingdom
T: +44 (0) 1492 582 323
E: support@robertson-geo.com
www.robertson-geo.com

ROBERTSON GEO
Unlocking Your GeoData

CERTIFICATE OF CONFORMITY

The probe detailed has been calibrated and then logged in the **ROBERTSON GEO** Test Borehole (Deganwy, UK). The resulting data falls within acceptable tolerances and meets all test criteria.

ROBERTSON GEO
Unlocking Your GeoData

Main Pass: 70-40m

Repeat Pass: 70-40m

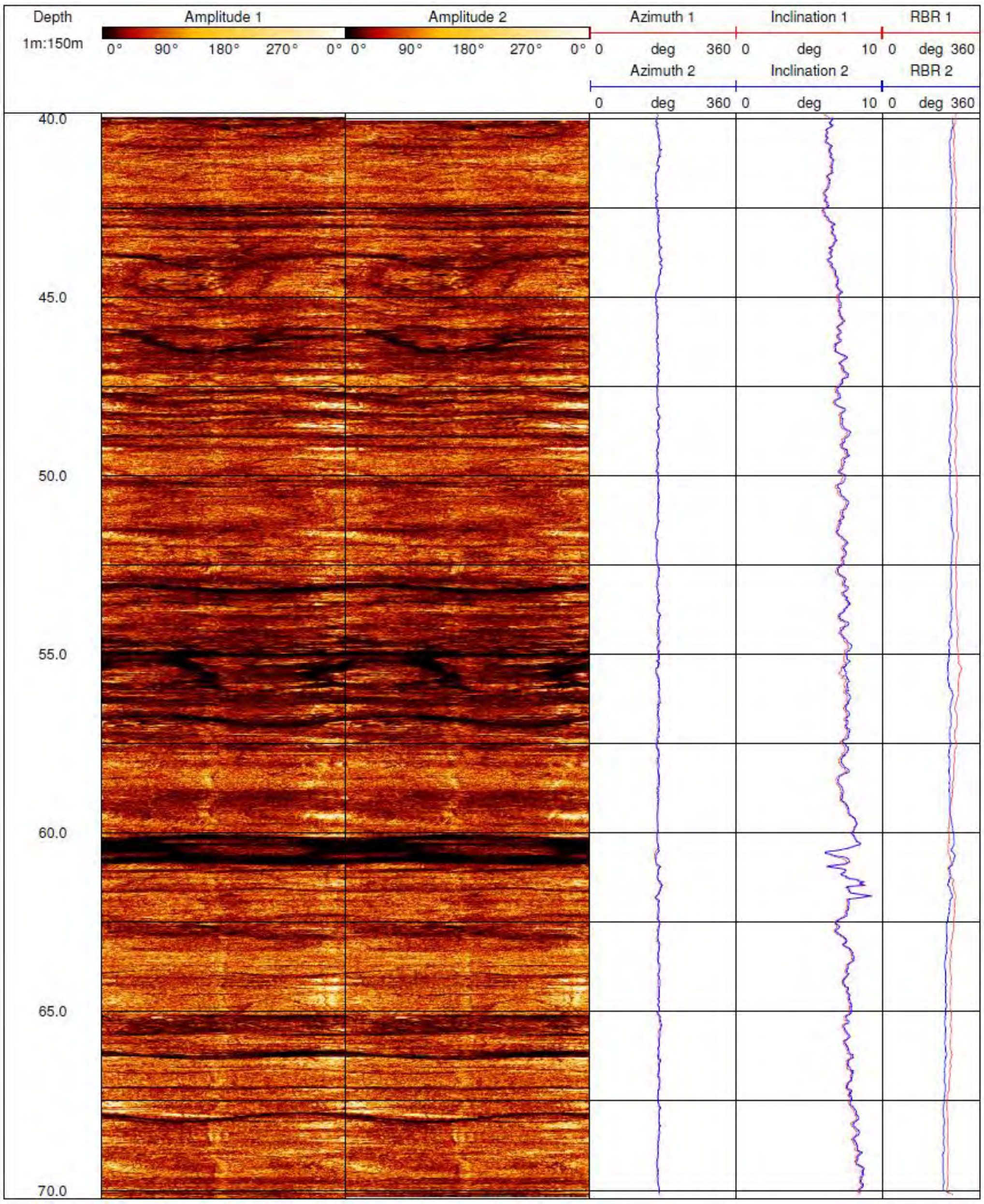

Robertson Geologging Ltd.
Deganwy, Conwy, LL31 9PX,
United Kingdom
T: +44 (0) 1492 582 323
E: growlands@robertson-geo.com
www.robertson-geo.com

ROBERTSON GEO
Unlocking Your GeoData

CERTIFICATE OF CONFORMITY

Certificate of Conformity

This is to certify that the following equipment conforms to the specification detailed below

ROBERTSON GEO
Unlocking Your GeoData

Equipment type: 3-Arm Caliper Probe (710mm range)

RG Order No: ORD00000

Serial No: 3ACS 11209

Comm. Type: Standard 4-Core

Quality Management System:
ISO 9001:2015
Certified by TÜV SÜD

Tested by: T Hamflett

Date: 30/08/19

Approved by:

[redacted]

Tim Hamflett | *Test Engineer*

Date: 30th August 2019

TÜV SÜD ISO 9001
ISO 9001
Certified
Quality Management System
www.tuv-sud.com/ms-cert

Robertson Geologging Ltd.
Deganwy, Conwy, LL31 9PX,
United Kingdom
T: +44 (0) 1492 582 323
E: support@robertson-geo.com
www.robertson-geo.com

ROBERTSON GEO
Unlocking Your GeoData

CERTIFICATE OF CONFORMITY

The probe detailed has been calibrated and then logged in the **ROBERTSON GEO** Test Borehole (Deganwy, UK). The resulting data falls within acceptable tolerances and meets all test criteria.

ROBERTSON GEO
Unlocking Your GeoData

Main Pass: 70-25m

Repeat Pass: 70-55m

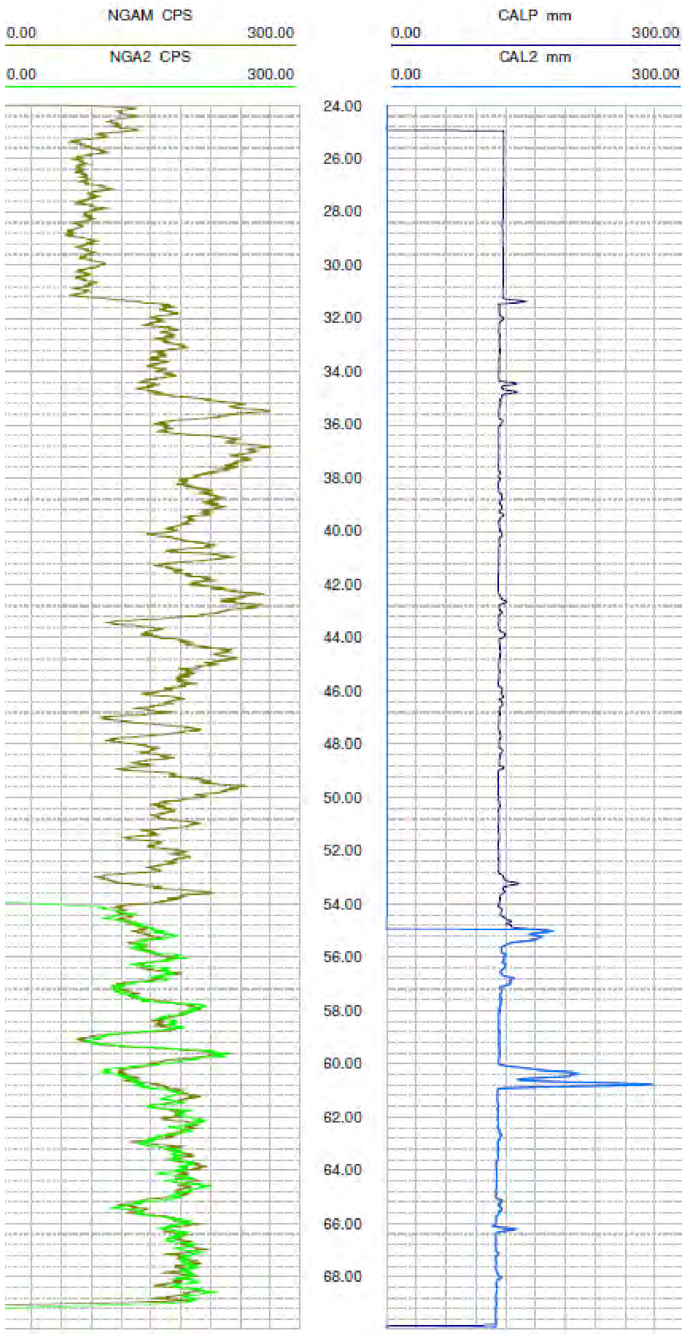

Channel	x^n	Coefficient
1 NGAM	0	0.0
	1	1.24517
	2	0.0
	3	0.0
2 CALP	0	-527.474
	1	9.20081E-2
	2	-2.03994E-6
	3	0.0
3	0	0.0
	1	1.0
	2	0.0
	3	0.0
4	0	0.0
	1	1.0
	2	0.0
	3	0.0
5	0	0.0
	1	1.0
	2	0.0
	3	0.0
6	0	0.0
	1	1.0
	2	0.0
	3	0.0
7	0	0.0
	1	1.0
	2	0.0
	3	0.0
8	0	0.0
	1	1.0
	2	0.0
	3	0.0
9	0	0.0
	1	1.0
	2	0.0
	3	0.0
10	0	0.0
	1	1.0
	2	0.0
	3	0.0
11	0	0.0
	1	1.0
	2	0.0
	3	0.0
12	0	0.0
	1	1.0
	2	0.0
	3	0.0

Calibrated Value=$ax^0+bx^1+cx^2+dx^3$

ISO 9001
Certified
Quality Management System
www.tuv-sud.com/ms-cert

Robertson Geologging Ltd.
Deganwy, Conwy, LL31 9PX,
United Kingdom
T: +44 (0) 1492 582 323
E: growlands@robertson-geo.com
www.robertson-geo.com

ROBERTSON GEO
Unlocking Your GeoData

CERTIFICATE OF CONFORMITY

Certificate of Conformity

This is to certify that the following equipment conforms to the specification detailed below

ROBERTSON GEO
Unlocking Your GeoData

Equipment type: Formation Density Probe

RG Order No: ORD00000

Serial No: FDGS 5386

Comm. Type: Standard 4-Core

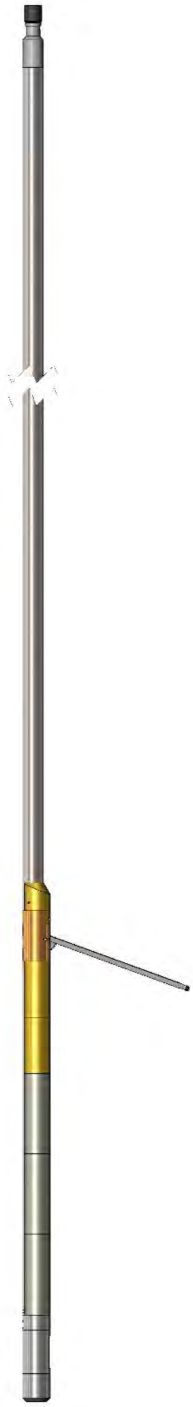

Quality Management System:
ISO 9001:2015
Certified by TÜV SÜD

Tested by: T Hamflett

Date: 10/07/19

Approved by:

[redacted]

Tim Hamflett | *Test Engineer*

Date: 10/07/19

TÜV SÜD ISO 9001
ISO 9001
Certified
Quality Management System
www.tuv-sud.com/ms-cert

Robertson Geologging Ltd.
Deganwy, Conwy, LL31 9PX,
United Kingdom
T: +44 (0) 1492 582 323
E: support@robertson-geo.com
www.robertson-geo.com

ROBERTSON GEO
Unlocking Your GeoData

CERTIFICATE OF CONFORMITY

The probe detailed has been calibrated and then logged in the **ROBERTSON GEO** Test Borehole (Deganwy, UK). The resulting data falls within acceptable tolerances and meets all test criteria.

Main Pass: 70-25m

Repeat Pass: 70-55m

Source Used: 5294GQ

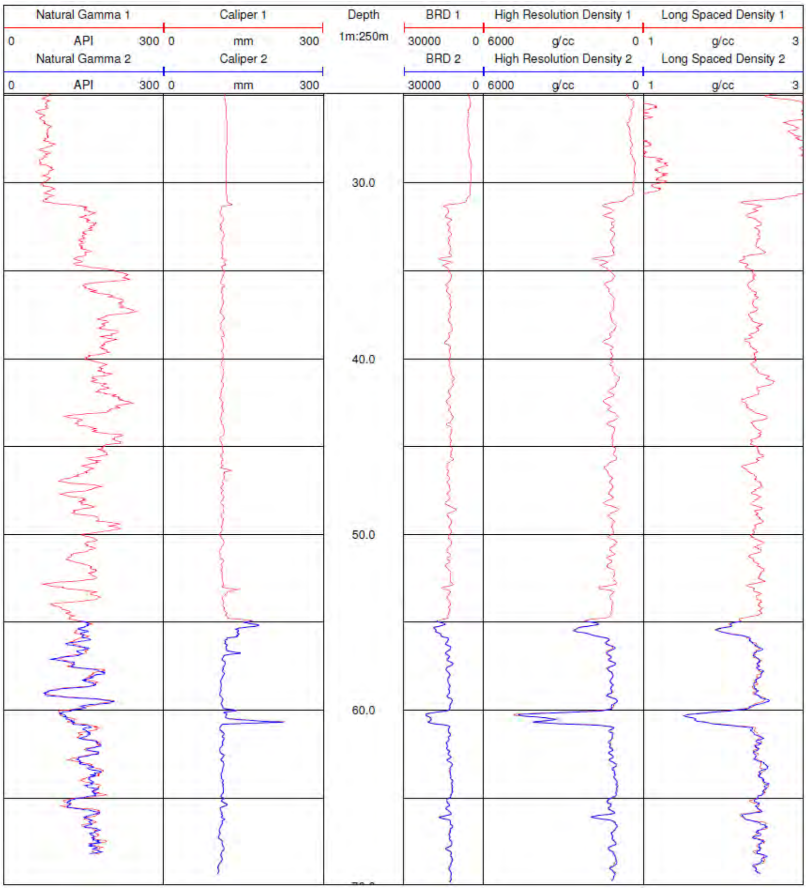

Channel	x^n	Coefficient
1 NGAM	0	0.0
	1	1.19444
	2	0.0
	3	0.0
2	0	0.0
	1	1.0
	2	0.0
	3	0.0
3 CALP	0	-88.5197
	1	0.0240289
	2	-2.65069
	3	0.0
4 LSD	0	5.72559
	1	1.45408
	2	0.0
	3	0.0
5 HRD	0	0.0
	1	1.0
	2	0.0
	3	0.0
6 BRD	0	0.0
	1	1.0
	2	0.0
	3	0.0
7	0	0.0
	1	1.0
	2	0.0
	3	0.0
8	0	0.0
	1	1.0
	2	0.0
	3	0.0
9	0	0.0
	1	1.0
	2	0.0
	3	0.0
10	0	0.0
	1	1.0
	2	0.0
	3	0.0
11	0	0.0
	1	1.0
	2	0.0
	3	0.0
12	0	0.0
	1	1.0
	2	0.0
	3	0.0

Calibrated Value=$ax^0+bx^1+cx^2+dx^3$

Robertson Geologging Ltd.
Deganwy, Conwy, LL31 9PX,
United Kingdom
T: +44 (0) 1492 582 323
E: growlands@robertson-geo.com
www.robertson-geo.com

CERTIFICATE OF CONFORMITY

Certificate of Conformity

This is to certify that the following equipment conforms to the specification detailed below

ROBERTSON GEO
Unlocking Your GeoData

Equipment type: Electric Log Probe

RG Order No: ORD00000

Serial No: ELTG 10894

Comm. Type: Standard 4-Core

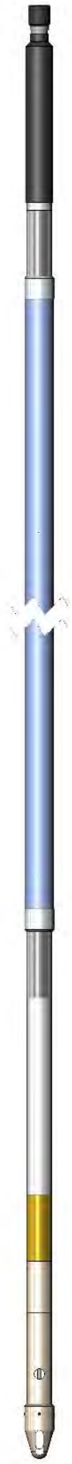

Quality Management System:
ISO 9001:2015
Certified by TÜV SÜD

Tested by: T Hamflett

Date: 25/06/19

Approved by:

[redacted]

Tim Hamflett | *Test Engineer*

Date: 25/06/19

CERTIFICATE OF CONFORMITY

The probe detailed has been calibrated and then logged in the **ROBERTSON GEO** Test Borehole (Deganwy, UK). The resulting data falls within acceptable tolerances and meets all test criteria.

ROBERTSON GEO
Unlocking Your GeoData

Main Pass: 70-25m

Repeat Pass: 70-55m

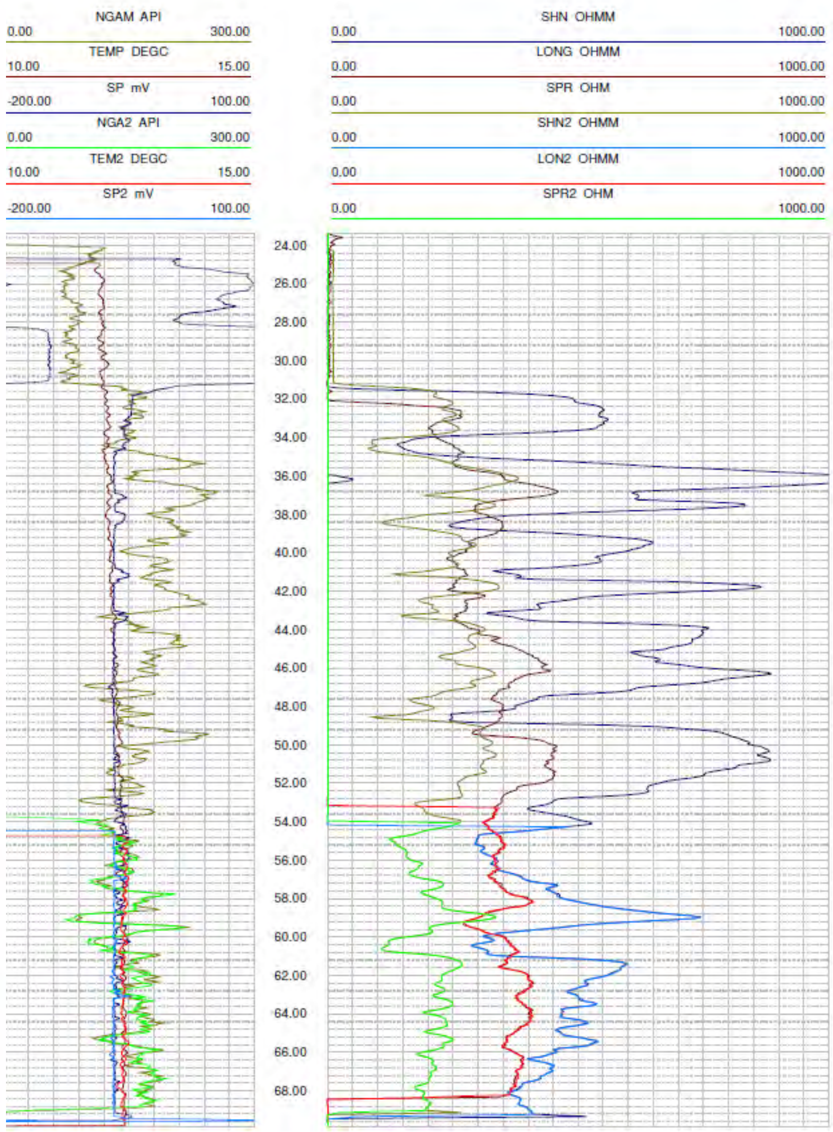

Channel	***x^n***	***Coefficient***
1 SHN	0	0.0
	1	0.2
	2	0.0
	3	0.0
2 LONG	0	0.0
	1	0.2
	2	0.0
	3	0.0
3 NGAM	0	0.0
	1	1.18566
	2	0.0
	3	0.0
4 TEMP	0	0.0
	1	1.0
	2	0.0
	3	0.0
5 SP	0	-1000.0
	1	0.1
	2	0.0
	3	0.0
6 SPR	0	0.0
	1	0.2
	2	0.0
	3	0.0
7	0	0.0
	1	1.0
	2	0.0
	3	0.0
8	0	0.0
	1	1.0
	2	0.0
	3	0.0
9	0	0.0
	1	1.0
	2	0.0
	3	0.0
10	0	0.0
	1	1.0
	2	0.0
	3	0.0
11	0	0.0
	1	1.0
	2	0.0
	3	0.0
12	0	0.0
	1	1.0
	2	0.0
	3	0.0

Calibrated Value=$ax^0+bx^1+cx^2+dx^3$

Robertson Geologging Ltd.
Deganwy, Conwy, LL31 9PX,
United Kingdom
T: +44 (0) 1492 582 323
E: growlands@robertson-geo.com
www.robertson-geo.com

ROBERTSON GEO
Unlocking Your GeoData

CERTIFICATE OF CONFORMITY

Certificate of Conformity

This is to certify that the following equipment conforms to the specification detailed below

ROBERTSON GEO
Unlocking Your GeoData

Equipment type: Temperature Conductivity Probe (standard mode)

RG Order No: ORD00000

Serial No: TCXS 1365

Comm. Type: Standard 4-Core

Quality Management System:
ISO 9001:2015
Certified by TÜV SÜD

Tested by: T Hamflett

Date: 18/06/19

Approved by:

[redacted]

Tim Hamflett | *Test Engineer*

Date: 18/06/19

ISO 9001
Certified
Quality Management System
www.tuv-sud.com/ms-cert

Robertson Geologging Ltd.
Deganwy, Conwy, LL31 9PX,
United Kingdom
T: +44 (0) 1492 582 323
E: support@robertson-geo.com
www.robertson-geo.com

ROBERTSON GEO
Unlocking Your GeoData

CERTIFICATE OF CONFORMITY

The probe detailed has been calibrated and then logged in the **ROBERTSON GEO** Test Borehole (Deganwy, UK). The resulting data falls within acceptable tolerances and meets all test criteria.

ROBERTSON GEO
Unlocking Your GeoData

Down Pass: 0-50m

Repeat Pass: 0-50m

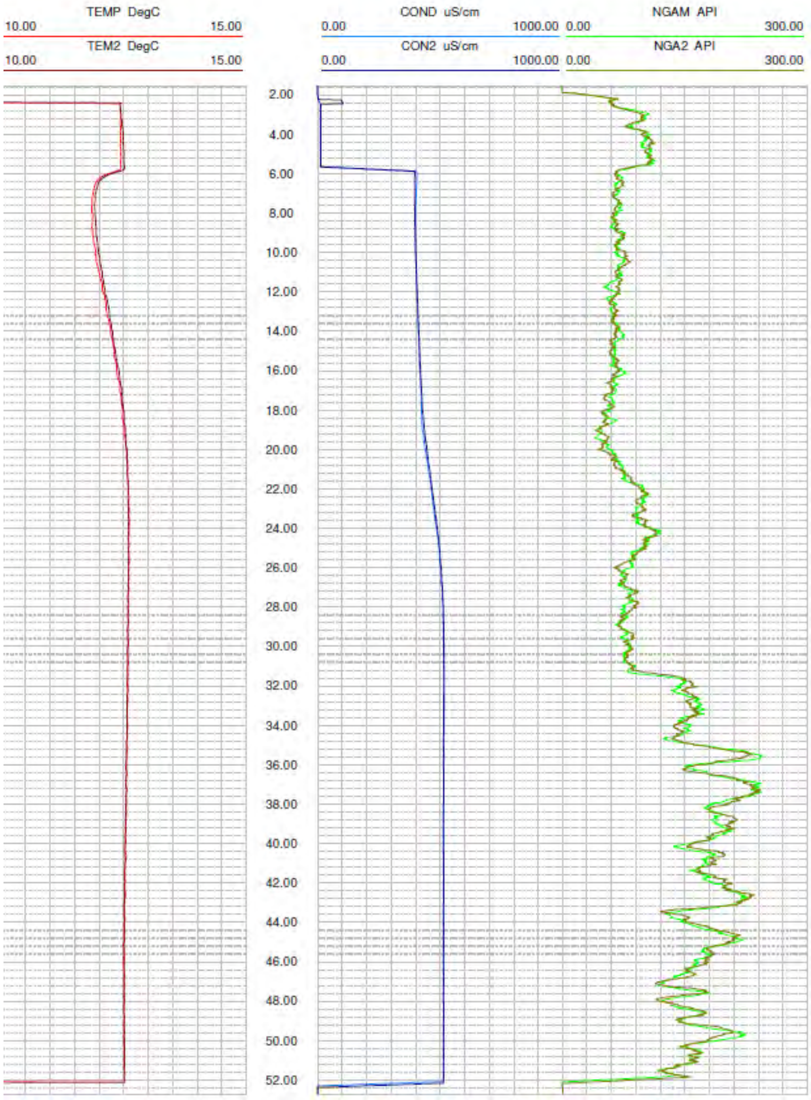

Channel	x^n	*Coefficient*
1 TEMP	0	-8.71562
	1	4.79188E-3
	2	0.0
	3	0.0
2 COND	0	2.92263
	1	0.915076
	2	5.97814E-7
	3	6.27746E-11
3 NGAM	0	0.0
	1	1.16848
	2	0.0
	3	0.0
4	0	0.0
	1	1.0
	2	0.0
	3	0.0
5	0	0.0
	1	1.0
	2	0.0
	3	0.0
6	0	0.0
	1	1.0
	2	0.0
	3	0.0
7	0	0.0
	1	1.0
	2	0.0
	3	0.0
8	0	0.0
	1	1.0
	2	0.0
	3	0.0
9	0	0.0
	1	1.0
	2	0.0
	3	0.0
10	0	0.0
	1	1.0
	2	0.0
	3	0.0
11	0	0.0
	1	1.0
	2	0.0
	3	0.0
12	0	0.0
	1	1.0
	2	0.0
	3	0.0

Calibrated Value= $ax^0+bx^1+cx^2+dx^3$

Robertson Geologging Ltd.
Deganwy, Conwy, LL31 9PX,
United Kingdom
T: +44 (0) 1492 582 323
E: growlands@robertson-geo.com
www.robertson-geo.com

ROBERTSON GEO
Unlocking Your GeoData

ROBERTSON GEO SERVICES
Unlocking Your Geodata

COMPANY	Geotechnical Engineering	
WELL ID	DSRC414	
FIELD	Barrow Wake viewpoint	
COUNTRY	England	
LOCATION		OTHER SERVICES
STATE		
SEC	TWP	RGE
PERMANENT DATUM	GL	ELEVATION
LOG MEAS FROM	GL	ABOVE PERM. DATUM
DRILLING MEAS. FROM	GL	
K.B.		
D.F.		
G.L.		
CO / WELL / FLD / CTY / STE / FILING No		

DATE	01.10.19	TYPE FLUID IN HOLE	Water
RUN No		SALINITY	
TYPE LOG	Flowmeter	DENSITY	
DEPTH-DRILLER	90	LEVEL	63.2
DEPTH-LOGGER	86.3	MAX. REC. TEMP	
BTM LOGGED INTERVAL	86.3		
TOP LOGGED INTERVAL	59.2	CASING SHOE	
OPERATING RIG TIME			
RECORDED BY	JB		
WITNESSED BY	KO		

BOREHOLE RECORD				CASING RECORD			
RUN NO.	BIT	FROM	TO	SIZE	WGT.	FROM	TO

CERTIFICATE OF CONFORMITY

Certificate of Conformity

This is to certify that the following equipment conforms to the specification detailed below

ROBERTSON GEO
Unlocking Your GeoData

Equipment type: 45mm Impeller Flowmeter Probe

RG Order No: ORD00000

Serial No: HRFM 11062

Comm. Type: Standard 4-Core

Quality Management System:
ISO 9001:2015
Certified by TÜV SÜD

Tested by: T Hamflett

Date: 30/04/19

Approved by:

[redacted]

Tim Hamflett | *Test Engineer*

Date: 30/04/19

CERTIFICATE OF CONFORMITY

The probe detailed has been calibrated and then logged in the **ROBERTSON GEO** Test Borehole (Deganwy, UK). The resulting data falls within acceptable tolerances and meets all test criteria.

ROBERTSON GEO
Unlocking Your GeoData

Down Pass x2: 7-1.8 m/min

Up Pass x2: 7-2.2 m/min

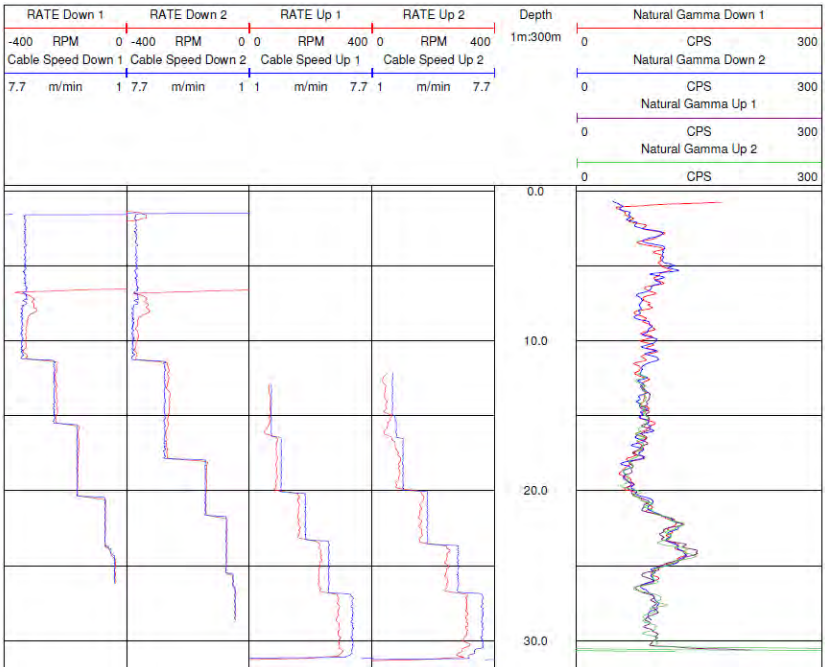

Channel	x^n	Coefficient
1 TFUP	0	0.0
	1	1.0
	2	0.0
	3	0.0
2 TFDN	0	0.0
	1	1.0
	2	0.0
	3	0.0
3 TSUP	0	0.0
	1	1.0
	2	0.0
	3	0.0
4 TSDN	0	0.0
	1	1.0
	2	0.0
	3	0.0
5 TIME	0	0.0
	1	1.0
	2	0.0
	3	0.0
6 NGAM	0	0.0
	1	1.39913
	2	0.0
	3	0.0
7	0	0.0
	1	1.0
	2	0.0
	3	0.0
8	0	0.0
	1	1.0
	2	0.0
	3	0.0
9	0	0.0
	1	1.0
	2	0.0
	3	0.0
10	0	0.0
	1	1.0
	2	0.0
	3	0.0
11	0	0.0
	1	1.0
	2	0.0
	3	0.0
12	0	0.0
	1	1.0
	2	0.0
	3	0.0

Calibrated Value=$ax^0+bx^1+cx^2+dx^3$

Robertson Geologging Ltd.
Deganwy, Conwy, LL31 9PX,
United Kingdom
T: +44 (0) 1492 582 323
E: growlands@robertson-geo.com
www.robertson-geo.com

ROBERTSON GEO
Unlocking Your GeoData

ROBERTSON GEO SERVICES
Unlocking Your GeoData

COMPANY	Geotechnical Engineering		
WELL ID	DSRC414		
FIELD	Barrow Wake vivewpoint		
COUNTRY	England	STATE	
LOCATION			OTHER SERVICES
SEC	TWP	RGE	

CO / WELL / FLD / CTY / STE / FILING No

PERMANENT DATUM	GL	ELEVATION	K.B.
LOG MEAS. FROM	GL	ABOVE PERM. DATUM	D.F.
DRILLING MEAS. FROM	GL		G.L.

DATE	01.10.19	TYPE FLUID IN HOLE	Water
RUN No		SALINITY	
TYPE LOG	Televiewer	DENSITY	
DEPTH-DRILLER	90	LEVEL	63.2
DEPTH-LOGGER	87.7	MAX. REC. TEMP.	
BTM LOGGED INTERVAL	87.7		
TOP LOGGED INTERVAL	2.1	CASING SHOE	
OPERATING RIG TIME			
RECORDED BY	JB		
WITNESSED BY	KO		

RUN	BOREHOLE RECORD			CASING RECORD			
NO.	BIT	FROM	TO	SIZE	WGT.	FROM	TO

Depth 1m:20m	Optical 0° 90° 180° 270° 0° / Features 0° 90° 180° 270° 0°	Amplitude 0° 90° 180° 270° 0° / Features 2 0° 90° 180° 270° 0°	Projection 0° 180°	Projection 2 90° 270°	Dips 0 90	Azimuth 0 Deg 360 / Inclination 0 Deg 5
1.2						
1.6						

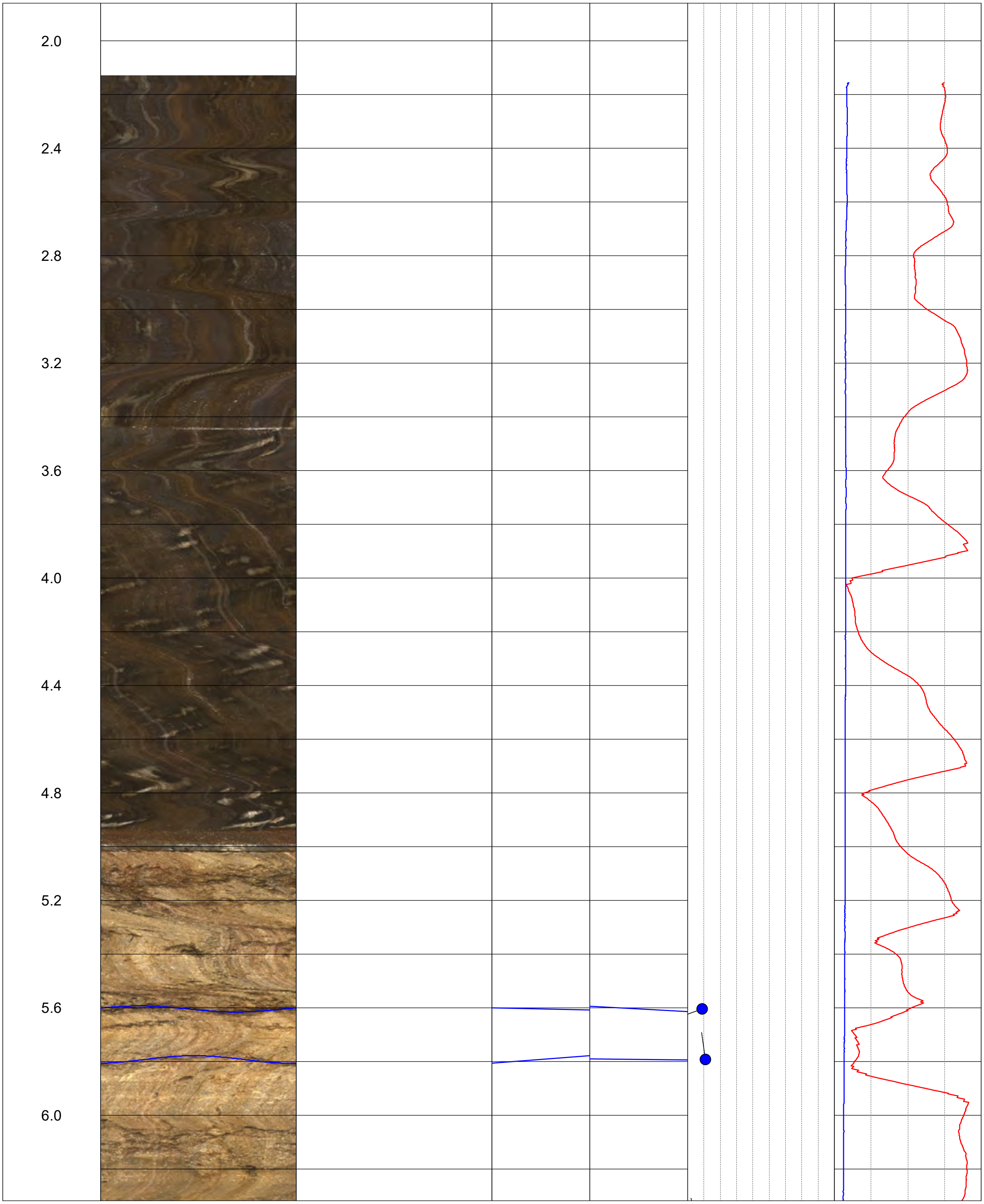
2.0
2.4
2.8
3.2
3.6
4.0
4.4
4.8
5.2
5.6
6.0

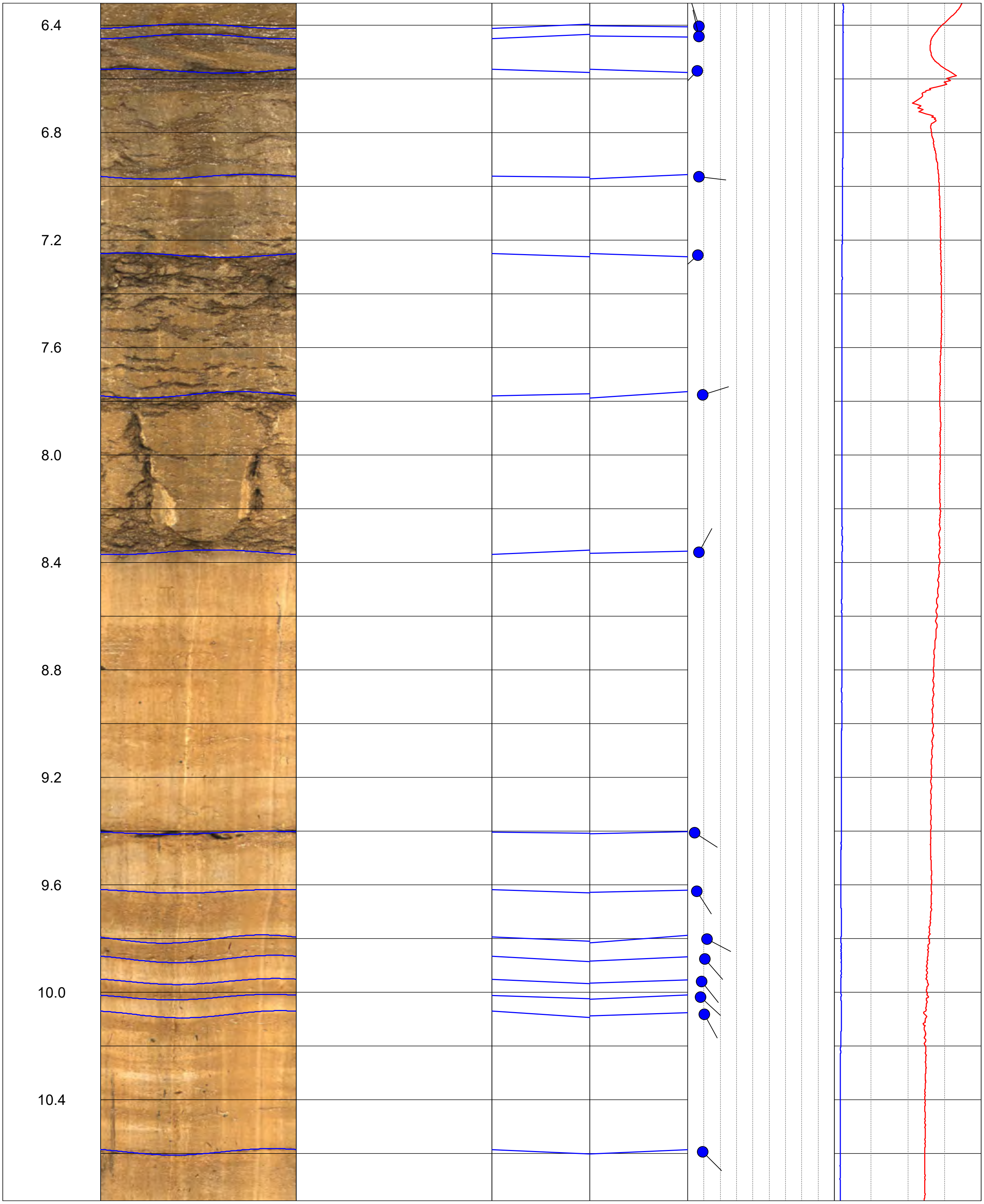
6.4
6.8
7.2
7.6
8.0
8.4
8.8
9.2
9.6
10.0
10.4

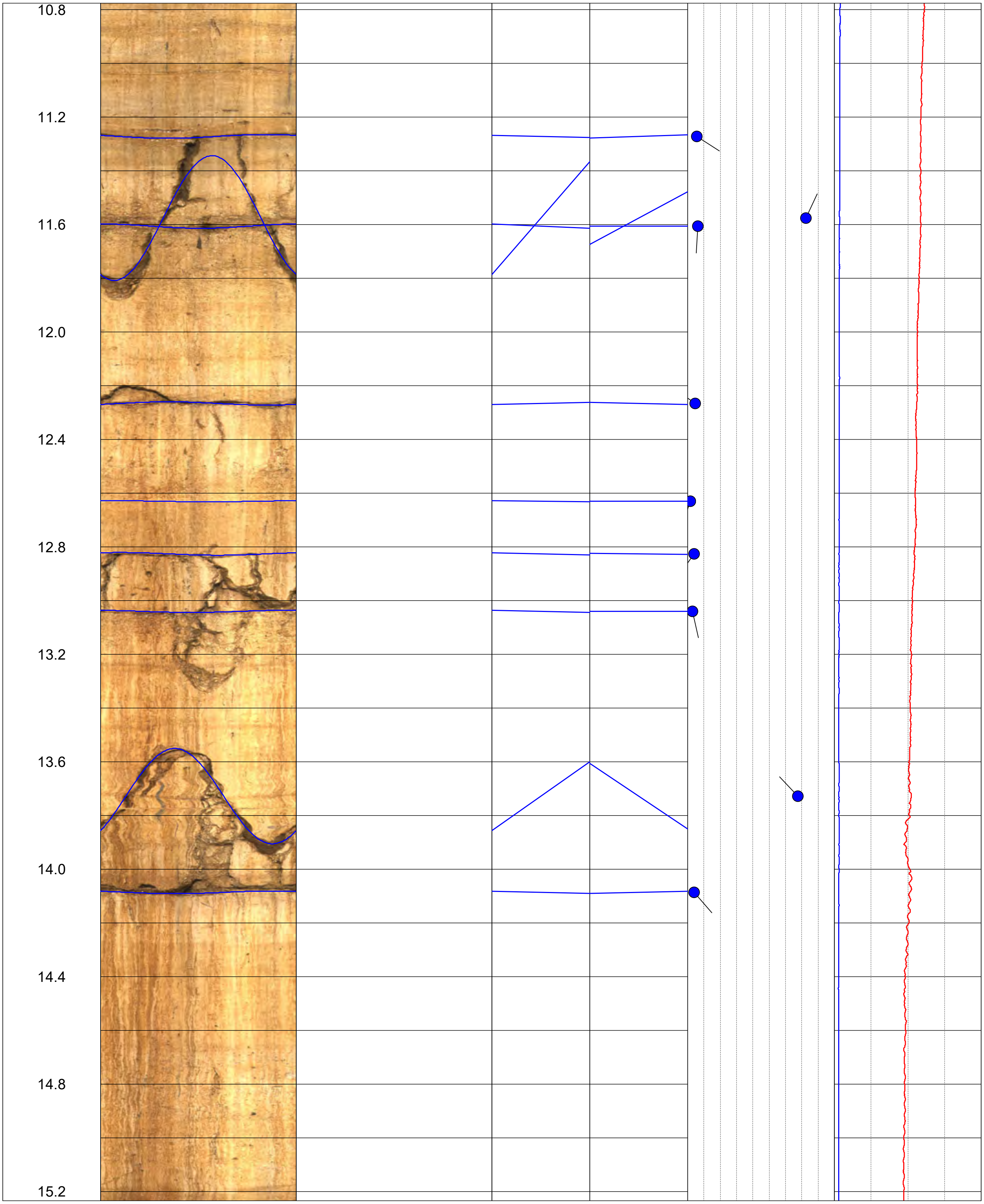
10.8
11.2
11.6
12.0
12.4
12.8
13.2
13.6
14.0
14.4
14.8
15.2

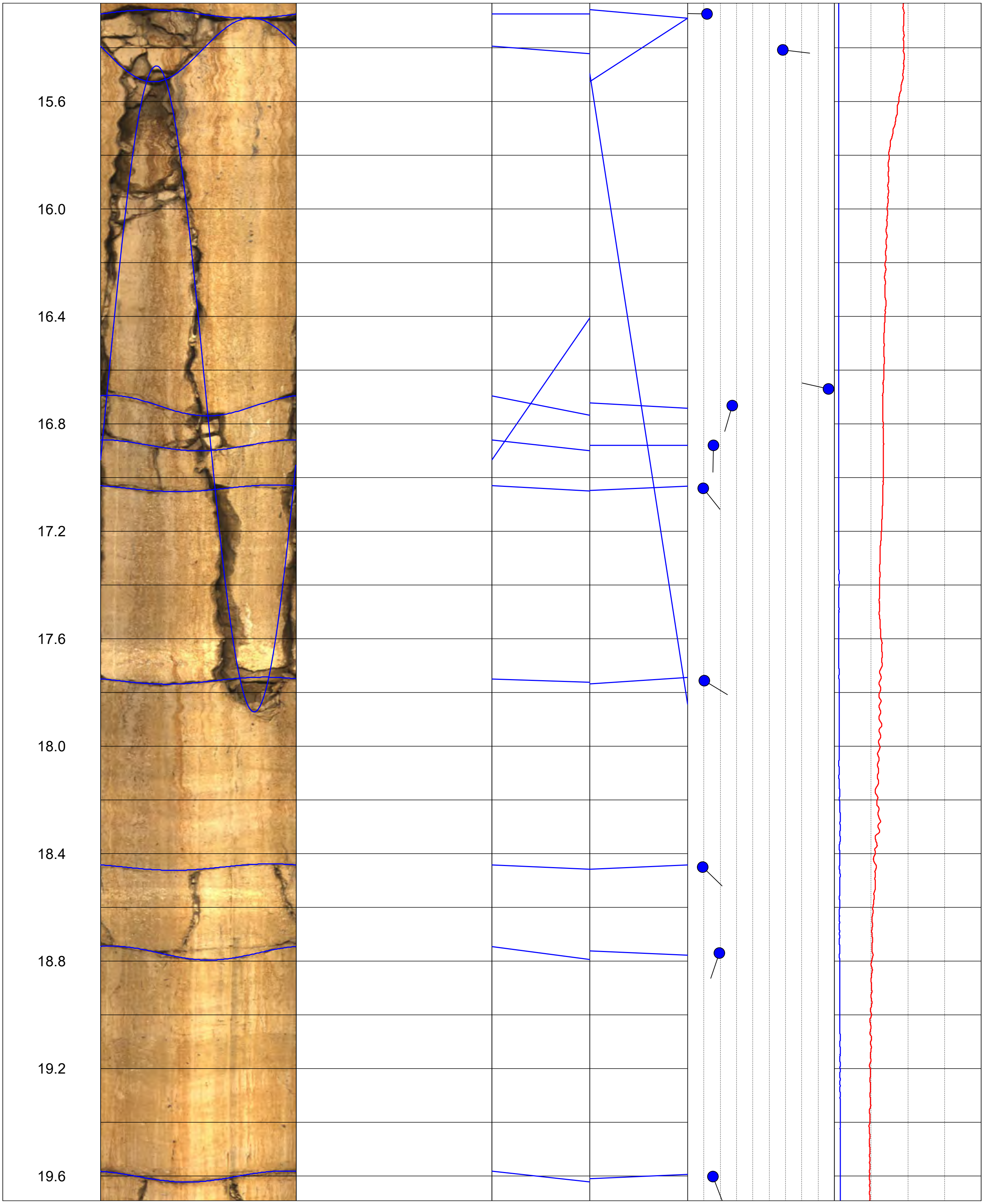

15.6
16.0
16.4
16.8
17.2
17.6
18.0
18.4
18.8
19.2
19.6

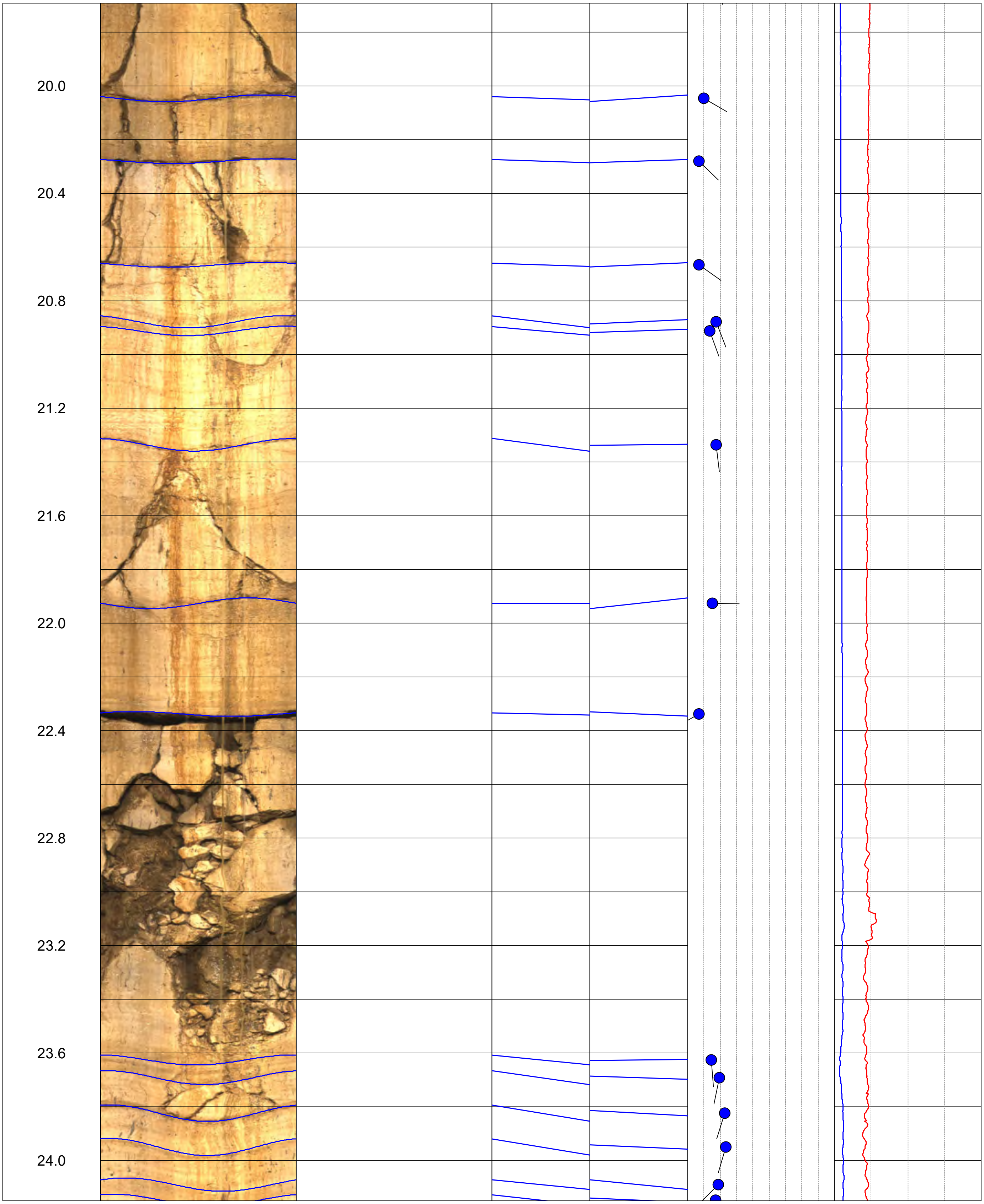
20.0
20.4
20.8
21.2
21.6
22.0
22.4
22.8
23.2
23.6
24.0

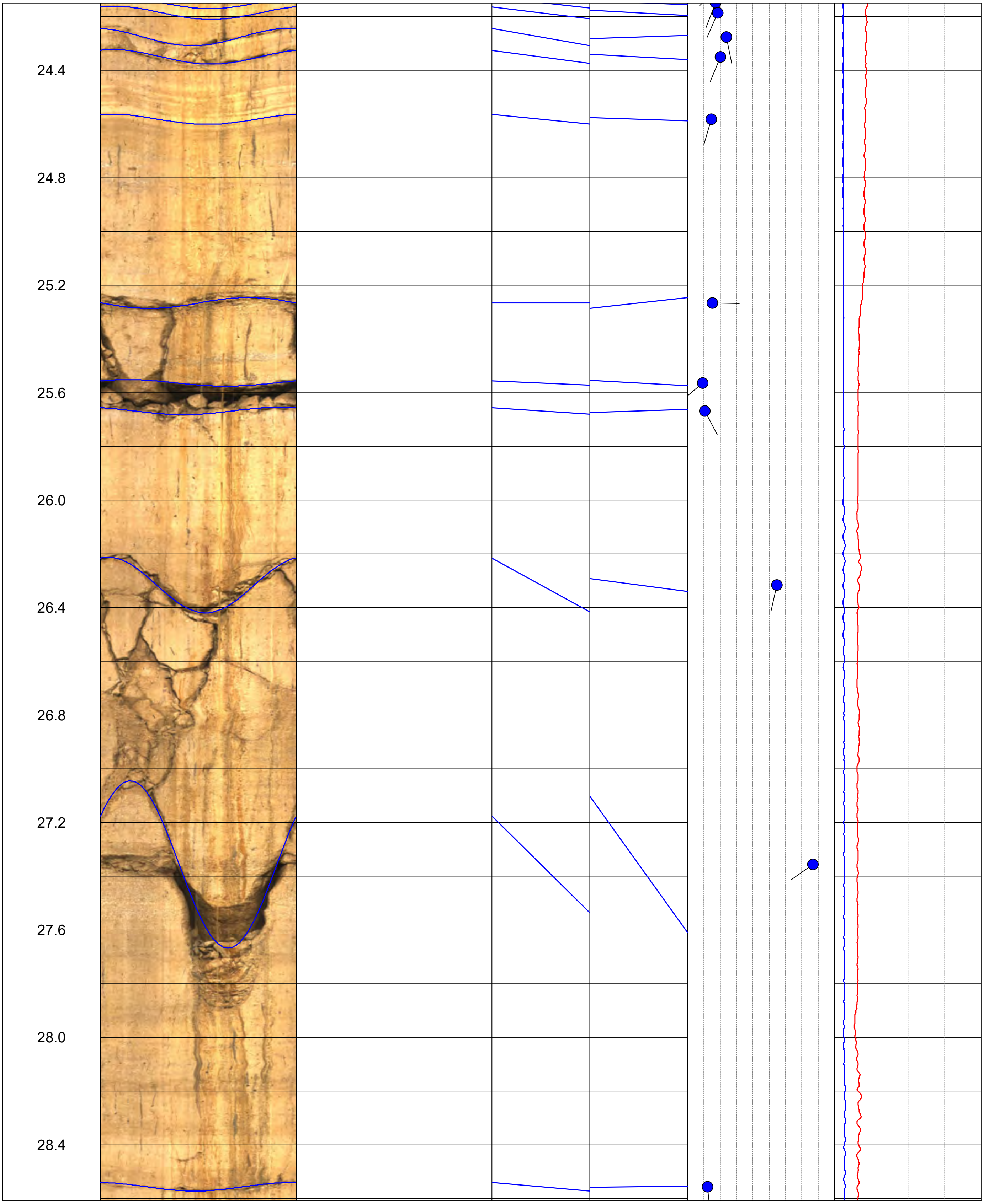
24.4
24.8
25.2
25.6
26.0
26.4
26.8
27.2
27.6
28.0
28.4

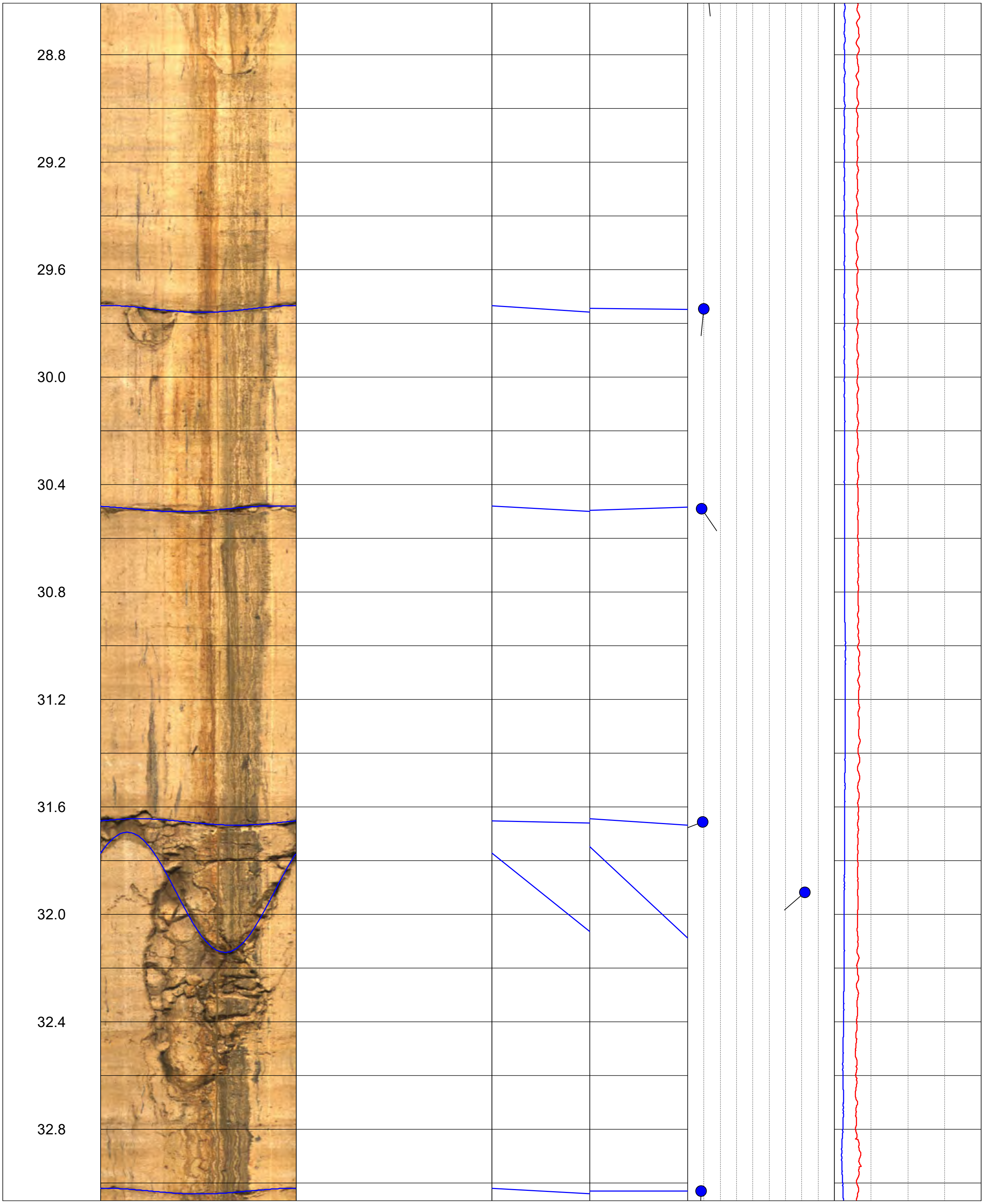
28.8
29.2
29.6
30.0
30.4
30.8
31.2
31.6
32.0
32.4
32.8

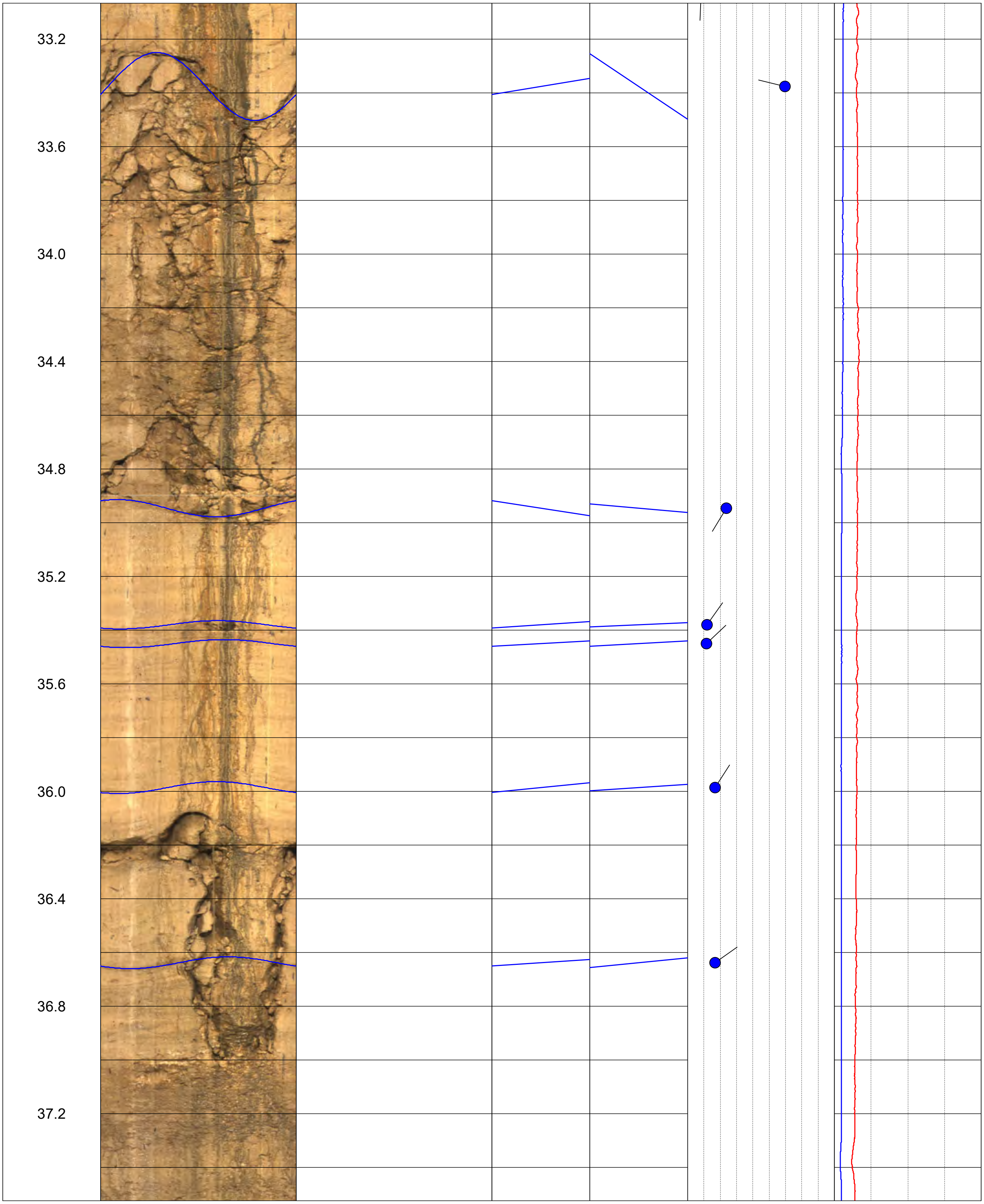
33.2
33.6
34.0
34.4
34.8
35.2
35.6
36.0
36.4
36.8
37.2

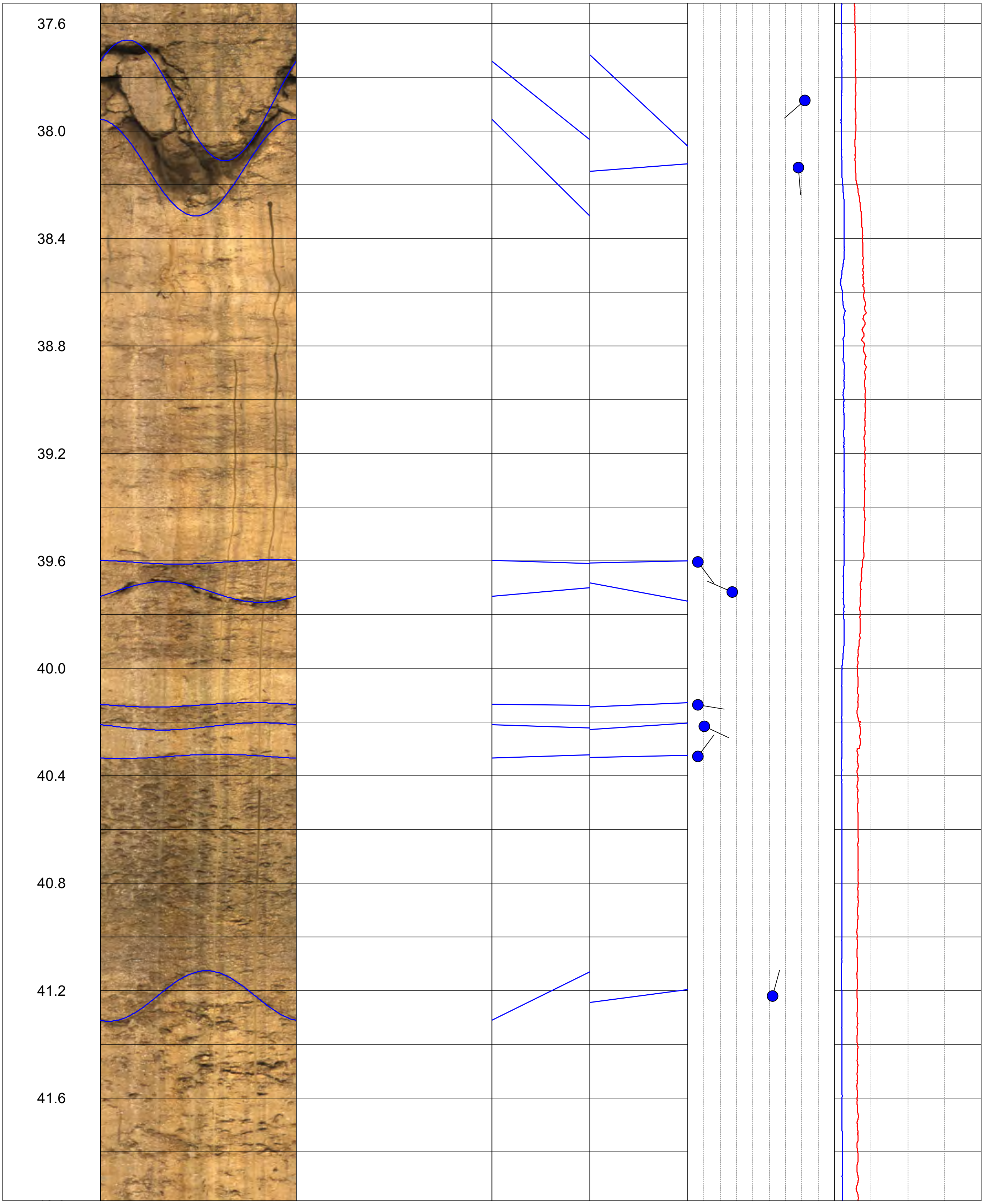
37.6
38.0
38.4
38.8
39.2
39.6
40.0
40.4
40.8
41.2
41.6

42.0
42.4
42.8
43.2
43.6
44.0
44.4
44.8
45.2
45.6
46.0
46.4

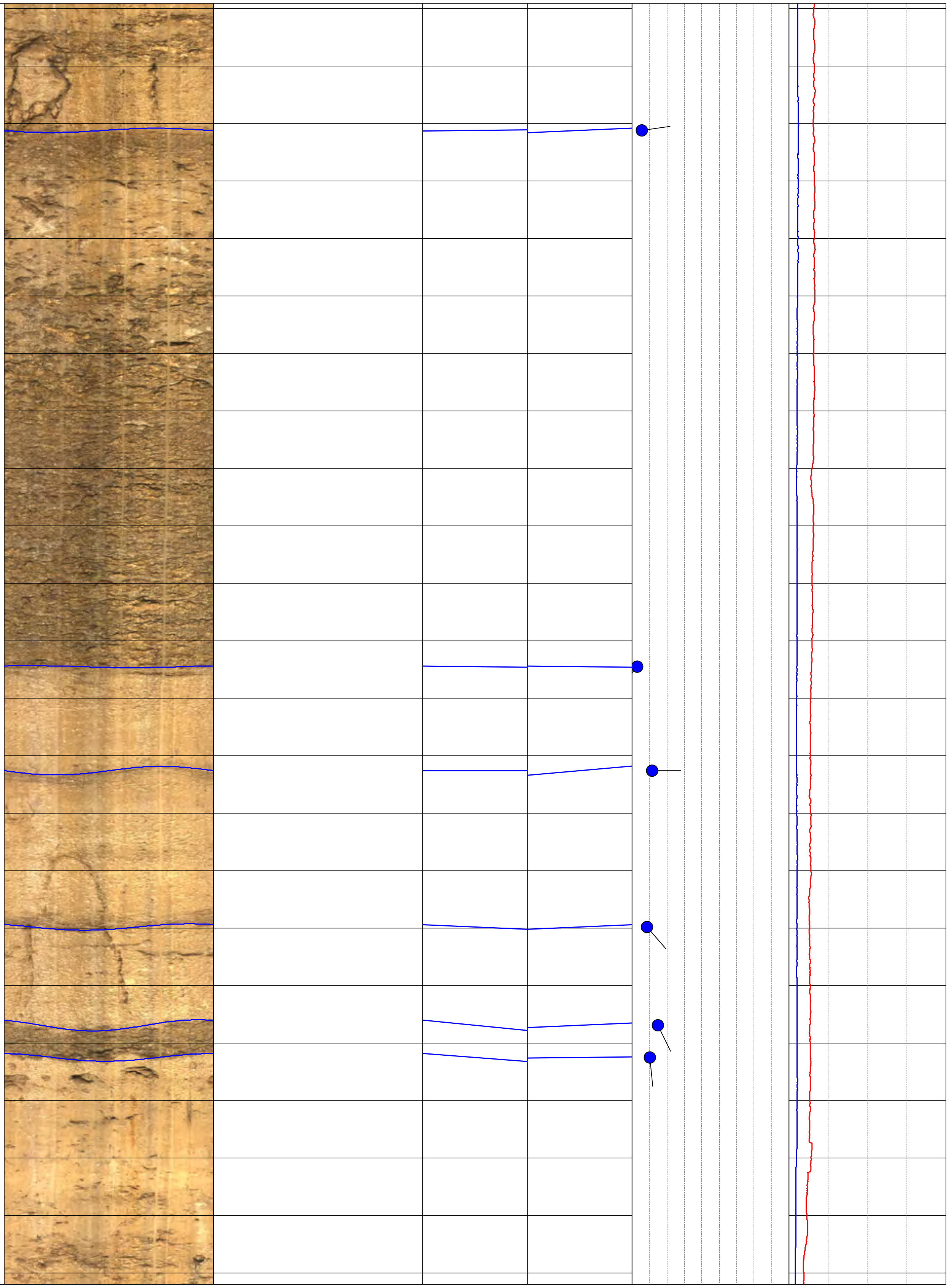

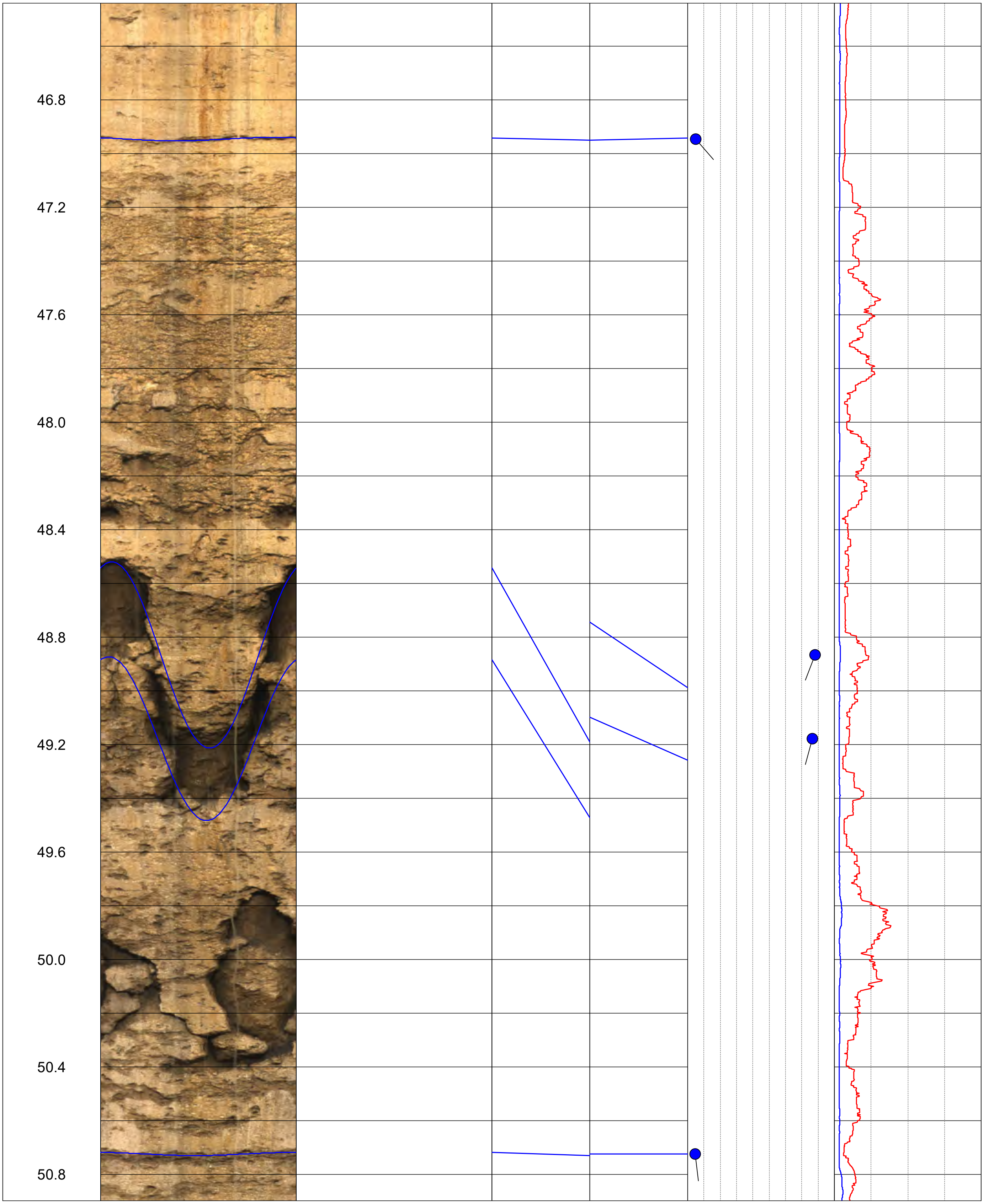

46.8
47.2
47.6
48.0
48.4
48.8
49.2
49.6
50.0
50.4
50.8

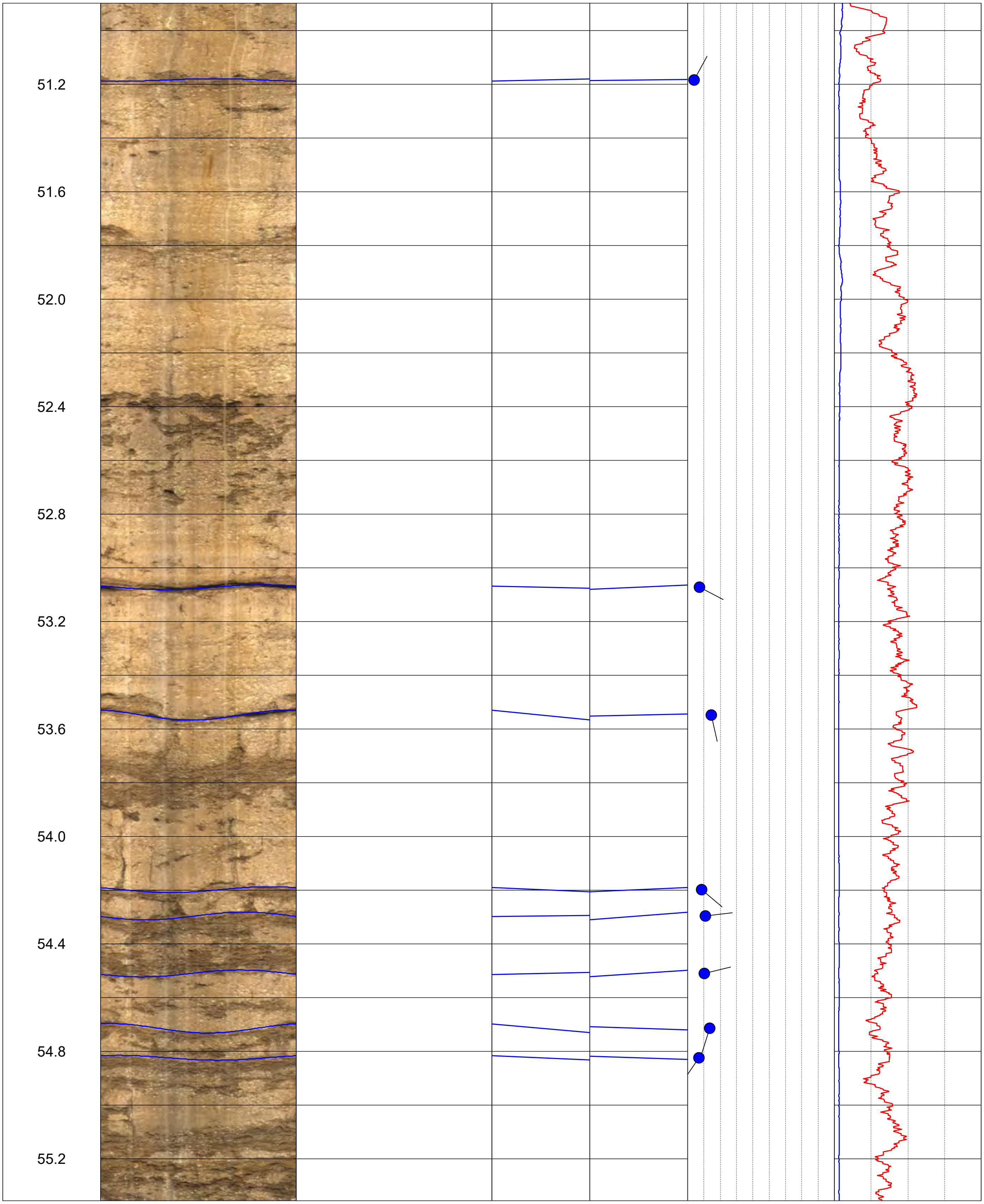
51.2
51.6
52.0
52.4
52.8
53.2
53.6
54.0
54.4
54.8
55.2

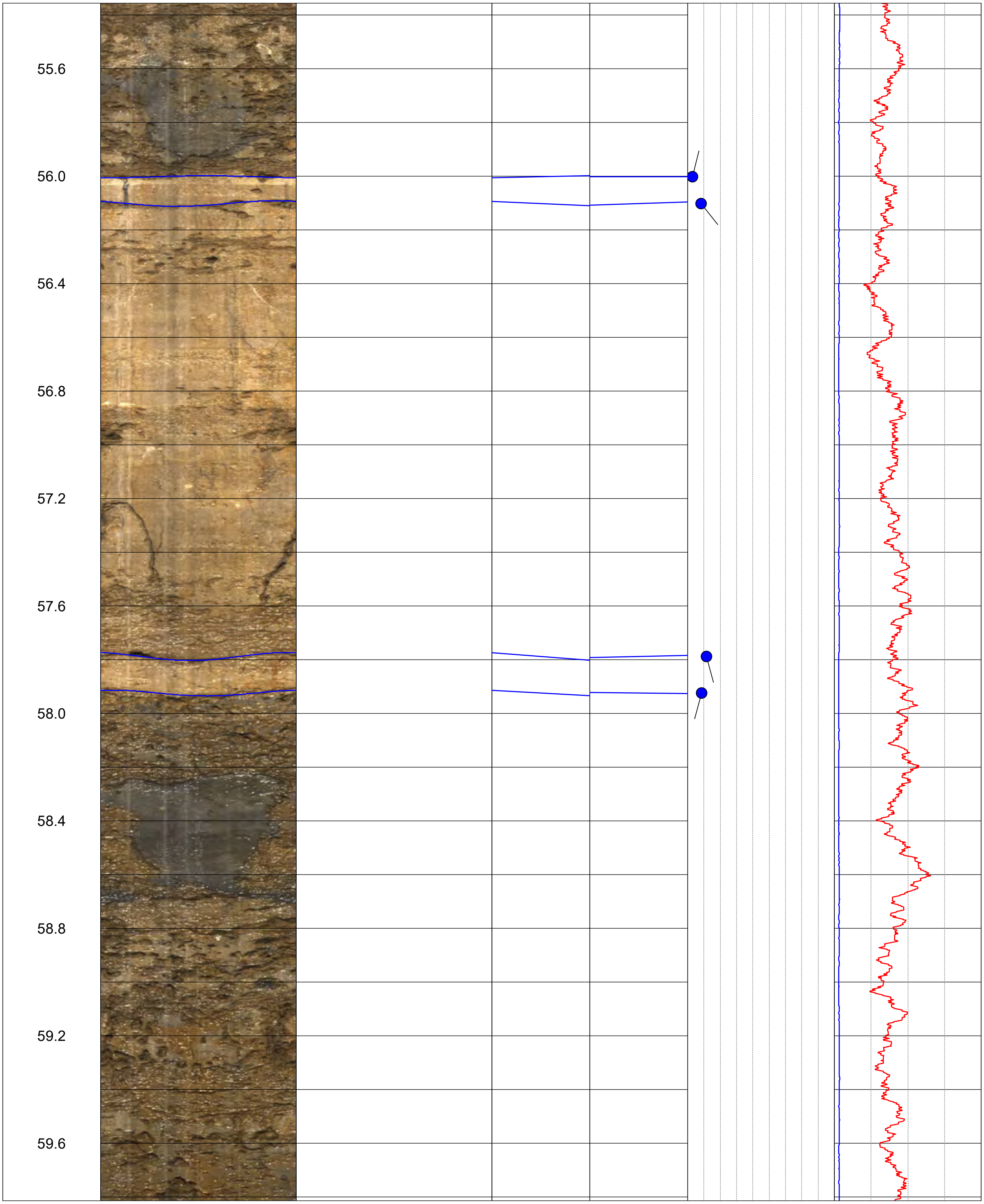
55.6
56.0
56.4
56.8
57.2
57.6
58.0
58.4
58.8
59.2
59.6

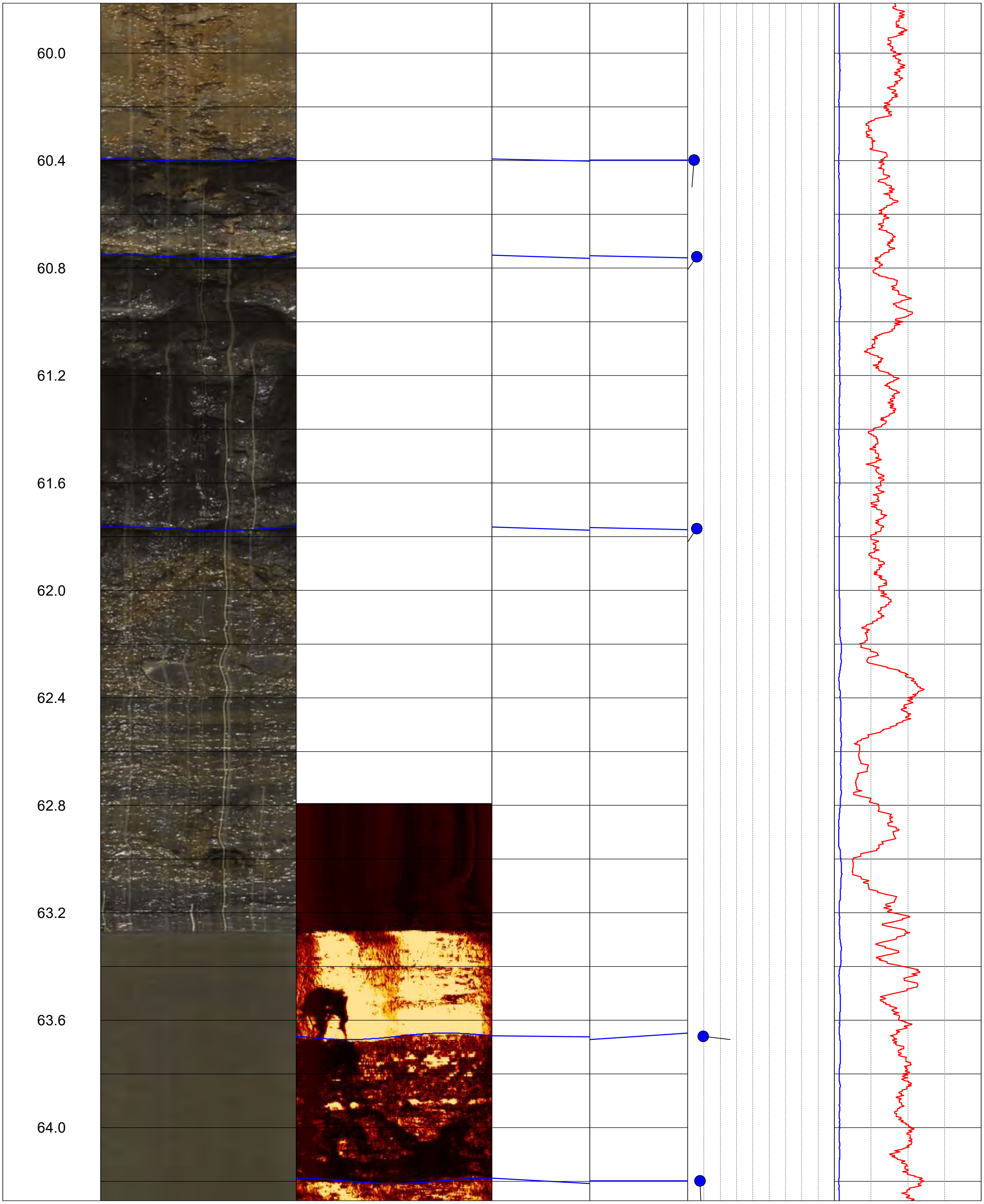
60.0
60.4
60.8
61.2
61.6
62.0
62.4
62.8
63.2
63.6
64.0

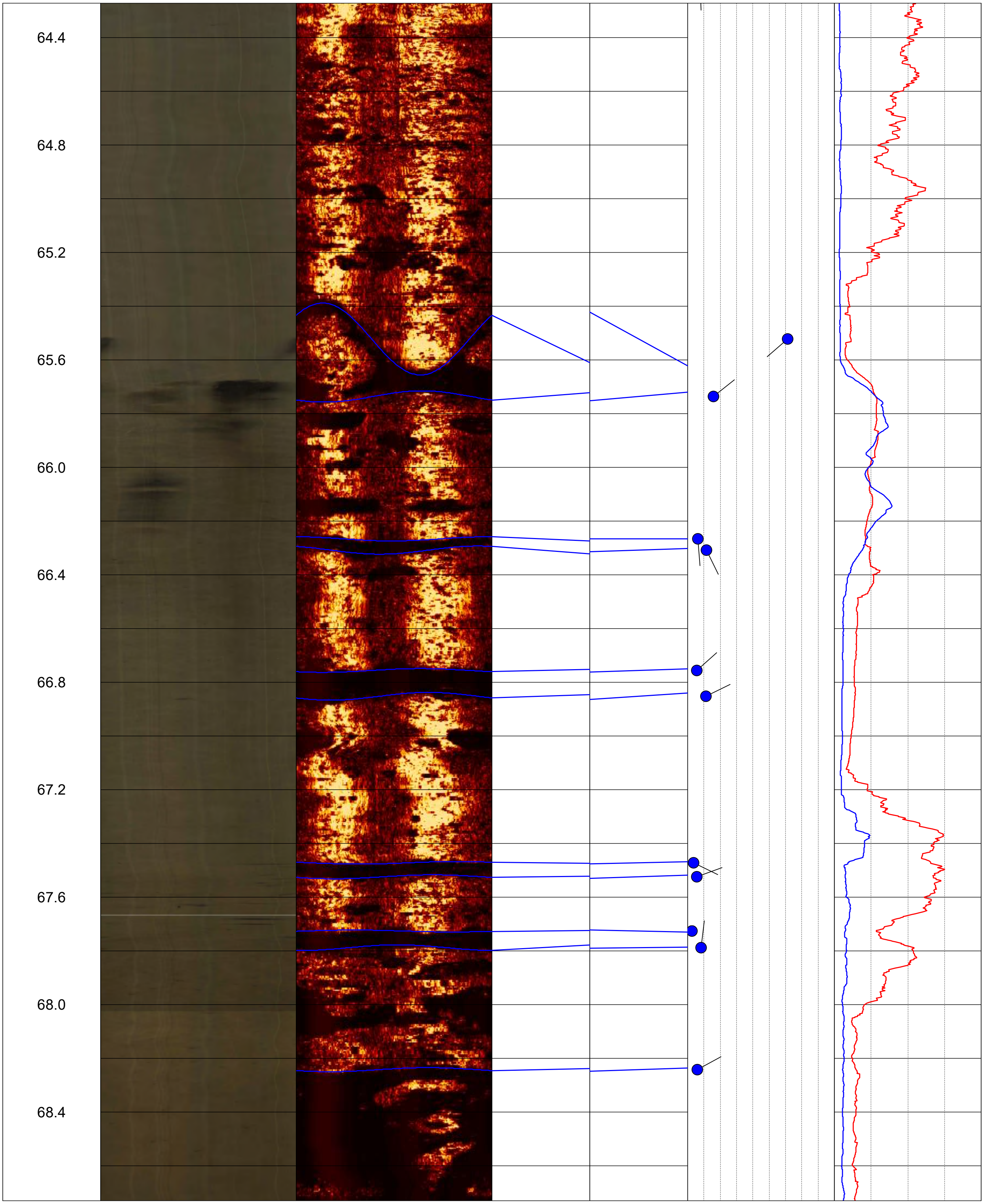
64.4
64.8
65.2
65.6
66.0
66.4
66.8
67.2
67.6
68.0
68.4

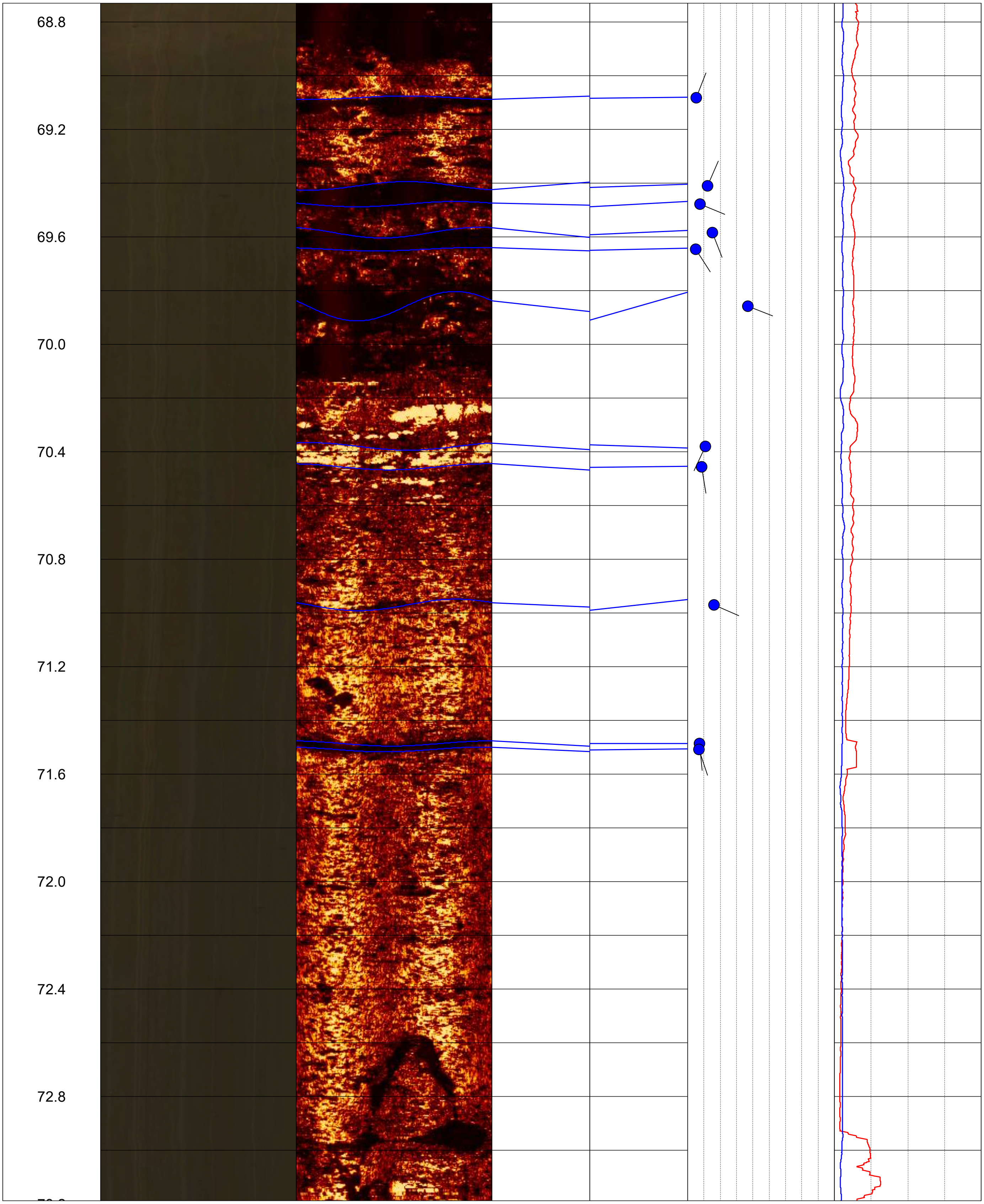
68.8
69.2
69.6
70.0
70.4
70.8
71.2
71.6
72.0
72.4
72.8

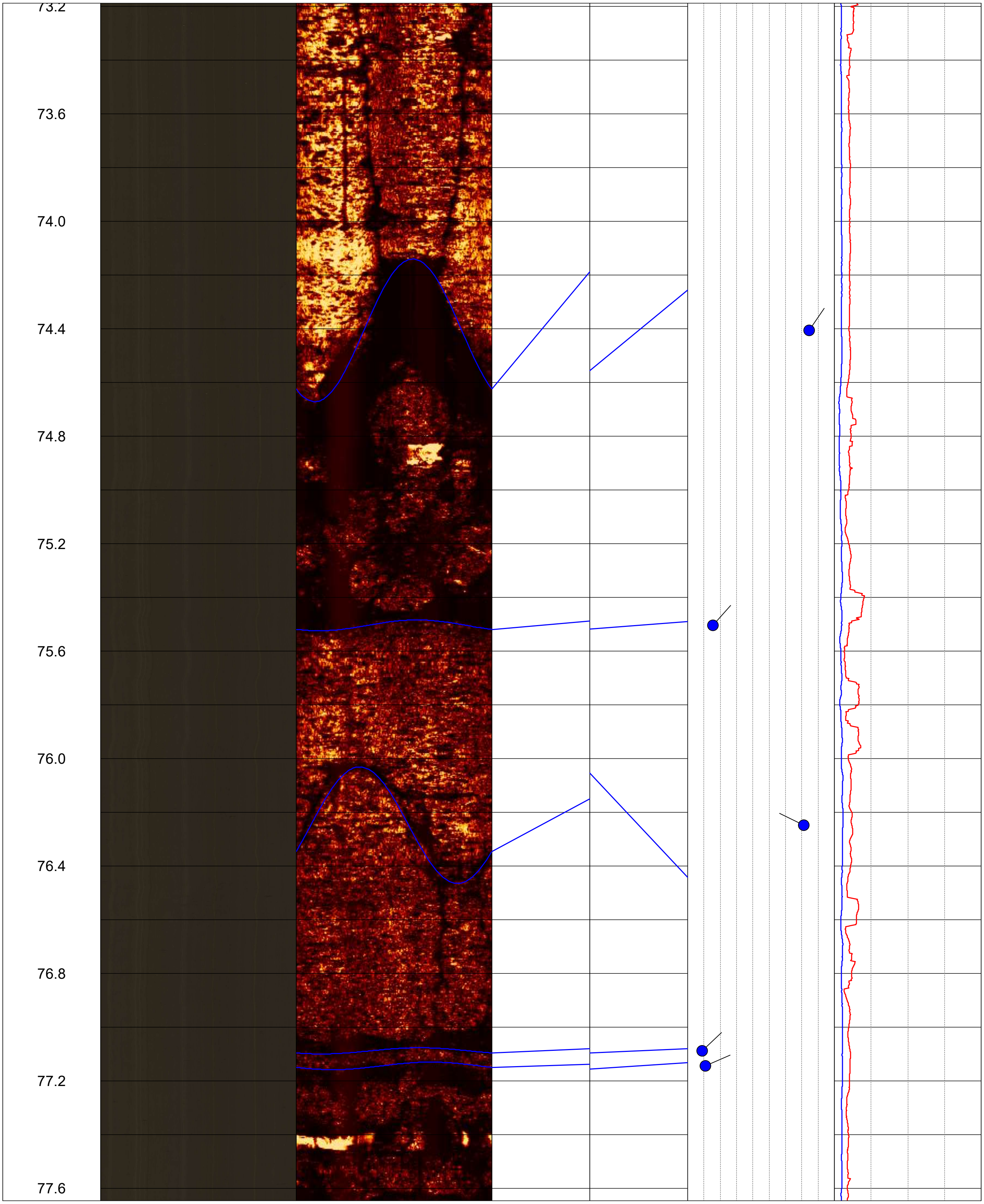
73.2
73.6
74.0
74.4
74.8
75.2
75.6
76.0
76.4
76.8
77.2
77.6

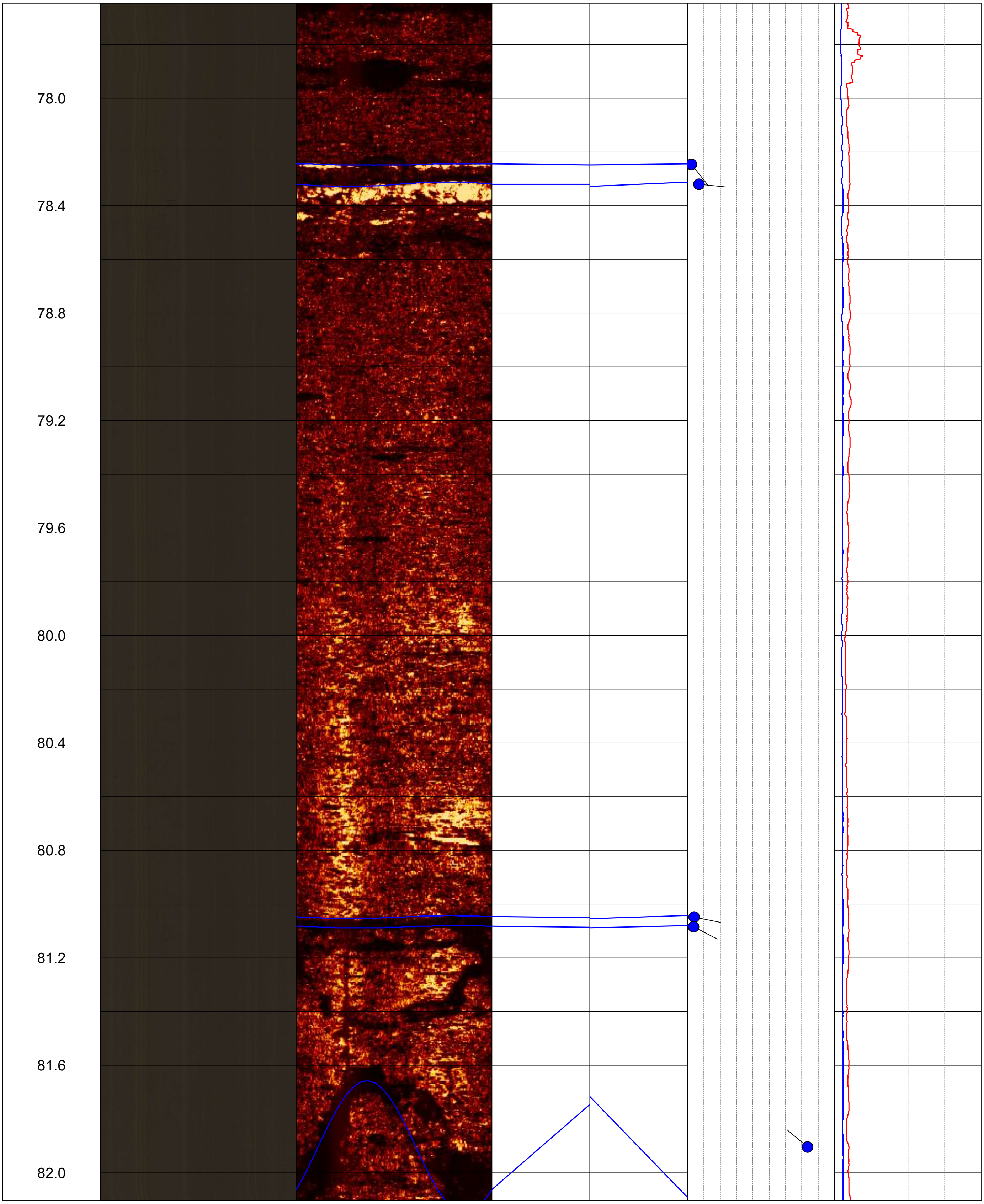
78.0
78.4
78.8
79.2
79.6
80.0
80.4
80.8
81.2
81.6
82.0

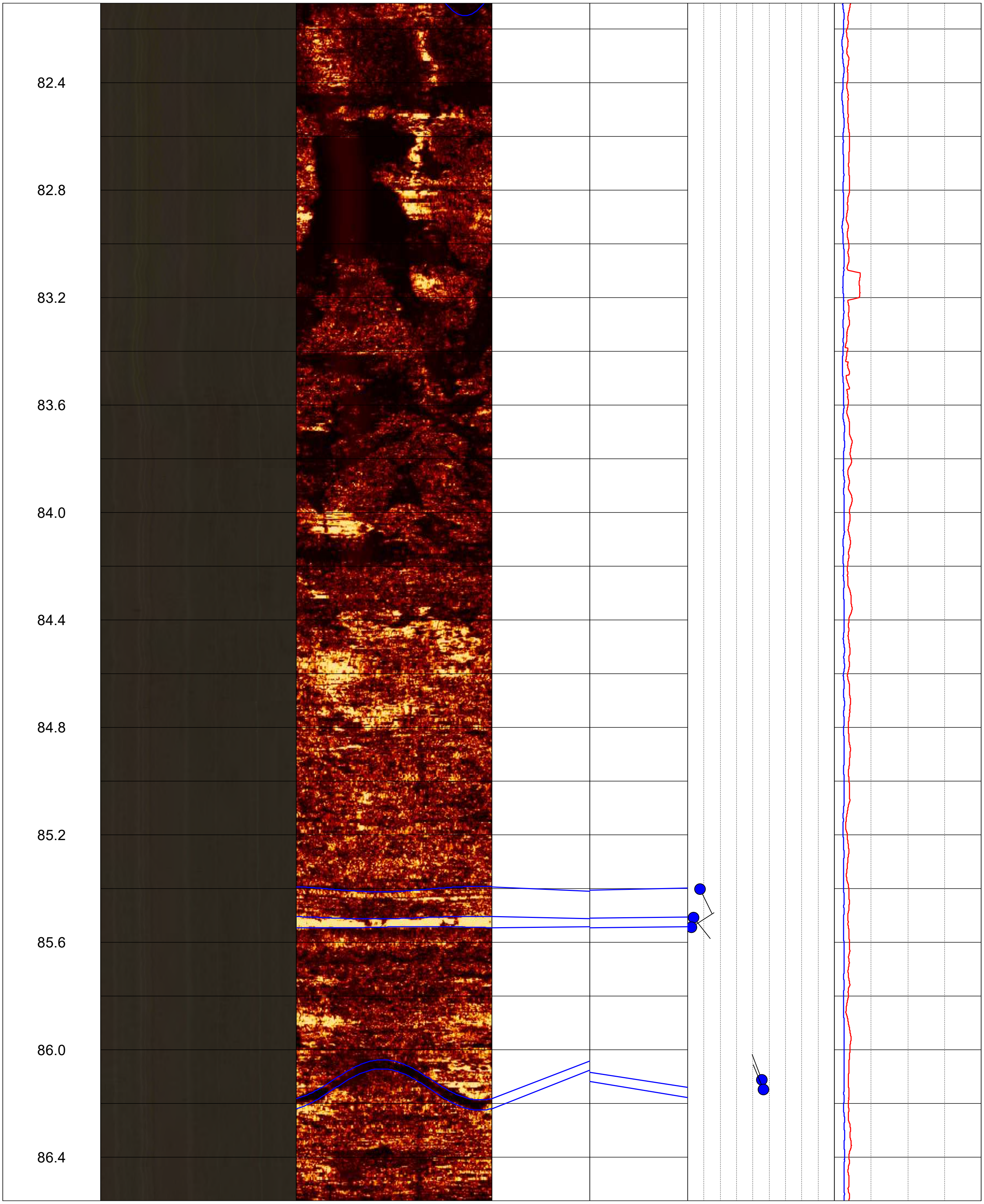
82.4
82.8
83.2
83.6
84.0
84.4
84.8
85.2
85.6
86.0
86.4

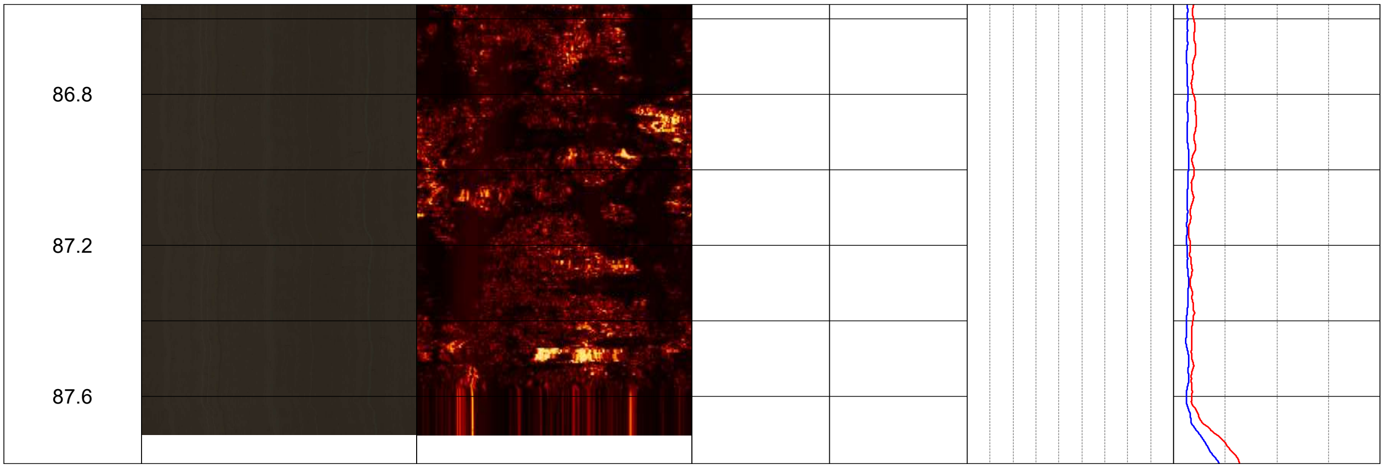
86.8
87.2
87.6

CERTIFICATE OF CONFORMITY

Certificate of Conformity

This is to certify that the following equipment conforms to the specification detailed below

ROBERTSON GEO®
Unlocking Your GeoData

Equipment type: High Resolution Optical Televiewer

RG Order No: ORD00000

Serial No: Hi-OPTV 11106

Comm. Type: Differential 4-Core/Coaxial

Quality Management System:
ISO 9001:2015
Certified by TÜV SÜD

Tested by: T Hamflett

Date: 16/07/19

Approved by:

[redacted]

Tim Hamflett | *Test Engineer*

Date: 16/07/19

TÜV SÜD ISO 9001
ISO 9001
Certified
Quality Management System
www.tuv-sud.com/ms-cert

Robertson Geologging Ltd.
Deganwy, Conwy, LL31 9PX,
United Kingdom
T: +44 (0) 1492 582 323
E: support@robertson-geo.com
www.robertson-geo.com

ROBERTSON GEO®
Unlocking Your GeoData

CERTIFICATE OF CONFORMITY

The probe detailed has been calibrated and then logged in the **ROBERTSON GEO** Test Borehole (Deganwy, UK). The resulting data falls within acceptable tolerances and meets all test criteria.

ROBERTSON GEO
Unlocking Your GeoData

Main Pass: 70-40m
Repeat Pass: 70-40m

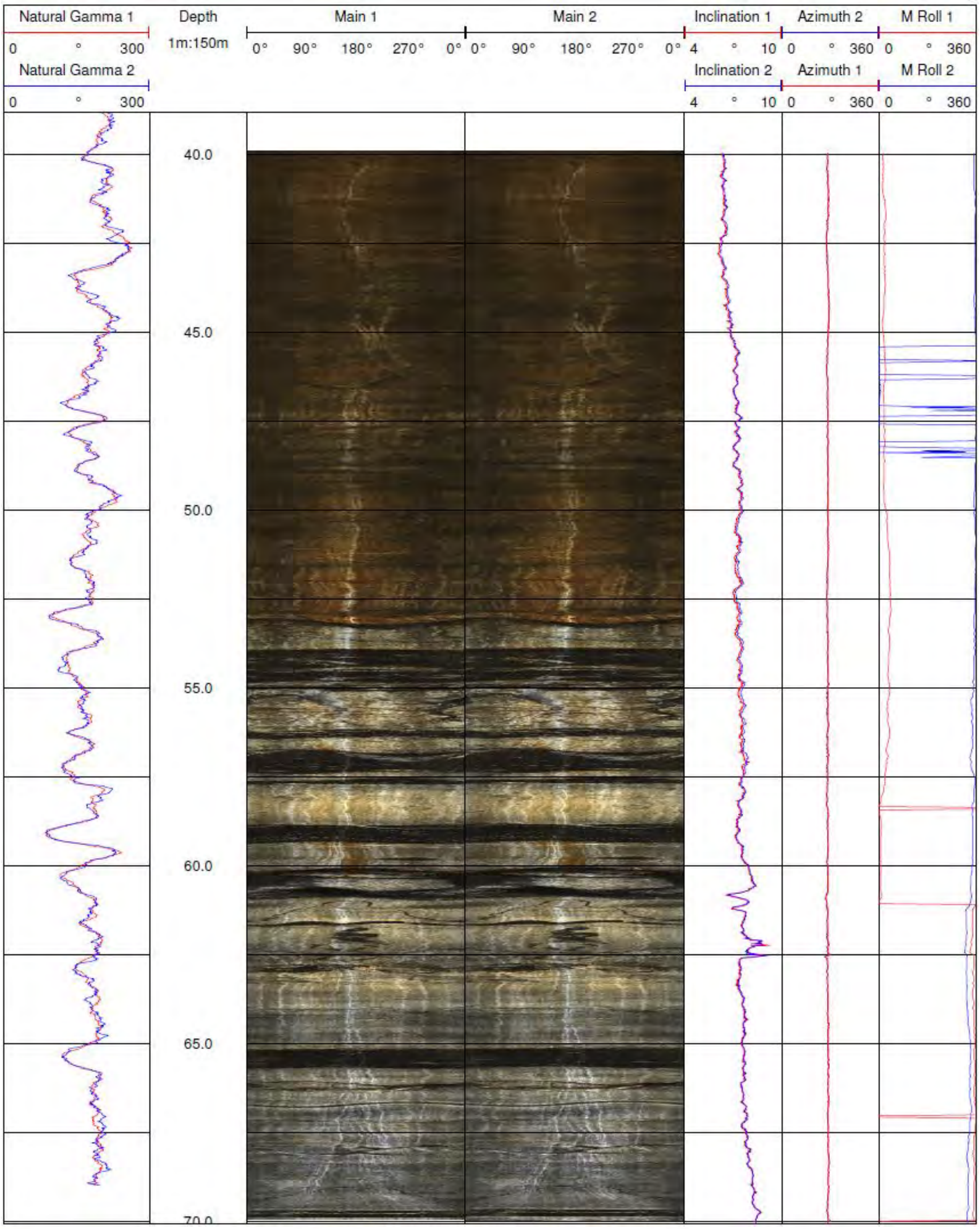

ISO 9001
Certified
Quality Management System
www.tuv-sud.com/ms-cert

Robertson Geologging Ltd.
Deganwy, Conwy, LL31 9PX,
United Kingdom
T: +44 (0) 1492 582 323
E: growlands@robertson-geo.com
www.robertson-geo.com

ROBERTSON GEO
Unlocking Your GeoData

CERTIFICATE OF CONFORMITY

Certificate of Conformity

This is to certify that the following equipment conforms to the specification detailed below

ROBERTSON GEO
Unlocking Your GeoData

Equipment type: High Resolution Acoustic Televiewer

RG Order No: ORD00000

Serial No: HiRAT 8237

Comm. Type: Standard 4-Core

Quality Management System:
ISO 9001:2015
Certified by TÜV SÜD

Tested by: T Hamflett

Date: 16/07/19

Approved by:

[redacted]

Tim Hamflett | *Test Engineer*

Date: 16/07/19

ISO 9001
Certified
Quality Management System
www.tuv-sud.com/ms-cert

Robertson Geologging Ltd.
Deganwy, Conwy, LL31 9PX,
United Kingdom
T: +44 (0) 1492 582 323
E: support@robertson-geo.com
www.robertson-geo.com

ROBERTSON GEO
Unlocking Your GeoData

CERTIFICATE OF CONFORMITY

The probe detailed has been calibrated and then logged in the **ROBERTSON GEO** Test Borehole (Deganwy, UK). The resulting data falls within acceptable tolerances and meets all test criteria.

ROBERTSON GEO®
Unlocking Your GeoData

Main Pass: 70-40m
Repeat Pass: 70-40m

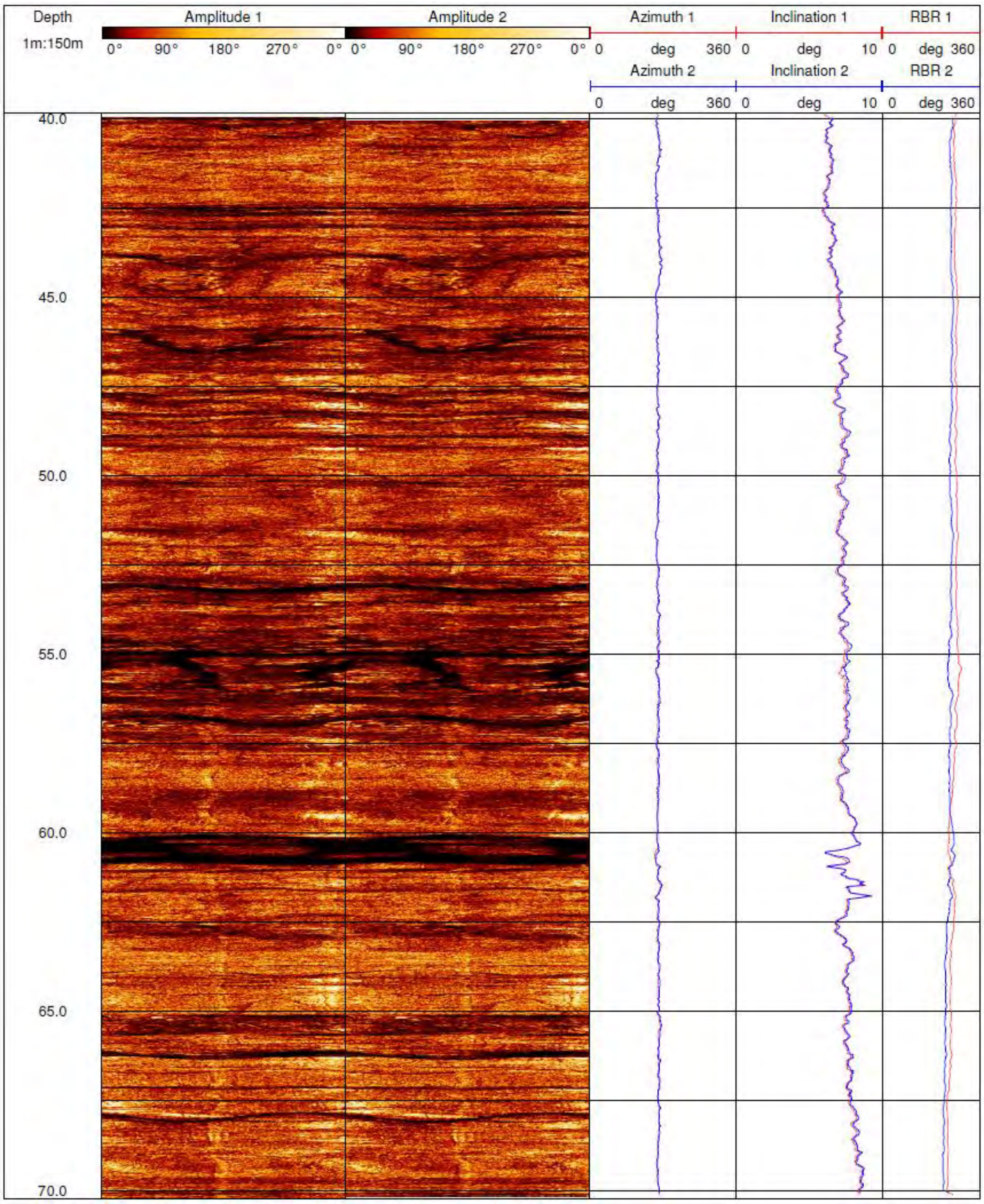

ISO 9001
Certified
Quality Management System
www.tuv-sud.com/ms-cert

Robertson Geologging Ltd.
Deganwy, Conwy, LL31 9PX,
United Kingdom
T: +44 (0) 1492 582 323
E: growlands@robertson-geo.com
www.robertson-geo.com

ROBERTSON GEO®
Unlocking Your GeoData

APPENDIX B

B2 SURFACE GEOPHYSICS

GEOPHYSICAL SURVEY REPORT

Project

Bedrock mapping and sediment characterisation

Location

A417, Birdlip

Client

Geotechnical Engineering

Head Office
Unit 1
Link Trade Park
Penarth Road
Cardiff CF11 8TQ
United Kingdom

Telephone: +44 (0)2920 700127
www.terradat.co.uk

TERRA DAT
down to earth geophysics

Job Reference: 6466
Date: July 2019
Version: 1

GEOPHYSICAL SURVEY REPORT

Project

Bedrock mapping and sediment characterisation

Location

A417, Birdlip

Client

Geotechnical Engineering

Project Geophysicist: J Hamlyn PhD MSc BSc FGS [redacted]

A Lewis BEng(Hon) MSc [redacted]

Reviewer: S Hughes PhD BSc FGS [redacted]

Job Reference: 6466

Date: August 2019

CONTENTS

Figures

Appendices

1 EXECUTIVE SUMMARY

A trial geophysical survey was carried out as part of the ground investigation for proposed improvements to the A417 near the village of Birdlip, south of the existing road. The survey work was commissioned by Geotechnical Engineering (the Client). The fieldwork was carried out in over four days in 2 phases: on the 3rd and 4th June 2019, and subsequently on the 16th and 17th July 2019. The work was designed to complement the invasive and geotechnical investigation in providing detailed information on the geology and ground conditions adjacent to the existing A417, with particular concern regarding potential landslide / landslip zones.

The geophysical survey consisted of an integrated survey approach utilising electromagnetic ground conductivity measurements, five targeted electrical resistivity tomography (ERT) profiles and two seismic P and S-wave refraction and Multichannel Analysis of Surface Waves (MASW) profiles along selected resistivity lines.

The electromagnetic ground conductivity and inphase results have successfully shown the distribution of granular/rocky material and limestone blocks identified in borehole CP-212, believed to be valley side and escarpment erosion material that has migrated down-slope. It has also shown areas of conductive clay-rich ground in the shallow sub-surface towards the north and east of the survey area that may represent a slip surface. An unmapped buried linear service has also been identified traversing east-west in the north of the survey area.

The modelled resistivity sections have identified an upper resistive layer across most of the site believed to represent the historical landslip material up to ~10-12 m thick. The depth of this material correlates well with the conductivity survey showing the deepest deposits in the south of the site. The resistivity models show an underlying conductive clay-rich overburden and argillaceous Lias bedrock that may be of concern with regards to slip zones. The resistivity models indicate the bedrock itself has a highly variable composition indicative of differential weathering and varying clay and water content.

The P and S-wave refraction have identified distinct velocity layers to assist with the bulk characterization of the shallow subsurface. The shear wave refraction appears to have been the most successful technique to resolve compositional and/or density variations in the overburden and the highly weathered bedrock. The P-wave refraction has more generally identified the unconsolidated surface/near-surface materials and the deep relatively competent bedrock. The MASW appears to have shown changes in ground stiffness that correspond to different materials in the overburden and what is believed to be the highly weathered soft Lias rockhead.

It has also identified a velocity inversion layer in profile 5 that is likely to represent a less dense or more clayey material not measured by the other techniques and again may represent a potential slip layer for the denser body of granular/rocky material above.

2 INTRODUCTION

This report describes a trial geophysical survey that was carried out as part of the ground investigation for proposed improvements to the A417 near the village of Birdlip. The survey work was commissioned by Geotechnical Engineering (the Client). The fieldwork was carried out in over four days in 2 phases: on the 3rd and 4th June 2019, and subsequently on the 16th and 17th July 2019.

The work was designed to complement the invasive and geotechnical investigation in providing detailed information on the geology and ground conditions adjacent to the existing A417, with particular concern regarding potential landslide / landslip zones.

2.1 Site description and history

The site (centred on 392750E, 215600E) is located across a 3.5 ha grassy field to the north of the village of Birdlip. The area is surrounded by two sections of the existing A417, as the road turns southwards along Barrow Wake Ridge (see Plate 1). Topographically, the field dips to the north, the relief is quite variable due to historical landslips and creep. Superimposed on the topography are significant ridge and furrows which trend northwest-southeast. During data collection, two drill rigs were operating on-site, data could not be acquired at these locations, and the associated surface metals (vehicles and fencing) will have masked any immediately adjacent subsurface features.

Plate 1: A) *Site location, survey area highlighted with a red line.* ***B)*** *Site conditions, photo looking east from the western boundary showing the slope of the site towards the A417.*

2.2 Geological setting

The Client has provided several borehole logs located within the survey area. The intrusive investigation has logged highly variable material comprising clay, mudstone, siltstone and limestone of the Lias Group and Inferior Oolite. The BGS Geoindex shows the site is comprised of the Lias Group and Inferior Oolite Group with argillaceous (clay-rich) sedimentary rocks. The Birdlip Limestone creates the topographic ridge and some escarpment exposure to the south and east of the site, where limestone erosional material has originated, to form part of the historical landslide debris seen as hummocky ground within the survey area.

According to the British Geological Survey (BGS) Geoindex, there are no superficial deposits in the vicinity of the site. All material overlying the bedrock is therefore believed to be bedrock erosion material from steep slopes and escarpments that has been transported by weather processes and landslide, down the valley side, and is referred to in this report as "overburden".

2.3 Survey objectives

The primary objectives of the survey were to provide detailed information on the shallow ground composition and deeper bedrock geology to assist with the ground investigation of the proposed road scheme. Of particular interest for engineering a new road cutting, is areas of shallow geology that may support further landslide movement of the overburden.

2.4 Survey design

Given the scope of the survey objectives, it was decided to adopt an integrated survey approach utilising the following geophysical methods:

- **Ground Conductivity**: to provide a ground conductivity map to characterise shallow overburden deposits and identify preferential water pathways such as gravel channels and clay rich layers.

- **Resistivity Tomography**: to provide electrical cross-sections along selected survey profiles that allow identification of geological or hydrological boundaries. The location of these profiles was based on the findings of the ground conductivity survey.

- **P-wave Seismic Refraction**: to provide seismic velocity (V_p) model sections that indicate the thickness of overburden deposits and the depth to competent bedrock, in correlation with standard tables.

- **S-wave Seismic Refraction**: to provide seismic velocity (V_s) model sections that indicate the depth of uncompacted and compacted sediments, weathered rockhead and more competent (higher shear strength) bedrock.

- **MASW (Multichannel Analysis of Surface Waves)**: to derive shear velocity ('S-wave' or 'V_s') from rolling surface waves that are related to the stiffness of the ground material. This technique is also useful where velocity inversions in the ground layers may be encountered.

2.5 Quality control

The geophysical data sets were collected in line with normal operating procedures as outlined by the instrument manufacturer and TerraDat company policy. On completion of the survey, the data were downloaded from the survey instrument on to a computer and backed up appropriately. The acquired data set was initially checked for errors that may be caused by instrument noise, low batteries, positional discrepancies, etc. and any field notes are either written up or incorporated in the initial data processing stage. The data set is then processed using the standard processing routines and once completed; the resulting plots are subject to peer review to ensure the integrity of the interpretation. Our quality control standards are BS EN ISO 9001: 2015 certified.

3 SURVEY DESCRIPTION

The survey was carried out using the following geophysical methods:

- EM - Ground conductivity and inphase mapping
- Electrical Resistivity Tomography (ERT)
- P-wave seismic refraction (employs compressional waves)
- S-wave seismic refraction (employs shear waves)
- MASW (Multichannel Analysis of Surface Waves)

The extents of the EM survey and resistivity and seismic profiles are shown in Figure 1. The ground conductivity mapping was conducted using a traverse spacing of 5 m. Five Electrical Resistivity Tomography (ERT) profiles were then collected over areas of interest identified by the survey. Seismic data were then collected along two selected ERT profiles (ERT-2 and ERT-5) approximately orthogonal to each other to achieve good spatial coverage.

Background information for the survey methods is provided in the appendices, while a description of the actual survey work is provided in the sections below.

3.1 Survey layout and topographic survey

The ground conductivity data were acquired under the positional control of an EGNOS dGPS system. The electrode locations of the ERT profiles, the geophone locations of the seismic lines and metallic structures/obstructions were surveyed using a Topcon Network RTK system. All measurements were referenced to National Grid (OSTN02) using the Topcon network correction.

3.2 Ground conductivity mapping

An electromagnetic ground conductivity survey involves the transmission of an electromagnetic field into the subsurface and then recording the returning signal via a receiver in the same instrument. Data are acquired on a grid covering the area of interest, and a contoured plan of the variation in ground conductivity response across the site is produced. The presence of conductive materials in the subsurface such as clay, water, mudstone, ash, metal, rebar, leachate, etc. will be evident as regions of high values on the ground conductivity plan. Materials such as coarse-grained sediments, dry zones, and many bedrock types will appear as regions of low values.

3.2.1 *Electromagnetic survey - field activity*

The conductivity data were acquired using a multi-frequency *Geophex GEM-2* instrument (Plate 2), and data were acquired under the control of an EGNOS corrected dGPS (accuracy +/- 0.5m) at a nominal 0.25m interval along a series of parallel 5 m spaced survey lines. The instrument was primarily configured to investigate depths of up to 3-5 m below ground level. The sensor was mounted on a cart and pulled behind an ATV.

Plate 2: *Ground conductivity data collection method. Geophex GEM-2 instrument mounted on a bespoke cart which was pulled across the site using an ATV, under the control of a GPS system. Library Photo.*

3.2.2 Electromagnetic survey – data processing

The conductivity data were downloaded from the data logger and compiled using dedicated software *WINGEM-3*. Initial editing was then carried out to remove positional errors and rogue values. The data were then exported as an 'XYZ' file and translated into the OSGB36 Coordinate system using the OSTN02 transformation. The software program *OASIS MONTAJ* was used to compile, edit and manipulate the data to enhance any features of interest. The colour contour plots were then integrated with the base plan information and the resulting plans exported to *CORELDRAW* for final annotation.

3.3 Electrical Resistivity Tomography (ERT)

An ERT survey involves the injection of DC electrical current into the ground at various electrode locations along a profile line. An electrical cross-section of the subsurface is then derived from the recorded data. A diverse range of features such as clay-rich sediments, fracture zones, infilled solution features, bedrock structure and mineralisation can be imaged in cross-section using a resistivity survey. A feature may be targeted using resistivity tomography given sufficient electrical contrast with its surroundings. A description of the field activity is provided below, and some background information on the survey method is found in the Appendix.

3.3.1 ERT survey field activity

A 72-channel *IRIS Syscal* resistivity system (Plate 3) was used to acquire five profiles across the survey area. The ERT profiles were acquired with an electrode spacing of 3 m or 2.5 m using a standard Wenner-Schlumberger array. A summary of the ERT profiles is given in Table 1.

ERT Profile No.	Start (OSGB)		End (OSGB)		Length (m)	Electrode Spacing (m)	~ Depth of penetration (m)
	Easting	Northing	Easting	Northing			
Line 1	392862.91	215714.86	392661.94	215646.54	213	3	30
Line 2	392865.33	215678.13	392664.64	215609.35	213	3	30
Line 3	392864.00	215674.68	392752.34	215493.64	213	3	30
Line 4	392889.09	215622.43	392708.18	215510.54	213	3	30
Line 5	392782.27	215486.36	392694.08	215637.80	175	2.5	25

Table 1: *ERT profile summary*

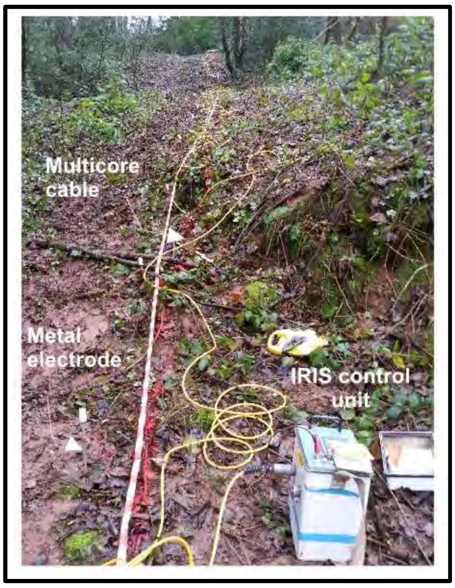

Plate 3: *Resistivity Tomography data collection. A 72 channel IRIS Syscal ERT system used to acquire five profiles across the site. Library Photo.*

3.3.2 *ERT survey data processing*

The data were processed using *Res2DInv* software to derive modelled electrical cross-sections of the subsurface. Elevation data were added to the models, using electrode positions surveyed using a TOPCON network RTK GPS. All topographic data were transformed into National Grid (OSGB36) using the OSTN02b transformation; elevations are given in m AOD. The ERT data was then exported into *Surfer 7* where it was gridded and presented as a 2D cross-sections of resistivity. These cross sections were then exported to *CorelDraw* for final annotation. All resistivity profiles are presented on the same colour scale and are not vertically exaggerated.

3.4 Seismic survey – P and S-wave refraction

3.4.1 Seismic survey field activity: P-wave refraction

P-wave seismic refraction data were acquired along two profile lines using a high precision 72 channel *GEODE* (Plate 4a) seismic system. To target the broad depth range, low frequency (4Hz) geophones were deployed at 2m intervals providing individual geophone spread lengths of 142m. The seismic wave was generated by a combination of sledgehammer striking a nylon plate and Seismic Impulse Device (SID) firing 12- and 8-gauge black powder cartridges (Plate 4b). To build up the refraction data set, seismic shots were taken at several positions along the geophone spread (usually every 6-12 geophones) and set distances beyond the geophone spread. For this particular survey, the 'offend' shots were limited by site constraints, but the maximum distance was 100 m.

Plate 4: *a) Field set-up and b) Seismic Impulse Source deployment (library picture).*

3.4.2 Seismic survey field activity: S-wave refraction (Shear)

S-wave seismic refraction data were also acquired using a 72 channel *GEODE* seismic system. Horizontally mounted geophones were deployed at 2m intervals producing individual geophone spread lengths of up to 142m. A weighted S-wave plate struck sideways with a sledgehammer was used as the energy source (Plate 5). At each shot location, the shot plate was aligned perpendicular to the profile line and subsequently struck on both ends to generate two sets of shear wave recordings that have opposite polarity. To build up the refraction data set, seismic shots were taken at several positions along the geophone spread (usually every 6-12 geophones) and set distances beyond the geophone spread. Due to the significant traffic noise affecting data quality, only 15 m off-ends were possible.

Plate 5: *S-wave source plate being struck (library photo)*

3.4.3 Seismic survey data processing: P and S-wave refraction

The data processing was carried out using *PICKWIN* and *PLOTREFA* software. The first stage involved the accurate determination of the first-arrival times of the seismic signal (time from the shot going off to each recording geophone) for every shot record using *PICKWIN*. Time-distance graphs showing the first-arrival times were then generated for each seismic line and analysed using *PLOTREFA* software to determine the number of seismic velocities layers. Modelled depth profiles for the observed seismic velocity layers were produced by a tomographic inversion procedure that was revised iteratively to develop a best-fit model.

The final output of a seismic refraction survey is a velocity model section of the subsurface based on an observed layer sequence. The measured velocities correspond to physical properties such as levels of compaction/saturation in the case of sediments and strength/rippability in the case of bedrock. A transitional velocity model will be considered if distinct layers are not expected, or velocity contrasts between layers are marginal. However, a layered model appears most appropriate to this site. The final sections were exported to *CORELDRAW* for annotation and presentation.

3.5 Seismic survey – MASW

Multichannel Analysis of Surface Waves (MASW) employs 'rolling' surface waves to derive shear velocity. This is achieved through analysis of the dispersion that occurs as surface wave energy propagates through the subsurface and separates into different frequencies travelling at different velocities depending on the stiffness of the sediments and/or rock encountered.

This technique utilises Rayleigh-type surface waves (normally considered noise in seismic refraction/reflection surveys and called "ground roll") recorded by multiple geophones deployed on an even spacing and connected to a common recording device (seismograph), as shown in Plate 6.

As the dispersion of the seismic wave can be dependent on the geology and ground conditions (i.e. variability, terrain, etc.), MASW profiles are usually limited to relatively flat areas or where the ground more homogenous.

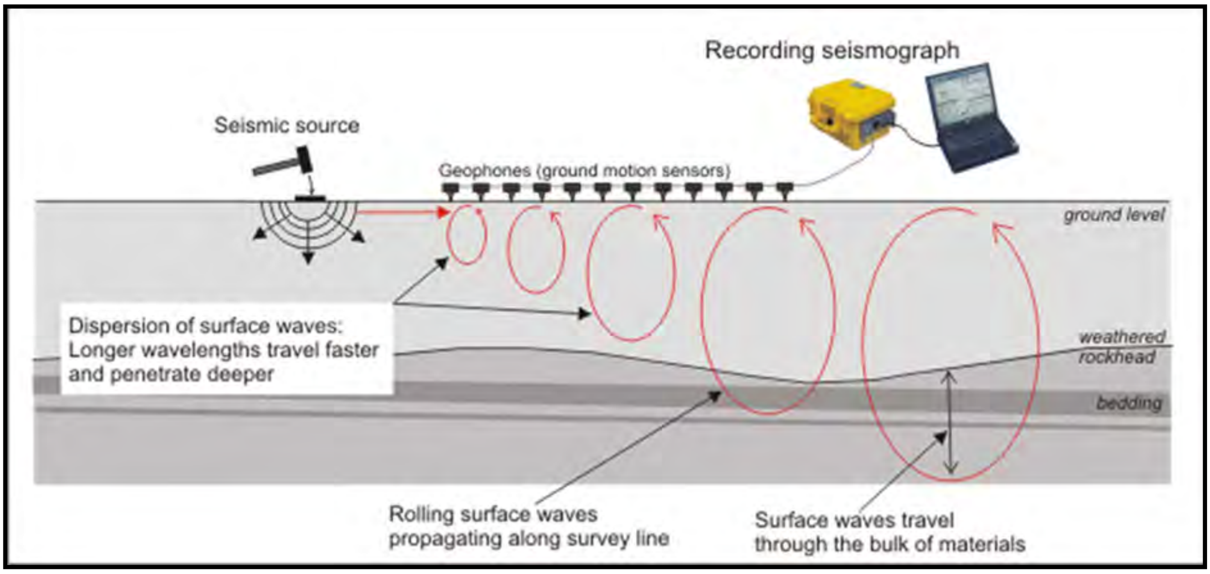

Plate 6: *MASW survey setup*

3.5.1 Seismic survey field activity: MASW

For this particular survey, the setup is very similar to the refraction set-up; however, instead of a discreet number of shot points, shots were acquired at every other geophone position along the profile. In this case, low frequency (4Hz) geophones were set at 2m intervals, and the data were acquired using the sledgehammer as the source. A one second record length was used to fully capture the frequency dispersion.

3.5.2 Seismic survey data processing - MASW

Analysis of surface waves recorded on multichannel shot records was carried out using SurfSeis software, which considers the dispersion properties of all types of waves (both body and surface waves) through a wave field transformation method. This directly converts the multichannel record into an image, where a dispersion pattern is recognised, and the necessary dispersion properties are extracted. These dispersion properties are used to generate modal dispersion curves that are subsequently inverted and used to produce the resultant shear-wave velocity (Vs) profile. The final velocity sections are created in SURFER then exported to CorelDraw for annotation and presentation.

4 RESULTS AND DISCUSSION

The results of the geophysical surveys are presented as a series of interpreted colour contour plots and scaled sections in Figures 1 - 6. A general description of the interpretation process is given below, followed by a summary of the findings in Sections 4.5 to 4.7.

4.1 Ground Conductivity

The results are presented as a colour contoured plot of ground conductivity (Figure 1a) and In-phase response (Figure 1b). Following a review of the electromagnetic data; it was decided only to consider the response of the 47,925 MHz frequency channel. A relative increase in conductivity values usually indicates a comparative increase in the clay/ash/water content, which could signify either a lateral change in lithology or a variation in bedrock depth. While the in-phase component (often referred to as 'metallic-response') is primarily influenced by the presence of metal or an increase in magnetic susceptibility, both of which can influence the ground conductivity plot. Extreme fluctuations in conductivity/in-phase values are usually indicative of instrument 'overload' due to high metal content. The interpretation of the conductivity data is based on both published electrical properties of typical sedimentary materials (Plate 7) and when available, correlation with on-site information.

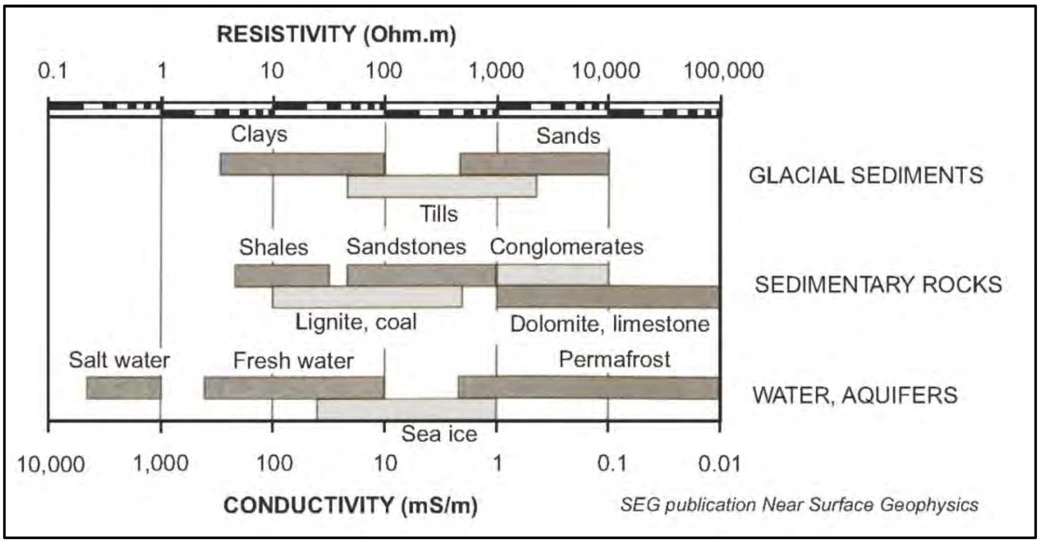

Plate 7: *Conductivity and resistivity values of common materials*

4.2 Resistivity tomography

The results of the resistivity survey are presented as a colour contoured scaled sections of the subsurface showing changes in resistivity in Figures 2 and 3, where blue colours represent low values, and red colours represent relatively high resistivity values. The vertical and horizontal axes display elevation and chainage along the profile line, respectively. The interpretation of the modelled resistivity sections is based on both published electrical properties of typical sub-surface materials (Plate 7) and when available, correlation with on-site information or observations. In principle, an increase in resistivity values usually indicates a relative decrease in the clay content or groundwater saturation. However, due to the non-uniqueness of the electrical properties (i.e. different material exhibiting same resistivity values), the final interpretation may be limited and may require addition calibration (i.e. drilling or other supplementary geophysical techniques).

The results of the ERT survey are discussed in the summary discussions, in conjunction with the results of the ground conductivity survey and seismic survey. To assist with the interpretation, the resistivity sections have been overlain with the interpreted seismic velocity boundaries where acquired.

4.3 Seismic Refraction – compressional (P) and shear (S) wave

Interpretation of the refraction sections is based on the widely understood and published velocities of typical sub-surface materials (provided in the appendices). It is beneficial to correlate model sections with on-site information/observations, but at the time of reporting, only limited borehole information was available.

4.3.1 Compressional (P) wave

Analysis of the P-wave refraction data has identified up to four distinct layers of contrasting velocity (V_p), and a typical description of each layer is given below and summarised in Table 2. It is worth noting that the seismic refraction section represents the measured bulk characteristics of the subsurface and in certain cases, it can prove difficult to correlate with point source data (boreholes/trial pits) where the underlying material is variable.

Layer	P-wave velocity	Sediment/Rock Description
P1 (pink)	300 m/s (low)	Thin dry loose surface soil, sand, gravel
P2 (orange)	~1100 m/s (medium low velocity)	Unconsolidated overburden material
P3 (light green)	1500-1800 m/s (medium velocity)	Compacted overburden material/ highly weathered Lias bedrock
P4 (Dark green)	2100 - 2300 m/s (medium high velocity)	Relatively competent Lias bedrock

Table 2: *A guide to the composition of the P-wave velocity layers identified*

Layers P1 has a low velocity that relates to loose, surface soil and uncompacted sands and gravels. Layer P2 typically reflects a relative increase in consolidation or compaction of the overburden material. Layer P3 can be more difficult to interpret as the overlap in velocities means that it can represent both overburden material (potentially wet, compact material) and weathered/weak/fractured bedrock. The most effective way to differentiate between sediment and rock type material is to consider the corresponding S-wave velocity, as discussed below. Layer P4 represents the highest (and deepest) velocity unit and is likely to reflect a more competent boundary within the bedrock strata.

4.3.2 Shear (S) wave

By carrying out an analysis of the S-wave refraction data, four distinct layers of contrasting velocity (V_s) have been identified and summarised in Table 3. They are characterised by their correlation with standard tables (see appendices).

In general, the shear-wave velocity (V_s) is much more sensitive than the P-wave velocity (V_p), where the ground becomes abruptly stiffer due to increases in rock strength. For this reason, it is possible to use the V_s to distinguish between sediments and 'rock' (i.e. cemented) material, which is particularly useful for grading the P-wave layer P3. A further advantage of shear waves is that they are unaffected by the groundwater table.

Layer	S-wave velocity	Sediment/Rock Description
S1	<100 m/s	Soft soils and loose sand and gravels
S2	190 - 230 m/s	Very weak, uncompacted overburden material
S3	440 – 510 m/s	Dense overburden, highly weathered bedrock
S4	620 - 730 m/s	Very dense overburden, very weak bedrock

Table 3: *A guide to the composition of the S-wave velocity layers identified*

When comparing the resulting P-wave and S-wave velocity sections, there is a rough 'rule of thumb' with regards to the ratio of the velocities. For unconsolidated sediment, V_p/V_s is usually between 4.0 to 8.0, while for consolidated rocks, the V_p/V_s ratio can vary between 1.5 to 2.0. Even though these are accepted values, they can vary between sites depending on the geology and ground conditions.

When correlating between the respective P-wave and S-wave refraction boundaries, in some instances there can be discrepancies in observed depth values. This depends on the prevailing geology and can reflect different survey parameters (horizontal/vertical polarised S-waves, spacing, etc.), weathering profile (vertical and horizontal), lithology or bedding structure. It has been noted on some sites that the S-wave refractor appears to correlate with internal bedding units as opposed to the general rock mass.

4.4 MASW

The results of the MASW survey are presented as colour contoured S-wave velocity panels showing changes in velocity (i.e. ground stiffness) below the surface. The seismic signal frequency dispersion required for the MASW technique has yielded reliable results to a depth of approximately 12m bgl. The persistent traffic noise from the A417 and the limited power of a sledgehammer energy source meant lower frequency dispersions (giving an increased depth of investigation) suffered from a high signal to noise ratio and were not suitable for modelling. The MASW sections have been colour scaled from white to red, with red representing the highest velocity modelled. The uncoloured MASW contours have been superimposed on the shear wave refraction model for direct ease of comparison of the two similar techniques.

4.5 Summary Discussion - Electromagnetic Survey

Ground conductivity (Figure 1a)

The ground conductivity survey, in conjunction with the trial pit and borehole information, appears to have accurately mapped the variation in the composition of the shallow overburden at the site. High conductivity (low resistivity) shown by blue and green colours, indicates a high clay and or water content and is seen towards the north (downslope) and east edge of the field (F2). Smaller areas of conductive ground can also be seen on the west side of the survey area, notably (F2a). The data here may have been influenced by the field boundary and increased vegetation.

The low conductivity (orange and red colours) appear to have mapped the thicker deposits of granular or blocky material that is likely escarpment erosion material that has migrated downslope. The main area of low conductivity (red and dark red colours) form two areas within a broad resistive zone characterised by elevated hummocky topography in the south half of the site (F1). These have been shown by the resistivity tomography and borehole CP212 to be comprised of up to 15 m of sands and gravels and limestone blocks. A localised resistive zone exists to the northeast (F3), which correlates with shallow limestone recorded in TP-207.

The surface of the northern and central areas undulated significantly due to the large ridge and furrow features, as a result, north-west to south-east lineations transect the data (F4).

At the time of surveying, service plans were not available, and it was not thought that any services ran through the site. However, the linear zone of instrument overload which transects the north of the site from west to east is most likely related to a significant metallic buried service (F5).

Inphase response (Figure 1b)

The in-phase response has been significantly affected by the presence of surface metals and shallow metals, finding anomalously high zones adjacent to the drill rigs and over the suspected service (F5).

As the inphase response is sensitive to the most conductive material, it has highlighted the most clay-rich ground, seen as yellow and orange colours (F6). This corresponds to the more conductive zones shown in Figure 1a. and clearly defines the shallow clay-rich overburden. Most significantly is a north-south zone, trending down-slope in the east of the site, that joins a broad zone in the north traversing most of the way across the site to the west. A smaller area corresponding to (F2a) can also be seen in the southwest.

4.6 Summary Discussion - Electrical Resistivity Tomography

The ERT sections are presented in Figures 2 and 3, and each one exhibits a number of different features which appears to reflect the variable nature of the ground conditions recorded in the borehole logs. Typically, areas of high resistivity indicate the presence of dry, granular, clay-deficient overburden material or intact clay-deficient, relatively dry bedrock. Areas of low resistivity indicate the presence of clay-rich material (including materials derived from weathering processes) and/or the presence of moisture. Zones of intermediate resistivity can represent transitional phases between these conditions.

The northern profiles (ERT 1 and 2) are characterised by two layers of different resistivity values; a more conductive (blue) material overlying a lower resistive layer (red). However, where profiles cross the south of the site (ERT 3, 4 and 5), an additional resistive layer is present at the surface that corresponds with feature (F1), observed in the ground conductivity data. The range of values recorded is limited, with a variation of approximately 300 Ohm.m across the site. Therefore, the ERT profiles are shown again in Figure 4, on a simplified colour scale to enhance the most significant changes in resistivity.

ERT1

ERT profile 1 appears to show a broad zone of conductive material within the central area of the section, with more resistive and variable material at each end. However, as this profile overlies the previously unknown buried service at an oblique angle, the west side of the profile may have been adversely affected, and interpretation of the conductive zone must be treated with caution. Shallower clay-rich ground can be seen between chainage ~50 m and 90 m.

ERT2

ERT profile 2 is characterised by 2 layers of significantly different resistivities: a layer of generally conductive material overlying a more resistive unit. The upper conductive layer has zones of more resistive material within it indicative of patches of granular sands and gravels in the overburden. The more laterally consistent conductive material (blue colours) may act as a slip zone where potentially wet clay-rich material would have a low friction surface for material to ride on top. The deeper resistive unit has high lateral variability and values within this zone vary from 30 to 300 Ohm.m. These variations reflect changes in bedrock composition assuming it is the bedrock unit, and indicate drier and/or more competent rock in contrast to more weathered or wet rock. There may also be an additional subvertical conductive feature which may relate to a change in lithology, differential weathering or a structural feature. At the far east end of the profile, chainage 0 m to 22 m, the edge of a resistive zone has been mapped that corresponds with ground conductivity anomaly (F3) and with shallow limestone mapped in Trial pit-207.

ERT3

The 2-layer scenario observed in ERT2 also exists to the northeast of profile ERT 3. However, to the south-west (between chainage 80 m to 210 m), there is an additional upper resistive zone above the conductive unit, creating a 3-layer scenario in the south of the site. This upper resistive zone extends to ~15 m bgl. in some areas and appears to be relatively homogeneous. This layer shows good correlation with the broad resistive zone observed in the conductivity data (F1) and correlates with the CP-212 showing it to be comprised of up to 15 m of sands and gravels and limestone blocks believed to be historical land-slide debris. The northeast end of the profile starts in the same area as ERT2 and has mapped the edge of the same resistive zone of shallow limestone blocks.

ERT4

ERT4 correlates well with ERT3 showing three distinct layers of resistivity values between chainage 70 m to 210 m. The section then becomes the 2-layer case between 0 m to 70 m. The variable lower resistivity unit shows a range of values from 30 to ~300 Ohm.m, an additional subvertical conductive feature bisects the unit at a chainage of 100 m, with similar characteristics to the feature observed in ERT2 and may be structurally related. The conductive unit (blue colours) appears to be is discreet zones ~2 to 5 m deep to the west and then deepens to 20 m bgl. in the east, where the overlying resistive unit is not observed. These conductive zones may be of wet clay-rich material that may act as slip zones for the overlying granular historical land-slide material.

ERT5

ERT5 was acquired with an electrode spacing of 2.5 m as opposed to 3 m, resulting in a slightly shallower depth of penetration of ~25 m, and as a result, the lower resistive zone may not have been well resolved. The upper resistive zone corresponding to ground conductivity feature (F1) is observed between chainage 0 m to 120 m and overlies the layer of more conductive material. A localised subvertical conductive feature exists at a chainage of ~60 m, and is related to either a change in lithology, differential weathering or a structural feature. Shallow clay rich ground can be seen towards the northwest end of the section that correlates with ERT2.

Simplified scale compilation plot

Figure 4 is a simplified representation of the different resistivity bodies identified, primarily showing the location and depth of the dry granular/rocky material believed to be slope and escarpment erosion material. This is located in the south of the survey area and manifests itself as hummocky ground at the surface. This can be seen to overlie clay-rich zones which may allow the migration of this material down the valley side in a northerly direction. The argillaceous nature of Lias bedrock has resistivity values indicative of very clay-rich material (<50 Ohm.m) and may also act as a slip plane, especially with the ingress of water potentially reaching an impermeable layer in the upper bedrock unit.

4.7 Summary Discussion - Seismic refraction and MASW

Seis-2 and ERT-2 (Figure 5)

Figure 5 shows the results of the seismic refraction and MASW surveys acquired along the same profile as ERT-2, with significant seismic boundaries overlain on the resistivity model.

Due to the apparent highly weak nature of the Lias bedrock in the area and the nature of the overburden, the shear wave refraction has appeared to better discern the geological units. The upper two layers S1 and S2, appear to represent the soils, granular material zones and uncompacted clay-rich overburden observed in ERT-2. Layer S3 with a velocity of V_s 441 m/s could represent dense overburden material or very soft rock. Unfortunately, there is no intrusive information close to the profile to prove the composition of S2 and S3, however, the resistivity and MASW both show a change in ground composition/structure that suggests a weak bedrock layer has been encountered. The change to higher resistivity values shown to be mudstone bedrock in ERT-4 and borehole CP-212 and the increase in ground stiffness shown in MASW indicate the likelihood of a highly weathered and variable composition Lias bedrock. Borehole DSRC207 is beyond the west end of the profile and appears to show an anomalously deep clay layer in this area of the site, although the siltstone shown in the base of this borehole may correlate with the lowest P and S wave boundaries indicating a more competent rock strata.

The profile traverses across the slope and generally shows laterally uniform layers that are sub-parallel to the ground surface. However, a slight deepening of the apparently weathered rockhead can be seen towards the west with a general shallow dip to the west of the marginally stronger bedrock layer S4.

The P-wave refraction survey has produced a four-layer model of increasing material compaction and competence. It correlates well with the shallow ERT-2 profile where P1 and P2 are indicative of loose soils and uncompacted granular material in the first few meters of ground, with the P2/P3 boundary representing the start of the clay-rich material shown in the resistivity model. Layer P3 encompasses most of S2, all of S3 and is deeper than S4 to the west showing all the corresponding shear wave layers have the same P-wave properties. A velocity of V_p 1550 m/s would usually relate to potentially wet, consolidated superficial material, but in this case the boundary between the overburden and the bedrock implied by the resistivity and shear wave surveys has not been observed, and therefore indicates extremely weak (slow velocity) Lias bedrock that is indiscernible from the overlying overburden material. Where the P4 layer deviates deeper that the S4 layer a more competent bedrock boundary has been observed. The deviation between the P and S-wave boundaries can be relatively common on sites where there are local variations in the weathering profile or subtle changes in lithology/groundwater. This forms a shallow 'bowl' profile with a maximum depth of ~30 m.

The MASW has worked relatively well at the site although the depth of penetration of the signal has probably been limited by the sledgehammer energy source and the high level of seismic noise generated by the continuous traffic on the nearby road. Good quality dispersion signal has been modelled to a depth of approximately 12 m bgl. and shows a two-layer case. This appears to correlate relatively well with the resistivity tomography to indicate the weak, poorly compacted overburden material, overlying the stiffer but highly weathered rock strata encountered at approximately 10 m bgl and deepening gently to the west.

Seis-5 and ERT-5 (Figure 6)

Figure 6 shows the results of the seismic refraction and MASW surveys acquired along the same profile as ERT-5, with significant seismic boundaries overlain on the resistivity model.

The shear wave model has given a four-layer case with S1 representing a very thin layer of loose surface soils. The S2 layer with a velocity of V_s 226 m/s represents uncompacted material that only forms a thin layer for the majority of the section, above the granular/rocky material shown in the ground conductivity and resistivity surveys. The S2 layer thickens rapidly between chainage 0 m to 40 m that correlates with the clay-rich conductive material in ERT-5 and observed in ERT-2. This supports the conclusion that a deeper zone of very weak clay-rich ground is situated in this part of the site.

The S3 layer (V_s 510 m/s) represents compacted ground up-slope believed to be dense granular and blocky material from eroded slopes that forms topographic surface mounds in the south of the site. This layer deepens at chainage 70 m to a depth of over 20 m at the north end of the profile. The MASW survey shows a change in ground stiffness at ~14 m bgl. that may represent the top of the weak bedrock, and the lower S3 boundary passes through this MASW boundary probably following a marginally more competent bedrock composition. The S4 layer shows the relatively more competent bedrock but with a velocity of V_s 625 m/s, is still a very soft rock composition.

The P-wave refraction has produced a four-layer model with relatively consistent layer thickness indicative of the main material strength changes with depth. The P1 and P2 layers are indicative of the loose soils and uncompacted granular material up to 5 m bgl. The P2/P3 boundary represents a change to more consolidated blocky material up-slope and the clay-rich layer shown in the north of the resistivity model (ERT-5 chainage 170 m to 135 m). Layer P3 with a velocity of V_p 1760 m/s represents well-compacted material that appears to encompass the overburden of dense slip material and clays, as well as the weak Lias bedrock. Layer P4 represents the more competent bedrock at a depth of ~25 m bgl.

MASW-5 was more compromised by the traffic noise at the northern end of the profile than the MASW-2 profile due to its orientation towards the road. However, it has identified zones of variable ground stiffness to a depth of approximately 12 m bgl. and shows a three-layer case where a velocity inversion is present beneath the believed granular/rocky slip material. The upper-velocity structure correlates well with the interpreted resistivity model indicating compacted, rocky slip material up-slope changing to clay-rich, low-velocity material at the down-slope end of the profile. The velocity inversion can be seen in the model as a layer a few meters thick represented as light grey colours, beneath the compacted rocky surface material and overlying the change to much stiffer ground (orange/red colours) believed to be the upper surface of the highly weathered bedrock. This lower velocity layer may represent a slip-zone for the overlying granular/rocky material and leads into the weak clay-rich material found at the downslope end of the profile. This layer may warrant further investigation to ascertain its potential for allowing overburden movement.

5 CONCLUSIONS

- The geophysical surveys have provided a non-invasive means for investigating the subsurface with a high degree of spatial coverage using the electromagnetic survey technique and detailed profile cross-sections of ground composition using resistivity tomography and seismic refraction and MASW.

- The electromagnetic survey has produced ground conductivity and inphase plots that show the distribution of granular/rocky material and limestone blocks believed to have migrated down-slope from eroded steep valley sides to the south. It has also shown areas of conductive clay-rich ground in the shallow sub-surface towards the north and east of the survey area.

- The electromagnetic survey has identified a previously unmapped buried service shown as a linear feature of extreme response.

- The modelled resistivity sections were characterised by zones of contrasting resistivity values that reflect lithological, hydrogeological, structural and weathering variations within the sub-surface. The sections are characterised by an upper resistive layer where present believed to represent the valley side erosion material that has migrated downthe slope and shown in boreholes to comprise of sand, gravels and limestone blocks. The depth of this material correlates well with the conductivity survey showing the deepest deposits in the south of the site. This material overlies conductive clay-rich overburden and argillaceous Lias bedrock. The resistivity models indicate the bedrock itself has a highly variable composition indicative of differential weathering and varying clay and water content.

- The analysis of both the P and S-wave refraction data has identified distinct velocity layers that have provided detailed information to assist with the bulk characterization of the shallow subsurface. The seismic refraction data is of good quality, but the MASW has limited depth penetration due to high signal to noise ratio caused by the persistent traffic noise from the nearby A417. The shear wave refraction appears to have been the most successful technique to resolve variations in the overburden and the highly weathered bedrock. The P-wave has more generally identified the unconsolidated surface/near-surface materials and the deep relatively competent bedrock.

- The MASW appears to have shown what is believed to be the highly weathered rockhead as a rapid increase in ground stiffness even where the shear wave has not appeared to follow this boundary due to the rock and overburden having the same shear strength.

- With regards to investigating potential landslip hazards, the ground conductivity has identified shallow clay rich material towards the bottom of the slope and on the east side of the survey area. The resistivity survey has also highlighted shallow clay-rich ground and highly weathered bedrock seen as a conductive layer that may act as a slip plane. MASW-5 orientated down the slope, has shown a velocity inversion of weak material beneath the granular valley-erosion deposits that may also represent a potential slip zone.

- If any additional borehole data becomes available, it may be possible to extend further/refine the interpretation and calibrate the acquired datasets.

Disclaimer

This report represents an opinionated interpretation of the geophysical data. It is intended for guidance with follow-up invasive investigation. Features that do not produce measurable geophysical anomalies or are hidden by other features may remain undetected. Geophysical surveys complement invasive/destructive methods and provide a tool for investigating the subsurface; they do not produce data that can be taken to represent all of the ground conditions found within the surveyed area. Areas that have not been surveyed due to obstructed access or any other reason are excluded from the interpretation.

FIGURES

a) Ground Conductivity

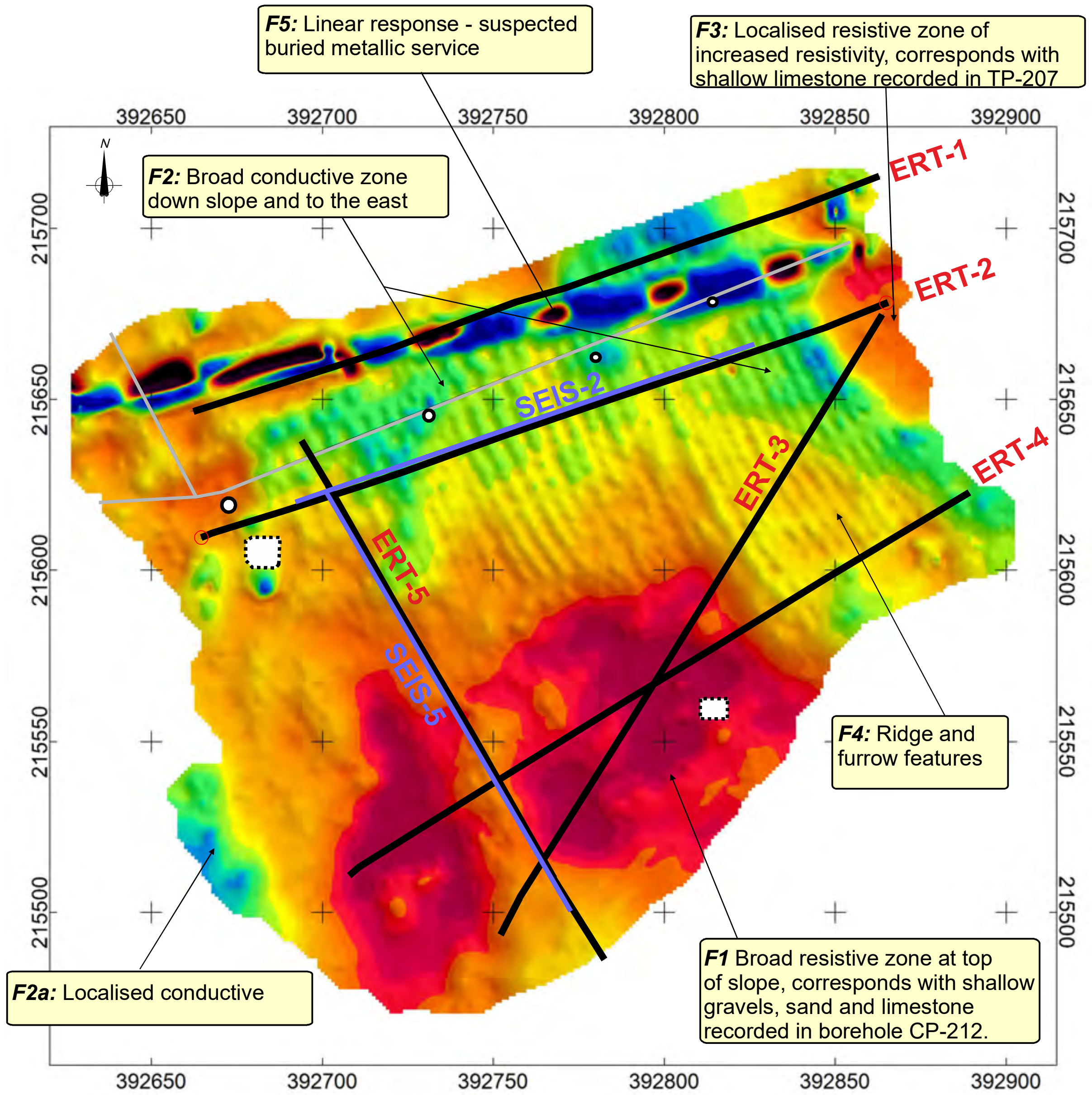

b) In-phase Response

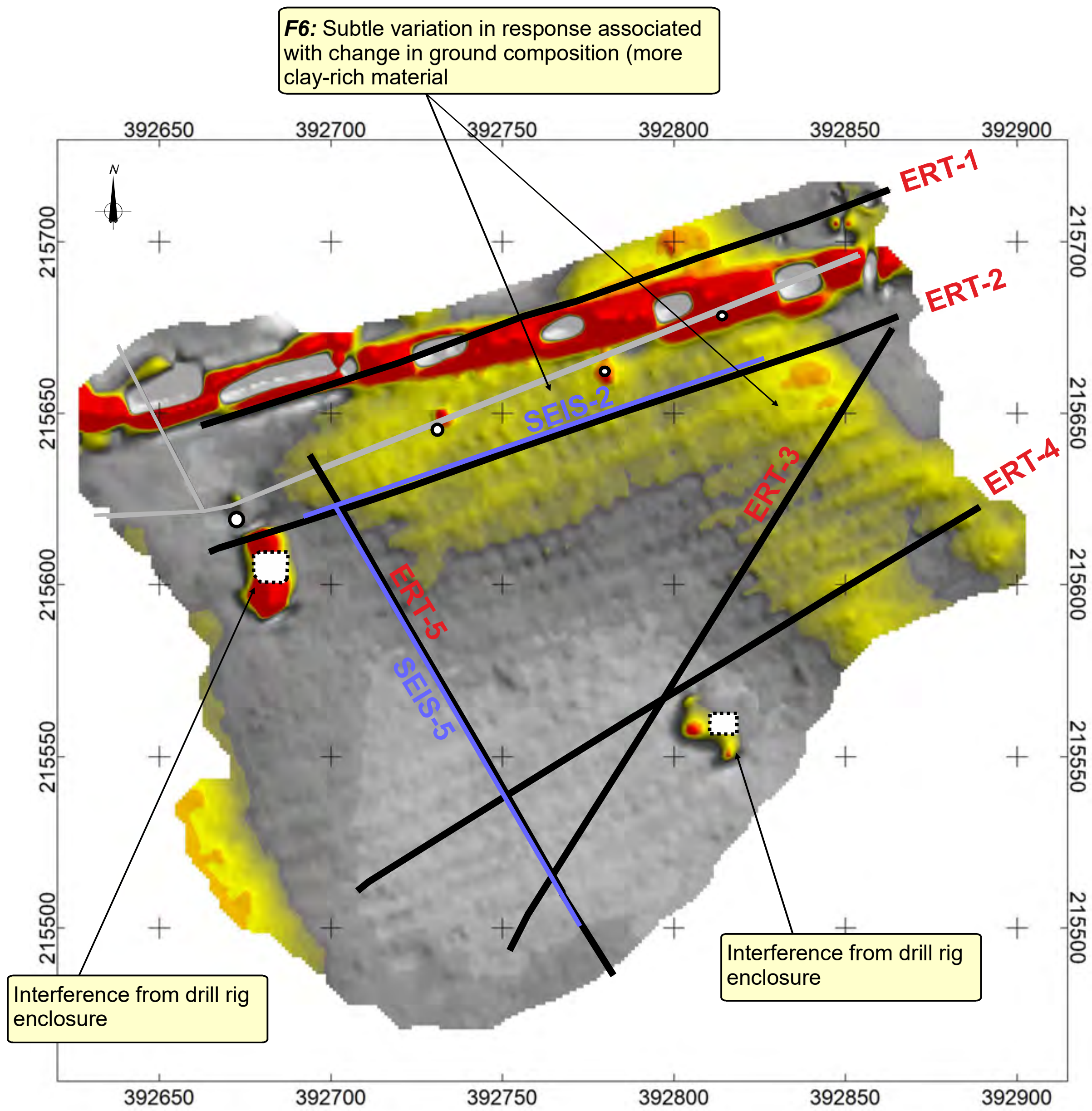

SATELLITE IMAGE

Google Earth *Not to Scale*

Approximate Site boundary

SCALE

1:2000

25 0 25 50

Metres

COLOUR SCALE

Electrical Conductivity (mS/m)

30 37 44 50 57 64 70 77 84 90 97 104 113 122

Increasing Conductivity

In-Phase Response (ppm)

-736 -479 -223 33 226 482 738 995 1251 1572

Increasing Response

KEY

Overhead power cables

ERT profiles

Locations of surface metals onsite (piles of metal fencing)

Location of intrusive data

TERRA DAT down to earth geophysics
Tel: +44 (0) 2920 700127
Web:www.terradat.co.uk
Email: web@terradat.co.uk

Title:

ELECTROMAGNETIC SURVEY RESULTS AND LOCATION OF RESISTIVITY AND SEISMIC PROFILES

Project:

A417 CRICKLEY HILL BIRDLIP

Scale: 1:2000 at A3	**FIGURE 1**
Drawn by/Ref: JH/6466/1	
Date: 19 JUNE 2019	

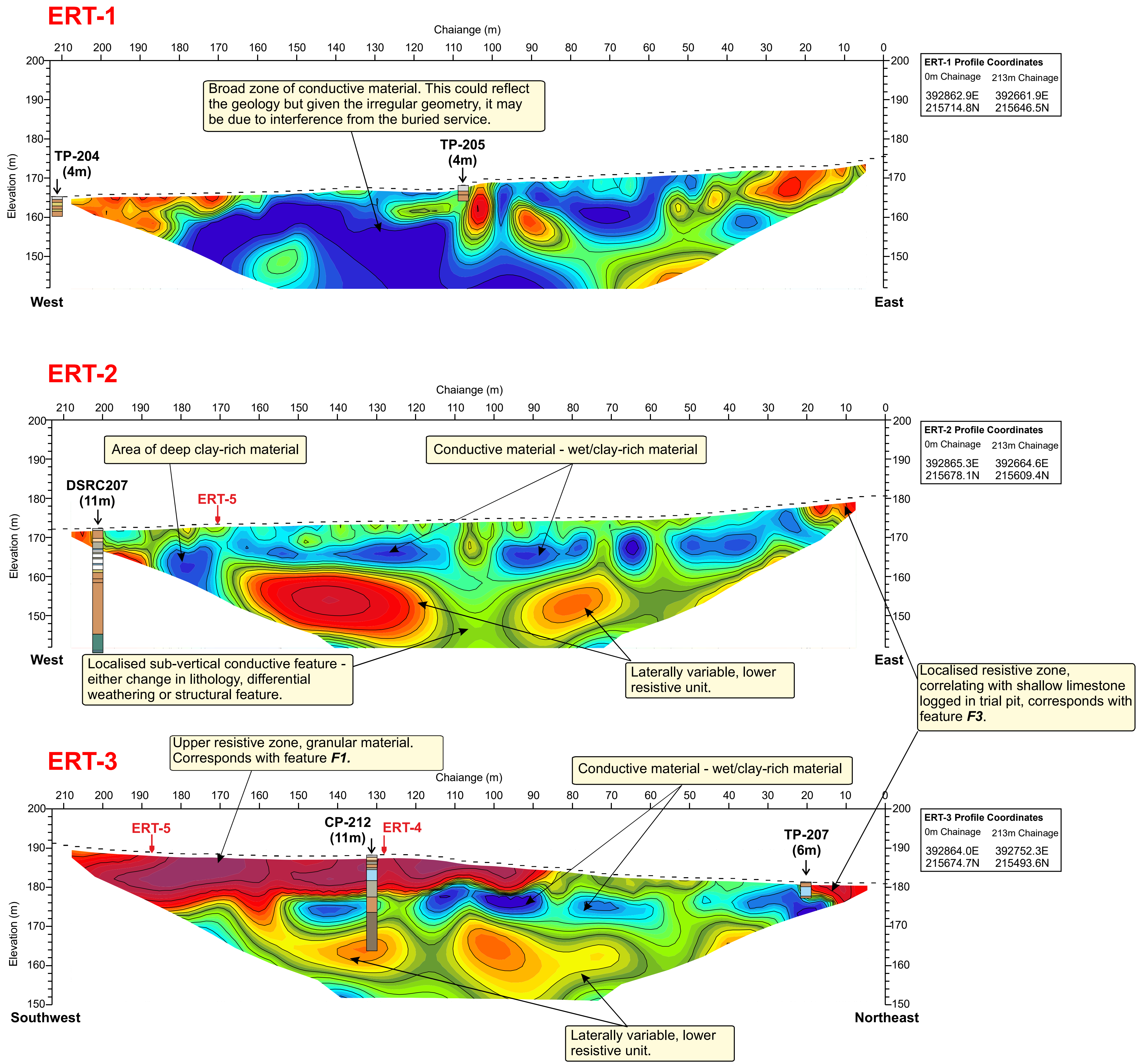

PROFILE LOCATIONS

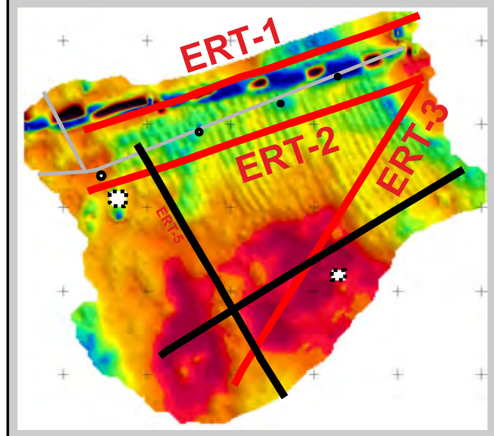

COLOUR SCALE

Electrical Resistvity (Ohm m)

9 19 24 28 33 40 51 90 302

Increasing Resistivity

BOREHOLE KEY

- Made ground
- Clay
- Silt
- Sand
- Gravel
- Sandstone
- Mudstone
- Siltstone
- Limestone
- Core loss

KEY

NOTES

TERRADAT down to earth geophysics

Tel: +44 (0) 2920 700127
Web:www.terradat.co.uk
Email: web@terradat.co.uk

Title: ELECTRICAL RESISTIVITY TOMOGRAPHY PROFILES 1 TO 3

Project: A417 CRICKLEY HILL BIRDLIP

Scale: 1:1000 at A3

Drawn by/Ref: JH/6466/2

Date: 19 JUNE 2019

FIGURE 2

PROFILE LOCATIONS

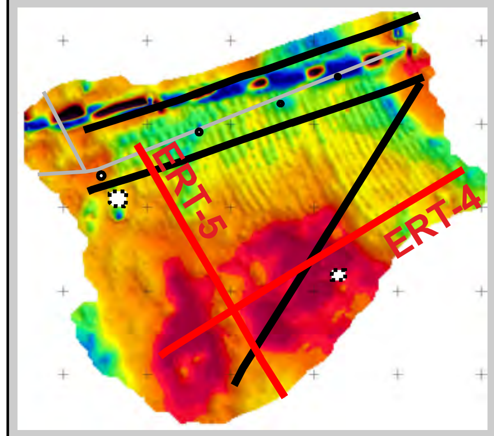

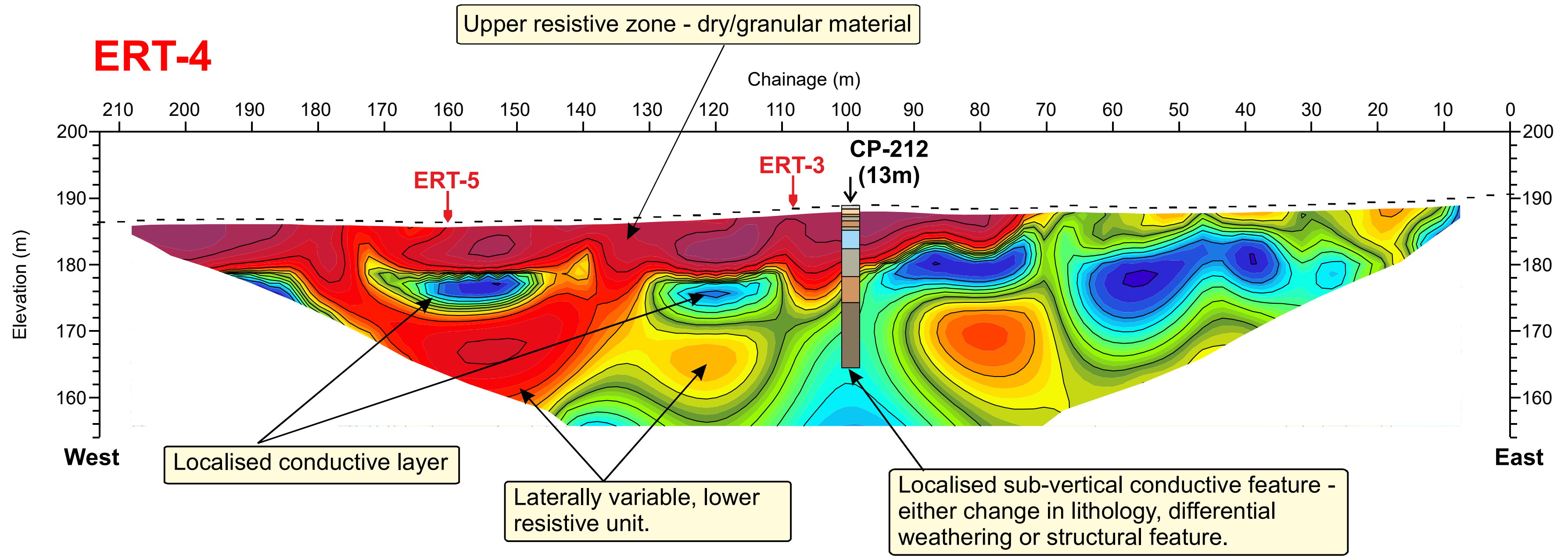

ERT-4 Profile Coordinates	
0m Chainage	213m Chainage
392889.1E 215622.4N	392708.2E 215510.5N

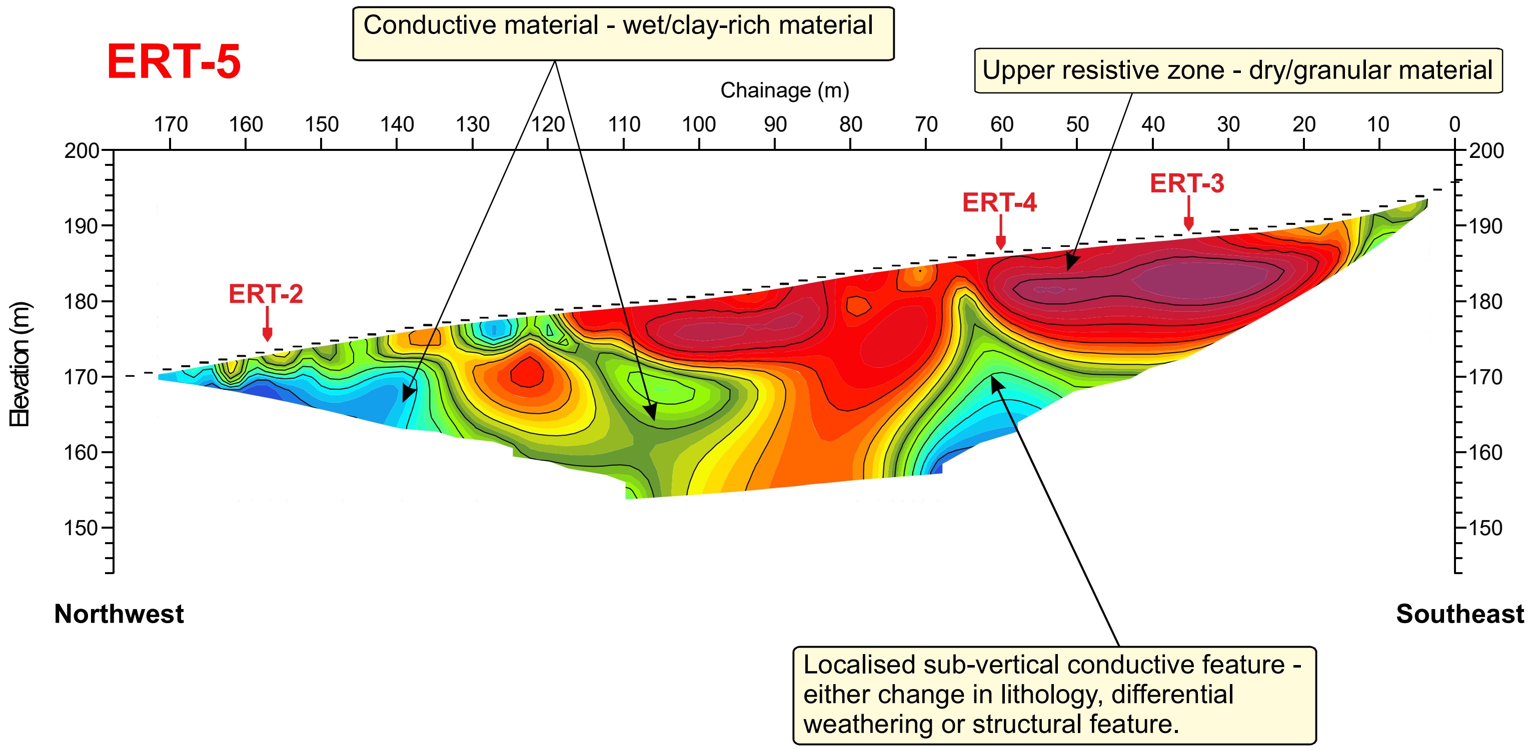

ERT-5 Profile Coordinates	
0m Chainage	175m Chainage
392782.3E 215486.4N	392694.1E 215637.8N

COLOUR SCALE

Electrical Resistivty (Ohm m)

9 19 24 28 33 40 51 90 302

Increasing Resistivity

BOREHOLE KEY

- Made ground
- Sandstone
- Clay
- Mudstone
- Silt
- Siltstone
- Sand
- Limestone
- Gravel
- Core loss

KEY

NOTES

TERRA DAT down to earth geophysics

Tel: +44 (0) 2920 700127
Web:www.terradat.co.uk
Email: web@terradat.co.uk

Title: ELECTRICAL RESISTIVITY TOMOGRAPHY PROFILES 4 AND 5

Project: A417 CRICKLEY HILL BIRDLIP

Scale: 1:1000 at A3

Drawn by/Ref: JH/6466/3

Date: 19 JUNE 2019

FIGURE 3

ERT-1

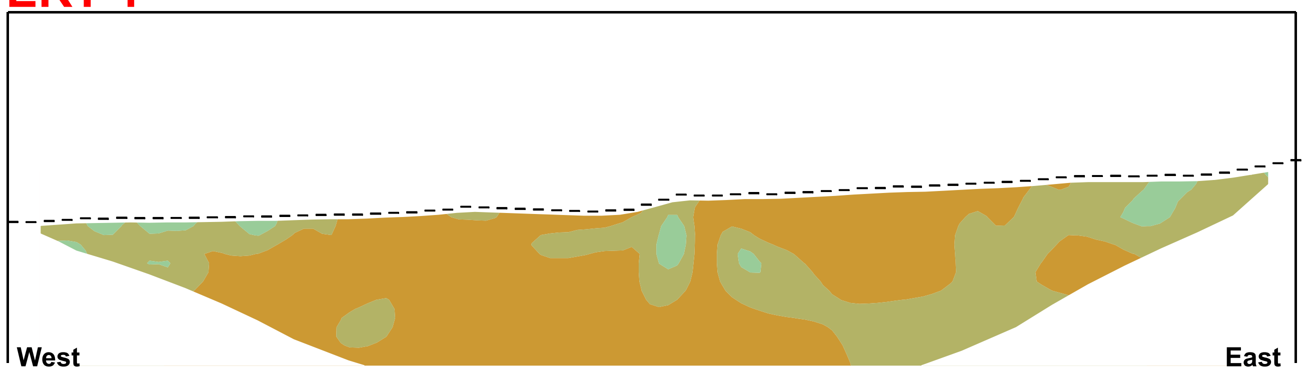

ERT-5

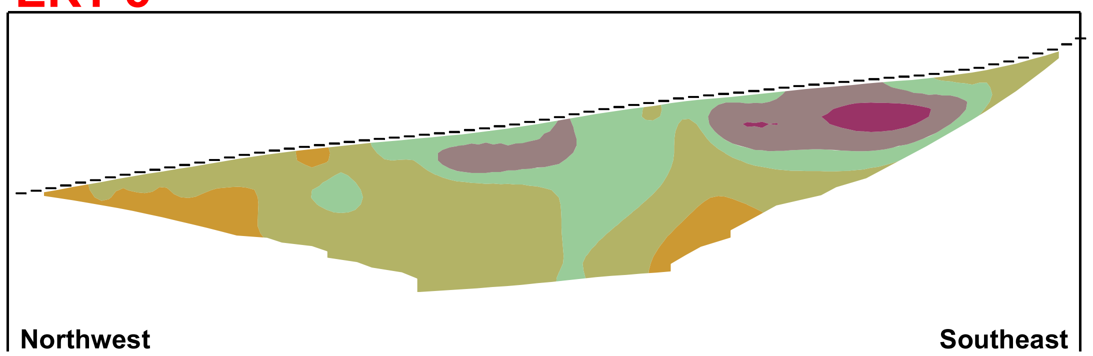

ERT-2

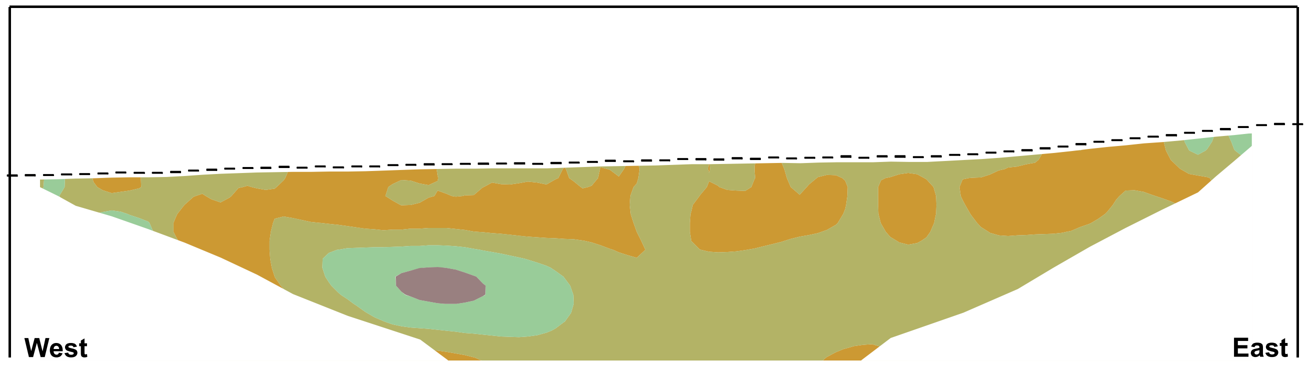

ERT-3

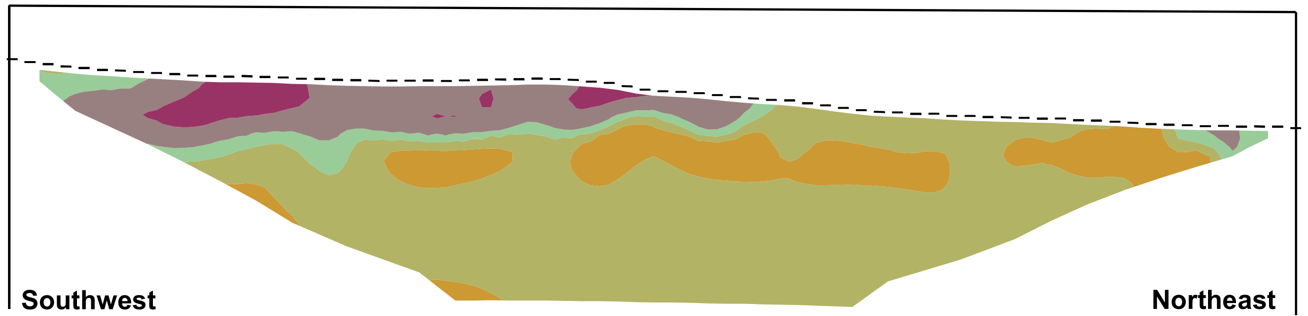

ERT-4

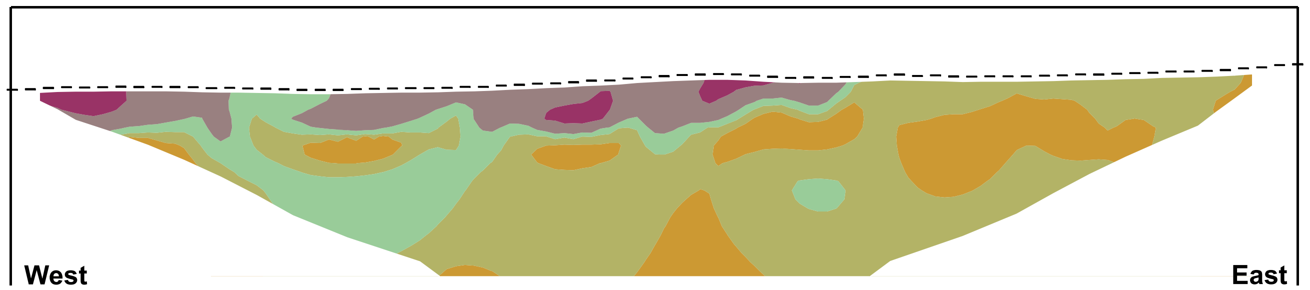

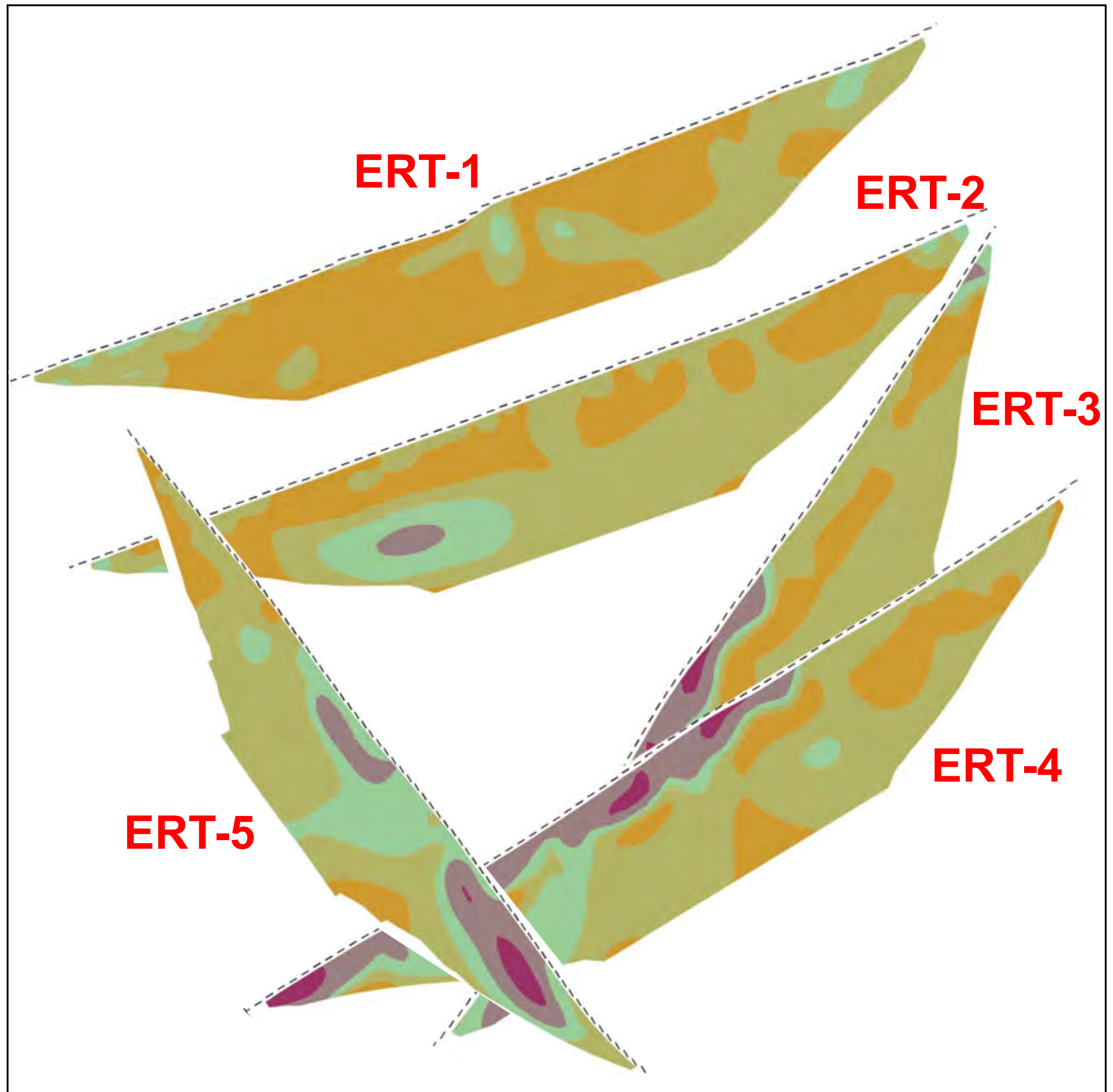

3D Representation

PROFILE LOCATIONS

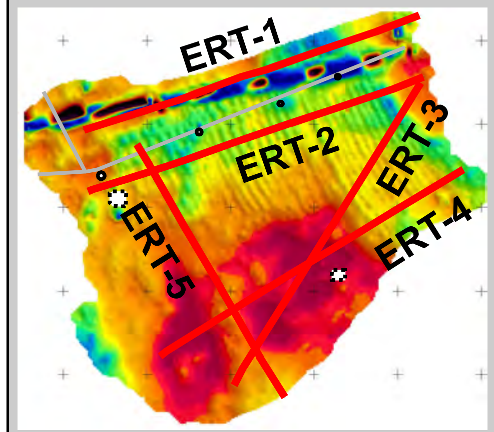

COLOUR SCALE

Electrical Resistvity (Ohm m)

Increasing Resistivity

KEY

NOTES

TERRA DAT down to earth geophysics
Tel: +44 (0) 2920 700127
Web:www.terradat.co.uk
Email: web@terradat.co.uk

Title: ELECTRICAL RESISTIVITY TOMOGRAPHY - SIMPLIFIED SCALE

Project: A417 CRICKLEY HILL BIRDLIP

Scale: 1:1250 at A3

Drawn by/Ref: JH/6466/4

Date: 19 JUNE 2019

FIGURE 4

ERT-2

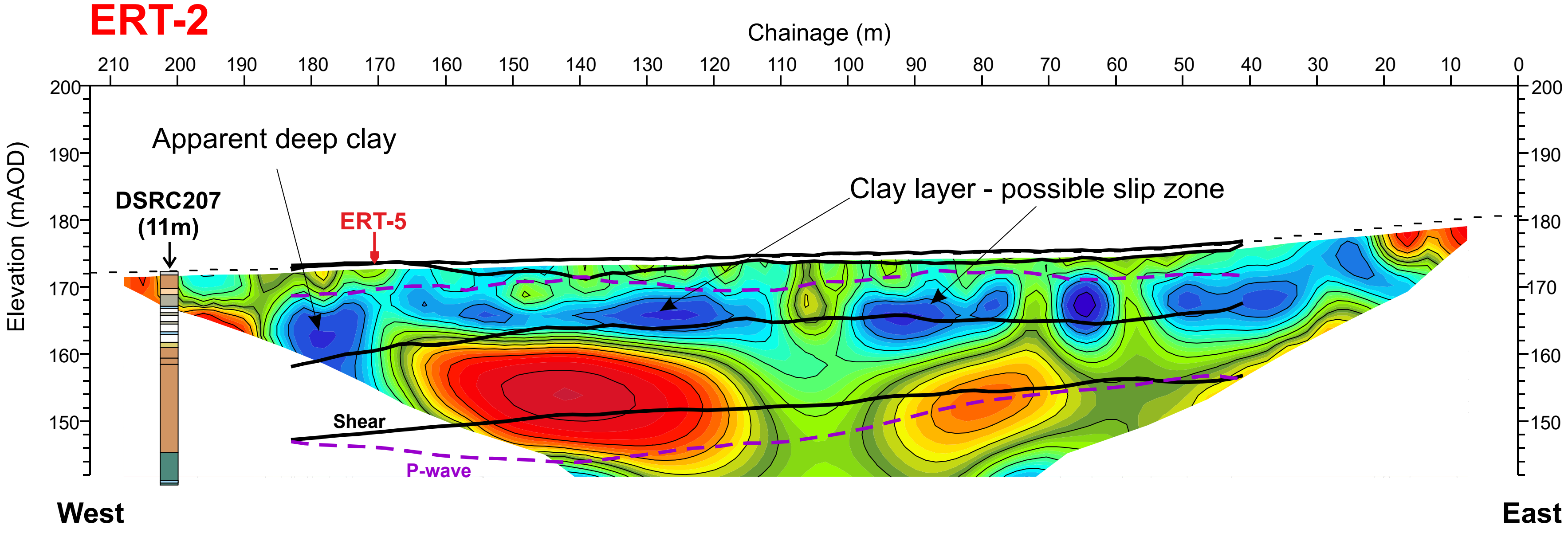

Cross Section Key

- S-wave refraction boundary (overlain on resistivity section) (overlain on masw section)
- P-wave refraction boundary (overlain on resistivity section)

Rock / Soil Description	S-wave velocity (m/s) Top 30m
Hard rock	> 1,500
Rock	760 - 1,500
Very dense soil / soft rock	360 - 760
Stiff soil	180 - 360
Soft soil	<180

from National Earthquake Hazard Reduction Prog.

Seis-2 Seismic shear wave refraction with MASW contours

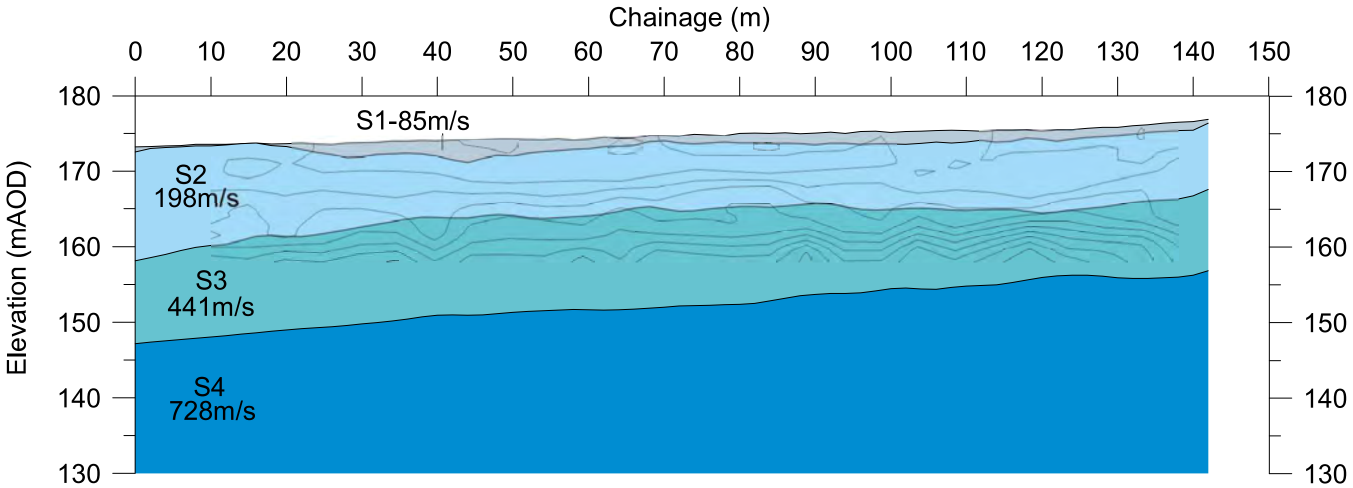

	S-wave seismic velocity	Description
S1	85 m/s	Dry, loose material - soil, uncompacted sand/gravel
S2	198 m/s	Uncompacted material - sands and gravels, escarpment erosion material and clay
S3	441 m/s	Likely bedrock lithology (based on CP212 bedrock depth) but needs proofing. Variable composition/ weathering shown in ERT-2
S4	728 m/s	Increased competence in bedrock possible change in lithology

MASW-2

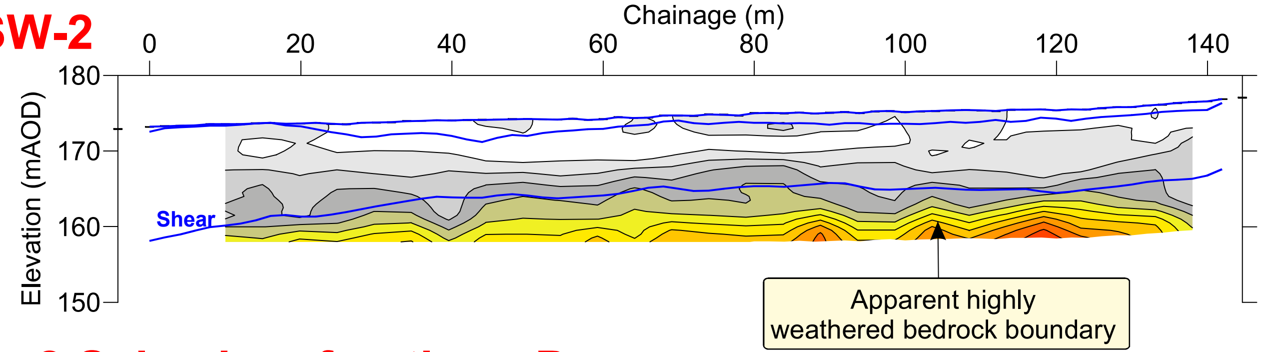

MASW-2 shows good quality results but with minimal penetration into the bedrock lithology. It has identified zones of variable compaction within the overburden material.
The MASW correlates well with the shear wave refraction showing unconsolidated material overlying what is believed to be weak bedrock, where the ground stiffness can be seen to increase significantly (yellow/red colors) at ~10m bgl. deepening slightly in the west

Seis-2 Seismic refraction - P-wave

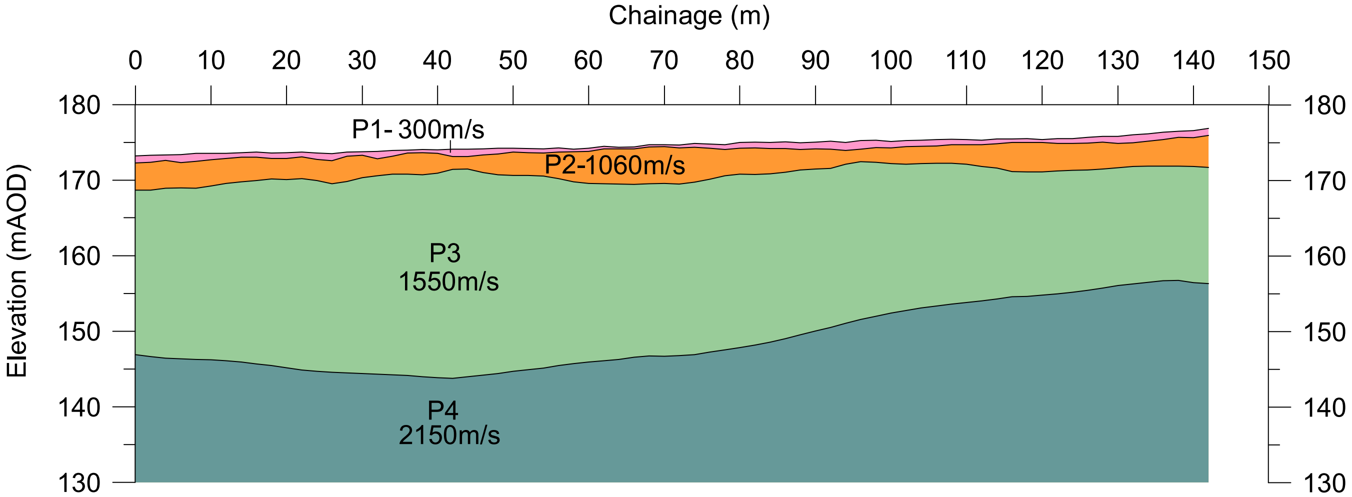

	P-wave seismic velocity	Description
P1	300 m/s	Dry, loose material - soil, uncompacted sand/gravel
P2	1060 m/s	Dry, unconsolidated material - predominantly sand and gravel or escarpment erosion with clay upper layer
P3	1550 m/s	Potentially wet, compacted material - clay/weathered bedrock and very weak bedrock
P4	2150 m/s	More competent rock - still relatively weak bedrock of mudstone and siltstone

PROFILE LOCATIONS

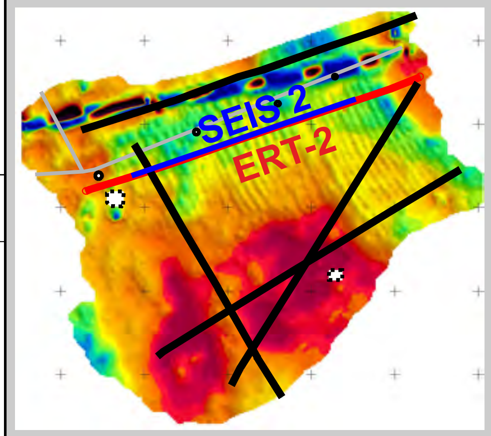

RESISTIVITY COLOR SCALE

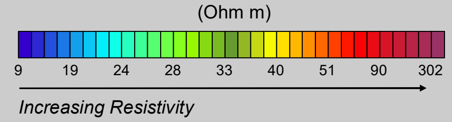

BOREHOLE KEY

- Made ground
- Sandstone
- Clay
- Mudstone
- Silt
- Siltstone
- Sand
- Limestone
- Gravel
- Core loss

MASW COLOR SCALE (m/s)

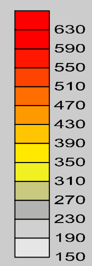

NOTES

TERRADAT down to earth geophysics
Tel: +44 (0) 2920 700127
Web:www.terradat.co.uk
Email: web@terradat.co.uk

Title: RESISTIVITY AND SEISMIC SURVEY RESULTS FOR PROFILE 2

Project: A417 CRICKLEY HILL BIRDLIP

Scale: 1:1000 at A3

Drawn by/Ref: AL/6466/5

Date: 31 JULY 2019

FIGURE 5

ERT-5

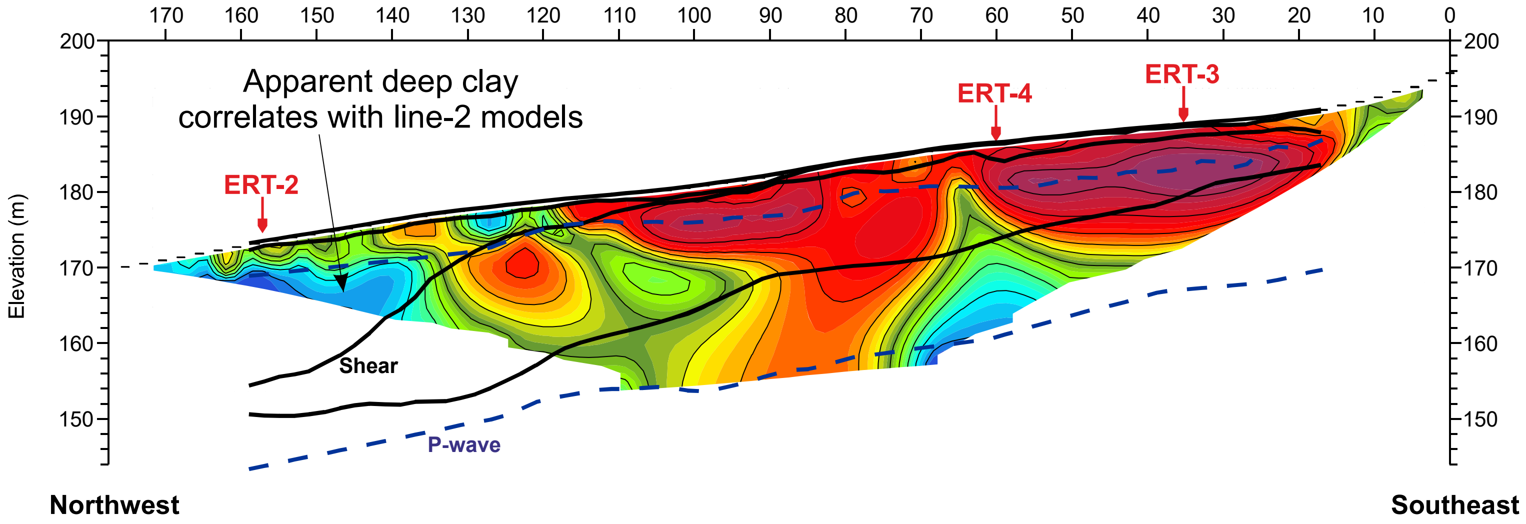

Seis-5 Seismic shear wave refraction with MASW contours

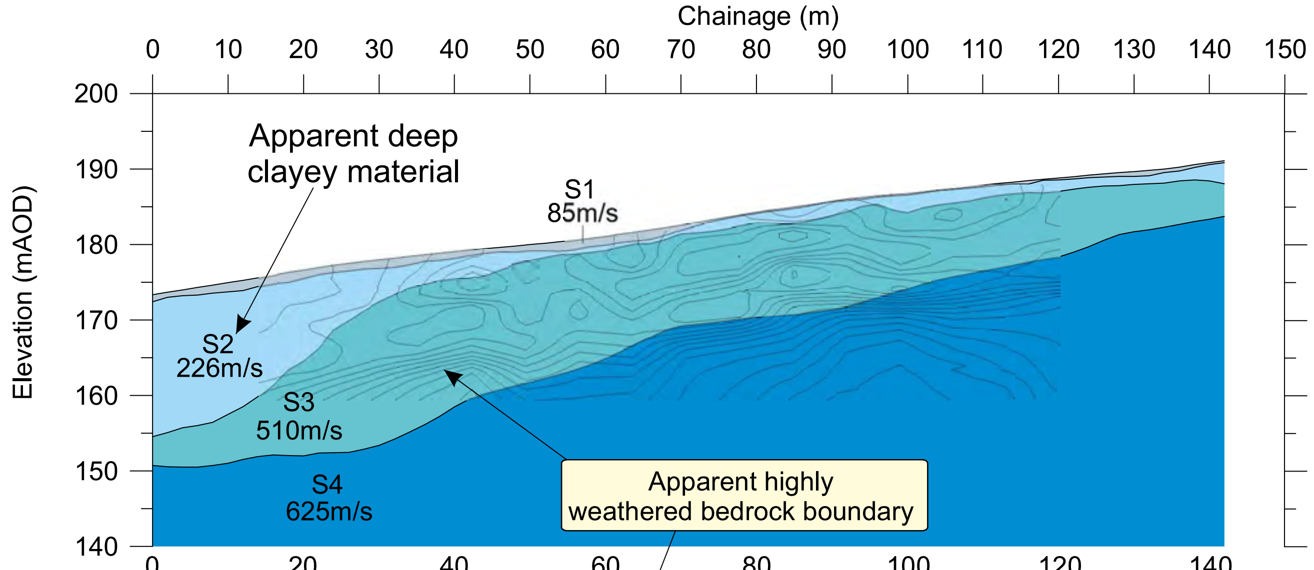

S-wave seismic velocity		Description
S1	85 m/s	Dry, loose material - soil, uncompacted sand/gravel
S2	226 m/s	Very weak material - likely clay rich overburden
S3	510 m/s	Compacted material that appears to represent the dry granular overburdon in the south (up slope topographic mounds) but may show a slightly more competent layer within the bedrock to the north with a highly weathered rockhead shown by stiffer material in the MASW survey.
S4	625 m/s	Increased competence in bedrock possible change in lithology

MASW-5

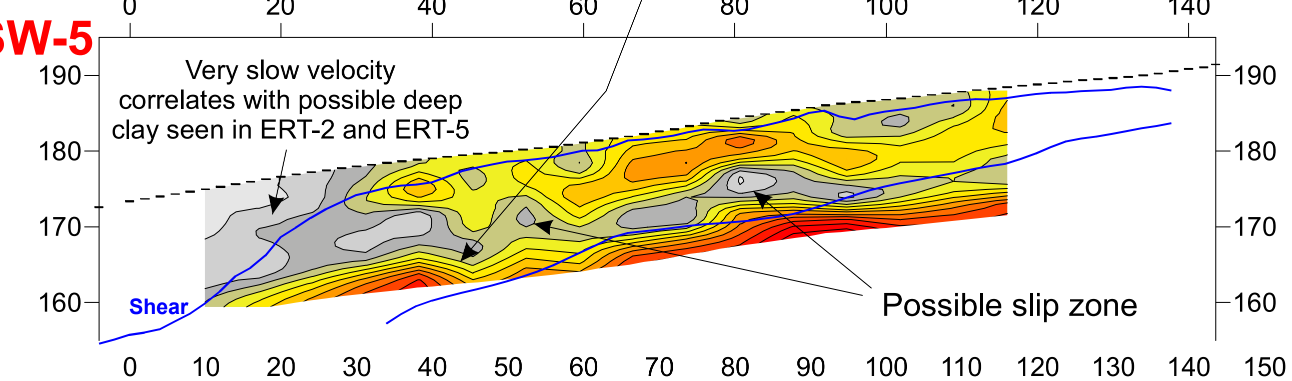

MASW-5 quality was compromised by traffic noise. The section represents the lowest error model. The model has identified zones of variable compaction within the overburden material, but with minimal penetration into the bedrock lithology. Of particular interest is the measured velocity inversion (grey colors beneath the yellow/orange colors), that shows a weaker layer, possibly overlying the bedrock, that could represent a possible slip zone.
The MASW correlates relatively well with the shear wave refraction model to the south showing unconsolidated material overlying what is believed to be weak bedrock. The MASW shows the more compacted material continues into the S3 layer possibly suggesting a highly weathered rockhead boundary

Seis-5 Seismic refraction (P-wave)

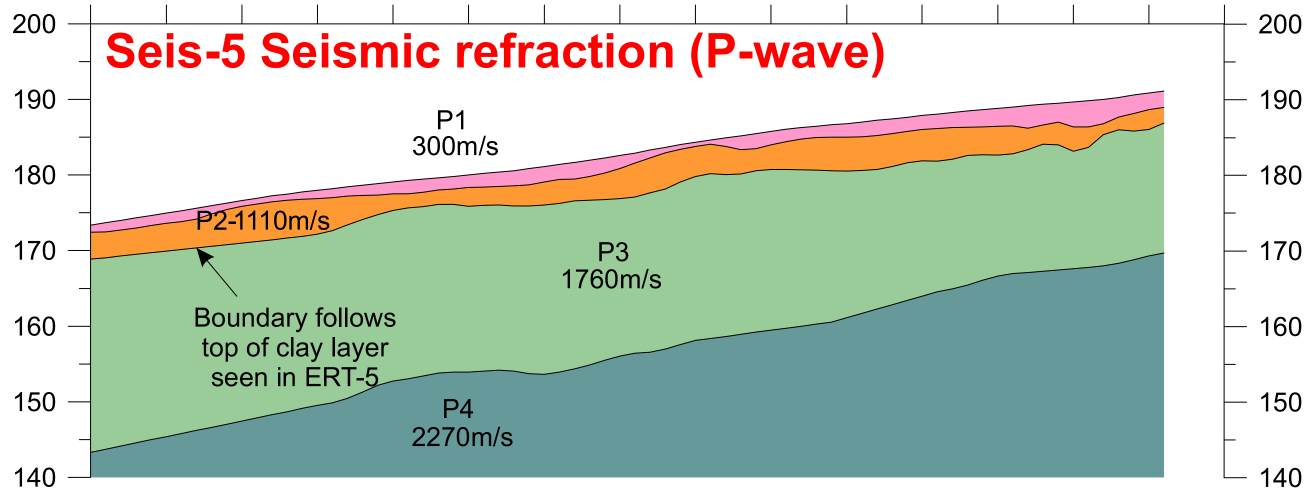

P-wave seismic velocity		Description
P1	300 m/s	Dry, loose material - soil, uncompacted sand/gravel
P2	1110 m/s	Dry, unconsolidated material - predominantly sand and gravel or escarpment erosion with clay upper layer
P3	1760 m/s	Potentially wet, compacted material - dense overburden weathered bedrock and very weak bedrock
P4	2270 m/s	More competent bedrock - still relatively weak bedrock of mudstone and siltstone

Cross Section Key

- S-wave refraction boundary (overlain on resistivity section) (overlain on masw section)
- P-wave refraction boundary (overlain on resistivity section)

Rock / Soil Description	S-wave velocity (m/s) Top 30m
Hard rock	> 1,500
Rock	760 - 1,500
Very dense soil / soft rock	360 - 760
Stiff soil	180 - 360
Soft soil	<180

from National Earthquake Hazard Reduction Prog.

PROFILE LOCATIONS

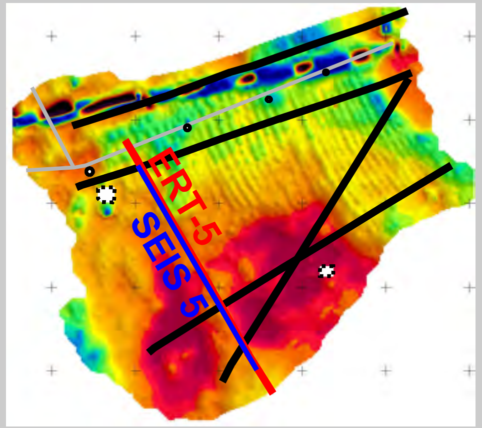

RESISTIVITY COLOR SCALE

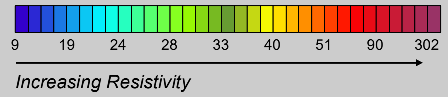

BOREHOLE KEY

Made ground	Sandstone
Clay	Mudstone
Silt	Siltstone
Sand	Limestone
Gravel	Core loss

MASW COLOR SCALE (m/s)

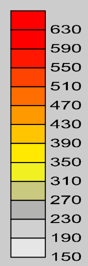

NOTES

TERRADAT down to earth geophysics
Tel: +44 (0) 2920 700127
Web:www.terradat.co.uk
Email: web@terradat.co.uk

Title: RESISTIVITY AND SEISMIC SURVEY RESULTS FOR PROFILE 5

Project: A417 CRICKLEY HILL BIRDLIP

Scale:	1:1000 at A3	FIGURE 6
Drawn by/Ref:	AL/6466/6	
Date:	31 JULY 2019	

Appendices

Appendix - Electromagnetic Survey

The electromagnetic (EM) technique involves the generation of an EM field at the surface and measuring the response of the ground as it propagates into the subsurface. The main components of an EM survey instrument are a transmitter (for the generation of primary field) and receiver (for measuring the induced secondary field). The instrument functions by inducing current into the ground via a transmitter coil which causes the generation of secondary electromagnetic fields in any ground conductors present within the depth range of the particular instrument. These secondary fields are measured at a receiver coil and the instrument can record ground conductivity and in-phase component (metal indicator) at each survey station.

Electromagnetic (EM) surveys are carried out using man-portable instruments with readings taken on a regular grid or along selected traverse lines. If site conditions permit, the EM instrument may be mounted/towed behind a quad bike and positional control is provided by dGPS. The selection of the particular EM instrument (GEM2/EM-38/EM-31/EM-34) is based on the required penetration depth of the survey.

The results from the EM survey can be presented as colour contoured plots of conductivity and inphase (metal response) data. In general terms, a relative increase in conductivity values usually indicates a local increase in clay content or water saturation. However, if there is a corresponding increase in the inphase response, the influence of some artificial source is likely (i.e. metal).

EM-38
(Exploration depth ~1.5m)

EM-31
(Exploration depth ~3 to 5m)

EM-34
(Exploration depth ~7.5 to 60m)

Towed EM-38 with dGPS

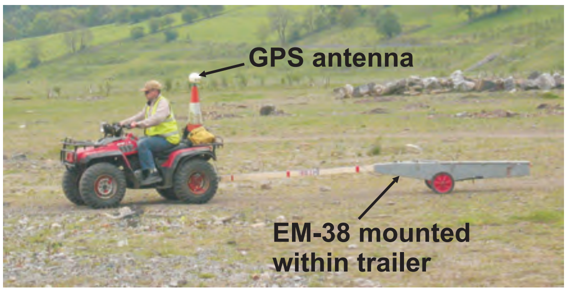

General principle of EM surveying

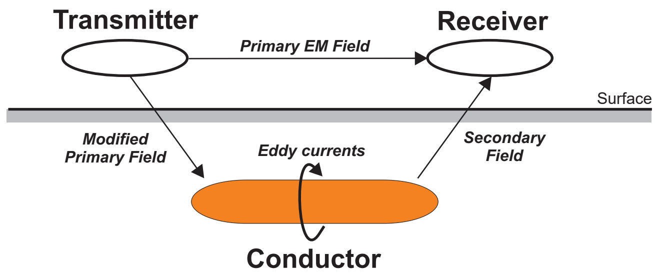

Mounted EM-31 with dGPS

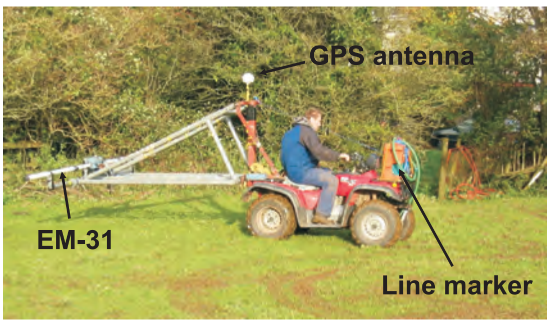

Conductivity data plot

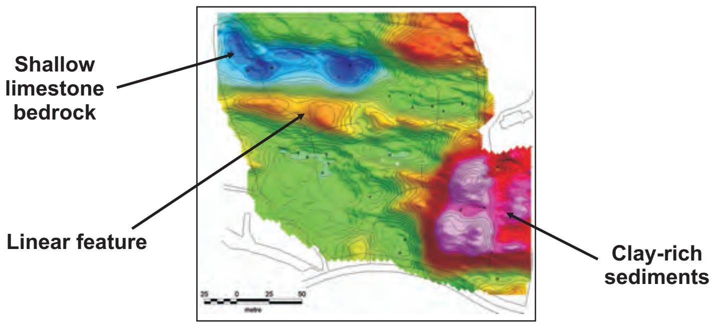

At the end of the survey, the data are downloaded to a field computer and corrected for instrument, diurnal and positional shifts. Additional editing may be carried out to remove non-essential or 'noisy' data values/positions. The dataset is then processed to enhance any identifiable anomalies .

Constraints
Power lines, buildings, metal structures (fences, rebar, vehicles, debris etc.) and buried services can interfere with the electro-magnetic measurements.

Appendix - Resistivity Tomography

The Resistivity technique is a useful method for characterising the sub-surface materials in terms of their electrical properties. Variations in electrical resistivity (or conductivity) typically correlate with variations in lithology, water saturation, fluid conductivity, porosity and permeability, which may be used to map stratigraphic units, geological structure, sinkholes, fractures and groundwater.

The acquisition of resistivity data involves the injection of current into the ground via a pair of electrodes and then the resulting potential field is measured by a corresponding pair of potential electrodes. The field set-up requires the deployment of an array of regularly spaced electrodes, which are connected to a central control unit via multi-core cables. Resistivity data are then recorded via complex combinations of current and potential electrode pairs to build up a pseudo cross-section of apparent resistivity beneath the survey line. The depth of investigation depends on the electrode separation and geometry, with greater electrode separations yielding bulk resistivity measurements from greater depths.

The recorded data are transferred to a PC for processing. In order to derive a cross-sectional model of true ground resistivity, the measured data are subject to a finite-difference inversion process via RES2DINV (ver 5.1) software.

General resistivity principle

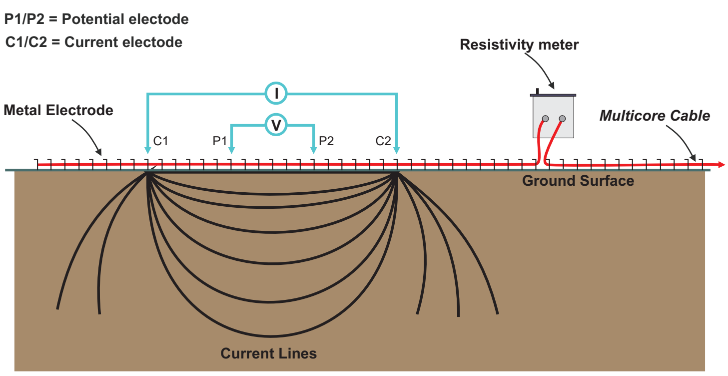

Typical field set-up

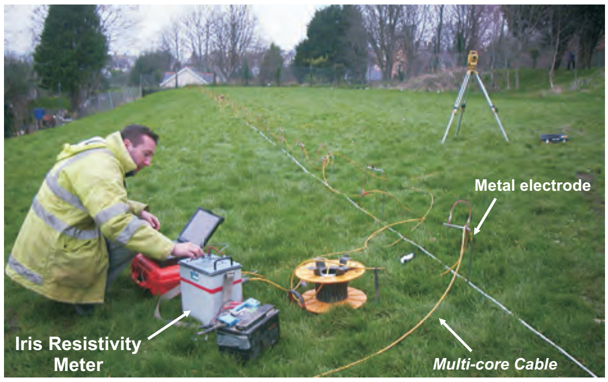

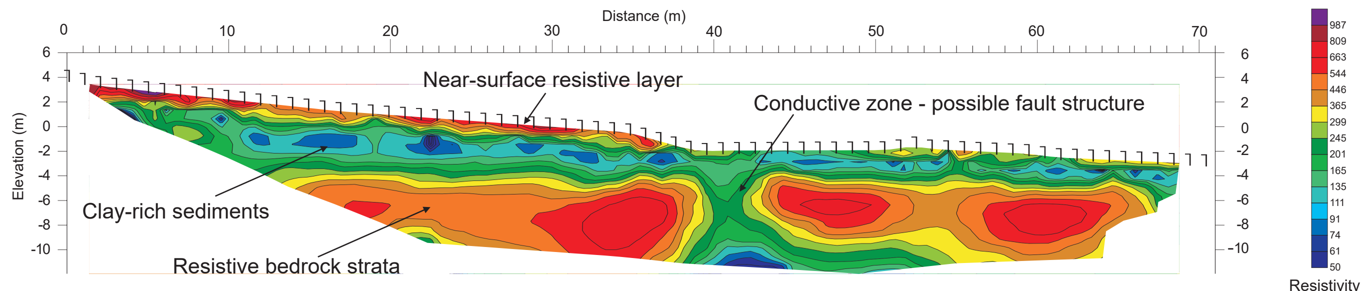

Modelled resistivity section

Data processing is based on an iterative routine involving determination of a two-dimensional (2D) simulated model of the subsurface, which is then compared to the observed data and revised. Convergence between theoretical and observed data is achieved by non-linear least squares optimisation. The extent to which the observed and calculated theoretical models agree is an indication of the validity of the true resistivity model (indicated by the final root-mean-squared (RMS) error).

The true resistivity models are presented as colour contour sections revealing spatial variation in subsurface resistivity. The 2D method of presenting resistivity data is limited where highly irregular or complex geological features are present and a 3D survey maybe required. Geological materials have characteristic resistivity values that enable identification of boundaries between distinct lithologies on resistivity cross-sections. At some sites, however, there are overlaps between the ranges of possible resistivity values for the targeted materials which therefore necessitates use of other geophysical surveys and/or drilling to confirm the nature of identified features.

Constraints:
Readings can be affected by poor electrical contact at the surface. An increased electrode array length is required to locate increased depths of interest therefore the site layout must permit long arrays. Resolution of target features decreases with increased depth of burial.

Appendix - Seismic Refraction Survey

Seismic refraction is a useful method for investigating geological structure and rock properties. The technique involves the observation of a seismic signal that has been refracted between layers of contrasting seismic velocity, i.e., at a geological boundary between a high velocity layer and an overlying lower velocity layer.

Shots are deployed at the surface and recordings made via a linear array of sensors (geophones or hydrophones). Refracted seismic signal travels laterally through the higher velocity layer (refractor) and generates a 'head-wave' that returns to surface. Beyond a certain distance away from the shot, the signal that has been refracted at depth is observed as first-arrival signal at the geophones. Observation of the travel-times of refracted signal from selectively deployed shots enables derivation of the depth profile of the refractor layer. Shots are typically fired at locations at and beyond both ends of the geophone spread and at regular intervals along its length.

The results of the seismic refraction survey are usually presented in the form of seismic velocity boundaries on interpreted cross-sections. Seismic sections represent the measured bulk properties of the subsurface and enable correlation between point source datasets (boreholes/trialpits) where underlying material is variable. Reference to the published seismic velocity tables enables derivation of rippability values.

Typical field set-up

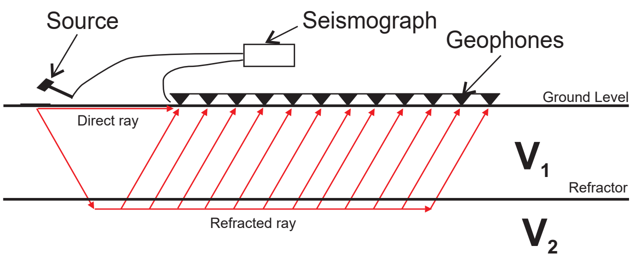

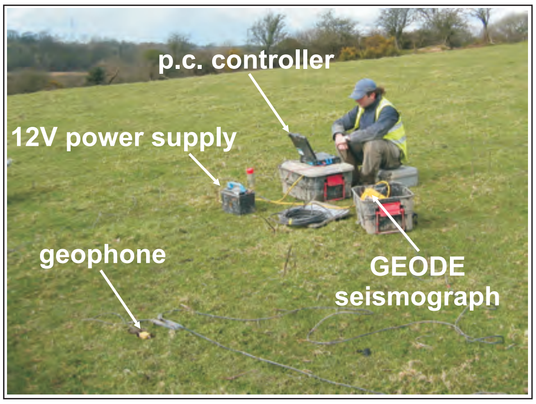

Travel-time curve

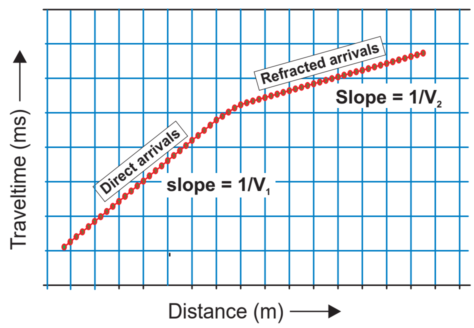

Modelled velocity section

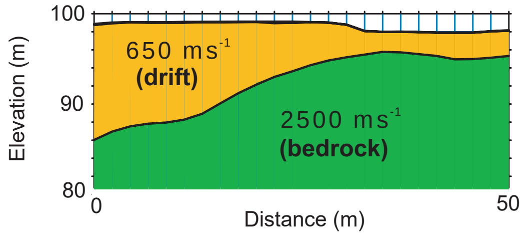

The data processing is carried out using PICKWIN & PLOTREFA (OYO ver2.2) software. The first stage involves accurate determination of the first-arrival times of the seismic signal (time from the hammer blow to each recording hydrophone) for every shot record, using PICKWIN. Time-distance graphs showing the first-arrival times were then generated for each seismic shot record and analysed using PLOTREFA software to determine the number of seismic velocity layers. Modelled depth profiles for the observed seismic velocity layers are produced by a tomographic inversion procedure that is revised iteratively to develop a best fit-model. The final output of a seismic refraction survey is a velocity model section of the subsurface based on an observed layer sequence with measured velocities that correspond to physical properties such as levels of compaction/ saturation in the case of sediments and strength/rippability in the case of bedrock.

Constraints
Layer velocity (density) must increase with depth; true in most instances. Layers must be of sufficient thickness to be detectable. Data collected directly over loose fill (landfills) or in the presence of excessive cultural noise may result in sub-standard results. In places where compact clay-rich tills and/or shallow water overly weak bedrock an S-wave survey may be used to profile rockhead where insufficient velocity contrast may prevent use of a P-wave survey.

TERRA DAT

Appendix - Surface Wave Surveys

MASW survey in progress

Hammer and plate source - the most

Multi-channel Analysis of Surface Waves (MASW) is a very useful method for investigating shallow geological structure and, in particular, the relative shear strength of subsurface materials. By incorporating density values for the local bedrock and overburden sediments it is possible to derive their shear modulus often referred to as dynamic ground stiffness.

The technique is based on the recording of seismic waves that roll much like a seawav e along the surface and extend down to depth beneath the survey line. At each new location it is essential to carry out initial tests to determine optimum acquisition parameters including geophone spacing and shot offset distances. Typically a hammer and plate or buffalo gun is used as the seismic source with the latter offering more power for difficult sites. Surface waves travel more slowly than other seismic signals and are recorded over long time intervals by comparison. The recorded data are first processed to produce dispersion curves for each shot. These curves are then modelled individually to produce 1D depth profiles of shear wave velocity and then combined to produce a depth cross-section revealing the shear wave velocity structure of the ground.

Typical Targets:

Dynamic stiffness modulus
Foundation strength for turbines/structures
Weak but cemented rockhead
Weathered rock beneath dense overburden
Shear strength of landslide materials

Benefits of MASW:

Low Cost
High productivity
Continuous profiles
Non-invasive
Environmentally friendly

MASW Survey procedure

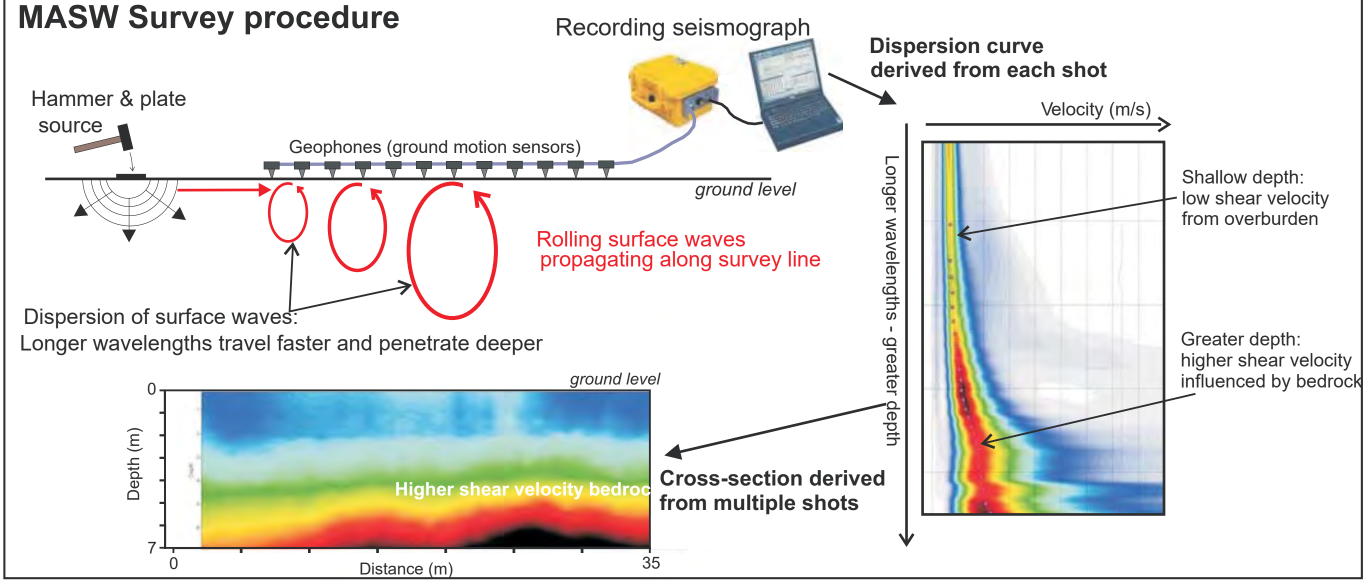

Combined MASW and Refraction Survey

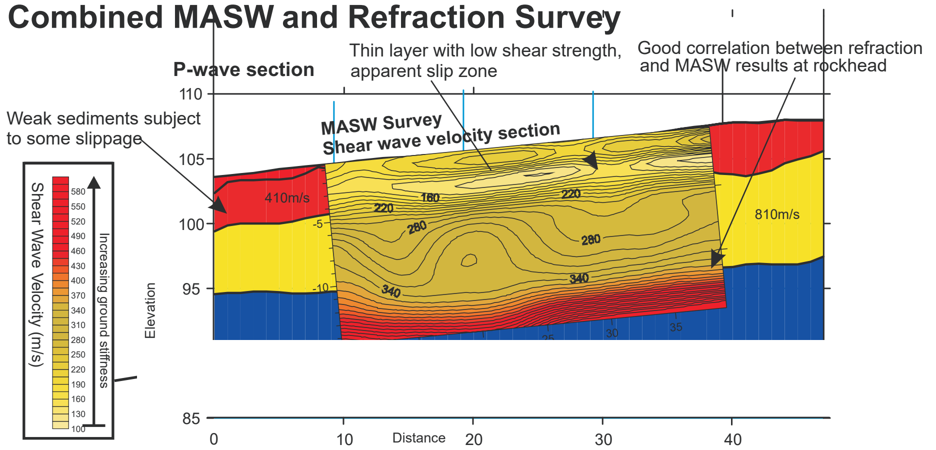

(ABOVE) A schematic illustration of the MASW data acquisition and processing procedure leading to a final section.

(LEFT) Results of a combined seismic refraction and MASW survey targeting shallow geological structure on an active landslide. The MASW survey results reveal spatial variation in shear wave velocity and dynamic ground stiffness. A shallow zone of low shear strength is clearly observed.

Appendix - Seismic velocity tables

Rippability Chart

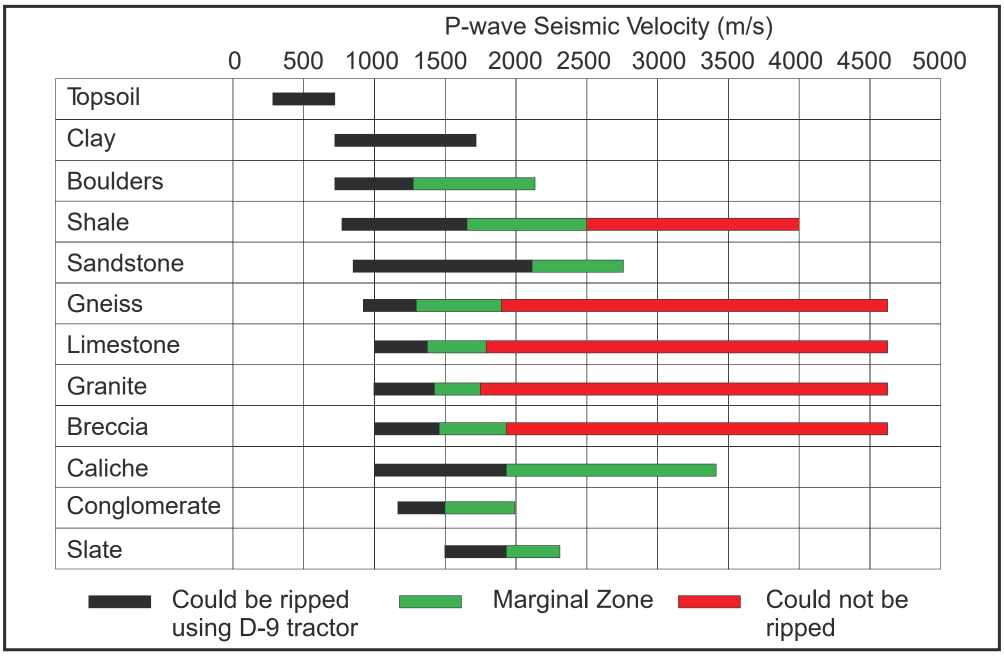

from Geology and Construction, 1995

Diggability Chart

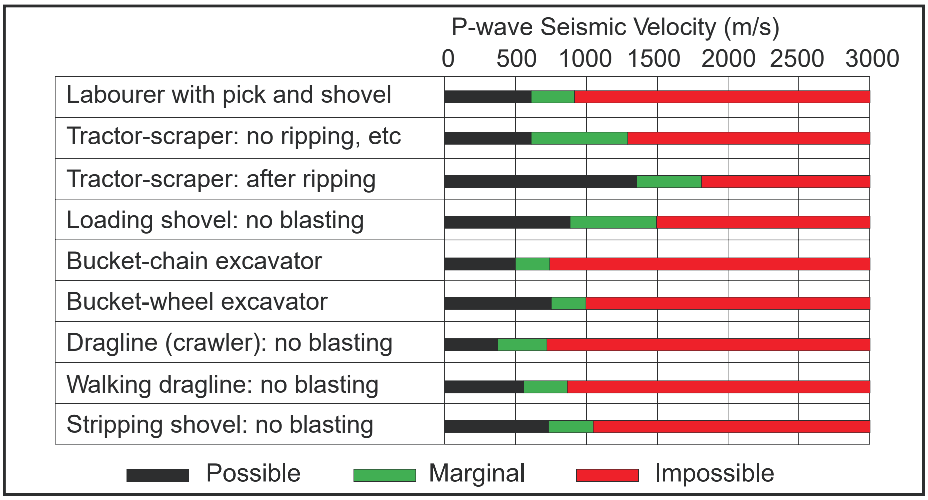

from Seismic velocities for determining diggability, Atkinson 1971

Shear Waves

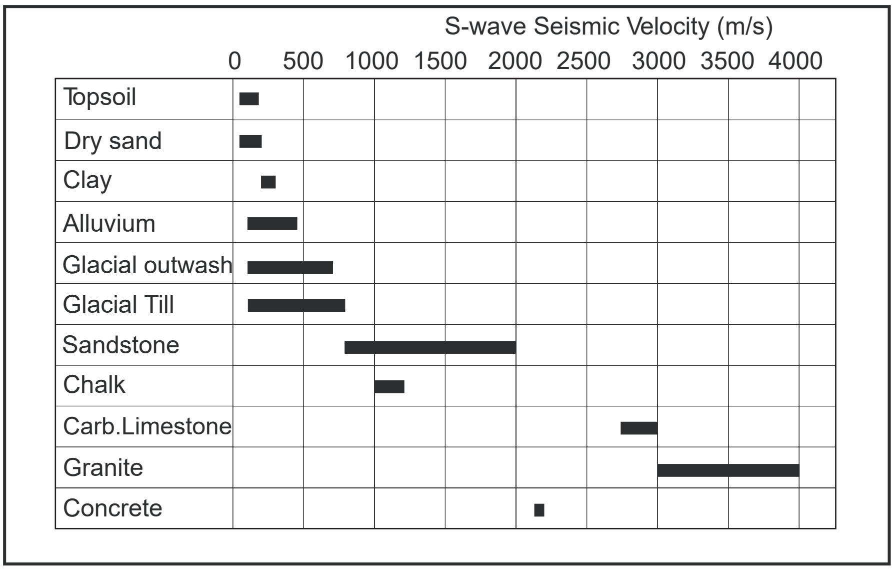

from a compilation of published sources

Rock / Soil Description	**S-wave velocity (m/s) Top 30m**
Hard rock	> 1,500
Rock	760 - 1,500
Very dense soil / soft rock	360 - 760
Stiff soil	180 - 360
Soft soil	<180

from National Earthquake Hazard Reduction Prog.

GEOPHYSICAL SURVEY REPORT

Project

Bedrock mapping and sediment characterisation

Location

Zone 1, A417, Birdlip

Client

Geotechnical Engineering

Head Office
Unit 1
Link Trade Park
Penarth Road
Cardiff CF11 8TQ
United Kingdom

Telephone: +44 (0)2920 700127
www.terradat.co.uk

down to earth **geophysics**

Job Reference: 6688
Date: December 2020
Version: 2

GEOPHYSICAL SURVEY REPORT

Project

Bedrock mapping and sediment characterisation

Location

Zone 1, A417, Birdlip

Client

Geotechnical Engineering

Project Geophysicist:	M Bottomley BSc MSc	[redacted]
Reviewer:	S Hughes PhD BSc FGS	[redacted]
Job Reference:	6688	
Date:	December 2020	

CONTENTS

Figures

Appendices

1 EXECUTIVE SUMMARY

A geophysical survey was carried out as part of the ground investigation for proposed improvements to the A417 near the village of Birdlip, south of the existing road. The survey work was commissioned by Geotechnical Engineering (the Client). The fieldwork was carried out during October 2019 and January 2020 and undertaken within an area defined by the Client as 'Zone 1', comprising seven targeted Electrical Resistivity Tomography (ERT) and seismic profiles, and an electromagnetic (EM) ground conductivity survey. The work was designed to complement the invasive and geotechnical investigation in providing detailed information on the geology and ground conditions adjacent to the existing A417, with particular concern regarding potential landslide/landslip zones.

The geophysical survey consisted of an integrated survey approach utilising electromagnetic ground conductivity measurements, seven targeted ERT profiles and seven seismic P and S-wave refraction and Multichannel Analysis of Surface Waves (MASW) profiles along all resistivity lines.

The results have been provided as a series of interpreted, colour-contoured plots (ground conductivity) and scaled sections (resistivity and seismic refraction), alongside a map showing the locations of the plots and profiles in relation to the underlying topographical features and bedrock geology as provided by Google Earth mapping and the British Geological Survey (BGS) Geology of Britain viewer.

2 INTRODUCTION

This report describes a geophysical survey that was carried out as part of the ground investigation for proposed improvements to the A417 near the village of Birdlip. The survey work was commissioned by Geotechnical Engineering (the Client). The fieldwork was carried out during October 2019 and January 2020 and undertaken within an area defined by the Client as 'Zone 1', comprising seven targeted Electrical Resistivity Tomography (ERT) and seismic profiles, as well as an electromagnetic (EM) ground conductivity survey.

The work was designed to complement the invasive and geotechnical investigation in providing detailed information on the geology and ground conditions adjacent to the existing A417, with particular concern regarding potential landslide/landslip zones.

2.1 Site description and history

Zone 1 (approx. centred on 393350E, 215940E) occupies an area of around 50 hectares, roughly 1.8 km northeast of the village of Birdlip. The survey area is located around the junction/roundabout between the A417 and A436 and encompasses woodland (owned by the National Trust) to the north of the A417, and open fields and hedge systems to the south. Profiles 13, 15, 17 and 19 are also located in fields immediately west of the Air Balloon pub. Topographically, the relief is not as steep as encountered within Zone 2.

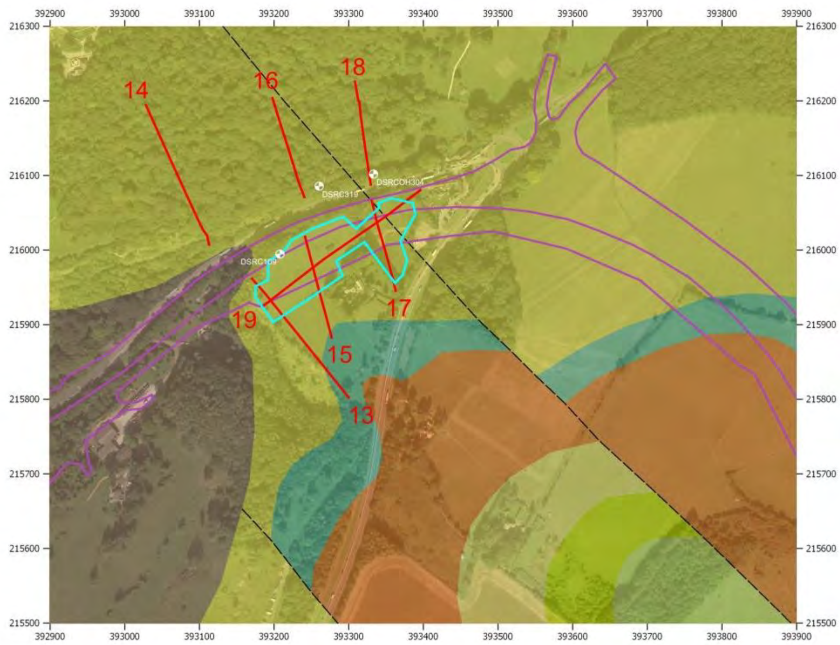

Plate 1. *Zone 1, showing the locations of the ERT and seismic profiles (red lines) and the extents of the EM ground conductivity survey (light blue).*

2.2 Geological setting

The Client has provided numerous borehole logs located within the 'Zone 1' survey area. The intrusive investigation has logged highly variable material comprising 20 to 30 m of clay and limestone of the Birdlip Limestone Formation, overlying mudstone and siltstone most likely from the Lias Group and Inferior Oolite. The British Geological Survey (BGS) Geoindex shows the survey area to fall mostly over the Birdlip Limestone Formation, rising onto the Aston and Salperton Limestone Formations to the south-east.

According to the BGS Geoindex, there are no superficial deposits in the vicinity of the site. All material overlying the bedrock is therefore believed to be bedrock erosion material from steep slopes and escarpments that has been transported by weather processes and landslide, down the valley side, and is referred to in this report as "overburden".

2.3 Survey objectives

The primary objectives of the survey were to provide detailed information on the shallow ground composition and deeper bedrock geology to assist with the ground investigation of the proposed road scheme. Of particular interest for engineering a new road cutting, are areas of shallow geology that may support further landslide movement of the overburden.

2.4 Survey design

Given the scope of the survey objectives, it was decided to adopt an integrated survey approach utilising the following geophysical methods:

- **Ground Conductivity**: to provide a ground conductivity map to characterise shallow overburden deposits and identify preferential water pathways such as gravel channels and clay-rich layers.

- **Resistivity Tomography**: to provide electrical cross-sections along selected survey profiles that allow identification of geological or hydrological boundaries.

- **P-wave Seismic Refraction**: to provide seismic velocity (V_p) model sections that indicate the thickness of overburden deposits and the depth to competent bedrock, in correlation with standard tables.

- **S-wave Seismic Refraction**: to provide seismic velocity (V_s) model sections that indicate the depth of uncompacted and compacted sediments, weathered rockhead and more competent (higher shear strength) bedrock.

- **MASW (Multichannel Analysis of Surface Waves)**: to derive shear velocity ('S-wave' or 'V_s') from rolling surface waves that are related to the stiffness of the ground material. This technique is also useful where velocity inversions in the ground layers may be encountered.

2.5 Quality control

The geophysical data sets were collected in line with normal operating procedures as outlined by the instrument manufacturer and TerraDat company policy. On completion of the survey, the data were downloaded from the survey instrument on to a computer and backed up appropriately. The acquired data set was initially checked for errors that may be caused by instrument noise, low batteries, positional discrepancies, etc. and any field notes are either written up or incorporated in the initial data processing stage. The data set is then processed using the standard processing routines and once completed; the resulting plots are subject to peer review to ensure the integrity of the interpretation. Our quality control standards are BS EN ISO 9001: 2015 certified.

3 SURVEY DESCRIPTION

The survey was carried out using the following geophysical methods:

- EM - Ground conductivity mapping
- Electrical Resistivity Tomography (ERT)
- P-wave seismic refraction (employs compressional waves)
- S-wave seismic refraction (employs shear waves)
- MASW (Multichannel Analysis of Surface Waves)

The extents of the EM survey, resistivity and seismic profiles are shown in Figure 1. Seven Electrical Resistivity Tomography (ERT) and seismic refraction profiles were deployed, in locations as specified by the Client.

Background information for the survey methods is provided in the appendices, while a description of the actual survey work is provided in the sections below.

3.1 Survey limitations and assumptions

Seismic refraction requires that the velocity of the materials in the subsurface increases with the depth of burial. This is normally the case since (i) the degree of compaction within the overburden typically increases with depth, and (ii) bedrock condition improves with depth as weathering is reduced, both of which lead to higher seismic velocities. Therefore, one limitation of the refraction method is the inability to resolve localised weak zones within rock where it resides at a depth below the competent non-weathered rock. One of the objectives of the resistivity tomography survey is to target such weak/broken zones in the rock where fines/water have infiltrated and reduced the local ground resistivity. The survey output from both the P and S-wave refraction surveys are cross-sectional models that describe the bulk physical properties of the ground in terms of superficials, weathered rock and competent rock layers. There will be local variations in rock strength within the interpreted weathered rock layer, and the fracture density / broken character of the rock will vary over very short lateral distances. Measuring the seismic velocity of the bedrock over tens of metres along each survey line determines the bulk properties of the shallow rock mass and enables targeted ground-truthing of any identified anomalous ground.

3.2 Survey layout and topographic survey

The ground conductivity data were acquired under the positional control of an EGNOS dGPS system. Where possible, a Topcon Hyper Pro RTK dGPS system was used to mark resistivity (electrode) and seismic profile (geophones and offend shots) locations with a survey accuracy of +/- 2.5 cm. In some cases, positional accuracy was not adequate due to extensive tree cover, and so a Trimble robotic total station was employed using dGPS established reference stations. All measurements were recorded in the Ordnance Survey National Grid coordinates.

3.3 Ground conductivity mapping

An electromagnetic ground conductivity survey involves the transmission of an electromagnetic field into the subsurface and then recording the returning signal via a receiver in the same instrument. Data are acquired on a grid covering the area of interest, and a contoured plan of the variation in ground conductivity response across the site is produced. The presence of conductive materials in the subsurface such as clay, water, mudstone, ash, metal, rebar, leachate, etc. will be evident as regions of high values on the ground conductivity plan. Materials such as coarse-grained sediments, dry zones, and many bedrock types will appear as regions of low values.

3.3.1 *Electromagnetic survey - field activity*

The conductivity data were acquired using a multi-frequency *Geophex GEM-2* instrument (Plate 2), and data were acquired under the control of an EGNOS corrected dGPS (accuracy +/- 0.5m) at a nominal 0.25 m interval along a series of parallel 5 m spaced survey lines. The instrument was primarily configured to investigate depths of up to 3 to 5 m below ground level. The sensor was mounted on a cart and pulled behind an ATV.

Plate 2. *Ground conductivity data collection method. Geophex GEM-2 instrument mounted on a bespoke cart which was pulled across the site using an ATV, under the control of a GPS system (library Photo).*

3.3.2 Electromagnetic survey – data processing

The conductivity data were downloaded from the data logger and compiled using dedicated software *WINGEM-3*. Initial editing was then carried out to remove positional errors and rogue values. The data were then exported as an 'XYZ' file and translated into the OSGB36 Coordinate system using the OSTN02 transformation. The software program *OASIS MONTAJ* was used to compile, edit and manipulate the data to enhance any features of interest. The colour contour plots were then integrated with the base plan information and the resulting plans exported to *CORELDRAW* for final annotation.

3.4 Electrical Resistivity Tomography (ERT)

An ERT survey involves the injection of DC electrical current into the ground at various electrode locations along a profile line. An electrical cross-section of the subsurface is then derived from the recorded data. A diverse range of features such as clay-rich sediments, fracture zones, infilled solution features, bedrock structure and mineralisation can be imaged in cross-section using a resistivity survey. A feature may be targeted using resistivity tomography given sufficient electrical contrast with its surroundings. A description of the field activity is provided below, and some background information on the survey method is found in the Appendix.

3.4.1 ERT survey field activity

A 72-channel *IRIS Syscal* resistivity system (Plate 3) was used to acquire seven profiles across the survey area, as shown in Figure 1. The ERT profiles were acquired with an electrode spacing of 2 or 3 m using a standard Wenner-Schlumberger array. For some of the profiles, 'roll-ons' were required to cover the required area of interest. A 'roll-on' simply involves adding one or two cables to the end of the initial 72-channel setup and then selecting the appropriate protocol file from the IRIS resistivity meter to continue data acquisition from the initial setup and into the new cables. A summary of the ERT profiles is given in Table 1.

ERT Profile No.	Fig.	Start (OSGB)		End (OSGB)		Length (m)	Electrode Spacing (m)	~ Depth of penetration (m)
		Easting	Northing	Easting	Northing			
Line 13	4	393300.0	215802.1	393169.2	215962.5	207	3	30
Line 14	5	393112.6	216008.0	393027.6	216195.4	214	2	20
Line 15	6	393240.9	216019.6	393276.9	215883.1	141	2	20
Line 16	7	393240.1	216071.7	393197.2	216204.9	142	2	20
Line 17	8	393330.8	216067.8	393362.6	215946.4	126	2	20
Line 18	9	393329.3	216088.1	393307.9	216227.0	142	2	20
Line 19	10A	393183.7	215923.6	393396.9	216081.9	266	3	30
Line 20*	-	-	-	-	-	-	-	-

**Line 20 could not be undertaken due to land access constraints, and will be undertaken once access becomes available.*

Table 1. *ERT profile summary.*

3.4.2 ERT survey data processing

The data were processed using *Res2DInv* software to derive modelled electrical cross-sections of the subsurface. Elevation data were added to the models, using electrode positions surveyed using a TOPCON network RTK GPS. All topographic data were transformed into National Grid (OSGB36) using the OSTN02b transformation; elevations are given in m AOD. The ERT data was then exported into *Surfer 7* where it was gridded and presented as a 2D cross-sections of resistivity. These cross-sections were then exported to *CorelDraw* for final annotation. All resistivity profiles are presented on the same colour scale and are not vertically exaggerated.

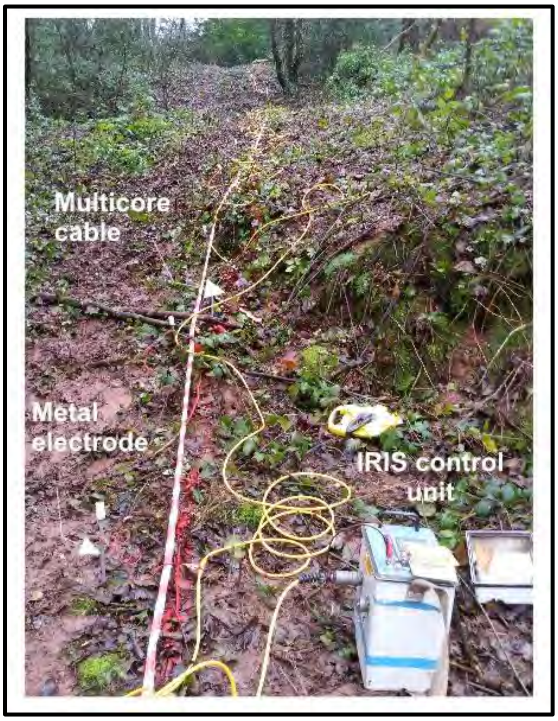

Plate 3. *Resistivity Tomography data collection. A 72 channel IRIS Syscal ERT system used to acquire eleven profiles across the site (library photo).*

3.5 Seismic survey – P and S-wave refraction

A seismic survey involves generating a shock wave signal at the surface to investigate the geological structure beneath a chosen profile line. A series of vibration sensors (geophones, or hydrophones in water) are deployed along the line and are used to record the travel times of incident seismic signal as it returns from below ground. Features such as rockhead, the water table, made ground, soft sediments and dense tills all have distinct velocity ranges and can be imaged in cross-section using a seismic refraction survey. A description of the field activity is provided below, and some further background information on the survey method is found in the appendices.

3.5.1 Seismic survey field activity: P-wave refraction

P-wave seismic refraction data were acquired along seven profile lines using a high precision 72 channel *GEODE* (Plate 4a) seismic system. To target the broad depth range, low frequency (4Hz) geophones were deployed at 2 m intervals providing individual geophone spread lengths of 142 m. For some profiles (e.g. Profiles 13 and 19), several setups were required to achieve full line coverage. The seismic wave was generated by a combination of sledgehammer striking a nylon plate and Seismic Impulse Device (SID) firing 12- and 8-gauge black powder cartridges (Plate 4b). To build up the refraction data set, seismic shots were taken at several positions along the geophone spread (usually every 6-12 geophones) and set distances beyond the geophone spread. For this particular survey, the 'offend' shots were limited by site constraints, but the maximum distance was 100 m. A summary of the seismic profiles is given in Table 2.

Plate 4. *a) Field setup and b) Seismic Impulse Source deployment (library photo).*

Seismic Profile No.	Fig.	Start (OSGB)		End (OSGB)		Length (m)	Geophone Spacing (m)	~ Depth of penetration (m)
		Easting	Northing	Easting	Northing			
Line 13	4	393285.6	215818.7	393169.2	215962.5	190	2	25
Line 14	5	393098.2	216038.3	393040.0	216167.3	142	2	25
Line 15	6	393239.9	216021.9	393276.6	215884.4	141	2	25
Line 16	7	393238.8	216077.1	393194.8	216211.3	142	2	25
Line 17	8	393365.7	215941.3	393331.6	216069.8	136	2	25
Line 18	9	393327.8	216104.7	393312.1	216197.5	94	2	20
Line 19	10B	393186.5	215925.6	393394.7	216079.0	260	2	25
Line 20*	-	-	-	-	-	-	-	-

**Line 20 could not be undertaken due to land access constraints, and will be undertaken once access becomes available.*

Table 2. *Seismic Profile summary.*

3.5.2 Seismic survey field activity: S-wave refraction (Shear)

S-wave seismic refraction data were also acquired using a 72 channel *GEODE* seismic system. Horizontally mounted geophones were deployed at 2 m intervals producing individual geophone spread lengths of up to 142 m. For some profiles (e.g. Profiles 13 and 19), several setups were required to achieve full line coverage. A weighted S-wave plate struck sideways with a sledgehammer was used as the energy source (Plate 5). At each shot location, the shot plate was aligned perpendicular to the profile line and subsequently struck on both ends to generate two sets of shear wave recordings that have opposite polarity. To build up the refraction data set, seismic shots were taken at several positions along the geophone spread (usually every 6-12 geophones) and set distances beyond the geophone spread.

Plate 5. *S-wave source plate being struck (library photo).*

3.5.3 Seismic survey data processing: P and S-wave refraction

The data processing was carried out using *PICKWIN* and *PLOTREFA* software. The first stage involved the accurate determination of the first-arrival times of the seismic signal (time from the shot going off to each recording geophone) for every shot record using *PICKWIN*. Time-distance graphs showing the first-arrival times were then generated for each seismic line and analysed using *PLOTREFA* software to determine the number of seismic velocities layers. Modelled depth profiles for the observed seismic velocity layers were produced by a tomographic inversion procedure that was revised iteratively to develop a best-fit model.

The final output of a seismic refraction survey is a velocity model section of the subsurface based on an observed layer sequence. The measured velocities correspond to physical properties such as levels of compaction/saturation in the case of sediments and strength/rippability in the case of bedrock. A transitional velocity model will be considered if distinct layers are not expected, or velocity contrasts between layers are marginal. However, a layered model appears most appropriate to this site. The final sections were exported to *CORELDRAW* for annotation and presentation.

3.6 Seismic survey – MASW

Multichannel Analysis of Surface Waves (MASW) employs 'rolling' surface waves to derive shear velocity. This is achieved through analysis of the dispersion that occurs as surface wave energy propagates through the subsurface and separates into different frequencies travelling at different velocities depending on the stiffness of the sediments and/or rock encountered.

This technique utilises Rayleigh-type surface waves (normally considered noise in seismic refraction/reflection surveys and called "ground roll") recorded by multiple geophones deployed on an even spacing and connected to a common recording device (seismograph), as shown in Plate 6.

As the dispersion of the seismic wave can be dependent on the geology and ground conditions (i.e. variability, terrain, etc.), MASW profiles are usually limited to relatively flat areas or where the ground is more homogenous.

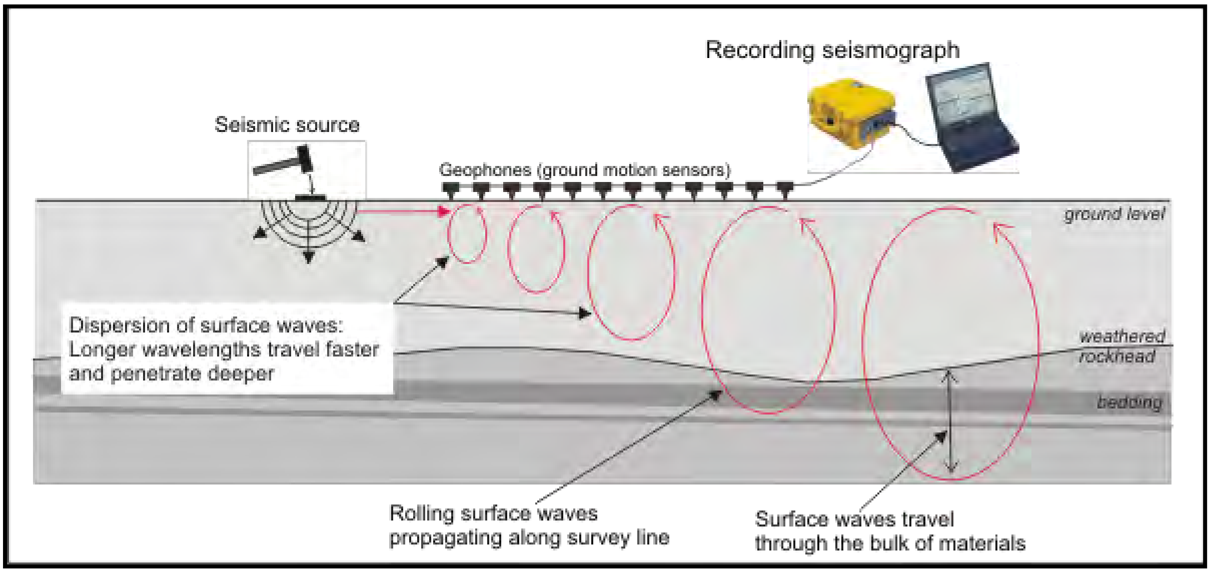

Plate 6. *MASW survey setup.*

3.6.1 Seismic survey field activity: MASW

For this particular survey, the setup is very similar to the refraction setup; however, instead of a discreet number of shot points, shots were acquired at every other geophone position along the profile. In this case, low frequency (4Hz) geophones were set at 2 m intervals, and the data were acquired using the sledgehammer as the source. A one-second record length was used to fully capture the frequency dispersion.

3.6.2 Seismic survey data processing - MASW

Analysis of surface waves recorded on multichannel shot records was carried out using SurfSeis software, which considers the dispersion properties of all types of waves (both body and surface waves) through a wave field transformation method. This directly converts the multichannel record into an image, where a dispersion pattern is recognised, and the necessary dispersion properties are extracted. These dispersion properties are used to generate modal dispersion curves that are subsequently inverted and used to produce the resultant shear-wave velocity (Vs) profile. The final velocity sections are created in SURFER then exported to CorelDraw for annotation and presentation.

4 RESULTS AND DISCUSSION

The results of the geophysical surveys are presented as a series of interpreted colour contour plots and scaled sections in Figures 3 to 10B. A general description of the interpretation process is given below, followed by a summary of the findings in Sections 4.5 and 4.6.

4.1 Ground Conductivity

The results are presented as a colour contoured plot of ground conductivity (Figure 3). Following a review of the electromagnetic data; it was decided only to consider the response of the 47,925 MHz frequency channel. A relative increase in conductivity values usually indicates a comparative increase in the clay/ash/water content, which could signify either a lateral change in lithology or a variation in bedrock depth. Extreme fluctuations in conductivity/in-phase values are usually indicative of instrument' overload' due to high metal content. The interpretation of the conductivity data is based on both published electrical properties of typical sedimentary materials (Plate 7) and when available, correlation with on-site information.

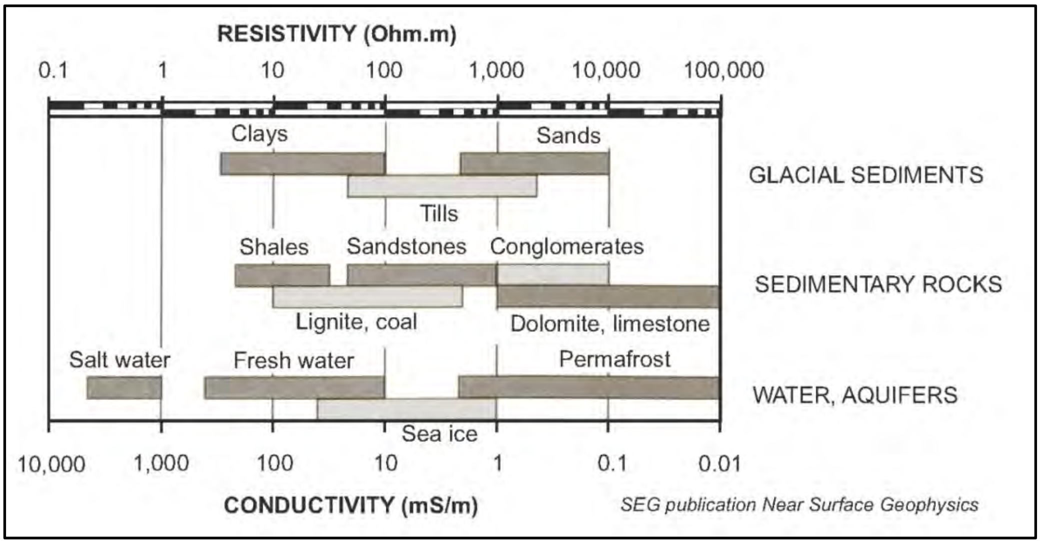

Plate 7. *Conductivity and resistivity values of common materials.*

4.2 Resistivity tomography

The results of the resistivity survey are presented as colour contoured scaled sections of the subsurface showing changes in resistivity, with blue colours representing low values, and red colours representing relatively high resistivity values. The vertical and horizontal axes display elevation and chainage along the profile line, respectively. The interpretation of the modelled resistivity sections is based on both published electrical properties of typical sub-surface materials (Plate 7) and, when available, correlation with on-site information or observations. In principle, an increase in resistivity values usually indicates a relative decrease in the clay content or groundwater saturation. However, due to the non-uniqueness of the electrical properties (i.e. different material exhibiting same resistivity values), the final interpretation may be limited and may require addition calibration (i.e. drilling or other supplementary geophysical techniques).

The results of the ERT survey are discussed in the summary discussions, in conjunction with the results of the seismic survey. To assist with the interpretation, the resistivity sections have been overlain with the interpreted seismic velocity boundaries where acquired.

4.3 Seismic Refraction – compressional (P) and shear (S) wave

Interpretation of the refraction sections is based on the widely understood and published velocities of typical sub-surface materials (provided in the appendices). It is beneficial to correlate model sections with on-site information/observations, but at the time of reporting, only limited borehole information was available.

4.3.1 Compressional (P) wave

Analysis of the P-wave refraction data has identified up to five distinct layers of contrasting velocity (V_p), and a typical description of each layer is given below and summarised in Table 3. It is worth noting that the seismic refraction section represents the measured bulk characteristics of the subsurface and, in certain cases, it can prove difficult to correlate with point source data (boreholes/trial pits) where the underlying material is variable. In such instances, the MASW results may be very useful.

Layer	P-wave velocity	Sediment/Rock Description
P1 (pink)	< 300 m/s (low)	Thin, dry loose surface soils and sediments
P2 (orange)	301 – 800 m/s (low to medium velocity)	Unconsolidated, dry overburden material
P3 (light green)	801 - 1400 m/s (medium velocity)	Compacted, dry overburden material
P4 (green)	1401 - 1900 m/s (medium to high velocity)	Compacted, saturated overburden material or highly weathered bedrock
P5 (dark green)	> 1901 m/s (high velocity)	Weathered to unweathered bedrock

Table 3. *A guide to the composition of the P-wave velocity layers identified.*

Layer P1 has a low velocity that relates to loose, surface soil and uncompacted sands and gravels. Layers P2 and P3 typically reflect a relative increase in consolidation or compaction of the still dry overburden material. Layer P4 can be more difficult to interpret as the overlap in velocities means that it can represent both overburden material (potentially wet, compact material) and weathered/weak/fractured bedrock. The most effective way to differentiate between sediment and rock type material is to consider the corresponding S-wave velocity, as discussed below. Layer P5 represents the highest (and deepest) velocity unit and is likely to reflect a more competent boundary within the bedrock strata.

4.3.2 Shear (S) wave

By carrying out an analysis of the S-wave refraction data, four distinct layers of contrasting velocity (V_s) have been identified and summarised in Table 4. They are characterised by their correlation with standard tables (see appendices).

In general, the shear-wave velocity (V_s) is much more sensitive than the P-wave velocity (V_p), where the ground becomes abruptly stiffer due to increases in rock strength. For this reason, it is possible to use the V_s to distinguish between sediments and 'rock' (i.e. cemented) material, which is particularly useful for grading the P-wave layer P4. A further advantage of shear waves is that they are unaffected by the groundwater table.

Layer	S-wave velocity	Sediment/Rock Description
S1	<180 m/s	Soft soils and loose sediments
S2	180 - 360 m/s	Stiff soils/overburden
S3	361 - 760 m/s	Very stiff, compacted overburden or highly weathered bedrock
S4	>761 m/s	Rock

Table 4. *A guide to the composition of the S-wave velocity layers identified.*

When comparing the resulting P-wave and S-wave velocity sections, there is a rough 'rule of thumb' with regards to the ratio of the velocities. For unconsolidated sediment, V_p/V_s is usually between 4.0 to 8.0, while for consolidated rocks, the V_p/V_s ratio can vary between 1.5 to 2.0. Even though these are accepted values, they can vary between sites depending on the geology and ground conditions.

When correlating between the respective P-wave and S-wave refraction boundaries, in some instances there can be discrepancies in observed depth values. This depends on the prevailing geology and can reflect different survey parameters (horizontal/vertical polarised S-waves, spacing, etc.), weathering profile (vertical and horizontal), lithology or bedding structure. It has been noted on some sites that the S-wave refractor appears to correlate with internal bedding units as opposed to the general rock mass.

4.4 MASW

The results of the MASW survey are presented as colour contoured S-wave velocity panels showing changes in velocity (i.e. ground stiffness) below the surface. The seismic signal frequency dispersion required for the MASW technique has yielded reliable results to a depth of up to approximately 20 m bgl. The persistent traffic noise from the A417 and the limited power of a sledgehammer energy source meant lower frequency dispersions (giving an increased depth of investigation) suffered from a high signal to noise ratio and were not suitable for modelling. The MASW sections have been colour scaled from white to red, with red representing the highest velocity modelled.

4.5 Summary Discussion – Ground Conductivity

Features or anomalies of interest have been listed and discussed in Table 5 below.

Zone	Feature	Description
1	F1	Linear, conductive feature (oriented NW to SE) is possibly indicative of underground service.
	F2	Area of elevated resistivity indicates a decrease of clay and/or water within the overburden or shallowing of the limestone bedrock.
	F3	Circular conductive feature indicates a localised increase in clay and/or water within the overburden.
	F4	Area of increased conductivity indicates an increase in clay and/or water within the overburden. This correlates very well with the ERT section for Profile 19. DSRC109 is located over material of a similar conductivity and reveals several metres of clay-rich sediments at the surface.
	F5	Linear zone (oriented NW to SE) of increased conductivity correlates very well with the position of the fault, indicating an increase in clay/water within the overburden, and possible deterioration in the underlying limestone bedrock condition.
	F6	Isolated, very conductive anomalies may be associated with surface metal.
	F7	Linear, very conductive feature (oriented NE to SW) is possibly indicative of a buried service.

Table 5. *Features and anomalies of interest as identified by the ground conductivity survey.*

4.6 Summary Discussion – ERT & Seismic Refraction

Features or anomalies of interest have been listed and discussed in Table 6 below.

Profile	Feature	Description
13	F13a	Isolated, slightly more conductive zones, likely indicating an increase of clay and/or water within the superficial deposits.
	F13b	The presence of much stiffer material on the MASW section correlates very well with the position of Layer S4 (i.e. limestone bedrock from the Birdlip Limestone Formation).

	F13c	Broader zone of increased conductivity indicates an increase of water/clay within the superficial deposits or change in sediment lithology. Borehole DSRC109 indicates the presence of clay-rich sediments overlying limestone.
	F13d	This resistive layer indicates a decrease of clay and/or water within the near-surface sediments (possible increase of silt, or gravel of weathered limestone).
	F13e	Poor correlation between Layers S4/P5, indicating that the seismic energy is travelling along different beddings or weathered zones, as is also observed in other profiles. This would not be surprising, considering Profile 13 crosses the expected boundary between the Aston Limestone Formation and the Birdlip Limestone Formation, and as such, off-end and interline shot locations will likely have been delivering seismic energy into different lithological units. Borehole DSRC109 is located too far away for direct comparison but would appear to suggest that Layer S4 could represent weathered limestone, and Layer P5 could represent deeper siltstone of the Lias Group. Of further note are the significantly higher Layer S4 velocities of 807 to 1015 m/s than seen in profiles to the west, indicating a stronger, more competent bedrock lithology.
	F13f	Increase of resistivity correlates with a transition into a more competent bedrock unit, which also corresponds with the position of Layer P5 (possibly siltstone of the Lias Group). This is less obvious further south, where the overlying bedrock is much more resistive.
	F13g	Significant, dipping conductive/resistive boundary coming to the surface at around 70m chainage may be associated with the transition from the Birdlip Limestone Formation into the Aston Limestone Formation to the south.
14	F14a	This resistive layer indicates a decrease of clay and/or water within the near-surface sediments and is also likely influenced by Layer S3, which is likely to represent weak, highly broken weathered limestone bedrock starting from around 2 m bgl.
	F14b	The presence of much stiffer material on the MASW section correlates very well with the positions of Layers S4, and P5 in particular. This also correlates with a decrease in resistivity, which suggests a weathered zone at the top of the bedrock, with the deeper, more competent bedrock indicated by an increase of resistivity below. Alternatively, the

		laterally continuous, dipping conductive/resistive bands could be mapping out different beds of mudstone (conductive) and limestone (more resistive).
	F14c	Isolated resistive feature also correlates with a 'step-up' in Layer S4 and an increase in material stiffness on the MASW section. Therefore this is likely to indicate a shallowing of the bedrock, or an isolated wedge of broken rock possibly originating from higher up the slope.
	F14d	Isolated, conductive zone within the bedrock, indicates a deterioration in bedrock condition (i.e. an increase of clay/water-bearing fractures) or change in bedrock lithology.
	F14e	Broad, laterally continuous zone of increased resistivity, indicating a decrease of clay and/or water within the bedrock (i.e. improved bedrock condition) and showing very good correlation with Layer S4/P5.
	F14f	Isolated, slightly more conductive zone, likely indicating an increase of clay and/or water within the superficial deposits.
	F14g	Poor correlation between Layers S4/P5 between 40 and 90m chainage, indicating that the seismic energy is travelling along different beddings or weathered zones, as is also observed in other profiles. Of further note are the significantly higher Layer S4 velocities to the south (1182 m/s), indicating a stronger, more competent bedrock to the south or change of bedrock lithology.
15	F15a	This resistive layer indicates a decrease of clay and/or water within the near-surface sediments (a possible increase of silt, or gravel of completely weathered limestone rock).
	F15b	The presence of much stiffer material on the MASW section correlates very well with the positions of Layers S4 and P5. This also correlates with a decrease in resistivity, which suggests a weathered zone at the top of the bedrock, or transition into the underlying Lias bedrock. Borehole DSRC109 indicates limestone bedrock but is located 38m away to the west. Alternatively, the laterally continuous and dipping resistive/conductive bands could be mapping out the different beds of limestone and siltstone/mudstone.
	F15c	Broader zone of increased conductivity indicates an increase of water/clay within the superficial deposits or change in sediment lithology. Borehole DSRC109 located 38m away indicates clay-rich sediments in the near-surface.

	F15d	Increase of resistivity correlates with a transition into a more competent bedrock unit, which also corresponds with the position of Layers S4/P5.
	F15e	Good correlation between Layers S4/P5 for the majority of the profile, indicating a transition into strong, competent bedrock given the high p-wave and s-wave velocities of 3283 m/s and 1176 m/s respectively. Overlying this is likely to be a weaker, more weathered limestone bedrock given the lower p-wave and s-wave velocities of 1662 m/s and 513 m/s respectively.
16	F16a	This resistive layer indicates a decrease of clay and/or water within the near-surface sediments and is also likely influenced by Layer S3, which is likely to represent weak, highly broken weathered limestone bedrock starting from around 2 m bgl.
	F16b	The presence of much stiffer material on the MASW section correlates very well with the positions of Layers S4 and P5 (particularly sharp boundary between 0 and 90 m chainage), and an increase of resistivity, revealing a significant improvement in bedrock (limestone) condition.
	F16c	Isolated, conductive zone within the bedrock, indicates a deterioration in bedrock condition (i.e. increase of clay/water-bearing fractures) or change in bedrock lithology (e.g. into Lias Group mudstones/siltstones)
	F16d	Broad, slightly more conductive zone, likely indicating an increase of clay and/or water within the superficial deposits. Borehole DSRC319 indicates clay-rich sediments at the surface.
	F16e	Good correlation between Layers S4/P5 for the majority of the profile. The correlation is lost towards the northern end of the section where there is a 'step-up' in Layer S4 only. Such discrepancies between bedrock boundaries can be due to the P and S-wave energy following different travel paths (e.g. different beddings within an interbedded bedrock, or different weathered zones, or faulting). The 'step-up' also correlates with a shallow, stiff zone in the MASW, likely indicating a shallower block of less weathered limestone.
17	F17a	This resistive layer indicates a decrease of clay and/or water within the near-surface sediments (silt or gravel of completely weathered limestone) and is also likely influenced by Layer S3, which is likely to represent weak, highly broken weathered limestone bedrock starting from around 2 m bgl.
	F17b	Broader zone of increased conductivity indicates an increase of

		water/clay within the superficial deposits or change in sediment lithology.
	F17c	The MASW section reveals a stiffer boundary, deeper than Layer S4 but above Layer P5, interpreted to be a stronger, more competent layer of limestone bedrock. Layer P5 may represent siltstones/mudstones from the underlying Lias Group (borehole DSRC109 indicates silt and siltstones at depth, underlying the limestone).
	F17d	Good correlation between Layer S4 and the MASW, indicating a transition into slightly stiffer bedrock. The corresponding decrease in resistivity may indicate a change of bedrock lithology.
	F17e	Abrupt, vertical boundary between conductive and resistive material possibly indicates the location of the NW-SE trending fault thought to pass very close to the northern end of Profile 17.
18	F18a	This resistive layer indicates a decrease of clay and/or water within the near-surface sediments (silt or gravel of completely weathered limestone) and is also likely influenced by Layer S3, which is likely to represent weak, highly broken weathered limestone bedrock starting from around 1 to 2 m bgl.
	F18b	Good correlation between Layer S4 and the MASW, indicating a transition into stiffer material, which given an s-wave velocity of 808 m/s represents moderately competent bedrock. The corresponding decrease in resistivity suggests a conductive bedrock unit rich in water and/or clay-bearing fractures or change of bedrock lithology.
	F18c	Broader zone of increased conductivity indicates an increase of water/clay within the superficial deposits or change in sediment lithology.
	F18d	Inclined, conductive feature may indicate a dipping bed of different lithology (e.g. mudstone) with limestone to the north and south, or a weaker zone of more conductive weathered limestone bedrock close to the fault.
	F18e	Isolated area of increased S-wave velocity, as noted on the MASW section, may indicate the presence of a block of limestone rock in the near-surface.
	F18f	Very good correlation between Layers S4 and P4. Although the s-wave velocity of 808 m/s indicates the presence of rock, the Layer P4 velocity is rather low for rock and is more typical of saturated, dense sediments.

		As such Layer P4 may possibly represent the top of a saturated zone/water table, which correlates with the top of the bedrock.
19	F19a	This resistive layer indicates a decrease of clay and/or water within the near-surface sediments (silt or gravel of completely weathered limestone) and is also likely influenced by Layer S3, which is likely to represent weak, highly broken weathered limestone bedrock starting from around 1 to 2 m bgl.
	F19b	Broader zone of increased conductivity indicates an increase of water/clay within the superficial deposits or change in sediment lithology.
	F19c	Isolated zone of increased resistivity, indicating a decrease of clay and/or water within the superficial deposits and/or underlying bedrock lithology, which is possibly related to the fault shown to pass close to the west. The feature may also be related to a number of highly resistive anomalies on the ground conductivity plot (F6).
	F19d	Laterally continuous increase in resistivity correlates very well with an increase in s-wave velocity and stiffness on the MASW section, as well as Layers S4/P4. This likely represents a transition onto competent limestone bedrock.
	F19e	Isolated zones of increased resistivity indicating localised improvements in bedrock condition (i.e. less water/clay-bearing fractures).
	F19f	Abrupt, vertical boundary between conductive and resistive material possibly indicates the location of a fault. This isn't shown on the BGS geology map, but may pass between Profiles 13 and 15 and be responsible for the sinuous shape shown to the Salperton and Aston Limestone Formations.
	F19g	Laterally continuous decrease in resistivity correlates very well with Layer P5, indicating a transition into a different bedrock lithology, likely siltstone or mudstone from the underlying Lias Group, given the results of borehole DSRC109, although this is located 43m away.
	F19h	Decrease in S-wave velocity to the east, from 1181 m/s to 837 m/s, is indicative of a deterioration in rock condition (e.g. increase of fractures). This appears to correlate with a general decrease in rock resistivity, and may be indicative of the NW to SE trending fault known to pass through this region, and which can be seen on the northern end of Profile 17.
	F19i	Layer S3 and the upper part of Layer S4 correlates with a laterally

		continuous conductive layer, which is likely to represent a weathered zone at the top of the limestone bedrock.

Table 6. *Features and anomalies of interest as identified by the seismic refraction and MASW surveys.*

5 CONCLUSIONS

- The geophysical surveys have provided a non-invasive means for investigating the subsurface with a high degree of 'spatial' coverage using the electromagnetic survey technique, and detailed profile cross-sections of ground composition using resistivity tomography and seismic refraction and MASW.

- The ground conductivity plots have revealed variations in near-surface sediment composition (notably clay content and saturation) and thickness, as well as mapping shallow bedrock. A number of services have also been shown to cross the surveyed areas, as highlighted.

- The modelled resistivity sections were characterised by zones of contrasting resistivity values that reflect lithological (including an increase/decrease in clay content), hydrogeological (e.g. groundwater level, saturated zones), structural (e.g. faults, steeply dipping beds) and weathering variations within the sub-surface.

- The analysis of both the P and S-wave refraction data has identified distinct velocity layers that have provided detailed information to assist with the bulk characterisation of the shallow subsurface and, in particular, the thickness of overburden sediments and depth to weathered and unweathered bedrock. In summary, five distinct layer boundaries have been identified by the P-wave refraction survey, with velocities ranging from <300 m/s (weak, loose sediments) to >1901 m/s (weathered to unweathered bedrock). This has been further characterised by the S-wave refraction survey, which has revealed up to four notable layers of increasing material stiffness from <180 m/s (weak, loose sediments) to >761 m/s (rock). Where layer velocities vary laterally, this may be due to structural changes such as faulting or steeply dipping bedding. Finally, zones of increased rock stiffness and/or deterioration in bedrock condition have been further highlighted by the results of the MASW survey.

- Available borehole data has been included on the cross-sections for direct correlation, and if any additional borehole data becomes available, it may be possible to extend further/refine the interpretation and calibrate the acquired datasets.

Disclaimer

This report represents an opinionated interpretation of the geophysical data. It is intended for guidance with follow-up invasive investigation. Features that do not produce measurable geophysical anomalies or are hidden by other features may remain undetected. Geophysical surveys complement invasive/destructive methods and provide a tool for investigating the subsurface; they do not produce data that can be taken to represent all of the ground conditions found within the surveyed area. Areas that have not been surveyed due to obstructed access or any other reason are excluded from the interpretation.

FIGURES

KEY

- Resistivity/Seismic Profile
- EM 'ground conductivity' survey extents
- Proposed road scheme

See individual line figures for start and end coordinates and profile orientation

KEY TO BGS GEOLOGY MAP

(Taken from the British Geological Survey Geology of Britain viewer, bedrock geology only)

- Lias
- Birdlip Limestone Formation
- Aston Limestone Formation
- Salperton Limestone Formation
- Fullers Earth Formation
- Hampen Formation
- White Limestone Formation
- Great Oolite Group
- Fault (expected location)

Source: Map data ©2020 Google.

Title: OVERALL LOCATION PLAN (ZONES 1 TO 4)	TERRA DAT down to earth geophysics		Tel: +44 (0) 2920 700127 Web:www.terradat.co.uk Email: web@terradat.co.uk
Project: A417 CRICKLEY HILL BIRDLIP	Scale: 1:15000 at A3 Drawn by/Ref: MB/6688/1 Date: 23 JULY 2020	FIGURE 1	

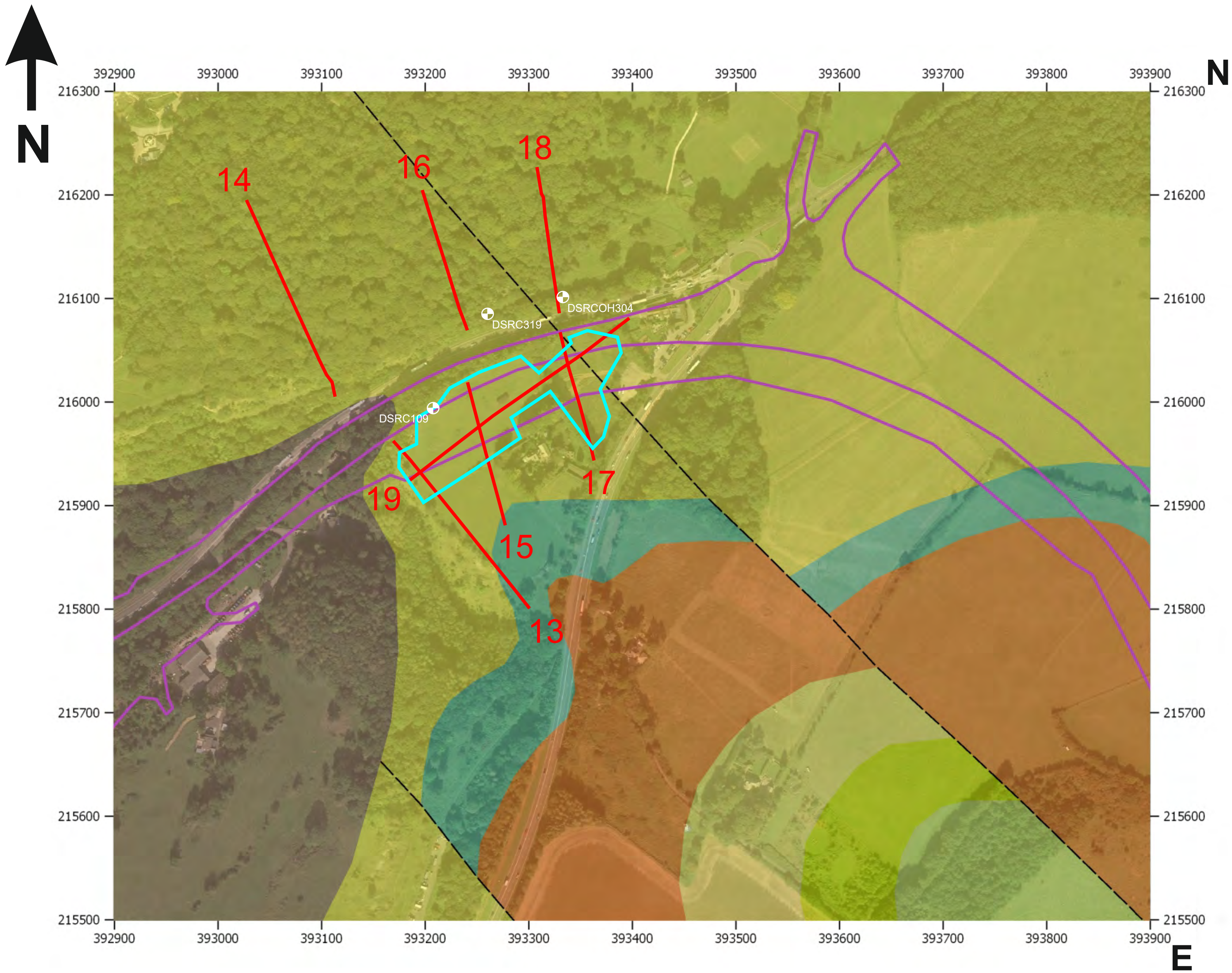

KEY

- Resistivity/Seismic Profile
- EM Survey Extents
- Proposed road scheme
- Borehole

KEY TO BGS GEOLOGY MAP

(Taken from the British Geological Survey Geology of Britain viewer, bedrock geology only)

- Lias
- Birdlip Limestone Formation
- Aston Limestone Formation
- Salperton Limestone Formation
- Fullers Earth Formation
- Hampen Formation
- --- Fault (expected location)

NOTES

1. See individual line figures for start and end coordinates and profile orientation

Source: Map data ©2020 Google.

Project: **BIRDLIP**

Title: **LOCATION MAP (ZONE 1)**

TERRA DAT down to earth geophysics

Tel: +44 (0) 2920 700127
Web:www.terradat.co.uk
Email: web@terradat.co.uk

Scale: 1:6000 at A4
Drawn by/Ref: MB/6688/2
Date: 09 JULY 2020

FIGURE 2

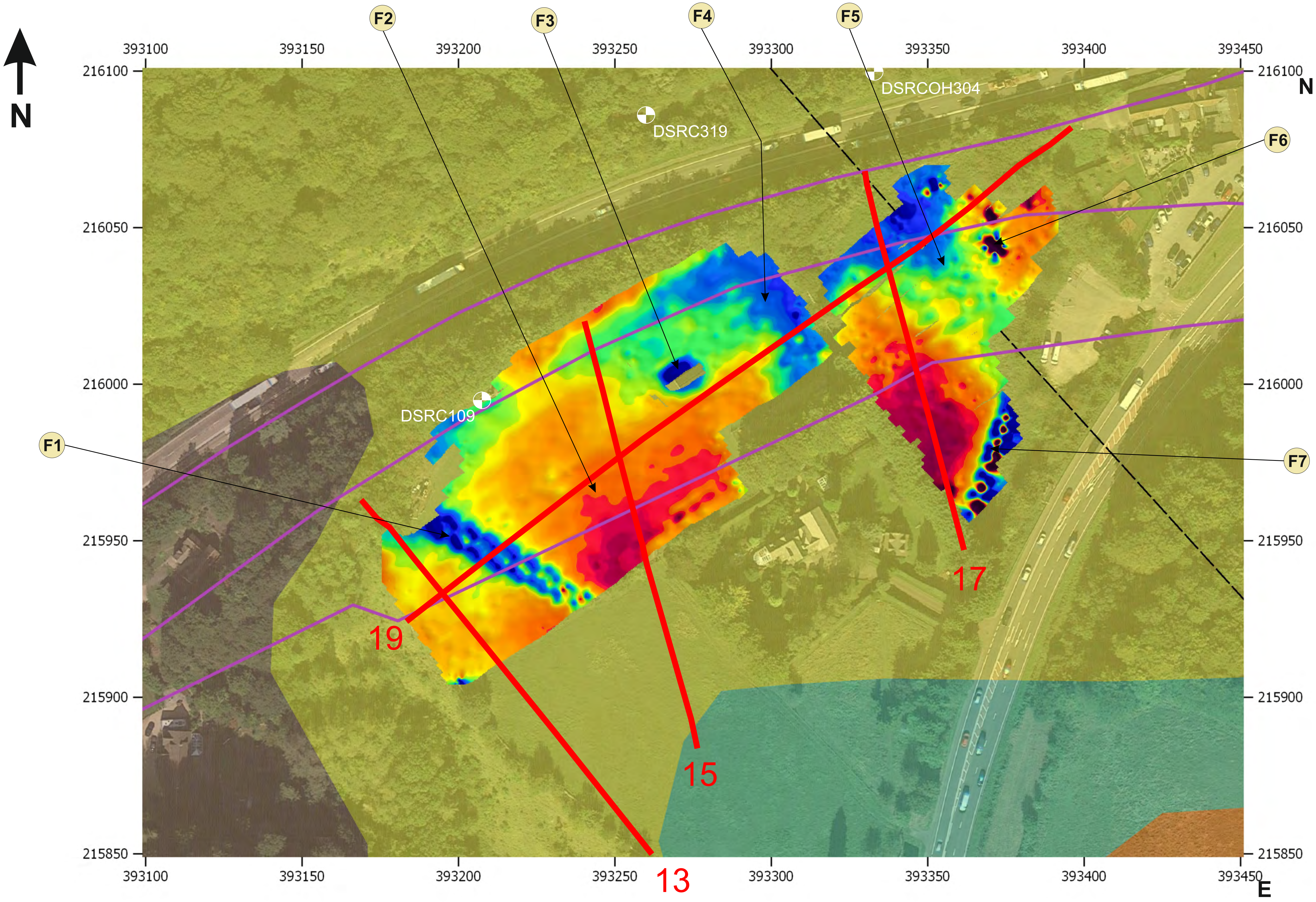

NOTES

1. See individual line figures for start and end coordinates

KEY TO BGS GEOLOGY MAP

(Taken from the British Geological Survey Geology of Britain viewer, bedrock geology only)

- Lias
- Birdlip Limestone Formation
- Aston Limestone Formation
- Salperton Limestone Formation
- Fullers Earth Formation
- Hampen Formation
- Fault (expected location)

COLOUR SCALE

CONDUCTIVITY (mS/m)

KEY

- Resistivity profile
- Proposed road scheme
- Borehole

Title:	EM GROUND CONDUCTIVITY (ZONE 1)
Project:	A417 CRICKLEY HILL BIRDLIP
Scale:	1:1250 @ A3
Drawn by/Ref:	MB/6688/3
Date:	14 JULY 2020

TERRA DAT down to earth geophysics

Tel: +44 (0) 2920 700127
Web:www.terradat.co.uk
Email: web@terradat.co.uk

FIGURE 3

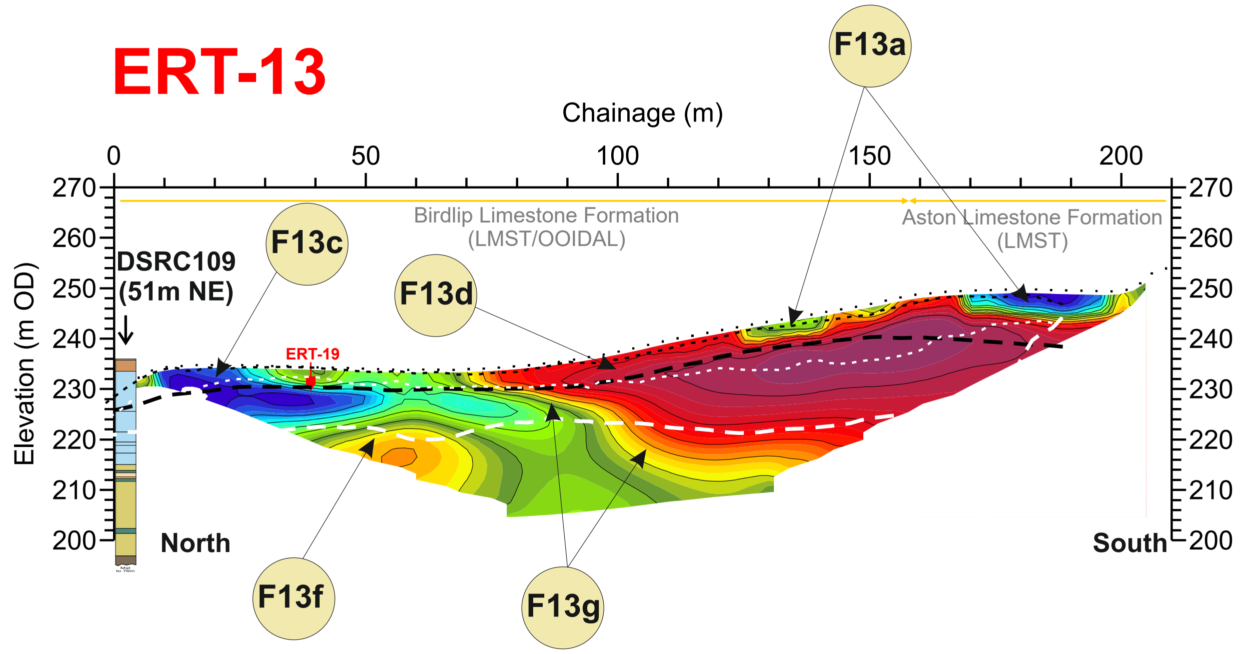

ERT-13 Profile Coordinates	
0m Chainage	207m Chainage
393169.2E 215962.5N	393300.0E 215802.1N

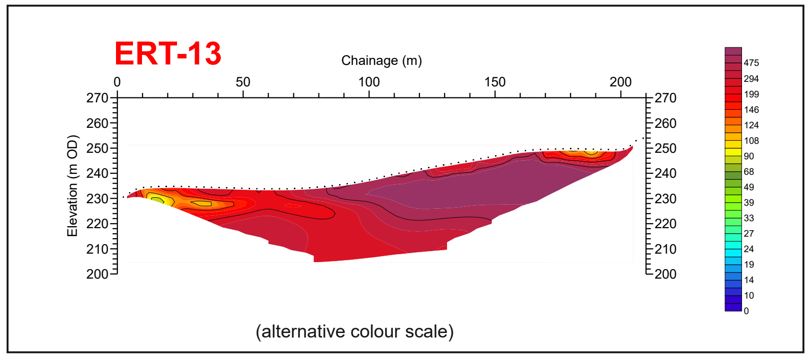

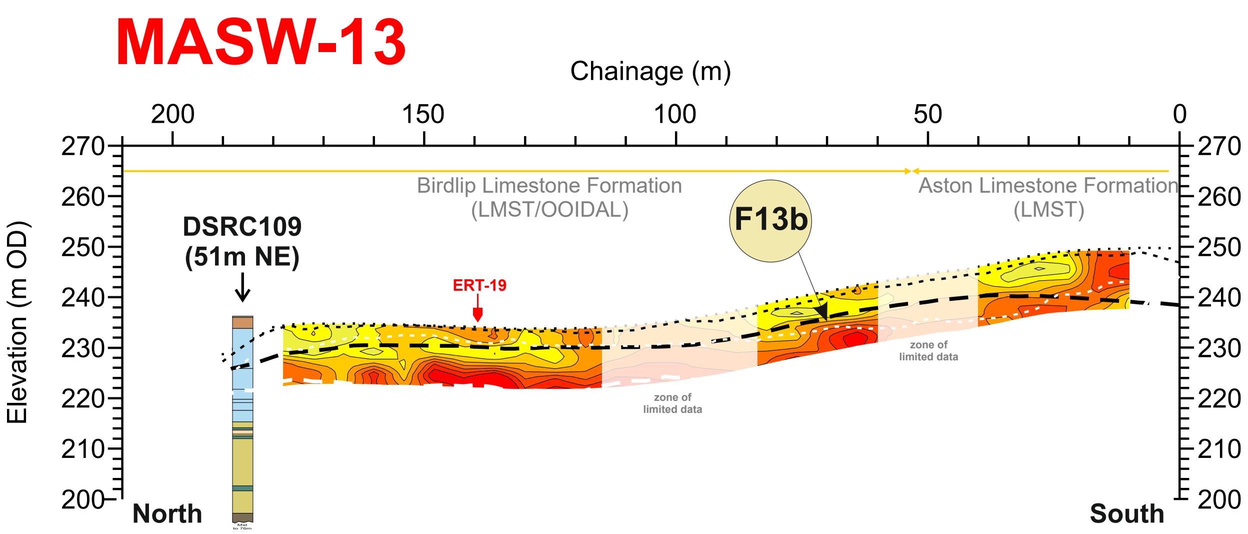

MASW-13 Profile Coordinates	
0m Chainage	190m Chainage
393285.6E 215818.7N	393169.2E 215962.5N

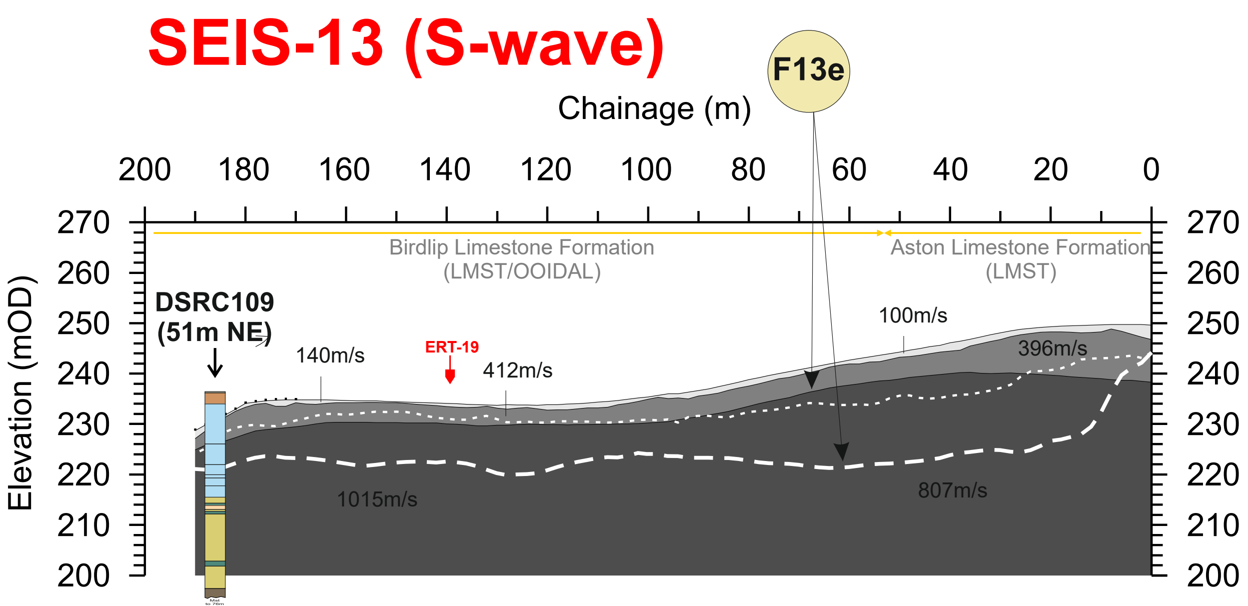

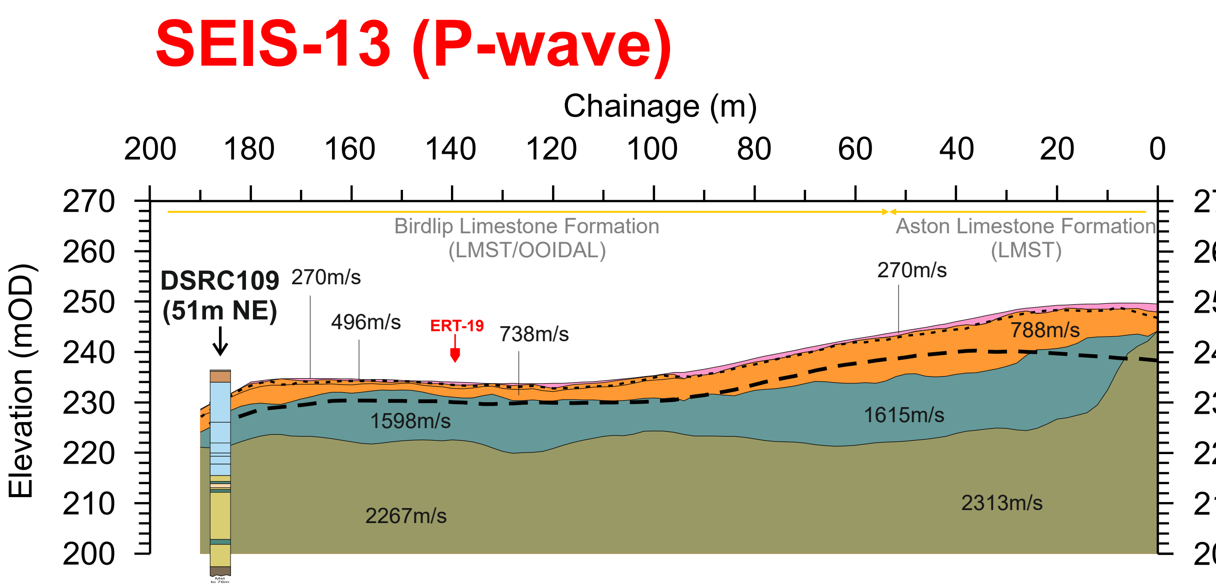

SEIS-13 Profile Coordinates	
0m Chainage	190m Chainage
393285.6E 215818.7N	393169.2E 215962.5N

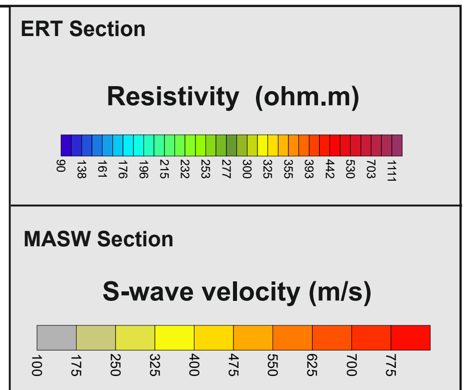

S-wave Refraction velocity layers

- Layer 1 (<180 m/s) SOFT SOIL*
- Layer 2 (180 - 360 m/s) STIFF SOIL*
- Layer 3 (361- 760 m/s) VERY DENSE SOIL / SOFT(WEAK**) ROCK*
- Layer 4 (>761 m/s) ROCK* (MODERATELY STRONG**)

S-wave boundaries shown on ERT, MASW and S-wave sections

**The NEHRP Recommended Provisions for seismic regulation for new buildings, (FEMA-222A and FEMA-223A, 1994)*

*** UK equivalent classification (Waltham, 1994)*

P-wave Refraction velocity layers

- Layer 1 (<300 m/s)
- Layer 2 (301 - 800 m/s)
- Layer 3 (801 - 1400 m/s)
- Layer 4 (1401- 1900m/s)
- Layer 5 (>1901 m/s)

P-wave boundaries shown on ERT, MASW and S-wave sections

BOREHOLE KEY

Made ground	Sandstone
Clay	Mudstone
Silt	Siltstone
Sand	Limestone
Gravel	Core loss

KEY

- Line 1 — Profile intersection
- Fault — Reported fault positions
- Bedrock geology subcrop

NOTES/OBSERVATIONS

Title: **ERT AND SEISMIC PROFILES**

Project: **A417 CRICKLEY HILL BIRDLIP**

TERRA DAT down to earth geophysics
Tel: +44 (0) 2920 700127
Web:www.terradat.co.uk
Email: web@terradat.co.uk

Scale: 1:1500 at A3
Drawn by/Ref: JT/6688/4
Date: 14 FEB 2020

FIGURE 4

ERT-14

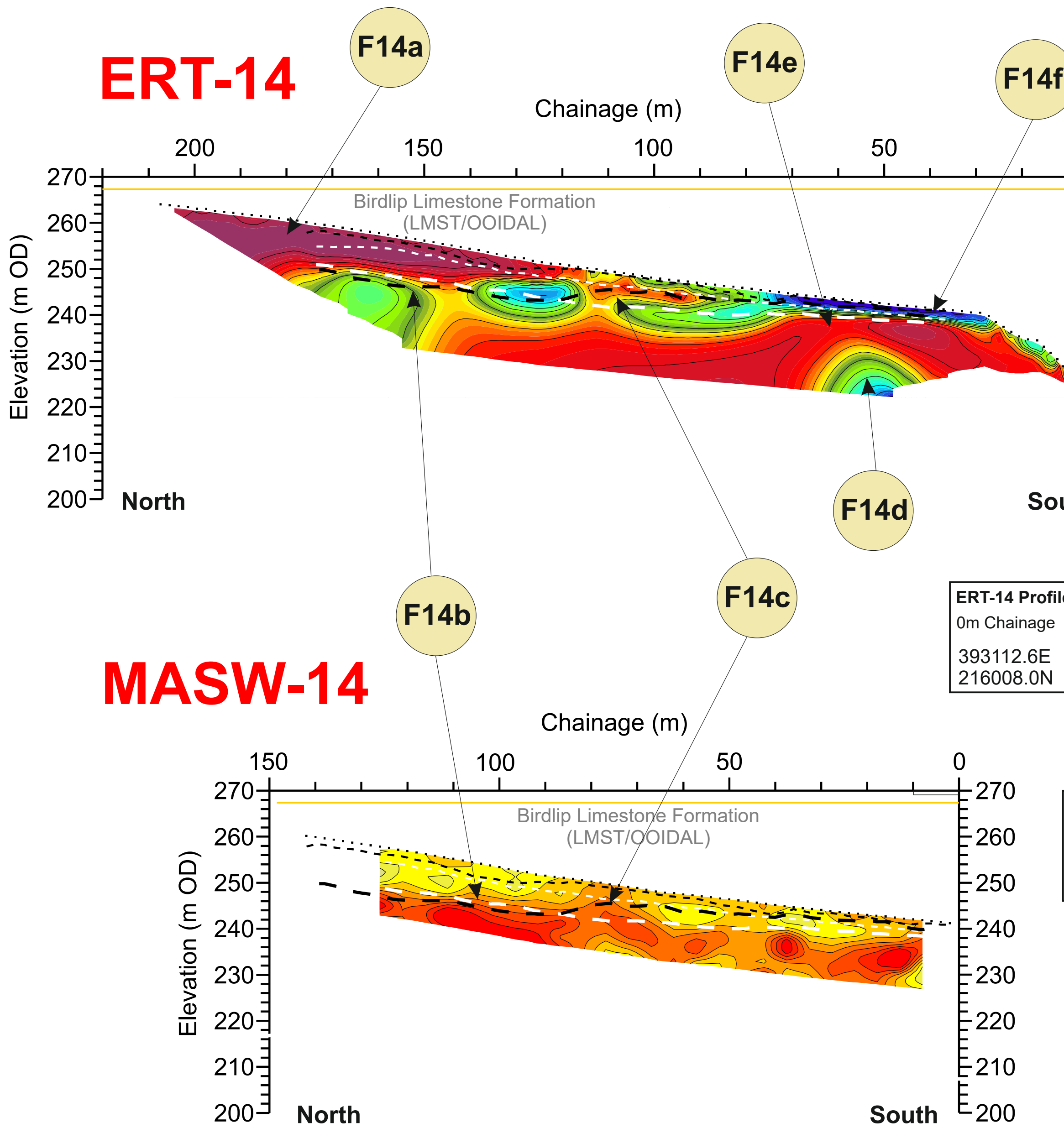

ERT-14 Profile Coordinates	
0m Chainage	214m Chainage
393112.6E 216008.0N	393027.6E 216195.4N

MASW-14 Profile Coordinates	
0m Chainage	142m Chainage
393098.2E 216038.3N	393040.0E 216167.3N

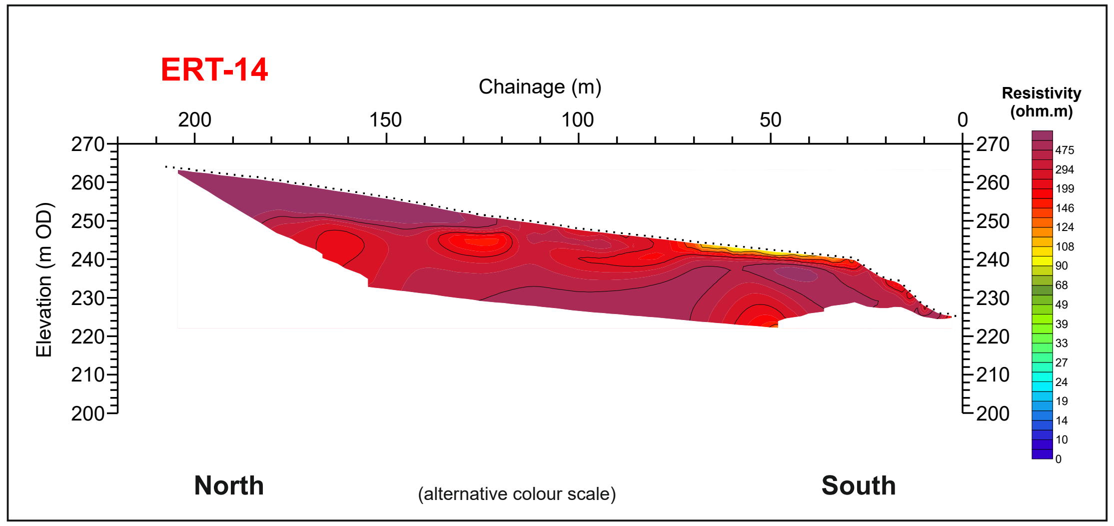

SEIS-14 (S-wave)

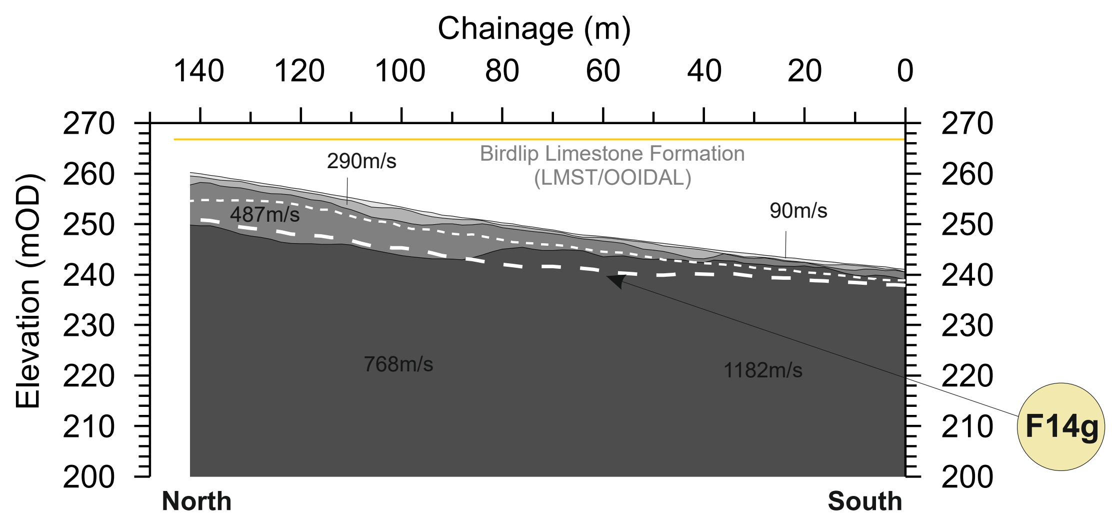

SEIS-14 (P-wave)

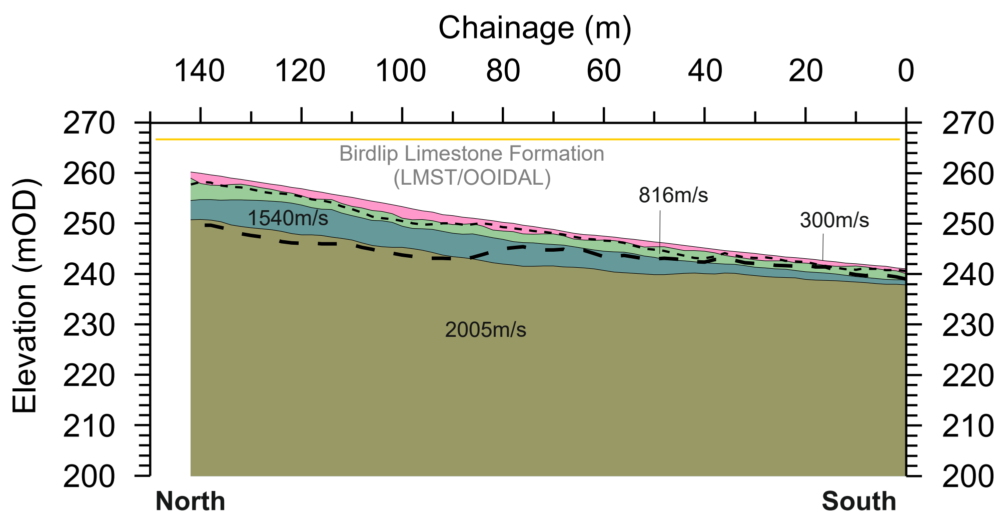

SEIS-14 Profile Coordinates	
0m Chainage	142m Chainage
393098.2E 216038.3N	393040.0E 216167.3N

ERT Section

Resistivity (ohm.m)

90 138 161 176 196 215 232 253 277 300 325 355 393 442 530 703 1111

MASW Section

S-wave velocity (m/s)

100 175 250 325 400 475 550 625 700 775

S-wave Refraction velocity layers

- Layer 1 (<180 m/s) SOFT SOIL*
- Layer 2 (180 - 360 m/s) STIFF SOIL*
- Layer 3 (361- 760 m/s) VERY DENSE SOIL / SOFT(WEAK**) ROCK*
- Layer 4 (>761 m/s) ROCK* (MODERATELY STRONG**)

S-wave boundaries shown on ERT, MASW and S-wave sections

*The NEHRP Recommended Provisions for seismic regulation for new buildings, (FEMA-222A and FEMA-223A, 1994)

** UK equivalent classification (Waltham, 1994)

P-wave Refraction velocity layers

- Layer 1 (<300 m/s)
- Layer 2 (301 - 800 m/s)
- Layer 3 (801 - 1400 m/s)
- Layer 4 (1401- 1900m/s)
- Layer 5 (>1901 m/s)

P-wave boundaries shown on ERT, MASW and S-wave sections

BOREHOLE KEY

Made ground	Sandstone
Clay	Mudstone
Silt	Siltstone
Sand	Limestone
Gravel	Core loss

KEY

- Line 1 — Profile intersection
- Fault — Reported fault positions
- Bedrock geology subcrop

NOTES/OBSERVATIONS

Title: ERT AND SEISMIC PROFILES

Project: A417 CRICKLEY HILL BIRDLIP

TERRA DAT down to earth geophysics

Tel: +44 (0) 2920 700127
Web:www.terradat.co.uk
Email: web@terradat.co.uk

Scale:	1:1500 at A3
Drawn by/Ref:	JT/6688/5
Date:	14 FEB 2020

FIGURE 5

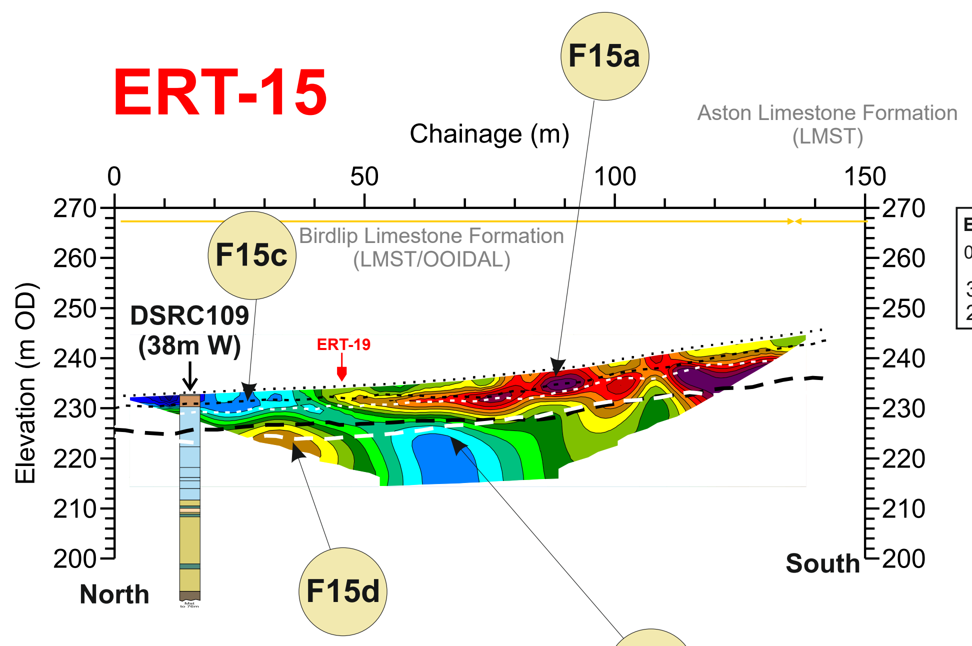

ERT-15 Profile Coordinates	
0m Chainage	141m Chainage
393240.9E 216019.6N	393276.9E 215883.1N

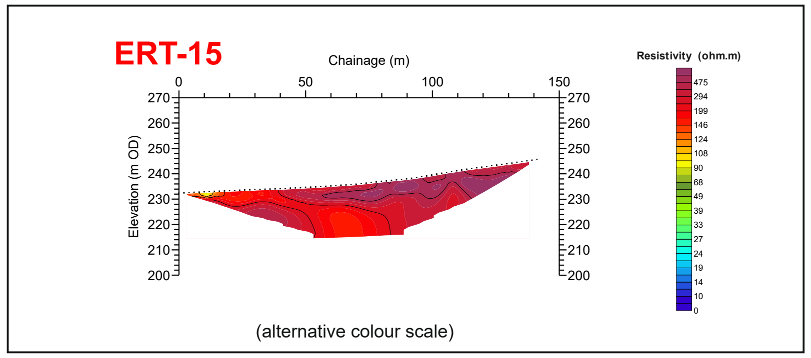

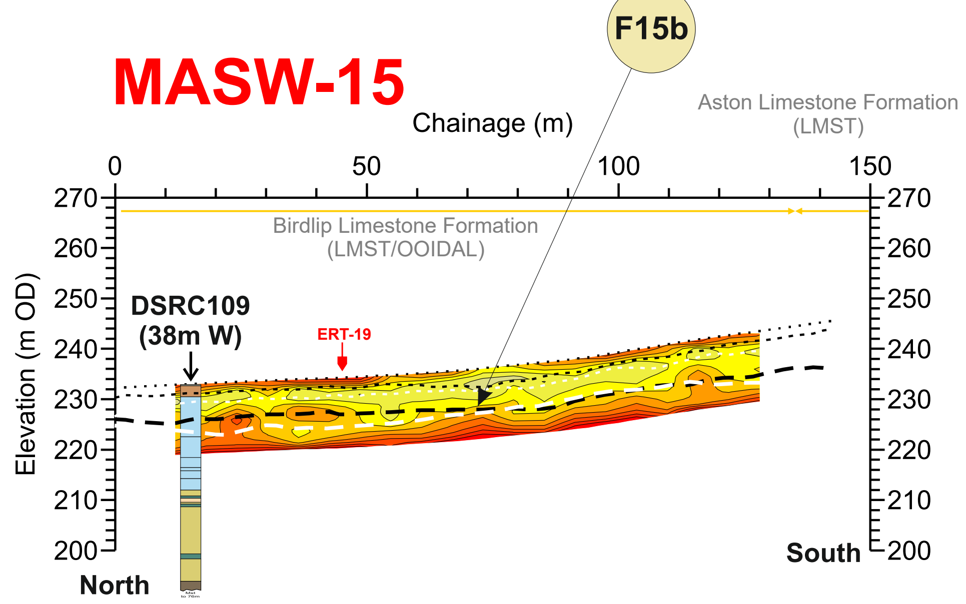

MASW-15 Profile Coordinates	
0m Chainage	141m Chainage
393239.9E 216021.9N	393276.6E 215884.4N

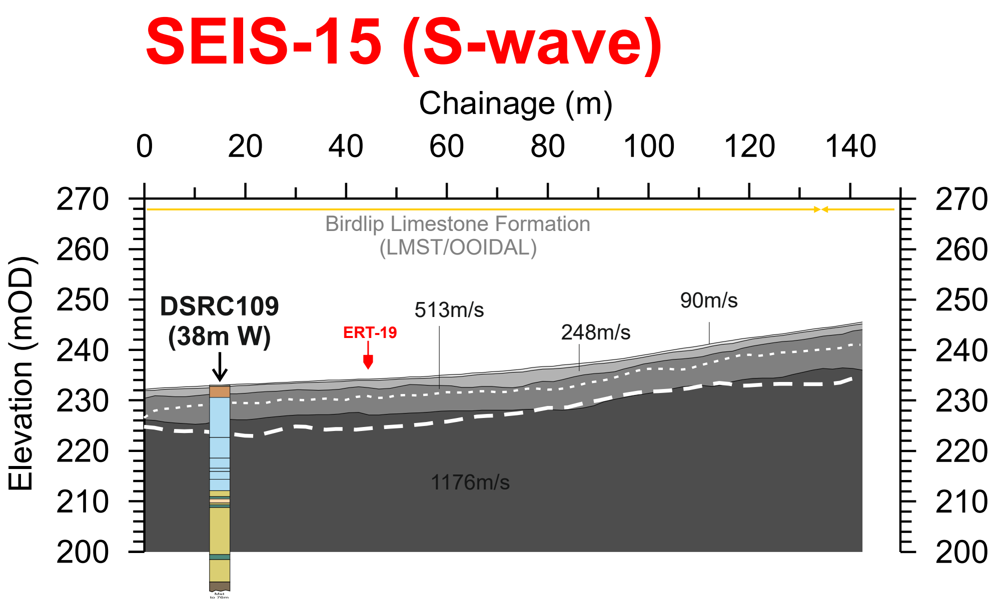

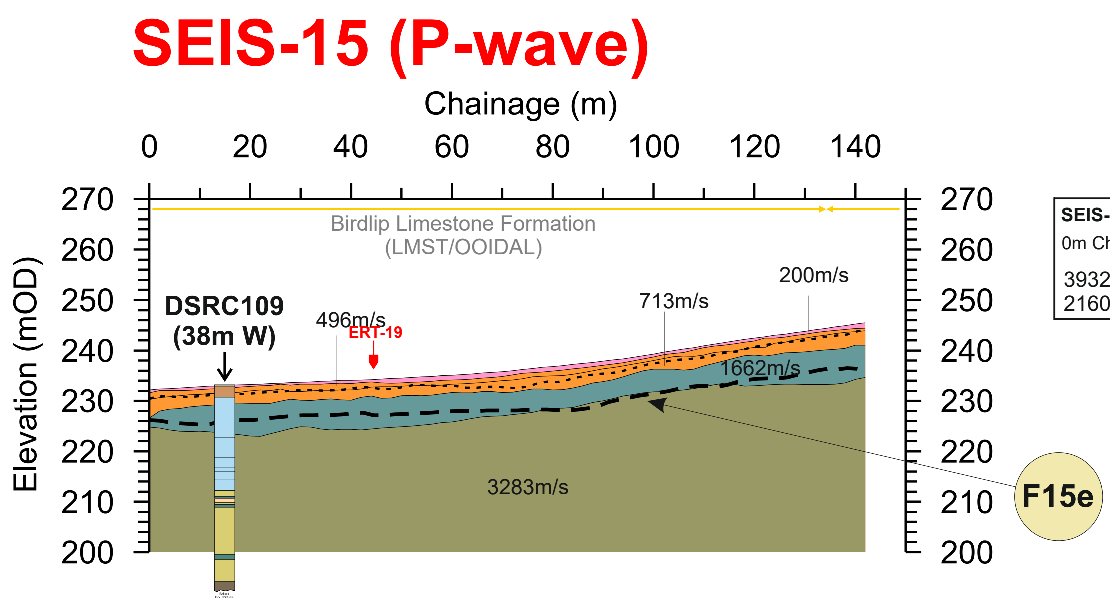

SEIS-15 Profile Coordinates	
0m Chainage	141m Chainage
393239.9E 216021.9N	393276.6E 215884.4N

ERT Section

Resistivity (ohm.m)

0, 95, 110, 127, 147, 169, 195, 225, 260, 300, 347, 400, 462, 533, 615, 710, 820, 1017

MASW Section

S-wave velocity (m/s)

100, 175, 250, 325, 400, 475, 550, 625, 700, 775

S-wave Refraction velocity layers

- Layer 1 (<180 m/s) SOFT SOIL*
- Layer 2 (180 - 360 m/s) STIFF SOIL*
- Layer 3 (361- 760 m/s) VERY DENSE SOIL / SOFT(WEAK**) ROCK*
- Layer 4 (>761 m/s) ROCK* (MODERATELY STRONG**)

S-wave boundaries shown on ERT, MASW and S-wave sections

*The NEHRP Recommended Provisions for seismic regulation for new buildings, (FEMA-222A and FEMA-223A, 1994)

** UK equivalent classification (Waltham, 1994)

P-wave Refraction velocity layers

- Layer 1 (<300 m/s)
- Layer 2 (301 - 800 m/s)
- Layer 3 (801 - 1400 m/s)
- Layer 4 (1401- 1900m/s)
- Layer 5 (>1901 m/s)

P-wave boundaries shown on ERT, MASW and S-wave sections

BOREHOLE KEY

Made ground, Clay, Silt, Sand, Gravel, Sandstone, Mudstone, Siltstone, Limestone, Core loss

KEY

Line 1 — Profile intersection

Fault — Reported fault positions

Bedrock geology subcrop

NOTES/OBSERVATIONS

Title: ERT AND SEISMIC PROFILES

Project: A417 CRICKLEY HILL BIRDLIP

TERRA DAT down to earth geophysics
Tel: +44 (0) 2920 700127
Web:www.terradat.co.uk
Email: web@terradat.co.uk

Scale: 1:1500 at A3

Drawn by/Ref: JT/6688/6

Date: 14 FEB 2020

FIGURE 6

ERT-16

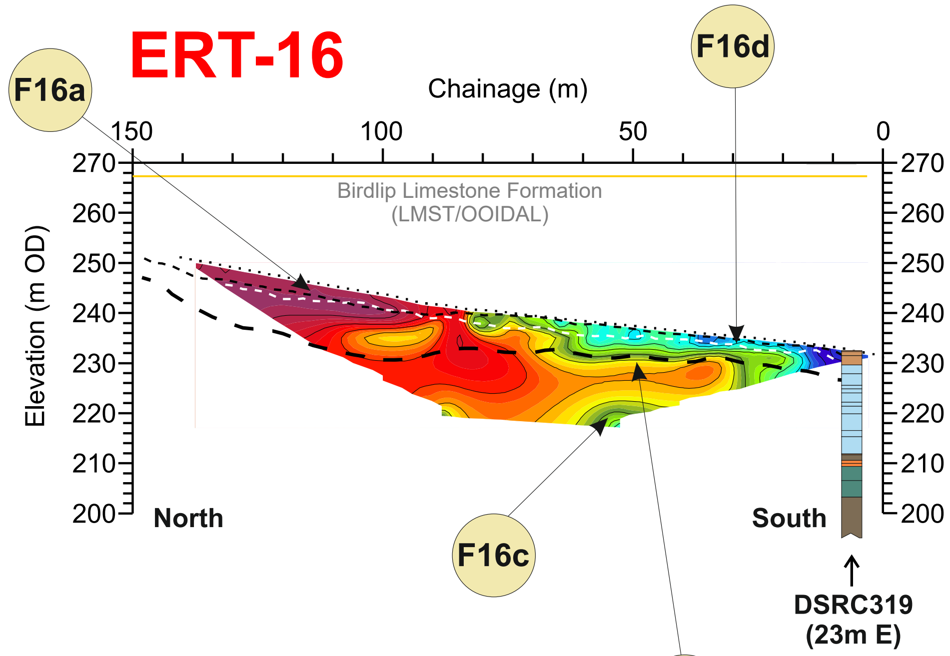

ERT-16 Profile Coordinates

0m Chainage	142m Chainage
393240.1E 216071.7N	393197.2E 216204.9N

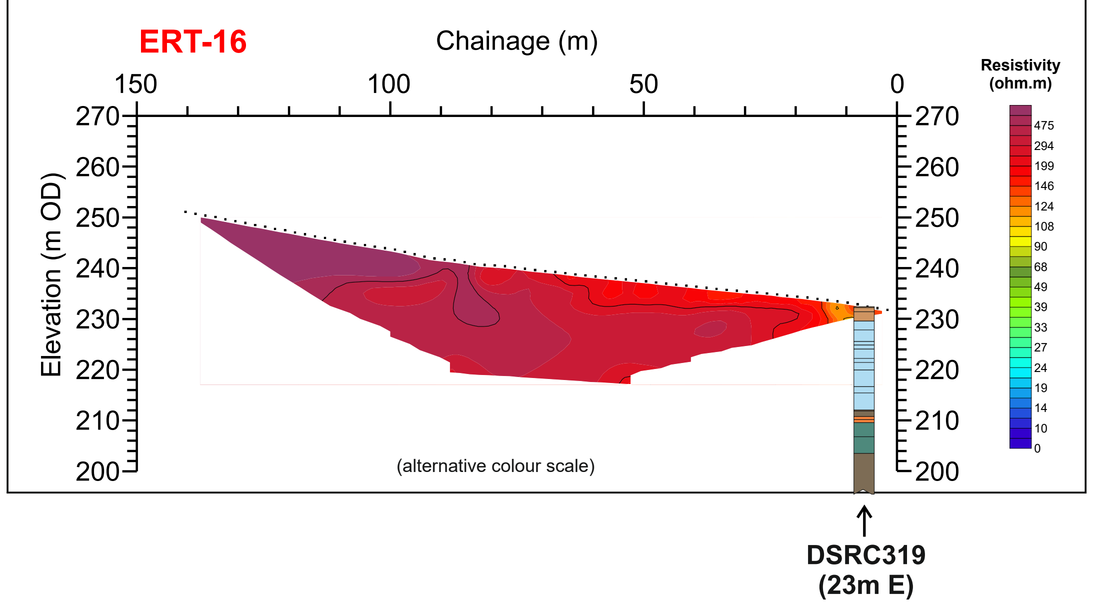

MASW-16

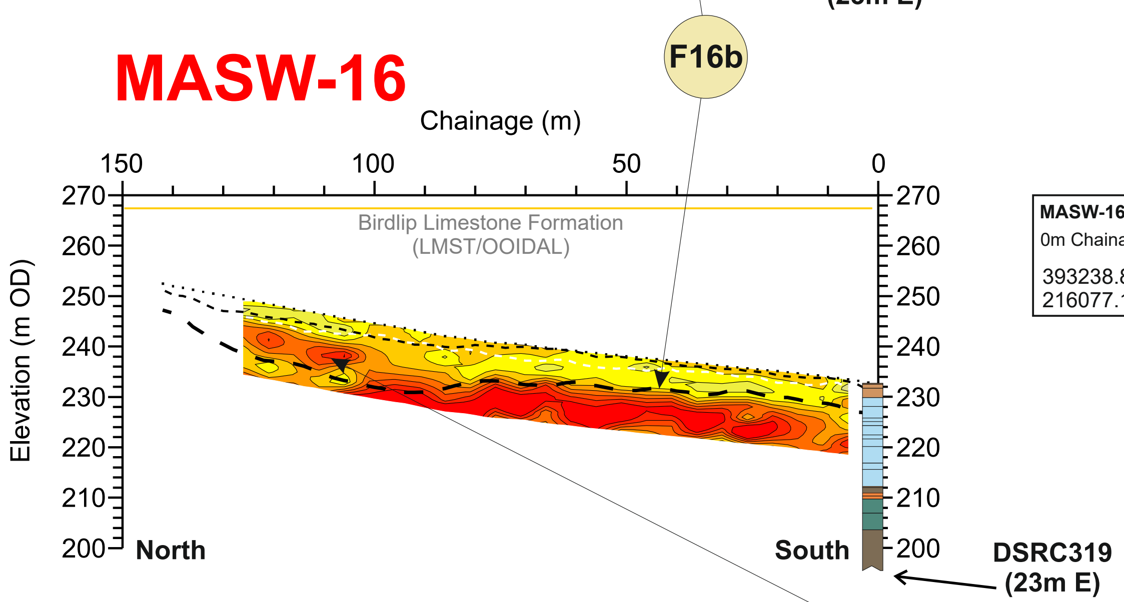

MASW-16 Profile Coordinates

0m Chainage	142m Chainage
393238.8E 216077.1N	393194.8E 216211.3N

SEIS-16 (S-wave)

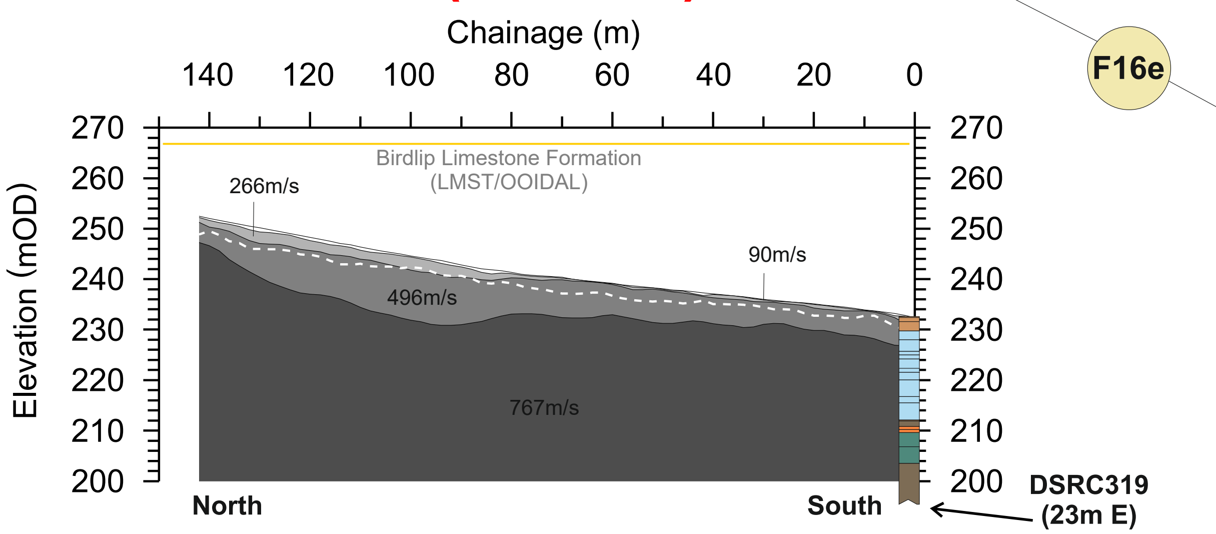

SEIS-16 (P-wave)

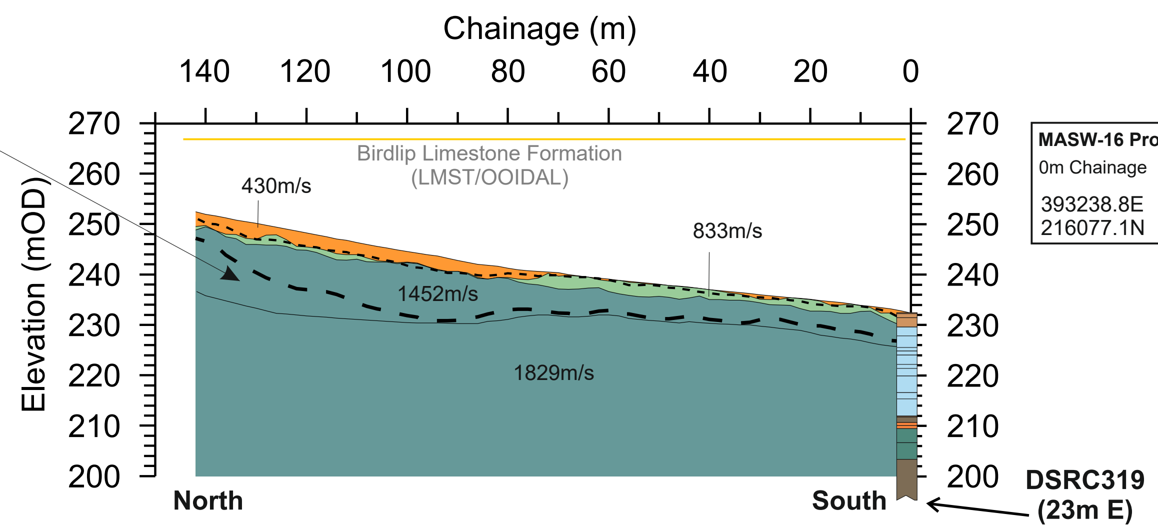

MASW-16 Profile Coordinates

0m Chainage	142m Chainage
393238.8E 216077.1N	393194.8E 216211.3N

ERT Section

Resistivity (ohm.m)

90, 138, 161, 176, 196, 215, 232, 253, 277, 300, 325, 355, 393, 442, 530, 703, 1111

MASW Section

S-wave velocity (m/s)

100, 175, 250, 325, 400, 475, 550, 625, 700, 775

S-wave Refraction velocity layers

- Layer 1 (<180 m/s) — SOFT SOIL*
- Layer 2 (180 - 360 m/s) — STIFF SOIL*
- Layer 3 (361- 760 m/s) — VERY DENSE SOIL / SOFT(WEAK**) ROCK*
- Layer 4 (>761 m/s) — ROCK* (MODERATELY STRONG**)

S-wave boundaries shown on ERT, MASW and S-wave sections

**The NEHRP Recommended Provisions for seismic regulation for new buildings, (FEMA-222A and FEMA-223A, 1994)*

*** UK equivalent classification (Waltham, 1994)*

P-wave Refraction velocity layers

- Layer 1 (<300 m/s)
- Layer 2 (301 - 800 m/s)
- Layer 3 (801 - 1400 m/s)
- Layer 4 (1401- 1900m/s)
- Layer 5 (>1901 m/s)

P-wave boundaries shown on ERT, MASW and S-wave sections

BOREHOLE KEY

Made ground	Sandstone
Clay	Mudstone
Silt	Siltstone
Sand	Limestone
Gravel	Core loss

KEY

- Line 1 — Profile intersection
- Fault — Reported fault positions
- Bedrock geology subcrop

NOTES/OBSERVATIONS

Title: ERT AND SEISMIC PROFILES

Project: A417 CRICKLEY HILL BIRDLIP

TERRA DAT
down to earth geophysics
Tel: +44 (0) 2920 700127
Web:www.terradat.co.uk
Email: web@terradat.co.uk

Scale:	1:1500 at A3
Drawn by/Ref:	JT/6688/7
Date:	14 FEB 2020

FIGURE 7

ERT-17

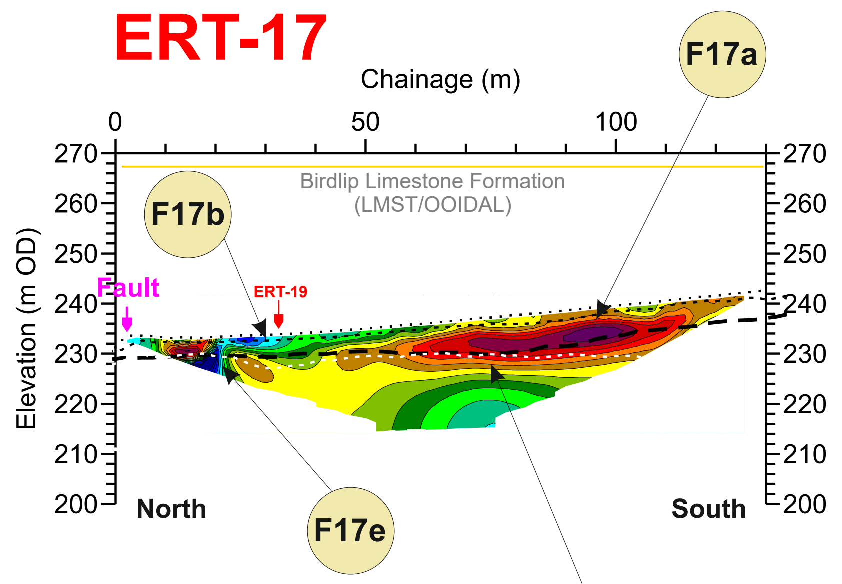

ERT-17 Profile Coordinates	
0m Chainage	126m Chainage
393330.8E 216067.8N	393362.6E 215946.4N

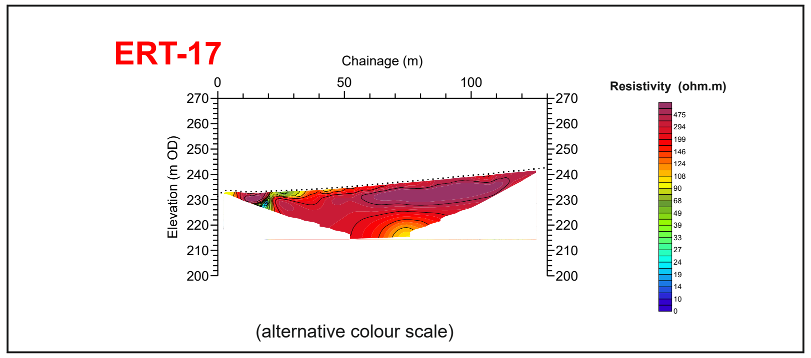

MASW-17

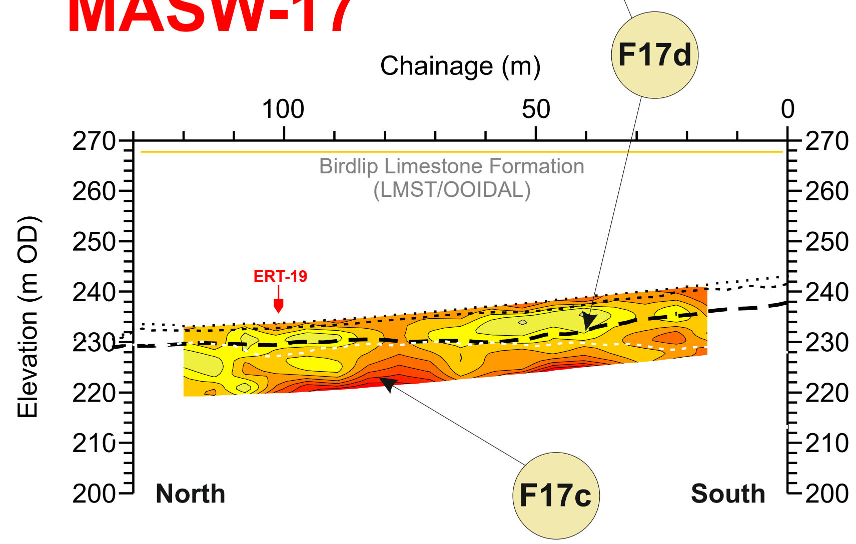

MASW-17 Profile Coordinates	
0m Chainage	136m Chainage
393365.7E 215941.3N	393331.6E 216069.8N

SEIS-17 (S-wave)

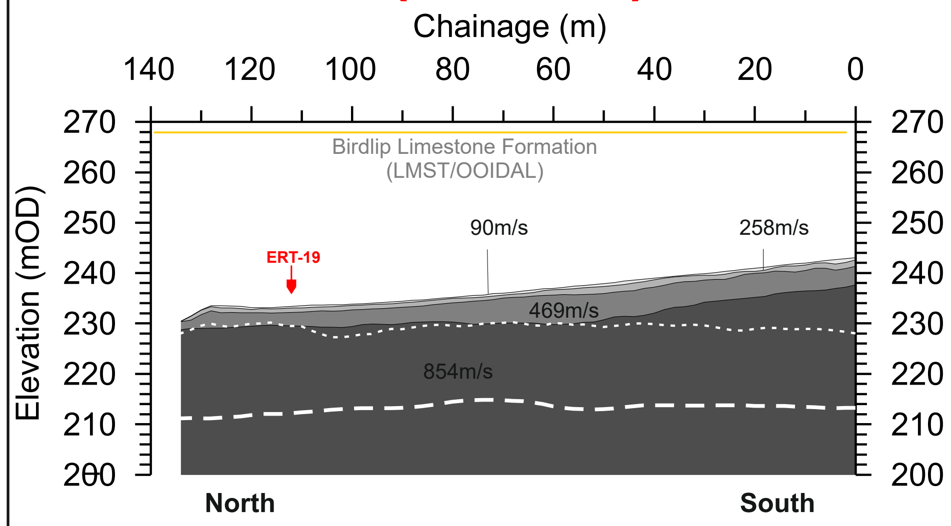

SEIS-17 (P-wave)

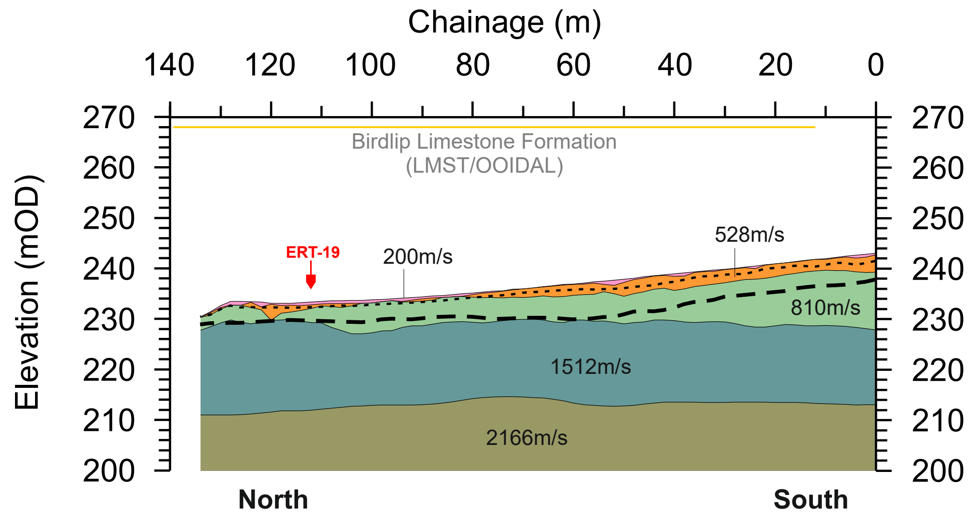

SEIS-17 Profile Coordinates	
0m Chainage	136m Chainage
393365.7E 215941.3N	393331.6E 216069.8N

ERT Section

Resistivity (ohm.m)

0, 29, 37, 48, 61, 78, 101, 129, 165, 212, 272, 349, 447, 573, 735, 943, 1209, 1757

MASW Section

S-wave velocity (m/s)

100, 175, 250, 325, 400, 475, 550, 625, 700, 775

S-wave Refraction velocity layers

- Layer 1 (<180 m/s) SOFT SOIL*
- Layer 2 (180 - 360 m/s) STIFF SOIL*
- Layer 3 (361- 760 m/s) VERY DENSE SOIL / SOFT(WEAK**) ROCK*
- Layer 4 (>761 m/s) ROCK* (MODERATELY STRONG**)

S-wave boundaries shown on ERT, MASW and S-wave sections

**The NEHRP Recommended Provisions for seismic regulation for new buildings, (FEMA-222A and FEMA-223A, 1994)*

*** UK equivalent classification (Waltham, 1994)*

P-wave Refraction velocity layers

- Layer 1 (<300 m/s)
- Layer 2 (301 - 800 m/s)
- Layer 3 (801 - 1400 m/s)
- Layer 4 (1401- 1900m/s)
- Layer 5 (>1901 m/s)

P-wave boundaries shown on ERT, MASW and S-wave sections

BOREHOLE KEY

Made ground, Sandstone, Clay, Mudstone, Silt, Siltstone, Sand, Limestone, Gravel, Core loss

KEY

- Line 1 — Profile intersection
- Fault — Reported fault positions
- Bedrock geology subcrop

NOTES/OBSERVATIONS

Title: ERT AND SEISMIC PROFILES

Project: A417 CRICKLEY HILL BIRDLIP

TERRA DAT — down to earth geophysics

Tel: +44 (0) 2920 700127
Web:www.terradat.co.uk
Email: web@terradat.co.uk

Scale:	1:1500 at A3
Drawn by/Ref:	JT/6688/8
Date:	14 FEB 2020

FIGURE 8

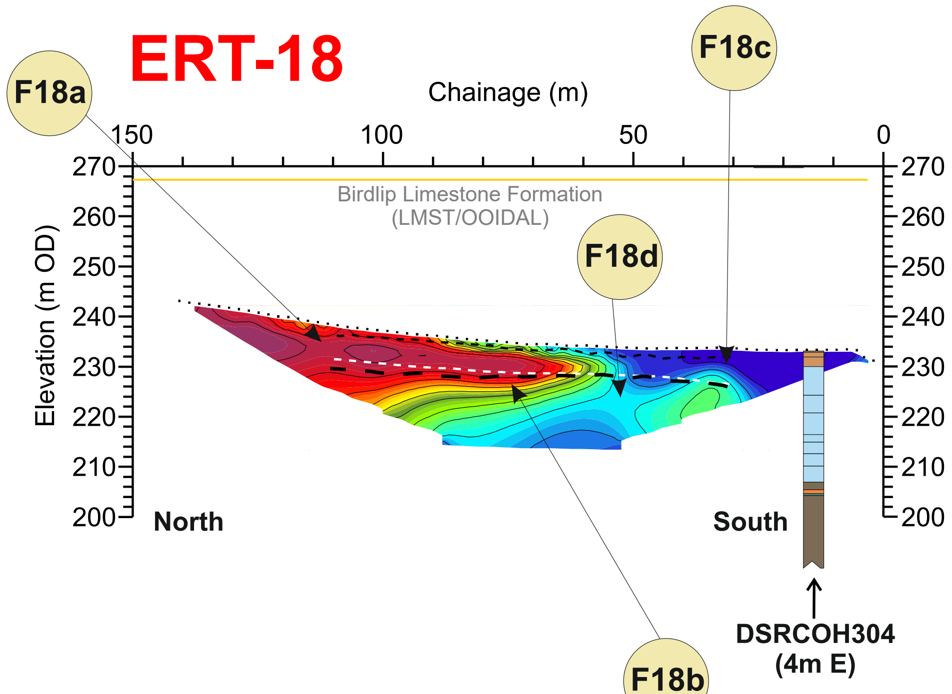

ERT-18 Profile Coordinates	
0m Chainage	142m Chainage
393329.3E 216088.1N	393307.9E 216227.0N

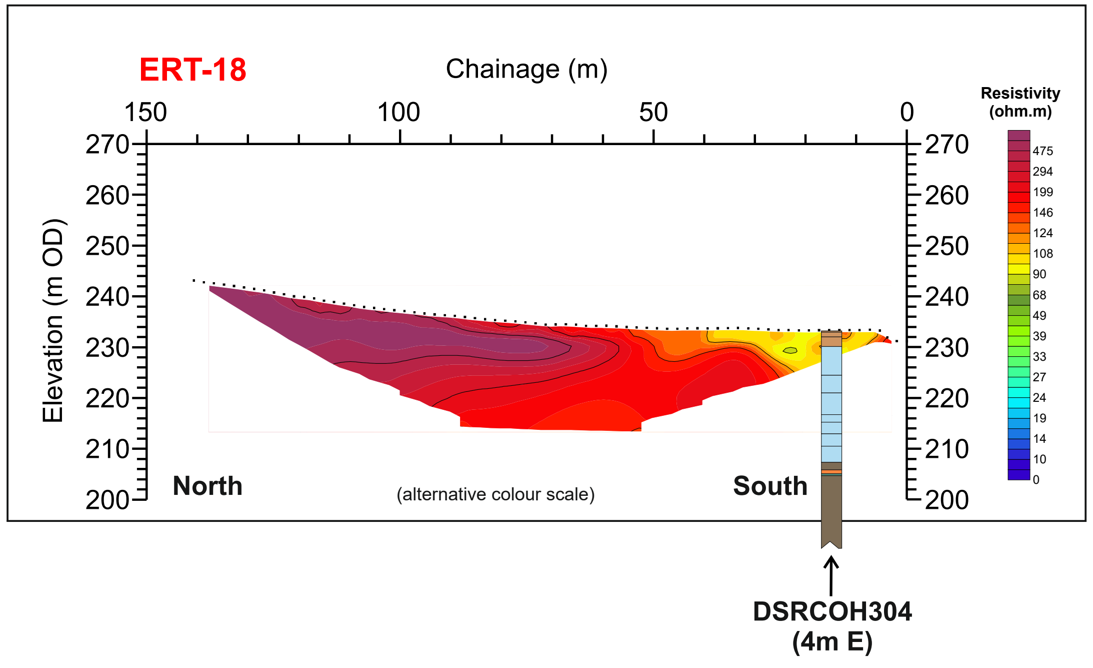

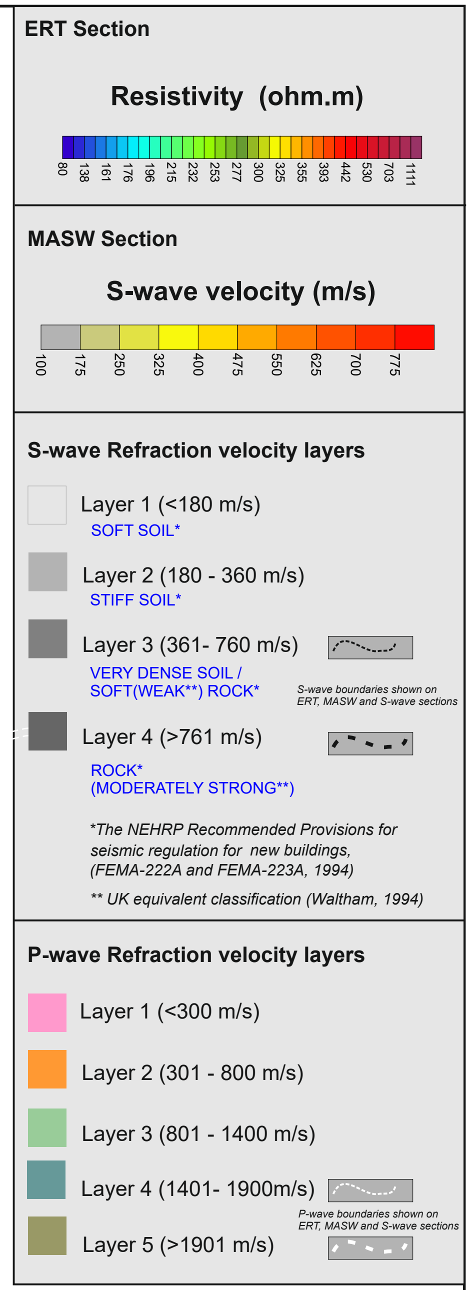

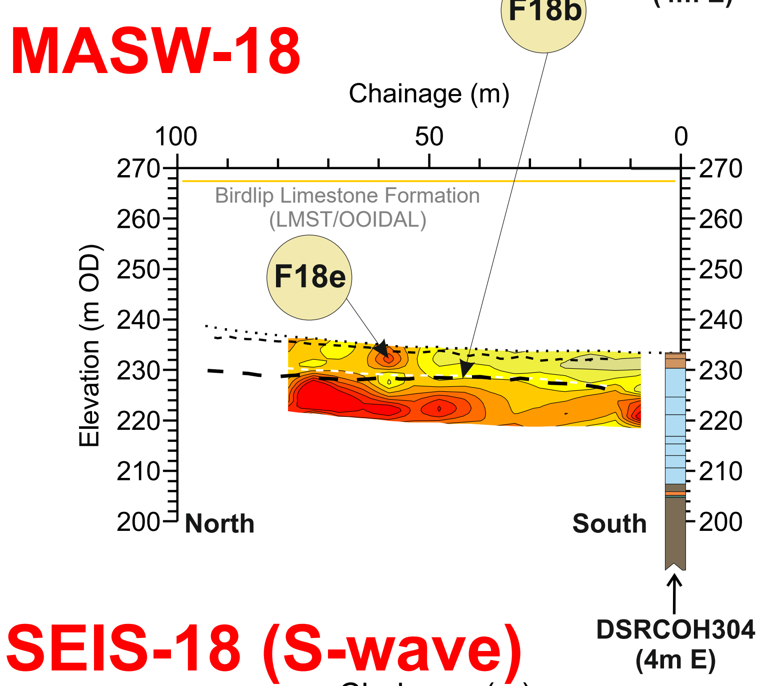

MASW-18 Profile Coordinates	
0m Chainage	94m Chainage
393327.8E 216104.6N	393312.1E 216197.5N

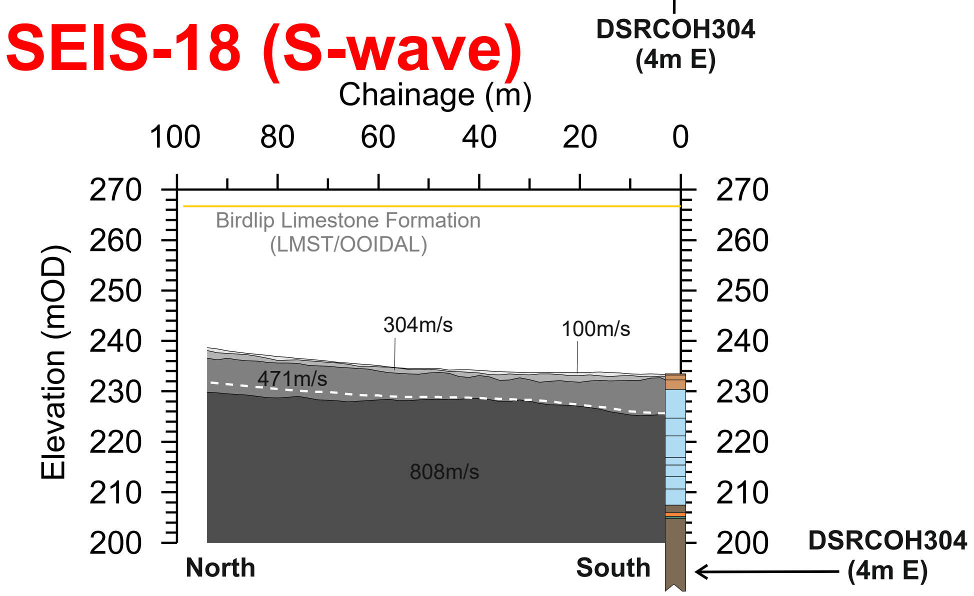

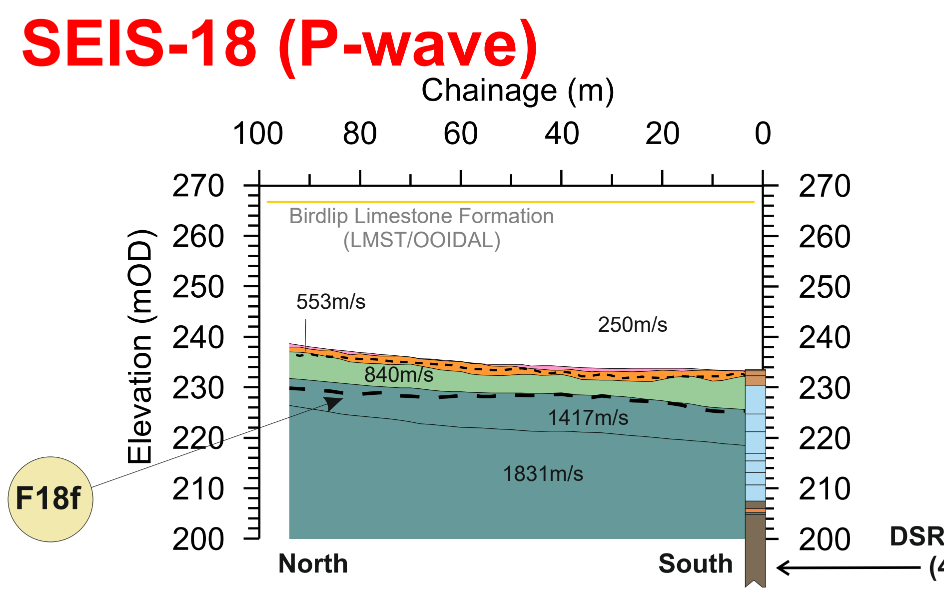

SEIS-18 Profile Coordinates	
0m Chainage	94m Chainage
393327.8E 216104.7N	393312.1E 216197.5N

KEY

Line 1 — Profile intersection

Fault — Reported fault positions

Bedrock geology subcrop

NOTES/OBSERVATIONS

Title: ERT AND SEISMIC PROFILES

Project: A417 CRICKLEY HILL BIRDLIP

TERRA DAT — down to earth geophysics

Tel: +44 (0) 2920 700127
Web:www.terradat.co.uk
Email: web@terradat.co.uk

Scale: 1:1500 at A3

Drawn by/Ref: JT/6688/9

Date: 14 FEB 2020

FIGURE 9

ERT-19

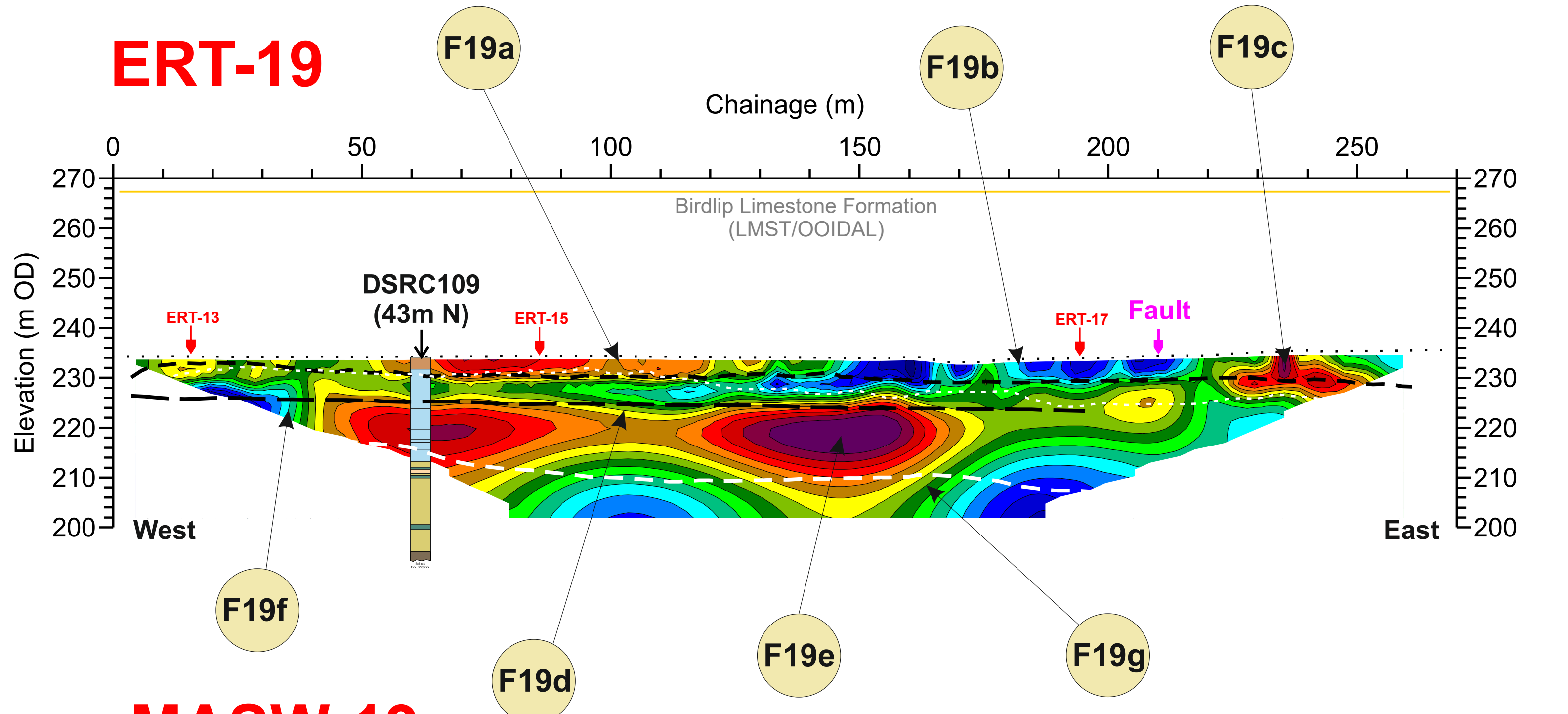

MASW-19

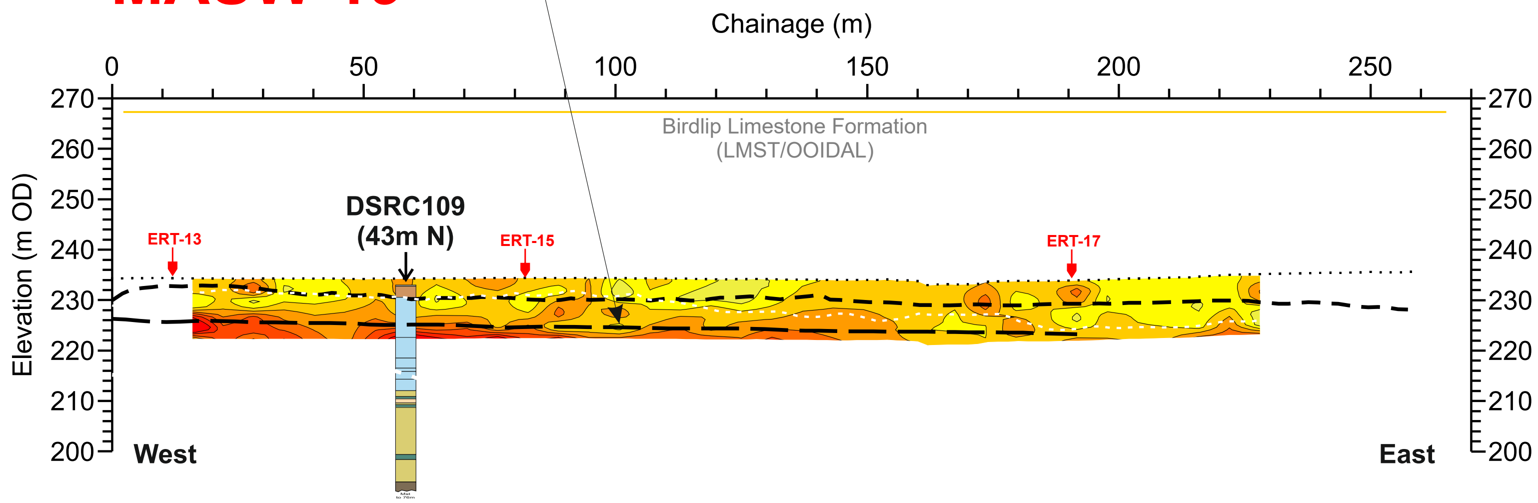

SEIS-19 (S-wave)

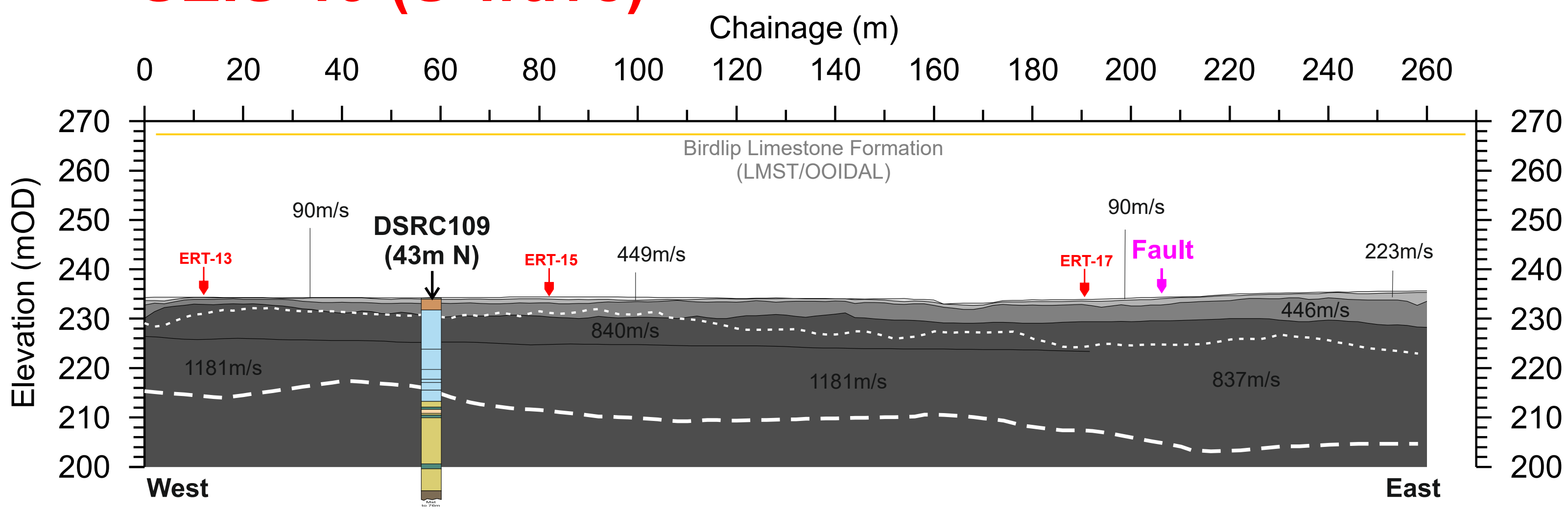

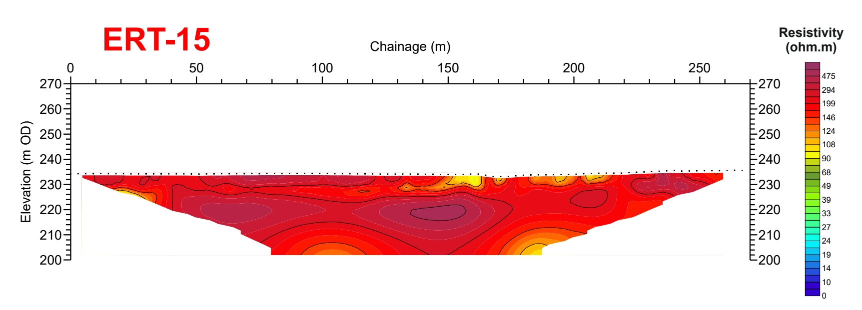

(alternative colour scale)

ERT-19 Profile Coordinates	
0m Chainage	266m Chainage
393183.7E 215923.6N	393396.9E 216081.9N

MASW-19 Profile Coordinates	
0m Chainage	260m Chainage
393186.5E 215925.6N	393394.7E 216079.0N

SEIS-19 Profile Coordinates	
0m Chainage	260m Chainage
393186.5E 215925.6N	393394.7E 216079.0N

ERT Section

Resistivity (ohm.m)

0 94 105 116 129 143 159 177 196 218 242 268 298 330 367 407 452 528

MASW Section

S-wave velocity (m/s)

100 175 250 325 400 475 550 625 700 775

S-wave Refraction velocity layers

- Layer 1 (<180 m/s) SOFT SOIL*
- Layer 2 (180 - 360 m/s) STIFF SOIL*
- Layer 3 (361- 760 m/s) VERY DENSE SOIL / SOFT(WEAK**) ROCK*
- Layer 4 (>761 m/s) ROCK* (MODERATELY STRONG**)

S-wave boundaries shown on ERT, MASW and S-wave sections

*The NEHRP Recommended Provisions for seismic regulation for new buildings, (FEMA-222A and FEMA-223A, 1994)

** UK equivalent classification (Waltham, 1994)

P-wave Refraction velocity layers

- Layer 1 (<300 m/s)
- Layer 2 (301 - 800 m/s)
- Layer 3 (801 - 1400 m/s)
- Layer 4 (1401- 1900m/s)
- Layer 5 (>1901 m/s)

P-wave boundaries shown on ERT, MASW and S-wave sections

BOREHOLE KEY

Made ground	Sandstone
Clay	Mudstone
Silt	Siltstone
Sand	Limestone
Gravel	Core loss

KEY

- Line 1 — Profile intersection
- Fault — Reported fault positions
- Bedrock geology subcrop

NOTES/OBSERVATIONS

Title: **ERT AND SEISMIC PROFILES**

Project: **A417 CRICKLEY HILL BIRDLIP**

TERRADAT down to earth geophysics
Tel: +44 (0) 2920 700127
Web:www.terradat.co.uk
Email: web@terradat.co.uk

Scale:	1:1500 at A3
Drawn by/Ref:	JT/6688/10A
Date:	14 FEB 2020

FIGURE 10A

SEIS-19 (S-wave)

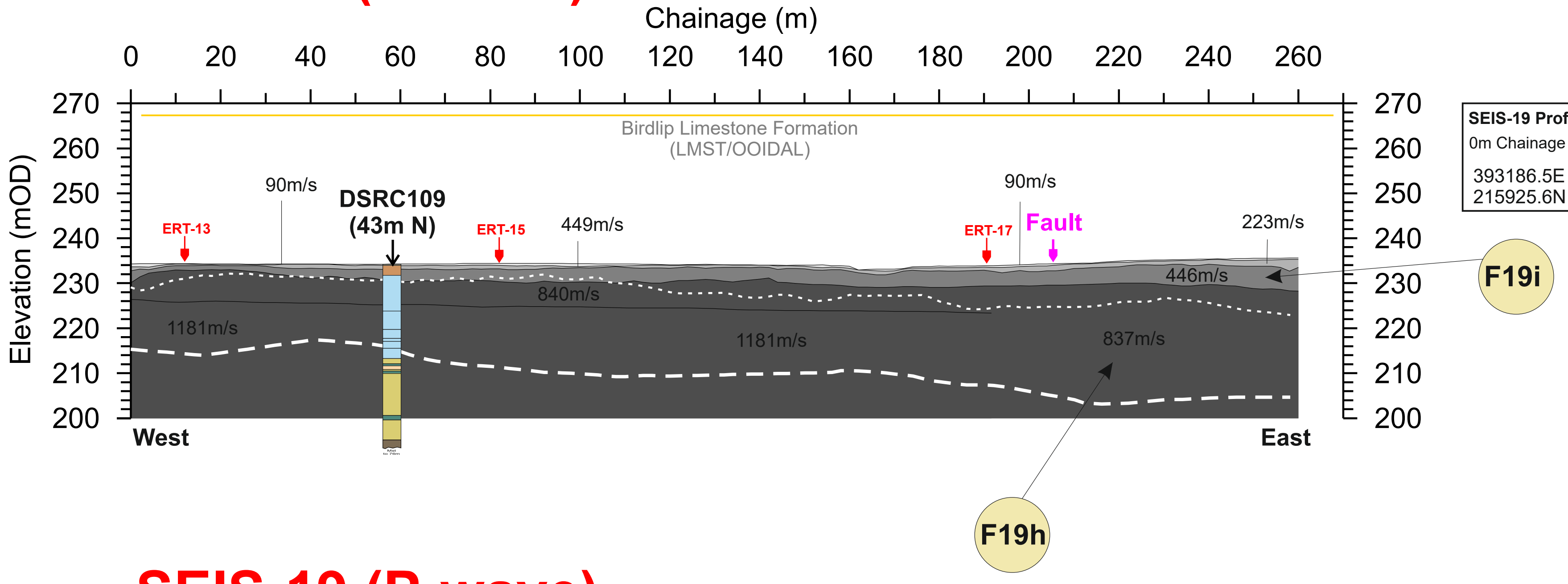

SEIS-19 Profile Coordinates	
0m Chainage	260m Chainage
393186.5E 215925.6N	393341.7E 216039.5N

SEIS-19 (P-wave)

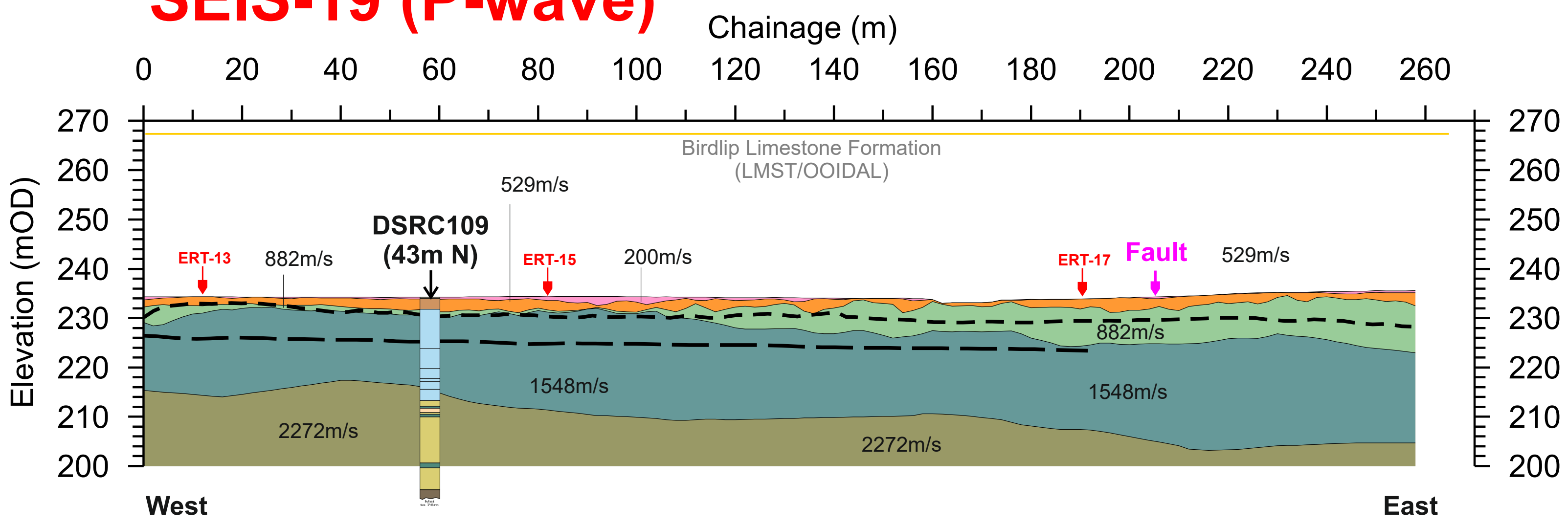

ERT Section

Resistivity (ohm.m)

0 10 14 19 24 27 33 39 49 68 90 108 124 146 199 294 475

MASW Section

S-wave velocity (m/s)

100 175 250 325 400 475 550 625 700 775

S-wave Refraction velocity layers

- Layer 1 (<180 m/s) SOFT SOIL*
- Layer 2 (180 - 360 m/s) STIFF SOIL*
- Layer 3 (361- 760 m/s) VERY DENSE SOIL / SOFT(WEAK**) ROCK*
- Layer 4 (>761 m/s) ROCK* (MODERATELY STRONG**)

S-wave boundaries shown on ERT, MASW and S-wave sections

**The NEHRP Recommended Provisions for seismic regulation for new buildings, (FEMA-222A and FEMA-223A, 1994)*

*** UK equivalent classification (Waltham, 1994)*

P-wave Refraction velocity layers

- Layer 1 (<300 m/s)
- Layer 2 (301 - 800 m/s)
- Layer 3 (801 - 1400 m/s)
- Layer 4 (1401- 1900m/s)
- Layer 5 (>1901 m/s)

P-wave boundaries shown on ERT, MASW and S-wave sections

BOREHOLE KEY

Made ground	Sandstone
Clay	Mudstone
Silt	Siltstone
Sand	Limestone
Gravel	Core loss

KEY

- Resistivity profile
- Fault — Reported fault positions
- Bedrock geology subcrop

NOTES/OBSERVATIONS

Title: SEISMIC REFRACTION PROFILES

Project: A417 CRICKLEY HILL BIRDLIP

TERRA DAT down to earth geophysics
Tel: +44 (0) 2920 700127
Web:www.terradat.co.uk
Email: web@terradat.co.uk

Scale: 1:1500 at A3

Drawn by/Ref: JT/6688/10B

Date: 14 FEB 2020

FIGURE 10B

APPENDICES

Appendix - Ground conductivity (EM) survey

A ground conductivity or electromagnetic (EM) survey involves the generation of an EM field at the surface and subsequent measuring of the response as it propagates through the subsurface. The main components of the instrument are a transmitter coil (to generate the primary EM field) and receiver coil (to measure the induced secondary EM field). The amplitude and phase-shift of the secondary field are recorded and are then converted into values for ground conductivity and in-phase component (metal indicator).

The ground conductivity (EM) instruments are either hand carried or mounted/towed behind a quad bike. Readings are usually taken on a regular grid or along selected traverse lines and positional control can be provided by dGPS if there is sufficient satellite coverage.

The selection of the particular EM instrument (EM-38/EM-31/GEM-2) is primarily based on the required penetration depth of the survey. However for most conductivity surveys the GEM-2 has replaced the more conventional EM-31 instrument due to its ability to simultaneously acquire data at different frequencies (i.e. different depth levels) and a greater depth of penetration. At the end of each survey, the survey data is downloaded to a field computer and corrected for instrument, diurnal and positional shifts. Additional editing may be carried out to remove any 'noisy' data values/positions.

The results from the EM survey can be presented as colour contoured plots of conductivity and inphase (metal response) data. In general terms, a relative increase in conductivity values usually indicates a local increase in clay content or water saturation. However, if there is a corresponding increase in the inphase response, the influence of some artificial source is likely (i.e. metal).

EM-38
Single frequency
Exploration depth ~1.5m

EM-31
Single frequency
Exploration depth ~3 to 5m

GEM-2
Multi-frequency
Exploration depth up to 10m

Towed EM-38 with dGPS

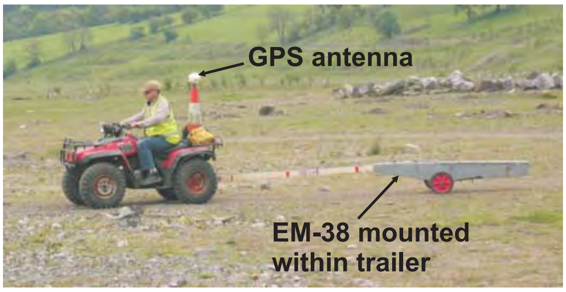

General principle of EM surveying

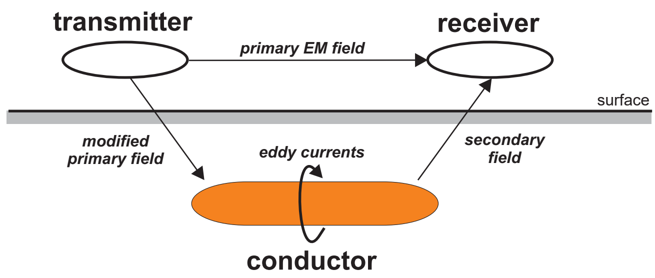

Mounted EM-31 with dGPS

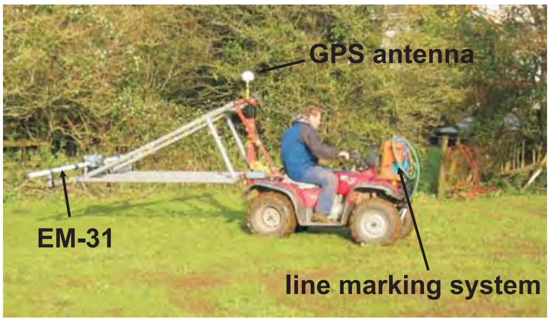

Ground conductivity data plot

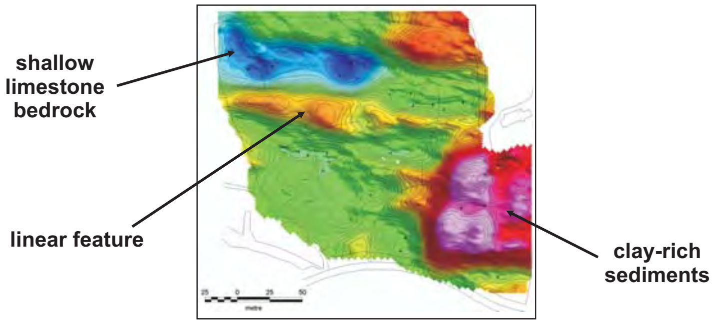

Constraints

Power lines, buildings, metal structures (fences, rebar, vehicles, debris etc.) and buried services can interfere with the electro-magnetic measurements.

TERRA DAT

Appendix - Resistivity Tomography

The Resistivity technique is a useful method for characterising the sub-surface materials in terms of their electrical properties. Variations in electrical resistivity (or conductivity) typically correlate with variations in lithology, water saturation, fluid conductivity, porosity and permeability, which may be used to map stratigraphic units, geological structure, sinkholes, fractures and groundwater.

The acquisition of resistivity data involves the injection of current into the ground via a pair of electrodes and then the resulting potential field is measured by a corresponding pair of potential electrodes. The field set-up requires the deployment of an array of regularly spaced electrodes, which are connected to a central control unit via multi-core cables. Resistivity data are then recorded via complex combinations of current and potential electrode pairs to build up a pseudo cross-section of apparent resistivity beneath the survey line. The depth of investigation depends on the electrode separation and geometry, with greater electrode separations yielding bulk resistivity measurements from greater depths.

The recorded data are transferred to a PC for processing. In order to derive a cross-sectional model of true ground resistivity, the measured data are subject to a finite-difference inversion process via RES2DINV (ver 5.1) software.

General resistivity principle

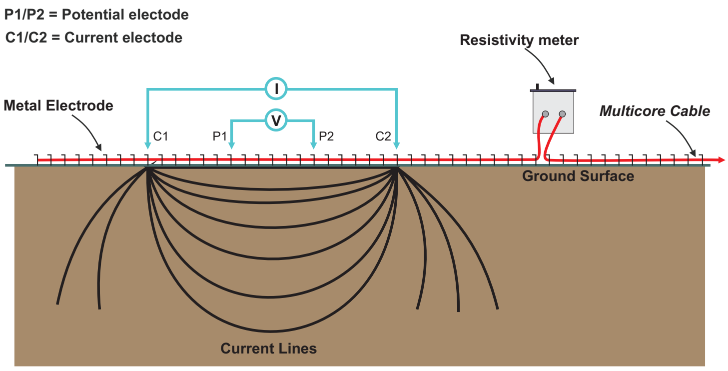

Typical field set-up

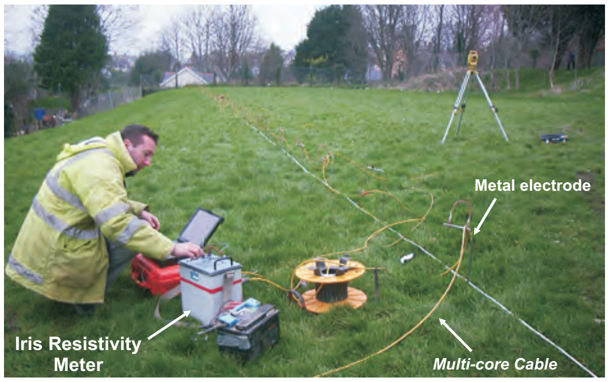

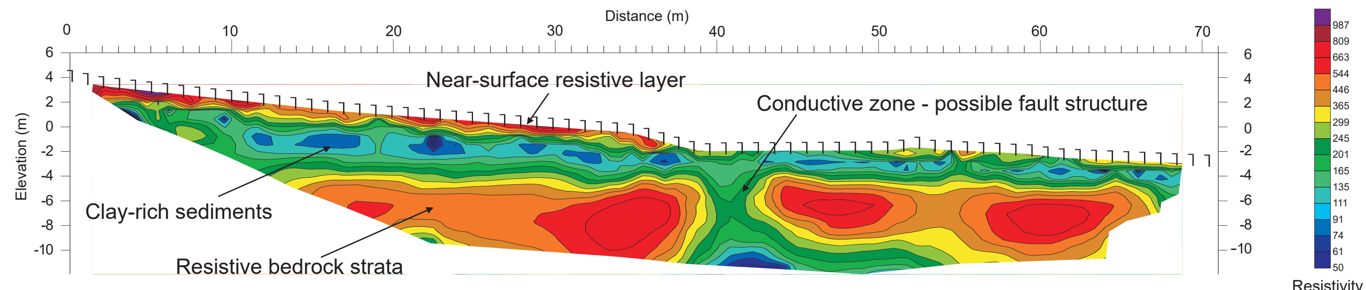

Modelled resistivity section

Data processing is based on an iterative routine involving determination of a two-dimensional (2D) simulated model of the subsurface, which is then compared to the observed data and revised. Convergence between theoretical and observed data is achieved by non-linear least squares optimisation. The extent to which the observed and calculated theoretical models agree is an indication of the validity of the true resistivity model (indicated by the final root-mean-squared (RMS) error).

The true resistivity models are presented as colour contour sections revealing spatial variation in subsurface resistivity. The 2D method of presenting resistivity data is limited where highly irregular or complex geological features are present and a 3D survey maybe required. Geological materials have characteristic resistivity values that enable identification of boundaries between distinct lithologies on resistivity cross-sections. At some sites, however, there are overlaps between the ranges of possible resistivity values for the targeted materials which therefore necessitates use of other geophysical surveys and/or drilling to confirm the nature of identified features.

Constraints:

Readings can be affected by poor electrical contact at the surface. An increased electrode array length is required to locate increased depths of interest therefore the site layout must permit long arrays. Resolution of target features decreases with increased depth of burial.

Appendix - Seismic Refraction Survey

Seismic refraction is a useful method for investigating geological structure and rock properties. The technique involves the observation of a seismic signal that has been refracted between layers of contrasting seismic velocity, i.e., at a geological boundary between a high velocity layer and an overlying lower velocity layer.

Shots are deployed at the surface and recordings made via a linear array of sensors (geophones or hydrophones). Refracted seismic signal travels laterally through the higher velocity layer (refractor) and generates a 'head-wave' that returns to surface. Beyond a certain distance away from the shot, the signal that has been refracted at depth is observed as first-arrival signal at the geophones. Observation of the travel-times of refracted signal from selectively deployed shots enables derivation of the depth profile of the refractor layer. Shots are typically fired at locations at and beyond both ends of the geophone spread and at regular intervals along its length.

The results of the seismic refraction survey are usually presented in the form of seismic velocity boundaries on interpreted cross-sections. Seismic sections represent the measured bulk properties of the subsurface and enable correlation between point source datasets (boreholes/trialpits) where underlying material is variable. Reference to the published seismic velocity tables enables derivation of rippability values.

Typical field set-up

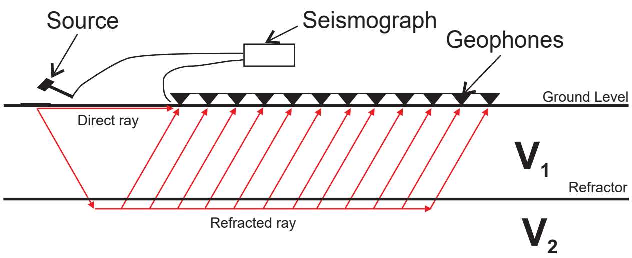

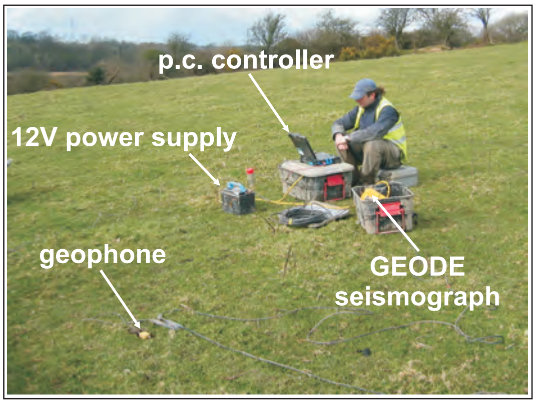

Travel-time curve

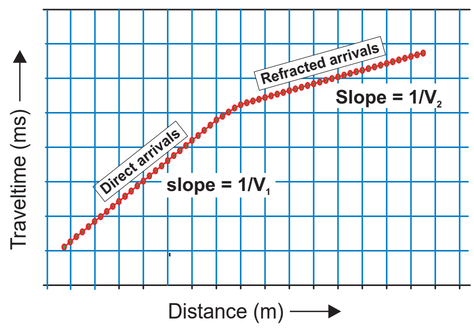

Modelled velocity section

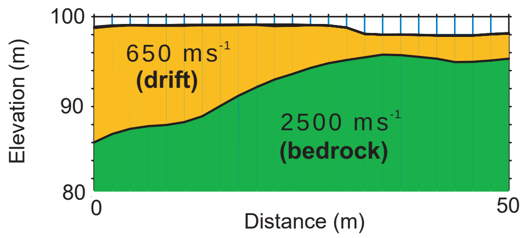

The data processing is carried out using PICKWIN & PLOTREFA (OYO ver2.2) software. The first stage involves accurate determination of the first-arrival times of the seismic signal (time from the hammer blow to each recording hydrophone) for every shot record, using PICKWIN. Time-distance graphs showing the first-arrival times were then generated for each seismic shot record and analysed using PLOTREFA software to determine the number of seismic velocity layers. Modelled depth profiles for the observed seismic velocity layers are produced by a tomographic inversion procedure that is revised iteratively to develop a best fit-model. The final output of a seismic refraction survey is a velocity model section of the subsurface based on an observed layer sequence with measured velocities that correspond to physical properties such as levels of compaction/ saturation in the case of sediments and strength/rippability in the case of bedrock.

Constraints

Layer velocity (density) must increase with depth; true in most instances. Layers must be of sufficient thickness to be detectable. Data collected directly over loose fill (landfills) or in the presence of excessive cultural noise may result in sub-standard results. In places where compact clay-rich tills and/or shallow water overly weak bedrock an S-wave survey may be used to profile rockhead where insufficient velocity contrast may prevent use of a P-wave survey.

Rippability Chart

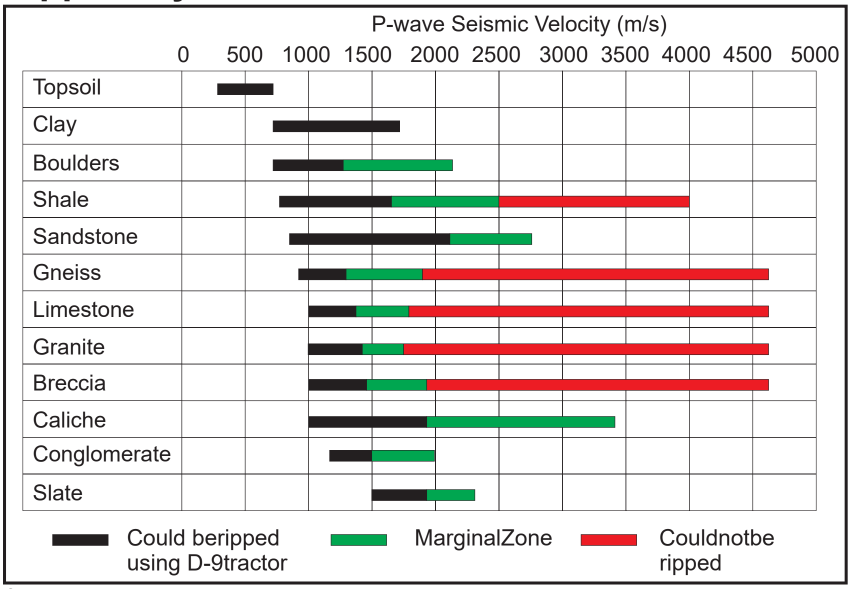

Ground preparation by ripping in open pit mining, Mining Magasine, 122, 458-469. Atkinson, 1970

Compressional P-wave velocity

Unconsolidated materials	***Vp (m/s)***
Sand (dry)	200 - 1000
Sand (water saturated)	1500 - 2000
Clay	1000 - 2500
Glacial till (water saturated)	1500 - 2500
Permafrost	3500 - 4000
Sedimentary rocks	
Sandstones	2000 - 6000
Tertiary sandstones	2000 - 2500
Pennant sandstone (Carboniferous)	4000 - 4500
Cambrian quartzite	5500 - 6000
Limestones	2000 - 6000
Cretaceous chalk	2000 - 2500
Jurassic limestones	3000 - 4000
Carboniferous limestones	5000 - 5500
Dolomites	2500 - 6500
Salt	4500 - 5000
Anhydrate	4500 - 6500
Gypsum	2000 - 3500
Igneous/Metamorphic rocks	
Granite	5500 - 6000
Gabbro	6500 - 7000
Ultramafic rocks	7500 - 8500
Serpentite	5500 - 6500
Other materials	
Steel	6100
Iron	5800
Aluminium	6600
Concrete	3600

An introduction to Geophysical Exploration 3rd Ed.
Kearey, Brooks & Hill: 2002

Diggability Chart

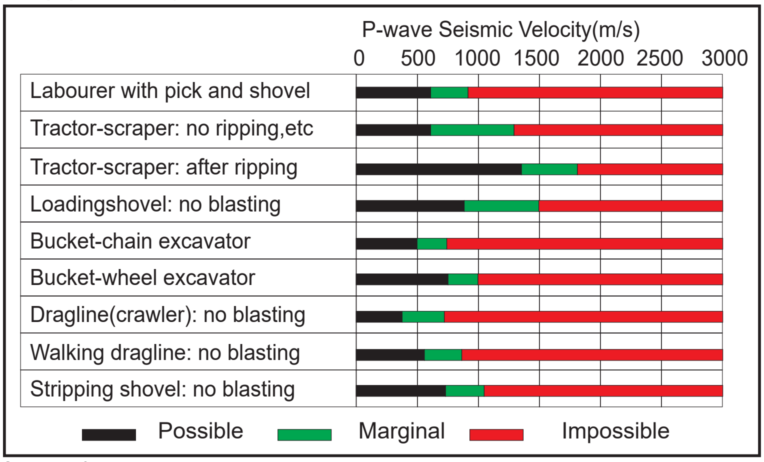

Selection of open pit excavation and loading equipment.
Transactions of the Institute of Mining and Metallurgy, 80, A101-A129, Atkinson 1971

Effect of ground water

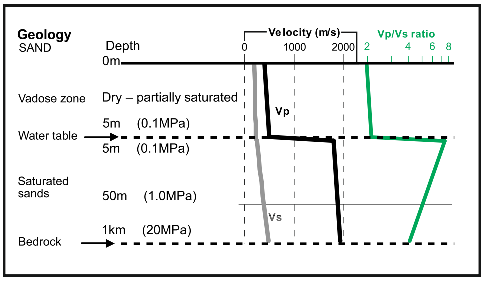

Prasad et al., Measurement of velocities and attenuation in shallow soils,
Near-Surface Geophysics Volume II Case Histories, SEG, Tulsa (2004)

Shear Waves

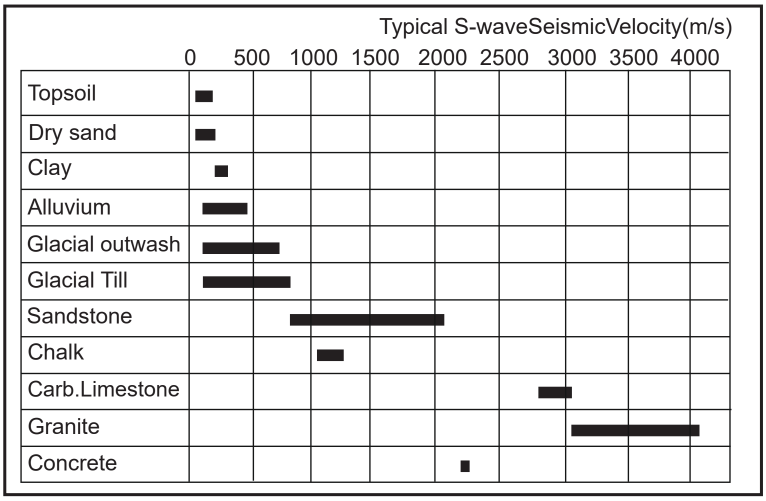

Rock / Soil Description (top 30m)	**S-wave velocity (m/s)**
Hard rock (*strong**)	> 1,500
Rock (*moderately strong**)	760 - 1,500
Very dense soil / soft (*weak**) rock	360 - 760
Stiff soil	180 - 360
Soft soil	<180

The NEHRP Recommended Provisions for seismic regulation for new buildings, (FEMA-222A and FEMA-223A, 1994)

** UK equivalent classification (Waltham, 1994)*

Applied Geophysics, Telford et al, 1990
Shear wave velocity determination of unlithified geologic materials (CUSEC region) Illinois State Geological Survey, Bauer, 2004.
Bauer et al., 2007, Illinois State Geological Survey.
Shear Wave Velocity, Geology and Geotechnical Data of Earth Materials in the Central U.S. Urban Hazard Mapping Areas.
An Introduction to Geophysical Exploration, 3rd Edition, Keary and Brooks, 2002.
Conceptual Overview of Rock and Fluid Factors that Impact Seismic Velocity and Impedance, Stanford Rock Physics Laboratory, n.d.

PUBLISHED SEISMIC VELOCITY TABLES

GEOPHYSICAL SURVEY REPORT

Project

Bedrock mapping and sediment characterisation

Location

Zone 2, A417, Birdlip

Client

Geotechnical Engineering

Head Office
Unit 1
Link Trade Park
Penarth Road
Cardiff CF11 8TQ
United Kingdom

Telephone: +44 (0)2920 700127
www.terradat.co.uk

TERRA DAT
down to earth **geophysics**

Job Reference: 6688
Date: December 2020
Version: 2

GEOPHYSICAL SURVEY REPORT

Project

Bedrock mapping and sediment characterisation

Location

Zone 2, A417, Birdlip

Client

Geotechnical Engineering

Project Geophysicist:	M Bottomley BSc MSc	[redacted]
Reviewer:	S Hughes PhD BSc FGS	_ [redacted]
Job Reference:	6688	
Date:	December 2020	

CONTENTS

Figures

Appendices

1 EXECUTIVE SUMMARY

A geophysical survey was carried out as part of the ground investigation for proposed improvements to the A417 near the village of Birdlip, south of the existing road. The survey work was commissioned by Geotechnical Engineering (the Client). The fieldwork was carried out during October/November 2019 and undertaken within an area defined by the Client as 'Zone 2' comprising eleven targeted Electrical Resistivity Tomography (ERT) and seismic profiles. The work was designed to complement the invasive and geotechnical investigation in providing detailed information on the geology and ground conditions adjacent to the existing A417, with particular concern regarding potential landslide/landslip zones.

The geophysical survey consisted of an integrated survey approach utilising eleven targeted ERT profiles and eleven seismic P and S-wave refraction and Multichannel Analysis of Surface Waves (MASW) profiles along all resistivity lines.

The results have been provided as a series of interpreted, colour-contoured and scaled sections (resistivity and seismic refraction), alongside a map showing the locations of the plots and profiles in relation to the underlying topographical features and bedrock geology, as provided by Google Earth mapping and the British Geological Survey (BGS) Geology of Britain viewer.

2 INTRODUCTION

This report describes a geophysical survey that was carried out as part of the ground investigation for proposed improvements to the A417 near the village of Birdlip. The survey work was commissioned by Geotechnical Engineering (the Client). The fieldwork was carried out during October/November 2019 and undertaken within an area defined by the Client as ‘Zone 2’ comprising eleven targeted Electrical Resistivity Tomography (ERT) and seismic profiles.

The work was designed to complement the invasive and geotechnical investigation in providing detailed information on the geology and ground conditions adjacent to the existing A417, with particular concern regarding potential landslide/landslip zones.

2.1 Site description and history

Zone 2 (approx. centred on 392800E, 215700E) occupies an area of around 60 hectares, 1 km north of the village of Birdlip. The survey area encompasses open fields, hedge systems and woodland to the north and south of the A417, up to the junction between the A417 and the A436 to the east. Topographically, land south of the A417 dips to the north-west and the relief is quite variable due to historical landslips and creep, with the steepest topography just west of the viewpoint at Barrows Wake. Superimposed on the topography are significant ridge and furrows which trend northwest-southeast.

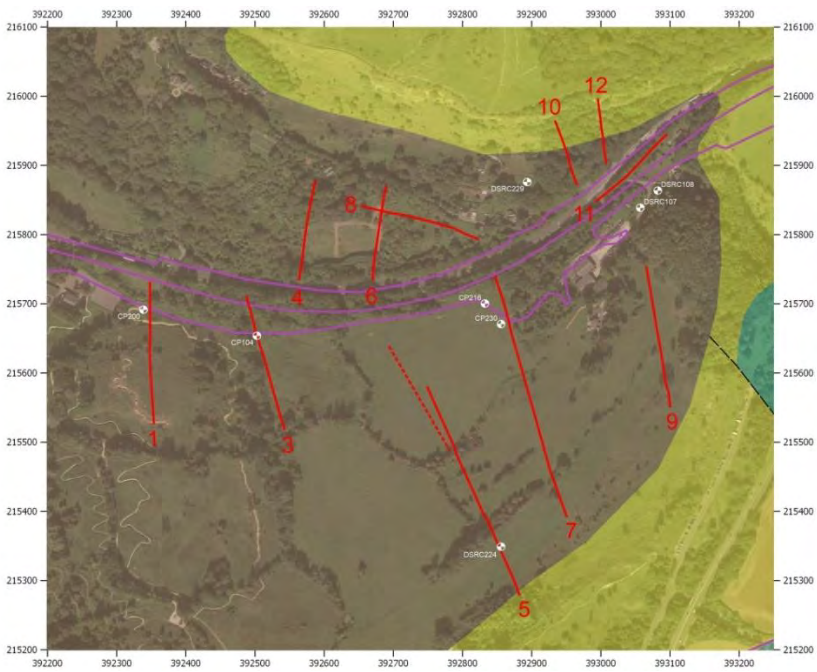

Plate 1. *Zone 2, showing the locations of the ERT and seismic profiles.*

Land north of the A417 dips to the south-west is more heavily wooded and the relief is generally steeper, with prominent limestone escarpments visible at around 250 m aOD.

2.2 Geological setting

The Client has provided numerous borehole logs located within the ‘Zone 2’ survey area. The intrusive investigation has logged highly variable material comprising clay, mudstone, siltstone and limestone of the Lias Group and Inferior Oolite. The British Geological Survey (BGS) Geoindex shows the site is comprised of the Lias Group and Inferior Oolite Group with argillaceous (clay-rich) sedimentary rocks. The Birdlip Limestone creates the topographic ridge and some escarpment exposure to the south and east of the site, where limestone erosional material has originated, to form part of the historical landslide debris seen as hummocky ground within the survey area.

According to the BGS Geoindex, there are no superficial deposits in the vicinity of the site. All material overlying the bedrock is therefore believed to be bedrock erosion material from steep slopes and escarpments that has been transported by weather processes and landslide, down the valley side, and is referred to in this report as “overburden”.

2.3 Survey objectives

The primary objectives of the survey were to provide detailed information on the shallow ground composition and deeper bedrock geology to assist with the ground investigation of the proposed road scheme. Of particular interest for engineering a new road cutting, is areas of shallow geology that may support further landslide movement of the overburden.

2.4 Survey design

Given the scope of the survey objectives, it was decided to adopt an integrated survey approach utilising the following geophysical methods:

- **Resistivity Tomography**: to provide electrical cross-sections along selected survey profiles that allow identification of geological or hydrological boundaries.

- **P-wave Seismic Refraction**: to provide seismic velocity (V_p) model sections that indicate the thickness of overburden deposits and the depth to competent bedrock, in correlation with standard tables.

- **S-wave Seismic Refraction**: to provide seismic velocity (V_s) model sections that indicate the depth of uncompacted and compacted sediments, weathered rockhead and more competent (higher shear strength) bedrock.

- **MASW (Multichannel Analysis of Surface Waves)**: to derive shear velocity ('S-wave' or 'V_s') from rolling surface waves that are related to the stiffness of the ground material. This technique is also useful where velocity inversions in the ground layers may be encountered.

2.5 Quality control

The geophysical data sets were collected in line with normal operating procedures as outlined by the instrument manufacturer and TerraDat company policy. On completion of the survey, the data were downloaded from the survey instrument on to a computer and backed up appropriately. The acquired data set was initially checked for errors that may be caused by instrument noise, low batteries, positional discrepancies, etc. and any field notes are either written up or incorporated in the initial data processing stage. The data set is then processed using the standard processing routines and once completed; the resulting plots are subject to peer review to ensure the integrity of the interpretation. Our quality control standards are BS EN ISO 9001: 2015 certified.

3 SURVEY DESCRIPTION

The survey was carried out using the following geophysical methods:

- Electrical Resistivity Tomography (ERT)
- P-wave seismic refraction (employs compressional waves)
- S-wave seismic refraction (employs shear waves)
- MASW (Multichannel Analysis of Surface Waves)

The extents of the resistivity and seismic profiles are shown in Figure 12. Eleven Electrical Resistivity Tomography (ERT) and seismic refraction profiles were deployed, in locations as specified by the Client.

Background information for the survey methods is provided in the appendices, while a description of the actual survey work is provided in the sections below.

3.1 Survey limitations and assumptions

Seismic refraction requires that the velocity of the materials in the subsurface increases with the depth of burial. This is normally the case since (i) the degree of compaction within the overburden typically increases with depth, and (ii) bedrock condition improves with depth as weathering is reduced, both of which lead to higher seismic velocities. Therefore, one limitation of the refraction method is the inability to resolve localised weak zones within rock where it resides at a depth below the competent non-weathered rock. One of the objectives of the resistivity tomography survey is to target such weak/broken zones in the rock where fines/water have infiltrated and reduced the local ground resistivity. The survey output from both the P and S-wave refraction surveys are cross-sectional models that describe the bulk physical properties of the ground in terms of superficials, weathered rock and competent rock layers. There will be local variations in rock strength within the interpreted weathered rock layer, and the fracture density / broken character of the rock will vary over very short lateral distances. Measuring the seismic velocity of the bedrock over tens of metres along each survey line determines the bulk properties of the shallow rock mass and enables targeted ground-truthing of any identified anomalous ground.

3.2 Survey layout and topographic survey

Where possible, a Topcon Hyper Pro RTK dGPS system was used to mark resistivity (electrode) and seismic profile (geophones and offend shots) locations with a survey accuracy of +/- 2.5cm. In some cases, positional accuracy was not adequate due to extensive tree cover, and so a Trimble robotic total station was employed using dGPS established reference stations. All measurements were recorded in Ordnance Survey National Grid coordinates.

3.3 Electrical Resistivity Tomography (ERT)

An ERT survey involves the injection of DC electrical current into the ground at various electrode locations along a profile line. An electrical cross-section of the subsurface is then derived from the recorded data. A diverse range of features such as clay-rich sediments, fracture zones, infilled solution features, bedrock structure and mineralisation can be imaged in cross-section using a resistivity survey. A feature may be targeted using resistivity tomography given sufficient electrical contrast with its surroundings. A description of the field activity is provided below, and some background information on the survey method is found in the Appendix.

3.3.1 ERT survey field activity

A 72-channel *IRIS Syscal* resistivity system (Plate 2) was used to acquire eleven profiles across the survey area, as shown in Figure 12. The ERT profiles were acquired with an electrode spacing of 1.5, 2 or 3 m using a standard Wenner-Schlumberger array. For some of the profiles, ‘roll-ons’ were required to cover the required area of interest. A ‘roll-on’ simply involves adding one or two cables to the end of the initial 72-channel setup and then selecting the appropriate protocol file from the IRIS resistivity meter to continue data acquisition from the initial setup and into the new cables. A summary of the ERT profiles is given in Table 1.

ERT Profile No.	Fig.	Start (OSGB)		End (OSGB)		Length (m)	Electrode Spacing (m)	~ Depth of penetration (m)
		Easting	Northing	Easting	Northing			
Line 1	13	392348.1	215731.4	392353.5	215527.0	204	3	30
Line 2*	-	-	-	-	-	-	-	-
Line 3	14	392487.5	215709.1	392543.2	215516.0	201	3	30
Line 4	15	392586.7	215875.5	392563.3	215732.8	145	2.5	25
Line 5	16A	392749.6	215578.5	392883.7	215277.4	330	3	30
Line 6	17	392689.4	215866.9	392670.5	215733.0	135	2	20
Line 7	18A	392848.1	215742.3	392951.9	215390.5	368	3	30
Line 8	19	392653.6	215840.6	392822.0	215793.6	175	2.5	25
Line 9	20	393066.1	215755.4	393100.8	215549.9	209	3	30
Line 10	21	392934.5	215964.6	392965.7	215873.4	96	1.5	15
Line 11	22	392994.9	215848.8	393096.5	215945.3	140	2	20
Line 12	23	392996.1	215996.0	393008.1	215903.8	94	1.5	15

**Line 2 could not be undertaken due to land access constraints, and will be undertaken once access becomes available.*

Table 1. *ERT profile summary.*

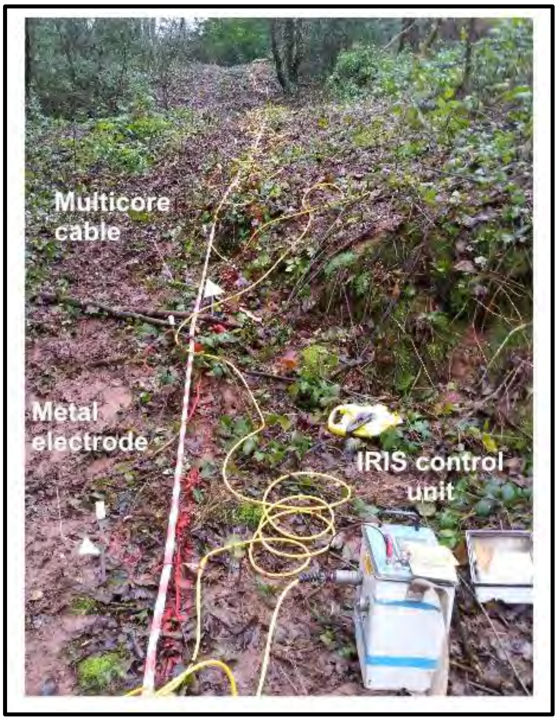

Plate 2. *Resistivity Tomography data collection. A 72 channel IRIS Syscal ERT system used to acquire eleven profiles across the site (Library photo).*

3.3.2 *ERT survey data processing*

The data were processed using *Res2DInv* software to derive modelled electrical cross-sections of the subsurface. Elevation data were added to the models, using electrode positions surveyed using a TOPCON network RTK GPS. All topographic data were transformed into National Grid (OSGB36) using the OSTN02b transformation; elevations are given in m AOD. The ERT data was then exported into *Surfer 7* where it was gridded and presented as a 2D cross-sections of resistivity. These cross-sections were then exported to *CorelDraw* for final annotation. All resistivity profiles are presented on the same colour scale and are not vertically exaggerated.

3.4 Seismic survey – P and S-wave refraction

A seismic survey involves generating a shock wave signal at the surface to investigate the geological structure beneath a chosen profile line. A series of vibration sensors (geophones, or hydrophones in water) are deployed along the line and are used to record the travel times of incident seismic signal as it returns from below ground. Features such as rockhead, the water table, made ground, soft sediments and dense tills all have distinct velocity ranges and can be imaged in cross-section using a seismic refraction survey. A description of the field activity is provided below, and some further background information on the survey method is found in the appendices.

3.4.1 Seismic survey field activity: P-wave refraction

P-wave seismic refraction data were acquired along eleven profile lines using a high precision 72 channel *GEODE* (Plate 3a) seismic system. To target the broad depth range, low frequency (4Hz) geophones were deployed at 2 m intervals providing individual geophone spread lengths of 142 m. For some profiles (e.g. Profiles 5 and 7), several setups were required to achieve full line coverage. The seismic wave was generated by a combination of sledgehammer striking a nylon plate and Seismic Impulse Device (SID) firing 12- and 8-gauge black powder cartridges (Plate 3b). To build up the refraction data set, seismic shots were taken at several positions along the geophone spread (usually every 6-12 geophones) and set distances beyond the geophone spread. For this particular survey, the ‘offend’ shots were limited by site constraints, but the maximum distance was 100 m. A summary of the seismic profiles is given in Table 2.

Plate 3. *a) Field setup and b) Seismic Impulse Source deployment (Library picture).*

Seismic Profile No.	Fig.	Start (OSGB)		End (OSGB)		Length (m)	Geophone Spacing (m)	~ Depth of penetration (m)
		Easting	Northing	Easting	Northing			
Line 1	13	392348.7	215594.5	392347.7	215731.3	137	2	25
Line 2*	-	-	-	-	-	-	-	-
Line 3	14	392493.3	215690.3	392544.1	215515.6	184	2	25
Line 4	15	392584.2	215867.8	392569.1	215763.5	110	2	20
Line 5	16B	392763.9	215543.7	392871.9	215305.1	330	2	25
Line 6	17	392688.0	215862.5	392674.3	215773.1	94	2	20
Line 7	18B	392851.8	215725.8	392959.2	215364.2	368	2	25
Line 8	19	392809.0	215796.6	392672.8	215835.8	142	2	25
Line 9	20	393065.1	215756.4	393089.6	215616.8	142	2	25
Line 10	21	392966.5	215874.2	392938.4	215955.2	86	2	15
Line 11	22	393004.8	215855.5	393071.5	215920.1	94	2	20
Line 12	23	393007.1	215907.0	392996.5	215990.7	85	2	15

**Line 2 could not be undertaken due to land access constraints, and will be undertaken once access becomes available.*

Table 2. *Seismic Profile summary.*

3.4.2 Seismic survey field activity: S-wave refraction (Shear)

S-wave seismic refraction data were also acquired using a 72 channel *GEODE* seismic system. Horizontally mounted geophones were deployed at 2 m intervals producing individual geophone spread lengths of up to 142 m. For some profiles (e.g. Profiles 5 and 7), several setups were required to achieve full line coverage. A weighted S-wave plate struck sideways with a sledgehammer was used as the energy source (Plate 4). At each shot location, the shot plate was aligned perpendicular to the profile line and subsequently struck on both ends to generate two sets of shear wave recordings that have opposite polarity. To build up the refraction data set, seismic shots were taken at several positions along the geophone spread (usually every 6-12 geophones) and set distances beyond the geophone spread.

Plate 4. *S-wave source plate being struck (Library photo).*

3.4.3 Seismic survey data processing: P and S-wave refraction

The data processing was carried out using *PICKWIN* and *PLOTREFA* software. The first stage involved the accurate determination of the first-arrival times of the seismic signal (time from the shot going off to each recording geophone) for every shot record using *PICKWIN*. Time-distance graphs showing the first-arrival times were then generated for each seismic line and analysed using *PLOTREFA* software to determine the number of seismic velocities layers. Modelled depth profiles for the observed seismic velocity layers were produced by a tomographic inversion procedure that was revised iteratively to develop a best-fit model.

The final output of a seismic refraction survey is a velocity model section of the subsurface based on an observed layer sequence. The measured velocities correspond to physical properties such as levels of compaction/saturation in the case of sediments and strength/rippability in the case of bedrock. A transitional velocity model will be considered if distinct layers are not expected, or velocity contrasts between layers are marginal. However, a layered model appears most appropriate to this site. The final sections were exported to *CORELDRAW* for annotation and presentation.

3.5 Seismic survey – MASW

Multichannel Analysis of Surface Waves (MASW) employs 'rolling' surface waves to derive shear velocity. This is achieved through analysis of the dispersion that occurs as surface wave energy propagates through the subsurface and separates into different frequencies travelling at different velocities depending on the stiffness of the sediments and/or rock encountered.

This technique utilises Rayleigh-type surface waves (normally considered noise in seismic refraction/reflection surveys and called 'ground roll' recorded by multiple geophones deployed on an even spacing and connected to a common recording device (seismograph), as shown in Plate 5.

As the dispersion of the seismic wave can be dependent on the geology and ground conditions (i.e. variability, terrain, etc.), MASW profiles are usually limited to relatively flat areas or where the ground more homogenous.

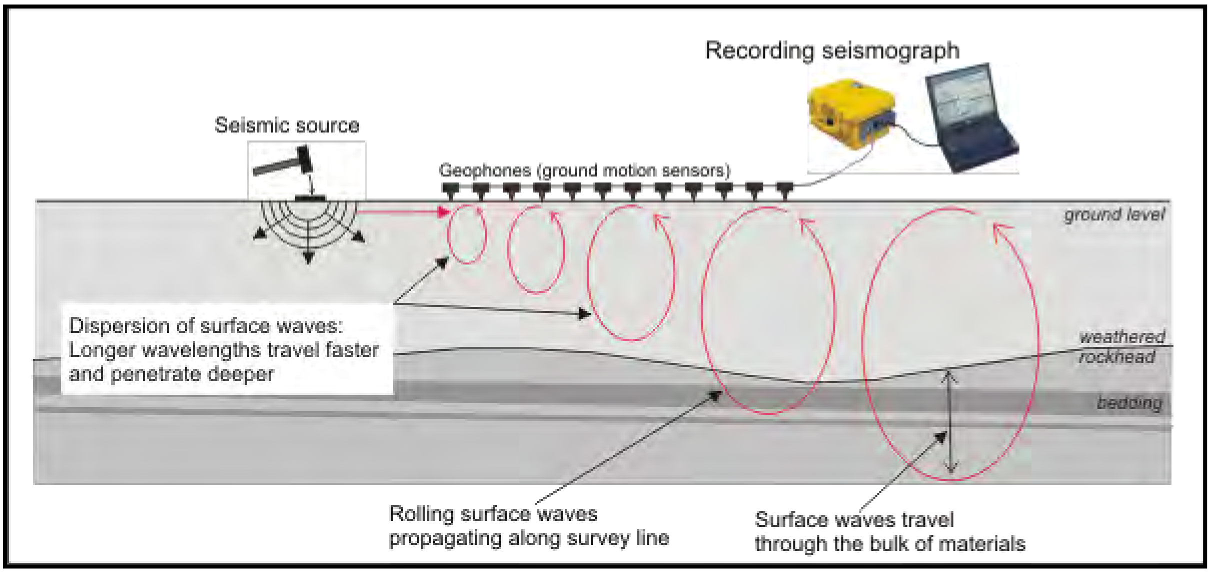

Plate 5. *MASW survey setup.*

3.5.1 Seismic survey field activity: MASW

For this particular survey, the setup is very similar to the refraction setup; however, instead of a discreet number of shot points, shots were acquired at every other geophone position along the profile. In this case, low frequency (4Hz) geophones were set at 2 m intervals, and the data were acquired using the sledgehammer as the source. A one-second record length was used to fully capture the frequency dispersion.

3.5.2 Seismic survey data processing - MASW

Analysis of surface waves recorded on multichannel shot records was carried out using SurfSeis software, which considers the dispersion properties of all types of waves (both body and surface waves) through a wave field transformation method. This directly converts the multichannel record into an image, where a dispersion pattern is recognised, and the necessary dispersion properties are extracted. These dispersion properties are used to generate modal dispersion curves that are subsequently inverted and used to produce the resultant shear-wave velocity (Vs) profile. The final velocity sections are created in SURFER then exported to CorelDraw for annotation and presentation.

4 RESULTS AND DISCUSSION

The results of the geophysical surveys are presented as a series of interpreted colour contour plots and scaled sections in Figures 13 to 23. A general description of the interpretation process is given below, followed by a summary of the findings in Section 4.4.

4.1 Resistivity tomography

The results of the resistivity survey are presented as colour contoured scaled sections of the subsurface showing changes in resistivity, with blue colours representing low values, and red colours representing relatively high resistivity values. The vertical and horizontal axes display elevation and chainage along the profile line, respectively. The interpretation of the modelled resistivity sections is based on both published electrical properties of typical sub-surface materials (Plate 6) and, when available, correlation with on-site information or observations. In principle, an increase in resistivity values usually indicates a relative decrease in the clay content or groundwater saturation. However, due to the non-uniqueness of the electrical properties (i.e. different material exhibiting same resistivity values), the final interpretation may be limited and may require addition calibration (i.e. drilling or other supplementary geophysical techniques).

The results of the ERT survey are discussed in the summary discussions, in conjunction with the results of the seismic survey. To assist with the interpretation, the resistivity sections have been overlain with the interpreted seismic velocity boundaries where acquired.

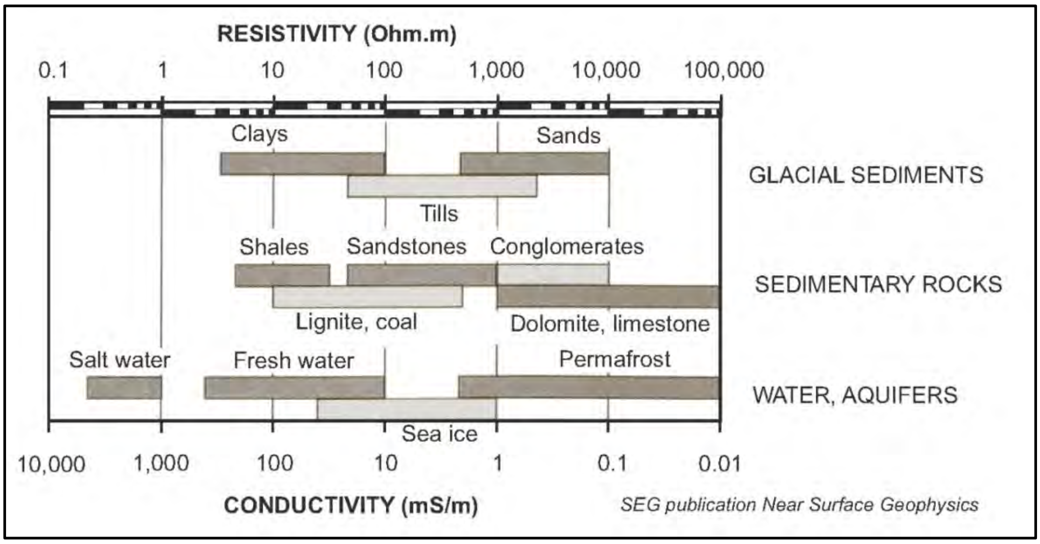

Plate 6. *Conductivity and resistivity values of common materials.*

4.2 Seismic Refraction – compressional (P) and shear (S) wave

Interpretation of the refraction sections is based on the widely understood and published velocities of typical sub-surface materials (provided in the appendices). It is beneficial to correlate model sections with on-site information/observations, but at the time of reporting, only limited borehole information was available.

4.2.1 Compressional (P) wave

Analysis of the P-wave refraction data has identified up to five distinct layers of contrasting velocity (V_p), and a typical description of each layer is given below and summarised in Table 3. It is worth noting that the seismic refraction section represents the measured bulk characteristics of the subsurface and in certain cases, it can prove difficult to correlate with point source data (boreholes/trial pits) where the underlying material is variable.

Layer	P-wave velocity	Sediment/Rock Description
P1 (pink)	< 300 m/s (low)	Thin, dry loose surface soils and sediments
P2 (orange)	301 – 800 m/s (low to medium velocity)	Unconsolidated, dry overburden material
P3 (light green)	801 - 1400 m/s (medium velocity)	Compacted, dry overburden material
P4 (green)	1401 - 1900 m/s (medium to high velocity)	Compacted, saturated overburden material or highly weathered bedrock
P5 (dark green)	> 1901 m/s (high velocity)	Weathered to unweathered bedrock

Table 3. *A guide to the composition of the P-wave velocity layers identified.*

Layers P1 has a low velocity that relates to loose, surface soil and uncompacted sands and gravels. Layers P2 and P3 typically reflect a relative increase in consolidation or compaction of the still dry overburden material. Layer P4 can be more difficult to interpret as the overlap in velocities means that it can represent both overburden material (potentially wet, compact material) and weathered/weak/fractured bedrock. The most effective way to differentiate between sediment and rock type material is to consider the corresponding S-wave velocity, as discussed below. Layer P5 represents the highest (and deepest) velocity unit and is likely to reflect a more competent boundary within the bedrock strata.

4.2.2 Shear (S) wave

By carrying out an analysis of the S-wave refraction data, four distinct layers of contrasting velocity (V_s) have been identified and summarised in Table 4. They are characterised by their correlation with standard tables (see appendices).

In general, the shear-wave velocity (V_s) is much more sensitive than the P-wave velocity (V_p), where the ground becomes abruptly stiffer due to increases in rock strength. For this reason, it is possible to use the V_s to distinguish between sediments and "rock" (i.e. cemented) material, which is particularly useful for grading the P-wave layer P4. A further advantage of shear waves is that they are unaffected by the groundwater table.

Layer	S-wave velocity	Sediment/Rock Description
S1	<180 m/s	Soft soils and loose sediments
S2	180 - 360 m/s	Stiff soils/overburden
S3	361 - 760 m/s	Very stiff, compacted overburden or highly weathered bedrock
S4	>761 m/s	Rock

Table 4. *A guide to the composition of the S-wave velocity layers identified.*

When comparing the resulting P-wave and S-wave velocity sections, there is a rough 'rule of thumb'' with regards to the ratio of the velocities. For unconsolidated sediment, V_p/V_s is usually between 4.0 to 8.0, while for consolidated rocks, the V_p/V_s ratio can vary between 1.5 to 2.0. Even though these are accepted values, they can vary between sites depending on the geology and ground conditions.

When correlating between the respective P-wave and S-wave refraction boundaries, in some instances there can be discrepancies in observed depth values. This depends on the prevailing geology and can reflect different survey parameters (horizontal/vertical polarised S-waves, spacing, etc.), weathering profile (vertical and horizontal), lithology or bedding structure. It has been noted on some sites that the S-wave refractor appears to correlate with internal bedding units as opposed to the general rock mass.

4.3 MASW

The results of the MASW survey are presented as colour contoured S-wave velocity panels showing changes in velocity (i.e. ground stiffness) below the surface. The seismic signal frequency dispersion required for the MASW technique has yielded reliable results to a depth of up to approximately 20 m bgl. The persistent traffic noise from the A417 and the limited power of a sledgehammer energy source meant lower frequency dispersions (giving an increased depth of investigation) suffered from a high signal to noise ratio and were not suitable for modelling. The MASW sections have been colour scaled from white to red, with red representing the highest velocity modelled.

4.4 Summary Discussion – ERT and Seismic Refraction

Features or anomalies of interest have been listed and discussed in Table 5 below.

Profile	Feature	Description
1	F1a	Isolated, slightly more conductive zone, likely indicating an increase of clay and/or water within the superficial deposits.
	F1b	Very good correlation between Layer P5 (2175 m/s) and transition into more conductive material, indicating conductive Lias bedrock, which is likely to be weak and highly weathered given the low S-wave velocity for Layer S4 of 591 m/s. The discrepancy between Layers S4/P5 may be due to Layer S4 representing a mudstone or limestone bed and Layer P5 representing a significant change in saturation (e.g. water table) or different lithology (e.g. mudstone) given the interbedded nature of the Lias bedrock.
	F1c	A region of increased S-wave velocity on the MASW section correlates with Layer S3 and is likely to represent a much stiffer zone of sediments. It is also located close to the transition zone with Layer S4, interpreted to be bedrock, and so this feature may be associated with a zone of very weak, broken rock.
	F1d	Broader zone of increased conductivity indicates an increase of water/clay within the superficial deposits or change in sediment lithology. The area is also a 'low-point' with a stream, and so is likely to be more saturated than the slope.
3	F3a	Broader zone of increased conductivity indicates an increase of

		water/clay within the superficial deposits or change in sediment lithology.
	F3b	Broad zone of increased resistivity, likely indicating a decrease of clay and/or water within the deeper superficial deposits and bedrock, or change in lithology, which may be dipping given the shape of the feature. In general, the section appears absent of any particularly resistive zones of interest, and resistivity values remain very low.
	F3c	Good correlation between Layer S3 and the MASW, indicating a transition into stiffer material which is likely to represent the Lias bedrock. Interestingly, CP104 terminates at Layer S3, possibly due to borehole refusal?
	F3d	Good correlation between CP104 and the S-wave section, in this case, showing Layer S1 to comprise very soft silt and Layer S2 to comprise much stiffer clay.
	F3e	Increase of resistivity correlates with a transition into weak, weathered Lias bedrock (Layers S3/P5), as indicated by low P-wave and S-wave velocities of 1955 m/s and 539 m/s respectively.
	F3f	The absence of Layer P5 beyond approximately 90 m chainage may indicate a change in geology and/or bedrock character (e.g. increase in water-bearing fractures). It must be noted that the velocities of Layers P4 and P5 are very similar and so the variations may be subtle, especially as no obvious variations are observed in the S-wave data.
4	F4a	This resistive layer indicates a decrease of clay and/or water within the near-surface sediments (increase of sand/silt/gravel?). A decrease in sediment saturation is likely given the steep nature of the slope (i.e. well-drained).
	F4b	Broader zone of increased conductivity indicates an increase of water/clay within the superficial deposits or change in sediment lithology.
	F4c	Good correlation between Layer S4 and the MASW, indicating a transition into stiffer material which is likely to represent the Lias bedrock although a borehole would be needed to confirm this, especially as the corresponding Layer P4 velocity (1473 m/s) is more indicative of dense, saturated sediments. As with profiles SEIS-1 and SEIS-3, an S-wave velocity of 503 m/s would suggest the presence of very weak, weathered mudstone bedrock.

	F4d	An increase in softer sediments lower down the slope, as also indicated by the MASW section, correlates with an increase in sediment conductivity.
	F4e	Layer P5 is likely to represent a change of bedrock lithology, given its location ~10 to 15 m deeper than Layer S4.
5	F5a	This thick, resistive layer indicates a decrease of clay and/or water within the near-surface sediments. This correlates with borehole DSRC224, which indicates the presence of gravel and silt.
	F5b	Very good correlation between the borehole log and resistivity section, showing the transition between more resistive gravel and silt and more conductive mudstone bedrock. Once again, the bedrock is likely to be highly weathered and rich in clay/water-bearing fractures given an S-wave velocity of 520 m/s and its conductive nature.
	F5c	Broad zone of increased resistivity, likely indicating a decrease of clay and/or water within the deeper superficial deposits, a structural feature (e.g. minor, vertical fault) or change in sediment lithology.
	F5d	Isolated zones of increased resistivity, likely indicating a decrease of clay and/or water within the superficial deposits, or change in sediment lithology. This could possibly be more granular silt and/or gravel (or less likely slipped blocks of limestone rock) originating from higher up the slope.
	F5e	Isolated resistive feature also correlates with a ‘step-up’ in Layer S4 and an increase in material stiffness on the MASW section. Therefore this is likely to indicate a shallowing of the mudstone bedrock, or change in Lias bedrock lithology (e.g. limestone?). A borehole would be required to confirm this.
	F5f	An increase in the thickness of Layer S2 (163 m/s) correlates with a zone of softer, less consolidated material on the MASW section (loose silt/gravel)
	F5g	Very good correlation between Layers S4/P5 for the majority of the profile. The correlation is lost towards both ends of the sections; at the north-western end where there is a ‘step-up’ in Layer S4 only and at the south-eastern end where Layer P5 appears to level off. Such discrepancies between bedrock boundaries can be due to the P and S-wave energy following different travel paths (e.g. different beddings within an interbedded bedrock, or different weathered zones). Layer S4

		also appears to be heading for a rock escarpment outcropping to the south-east, and it should be noted that off-end shot locations located off the south-eastern end of the profile are above the Birdlip Limestone Formation, and so this too may have influenced P and S-wave travel paths within the subsurface.
6	F6a	Isolated zones of increased resistivity, likely indicating a decrease of clay and/or water within the superficial deposits, or change in sediment lithology. This could possibly be more granular silt and/or gravel originating from higher up the slope.
	F6b	Broader zone of increased conductivity indicates an increase of water/clay within the superficial deposits or change in sediment lithology.
	F6c	An increase in the thickness of Layer S2 (171 m/s) correlates with a zone of softer, less consolidated material on the MASW section.
	F6d	Given the velocity of 541 m/s, and through comparison with Profiles 1 to 5, Layer S4 is likely to represent the Lias bedrock. Layer P5 can be seen around 6 to 10 m deeper, and likely indicates different bedding of mudstone, siltstone or potentially limestone bedrock.
	F6e	Notable increase in the thickness of Layer P3 to the south, indicating a thickening of dry, stiff superficial deposits.
7	F7a	Isolated zones of increased resistivity, likely indicating a decrease of clay and/or water within the superficial deposits, or change in sediment lithology. This could possibly be more granular silt and/or gravel (or less likely slipped blocks of limestone rock) originating from higher up the slope.
	F7b	This thick, resistive layer indicates a decrease of clay and/or water within the near-surface sediments. Comparison with the nearby Profile 5 suggests this could comprise gravel and silt.
	F7c	An increase in the thickness of Layer S2 (172 to 190 m/s) correlates with zones of softer, less consolidated material on the MASW section (e.g. loose silt/gravel)
	F7d	Very good correlation between the borehole log and resistivity section, showing the transition between more resistive gravel, clay and possible limestone blocks, and more conductive mudstone bedrock beneath. Once again, the bedrock is likely to be highly weathered and rich in clay/water-bearing fractures given an S-wave velocity of 650 m/s and its

		conductive nature. The s-wave velocity is higher than observed along Profile 5, suggesting the bedrock to be slightly more competent along Profile 7.
	F7e	Broad zone of increased resistivity, likely indicating a decrease of clay and/or water within the deeper superficial deposits, a structural feature or change in sediment lithology. This may be related to a similar feature observed along Profile 5 (F5c).
	F7f	Differences between closely spaced borehole logs may be indicative of dipping or thinning out beds, or faulting. In this case, CP-216 reveals a predominantly siltstone bedrock as opposed to CP-230 which reveals a predominantly mudstone bedrock.
	F7g	Good correlation between Layers S4/P5 for the majority of the profile. The correlation is lost towards the southern end of the section where there is a ‘step-up’ in Layer S4 only. Such discrepancies between bedrock boundaries can be due to the P and S-wave energy following different travel paths (e.g. different beddings within an interbedded bedrock, or different weathered zones, or faulting). Layer S4 also appears to be heading for a rock escarpment outcropping to the south-east, and it should be noted that off-end shot locations located off the south-eastern end of the profile are above the Birdlip Limestone Formation, and so this too may have influenced P and S-wave travel paths within the subsurface.
	F7h	Isolated resistive feature also correlates with a ‘step-up’ in Layer S4 and an increase in material stiffness on the MASW section. Therefore this is likely to indicate a shallowing of the mudstone bedrock, or change in Lias bedrock lithology (e.g. limestone?). A borehole would be required to confirm this.
	F7i	Broader zone of increased conductivity indicates an increase of water/clay within the superficial deposits or change in sediment lithology. Both CP-216 and CP-230 lower down the slope indicate the presence of clay-rich sediments underlying near-surface silts/gravels.
	F7j	Good correlation between Layer S4 and the MASW (increased velocity and stiffening) as well as the boreholes, indicating a transition into stiffer material interpreted to be the Lias bedrock.
8	F8a	Broad, laterally continuous zone of increased resistivity, indicating a decrease of clay and/or water and showing good correlation with Layer

		S4. In general, the section appears absent of any particularly resistive zones of interest, and resistivity values remain very low, which would be indicative of a weak Lias bedrock lithology.
	F8b	Broad, laterally continuous zone of increased conductivity indicates an increase of water/clay within the superficial deposits, or change in sediment lithology (e.g. transition from silt or gravel, to clay-rich sediments).
	F8c	Good correlation between Layer S4 and the MASW, indicating a transition into stiffer material which is likely to represent the Lias bedrock although a borehole would be needed to confirm this, especially as the corresponding Layer P4 velocity (1586 m/s) is more indicative of dense, saturated sediments. However, it is possible that Layer P4 represents the position of the water table. As with other adjacent profiles, an S-wave velocity of 556 m/s would suggest the presence of very weak, weathered mudstone bedrock.
	F8d	In general, there is a very good correlation between Profiles 6 and 8 at the intersection point. One notable observation is the lack of Layer P5 in Profile 8, which is likely due to the fact that this layer is hovering around the limit of depth penetration for this particular survey setup.
9	F9a	This thick, resistive layer indicates a decrease of clay and/or water within the near-surface sediments. Comparison with the nearby Profiles 5 and 7 suggests this could comprise gravel and silt.
	F9b	Broad zone of increased conductivity indicates an increase of water/clay within the superficial deposits, or change in sediment lithology (e.g. clay-rich sediments, as is observed at the northern end of Profile 7).
	F9c	Very good correlation between Layers S4/P5 for the majority of the profile. The correlation is lost towards the northern end where Layer P5 appears to deepen. Such discrepancies between bedrock boundaries can be due to the P and S-wave energy following different travel paths (e.g. different beddings within an interbedded bedrock, or different weathered zones). The Layer S4 velocity is lower than average (495 m/s), suggesting a much weaker, weathered bedrock lithology.
	F9d	Very good correlation between Layer P5 and transition into more conductive material, indicating conductive Lias, likely mudstone bedrock.
10	F10a	This thick, resistive zone, possibly extending north beyond the end of

		the section indicates a decrease of clay and/or water within the near-surface sediments (possible silt, sand or gravel-rich sediments).
	F10b	Isolated zones of increased resistivity, likely indicating a decrease of clay and/or water within the superficial deposits, or change in sediment lithology. This could possibly be more granular silt and/or gravel (or less likely slipped blocks of limestone rock) originating from higher up the slope, and which has accumulated on a level bench in the topography.
	F10c	Isolated, slightly more conductive zone, likely indicating an increase of clay and/or water within the superficial deposits. The feature located at approximately 80m chainage may be associated with a nearby spring, while the feature located at approximately 50 to 60m chainage may be associated with a zone of 'softer' sediments on the MASW section.
	F10d	Poor correlation between Layers S4/P5, indicating that the seismic energy is travelling along different beddings or weathered zones, as is also observed in other profiles. This would not be surprising, considering Profile 10 crosses the expected boundary between the Lias and the Birdlip Limestone Formation, and as such, offend and interline shot locations will likely have been delivering seismic energy into different lithological units. Borehole DSRC229 is located too far away for a direct comparison but would suggest deep, superficial silt and clay-rich sediments (>20m).
	F10e	Although DSRC229 is located too far away for a direct comparison, there is an interesting correlation shown with the MASW, where a transition into stiffer material (as indicated by the increase in S-wave velocity) may represent the transition from soft silts into stiff, conductive clay-rich sediments.
11	F11a	Broad, laterally continuous zone of increased conductivity indicates an increase of water/clay within the superficial deposits or change in sediment lithology. Boreholes DSRC107 and 108 are located too far away for direct comparison but would suggest clay-rich sediments underlying more resistive made ground material.
	F11b	Dipping resistive/conductive boundary correlates with nearby boreholes, suggesting a thickening of clay-rich sediments to the west, and also possibly to the east beyond 100 m chainage (therefore conductive feature may be a ridge in the Lias mudstone bedrock).
	F11c	Isolated zone of increased resistivity, likely indicating a decrease of clay

		and/or water within the superficial deposits, or change in sediment lithology. This could possibly be made ground associated with the road.
	F11d	Layer P5 is likely to represent a transition into more competent Lias, mudstone bedrock, given the results of nearby boreholes.
12	F12a	This thick, resistive layer, possibly extending north beyond the end of the section indicates a decrease of clay and/or water within the near-surface sediments (possible silt, sand, or gravel-rich sediments, or given the shallowing of Layer S4, this could be in-situ limestone bedrock).
	F12b	Isolated zones of increased resistivity, likely indicating a decrease of clay and/or water within the superficial deposits, or change in sediment lithology. This could possibly be more granular silt and/or gravel (or less likely slipped blocks of limestone rock) originating from higher up the slope, and which has accumulated on a level bench in the topography.
	F12c	Isolated, slightly more conductive zone, likely indicating an increase of clay and/or water (possibly from nearby springs) within the superficial deposits. The feature located at approximately 60 to 70m chainage may be associated with a zone of 'softer' sediments on the MASW section.
	F12d	Poor correlation between Layers S4/P5, indicating that the seismic energy is travelling along different beddings or weathered zones, as is also observed in other profiles. This would not be surprising, considering Profile 12 crosses the expected boundary between the Lias and the Birdlip Limestone Formation, and as such, offend and interline shot locations will likely have been delivering seismic energy into different lithological units. Profile 10 and borehole DSRC229 are located too far away for a direct comparison but would suggest deep, superficial silt and clay-rich sediments (>20m). Notably, Layer S4 appears to show a more 'stepped' profile than seen along Profile 10.
	F12e	Good correlation between Layer S4 and the MASW, indicating a transition into stiffer material which is likely to represent the bedrock from the Birdlip Limestone Formation although a borehole would be needed to confirm this, especially given the corresponding low P-wave velocities which are more indicative of dense, saturated sediments. An S-wave velocity of 503 m/s would suggest the presence of very weak, weathered mudstone bedrock.

Table 5. *Features and anomalies of interest as identified by the seismic refraction and MASW surveys.*

5 CONCLUSIONS

- The geophysical surveys have provided a non-invasive means for investigating the subsurface yielding detailed profile cross-sections of ground composition using resistivity tomography, seismic refraction, and MASW.

- The modelled resistivity sections were characterised by zones of contrasting resistivity values that reflect lithological (including an increase/decrease in clay content), hydrogeological (e.g. groundwater level, saturated zones), structural (e.g. faults, steeply dipping beds) and weathering variations within the sub-surface.

- The analysis of both the P and S-wave refraction data has identified distinct velocity layers that have provided detailed information to assist with the bulk characterisation of the shallow subsurface and, in particular, the thickness of overburden sediments and depth to weathered and unweathered bedrock. In summary, five distinct layer boundaries have been identified by the P-wave refraction survey, with velocities ranging from <300 m/s (weak, loose sediments) to >1901 m/s (weathered to unweathered bedrock). This has been further characterised by the S-wave refraction survey, which has revealed up to four notable layers of increasing material stiffness from <180 m/s (weak, loose sediments) to >761 m/s (rock). Where layer velocities vary laterally, this may be due to structural changes such as faulting or steeply dipping bedding. Finally, zones of increased rock stiffness and/or deterioration in bedrock condition have been further highlighted by the results of the MASW survey.

- Available borehole data has been included on the cross-sections for direct correlation, and if any additional borehole data becomes available, it may be possible to extend further/refine the interpretation and calibrate the acquired datasets.

Disclaimer

This report represents an opinionated interpretation of the geophysical data. It is intended for guidance with follow-up invasive investigation. Features that do not produce measurable geophysical anomalies or are hidden by other features may remain undetected. Geophysical surveys complement invasive/destructive methods and provide a tool for investigating the subsurface; they do not produce data that can be taken to represent all of the ground conditions found within the surveyed area. Areas that have not been surveyed due to obstructed access or any other reason are excluded from the interpretation.

FIGURES

KEY

- Resistivity/Seismic Profile
- EM 'ground conductivity' survey extents
- Proposed road scheme

See individual line figures for start and end coordinates and profile orientation

KEY TO BGS GEOLOGY MAP

(Taken from the British Geological Survey Geology of Britain viewer, bedrock geology only)

Source: Map data ©2020 Google.

- Lias
- Birdlip Limestone Formation
- Aston Limestone Formation
- Salperton Limestone Formation
- Fullers Earth Formation
- Hampen Formation
- White Limestone Formation
- Great Oolite Group
- Fault (expected location)

Title:

OVERALL LOCATION PLAN (ZONES 1 TO 4)

Project:

A417 CRICKLEY HILL BIRDLIP

TERRA DAT
down to earth geophysics

Tel: +44 (0) 2920 700127
Web:www.terradat.co.uk
Email: web@terradat.co.uk

Scale: 1:15000 at A3
Drawn by/Ref: MB/6688/1
Date: 23 JULY 2020

FIGURE 11

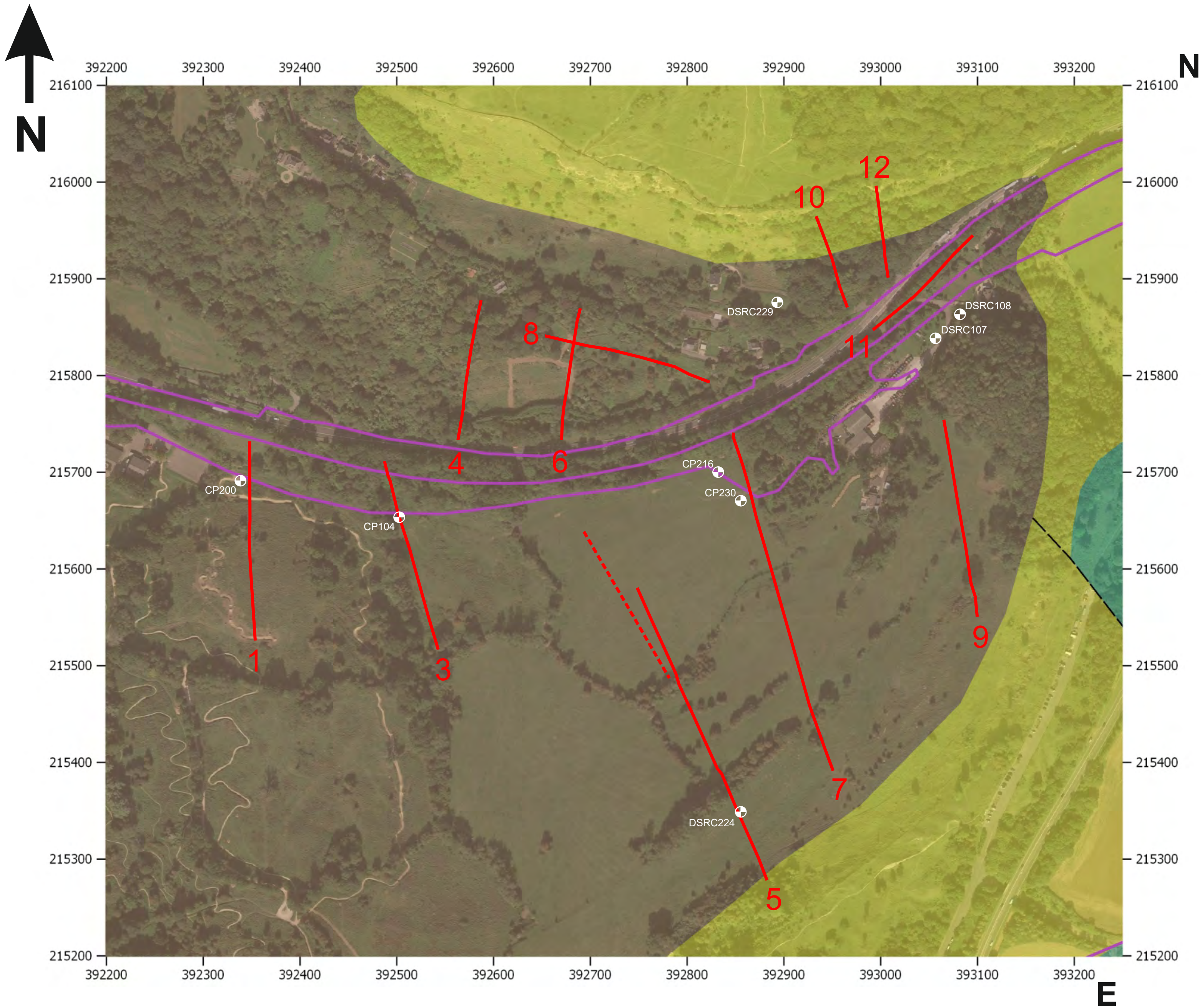

KEY

- Resistivity/Seismic Profile
- GEM Survey Extents
- Proposed road scheme
- Borehole

KEY TO BGS GEOLOGY MAP

(Taken from the British Geological Survey Geology of Britain viewer, bedrock geology only)

- Lias
- Birdlip Limestone Formation
- Aston Limestone Formation

NOTES

1. See individual line figures for start and end coordinates and profile orientation

Source: Map data ©2020 Google.

Project: **BIRDLIP**

Title: **LOCATION MAP (ZONE 2)**

TERRA DAT down to earth geophysics

Tel: +44 (0) 2920 700127
Web:www.terradat.co.uk
Email: web@terradat.co.uk

Scale: 1:6000 at A4
Drawn by/Ref: MB/6688/12
Date: 09 JULY 2020

FIGURE 12

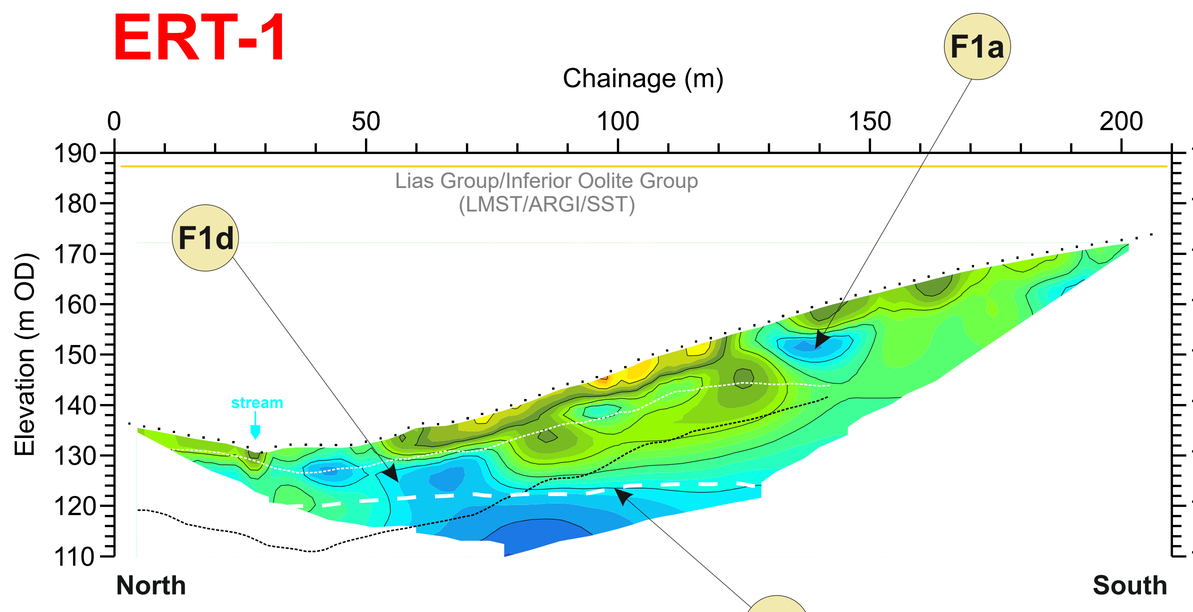

ERT-1 Profile Coordinates	
0m Chainage	204m Chainage
392348.1E 215731.4N	392353.5E 215527.0N

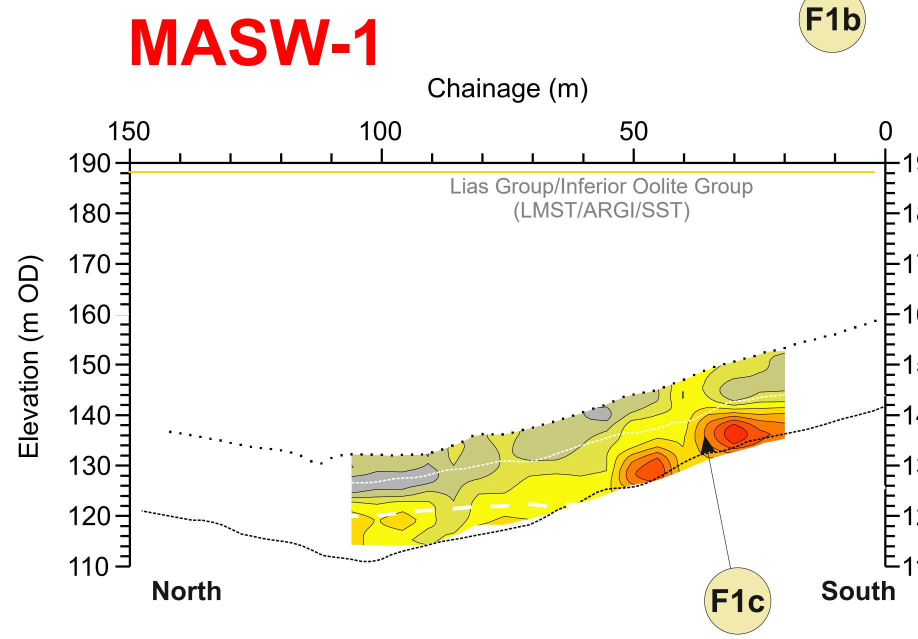

MASW-1 Profile Coordinates	
0m Chainage	142m Chainage
392348.7E 215594.5N	392347.7E 215731.8N

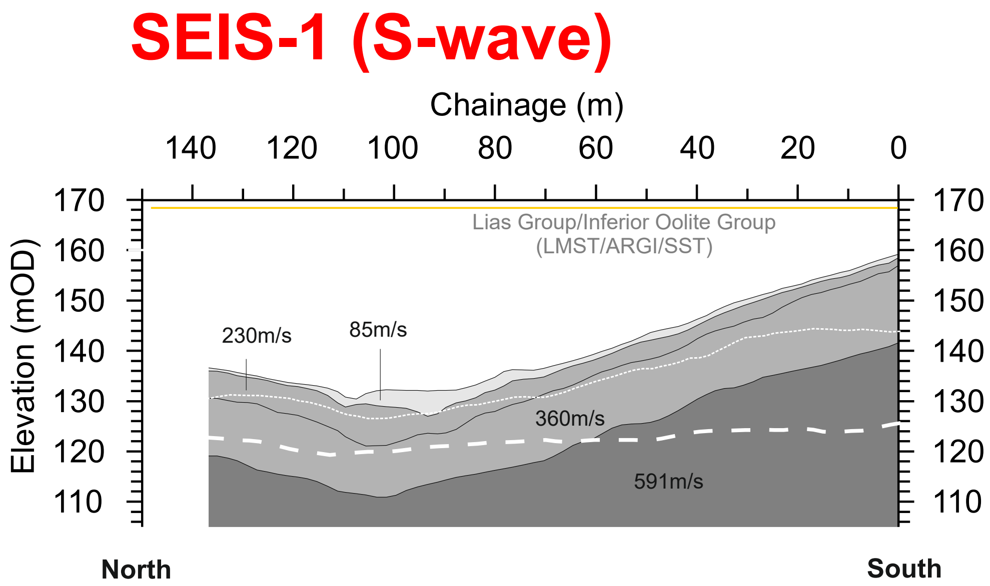

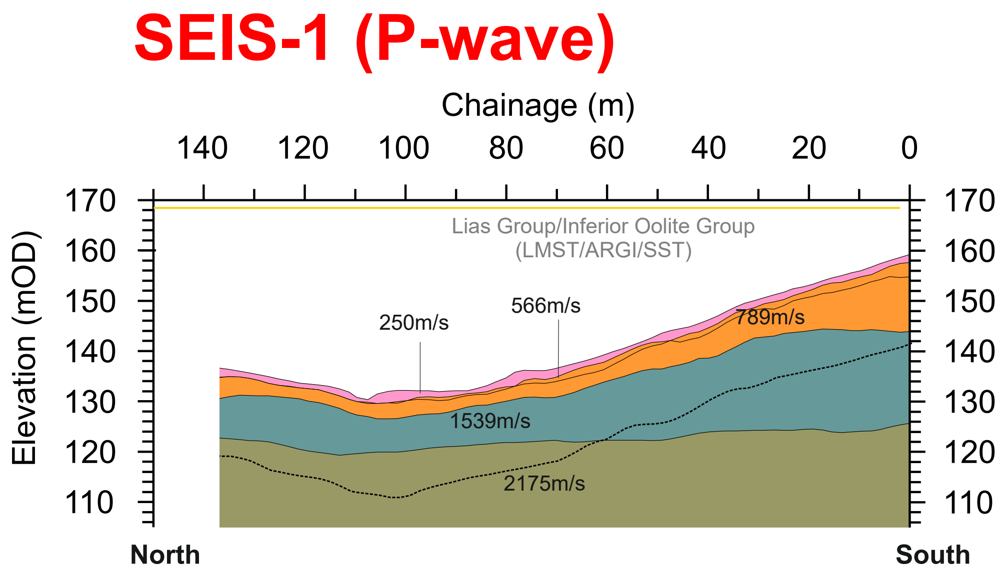

SEIS-1 Profile Coordinates	
0m Chainage	137m Chainage
392348.68E 215594.53N	392347.74E 215731.33N

ERT Section

Resistivity (ohm.m)

0, 10, 14, 19, 24, 27, 33, 39, 49, 68, 90, 108, 124, 146, 199, 294, 475

MASW Section

S-wave velocity (m/s)

100, 175, 250, 325, 400, 475, 550, 625, 700, 775

S-wave Refraction velocity layers

- Layer 1 (<180 m/s) — SOFT SOIL*
- Layer 2 (180 - 360 m/s) — STIFF SOIL*
- Layer 3 (361- 760 m/s) — VERY DENSE SOIL / SOFT(WEAK**) ROCK*
- Layer 4 (>761 m/s) — ROCK* (MODERATELY STRONG**)

S-wave boundaries shown on ERT, MASW and S-wave sections

*The NEHRP Recommended Provisions for seismic regulation for new buildings, (FEMA-222A and FEMA-223A, 1994)

** UK equivalent classification (Waltham, 1994)

P-wave Refraction velocity layers

- Layer 1 (<300 m/s)
- Layer 2 (301 - 800 m/s)
- Layer 3 (801 - 1400 m/s)
- Layer 4 (1401- 1900m/s)
- Layer 5 (>1901 m/s)

P-wave boundaries shown on ERT, MASW and S-wave sections

BOREHOLE KEY

Made ground	Sandstone
Clay	Mudstone
Silt	Siltstone
Sand	Limestone
Gravel	Core loss

KEY

- Line 1 — Profile intersection
- Fault — Reported fault positions
- Bedrock geology subcrop

NOTES/OBSERVATIONS

Title: **RESISTIVITY TOMOGRAPHY (ERT) PROFILES**

Project: **A417 CRICKLEY HILL BIRDLIP**

TERRA DAT — down to earth geophysics

Tel: +44 (0) 2920 700127
Web:www.terradat.co.uk
Email: web@terradat.co.uk

Scale: 1:1500 at A3

Drawn by/Ref: JT/6688/13

Date: 14 FEB 2020

FIGURE 13

ERT-3

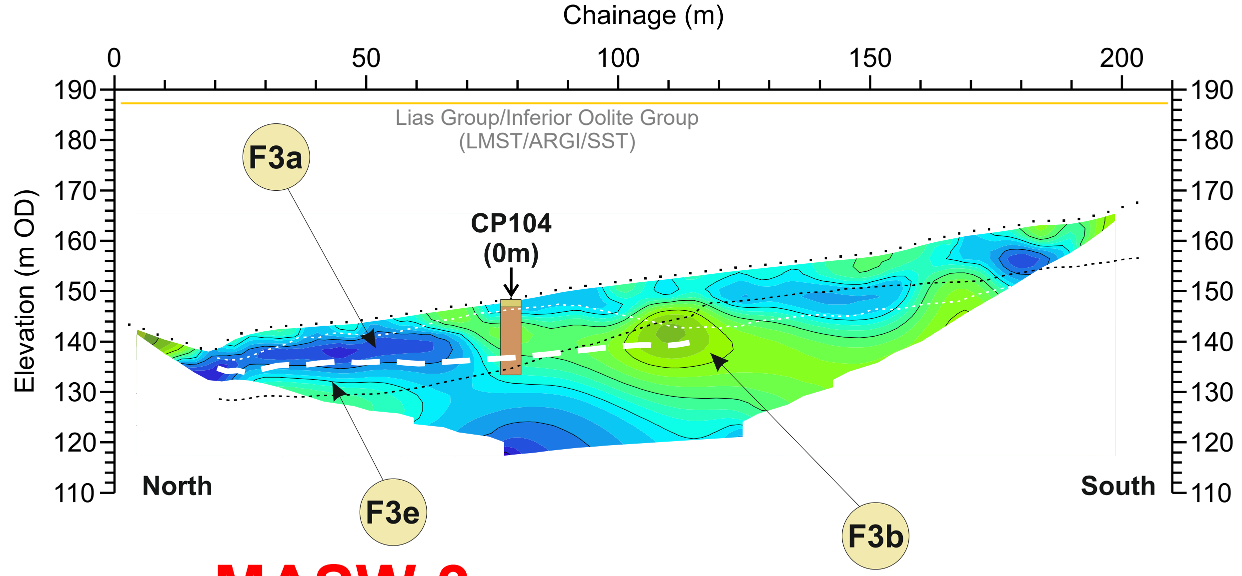

ERT-3 Profile Coordinates	
0m Chainage	201m Chainage
392487.5E 215709.1N	392543.2E 215516.0N

MASW-3

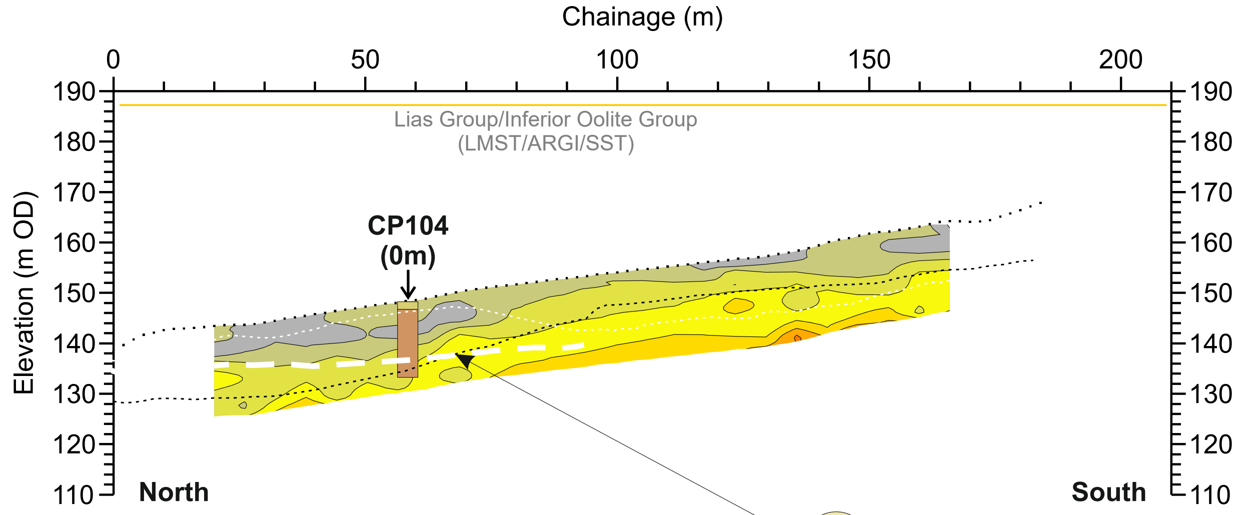

MASW-3 Profile Coordinates	
0m Chainage	184m Chainage
392493.3E 215690.3N	392544.1E 215515.6N

SEIS-3 (S-wave)

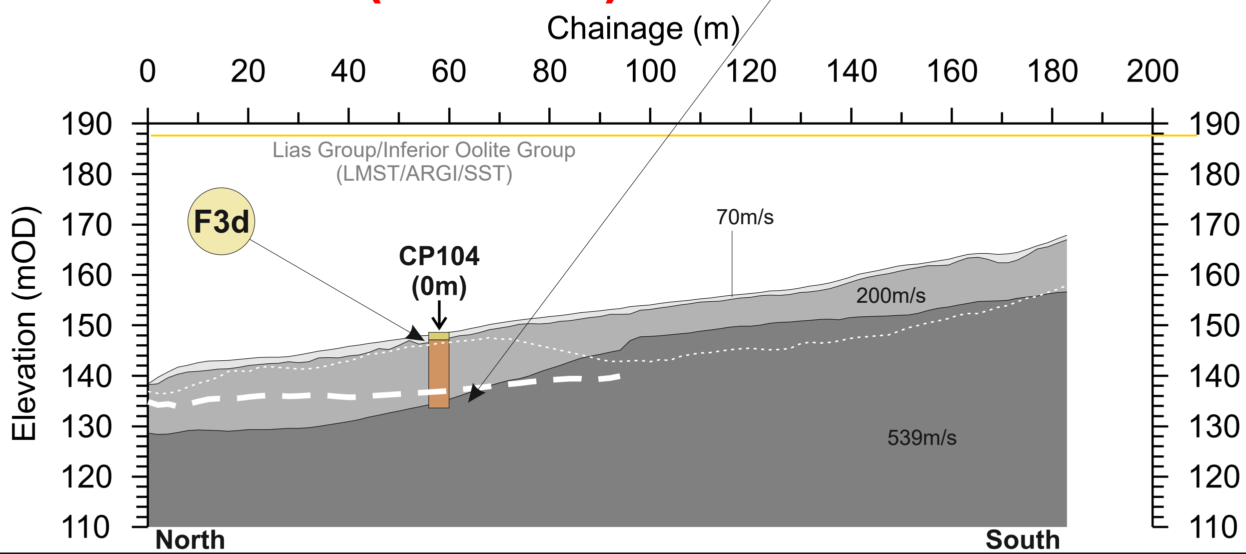

SEIS-3 (P-wave)

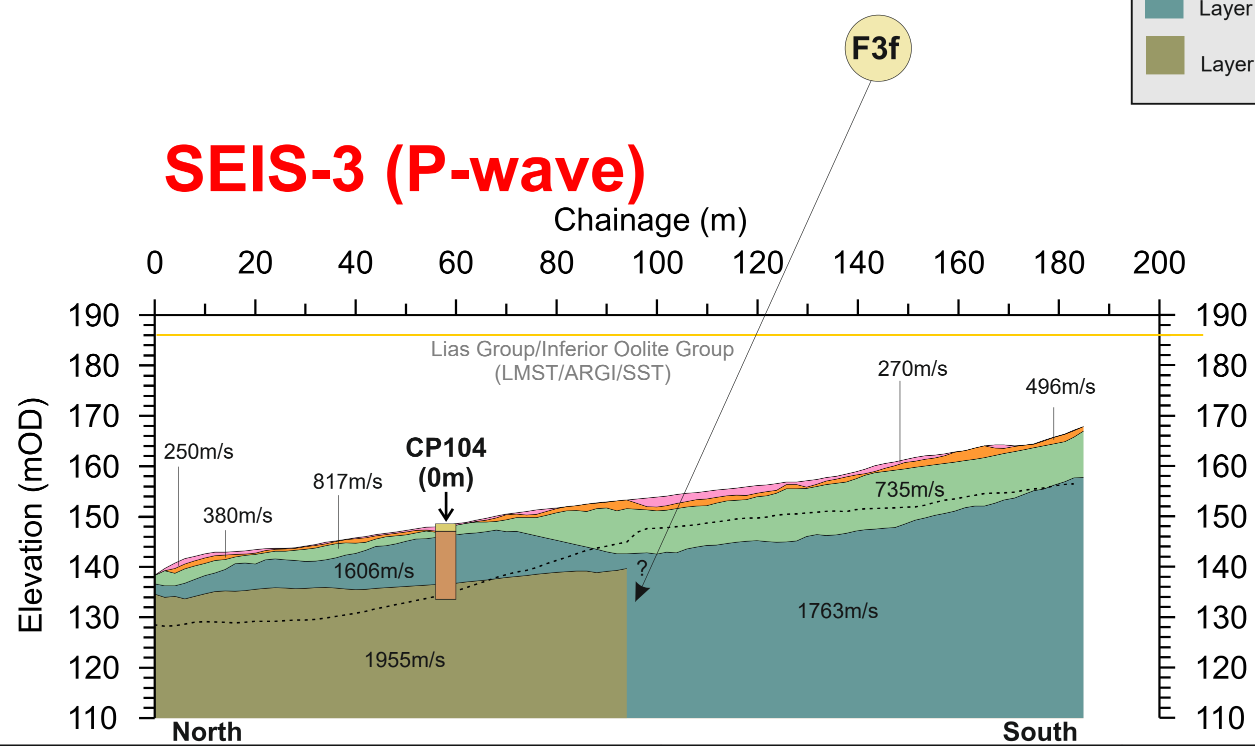

SEIS-3 Profile Coordinates	
0m Chainage	184m Chainage
392493.3E 215690.3N	392544.1E 215515.6N

ERT Section

Resistivity (ohm.m)

0, 10, 14, 19, 24, 27, 33, 39, 49, 68, 90, 108, 124, 146, 199, 294, 475

MASW Section

S-wave velocity (m/s)

100, 175, 250, 325, 400, 475, 550, 625, 700, 775

S-wave Refraction velocity layers

- Layer 1 (<180 m/s) — SOFT SOIL*
- Layer 2 (180 - 360 m/s) — STIFF SOIL*
- Layer 3 (361- 760 m/s) — VERY DENSE SOIL / SOFT(WEAK**) ROCK*
- Layer 4 (>761 m/s) — ROCK* (MODERATELY STRONG**)

S-wave boundaries shown on ERT, MASW and S-wave sections

*The NEHRP Recommended Provisions for seismic regulation for new buildings, (FEMA-222A and FEMA-223A, 1994)

** UK equivalent classification (Waltham, 1994)

P-wave Refraction velocity layers

- Layer 1 (<300 m/s)
- Layer 2 (301 - 800 m/s)
- Layer 3 (801 - 1400 m/s)
- Layer 4 (1401- 1900m/s)
- Layer 5 (>1901 m/s)

P-wave boundaries shown on ERT, MASW and S-wave sections

BOREHOLE KEY

Made ground	Sandstone
Clay	Mudstone
Silt	Siltstone
Sand	Limestone
Gravel	Core loss

KEY

- Line 1 — Profile intersection
- Fault — Reported fault positions
- Bedrock geology subcrop

NOTES/OBSERVATIONS

Title: **ERT AND SEISMIC PROFILES**

Project: **A417 CRICKLEY HILL BIRDLIP**

TERRA DAT
down to earth geophysics
Tel: +44 (0) 2920 700127
Web:www.terradat.co.uk
Email: web@terradat.co.uk

Scale: 1:1500 at A3

Drawn by/Ref: JT/6688/14

Date: 14 FEB 2020

FIGURE 14

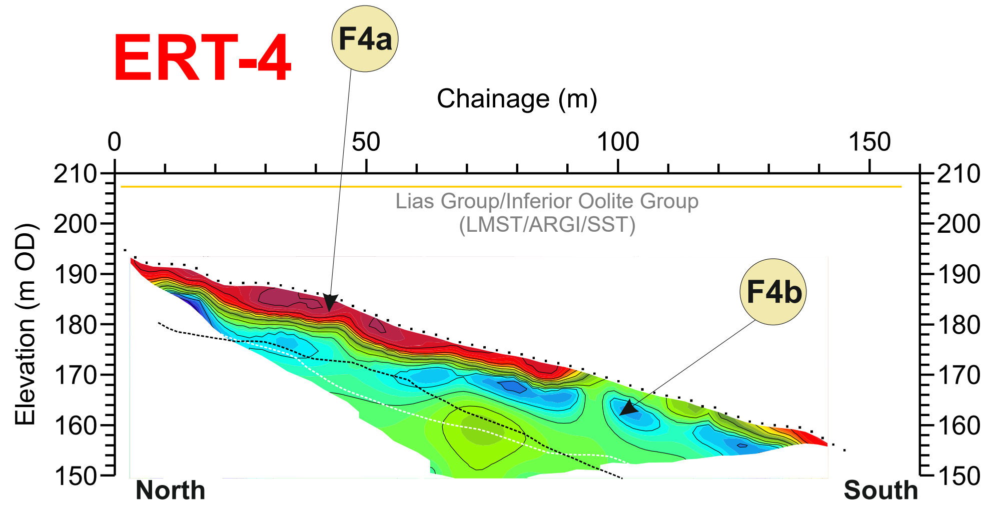

ERT-4 Profile Coordinates	
0m Chainage	145m Chainage
392586.7E 215875.5N	392563.3E 215732.8N

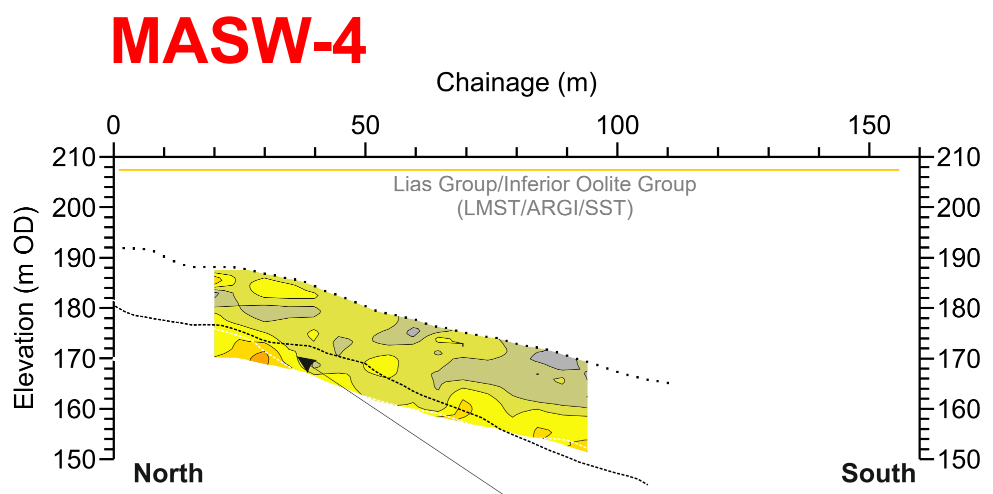

MASW-4 Profile Coordinates	
0m Chainage	110m Chainage
392584.2E 215867.8N	392569.1E 215763.5N

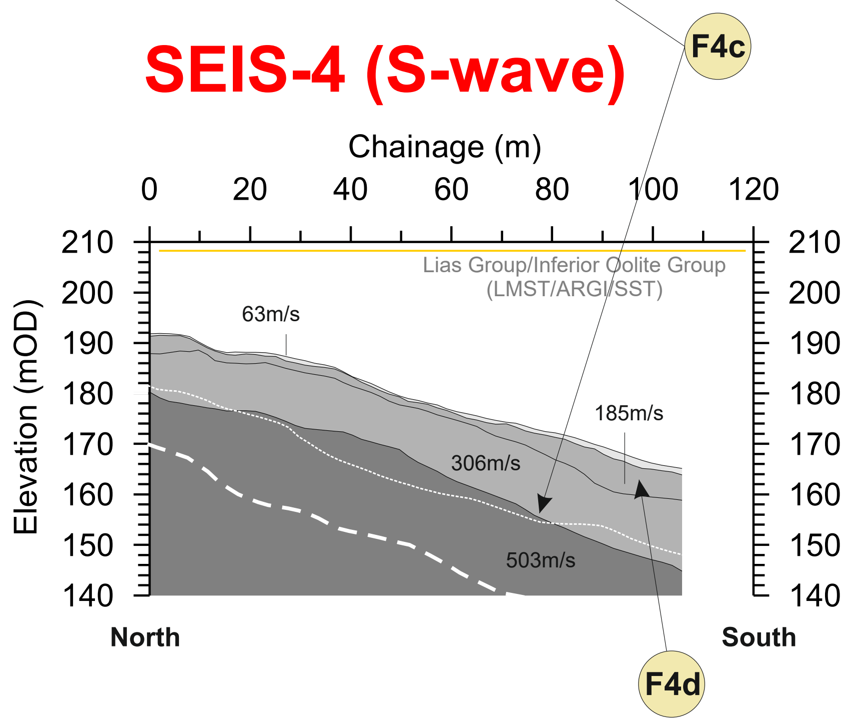

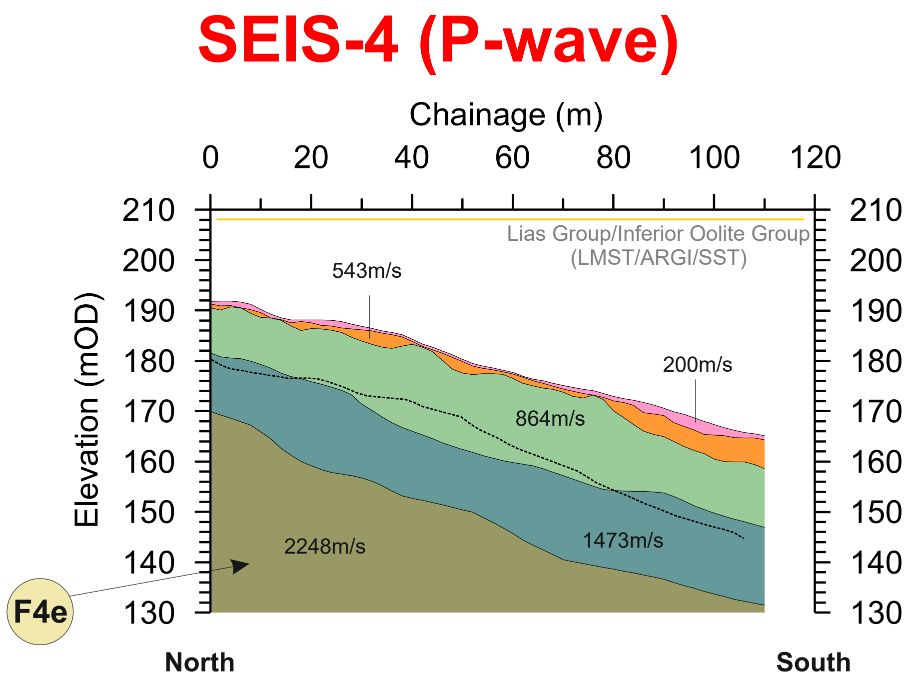

SEIS-4 Profile Coordinates	
0m Chainage	110m Chainage
392584.2E 215867.8N	392569.1E 215763.5N

ERT Section

Resistivity (ohm.m)

0 10 14 19 24 27 33 39 49 68 90 108 124 146 199 294 475

MASW Section

S-wave velocity (m/s)

100 175 250 325 400 475 550 625 700 775

S-wave Refraction velocity layers

- Layer 1 (<180 m/s) SOFT SOIL*
- Layer 2 (180 - 360 m/s) STIFF SOIL*
- Layer 3 (361- 760 m/s) VERY DENSE SOIL / SOFT(WEAK**) ROCK*
- Layer 4 (>761 m/s) ROCK* (MODERATELY STRONG**)

S-wave boundaries shown on ERT, MASW and S-wave sections

**The NEHRP Recommended Provisions for seismic regulation for new buildings, (FEMA-222A and FEMA-223A, 1994)*

*** UK equivalent classification (Waltham, 1994)*

P-wave Refraction velocity layers

- Layer 1 (<300 m/s)
- Layer 2 (301 - 800 m/s)
- Layer 3 (801 - 1400 m/s)
- Layer 4 (1401- 1900m/s)
- Layer 5 (>1901 m/s)

P-wave boundaries shown on ERT, MASW and S-wave sections

BOREHOLE KEY

Made ground	Sandstone
Clay	Mudstone
Silt	Siltstone
Sand	Limestone
Gravel	Core loss

KEY

- Line 1 — Profile intersection
- Fault — Reported fault positions
- Bedrock geology subcrop

NOTES/OBSERVATIONS

Title: ERT AND SEISMIC PROFILES

Project: A417 CRICKLEY HILL BIRDLIP

TERRA DAT down to earth geophysics

Tel: +44 (0) 2920 700127
Web:www.terradat.co.uk
Email: web@terradat.co.uk

Scale: 1:1500 at A3
Drawn by/Ref: JT/6688/15
Date: 14 FEB 2020

FIGURE 15

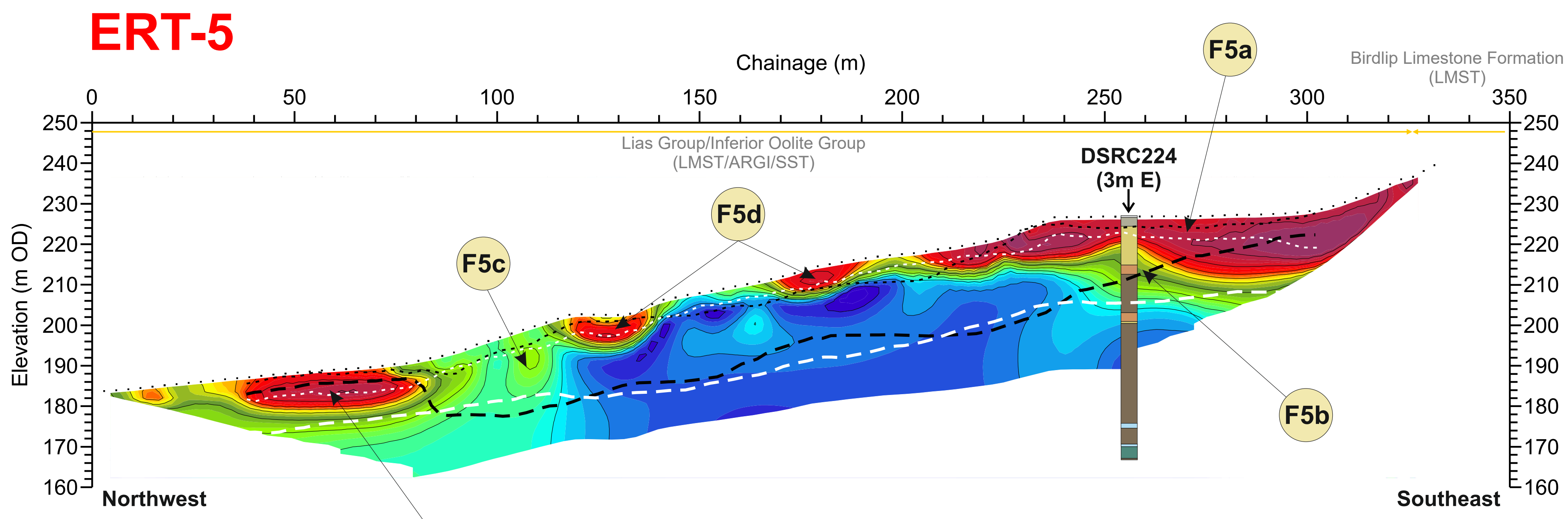

ERT-5 Profile Coordinates	
0m Chainage	330m Chainage
392749.6E 215578.5N	392883.7E 215277.4N

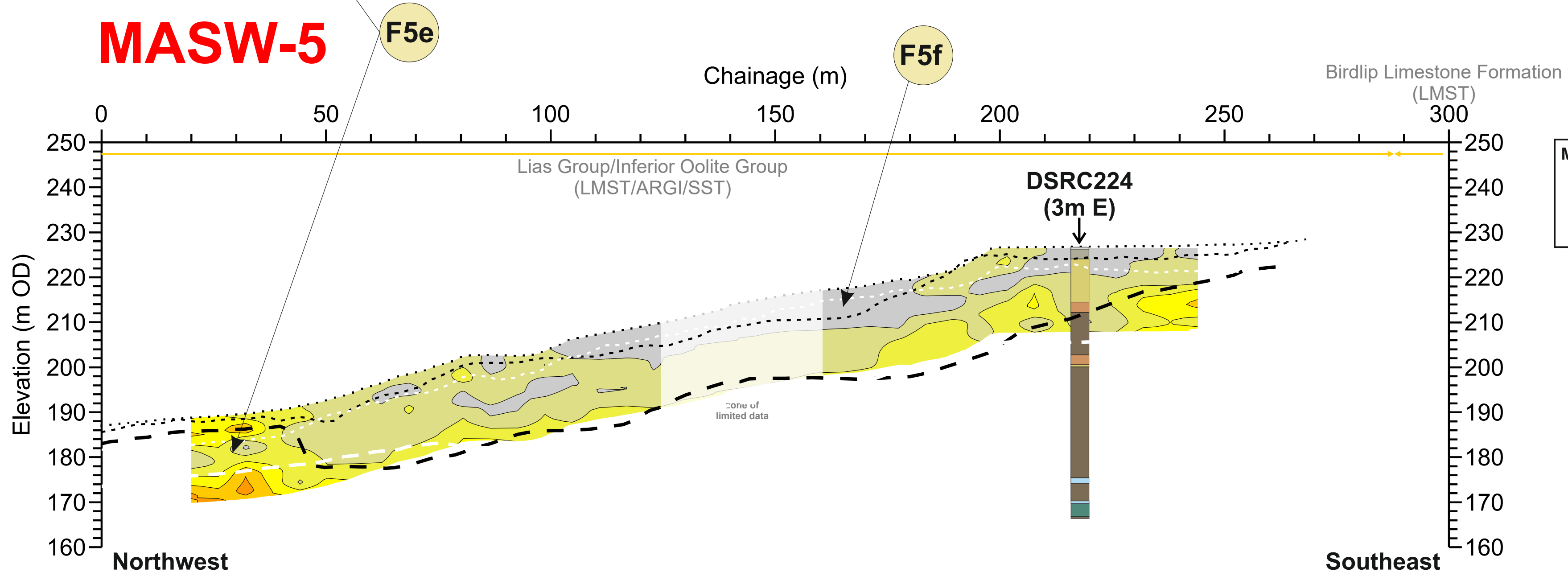

MASW-5 Profile Coordinates	
0m Chainage	330m Chainage
392763.9E 215543.7N	392871.9E 215305.1N

ERT Section

Resistivity (ohm.m)

0 10 14 19 24 27 33 39 49 68 90 108 124 146 199 294 475

MASW Section

S-wave velocity (m/s)

100 175 250 325 400 475 550 625 700 775

S-wave Refraction velocity layers

- Layer 1 (<180 m/s) SOFT SOIL*
- Layer 2 (180 - 360 m/s) STIFF SOIL*
- Layer 3 (361- 760 m/s) VERY DENSE SOIL / SOFT(WEAK**) ROCK*
- Layer 4 (>761 m/s) ROCK* (MODERATELY STRONG**)

S-wave boundaries shown on ERT, MASW and S-wave sections

**The NEHRP Recommended Provisions for seismic regulation for new buildings, (FEMA-222A and FEMA-223A, 1994)*

*** UK equivalent classification (Waltham, 1994)*

P-wave Refraction velocity layers

- Layer 1 (<300 m/s)
- Layer 2 (301 - 800 m/s)
- Layer 3 (801 - 1400 m/s)
- Layer 4 (1401- 1900m/s)
- Layer 5 (>1901 m/s)

P-wave boundaries shown on ERT, MASW and S-wave sections

COLOUR SCALE

Resistivity (ohm.m)

0 10 14 19 24 27 33 39 49 68 90 108 124 146 199 294 475

COLOUR SCALE - MASW

S-wave velocity (m/s)

100 175 250 325 400 475 550 625 700 775

BOREHOLE KEY

Made ground, Sandstone, Clay, Mudstone, Silt, Siltstone, Sand, Limestone, Gravel, Core loss

KEY

Line 1 — Resistivity profile / Refraction line

Fault — Reported fault positions

Bedrock geology subcrop

NOTES/OBSERVATIONS

Title: **ERT AND SEISMIC PROFILES**

Project: **A417 CRICKLEY HILL BIRDLIP**

TERRA DAT down to earth geophysics

Tel: +44 (0) 2920 700127
Web:www.terradat.co.uk
Email: web@terradat.co.uk

Scale: 1:1500 at A3
Drawn by/Ref: JT/6688/16A
Date: 14 FEB 2020

FIGURE 16A

SEIS-5 (S-wave)

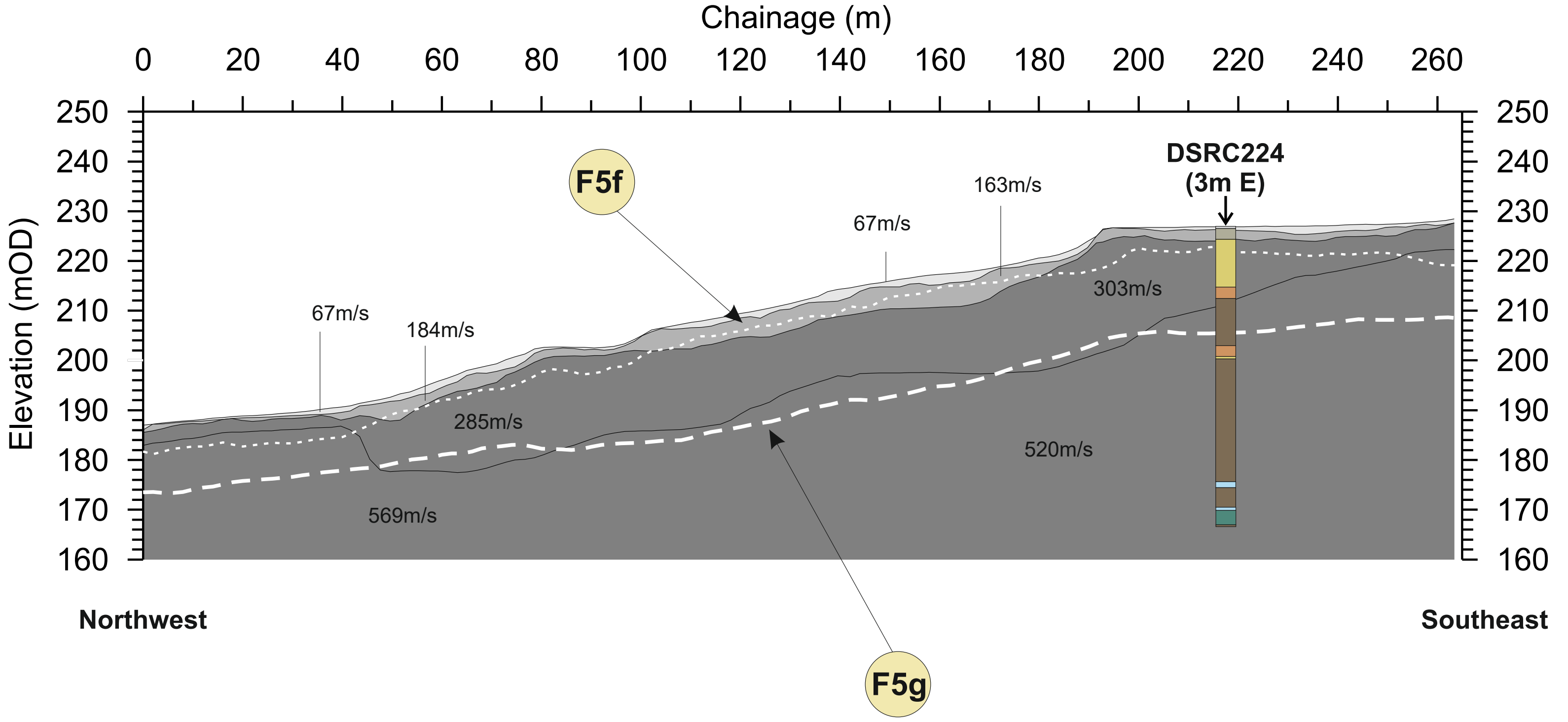

SEIS-5 (P-wave)

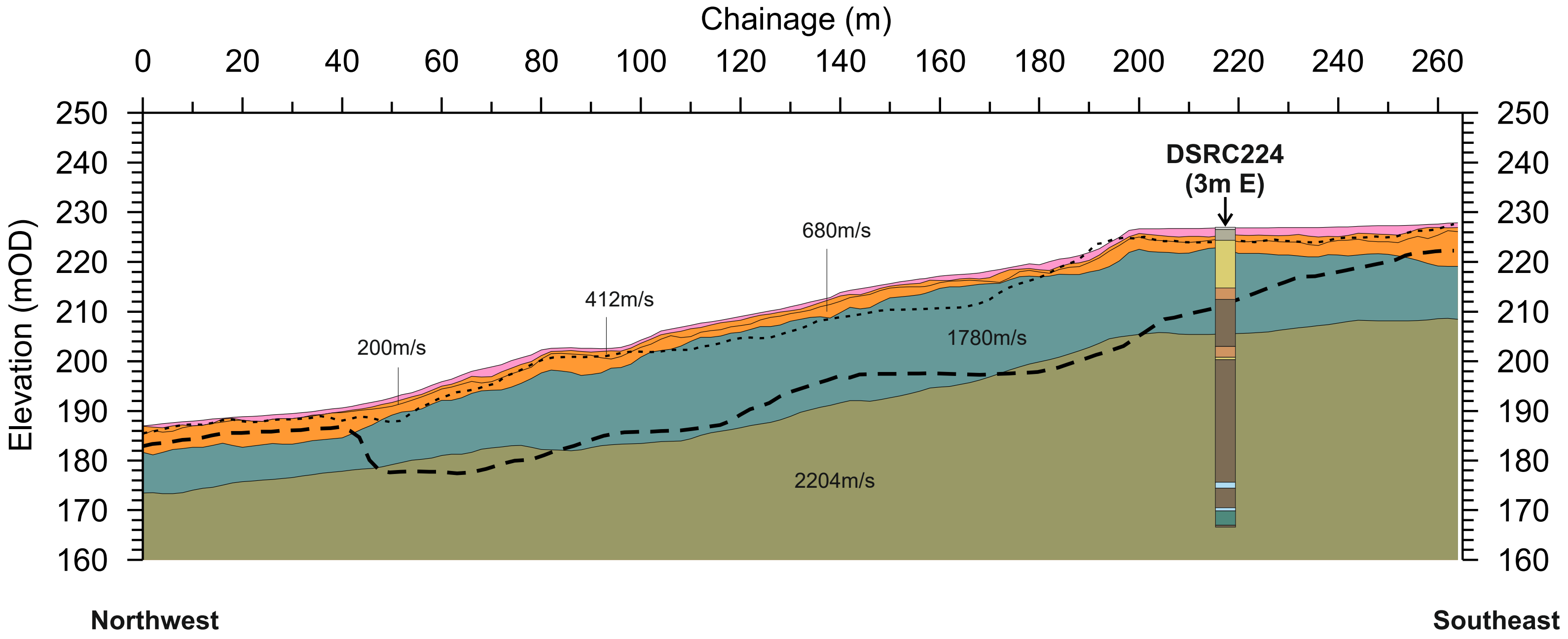

SEIS-5 Profile Coordinates	
0m Chainage	330m Chainage
392763.9E 215543.7N	392871.9E 215305.1N

ERT Section

Resistivity (ohm.m)

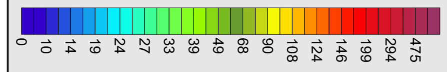

MASW Section

S-wave velocity (m/s)

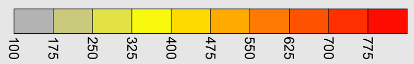

S-wave Refraction velocity layers

- Layer 1 (<180 m/s) — SOFT SOIL*
- Layer 2 (180 - 360 m/s) — STIFF SOIL*
- Layer 3 (361- 760 m/s) — VERY DENSE SOIL / SOFT(WEAK**) ROCK*
- Layer 4 (>761 m/s) — ROCK* (MODERATELY STRONG**)

S-wave boundaries shown on ERT, MASW and S-wave sections

*The NEHRP Recommended Provisions for seismic regulation for new buildings, (FEMA-222A and FEMA-223A, 1994)

** UK equivalent classification (Waltham, 1994)

P-wave Refraction velocity layers

- Layer 1 (<300 m/s)
- Layer 2 (301 - 800 m/s)
- Layer 3 (801 - 1400 m/s)
- Layer 4 (1401- 1900m/s)
- Layer 5 (>1901 m/s)

P-wave boundaries shown on ERT, MASW and S-wave sections

BOREHOLE KEY

Made ground, Sandstone, Clay, Mudstone, Silt, Siltstone, Sand, Limestone, Gravel, Core loss

KEY

Line 1 — Resistivity profile

Fault — Reported fault positions

Bedrock geology subcrop

NOTES/OBSERVATIONS

Title: SEISMIC REFRACTION PROFILES

Project: A417 CRICKLEY HILL BIRDLIP

TERRA DAT — down to earth geophysics

Tel: +44 (0) 2920 700127
Web:www.terradat.co.uk
Email: web@terradat.co.uk

Scale: 1:1500 at A3

Drawn by/Ref: JT/6688/16B

Date: 14 FEB 2020

FIGURE 16B

ERT-6

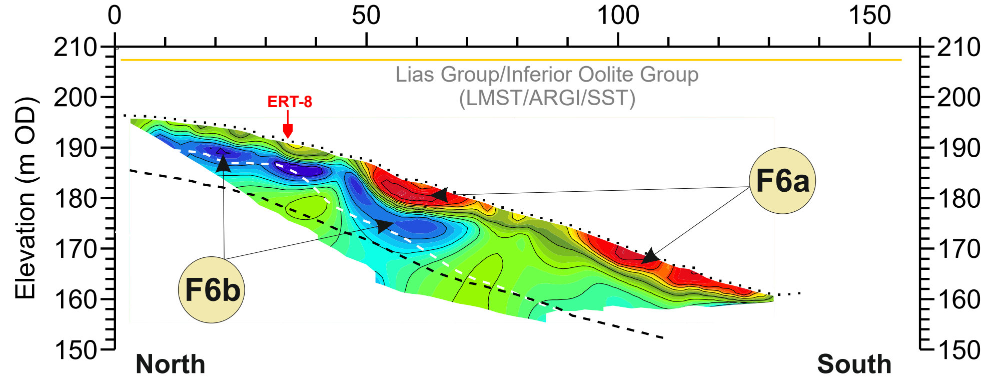

ERT-6 Profile Coordinates	
0m Chainage	135m Chainage
392689.4E	392670.5E
215866.9N	215733.0N

MASW-6

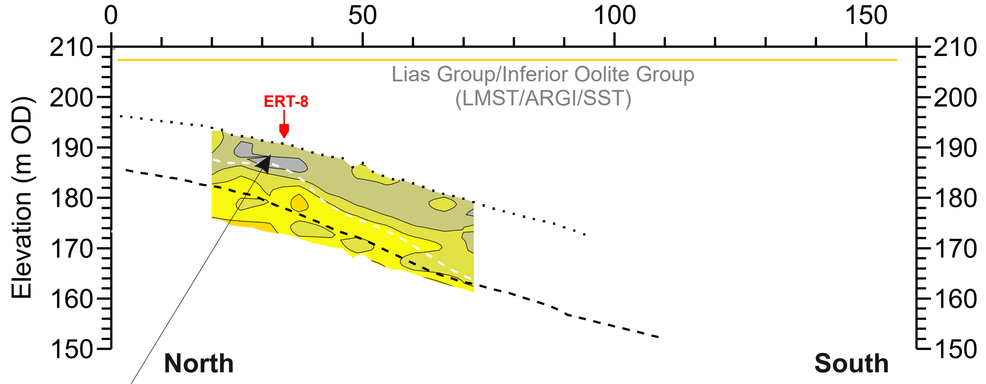

MASW-6 Profile Coordinates	
0m Chainage	94m Chainage
392688.0E	392674.3E
215862.5N	215773.1N

SEIS-6 (S-wave)

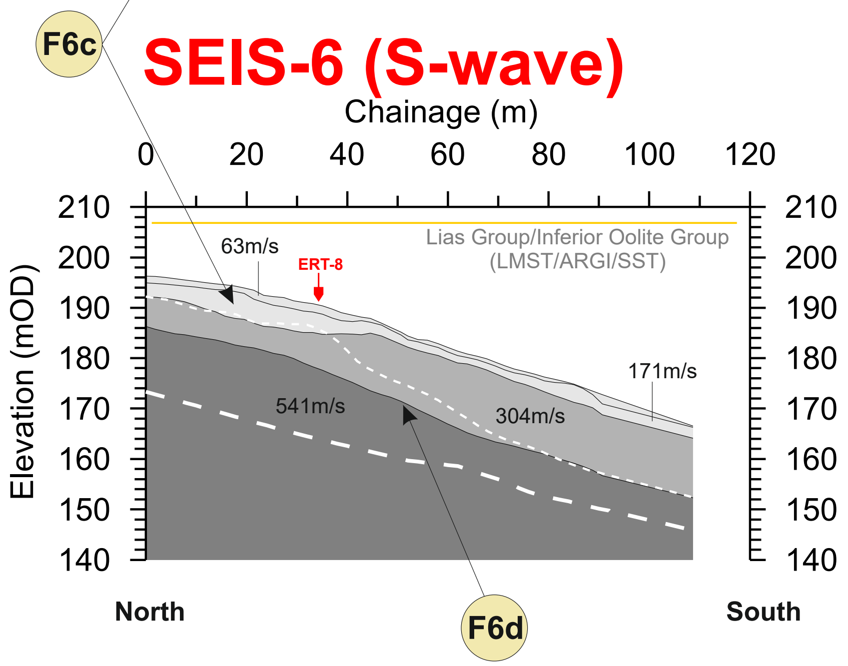

SEIS-6 (P-wave)

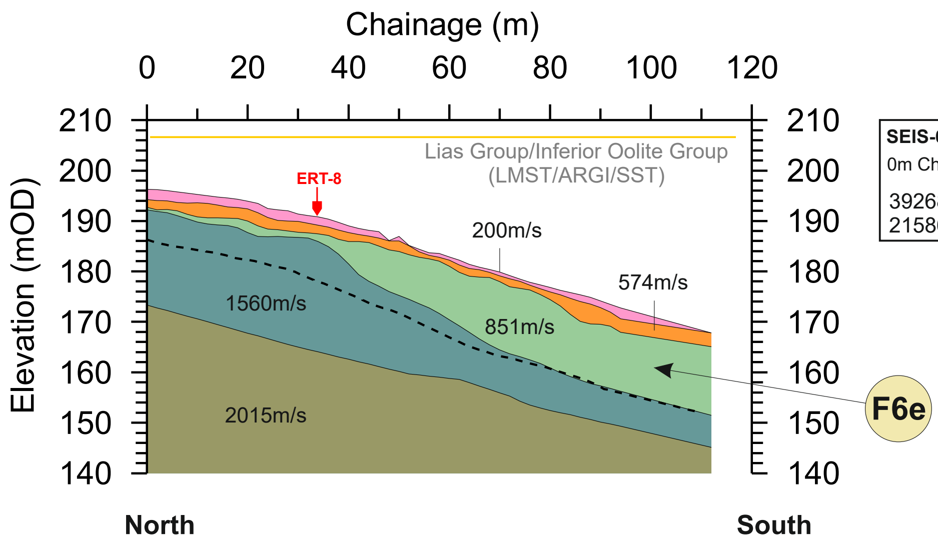

SEIS-6 Profile Coordinates	
0m Chainage	94m Chainage
392688.0E	392674.3E
215862.5N	215773.1N

ERT Section

Resistivity (ohm.m)

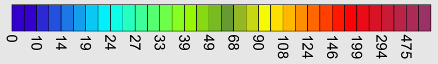

MASW Section

S-wave velocity (m/s)

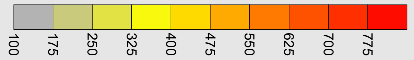

S-wave Refraction velocity layers

- Layer 1 (<180 m/s) SOFT SOIL*
- Layer 2 (180 - 360 m/s) STIFF SOIL*
- Layer 3 (361- 760 m/s) VERY DENSE SOIL / SOFT(WEAK**) ROCK*
- Layer 4 (>761 m/s) ROCK* (MODERATELY STRONG**)

S-wave boundaries shown on ERT, MASW and S-wave sections

**The NEHRP Recommended Provisions for seismic regulation for new buildings, (FEMA-222A and FEMA-223A, 1994)*

*** UK equivalent classification (Waltham, 1994)*

P-wave Refraction velocity layers

- Layer 1 (<300 m/s)
- Layer 2 (301 - 800 m/s)
- Layer 3 (801 - 1400 m/s)
- Layer 4 (1401- 1900m/s)
- Layer 5 (>1901 m/s)

P-wave boundaries shown on ERT, MASW and S-wave sections

BOREHOLE KEY

Made ground	Sandstone
Clay	Mudstone
Silt	Siltstone
Sand	Limestone
Gravel	Core loss

KEY

- Resistivity profile
- Fault — Reported fault positions
- Bedrock geology subcrop

NOTES/OBSERVATIONS

Title: **ERT AND SEISMIC PROFILES**

Project: **A417 CRICKLEY HILL BIRDLIP**

TERRADAT down to earth geophysics
Tel: +44 (0) 2920 700127
Web:www.terradat.co.uk
Email: web@terradat.co.uk

Scale: 1:1500 at A3
Drawn by/Ref: JT/6688/17
Date: 14 FEB 2020

FIGURE 17

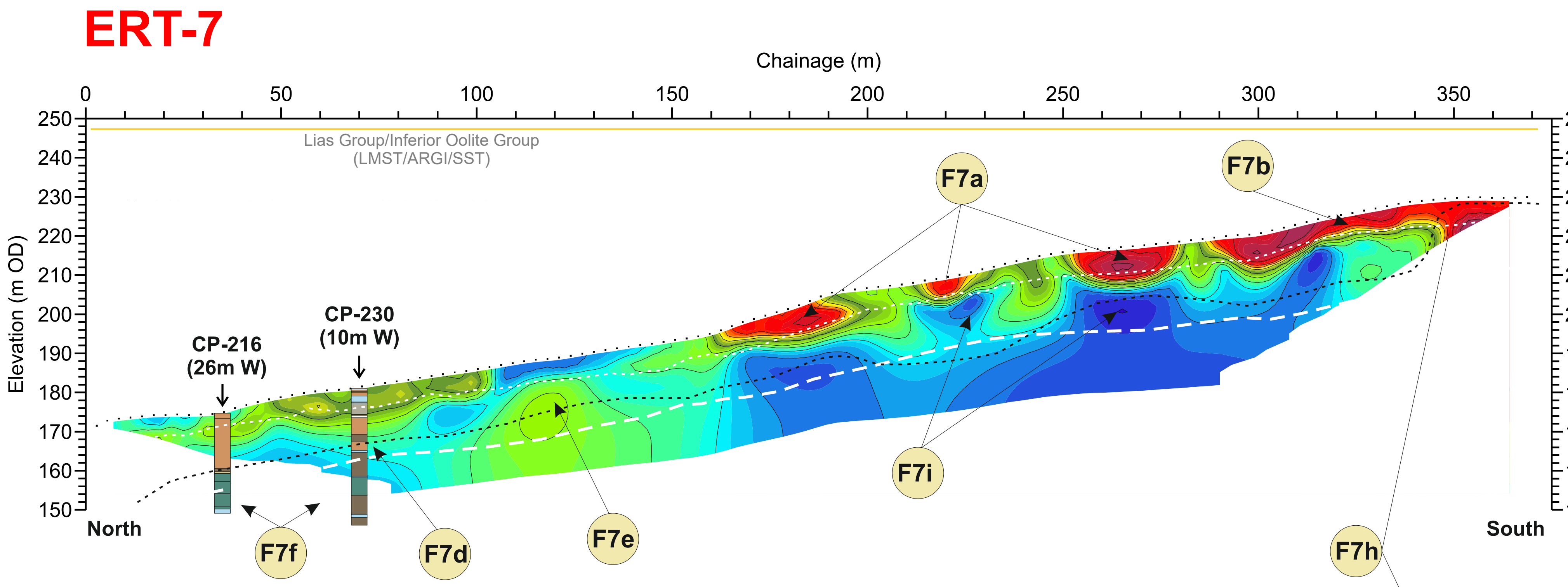

ERT-7 Profile Coordinates

0m Chainage	368m Chainage
392848.1E	392951.9E
215742.3N	215390.5N

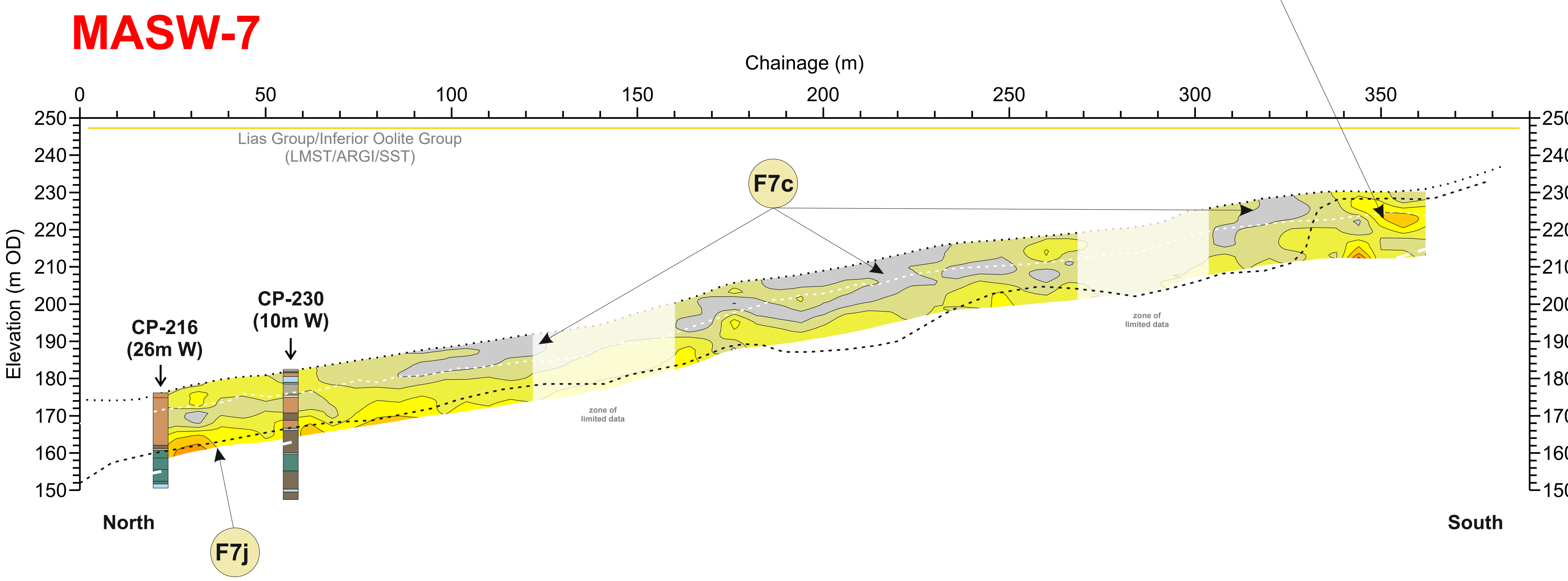

MASW-7 Profile Coordinates

0m Chainage	368m Chainage
392851.8E	392959.2E
215725.8N	215364.2N

ERT Section

Resistivity (ohm.m)

0, 10, 14, 19, 24, 27, 33, 39, 49, 68, 90, 108, 124, 146, 199, 294, 475

MASW Section

S-wave velocity (m/s)

100, 175, 250, 325, 400, 475, 550, 625, 700, 775

S-wave Refraction velocity layers

- Layer 1 (<180 m/s) SOFT SOIL*
- Layer 2 (180 - 360 m/s) STIFF SOIL*
- Layer 3 (361- 760 m/s) VERY DENSE SOIL / SOFT(WEAK**) ROCK*
- Layer 4 (>761 m/s) ROCK* (MODERATELY STRONG**)

S-wave boundaries shown on ERT, MASW and S-wave sections

**The NEHRP Recommended Provisions for seismic regulation for new buildings, (FEMA-222A and FEMA-223A, 1994)*

*** UK equivalent classification (Waltham, 1994)*

P-wave Refraction velocity layers

- Layer 1 (<300 m/s)
- Layer 2 (301 - 800 m/s)
- Layer 3 (801 - 1400 m/s)
- Layer 4 (1401- 1900m/s)
- Layer 5 (>1901 m/s)

P-wave boundaries shown on ERT, MASW and S-wave sections

BOREHOLE KEY

Made ground	Sandstone
Clay	Mudstone
Silt	Siltstone
Sand	Limestone
Gravel	Core loss

KEY

- Line 1 — Profile intersection
- Fault — Reported fault positions
- Bedrock geology subcrop

NOTES/OBSERVATIONS

Title: **ERT AND SEISMIC PROFILES**

Project: **A417 CRICKLEY HILL BIRDLIP**

TERRA DAT down to earth geophysics
Tel: +44 (0) 2920 700127
Web:www.terradat.co.uk
Email: web@terradat.co.uk

Scale: 1:1500 at A3

Drawn by/Ref: JT/6688/18A

Date: 14 FEB 2020

FIGURE 18A

SEIS-7 (S-wave)

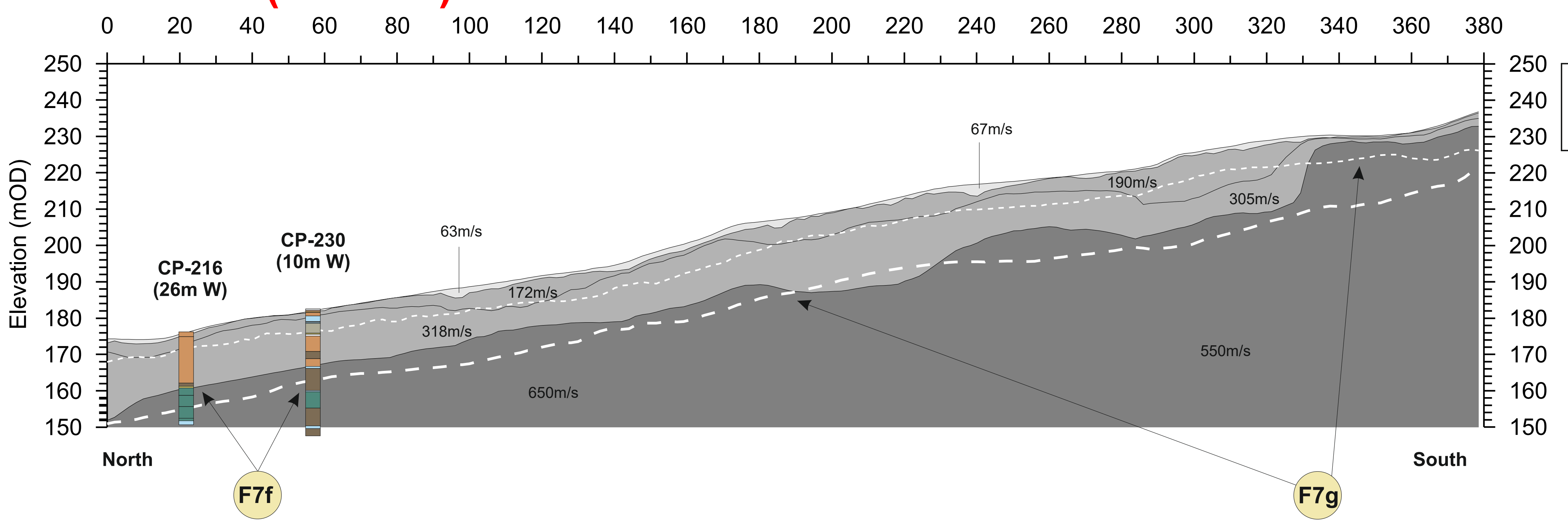

SEIS-7 Profile Coordinates

0m Chainage	368m Chainage
392851.8E 215725.8N	392959.2E 215364.2N

SEIS-7 (P-wave)

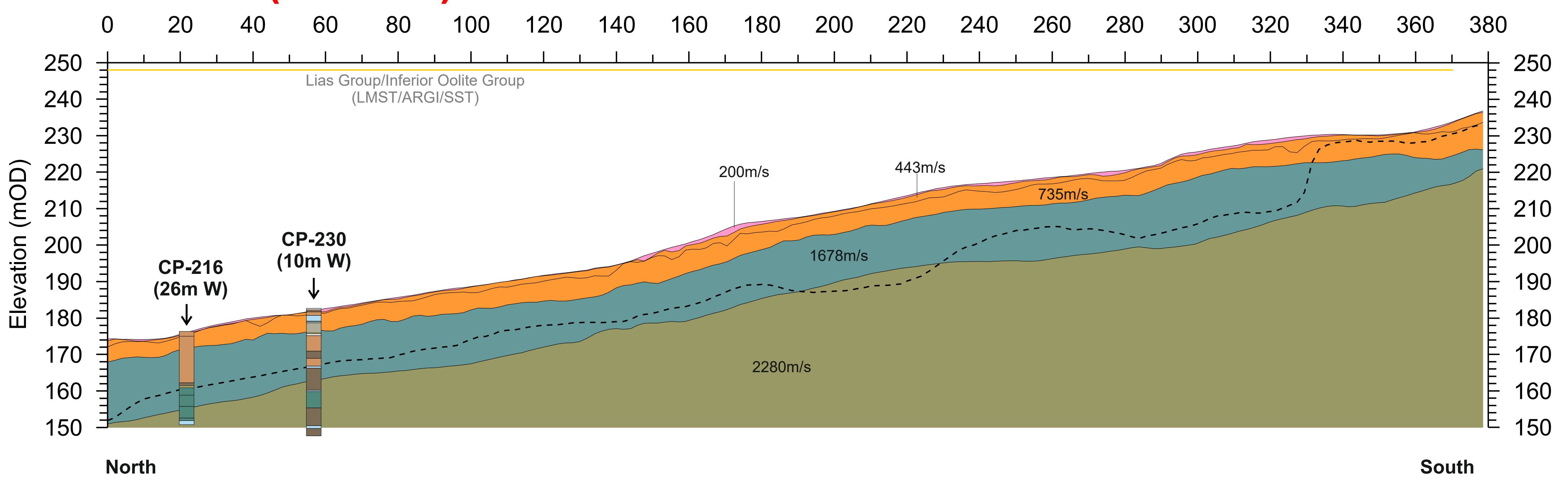

ERT Section

Resistivity (ohm.m)

0 10 14 19 24 27 33 39 49 68 90 108 124 146 199 294 475

MASW Section

S-wave velocity (m/s)

100 175 250 325 400 475 550 625 700 775

S-wave Refraction velocity layers

- Layer 1 (<180 m/s) — SOFT SOIL*
- Layer 2 (180 - 360 m/s) — STIFF SOIL*
- Layer 3 (361- 760 m/s) — VERY DENSE SOIL / SOFT(WEAK**) ROCK*
- Layer 4 (>761 m/s) — ROCK* (MODERATELY STRONG**)

S-wave boundaries shown on ERT, MASW and S-wave sections

**The NEHRP Recommended Provisions for seismic regulation for new buildings, (FEMA-222A and FEMA-223A, 1994)*

*** UK equivalent classification (Waltham, 1994)*

P-wave Refraction velocity layers

- Layer 1 (<300 m/s)
- Layer 2 (301 - 800 m/s)
- Layer 3 (801 - 1400 m/s)
- Layer 4 (1401- 1900m/s)
- Layer 5 (>1901 m/s)

P-wave boundaries shown on ERT, MASW and S-wave sections

BOREHOLE KEY

Made ground	Sandstone
Clay	Mudstone
Silt	Siltstone
Sand	Limestone
Gravel	Core loss

KEY

- Line 1 — Profile intersection
- Fault — Reported fault positions
- Bedrock geology subcrop

NOTES/OBSERVATIONS

Title: SEISMIC REFRACTION PROFILES

Project: A417 CRICKLEY HILL BIRDLIP

TERRA DAT
down to earth geophysics
Tel: +44 (0) 2920 700127
Web:www.terradat.co.uk
Email: web@terradat.co.uk

Scale:	1:1500 at A3
Drawn by/Ref:	JT/6688/18B
Date:	14 FEB 2020

FIGURE 18B

ERT-8

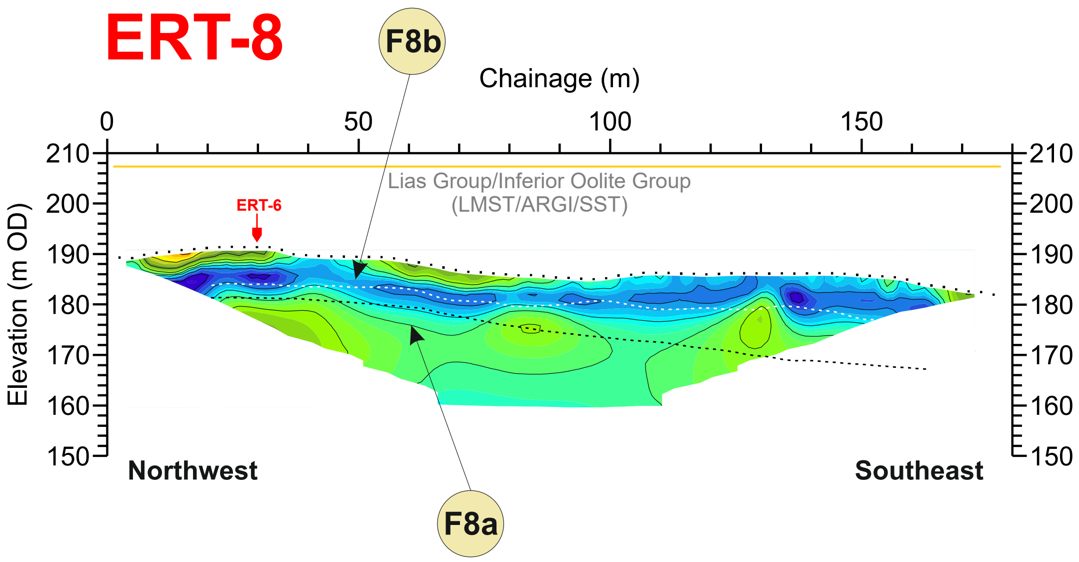

ERT-8 Profile Coordinates	
0m Chainage	175m Chainage
392653.6E 215840.6N	392822.0E 215793.6N

MASW-8

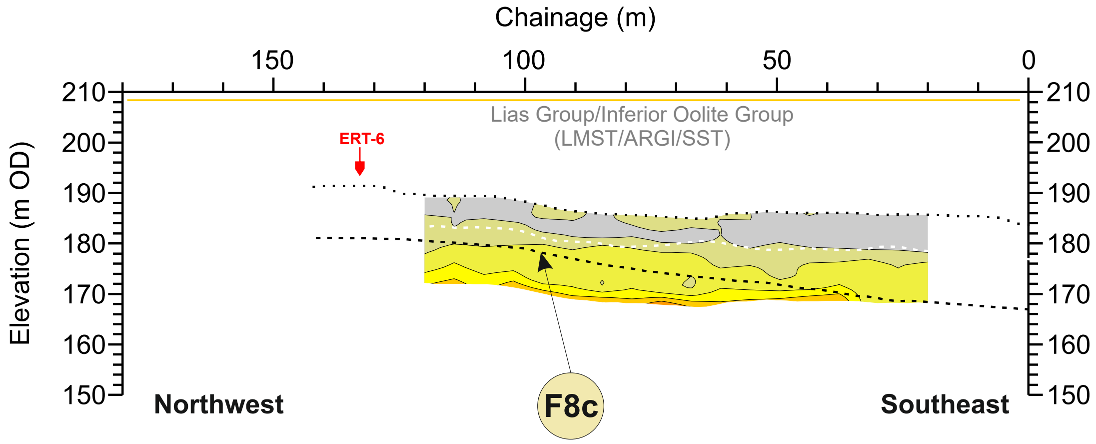

MASW-8 Profile Coordinates	
0m Chainage	142m Chainage
392809.0E 215796.6N	392672.8E 215835.8N

SEIS-8 (S-wave)

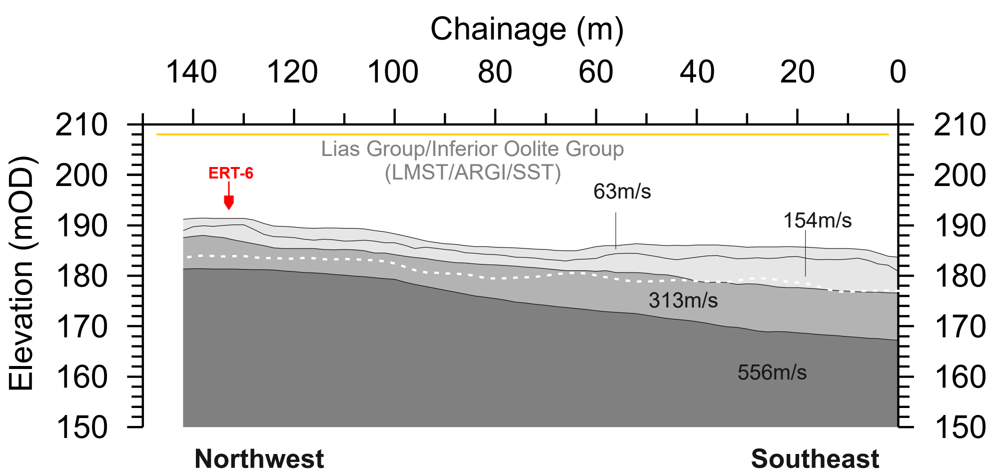

SEIS-8 (P-wave)

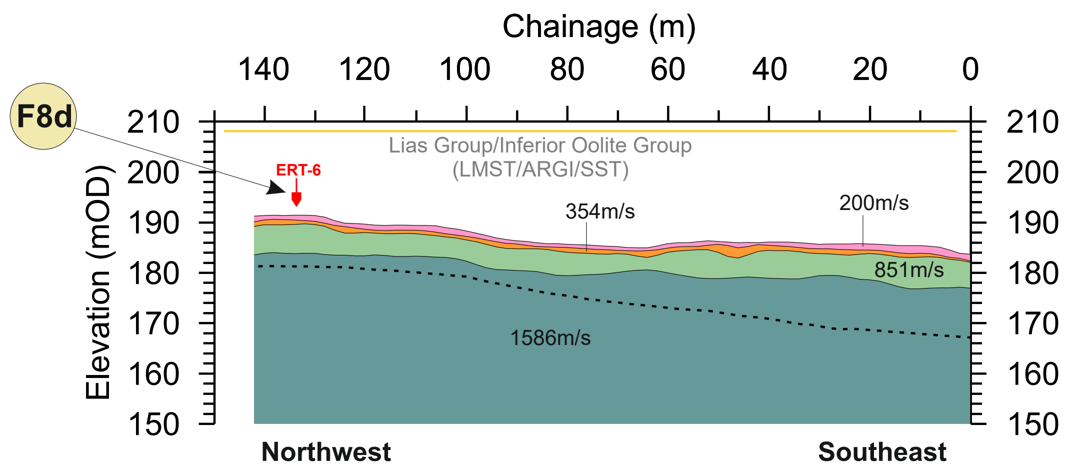

SEIS-8 Profile Coordinates	
0m Chainage	142m Chainage
392809.0E 215796.6N	392672.8E 215835.8N

ERT Section

Resistivity (ohm.m)

0, 10, 14, 19, 24, 27, 33, 39, 49, 68, 90, 108, 124, 146, 199, 294, 475

MASW Section

S-wave velocity (m/s)

100, 175, 250, 325, 400, 475, 550, 625, 700, 775

S-wave Refraction velocity layers

- Layer 1 (<180 m/s) SOFT SOIL*
- Layer 2 (180 - 360 m/s) STIFF SOIL*
- Layer 3 (361- 760 m/s) VERY DENSE SOIL / SOFT(WEAK**) ROCK*
- Layer 4 (>761 m/s) ROCK* (MODERATELY STRONG**)

S-wave boundaries shown on ERT, MASW and S-wave sections

**The NEHRP Recommended Provisions for seismic regulation for new buildings, (FEMA-222A and FEMA-223A, 1994)*

*** UK equivalent classification (Waltham, 1994)*

P-wave Refraction velocity layers

- Layer 1 (<300 m/s)
- Layer 2 (301 - 800 m/s)
- Layer 3 (801 - 1400 m/s)
- Layer 4 (1401- 1900m/s)
- Layer 5 (>1901 m/s)

P-wave boundaries shown on ERT, MASW and S-wave sections

BOREHOLE KEY

Made ground, Sandstone, Clay, Mudstone, Silt, Siltstone, Sand, Limestone, Gravel, Core loss

KEY

- Resistivity profile
- Fault — Reported fault positions
- Bedrock geology subcrop

NOTES/OBSERVATIONS

Title: **ERT AND SEISMIC PROFILES**

Project: **A417 CRICKLEY HILL BIRDLIP**

TERRA DAT down to earth geophysics

Tel: +44 (0) 2920 700127
Web:www.terradat.co.uk
Email: web@terradat.co.uk

Scale: 1:1500 at A3
Drawn by/Ref: JT/6688/19
Date: 14 FEB 2020

FIGURE 19

ERT-9

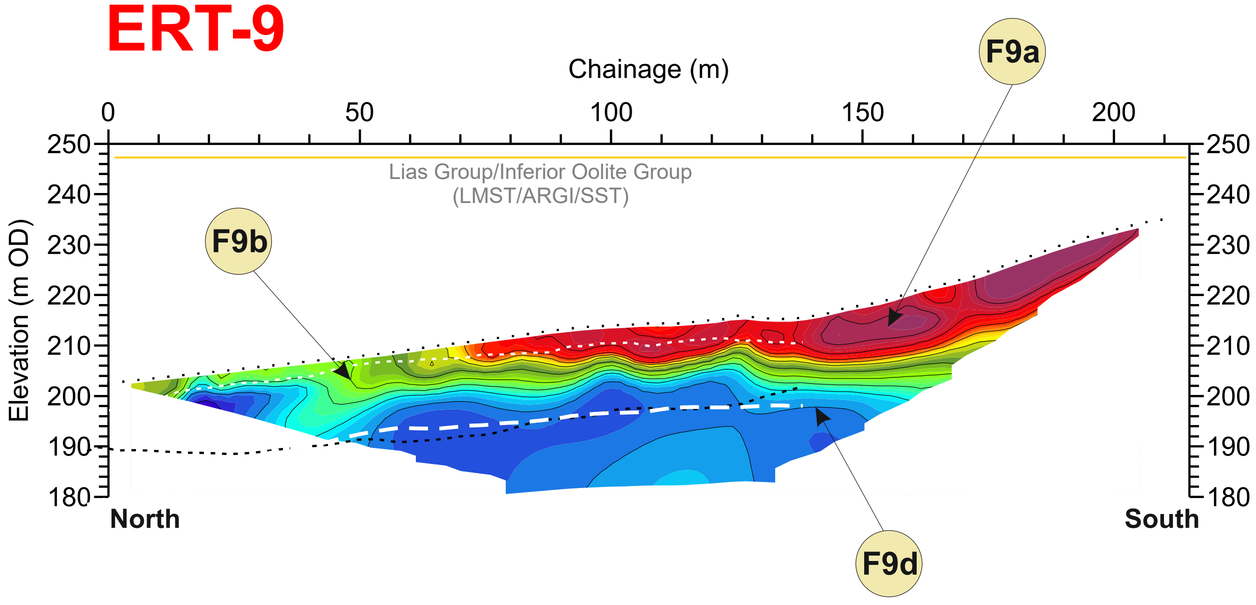

ERT-9 Profile Coordinates	
0m Chainage	209m Chainage
393066.1E 215755.4N	393100.8E 215549.9N

MASW-9

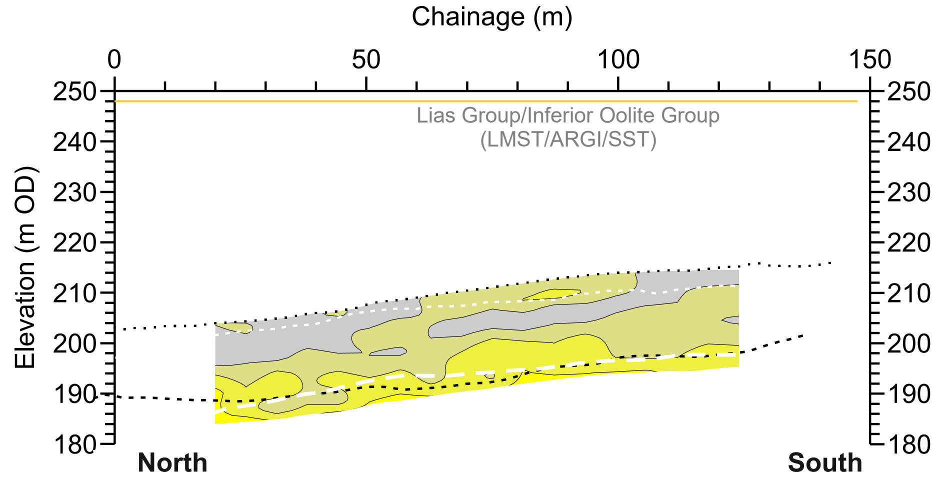

MASW-9 Profile Coordinates	
0m Chainage	142m Chainage
393065.1E 215756.4N	393089.6E 215616.8N

SEIS-9 (S-wave)

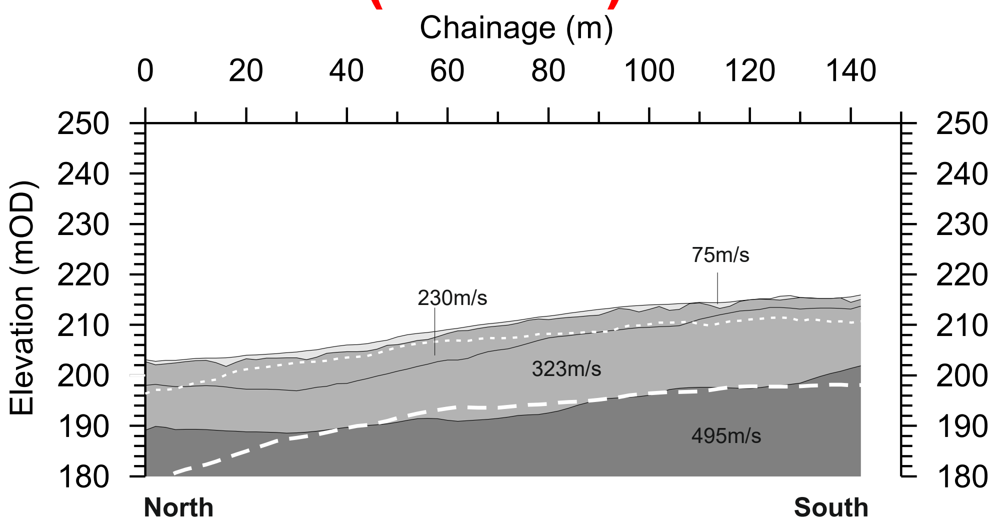

SEIS-9 (P-wave)

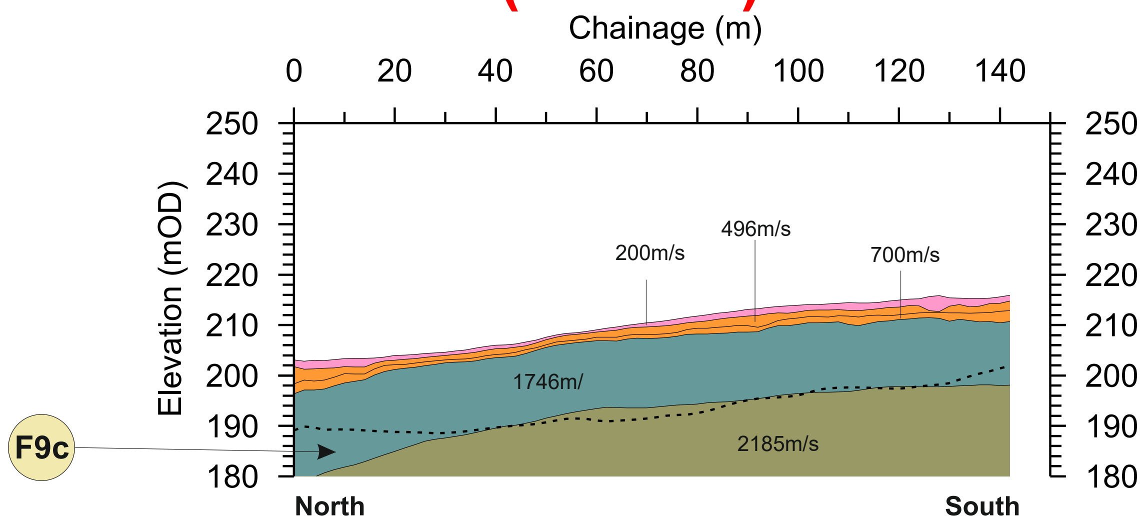

SEIS-9 Profile Coordinates	
0m Chainage	142m Chainage
393065.1E 215756.4N	393089.6E 215616.8N

ERT Section

Resistivity (ohm.m)

0, 10, 14, 19, 24, 27, 33, 39, 49, 68, 90, 108, 124, 146, 199, 294, 475

MASW Section

S-wave velocity (m/s)

100, 175, 250, 325, 400, 475, 550, 625, 700, 775

S-wave Refraction velocity layers

- Layer 1 (<180 m/s) SOFT SOIL*
- Layer 2 (180 - 360 m/s) STIFF SOIL*
- Layer 3 (361- 760 m/s) VERY DENSE SOIL / SOFT(WEAK**) ROCK*
- Layer 4 (>761 m/s) ROCK* (MODERATELY STRONG**)

S-wave boundaries shown on ERT, MASW and S-wave sections

*The NEHRP Recommended Provisions for seismic regulation for new buildings, (FEMA-222A and FEMA-223A, 1994)

** UK equivalent classification (Waltham, 1994)

P-wave Refraction velocity layers

- Layer 1 (<300 m/s)
- Layer 2 (301 - 800 m/s)
- Layer 3 (801 - 1400 m/s)
- Layer 4 (1401- 1900m/s)
- Layer 5 (>1901 m/s)

P-wave boundaries shown on ERT, MASW and S-wave sections

BOREHOLE KEY

Made ground, Sandstone, Clay, Mudstone, Silt, Siltstone, Sand, Limestone, Gravel, Core loss

KEY

Line 1 — Profile intersection

Fault — Reported fault positions

Bedrock geology subcrop

NOTES/OBSERVATIONS

Title: ERT AND SEISMIC PROFILES

Project: A417 CRICKLEY HILL BIRDLIP

TERRA DAT down to earth geophysics

Tel: +44 (0) 2920 700127
Web:www.terradat.co.uk
Email: web@terradat.co.uk

Scale: 1:1500 at A3
Drawn by/Ref: JT/6688/20
Date: 14 FEB 2020

FIGURE 20

ERT-10

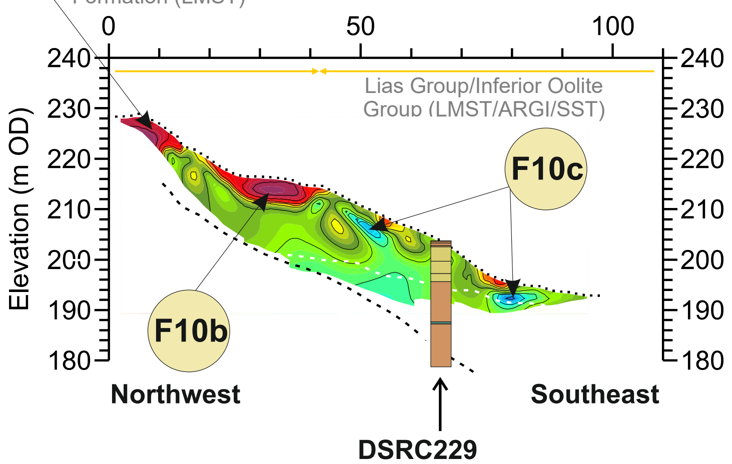

ERT-10 Profile Coordinates	
0m Chainage	96m Chainage
392934.5E 215964.6N	392965.7E 215873.4N

MASW-10

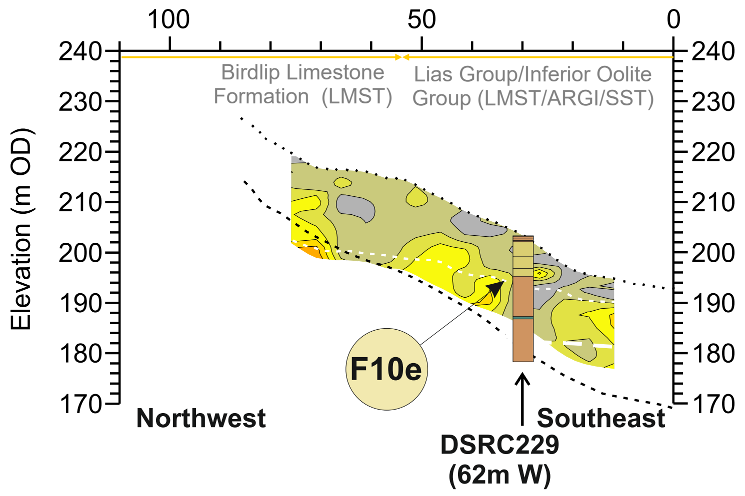

MASW-10 Profile Coordinates	
0m Chainage	85m Chainage
392966.5E 215874.2N	392938.4E 215955.2N

SEIS-10 (S-wave)

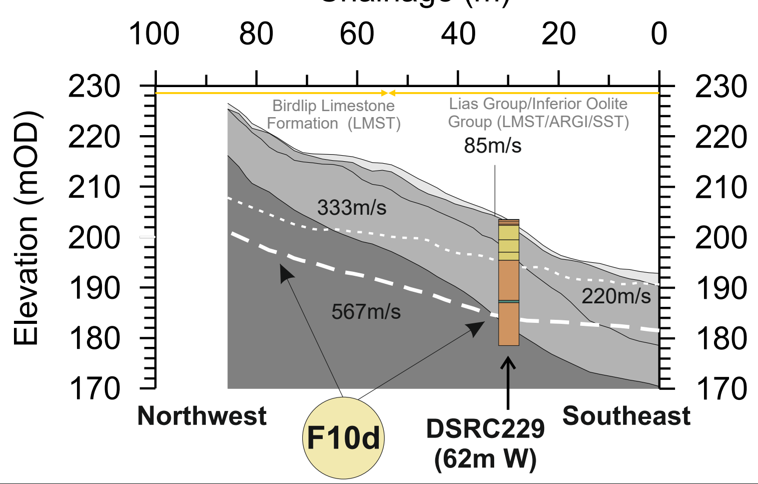

SEIS-10 (P-wave)

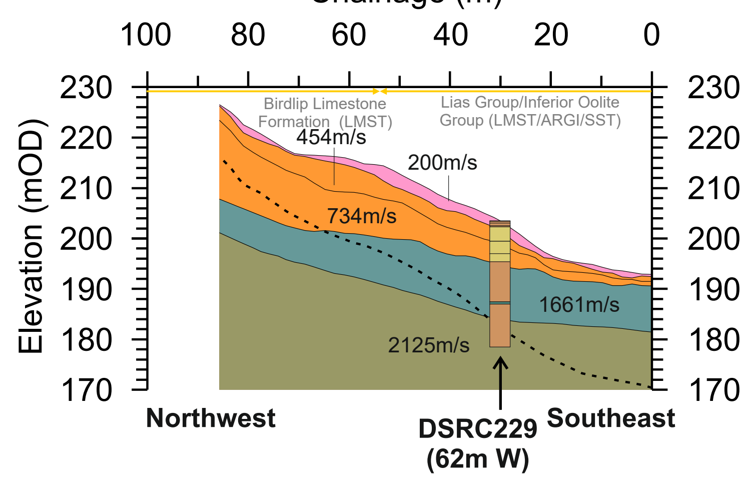

SEIS-10 Profile Coordinates	
0m Chainage	86m Chainage
392966.54E 215874.2N	392938.39E 215955.16N

ERT Section

Resistivity (ohm.m)

0, 10, 14, 19, 24, 27, 33, 39, 49, 68, 90, 108, 124, 146, 199, 294, 475

MASW Section

S-wave velocity (m/s)

100, 175, 250, 325, 400, 475, 550, 625, 700, 775

S-wave Refraction velocity layers

- Layer 1 (<180 m/s) — SOFT SOIL*
- Layer 2 (180 - 360 m/s) — STIFF SOIL*
- Layer 3 (361- 760 m/s) — VERY DENSE SOIL / SOFT(WEAK**) ROCK*
- Layer 4 (>761 m/s) — ROCK* (MODERATELY STRONG**)

S-wave boundaries shown on ERT, MASW and S-wave sections

*The NEHRP Recommended Provisions for seismic regulation for new buildings, (FEMA-222A and FEMA-223A, 1994)

** UK equivalent classification (Waltham, 1994)

P-wave Refraction velocity layers

- Layer 1 (<300 m/s)
- Layer 2 (301 - 800 m/s)
- Layer 3 (801 - 1400 m/s)
- Layer 4 (1401- 1900m/s)
- Layer 5 (>1901 m/s)

P-wave boundaries shown on ERT, MASW and S-wave sections

BOREHOLE KEY

Made ground	Sandstone
Clay	Mudstone
Silt	Siltstone
Sand	Limestone
Gravel	Core loss

KEY

- Line 1 — Profile intersection
- Fault — Reported fault positions
- Bedrock geology subcrop

NOTES/OBSERVATIONS

Title: **ERT AND SEISMIC PROFILES**

Project: **A417 CRICKLEY HILL BIRDLIP**

TERRA DAT down to earth geophysics
Tel: +44 (0) 2920 700127
Web:www.terradat.co.uk
Email: web@terradat.co.uk

Scale: 1:1500 at A3
Drawn by/Ref: JT/6688/21
Date: 14 FEB 2020

FIGURE 21

ERT-11

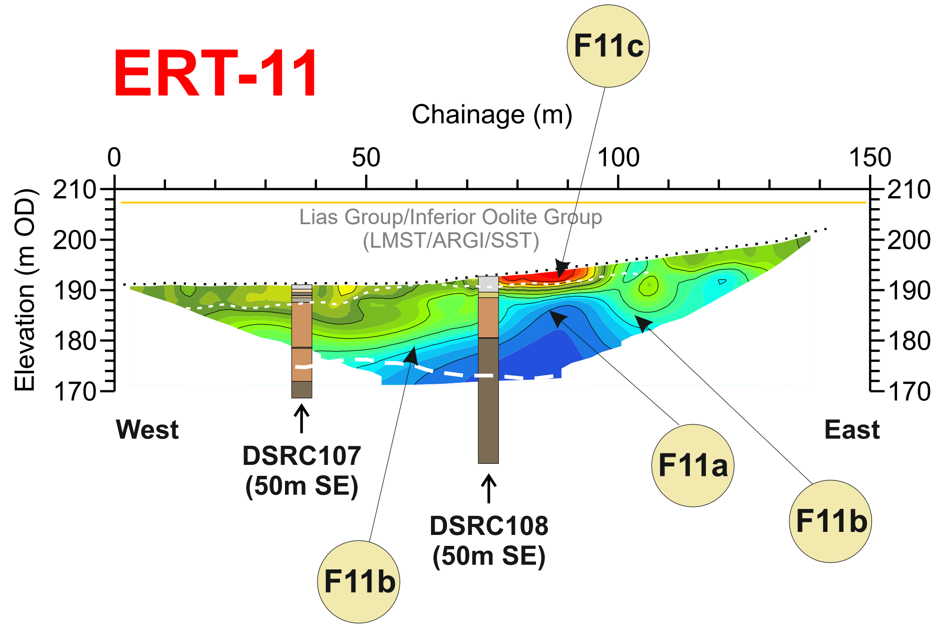

ERT-11 Profile Coordinates	
0m Chainage	140m Chainage
392994.9E 215848.8N	393096.5E 215945.3N

MASW-11

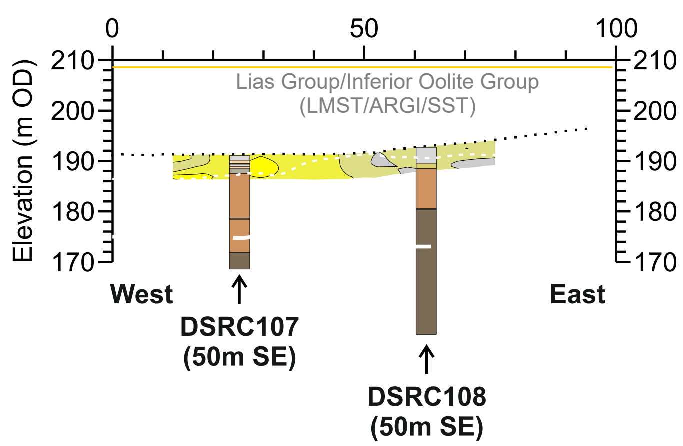

MASW-11 Profile Coordinates	
0m Chainage	94m Chainage
393004.8E 215855.5N	393071.5E 215920.1N

SEIS-11 (S-wave)

Poor data due to adverse vibrational noise from the road traffic

SEIS-11 (P-wave)

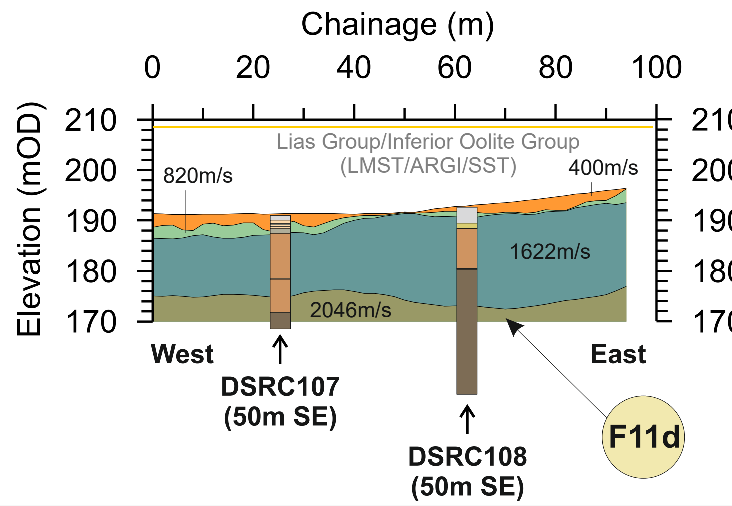

SEIS-11 Profile Coordinates	
0m Chainage	94m Chainage
393004.8E 215855.5N	393071.5E 215920.1N

ERT Section

Resistivity (ohm.m)

0 10 14 19 24 27 33 39 49 68 90 108 124 146 199 294 475

MASW Section

S-wave velocity (m/s)

100 175 250 325 400 475 550 625 700 775

S-wave Refraction velocity layers

- Layer 1 (<180 m/s) SOFT SOIL*
- Layer 2 (180 - 360 m/s) STIFF SOIL*
- Layer 3 (361- 760 m/s) VERY DENSE SOIL / SOFT(WEAK**) ROCK*
- Layer 4 (>761 m/s) ROCK* (MODERATELY STRONG**)

S-wave boundaries shown on ERT, MASW and S-wave sections

**The NEHRP Recommended Provisions for seismic regulation for new buildings, (FEMA-222A and FEMA-223A, 1994)*

*** UK equivalent classification (Waltham, 1994)*

P-wave Refraction velocity layers

- Layer 1 (<300 m/s)
- Layer 2 (301 - 800 m/s)
- Layer 3 (801 - 1400 m/s)
- Layer 4 (1401- 1900m/s)
- Layer 5 (>1901 m/s)

P-wave boundaries shown on ERT, MASW and S-wave sections

BOREHOLE KEY

Made ground	Sandstone
Clay	Mudstone
Silt	Siltstone
Sand	Limestone
Gravel	Core loss

KEY

- Line 1 — Profile intersection
- Fault — Reported fault positions
- Bedrock geology subcrop

NOTES/OBSERVATIONS

Title: ERT AND SEISMIC PROFILES

Project: A417 CRICKLEY HILL BIRDLIP

TERRA DAT down to earth geophysics
Tel: +44 (0) 2920 700127
Web:www.terradat.co.uk
Email: web@terradat.co.uk

Scale:	1:1500 at A3
Drawn by/Ref:	JT/6688/22
Date:	14 FEB 2020

FIGURE 22

ERT-12

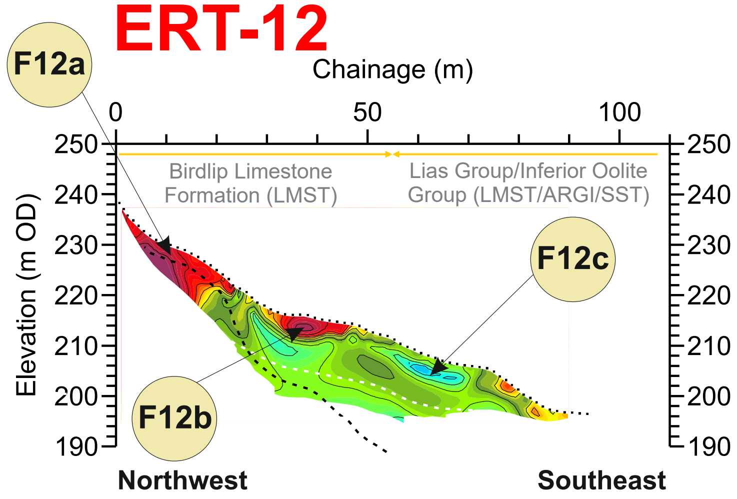

ERT-12 Profile Coordinates	
0m Chainage	94m Chainage
392996.1E 215996.0N	393008.1E 215903.8N

MASW-12

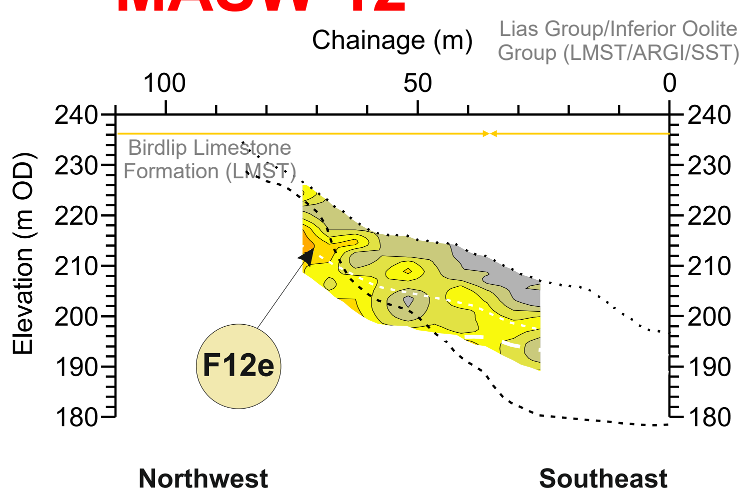

MASW-12 Profile Coordinates	
0m Chainage	94m Chainage
392007.1E 215907.0N	392996.5E 215990.7N

SEIS-12 (S-wave)

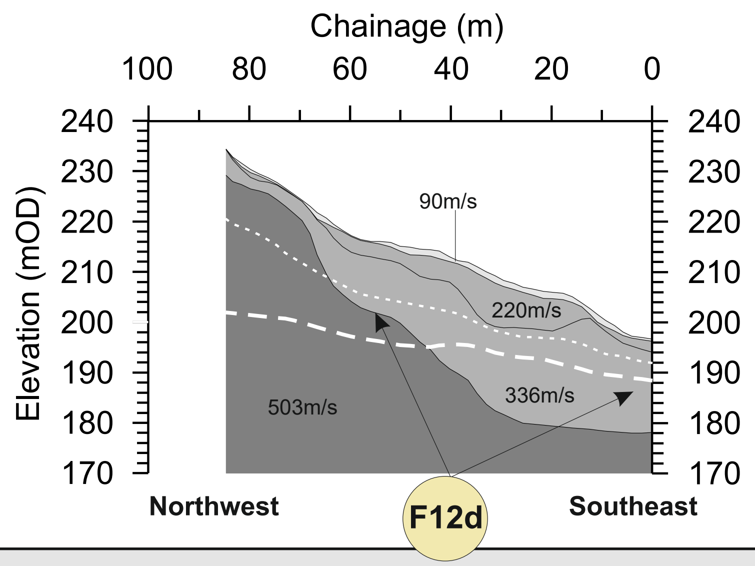

SEIS-12 (P-wave)

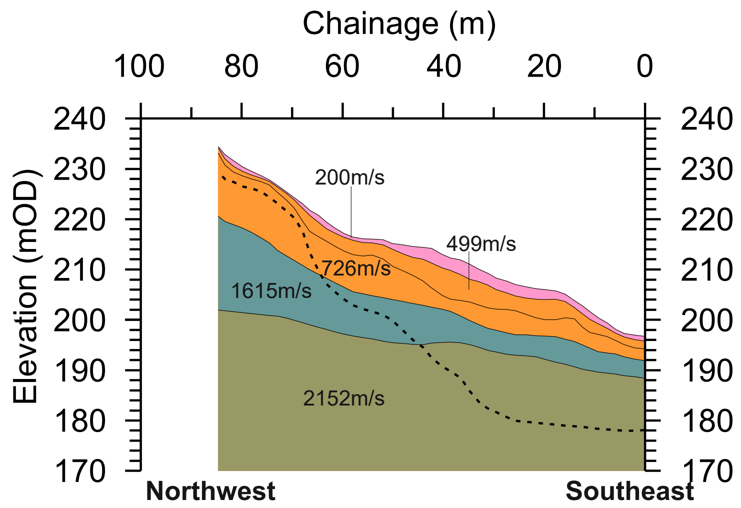

SEIS-12 Profile Coordinates	
0m Chainage	85m Chainage
393007.13E 215907.01N	392996.52E 215990.74N

ERT Section

Resistivity (ohm.m)

0 10 14 19 24 27 33 39 49 68 90 108 124 146 199 294 475

MASW Section

S-wave velocity (m/s)

100 175 250 325 400 475 550 625 700 775

S-wave Refraction velocity layers

- Layer 1 (<180 m/s) SOFT SOIL*
- Layer 2 (180 - 360 m/s) STIFF SOIL*
- Layer 3 (361- 760 m/s) VERY DENSE SOIL / SOFT(WEAK**) ROCK*
- Layer 4 (>761 m/s) ROCK* (MODERATELY STRONG**)

S-wave boundaries shown on ERT, MASW and S-wave sections

*The NEHRP Recommended Provisions for seismic regulation for new buildings, (FEMA-222A and FEMA-223A, 1994)

** UK equivalent classification (Waltham, 1994)

P-wave Refraction velocity layers

- Layer 1 (<300 m/s)
- Layer 2 (301 - 800 m/s)
- Layer 3 (801 - 1400 m/s)
- Layer 4 (1401- 1900m/s)
- Layer 5 (>1901 m/s)

P-wave boundaries shown on ERT, MASW and S-wave sections

BOREHOLE KEY

Made ground, Sandstone, Clay, Mudstone, Silt, Siltstone, Sand, Limestone, Gravel, Core loss

KEY

- Line 1 — Profile intersection
- Fault — Reported fault positions
- Bedrock geology subcrop

NOTES/OBSERVATIONS

Title: **RESISTIVITY TOMOGRAPHY (ERT) PROFILES**

Project: **A417 CRICKLEY HILL BIRDLIP**

TERRA DAT — down to earth geophysics

Tel: +44 (0) 2920 700127
Web:www.terradat.co.uk
Email: web@terradat.co.uk

Scale: 1:1500 at A3
Drawn by/Ref: JT/6688/23
Date: 14 FEB 2020

FIGURE 23

APPENDICES

Appendix - Resistivity Tomography

The Resistivity technique is a useful method for characterising the sub-surface materials in terms of their electrical properties. Variations in electrical resistivity (or conductivity) typically correlate with variations in lithology, water saturation, fluid conductivity, porosity and permeability, which may be used to map stratigraphic units, geological structure, sinkholes, fractures and groundwater.

The acquisition of resistivity data involves the injection of current into the ground via a pair of electrodes and then the resulting potential field is measured by a corresponding pair of potential electrodes. The field set-up requires the deployment of an array of regularly spaced electrodes, which are connected to a central control unit via multi-core cables. Resistivity data are then recorded via complex combinations of current and potential electrode pairs to build up a pseudo cross-section of apparent resistivity beneath the survey line. The depth of investigation depends on the electrode separation and geometry, with greater electrode separations yielding bulk resistivity measurements from greater depths.

The recorded data are transferred to a PC for processing. In order to derive a cross-sectional model of true ground resistivity, the measured data are subject to a finite-difference inversion process via RES2DINV (ver 5.1) software.

General resistivity principle

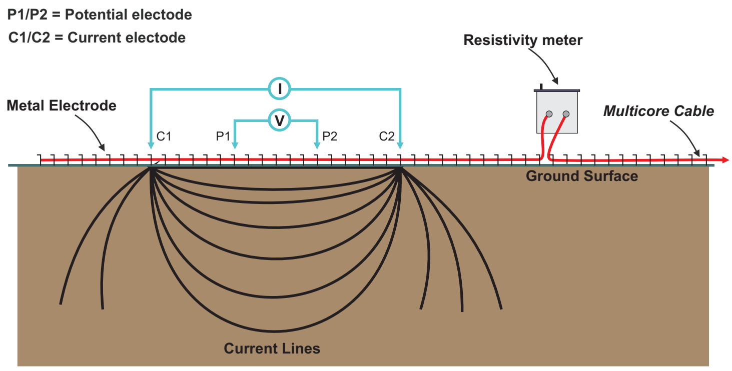

Typical field set-up

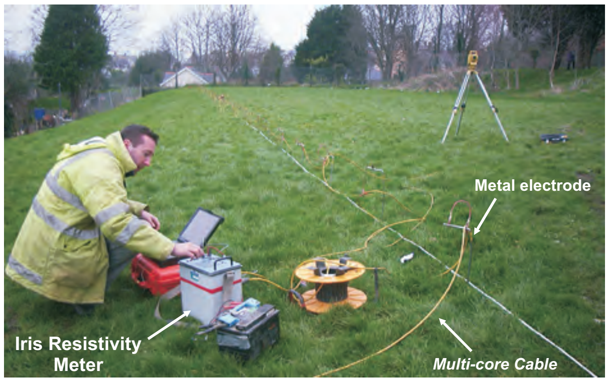

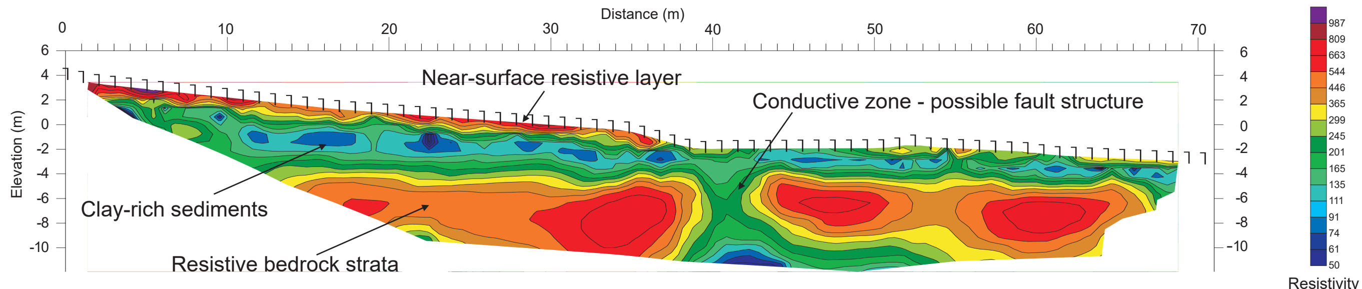

Modelled resistivity section

Data processing is based on an iterative routine involving determination of a two-dimensional (2D) simulated model of the subsurface, which is then compared to the observed data and revised. Convergence between theoretical and observed data is achieved by non-linear least squares optimisation. The extent to which the observed and calculated theoretical models agree is an indication of the validity of the true resistivity model (indicated by the final root-mean-squared (RMS) error).

The true resistivity models are presented as colour contour sections revealing spatial variation in subsurface resistivity. The 2D method of presenting resistivity data is limited where highly irregular or complex geological features are present and a 3D survey maybe required. Geological materials have characteristic resistivity values that enable identification of boundaries between distinct lithologies on resistivity cross-sections. At some sites, however, there are overlaps between the ranges of possible resistivity values for the targeted materials which therefore necessitates use of other geophysical surveys and/or drilling to confirm the nature of identified features.

Constraints:

Readings can be affected by poor electrical contact at the surface. An increased electrode array length is required to locate increased depths of interest therefore the site layout must permit long arrays. Resolution of target features decreases with increased depth of burial.

Appendix - Seismic Refraction Survey

Seismic refraction is a useful method for investigating geological structure and rock properties. The technique involves the observation of a seismic signal that has been refracted between layers of contrasting seismic velocity, i.e., at a geological boundary between a high velocity layer and an overlying lower velocity layer.

Shots are deployed at the surface and recordings made via a linear array of sensors (geophones or hydrophones). Refracted seismic signal travels laterally through the higher velocity layer (refractor) and generates a 'head-wave' that returns to surface. Beyond a certain distance away from the shot, the signal that has been refracted at depth is observed as first-arrival signal at the geophones. Observation of the travel-times of refracted signal from selectively deployed shots enables derivation of the depth profile of the refractor layer. Shots are typically fired at locations at and beyond both ends of the geophone spread and at regular intervals along its length.

The results of the seismic refraction survey are usually presented in the form of seismic velocity boundaries on interpreted cross-sections. Seismic sections represent the measured bulk properties of the subsurface and enable correlation between point source datasets (boreholes/trialpits) where underlying material is variable. Reference to the published seismic velocity tables enables derivation of rippability values.

Typical field set-up

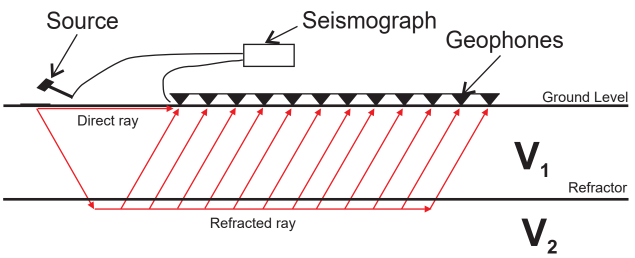

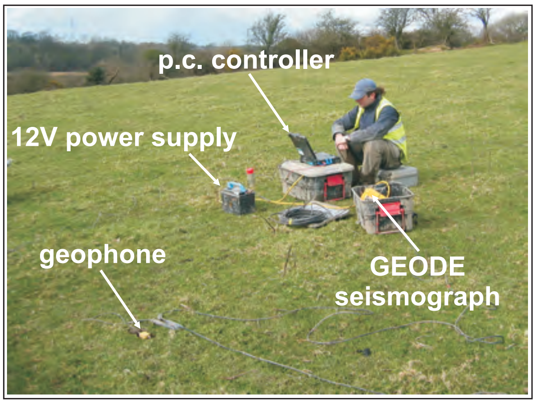

Travel-time curve

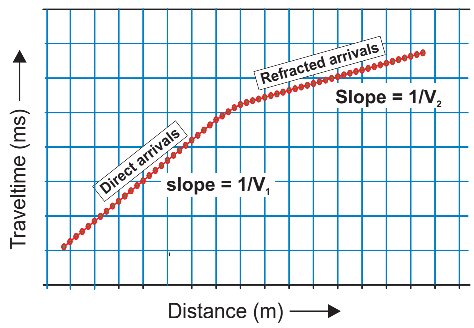

Modelled velocity section

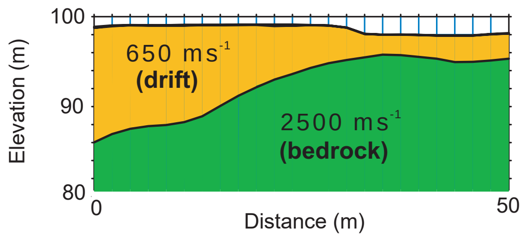

The data processing is carried out using PICKWIN & PLOTREFA (OYO ver2.2) software. The first stage involves accurate determination of the first-arrival times of the seismic signal (time from the hammer blow to each recording hydrophone) for every shot record, using PICKWIN. Time-distance graphs showing the first-arrival times were then generated for each seismic shot record and analysed using PLOTREFA software to determine the number of seismic velocity layers. Modelled depth profiles for the observed seismic velocity layers are produced by a tomographic inversion procedure that is revised iteratively to develop a best fit-model. The final output of a seismic refraction survey is a velocity model section of the subsurface based on an observed layer sequence with measured velocities that correspond to physical properties such as levels of compaction/ saturation in the case of sediments and strength/rippability in the case of bedrock.

Constraints
Layer velocity (density) must increase with depth; true in most instances. Layers must be of sufficient thickness to be detectable. Data collected directly over loose fill (landfills) or in the presence of excessive cultural noise may result in sub-standard results. In places where compact clay-rich tills and/or shallow water overly weak bedrock an S-wave survey may be used to profile rockhead where insufficient velocity contrast may prevent use of a P-wave survey.

Rippability Chart

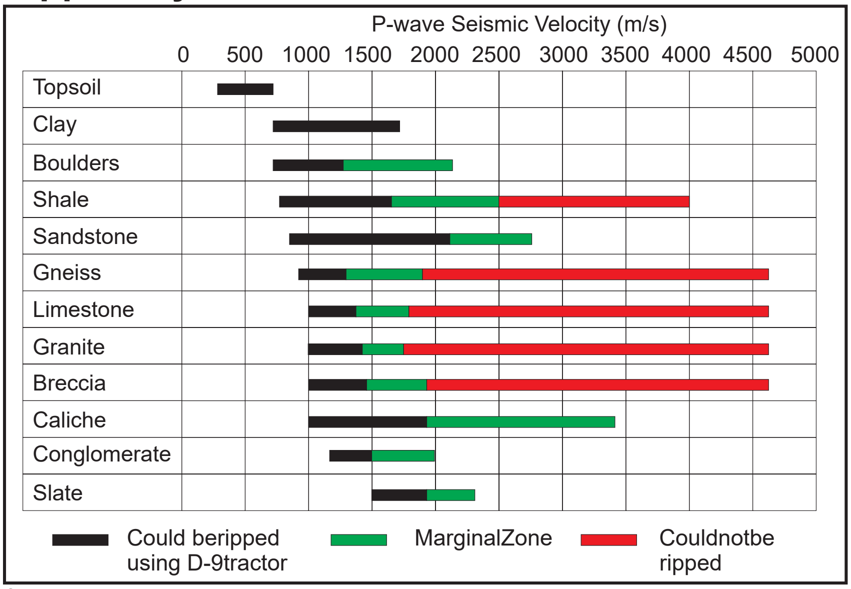

Ground preparation by ripping in open pit mining, Mining Magasine, 122, 458-469. Atkinson, 1970

Compressional P-wave velocity

Unconsolidated materials	***Vp (m/s)***
Sand (dry)	200 - 1000
Sand (water saturated)	1500 - 2000
Clay	1000 - 2500
Glacial till (water saturated)	1500 - 2500
Permafrost	3500 - 4000
Sedimentary rocks	
Sandstones	2000 - 6000
Tertiary sandstones	2000 - 2500
Pennant sandstone (Carboniferous)	4000 - 4500
Cambrian quartzite	5500 - 6000
Limestones	2000 - 6000
Cretaceous chalk	2000 - 2500
Jurassic limestones	3000 - 4000
Carboniferous limestones	5000 - 5500
Dolomites	2500 - 6500
Salt	4500 - 5000
Anhydrate	4500 - 6500
Gypsum	2000 - 3500
Igneous/Metamorphic rocks	
Granite	5500 - 6000
Gabbro	6500 - 7000
Ultramafic rocks	7500 - 8500
Serpentite	5500 - 6500
Other materials	
Steel	6100
Iron	5800
Aluminium	6600
Concrete	3600

An introduction to Geophysical Exploration 3rd Ed.
Kearey, Brooks & Hill: 2002

Diggability Chart

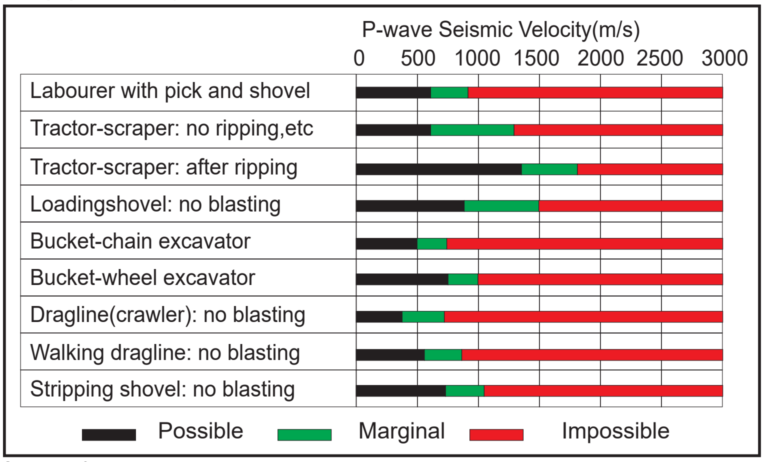

Selection of open pit excavation and loading equipment.
Transactions of the Institute of Mining and Metallurgy, 80, A101-A129, Atkinson 1971

Effect of ground water

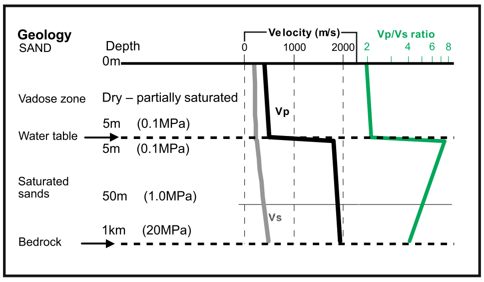

Prasad et al., Measurement of velocities and attenuation in shallow soils,
Near-Surface Geophysics Volume II Case Histories, SEG, Tulsa (2004)

Shear Waves

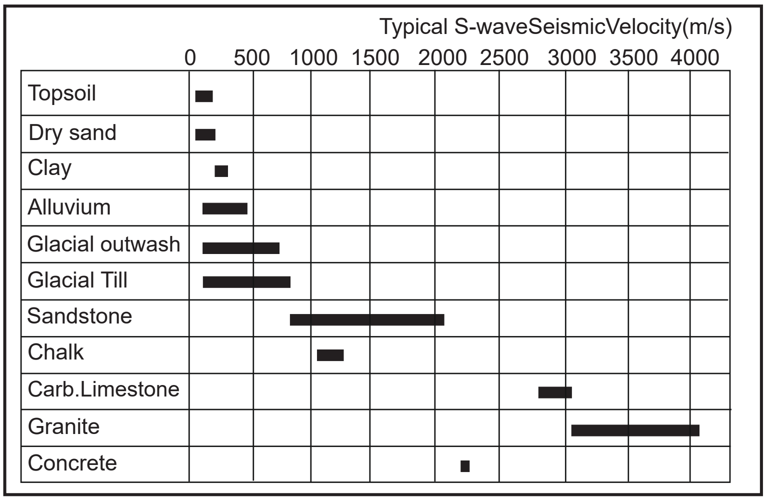

Rock / Soil Description (top 30m)	**S-wave velocity (m/s)**
Hard rock (*strong**)	> 1,500
Rock (*moderately strong**)	760 - 1,500
Very dense soil / soft (*weak**) rock	360 - 760
Stiff soil	180 - 360
Soft soil	<180

The NEHRP Recommended Provisions for seismic regulation for new buildings, (FEMA-222A and FEMA-223A, 1994)

** UK equivalent classification (Waltham, 1994)*

Applied Geophysics, Telford et al, 1990
Shear wave velocity determination of unlithified geologic materials (CUSEC region) Illinois State Geological Survey, Bauer, 2004.
Bauer et al., 2007, Illinois State Geological Survey.
Shear Wave Velocity, Geology and Geotechnical Data of Earth Materials in the Central U.S. Urban Hazard Mapping Areas.
An Introduction to Geophysical Exploration, 3rd Edition, Keary and Brooks, 2002.
Conceptual Overview of Rock and Fluid Factors that Impact Seismic Velocity and Impedance, Stanford Rock Physics Laboratory, n.d.

PUBLISHED SEISMIC VELOCITY TABLES

GEOPHYSICAL SURVEY REPORT

Project

Bedrock mapping and sediment characterisation

Location

Zone 3, A417, Birdlip

Client

Geotechnical Engineering

Head Office
Unit 1
Link Trade Park
Penarth Road
Cardiff CF11 8TQ
United Kingdom

Telephone: +44 (0)2920 700127
www.terradat.co.uk

TERRA DAT
down to earth **geophysics**

Job Reference: 6688
Date: November 2020
Version: 1

GEOPHYSICAL SURVEY REPORT

Project

Bedrock mapping and sediment characterisation

Location

Zone 3, A417, Birdlip

Client

Geotechnical Engineering

Project Geophysicist:	M Bottomley BSc MSc	[redacted]
Reviewer:	S Hughes PhD BSc FGS	[redacted]
Job Reference:	6688	
Date:	November 2020	

CONTENTS

Figures

Appendices

1 EXECUTIVE SUMMARY

A geophysical survey was carried out as part of the ground investigation for proposed improvements to the A417 near the village of Birdlip, south of the existing road. The survey work was commissioned by Geotechnical Engineering (the Client). The fieldwork was carried out during November 2019 and July 2020 and undertaken within an area defined by the Client as 'Zone 3', comprising four targeted Electrical Resistivity Tomography (ERT) and seismic profiles, and an electromagnetic (EM) ground conductivity survey. The work was designed to complement the invasive and geotechnical investigation in providing detailed information on the geology and ground conditions adjacent to the existing A417, with particular concern regarding potential landslide/landslip zones.

The geophysical survey consisted of an integrated survey approach utilising electromagnetic ground conductivity measurements, four targeted ERT profiles and four seismic P and S-wave refraction and Multichannel Analysis of Surface Waves (MASW) profiles along all resistivity lines.

The results have been provided as a series of interpreted, colour-contoured plots (ground conductivity) and scaled sections (resistivity and seismic refraction), alongside a map showing the locations of the plots and profiles in relation to the underlying topographical features and bedrock geology as provided by Google Earth mapping and the British Geological Survey (BGS) Geology of Britain viewer.

2 INTRODUCTION

This report describes a geophysical survey that was carried out as part of the ground investigation for proposed improvements to the A417 near the village of Birdlip. The survey work was commissioned by Geotechnical Engineering (the Client). The fieldwork was carried out during November 2019 and July 2020 and undertaken within an area defined by the Client as ‘Zone 3’, comprising four targeted Electrical Resistivity Tomography (ERT) and seismic profiles, as well as an electromagnetic (EM) ground conductivity survey.

The work was designed to complement the invasive and geotechnical investigation in providing detailed information on the geology and ground conditions adjacent to the existing A417, with particular concern regarding potential landslide/landslip zones.

2.1 Site description and history

Zone 3 (approx. centred on 394000E, 215150E) occupies an area of around 70 hectares, roughly 1.3 km northeast of the village of Birdlip. The survey area is east of the A417 and encompasses open fields and hedge systems as well as scatterings of woodland.

Plate 1. *Zone 3, showing the locations of the ERT and seismic profiles (red lines) and the extents of the EM ground conductivity survey (light blue).*

Topographically, the survey area is at the top of the hill and exhibits relatively minor variations in relief although the ground begins to steepen to the north and north-east beyond Shab Hill.

2.2 Geological setting

The Client has provided numerous borehole logs located within the 'Zone 3' survey area. The intrusive investigation has logged highly variable material comprising 1 to 4 m of clay overlying thick limestones of the (*in order from the top of the hill*) White Limestone Formation, Hampen Formation, Salperton Formation, Aston Formation, and Birdlip Limestone Formation. Borehole DSRC315 reveals a transition into much deeper mudstones and siltstones, most likely belonging to the Lias Group and Inferior Oolite at >50 m bgl. Mudstone layers, as revealed by borehole RC520 within the upper 30 m of the subsurface may belong to the Fullers Earth Formation, located between the Salperton and Hampen Formations. The survey area is also transected by two significant faults, the expected locations for which are shown on Plate 1 and Figure 25.

According to the British Geological Survey (BGS) Geoindex, there are no superficial deposits in the vicinity of the site. All material overlying the bedrock is therefore believed to be bedrock erosion material from steep slopes and escarpments that has been transported by weather processes and landslide, down the valley side, and is referred to in this report as "overburden".

2.3 Survey objectives

The primary objectives of the survey were to provide detailed information on the shallow ground composition and deeper bedrock geology to assist with the ground investigation of the proposed road scheme. Of particular interest for engineering a new road cutting, is areas of shallow geology that may support further landslide movement of the overburden.

2.4 Survey design

Given the scope of the survey objectives, it was decided to adopt an integrated survey approach utilising the following geophysical methods:

- **Ground Conductivity**: to provide a ground conductivity map to characterise shallow overburden deposits and identify preferential water pathways such as gravel channels and clay-rich layers.

- **Resistivity Tomography**: to provide electrical cross-sections along selected survey profiles that allow identification of geological or hydrological boundaries.

- **P-wave Seismic Refraction**: to provide seismic velocity (V_p) model sections that indicate the thickness of overburden deposits and the depth to competent bedrock, in correlation with standard tables.

- **S-wave Seismic Refraction**: to provide seismic velocity (V_s) model sections that indicate the depth of uncompacted and compacted sediments, weathered rockhead and more competent (higher shear strength) bedrock.

- **MASW (Multichannel Analysis of Surface Waves)**: to derive shear velocity ('S-wave' or 'V_s') from rolling surface waves that are related to the stiffness of the ground material. This technique is also useful where velocity inversions in the ground layers may be encountered.

2.5 Quality control

The geophysical data sets were collected in line with normal operating procedures as outlined by the instrument manufacturer and TerraDat company policy. On completion of the survey, the data were downloaded from the survey instrument on to a computer and backed up appropriately. The acquired data set was initially checked for errors that may be caused by instrument noise, low batteries, positional discrepancies, etc. and any field notes are either written up or incorporated in the initial data processing stage. The data set is then processed using the standard processing routines and once completed; the resulting plots are subject to peer review to ensure the integrity of the interpretation. Our quality control standards are BS EN ISO 9001: 2015 certified.

3 SURVEY DESCRIPTION

The survey was carried out using the following geophysical methods:

- EM - Ground conductivity mapping
- Electrical Resistivity Tomography (ERT)
- P-wave seismic refraction (employs compressional waves)
- S-wave seismic refraction (employs shear waves)
- MASW (Multichannel Analysis of Surface Waves)

The extents of the EM survey, resistivity and seismic profiles are shown in Figure 25. Four Electrical Resistivity Tomography (ERT) and seismic refraction profiles were deployed, in locations as specified by the Client.

Background information for the survey methods is provided in the appendices, while a description of the actual survey work is provided in the sections below.

3.1 Survey limitations and assumptions

Seismic refraction requires that the velocity of the materials in the subsurface increases with the depth of burial. This is normally the case since (i) the degree of compaction within the overburden typically increases with depth, and (ii) bedrock condition improves with depth as weathering is reduced, both of which lead to higher seismic velocities. Therefore, one limitation of the refraction method is the inability to resolve localised weak zones within rock where it resides at a depth below the competent non-weathered rock. One of the objectives of the resistivity tomography survey is to target such weak/broken zones in the rock where fines/water have infiltrated and reduced the local ground resistivity. The survey output from both the P and S-wave refraction surveys are cross-sectional models that describe the bulk physical properties of the ground in terms of superficials, weathered rock and competent rock layers. There will be local variations in rock strength within the interpreted weathered rock layer, and the fracture density / broken character of the rock will vary over very short lateral distances. Measuring the seismic velocity of the bedrock over tens of metres along each survey line determines the bulk properties of the shallow rock mass and enables targeted ground-truthing of any identified anomalous ground.

3.2 Survey layout and topographic survey

The ground conductivity data were acquired under the positional control of an EGNOS dGPS system. Where possible, a Topcon Hyper Pro RTK dGPS system was used to mark resistivity (electrode) and seismic profile (geophones and offend shots) locations with a survey accuracy of +/- 2.5 cm. In some cases, positional accuracy was not adequate due to extensive tree cover, and so a Trimble robotic total station was employed using dGPS established reference stations. All measurements were recorded in Ordnance Survey National Grid coordinates.

3.3 Ground conductivity mapping

An electromagnetic ground conductivity survey involves the transmission of an electromagnetic field into the subsurface and then recording the returning signal via a receiver in the same instrument. Data are acquired on a grid covering the area of interest, and a contoured plan of the variation in ground conductivity response across the site is produced. The presence of conductive materials in the subsurface such as clay, water, mudstone, ash, metal, rebar, leachate, etc. will be evident as regions of high values on the ground conductivity plan. Materials such as coarse-grained sediments, dry zones, and many bedrock types will appear as regions of low values.

3.3.1 *Electromagnetic survey - field activity*

The conductivity data were acquired using a multi-frequency *Geophex GEM-2* instrument (Plate 2), and data were acquired under the control of an EGNOS corrected dGPS (accuracy +/- 0.5m) at a nominal 0.25 m interval along a series of parallel 5 m spaced survey lines. The instrument was primarily configured to investigate depths of up to 3 to 5 m below ground level. The sensor was mounted on a cart and pulled behind an ATV.

Plate 2. *Ground conductivity data collection method. Geophex GEM-2 instrument mounted on a bespoke cart which was pulled across the site using an ATV, under the control of a GPS system (Library photo).*

3.3.2 Electromagnetic survey – data processing

The conductivity data were downloaded from the data logger and compiled using dedicated software *WINGEM-3*. Initial editing was then carried out to remove positional errors and rogue values. The data were then exported as an 'XYZ' file and translated into the OSGB36 Coordinate system using the OSTN02 transformation. The software program *OASIS MONTAJ* was used to compile, edit and manipulate the data to enhance any features of interest. The colour contour plots were then integrated with the base plan information and the resulting plans exported to *CORELDRAW* for final annotation.

3.4 Electrical Resistivity Tomography (ERT)

An ERT survey involves the injection of DC electrical current into the ground at various electrode locations along a profile line. An electrical cross-section of the subsurface is then derived from the recorded data. A diverse range of features such as clay-rich sediments, fracture zones, infilled solution features, bedrock structure and mineralisation can be imaged in cross-section using a resistivity survey. A feature may be targeted using resistivity tomography given sufficient electrical contrast with its surroundings. A description of the field activity is provided below, and some background information on the survey method is found in the Appendix.

3.4.1 ERT survey field activity

A 72-channel *IRIS Syscal* resistivity system (Plate 3) was used to acquire four profiles across the survey area, as shown in Figure 25. The ERT profiles were acquired with an electrode spacing of 3 m using a standard Wenner-Schlumberger array. For all of the profiles, 'roll-ons' were required to cover the required area of interest. A 'roll-on' simply involves adding one or two cables to the end of the initial 72-channel setup and then selecting the appropriate protocol file from the IRIS resistivity meter to continue data acquisition from the initial setup and into the new cables. A summary of the ERT profiles is given in Table 1.

ERT Profile No.	Fig.	Start (OSGB)		End (OSGB)		Length (m)	Electrode Spacing (m)	~ Depth of penetration (m)
		Easting	Northing	Easting	Northing			
Line 21	27A	393723.1	215438.4	394058.1	215702.7	429	3	30
Line 22	28A	393594.7	215109.7	394015.6	215430.3	531	3	30
Line 23	29A	394046.5	215331.1	394104.7	214858.4	476	3	30
Line 24	30A	394251.7	215182.0	394077.3	214736.2	479	3	30

Table 1. *ERT profile summary.*

3.4.2 *ERT survey data processing*

The data were processed using *Res2DInv* software to derive modelled electrical cross-sections of the subsurface. Elevation data were added to the models, using electrode positions surveyed using a TOPCON network RTK GPS. All topographic data were transformed into National Grid (OSGB36) using the OSTN02b transformation; elevations are given in m AOD. The ERT data was then exported into *Surfer 7* where it was gridded and presented as a 2D cross-sections of resistivity. These cross-sections were then exported to *CorelDraw* for final annotation. All resistivity profiles are presented on the same colour scale and are not vertically exaggerated.

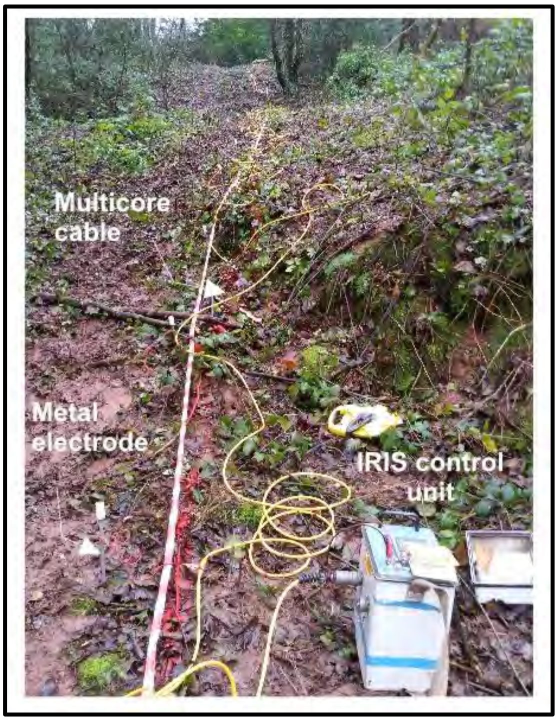

Plate 3. *Resistivity Tomography data collection. A 72 channel IRIS Syscal ERT system used to acquire eleven profiles across the site (Library photo).*

3.5 Seismic survey – P and S-wave refraction

A seismic survey involves generating a shock wave signal at the surface to investigate the geological structure beneath a chosen profile line. A series of vibration sensors (geophones, or hydrophones in water) are deployed along the line and are used to record the travel times of incident seismic signal as it returns from below ground. Features such as rockhead, the water table, made ground, soft sediments and dense tills all have distinct velocity ranges and can be imaged in cross-section using a seismic refraction survey. A description of the field activity is provided below, and some further background information on the survey method is found in the appendices.

3.5.1 Seismic survey field activity: P-wave refraction

P-wave seismic refraction data were acquired along four profile lines using a high precision 72 channel *GEODE* (Plate 4a) seismic system. To target the broad depth range, low frequency (4Hz) geophones were deployed at 2 m intervals providing individual geophone spread lengths of 142 m. For all profiles, several setups were required to achieve full line coverage. The seismic wave was generated by a combination of sledgehammer striking a nylon plate and Seismic Impulse Device (SID) firing 12- and 8-gauge black powder cartridges (Plate 4b).

To build up the refraction data set, seismic shots were taken at several positions along the geophone spread (usually every 6-12 geophones) and set distances beyond the geophone spread. For this particular survey, the 'offend' shots were limited by site constraints, but the maximum distance was 100 m. A summary of the seismic profiles is given in Table 2.

Plate 4. *a) Field setup and b) Seismic Impulse Source deployment (Library photo).*

Seismic Profile No.	Fig.	Start (OSGB)		End (OSGB)		Length (m)	Geophone Spacing (m)	~ Depth of penetration (m)
		Easting	Northing	Easting	Northing			
Line 21	27B	393722.5	215437.7	394059.2	215707.6	430	2	25
Line 22	28C	393594.2	215108.9	394084.7	215495.9	622	2	25
Line 23	29B	394104.6	214858.4	394047.2	215327.2	478	2	25
Line 24	30B	394248.7	215182.0	394061.2	214694.6	475	2	25

Table 2. *Seismic Profile summary.*

3.5.2 Seismic survey field activity: S-wave refraction (Shear)

S-wave seismic refraction data were also acquired using a 72 channel *GEODE* seismic system. Horizontally mounted geophones were deployed at 2 m intervals producing individual geophone spread lengths of up to 142 m. For all profiles, several setups were required to achieve full line coverage. A weighted S-wave plate struck sideways with a sledgehammer was used as the energy source (Plate 5). At each shot location, the shot plate was aligned perpendicular to the profile line and subsequently struck on both ends to generate two sets of shear wave recordings that have opposite polarity. To build up the refraction data set, seismic shots were taken at several positions along the geophone spread (usually every 6-12 geophones) and set distances beyond the geophone spread.

Plate 5. *S-wave source plate being struck (Library photo).*

3.5.3 Seismic survey data processing: P and S-wave refraction

The data processing was carried out using *PICKWIN* and *PLOTREFA* software. The first stage involved the accurate determination of the first-arrival times of the seismic signal (time from the shot going off to each recording geophone) for every shot record using *PICKWIN*. Time-distance graphs showing the first-arrival times were then generated for each seismic line and analysed using *PLOTREFA* software to determine the number of seismic velocities layers. Modelled depth profiles for the observed seismic velocity layers were produced by a tomographic inversion procedure that was revised iteratively to develop a best-fit model.

The final output of a seismic refraction survey is a velocity model section of the subsurface based on an observed layer sequence. The measured velocities correspond to physical properties such as levels of compaction/saturation in the case of sediments and strength/rippability in the case of bedrock. A transitional velocity model will be considered if distinct layers are not expected, or velocity contrasts between layers are marginal. However, a layered model appears most appropriate to this site. The final sections were exported to *CORELDRAW* for annotation and presentation.

3.6 Seismic survey – MASW

Multichannel Analysis of Surface Waves (MASW) employs 'rolling' surface waves to derive shear velocity. This is achieved through analysis of the dispersion that occurs as surface wave energy propagates through the subsurface and separates into different frequencies travelling at different velocities depending on the stiffness of the sediments and/or rock encountered.

This technique utilises Rayleigh-type surface waves (normally considered noise in seismic refraction/reflection surveys and called "ground roll") recorded by multiple geophones deployed on an even spacing and connected to a common recording device (seismograph), as shown in Plate 6.

As the dispersion of the seismic wave can be dependent on the geology and ground conditions (i.e. variability, terrain, etc.), MASW profiles are usually limited to relatively flat areas or where the ground more homogenous.

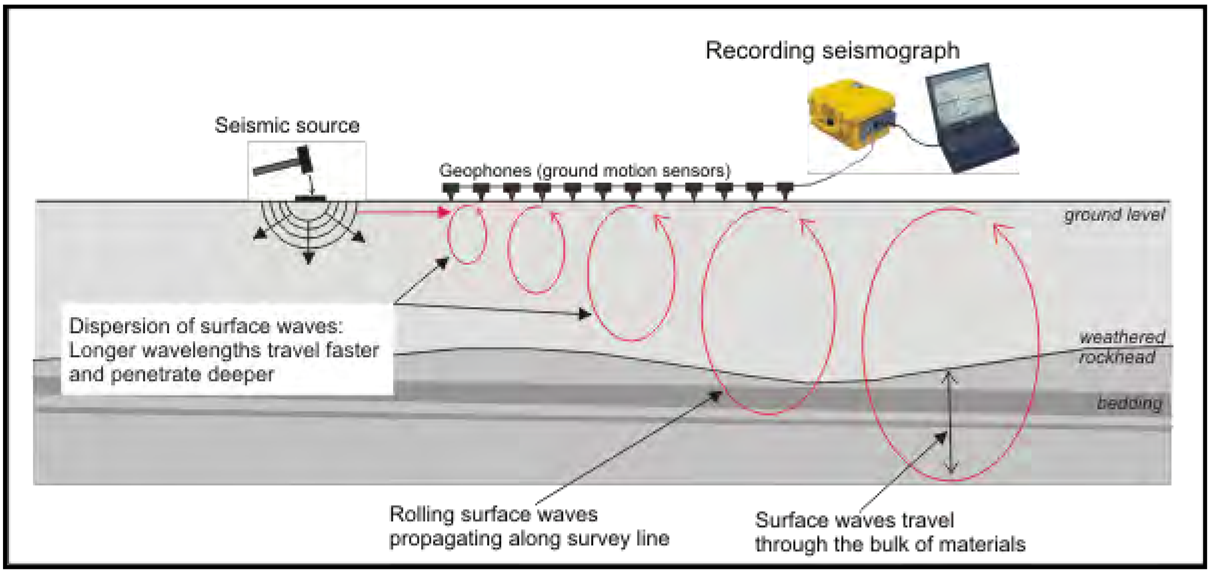

Plate 6. *MASW survey setup.*

3.6.1 Seismic survey field activity: MASW

For this particular survey, the setup is very similar to the refraction setup; however, instead of a discreet number of shot points, shots were acquired at every other geophone position along the profile. In this case, low frequency (4Hz) geophones were set at 2 m intervals, and the data were acquired using the sledgehammer as the source. A one-second record length was used to fully capture the frequency dispersion.

3.6.2 Seismic survey data processing - MASW

Analysis of surface waves recorded on multichannel shot records was carried out using SurfSeis software, which considers the dispersion properties of all types of waves (both body and surface waves) through a wave field transformation method. This directly converts the multichannel record into an image, where a dispersion pattern is recognised, and the necessary dispersion properties are extracted. These dispersion properties are used to generate modal dispersion curves that are subsequently inverted and used to produce the resultant shear-wave velocity (Vs) profile. The final velocity sections are created in SURFER then exported to CorelDraw for annotation and presentation.

4 RESULTS AND DISCUSSION

The results of the geophysical surveys are presented as a series of interpreted colour contour plots and scaled sections in Figures 26 to 30B. A general description of the interpretation process is given below, followed by a summary of the findings in Sections 4.5 and 4.6.

4.1 Ground Conductivity

The results are presented as a colour contoured plot of ground conductivity (Figure 26). Following a review of the electromagnetic data; it was decided only to consider the response of the 47,925 MHz frequency channel. A relative increase in conductivity values usually indicates a comparative increase in the clay/ash/water content, which could signify either a lateral change in lithology or a variation in bedrock depth. Extreme fluctuations in conductivity/in-phase values are usually indicative of instrument 'overload' due to high metal content. The interpretation of the conductivity data is based on both published electrical properties of typical sedimentary materials (Plate 7) and when available, correlation with on-site information.

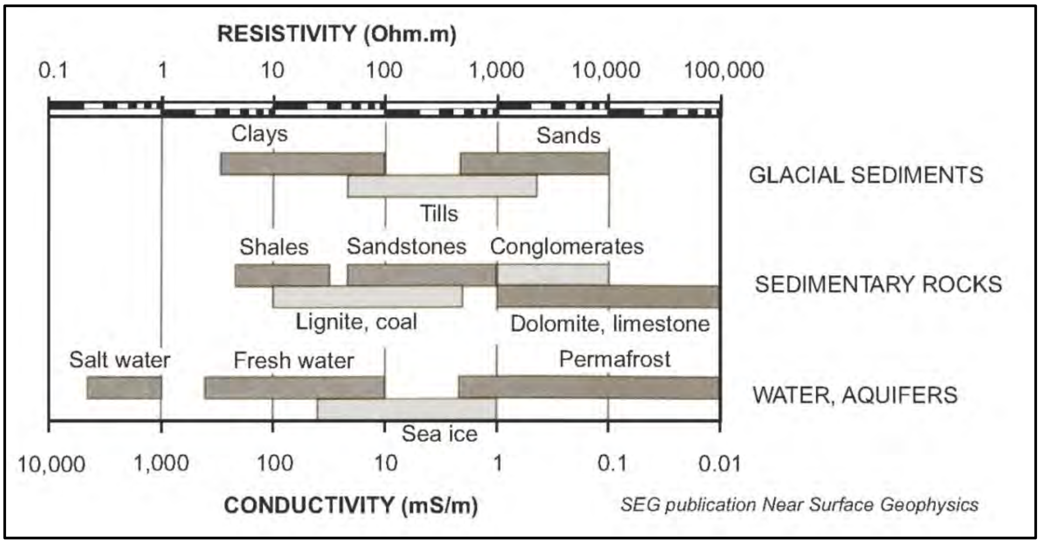

Plate 7. *Conductivity and resistivity values of common materials.*

4.2 Resistivity tomography

The results of the resistivity survey are presented as colour contoured scaled sections of the subsurface showing changes in resistivity, with blue colours representing low values, and red colours representing relatively high resistivity values. The vertical and horizontal axes display elevation and chainage along the profile line, respectively. The interpretation of the modelled resistivity sections is based on both published electrical properties of typical sub-surface materials (Plate 7) and when available, correlation with on-site information or observations. In principle, an increase in resistivity values usually indicates a relative decrease in the clay content or groundwater saturation. However, due to the non-uniqueness of the electrical properties (i.e. different material exhibiting same resistivity values), the final interpretation may be limited and may require addition calibration (i.e. drilling or other supplementary geophysical techniques).

The results of the ERT survey are discussed in the summary discussions, in conjunction with the results of the seismic survey. To assist with the interpretation, the resistivity sections have been overlain with the interpreted seismic velocity boundaries where acquired.

4.3 Seismic Refraction – compressional (P) and shear (S) wave

Interpretation of the refraction sections is based on the widely understood and published velocities of typical sub-surface materials (provided in the appendices). It is beneficial to correlate model sections with on-site information/observations, but at the time of reporting, only limited borehole information was available.

4.3.1 Compressional (P) wave

Analysis of the P-wave refraction data has identified up to five distinct layers of contrasting velocity (V_p), and a typical description of each layer is given below and summarised in Table 3. It is worth noting that the seismic refraction section represents the measured bulk characteristics of the subsurface and in certain cases, it can prove difficult to correlate with point source data (boreholes/trial pits) where the underlying material is variable.

Layer	P-wave velocity	Sediment/Rock Description
P1 (pink)	< 300 m/s (low)	Thin, dry loose surface soil and sediments
P2 (orange)	301 – 800 m/s (low to medium velocity)	Unconsolidated, dry overburden material
P3 (light green)	801 - 1400 m/s (medium velocity)	Compacted, dry overburden material
P4 (green)	1401 - 1900 m/s (medium to high velocity)	Compacted, saturated overburden material or highly weathered bedrock
P5 (dark green)	> 1901 m/s (high velocity)	Weathered to unweathered bedrock

Table 3. *A guide to the composition of the P-wave velocity layers identified.*

Layers P1 has a low velocity that relates to loose, surface soil and uncompacted sands and gravels. Layers P2 and P3 typically reflect a relative increase in consolidation or compaction of the still dry overburden material. Layer P4 can be more difficult to interpret as the overlap in velocities means that it can represent both overburden material (potentially wet, compact material) and weathered/weak/fractured bedrock. The most effective way to differentiate between sediment and rock type material is to consider the corresponding S-wave velocity, as discussed below. Layer P5 represents the highest (and deepest) velocity unit and is likely to reflect a more competent boundary within the bedrock strata.

4.3.2 Shear (S) wave

By carrying out an analysis of the S-wave refraction data, four distinct layers of contrasting velocity (V_s) have been identified and summarised in Table 4. They are characterised by their correlation with standard tables (see appendices).

In general, the shear-wave velocity (V_s) is much more sensitive than the P-wave velocity (V_p), where the ground becomes abruptly stiffer due to increases in rock strength. For this reason, it is possible to use the V_s to distinguish between sediments and 'rock' (i.e. cemented) material, which is particularly useful for grading the P-wave layer P4. A further advantage of shear waves is that they are unaffected by the groundwater table.

Layer	S-wave velocity	Sediment/Rock Description
S1	<180 m/s	Soft soils and loose sediments
S2	180 - 360 m/s	Stiff soils/overburden
S3	361 - 760 m/s	Very stiff, compacted overburden or highly weathered bedrock
S4	>761 m/s	Rock

Table 4. *A guide to the composition of the S-wave velocity layers identified.*

When comparing the resulting P-wave and S-wave velocity sections, there is a rough 'rule of thumb' with regards to the ratio of the velocities. For unconsolidated sediment, V_p/V_s is usually between 4.0 to 8.0, while for consolidated rocks, the V_p/V_s ratio can vary between 1.5 to 2.0. Even though these are accepted values, they can vary between sites depending on the geology and ground conditions.

When correlating between the respective P-wave and S-wave refraction boundaries, in some instances there can be discrepancies in observed depth values. This depends on the prevailing geology and can reflect different survey parameters (horizontal/vertical polarised S-waves, spacing, etc.), weathering profile (vertical and horizontal), lithology or bedding structure. It has been noted on some sites that the S-wave refractor appears to correlate with internal bedding units as opposed to the general rock mass.

4.4 MASW

The results of the MASW survey are presented as colour contoured S-wave velocity panels showing changes in velocity (i.e. ground stiffness) below the surface. The seismic signal frequency dispersion required for the MASW technique has yielded reliable results to a depth of up to approximately 20 m bgl. The persistent traffic noise from the A417 and the limited power of a sledgehammer energy source meant lower frequency dispersions (giving an increased depth of investigation) suffered from a high signal to noise ratio and were not suitable for modelling. The MASW sections have been colour scaled from white to red, with red representing the highest velocity modelled.

4.5 Summary Discussion – Ground Conductivity

Features or anomalies of interest have been listed and discussed in Table 5 below.

Zone	Feature	Description
3	F8	Resistive zone indicates a decrease of clay and/or water within the overburden, possibly associated with a change of lithology given the proximity of the fault.
	F9	South of the fault, the overburden is more conductive, indicating an increase of clay and/or water within the overburden. TP605 and TP210, for example, indicate clay-rich sediments.
	F10	Area of elevated resistivity indicates a decrease of clay and/or water within the overburden. TP618 and TP638 indicate limestone bedrock at or close to surface, and so the resistive zones can be interpreted as mapping the shallowing of the limestone bedrock.
	F11	Extremely good correlation between interpreted fault location, and the transition between conductive/resistive near-surface material. It is likely that to the south of the fault, there is a deepening of the limestone bedrock, with clay-rich overburden at the surface as indicated by TP619.

Table 5. *Features and anomalies of interest as identified by the ground conductivity survey.*

4.6 Summary Discussion – ERT and Seismic Refraction

Features or anomalies of interest have been listed and discussed in Table 6 below.

Profile	Feature	Description
21	F21a	This resistive layer indicates a decrease of clay and/or water within the near-surface sediments (possible increase of silt or gravel). The corresponding S-wave data also reveals the presence of very stiff sediments and/or highly weathered, broken rock (V_s of 442 m/s). This resistive zone also correlates with a layer of increased stiffness on the MASW section.
	F21b	Abrupt, vertical boundary between conductive and resistive material indicates the location of a fault, with the Salperton/Aston Limestone Formation to the north-east and White/Hampen Limestone Formation to the south-west.

	F21c	Decrease in resistivity indicates transition into more conductive bedrock, possibly mudstone from the Fullers Earth Formation underlying the more resistive White and Hampen Limestone Formations.
	F21d	Homogenous, resistive subsurface to the north-east of the fault. The S-wave results reveal shallow, weathered limestone bedrock (V_s of 693 m/s) overlying a more competent, stronger bedrock layer (V_s of 947 m/s).
	F21e	Isolated conductive zones within the bedrock likely indicate localised deteriorations in bedrock condition and increase of clay/water-bearing fractures.
	F21f	Very good correlation shown between P and S-wave seismic boundaries, and transitions into stiffer, likely dipping layers of limestone bedrock as shown on the MASW section.
	F21g	Decrease of MASW S-wave velocity indicates a decrease in stiffness and likely deterioration in bedrock condition. Possibly related to a conductive zone shown on the resistivity section (F21e).
	F21h	Stiff zone on the MASW section correlates with the position of a very stiff region or ridge of bedrock (V_s of 1586 m/s), which is present here, before dipping beyond the depth limit of investigation to the north-east and south-west (see also F21k).
	F21i	Bedrock to the south-west of the fault is shown to be generally less stiff (mudstone from Fullers Earth Formation?)
	F21j	Very good correlation shown between the S-wave section and borehole RC516 located 53 m away to the east. Layers S1 is interpreted to comprise clay-rich sediments, while Layers S2-S4 are interpreted to comprise limestone from the Salperton and Aston Limestone Formations in particular at least to the north-east of the fault.
	F21k	Both the P and S-wave sections reveal a stronger, stiffer and more competent zone of bedrock to the immediate north-east of the fault. Borehole RC516 suggests this to be limestone, which has possibly undergone structural changes (e.g. compression) due to the influence of the fault. The boundary is lost to the north-east and south-west as it dips beyond the depth of investigation for this particular survey setup.
22	F22a	This resistive layer indicates a decrease of clay and/or water within the near-surface sediments and shallow limestone rock (Salperton/Hampen Limestone Formation) as indicated by TP636 located 27 m away to the

		east.
	F22b	Decrease in resistivity indicates transition into more conductive bedrock, likely mudstone from the underlying Fullers Earth Formation. The inclined nature of the resistive/conductive boundary may be indicative of the dipping bedrock lithology.
	F22c	Abrupt, vertical boundary between conductive and resistive material likely indicates the location of a fault, with a more competent bedrock lithology to the south-west as indicated by the increase of resistivity. The MASW section shows a corresponding increase in rock stiffness to the south-west of the suspected fault.
	F22d	Increase in resistivity indicates a transition into more competent bedrock. This correlates very well with a stiffer zone on the MASW section, as well as a shallowing of Layers S3/S4/P5, with S-wave velocities of 967 m/s and 1454 m/s indicating the presence of strong to very strong, competent bedrock.
	F22e	Decrease in resistivity indicates transition into more conductive bedrock, again, likely to be mudstone from the Fullers Earth Formation. The dipping nature of the resistive/conductive boundary may be indicative of the dipped bedrock lithology.
	F22f	Abrupt, vertical boundary between conductive and resistive material likely indicates the location of a fault (~40 m away from the expected fault location), with a more, competent bedrock lithology to the south-west (Salperton Limestone Formation) as indicated by the increase of resistivity. The MASW section also reveals a corresponding sharp increase in rock stiffness to the south-west of the suspected fault.
	F22g	Isolated, slightly more conductive zone, likely indicating an increase of clay and/or water within the superficial deposits, or weaker broken rock.
	F22h	Abrupt, vertical conductive feature possibly indicates the location of a fault, although this is marked as being 60 m to the south-west.
	F22i	A stiffer layer is evident beyond approximately 450 m chainage and correlates with the resistive zone (F22a) indicating a likely improvement in bedrock condition and decrease in water/clay-bearing fractures.
	F22j	Good correlation shown between the resistivity. The lower P and S-wave bedrock boundaries and an increase in rock stiffness as indicate by the MASW.
	F22k	Zone of decreased MASW S-wave velocity (and therefore rock

		stiffness), indicating a possible change of bedding lithology or deterioration in rock condition.
	F22l	Good correlation shown between P and S-wave boundaries, indicating shallow, strong and competent bedrock between 0-40 m, 160-320 m and 560-622 m approximately, deepening in between.
	F22m	Layer of very stiff sediments, or more likely, soft, highly weathered limestone. This correlates very well with soft, conductive zones shown on the MASW and resistivity sections respectively.
23	F23a	Broader zone of increased conductivity indicates an increase of water/clay within the superficial deposits or change in sediment lithology. TP603 indicates the presence of clay-rich sediments overlying the shallow limestone bedrock (interpreted Hampen Formation).
	F23b	Very good correlation between Layers S3/S4/P5 and a transition into more resistive, competent limestone bedrock.
	F23c	Abrupt, vertical conductive/resistive boundary is likely to indicate the location of a fault. To the south of the fault, the deeper bedrock lithologies (possibly dipping beds as suggested by the angle of the contours) appear to be more conductive, likely due to fracturing associated with the fault or a change of bedrock formation (i.e. conductive mudstone from the Fullers Earth Formation).
	F23d	Very good correlation between Layers S4/P5 and a transition into more conductive bedrock (i.e. conductive mudstone from the Fullers Earth Formation).
	F23e	Isolated, conductive zone within the bedrock, indicates a deterioration in bedrock condition (i.e. increase of clay/water-bearing fractures) or change in bedrock lithology (e.g. into mudstone from the Fullers Earth Formation).
	F23f	Isolated, slightly more conductive zone, likely indicating an increase of clay and/or water within the superficial deposits.
	F23g	This area is generally more resistive, indicating a decrease in clay/water-bearing fractures within the weathered limestone (Hampen Formation) bedrock and superficial deposits. This correlates with an increase in S-wave velocity from 623m/s to 734m/s, and also an area of increased velocity and stiffness on the MASW section between 130 and 210 m approximately. The stiff zone shown on the MASW section appears to end at the location of the fault, with less stiff bedrock (likely

		mudstone from the Fullers Earth Formation) to the south of the fault.
	F23h	Abrupt, vertical conductive/resistive boundary is likely to indicate the location of a fault. To the south of the fault, the deeper bedrock lithologies (possibly dipping beds as suggested by the angle of the contours) appear to be more conductive, possibly due to fracturing associated with the fault or a change of bedrock formation (i.e. conductive mudstone from the Fullers Earth Formation).
	F23i	Broader zone of increased conductivity indicates an increase of water/clay within the superficial deposits or change in sediment lithology.
	F23j	Good correlation between Layers S4/P5 for the majority of the profile. Discrepancies between bedrock boundaries can be due to the P and S-wave energy following different travel paths (e.g. different beddings within an interbedded mudstone/limestone bedrock, or different weathered zones, or faulting).
24	F24a	This significant resistive zone correlates very well with the position of the Hampen Formation, and indicates a decrease of clay and/or water within the near-surface sediments (possible silt, or gravel of completely weathered limestone), overlying a homogenously resistive limestone bedrock, except for an isolated conductive anomaly at approximately 160 m chainage (small zone of weaker, broken rock).
	F24b	Broad conductive zone likely indicates a transition into mudstone bedrock from the Fullers Earth Formation. There is a very good correlation with Layer P4 (1447 m/s) with the corresponding S-wave velocity (342-394 m/s) indicating a highly weathered bedrock. Borehole DSRC315 is located too far away for direct correlation and is located on the Hampen Formation (limestone).
	F24c	Broader zone of increased conductivity indicates an increase of water/clay within the superficial deposits or change in sediment lithology. This also correlates with a zone of decreased s-wave velocity/stiffness on the MASW section, indicating the presence of softer, less consolidated sediments.
	F24d	Dipping conductive/resistive boundary likely marks the transition from conductive mudstone from the Fullers Earth Formation into more resistive limestone from the Hampen Formation. The increase in resistivity is possibly due to a decrease in water/clay as opposed to an

		increase in competence/bedrock condition, given the still low s-wave velocities (<600m/s).
	F24e	An increase of conductivity at depth indicates a transition into a different bedrock lithology (e.g. mudstone), or an increase in clay/water content within the bedrock.
	F24f	Abrupt, vertical conductive/resistive boundary is likely to indicate the location of a fault. To the south-west of the fault, the deeper bedrock lithologies (dipping beds as suggested by the angle of the contours) appear to be more conductive (i.e. mudstone from Fullers Earth Formation). The marked fault location is approximately 20 m to the north-east.
	F24g	Broader zone of increased conductivity to the south-west of the fault indicates an increase of water/clay within the superficial deposits or change in sediment lithology.
	F24h	Dipping conductive feature possibly represents a bed of more conductive mudstone from the Great Oolite Group.
	F24i	Dipping resistive feature possibly represents a bed of more resistive limestone from the Great Oolite Group.
	F24j	Region of elevated s-wave velocity indicates a stiffer zone within the bedrock, close to the fault position. The S-wave section does also indicate an increase in bedrock velocity up to 1079m/s in the vicinity of the stiff zone, suggesting much more competent rock here at depth (possible ridge).
	F24k	Decrease in near-surface, Layer P2 p-wave velocity indicating a change of sediment lithology, possibly into less consolidated sediments, as also suggested by ‘softer’ zones on the MASW section, and an increase in Layer S1/S2 layer thickness.
	F24l	Abrupt boundary indicating an increase in sediment/soft rock stiffness to the south-west.
	F24m	Increase in s-wave velocity indicates the presence of more competent bedrock at depth, with the boundary dropping off sharply in both directions possibly indicating the presence of a ridge.

Table 6. *Features and anomalies of interest as identified by the seismic refraction and MASW surveys.*

5 CONCLUSIONS

- The geophysical surveys have provided a non-invasive means for investigating the subsurface with a high degree of 'spatial' coverage using the electromagnetic survey technique. Detailed profile cross-sections of ground composition have been provided using resistivity tomography, seismic refraction and MASW.

- The ground conductivity plots have revealed variations in near-surface sediment composition (notably clay content and saturation) and thickness, as well as mapping shallow bedrock. A number of services have also been shown to cross the surveyed areas, as highlighted.

- The modelled resistivity sections were characterised by zones of contrasting resistivity values that reflect lithological (including an increase/decrease in clay content), hydrogeological (e.g. groundwater level, saturated zones), structural (e.g. faults, steeply dipping beds) and weathering variations within the sub-surface.

- The analysis of both the P and S-wave refraction data has identified distinct velocity layers that have provided detailed information to assist with the bulk characterisation of the shallow subsurface and, in particular, the thickness of overburden sediments and depth to weathered and unweathered bedrock. In summary, five distinct layer boundaries have been identified by the P-wave refraction survey, with velocities ranging from <300 m/s (weak, loose sediments) to >1901 m/s (weathered to unweathered bedrock). This has been further characterised by the S-wave refraction survey, which has revealed up to four notable layers of increasing material stiffness from <180 m/s (weak, loose sediments) to >761 m/s (rock). Where layer velocities vary laterally, this may be due to structural changes such as faulting or steeply dipping bedding. Finally, zones of increased rock stiffness and/or deterioration in bedrock condition have been further highlighted by the results of the MASW survey.

- Available borehole data has been included on the cross-sections for direct correlation, and if any additional borehole data becomes available, it may be possible to extend further/refine the interpretation and calibrate the acquired datasets.

Disclaimer

This report represents an opinionated interpretation of the geophysical data. It is intended for guidance with follow-up invasive investigation. Features that do not produce measurable geophysical anomalies or are hidden by other features may remain undetected. Geophysical surveys complement invasive/destructive methods and provide a tool for investigating the subsurface; they do not produce data that can be taken to represent all of the ground conditions found within the surveyed area. Areas that have not been surveyed due to obstructed access or any other reason are excluded from the interpretation.

FIGURES

KEY

- Resistivity/Seismic Profile
- EM 'ground conductivity' survey extents
- Proposed road scheme

See individual line figures for start and end coordinates and profile orientation

KEY TO BGS GEOLOGY MAP

(Taken from the British Geological Survey Geology of Britain viewer, bedrock geology only)

Source: Map data ©2020 Google.

- Lias
- Birdlip Limestone Formation
- Aston Limestone Formation
- Salperton Limestone Formation
- Fullers Earth Formation
- Hampen Formation
- White Limestone Formation
- Great Oolite Group
- Fault (expected location)

Title: **OVERALL LOCATION PLAN (ZONES 1 TO 4)**

Project: **A417 CRICKLEY HILL BIRDLIP**

TERRADAT down to earth geophysics

Tel: +44 (0) 2920 700127
Web:www.terradat.co.uk
Email: web@terradat.co.uk

Scale:	1:15000 at A3
Drawn by/Ref:	MB/6688/1
Date:	23 JULY 2020

FIGURE 24

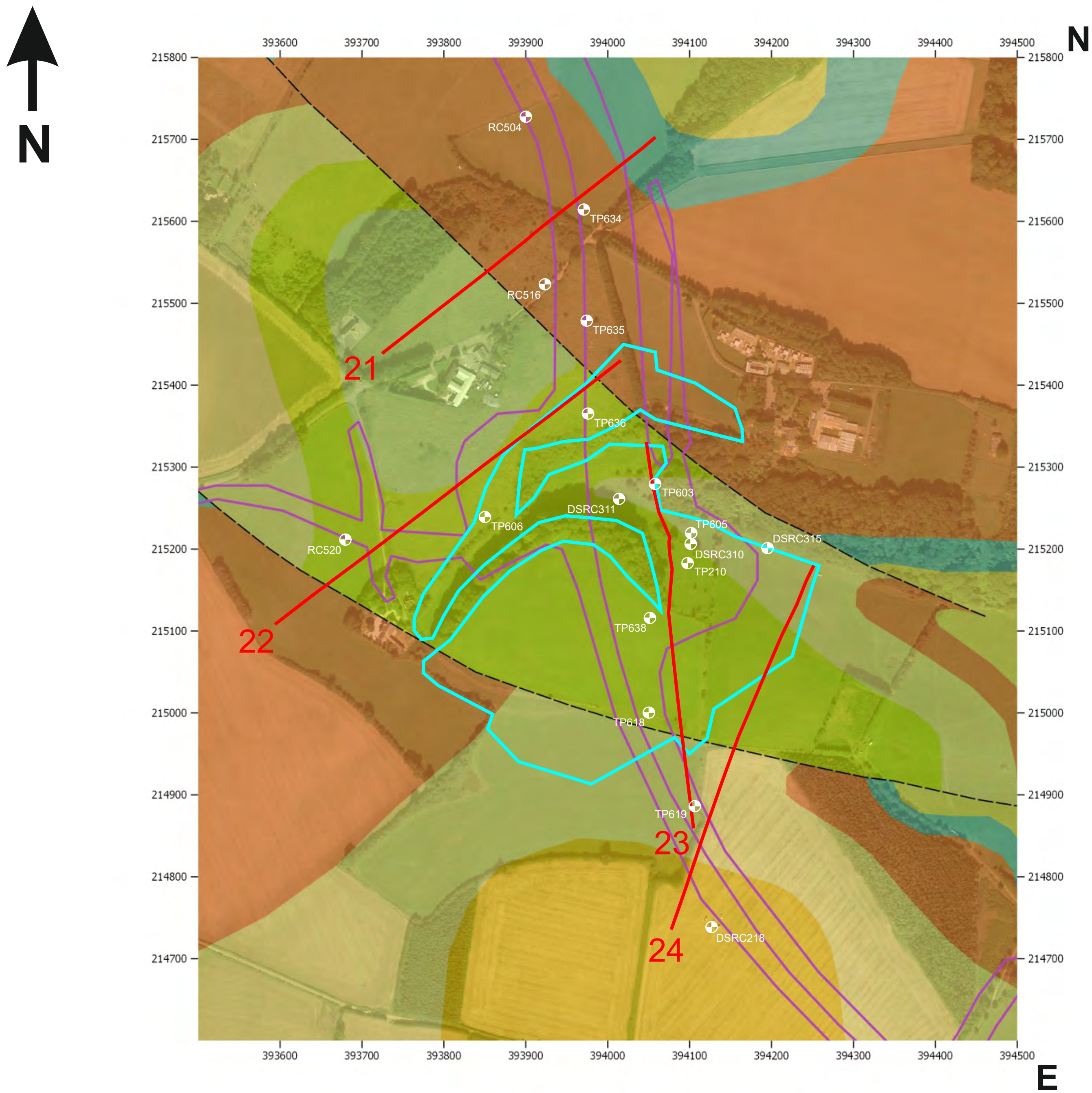

KEY

- Resistivity/Seismic Profile
- EM Survey Extents
- Proposed road scheme
- Borehole/Trial Pit

KEY TO BGS GEOLOGY MAP

(Taken from the British Geological Survey Geology of Britain viewer, bedrock geology only)

- Lias
- Birdlip Limestone Formation
- Aston Limestone Formation
- Salperton Limestone Formation
- Fullers Earth Formation
- Hampen Formation
- White Limestone Formation
- Great Oolite Group
- Fault (expected location)

NOTES

1. See individual line figures for start and end coordinates and profile orientation

Source: Map data ©2020 Google.

Project: **BIRDLIP**

Title: **LOCATION MAP (ZONE 3)**

TERRA DAT down to earth geophysics
Tel: +44 (0) 2920 700127
Web:www.terradat.co.uk
Email: web@terradat.co.uk

Scale: 1:7500 at A4

Drawn by/Ref: MB/6688/25

Date: 09 JULY 2020

FIGURE 25

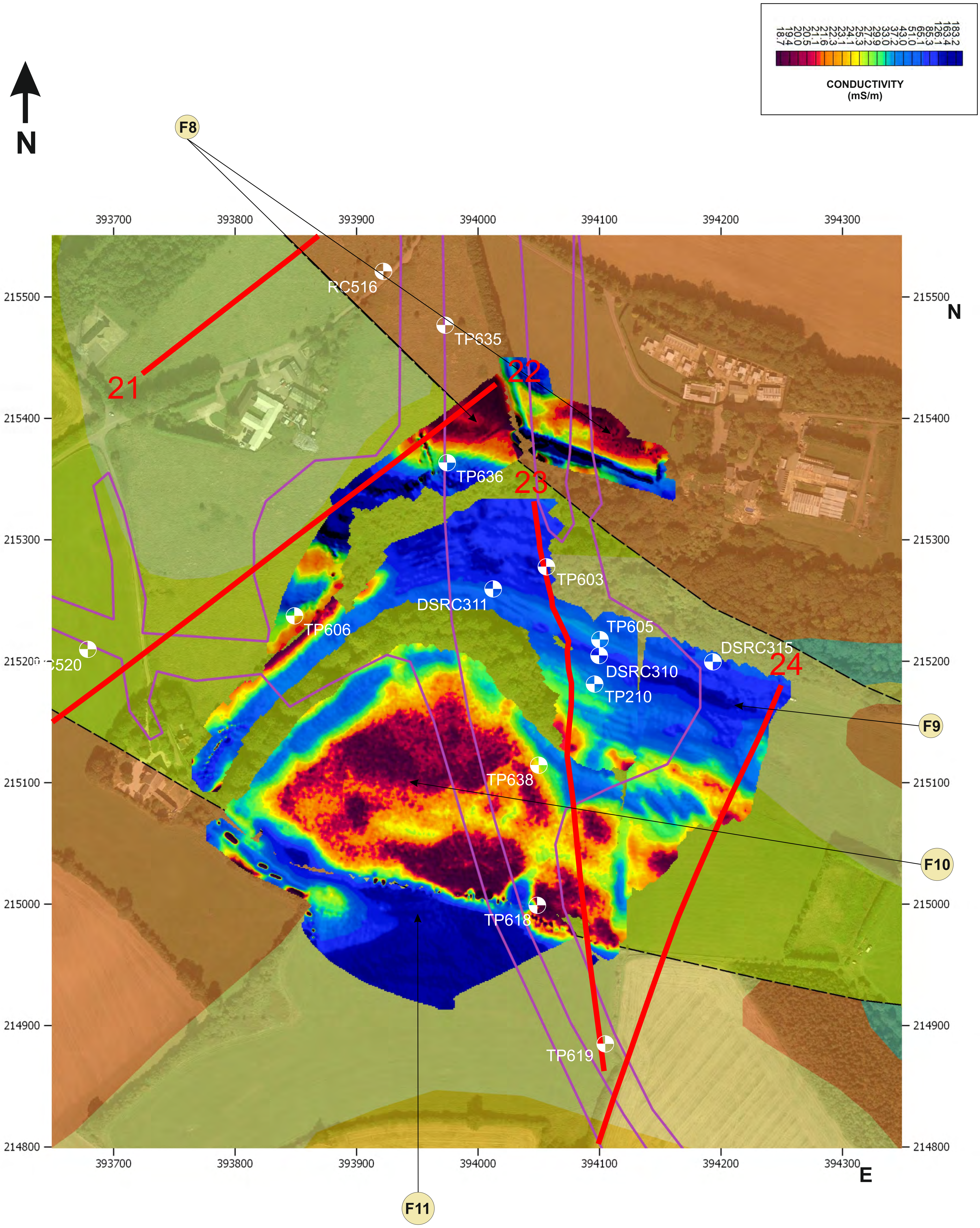

NOTES

1. See individual line figures for start and end coordinates and line orientation.

KEY TO BGS GEOLOGY MAP

(Taken from the British Geological Survey Geology of Britain viewer, bedrock geology)

- Lias
- Birdlip Limestone Formation
- Aston Limestone Formation
- Salperton Limestone Formation
- Fullers Earth Formation
- Hampen Formation
- White Limestone Formation
- Great Oolite Group
- Fault (expected location)

KEY

- Resistivity profile
- Proposed road scheme
- Borehole

Title: **GROUND CONDUCTIVITY (ZONE 3)**

Project: **A417 CRICKLEY HILL BIRDLIP**

TERRA DAT down to earth geophysics

Tel: +44 (0) 2920 700127
Web:www.terradat.co.uk
Email: web@terradat.co.uk

Scale: 1:1500 @ A3
Drawn by/Ref: MB/6688/26
Date: 14 JULY 2020

FIGURE 26

ERT-21

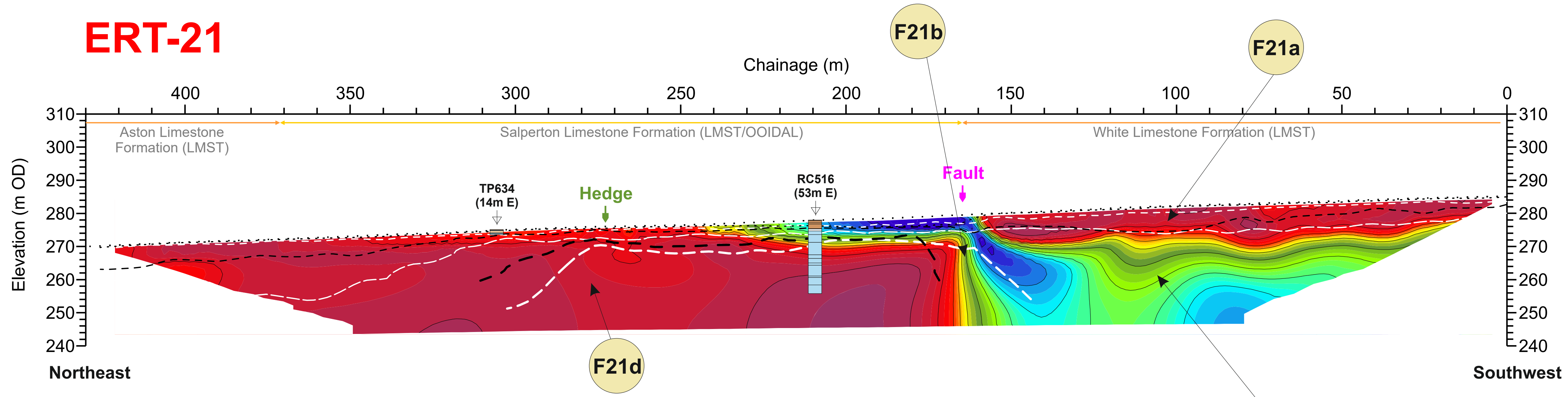

ERT-21 Profile Coordinates	
0m Chainage	429m Chainage
393723.1E 215438.4N	394058.1E 215702.7N

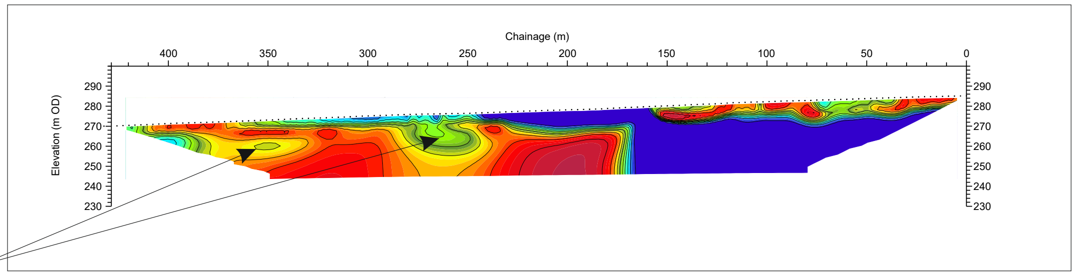

MASW-21

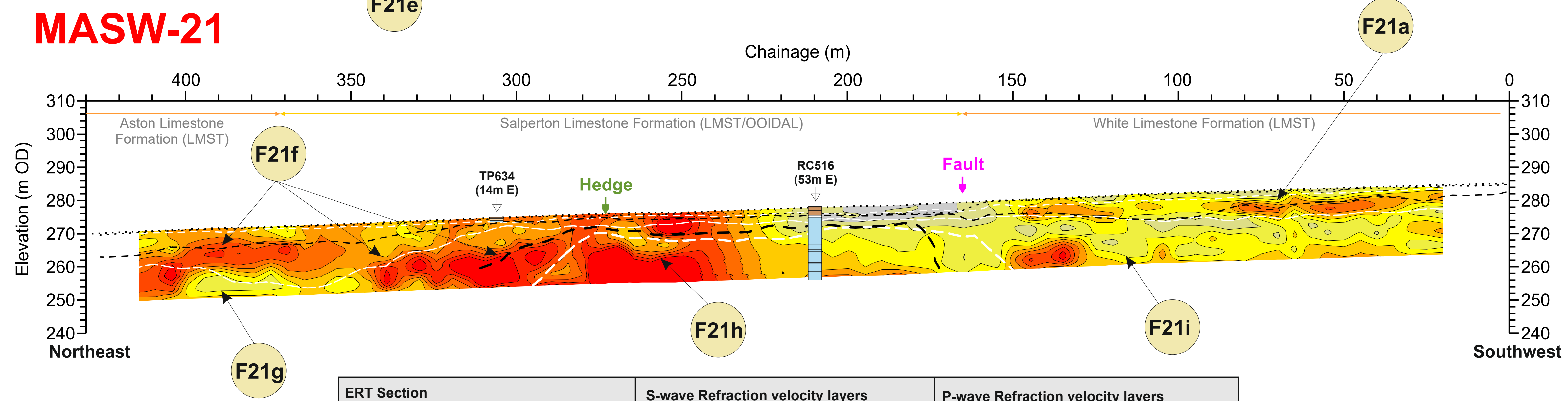

MASW-21 Profile Coordinates	
0m Chainage	430m Chainage
393722.5E 215437.7N	394059.2E 215707.6N

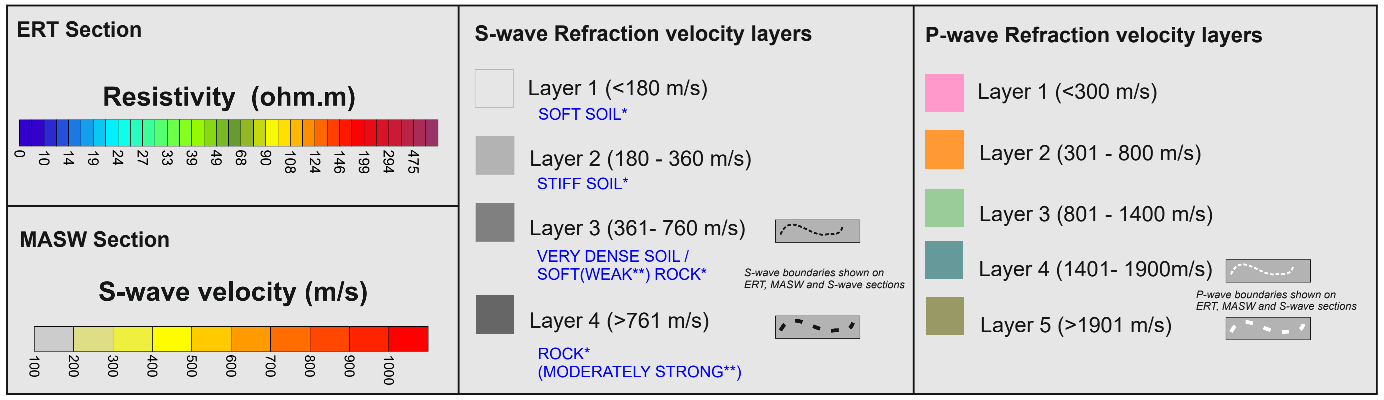

BOREHOLE KEY

Made ground, Sandstone, Clay, Mudstone, Silt, Siltstone, Sand, Limestone, Gravel, Core loss

KEY

- Line 1 — Profile intersection
- Fault — Reported fault positions
- Bedrock geology subcrop

NOTES/OBSERVATIONS

*The NEHRP Recommended Provisions for seismic regulation for new buildings, (FEMA-222A and FEMA-223A, 1994)

** UK equivalent classification (Waltham, 1994)

Title: **ERT AND SEISMIC PROFILES**

Project: **A417 CRICKLEY HILL BIRDLIP**

TERRA DAT — down to earth geophysics

Tel: +44 (0) 2920 700127
Web:www.terradat.co.uk
Email: web@terradat.co.uk

Scale: 1:1500 at A3
Drawn by/Ref: JT/6688/*
Date: 07 AUG 2020

FIGURE 27A

SEIS-21 (S-wave)

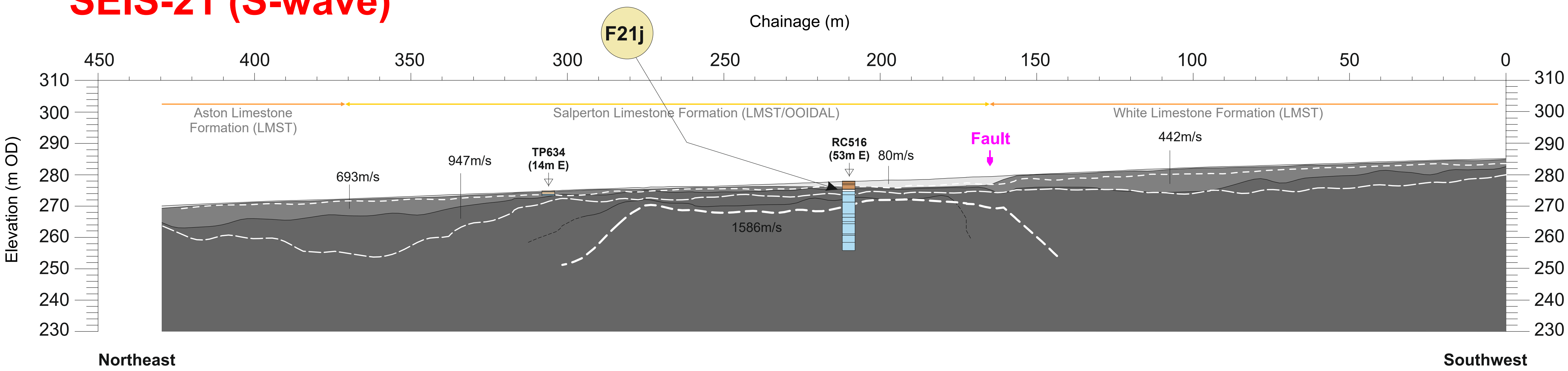

SEIS-21 Profile Coordinates	
0m Chainage	430m Chainage
393722.5E 215437.7N	394059.2E 215707.6N

SEIS-21 (P-wave)

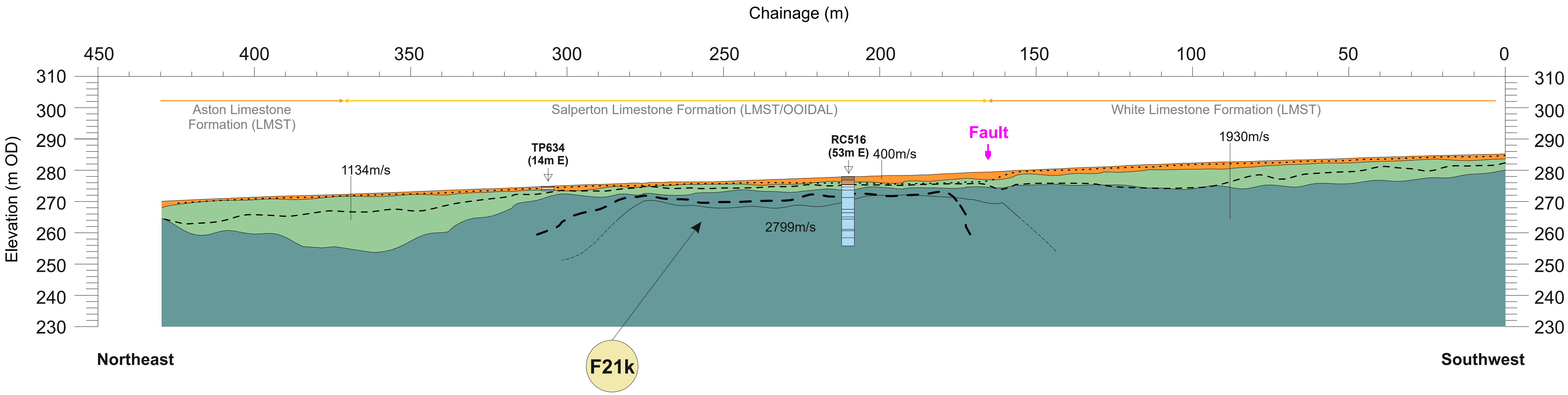

ERT Section

Resistivity (ohm.m)

0 10 14 19 24 27 33 39 49 68 90 108 124 146 199 294 475

MASW Section

S-wave velocity (m/s)

100 175 250 325 400 475 550 625 700 775

S-wave Refraction velocity layers

- Layer 1 (<180 m/s) SOFT SOIL*
- Layer 2 (180 - 360 m/s) STIFF SOIL*
- Layer 3 (361- 760 m/s) VERY DENSE SOIL / SOFT(WEAK**) ROCK*
- Layer 4 (>761 m/s) ROCK* (MODERATELY STRONG**)

S-wave boundaries shown on ERT, MASW and S-wave sections

P-wave Refraction velocity layers

- Layer 1 (<300 m/s)
- Layer 2 (301 - 800 m/s)
- Layer 3 (801 - 1400 m/s)
- Layer 4 (1401- 1900m/s)
- Layer 5 (>1901 m/s)

P-wave boundaries shown on ERT, MASW and S-wave sections

BOREHOLE KEY

Made ground, Clay, Silt, Sand, Gravel, Sandstone, Mudstone, Siltstone, Limestone, Core loss

KEY

- Line 1 — Profile intersection
- Fault — Reported fault positions
- Bedrock geology subcrop

NOTES/OBSERVATIONS

*The NEHRP Recommended Provisions for seismic regulation for new buildings, (FEMA-222A and FEMA-223A, 1994)

** UK equivalent classification (Waltham, 1994)

Title: ERT AND SEISMIC PROFILES

Project: A417 CRICKLEY HILL BIRDLIP

TERRADAT down to earth geophysics

Tel: +44 (0) 2920 700127
Web:www.terradat.co.uk
Email: web@terradat.co.uk

Scale: 1:1500 at A3

Drawn by/Ref: JT/6688/*

Date: 29 JUN 2020

FIGURE 27B

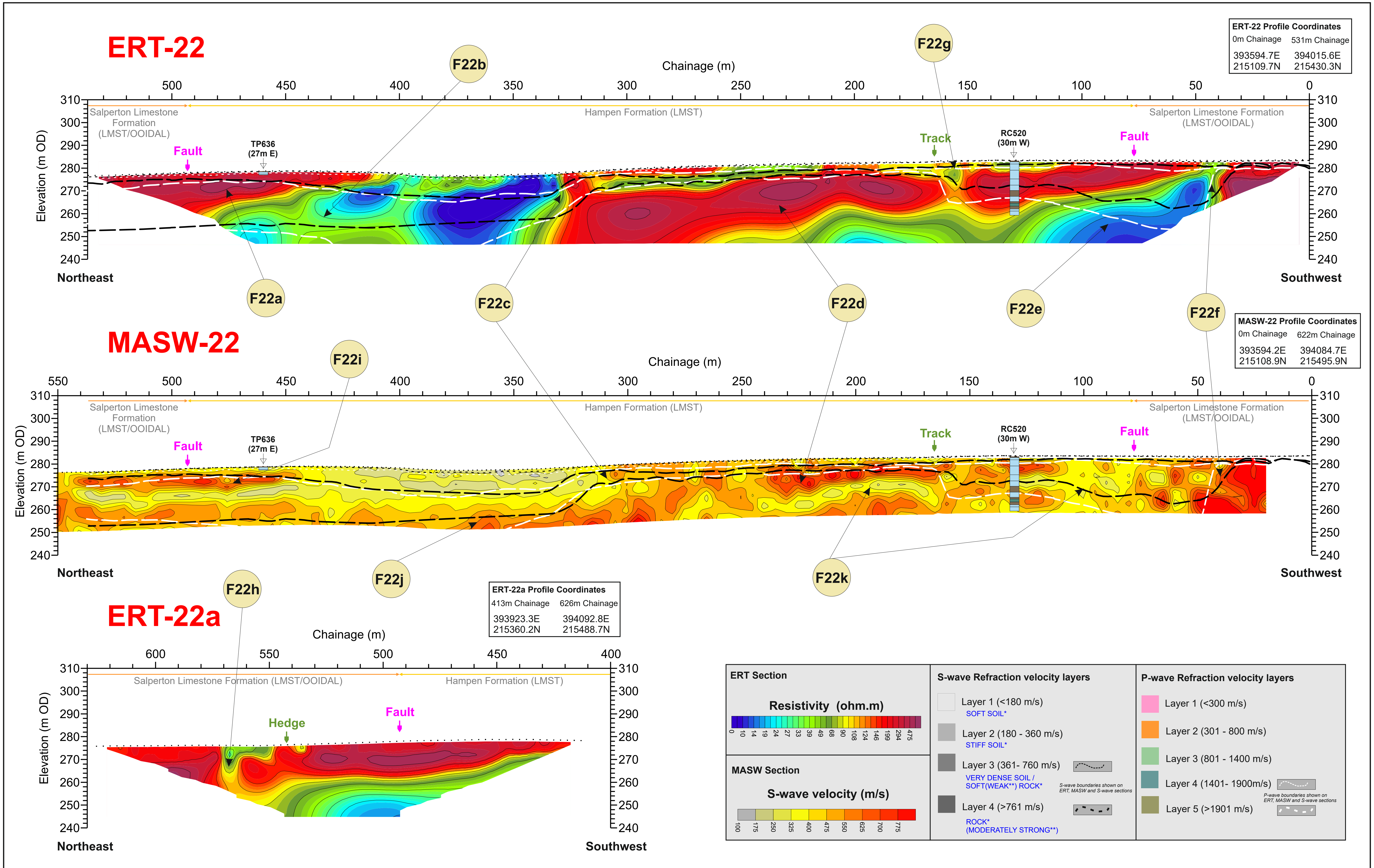

BOREHOLE KEY

Made ground	Sandstone
Clay	Mudstone
Silt	Siltstone
Sand	Limestone
Gravel	Core loss

KEY

Line 1 – Profile intersection

Fault – Reported fault positions

Bedrock geology subcrop

NOTES/OBSERVATIONS

*The NEHRP Recommended Provisions for seismic regulation for new buildings, (FEMA-222A and FEMA-223A, 1994)

** UK equivalent classification (Waltham, 1994)

Title: **ERT AND SEISMIC PROFILES**

Project: **A417 CRICKLEY HILL BIRDLIP**

TERRA DAT down to earth geophysics

Tel: +44 (0) 2920 700127
Web:www.terradat.co.uk
Email: web@terradat.co.uk

Scale: 1:1500 at A3
Drawn by/Ref: JT/6688/*
Date: 17 AUG 2020

FIGURE 28A

ERT-22a

ERT-22a Profile Coordinates	
413m Chainage	626m Chainage
393923.3E 215360.2N	394092.8E 215488.7N

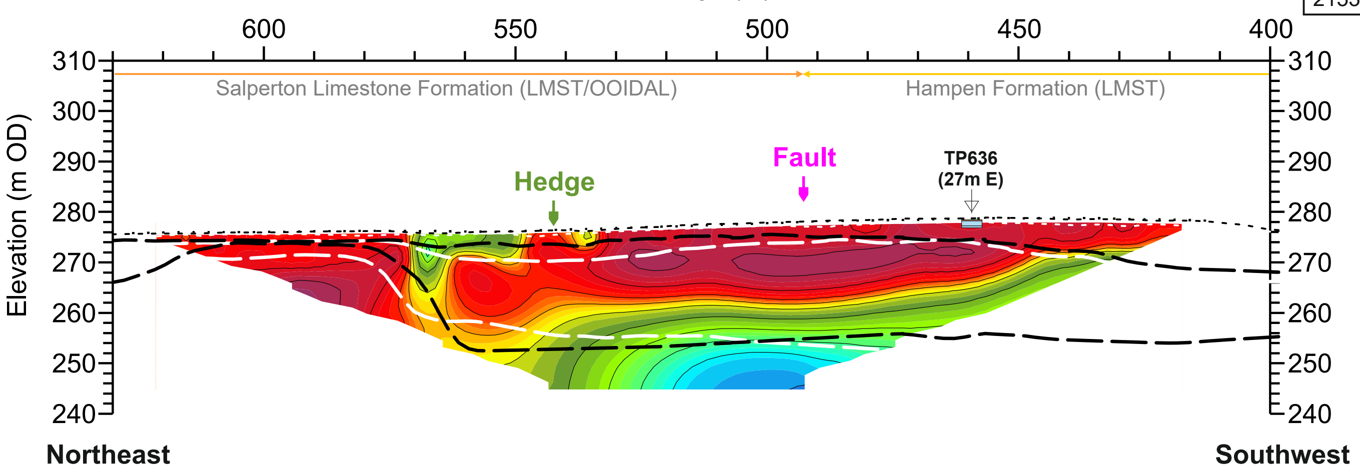

ERT Section	S-wave Refraction velocity layers	P-wave Refraction velocity layers
Resistivity (ohm.m): 0, 10, 14, 19, 24, 27, 33, 39, 49, 68, 90, 108, 124, 146, 199, 294, 475	Layer 1 (<180 m/s) SOFT SOIL*	Layer 1 (<300 m/s)
	Layer 2 (180 - 360 m/s) STIFF SOIL*	Layer 2 (301 - 800 m/s)
MASW Section	Layer 3 (361- 760 m/s) VERY DENSE SOIL / SOFT(WEAK**) ROCK*	Layer 3 (801 - 1400 m/s)
S-wave velocity (m/s): 100, 175, 250, 325, 400, 475, 550, 625, 700, 775	*S-wave boundaries shown on ERT, MASW and S-wave sections*	Layer 4 (1401- 1900m/s)
	Layer 4 (>761 m/s) ROCK* (MODERATELY STRONG**)	*P-wave boundaries shown on ERT, MASW and S-wave sections*
		Layer 5 (>1901 m/s)

MASW-22 (continued)

MASW-22 Profile Coordinates	
0m Chainage	622m Chainage
393594.2E 215108.9N	394084.7E 215495.9N

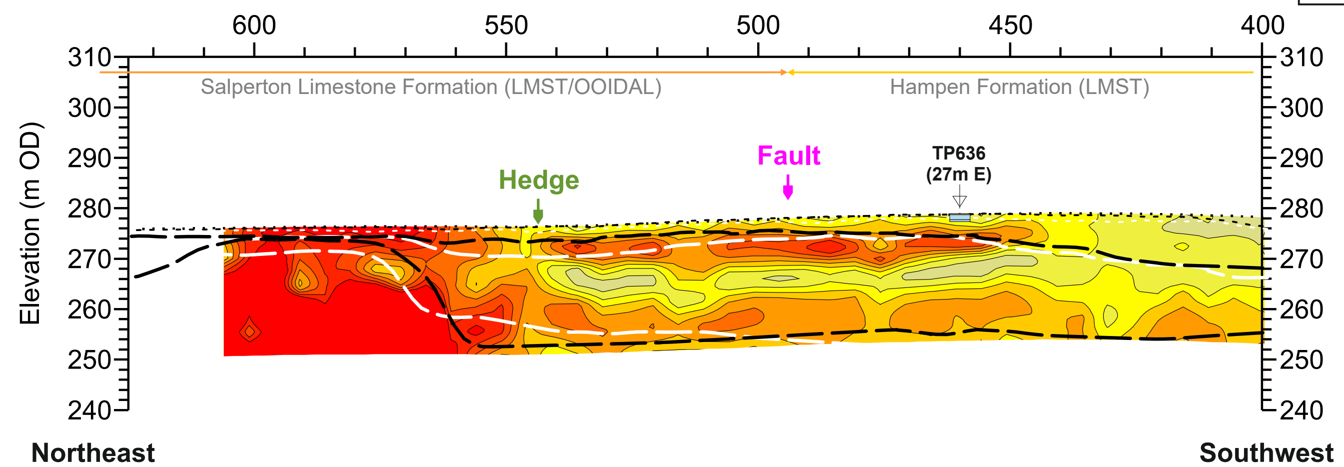

MASW-22 (complete)

MASW-22 Profile Coordinates	
0m Chainage	622m Chainage
393594.2E 215108.9N	394084.7E 215495.9N

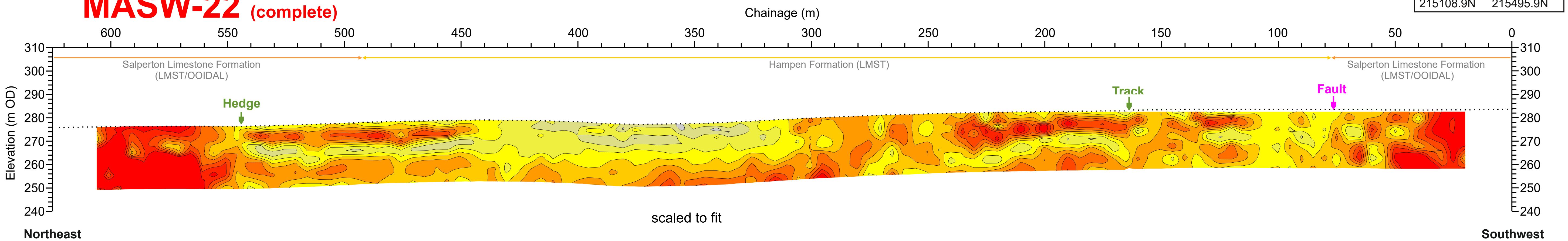

BOREHOLE KEY

Made ground, Clay, Silt, Sand, Gravel, Sandstone, Mudstone, Siltstone, Limestone, Core loss

KEY

Line 1 — Profile intersection

Fault — Reported fault positions

Bedrock geology subcrop

NOTES/OBSERVATIONS

**The NEHRP Recommended Provisions for seismic regulation for new buildings, (FEMA-222A and FEMA-223A, 1994)*

*** UK equivalent classification (Waltham, 1994)*

Title: **ERT AND SEISMIC PROFILES**

Project: **A417 CRICKLEY HILL BIRDLIP**

TERRADAT down to earth geophysics

Tel: +44 (0) 2920 700127
Web:www.terradat.co.uk
Email: web@terradat.co.uk

Scale: 1:1500 at A3

Drawn by/Ref: JT/6688/*

Date: 17 AUG 2020

FIGURE 28B

SEIS-22 (S-wave)

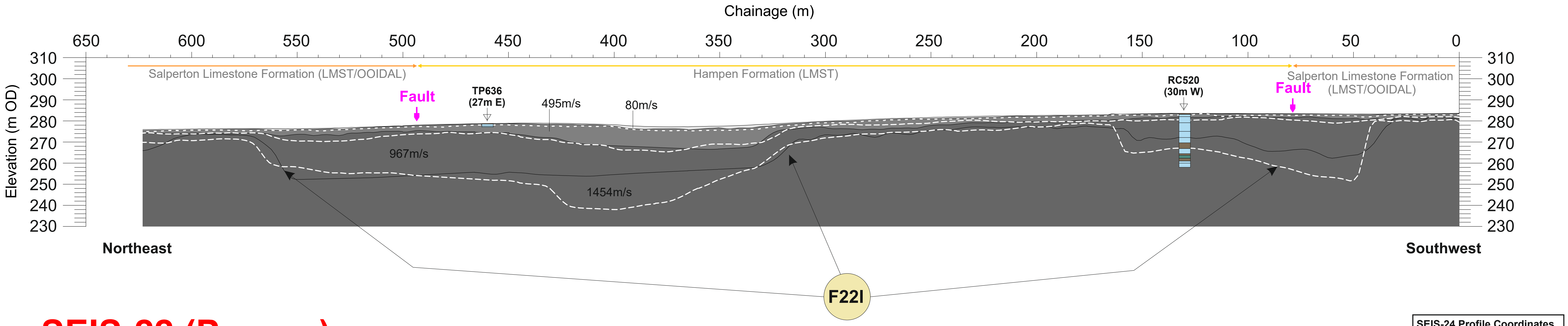

SEIS-22 (P-wave)

SEIS-24 Profile Coordinates	
0m Chainage	622m Chainage
393594.2E 215108.9N	394084.7E 215495.9N

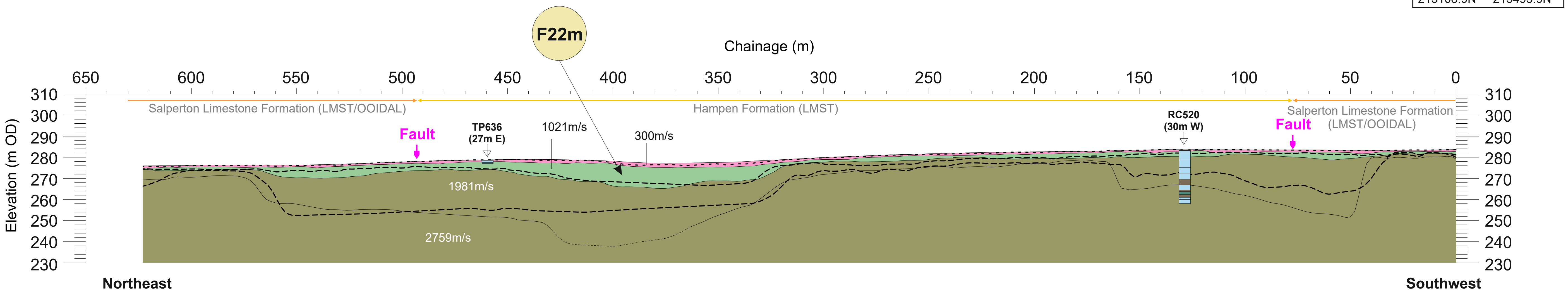

ERT Section

Resistivity (ohm.m)

0 10 14 19 24 27 33 39 49 68 90 108 124 146 199 294 475

MASW Section

S-wave velocity (m/s)

100 175 250 325 400 475 550 625 700 775

S-wave Refraction velocity layers

- Layer 1 (<180 m/s) SOFT SOIL*
- Layer 2 (180 - 360 m/s) STIFF SOIL*
- Layer 3 (361- 760 m/s) VERY DENSE SOIL / SOFT(WEAK**) ROCK*
- Layer 4 (>761 m/s) ROCK* (MODERATELY STRONG**)

S-wave boundaries shown on ERT, MASW and S-wave sections

P-wave Refraction velocity layers

- Layer 1 (<300 m/s)
- Layer 2 (301 - 800 m/s)
- Layer 3 (801 - 1400 m/s)
- Layer 4 (1401- 1900m/s)
- Layer 5 (>1901 m/s)

P-wave boundaries shown on ERT, MASW and S-wave sections

BOREHOLE KEY

Made ground, Clay, Silt, Sand, Gravel, Sandstone, Mudstone, Siltstone, Limestone, Core loss

KEY

Line 1 — Profile intersection

Fault — Reported fault positions

Bedrock geology subcrop

NOTES/OBSERVATIONS

*The NEHRP Recommended Provisions for seismic regulation for new buildings, (FEMA-222A and FEMA-223A, 1994)

** UK equivalent classification (Waltham, 1994)

Title: **ERT AND SEISMIC PROFILES**

Project: **A417 CRICKLEY HILL BIRDLIP**

TERRA DAT down to earth geophysics

Tel: +44 (0) 2920 700127
Web:www.terradat.co.uk
Email: web@terradat.co.uk

Scale: 1:2000 at A3
Drawn by/Ref: JT/6688/*
Date: 29 JUN 2020

FIGURE 28C

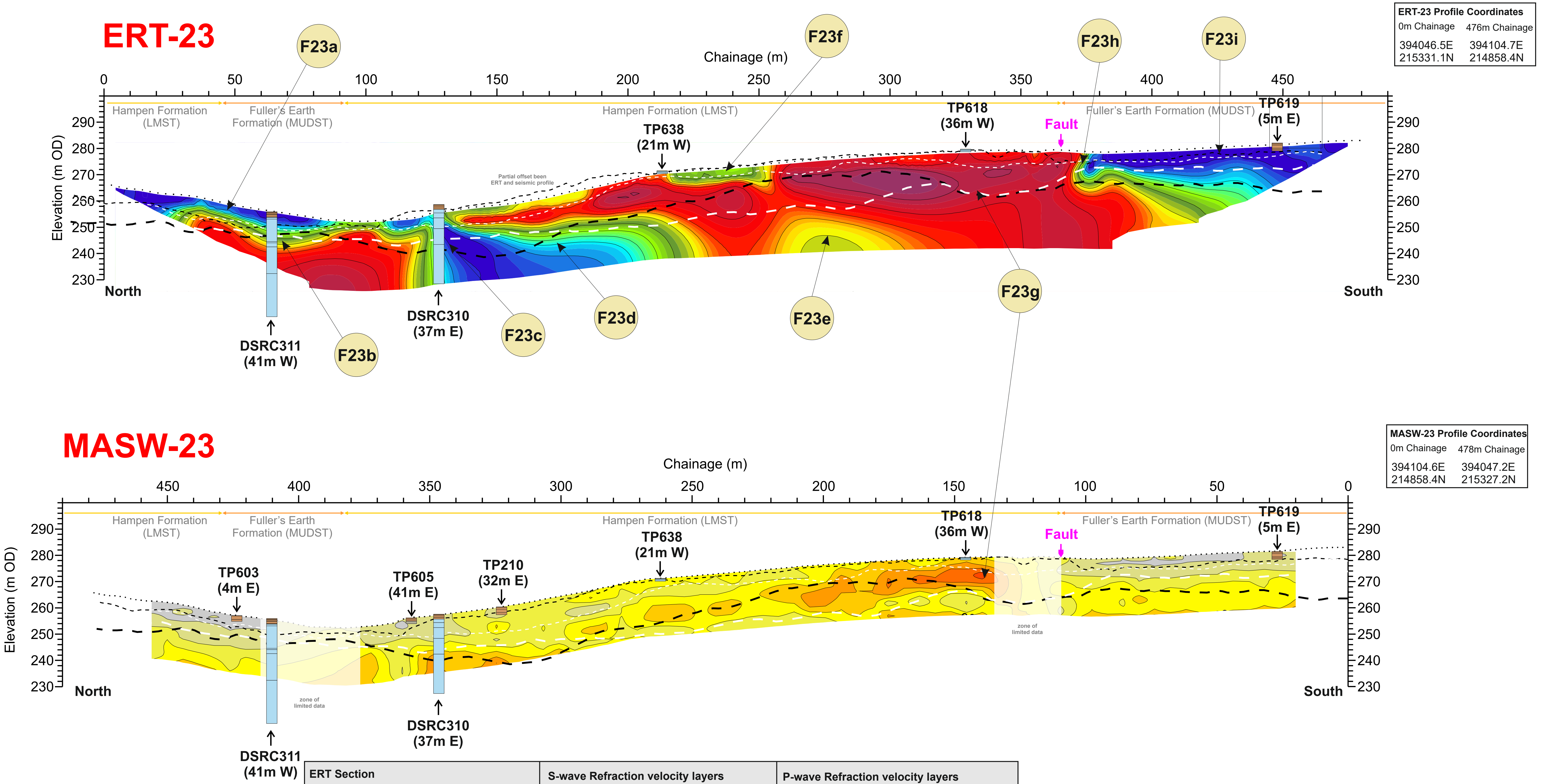

ERT Section

Resistivity (ohm.m)

0 10 14 19 24 27 33 39 49 68 90 108 124 146 199 294 475

MASW Section

S-wave velocity (m/s)

100 175 250 325 400 475 550 625 700 775

S-wave Refraction velocity layers

- Layer 1 (<180 m/s) SOFT SOIL*
- Layer 2 (180 - 360 m/s) STIFF SOIL*
- Layer 3 (361- 760 m/s) VERY DENSE SOIL / SOFT(WEAK**) ROCK*
- Layer 4 (>761 m/s) ROCK* (MODERATELY STRONG**)

S-wave boundaries shown on ERT, MASW and S-wave sections

P-wave Refraction velocity layers

- Layer 1 (<300 m/s)
- Layer 2 (301 - 800 m/s)
- Layer 3 (801 - 1400 m/s)
- Layer 4 (1401- 1900m/s)
- Layer 5 (>1901 m/s)

P-wave boundaries shown on ERT, MASW and S-wave sections

BOREHOLE KEY

Made ground, Sandstone, Clay, Mudstone, Silt, Siltstone, Sand, Limestone, Gravel, Core loss

KEY

- Line 1 — Profile intersection
- Fault — Reported fault positions
- Bedrock geology subcrop

NOTES/OBSERVATIONS

*The NEHRP Recommended Provisions for seismic regulation for new buildings, (FEMA-222A and FEMA-223A, 1994)

** UK equivalent classification (Waltham, 1994)

Title: **ERT AND SEISMIC PROFILES**

Project: **A417 CRICKLEY HILL BIRDLIP**

TERRA DAT down to earth geophysics

Tel: +44 (0) 2920 700127
Web:www.terradat.co.uk
Email: web@terradat.co.uk

Scale: 1:1500 at A3
Drawn by/Ref: JT/6688/29A
Date: 14 FEB 2020

FIGURE 29A

SEIS-23 (S-wave)

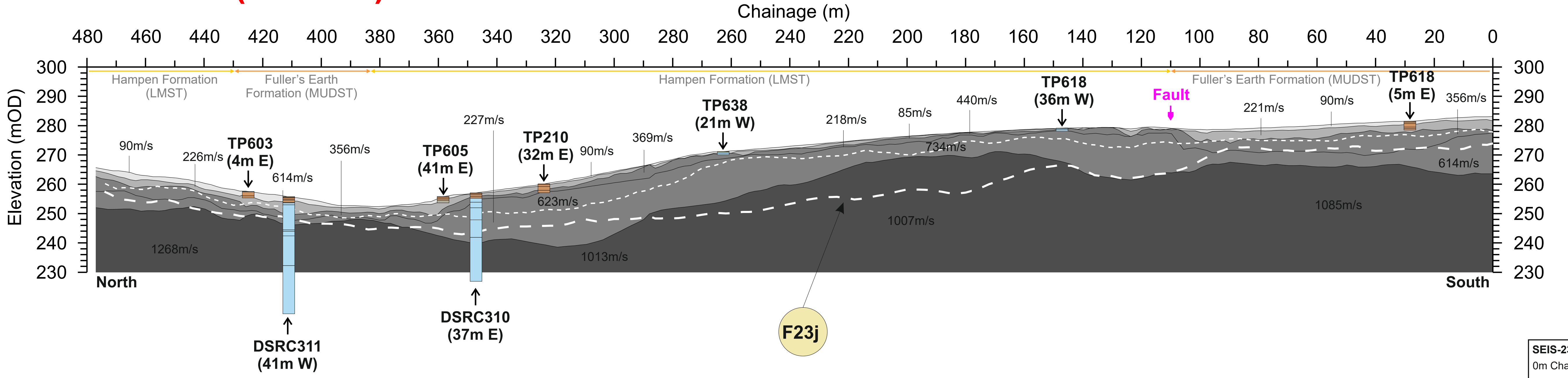

SEIS-23 Profile Coordinates	
0m Chainage	478m Chainage
394104.6E 214858.4N	394047.2E 215327.2N

SEIS-23 (P-wave)

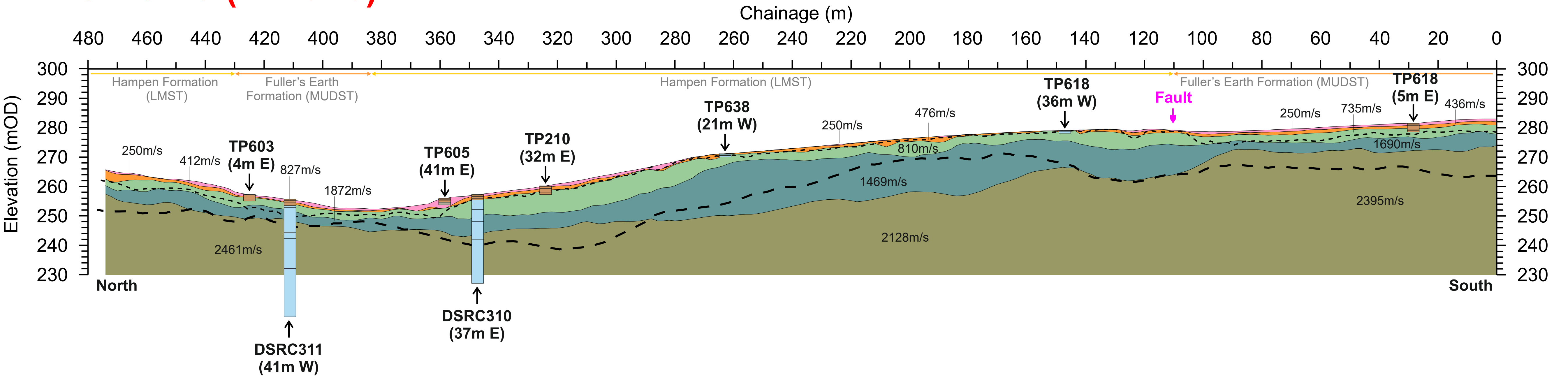

ERT Section

Resistivity (ohm.m)

0 10 14 19 24 27 33 39 49 68 90 108 124 146 199 294 475

MASW Section

S-wave velocity (m/s)

100 175 250 325 400 475 550 625 700 775

S-wave Refraction velocity layers

- Layer 1 (<180 m/s) SOFT SOIL*
- Layer 2 (180 - 360 m/s) STIFF SOIL*
- Layer 3 (361- 760 m/s) VERY DENSE SOIL / SOFT(WEAK**) ROCK*
- Layer 4 (>761 m/s) ROCK* (MODERATELY STRONG**)

S-wave boundaries shown on ERT, MASW and S-wave sections

P-wave Refraction velocity layers

- Layer 1 (<300 m/s)
- Layer 2 (301 - 800 m/s)
- Layer 3 (801 - 1400 m/s)
- Layer 4 (1401- 1900m/s)
- Layer 5 (>1901 m/s)

P-wave boundaries shown on ERT, MASW and S-wave sections

BOREHOLE KEY

Made ground, Clay, Silt, Sand, Gravel, Sandstone, Mudstone, Siltstone, Limestone, Core loss

KEY

Line 1 — Profile intersection

Fault — Reported fault positions

Bedrock geology subcrop

NOTES/OBSERVATIONS

*The NEHRP Recommended Provisions for seismic regulation for new buildings, (FEMA-222A and FEMA-223A, 1994)

** UK equivalent classification (Waltham, 1994)

Title: SEISMIC REFRACTION PROFILES

Project: A417 CRICKLEY HILL BIRDLIP

TERRA DAT down to earth geophysics
Tel: +44 (0) 2920 700127
Web:www.terradat.co.uk
Email: web@terradat.co.uk

Scale:	1:1500 at A3
Drawn by/Ref:	JT/6688/29B
Date:	14 FEB 2020

FIGURE 29B

ERT-24

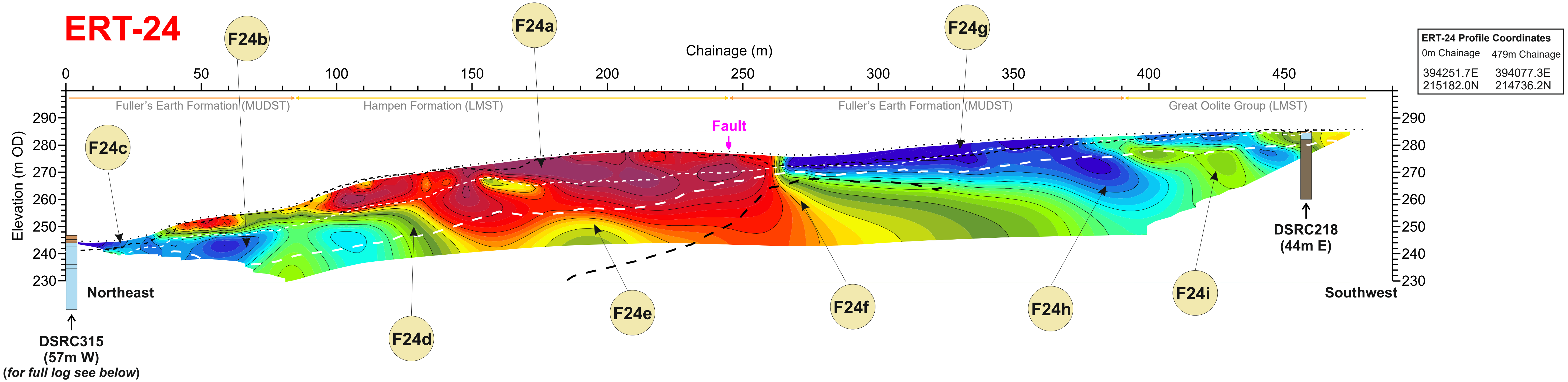

ERT-24 Profile Coordinates	
0m Chainage	479m Chainage
394251.7E	394077.3E
215182.0N	214736.2N

MASW-24

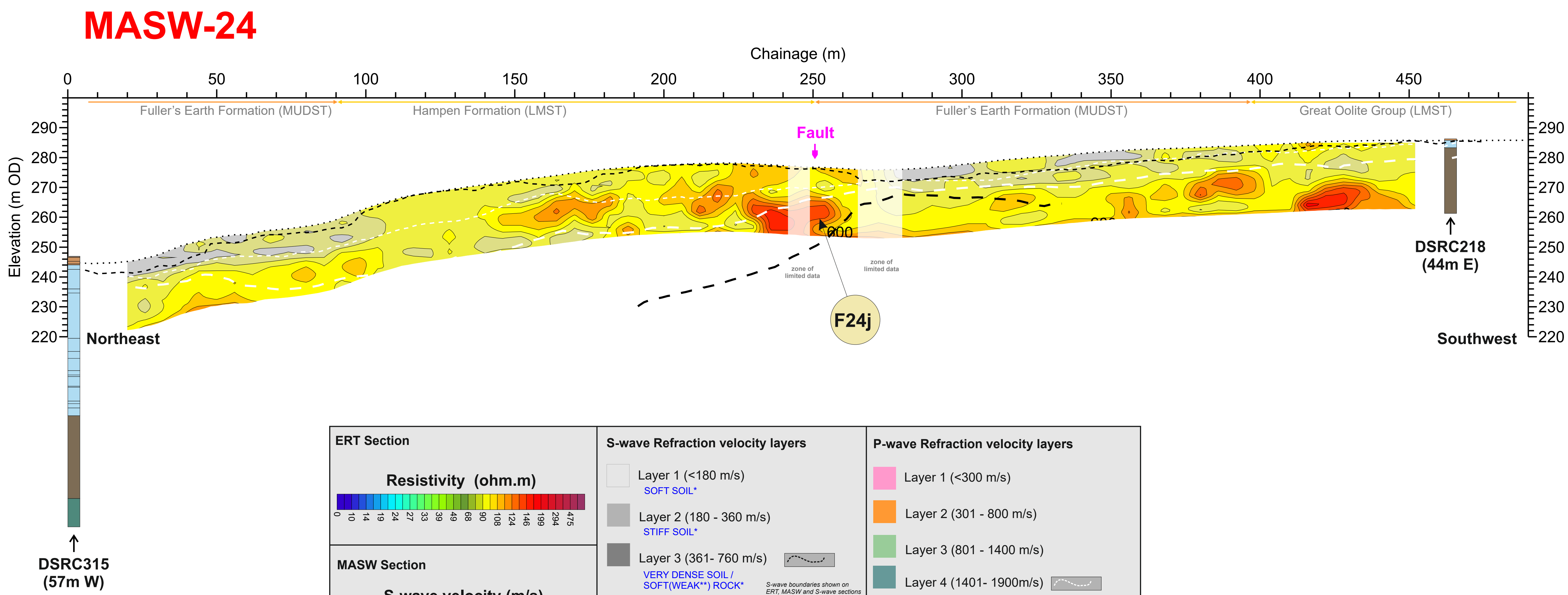

MASW-24 Profile Coordinates	
0m Chainage	526m Chainage
394248.7E	394061.2E
215182.0N	214694.6N

ERT Section

Resistivity (ohm.m)

0, 10, 14, 19, 24, 27, 33, 39, 49, 68, 90, 108, 124, 146, 199, 294, 475

MASW Section

S-wave velocity (m/s)

100, 175, 250, 325, 400, 475, 550, 625, 700, 775

S-wave Refraction velocity layers

- Layer 1 (<180 m/s) SOFT SOIL*
- Layer 2 (180 - 360 m/s) STIFF SOIL*
- Layer 3 (361- 760 m/s) VERY DENSE SOIL / SOFT(WEAK**) ROCK*
- Layer 4 (>761 m/s) ROCK* (MODERATELY STRONG**)

S-wave boundaries shown on ERT, MASW and S-wave sections

P-wave Refraction velocity layers

- Layer 1 (<300 m/s)
- Layer 2 (301 - 800 m/s)
- Layer 3 (801 - 1400 m/s)
- Layer 4 (1401- 1900m/s)
- Layer 5 (>1901 m/s)

P-wave boundaries shown on ERT, MASW and S-wave sections

BOREHOLE KEY

Made ground, Sandstone, Clay, Mudstone, Silt, Siltstone, Sand, Limestone, Gravel, Core loss

KEY

- Line 1 — Profile intersection
- Fault — Reported fault positions
- Bedrock geology subcrop

NOTES/OBSERVATIONS

Title: ERT AND SEISMIC PROFILES

Project: A417 CRICKLEY HILL BIRDLIP

TERRA DAT down to earth geophysics

Tel: +44 (0) 2920 700127
Web:www.terradat.co.uk
Email: web@terradat.co.uk

Scale: 1:1500 at A3
Drawn by/Ref: JT/6688/30A
Date: 14 FEB 2020

FIGURE 30A

ERT-24

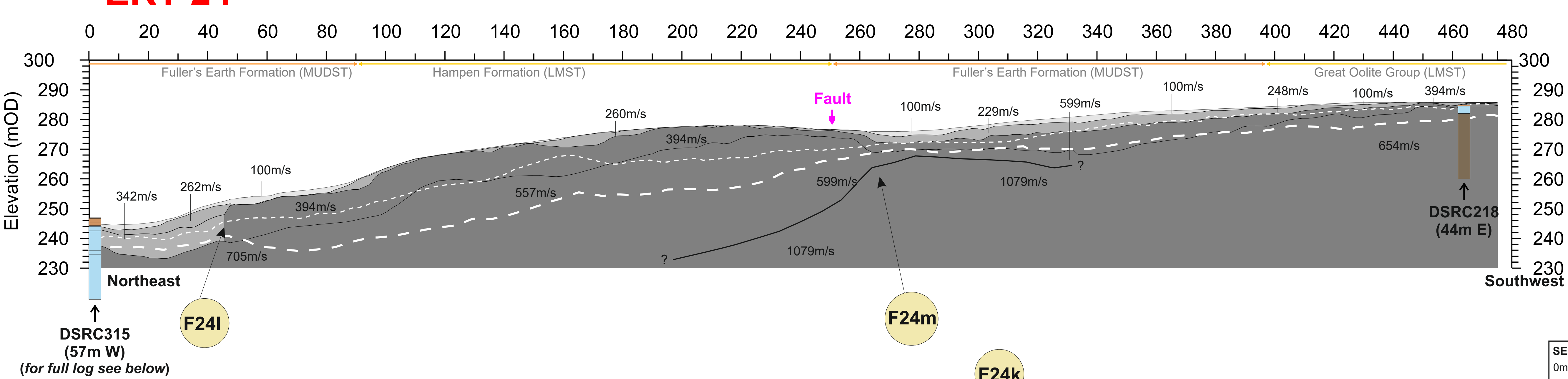

SEIS-24 Profile Coordinates	
0m Chainage	475m Chainage
394248.7E	394061.2E
215182.0N	214694.6N

SEIS-24 (P-wave)

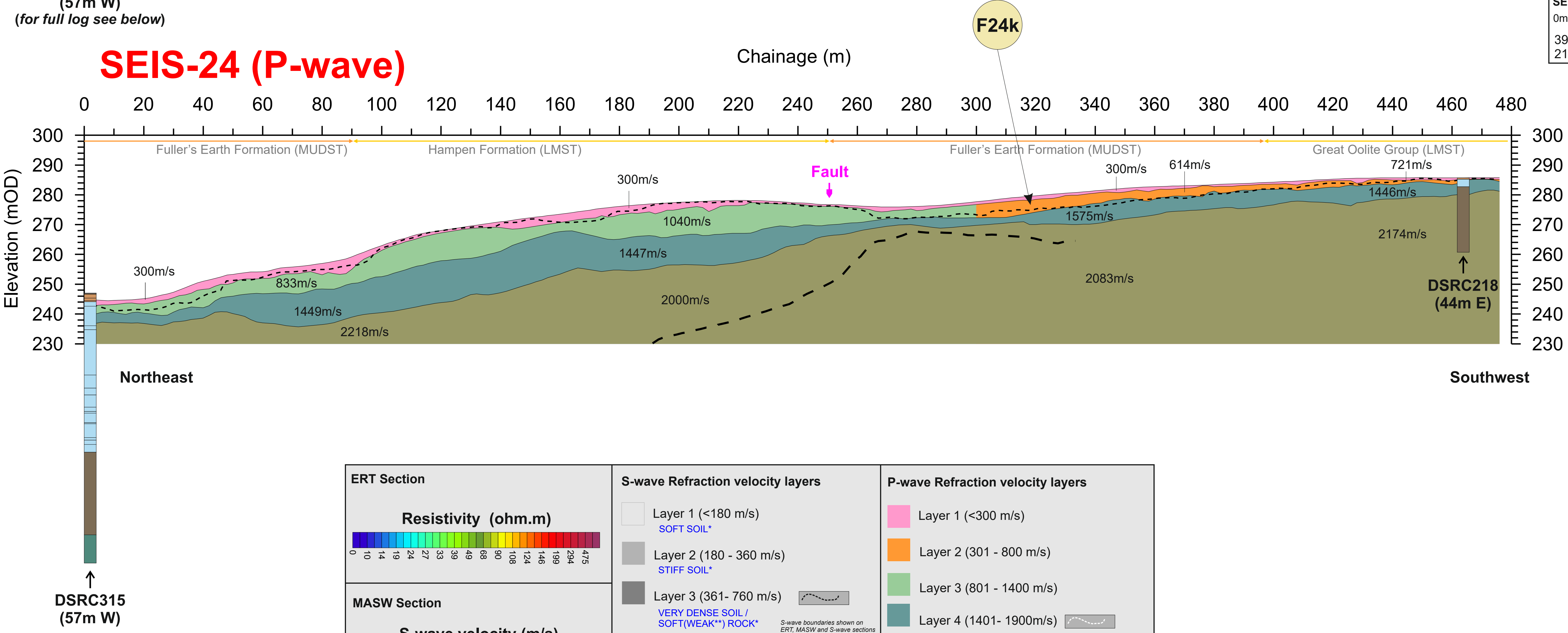

ERT Section

Resistivity (ohm.m)

0 10 14 19 24 27 33 39 49 68 90 108 124 146 199 294 475

MASW Section

S-wave velocity (m/s)

100 175 250 325 400 475 550 625 700 775

S-wave Refraction velocity layers

- Layer 1 (<180 m/s) — SOFT SOIL*
- Layer 2 (180 - 360 m/s) — STIFF SOIL*
- Layer 3 (361- 760 m/s) — VERY DENSE SOIL / SOFT(WEAK**) ROCK*
- Layer 4 (>761 m/s) — ROCK* (MODERATELY STRONG**)

S-wave boundaries shown on ERT, MASW and S-wave sections

P-wave Refraction velocity layers

- Layer 1 (<300 m/s)
- Layer 2 (301 - 800 m/s)
- Layer 3 (801 - 1400 m/s)
- Layer 4 (1401- 1900m/s)
- Layer 5 (>1901 m/s)

P-wave boundaries shown on ERT, MASW and S-wave sections

BOREHOLE KEY

Made ground	Sandstone
Clay	Mudstone
Silt	Siltstone
Sand	Limestone
Gravel	Core loss

KEY

- Line 1 — Profile intersection
- Fault — Reported fault positions
- Bedrock geology subcrop

NOTES/OBSERVATIONS

Title: **SEISMIC REFRACTION PROFILES**

Project: **A417 CRICKLEY HILL BIRDLIP**

TERRA DAT down to earth geophysics
Tel: +44 (0) 2920 700127
Web:www.terradat.co.uk
Email: web@terradat.co.uk

Scale:	1:1500 at A3
Drawn by/Ref:	JT/6688/30B
Date:	14 FEB 2020

FIGURE 30B

APPENDICES

Appendix - Ground conductivity (EM) survey

A ground conductivity or electromagnetic (EM) survey involves the generation of an EM field at the surface and subsequent measuring of the response as it propagates through the subsurface. The main components of the instrument are a transmitter coil (to generate the primary EM field) and receiver coil (to measure the induced secondary EM field). The amplitude and phase-shift of the secondary field are recorded and are then converted into values for ground conductivity and in-phase component (metal indicator).

The ground conductivity (EM) instruments are either hand carried or mounted/towed behind a quad bike. Readings are usually taken on a regular grid or along selected traverse lines and positional control can be provided by dGPS if there is sufficient satellite coverage.

The selection of the particular EM instrument (EM-38/EM-31/GEM-2) is primarily based on the required penetration depth of the survey. However for most conductivity surveys the GEM-2 has replaced the more conventional EM-31 instrument due to its ability to simultaneously acquire data at different frequencies (i.e. different depth levels) and a greater depth of penetration. At the end of each survey, the survey data is downloaded to a field computer and corrected for instrument, diurnal and positional shifts. Additional editing may be carried out to remove any 'noisy' data values/positions.

The results from the EM survey can be presented as colour contoured plots of conductivity and inphase (metal response) data. In general terms, a relative increase in conductivity values usually indicates a local increase in clay content or water saturation. However, if there is a corresponding increase in the inphase response, the influence of some artificial source is likely (i.e. metal).

EM-38
Single frequency
Exploration depth ~1.5m

EM-31
Single frequency
Exploration depth ~3 to 5m

GEM-2
Multi-frequency
Exploration depth up to 10m

Towed EM-38 with dGPS

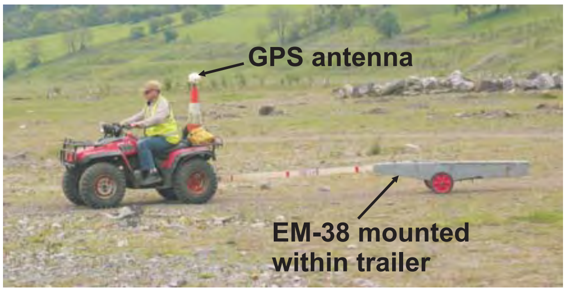

General principle of EM surveying

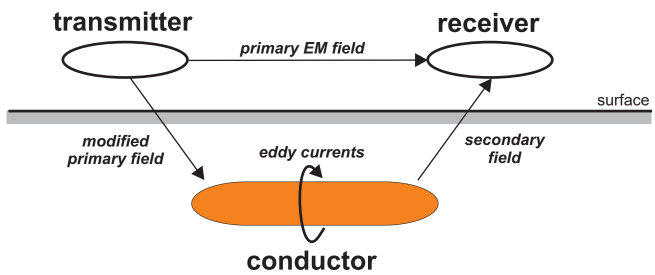

Mounted EM-31 with dGPS

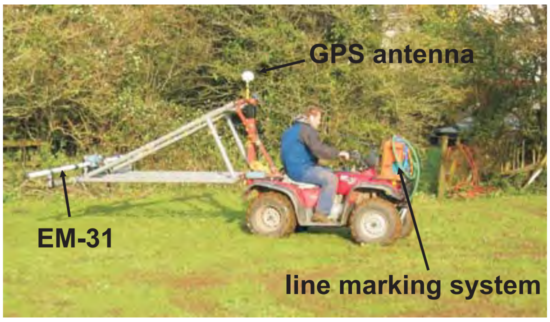

Ground conductivity data plot

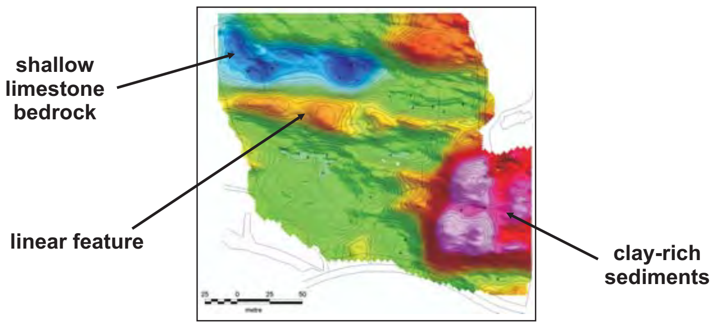

Constraints
Power lines, buildings, metal structures (fences, rebar, vehicles, debris etc.) and buried services can interfere with the electro-magnetic measurements.

Appendix - Resistivity Tomography

The Resistivity technique is a useful method for characterising the sub-surface materials in terms of their electrical properties. Variations in electrical resistivity (or conductivity) typically correlate with variations in lithology, water saturation, fluid conductivity, porosity and permeability, which may be used to map stratigraphic units, geological structure, sinkholes, fractures and groundwater.

The acquisition of resistivity data involves the injection of current into the ground via a pair of electrodes and then the resulting potential field is measured by a corresponding pair of potential electrodes. The field set-up requires the deployment of an array of regularly spaced electrodes, which are connected to a central control unit via multi-core cables. Resistivity data are then recorded via complex combinations of current and potential electrode pairs to build up a pseudo cross-section of apparent resistivity beneath the survey line. The depth of investigation depends on the electrode separation and geometry, with greater electrode separations yielding bulk resistivity measurements from greater depths.

The recorded data are transferred to a PC for processing. In order to derive a cross-sectional model of true ground resistivity, the measured data are subject to a finite-difference inversion process via RES2DINV (ver 5.1) software.

General resistivity principle

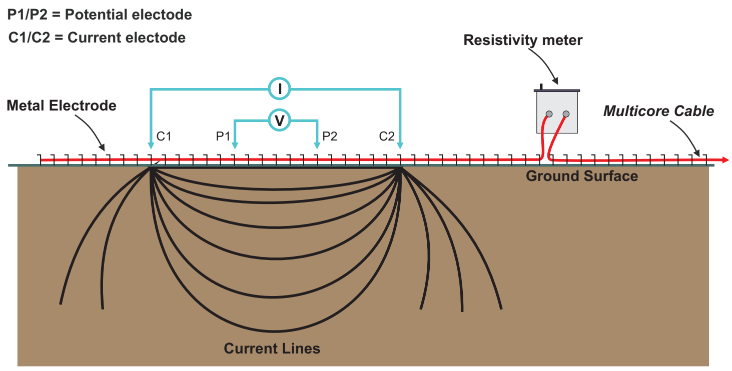

Typical field set-up

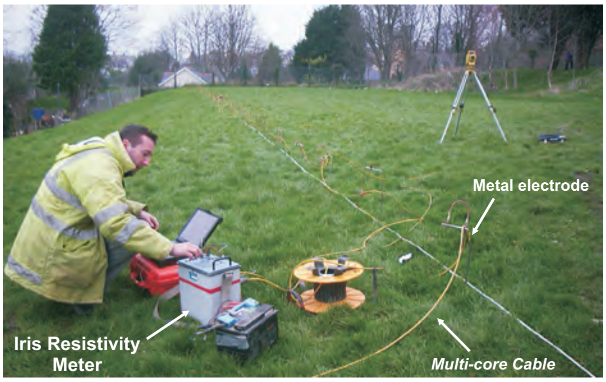

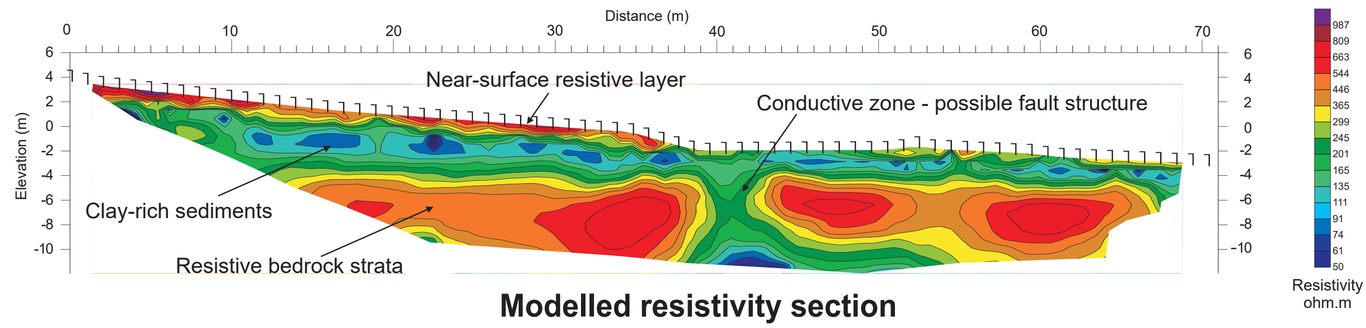

Modelled resistivity section

Data processing is based on an iterative routine involving determination of a two-dimensional (2D) simulated model of the subsurface, which is then compared to the observed data and revised. Convergence between theoretical and observed data is achieved by non-linear least squares optimisation. The extent to which the observed and calculated theoretical models agree is an indication of the validity of the true resistivity model (indicated by the final root-mean-squared (RMS) error).

The true resistivity models are presented as colour contour sections revealing spatial variation in subsurface resistivity. The 2D method of presenting resistivity data is limited where highly irregular or complex geological features are present and a 3D survey maybe required. Geological materials have characteristic resistivity values that enable identification of boundaries between distinct lithologies on resistivity cross-sections. At some sites, however, there are overlaps between the ranges of possible resistivity values for the targeted materials which therefore necessitates use of other geophysical surveys and/or drilling to confirm the nature of identified features.

Constraints:
Readings can be affected by poor electrical contact at the surface. An increased electrode array length is required to locate increased depths of interest therefore the site layout must permit long arrays. Resolution of target features decreases with increased depth of burial.

Appendix - Seismic Refraction Survey

Seismic refraction is a useful method for investigating geological structure and rock properties. The technique involves the observation of a seismic signal that has been refracted between layers of contrasting seismic velocity, i.e., at a geological boundary between a high velocity layer and an overlying lower velocity layer.

Shots are deployed at the surface and recordings made via a linear array of sensors (geophones or hydrophones). Refracted seismic signal travels laterally through the higher velocity layer (refractor) and generates a 'head-wave' that returns to surface. Beyond a certain distance away from the shot, the signal that has been refracted at depth is observed as first-arrival signal at the geophones. Observation of the travel-times of refracted signal from selectively deployed shots enables derivation of the depth profile of the refractor layer. Shots are typically fired at locations at and beyond both ends of the geophone spread and at regular intervals along its length.

The results of the seismic refraction survey are usually presented in the form of seismic velocity boundaries on interpreted cross-sections. Seismic sections represent the measured bulk properties of the subsurface and enable correlation between point source datasets (boreholes/trialpits) where underlying material is variable. Reference to the published seismic velocity tables enables derivation of rippability values.

Typical field set-up

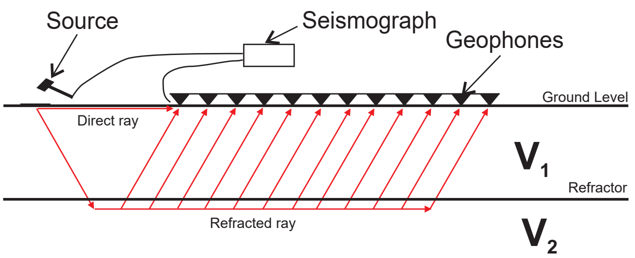

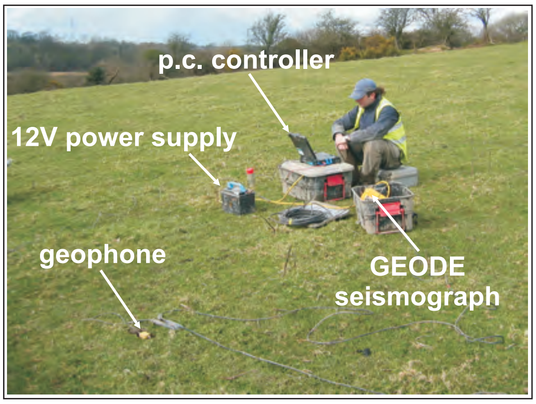

Travel-time curve

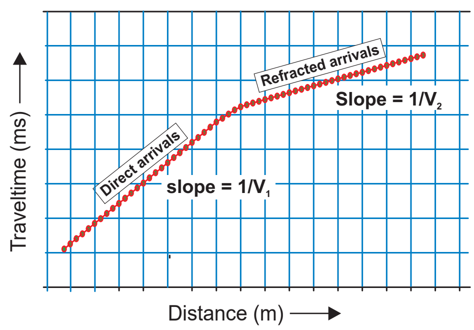

Modelled velocity section

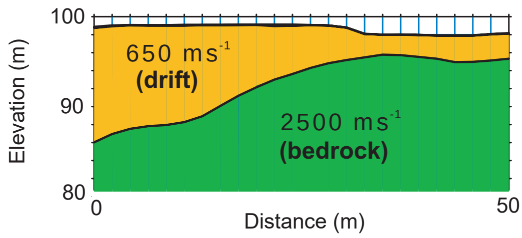

The data processing is carried out using PICKWIN & PLOTREFA (OYO ver2.2) software. The first stage involves accurate determination of the first-arrival times of the seismic signal (time from the hammer blow to each recording hydrophone) for every shot record, using PICKWIN. Time-distance graphs showing the first-arrival times were then generated for each seismic shot record and analysed using PLOTREFA software to determine the number of seismic velocity layers. Modelled depth profiles for the observed seismic velocity layers are produced by a tomographic inversion procedure that is revised iteratively to develop a best fit-model. The final output of a seismic refraction survey is a velocity model section of the subsurface based on an observed layer sequence with measured velocities that correspond to physical properties such as levels of compaction/ saturation in the case of sediments and strength/rippability in the case of bedrock.

Constraints

Layer velocity (density) must increase with depth; true in most instances. Layers must be of sufficient thickness to be detectable. Data collected directly over loose fill (landfills) or in the presence of excessive cultural noise may result in sub-standard results. In places where compact clay-rich tills and/or shallow water overly weak bedrock an S-wave survey may be used to profile rockhead where insufficient velocity contrast may prevent use of a P-wave survey.

Rippability Chart

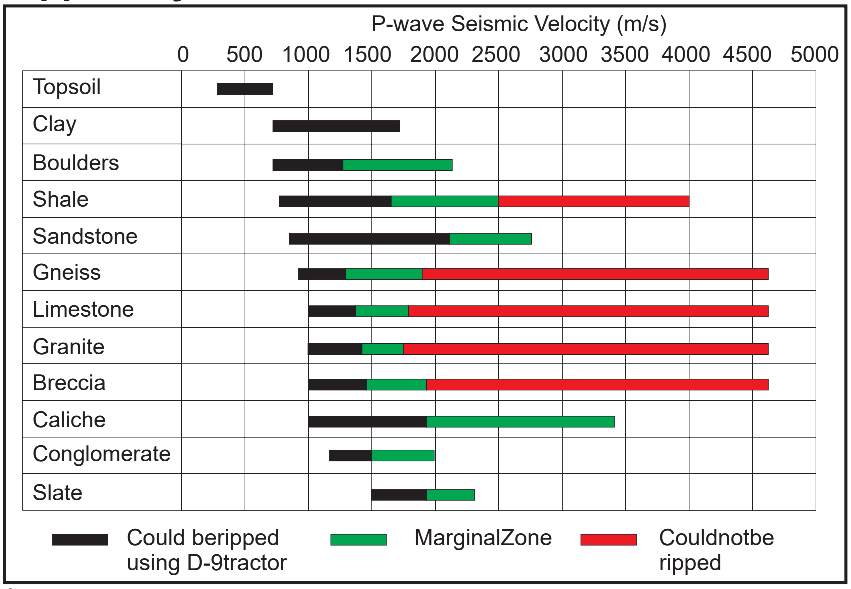

Ground preparation by ripping in open pit mining, Mining Magasine, 122, 458-469. Atkinson, 1970

Compressional P-wave velocity

Unconsolidated materials	***Vp (m/s)***
Sand (dry)	200 - 1000
Sand (water saturated)	1500 - 2000
Clay	1000 - 2500
Glacial till (water saturated)	1500 - 2500
Permafrost	3500 - 4000
Sedimentary rocks	
Sandstones	2000 - 6000
Tertiary sandstones	2000 - 2500
Pennant sandstone (Carboniferous)	4000 - 4500
Cambrian quartzite	5500 - 6000
Limestones	2000 - 6000
Cretaceous chalk	2000 - 2500
Jurassic limestones	3000 - 4000
Carboniferous limestones	5000 - 5500
Dolomites	2500 - 6500
Salt	4500 - 5000
Anhydrate	4500 - 6500
Gypsum	2000 - 3500
Igneous/Metamorphic rocks	
Granite	5500 - 6000
Gabbro	6500 - 7000
Ultramafic rocks	7500 - 8500
Serpentite	5500 - 6500
Other materials	
Steel	6100
Iron	5800
Aluminium	6600
Concrete	3600

An introduction to Geophysical Exploration 3rd Ed.
Kearey, Brooks & Hill: 2002

Diggability Chart

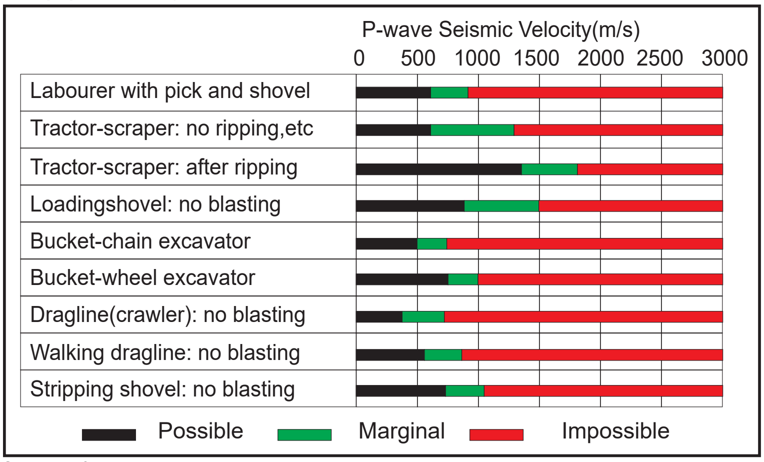

Selection of open pit excavation and loading equipment.
Transactions of the Institute of Mining and Metallurgy, 80, A101-A129, Atkinson 1971

Effect of ground water

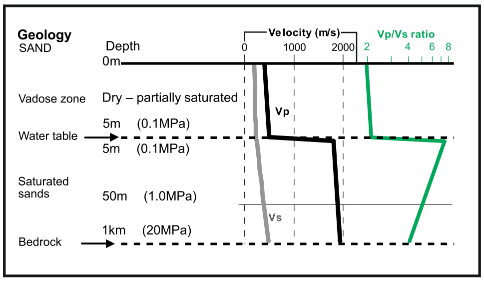

Prasad et al., Measurement of velocities and attenuation in shallow soils,
Near-Surface Geophysics Volume II Case Histories, SEG, Tulsa (2004)

Shear Waves

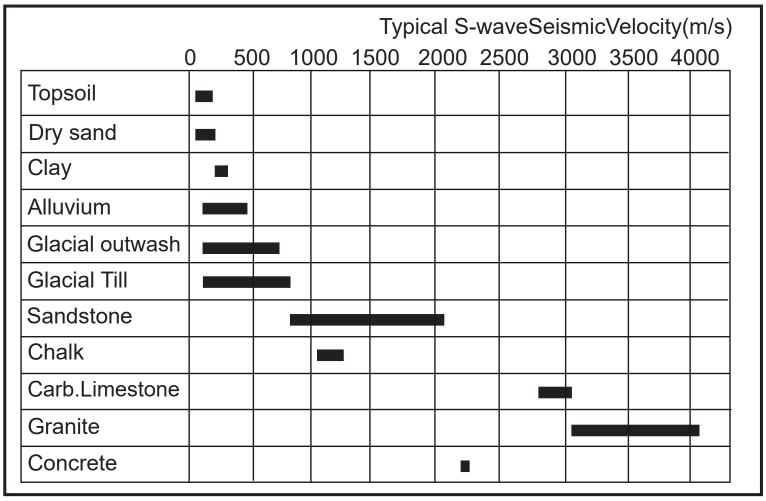

Rock / Soil Description (top 30m)	**S-wave velocity (m/s)**
Hard rock (*strong**)	> 1,500
Rock (*moderately strong**)	760 - 1,500
Very dense soil / soft (*weak**) rock	360 - 760
Stiff soil	180 - 360
Soft soil	<180

The NEHRP Recommended Provisions for seismic regulation for new buildings, (FEMA-222A and FEMA-223A, 1994)

** UK equivalent classification (Waltham, 1994)*

Applied Geophysics, Telford et al, 1990
Shear wave velocity determination of unlithified geologic materials (CUSEC region) Illinois State Geological Survey, Bauer, 2004.
Bauer et al., 2007, Illinois State Geological Survey.
Shear Wave Velocity, Geology and Geotechnical Data of Earth Materials in the Central U.S. Urban Hazard Mapping Areas.
An Introduction to Geophysical Exploration, 3rd Edition, Keary and Brooks, 2002.
Conceptual Overview of Rock and Fluid Factors that Impact Seismic Velocity and Impedance, Stanford Rock Physics Laboratory, n.d.

PUBLISHED SEISMIC VELOCITY TABLES

TERRA DAT
down to earth geophysics

GEOPHYSICAL SURVEY REPORT

Project

Bedrock mapping and sediment characterisation

Location

Zone 4, A417, Birdlip

Client

Geotechnical Engineering

Head Office
Unit 1
Link Trade Park
Penarth Road
Cardiff CF11 8TQ
United Kingdom

Telephone: +44 (0)2920 700127
www.terradat.co.uk

TERRA DAT
down to earth **geophysics**

Job Reference: 6688
Date: November 2020
Version: 1

GEOPHYSICAL SURVEY REPORT

Project

Bedrock mapping and sediment characterisation

Location

Zone 4, A417, Birdlip

Client

Geotechnical Engineering

Project Geophysicist:	M Bottomley BSc MSc	[redacted]
Reviewer:	S Hughes PhD BSc FGS	_ [redacted]
Job Reference:	6688	
Date:	November 2020	

CONTENTS

Figures

Appendices

1 EXECUTIVE SUMMARY

A geophysical survey was carried out as part of the ground investigation for proposed improvements to the A417 near the village of Birdlip, south of the existing road. The survey work was commissioned by Geotechnical Engineering (the Client). The fieldwork was carried out during October 2019 and undertaken within an area defined by the Client as 'Zone 4', comprising two targeted Electrical Resistivity Tomography (ERT) and seismic profiles, and an electromagnetic (EM) ground conductivity survey. The work was designed to complement the invasive and geotechnical investigation in providing detailed information on the geology and ground conditions adjacent to the existing A417, with particular concern regarding potential landslide/landslip zones.

The geophysical survey consisted of an integrated survey approach utilising electromagnetic ground conductivity measurements, two targeted ERT profiles and two seismic P and S-wave refraction and Multichannel Analysis of Surface Waves (MASW) profiles along all resistivity lines.

The results have been provided as a series of interpreted, colour-contoured plots (ground conductivity) and scaled sections (resistivity and seismic refraction), alongside a map showing the locations of the plots and profiles in relation to the underlying topographical features and bedrock geology as provided by Google Earth mapping and the British Geological Survey (BGS) Geology of Britain viewer.

2 INTRODUCTION

This report describes a geophysical survey that was carried out as part of the ground investigation for proposed improvements to the A417 near the village of Birdlip. The survey work was commissioned by Geotechnical Engineering (the Client). The fieldwork was carried out during October 2019 and undertaken within an area defined by the Client as 'Zone 4', comprising two targeted Electrical Resistivity Tomography (ERT) and seismic profiles, as well as an electromagnetic (EM) ground conductivity survey.

The work was designed to complement the invasive and geotechnical investigation in providing detailed information on the geology and ground conditions adjacent to the existing A417, with particular concern regarding potential landslide landslip zones.

2.1 Site description and history

Zone 4 (approx. centred on 394000E, 215150E) occupies an area of around 25 hectares, roughly 2 km east of the village of Birdlip. The survey area is located immediately north of the A417 and encompasses open fields and hedge systems, as well as a track which the profiles cross.

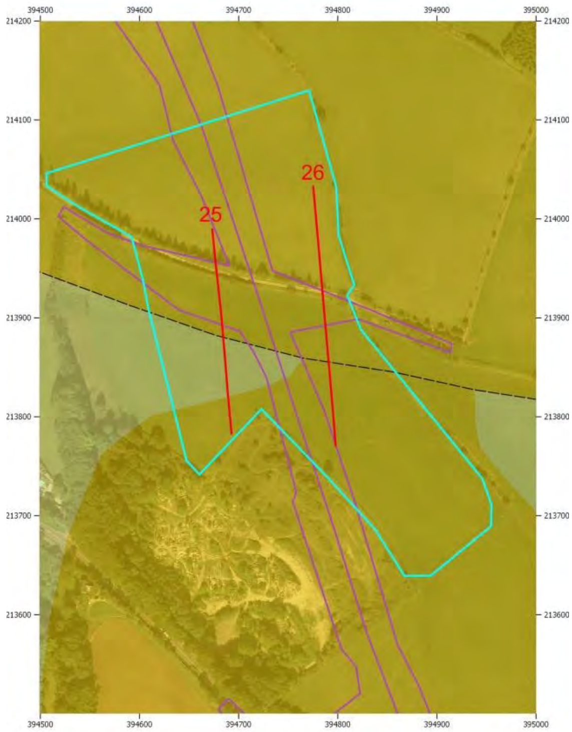

Plate 1. *Zone 4, showing the locations of the ERT and seismic profiles (red lines) and the extents of the EM ground conductivity survey (light blue).*

Topographically, the survey area is located on a broad ridge next to the disused Birdlip Quarry, and exhibits relatively minor variations in relief in the vicinity of the profiles, although the ground begins to quickly steepen to the west.

2.2 Geological setting

According to the British Geological Survey (BGS) Geoindex, the survey area is located on bedrock from the Great Oolite Group and the Fullers Earth Formation, and so limestones and mudstones are expected in the near-surface, likely underlain with limestones from the Salperton and Aston Formations. The survey area is also transected by one significant fault, oriented west to east, the expected location for which is shown on Plate 1 and Figure 32.

According to the BGS Geoindex, there are no superficial deposits in the vicinity of the site. All material overlying the bedrock is therefore believed to be bedrock erosion material from steep slopes and escarpments that has been transported by weather processes and landslide, down the valley side, and is referred to in this report as "overburden".

2.3 Survey objectives

The primary objectives of the survey were to provide detailed information on the shallow ground composition and deeper bedrock geology to assist with the ground investigation of the proposed road scheme. Of particular interest for engineering a new road cutting, is areas of shallow geology that may support further landslide movement of the overburden.

2.4 Survey design

Given the scope of the survey objectives, it was decided to adopt an integrated survey approach utilising the following geophysical methods:

- **Ground Conductivity**: to provide a ground conductivity map to characterise shallow overburden deposits and identify preferential water pathways such as gravel channels and clay-rich layers.

- **Resistivity Tomography**: to provide electrical cross-sections along selected survey profiles that allow identification of geological or hydrological boundaries.

- **P-wave Seismic Refraction**: to provide seismic velocity (V_p) model sections that indicate the thickness of overburden deposits and the depth to competent bedrock, in correlation with standard tables.

- **S-wave Seismic Refraction**: to provide seismic velocity (V_s) model sections that indicate the depth of uncompacted and compacted sediments, weathered rockhead and more competent (higher shear strength) bedrock.

- **MASW (Multichannel Analysis of Surface Waves)**: to derive shear velocity ('S-wave' or 'V_s') from rolling surface waves that are related to the stiffness of the ground material. This technique is also useful where velocity inversions in the ground layers may be encountered.

2.5 Quality control

The geophysical data sets were collected in line with normal operating procedures as outlined by the instrument manufacturer and TerraDat company policy. On completion of the survey, the data were downloaded from the survey instrument on to a computer and backed up appropriately. The acquired data set was initially checked for errors that may be caused by instrument noise, low batteries, positional discrepancies, etc. and any field notes are either written up or incorporated in the initial data processing stage. The data set is then processed using the standard processing routines and once completed; the resulting plots are subject to peer review to ensure the integrity of the interpretation. Our quality control standards are BS EN ISO 9001: 2015 certified.

3 SURVEY DESCRIPTION

The survey was carried out using the following geophysical methods:

- EM - Ground conductivity mapping
- Electrical Resistivity Tomography (ERT)
- P-wave seismic refraction (employs compressional waves)
- S-wave seismic refraction (employs shear waves)
- MASW (Multichannel Analysis of Surface Waves)

The extents of the EM survey, resistivity and seismic profiles are shown in Figure 32. Two Electrical Resistivity Tomography (ERT) and seismic refraction profiles were deployed, in locations as specified by the Client.

Background information for the survey methods is provided in the appendices, while a description of the actual survey work is provided in the sections below.

3.1 Survey limitations and assumptions

Seismic refraction requires that the velocity of the materials in the subsurface increases with the depth of burial. This is normally the case since (i) the degree of compaction within the overburden typically increases with depth, and (ii) bedrock condition improves with depth as weathering is reduced, both of which lead to higher seismic velocities. Therefore, one limitation of the refraction method is the inability to resolve localised weak zones within rock where it resides at a depth below the competent non-weathered rock. One of the objectives of the resistivity tomography survey is to target such weak/broken zones in the rock where fines/water have infiltrated and reduced the local ground resistivity. The survey output from both the P and S-wave refraction surveys are cross-sectional models that describe the bulk physical properties of the ground in terms of superficials, weathered rock and competent rock layers. There will be local variations in rock strength within the interpreted weathered rock layer, and the fracture density / broken character of the rock will vary over very short lateral distances. Measuring the seismic velocity of the bedrock over tens of metres along each survey line determines the bulk properties of the shallow rock mass and enables targeted ground-truthing of any identified anomalous ground.

3.2 Survey layout and topographic survey

The ground conductivity data were acquired under the positional control of an EGNOS dGPS system. Where possible, a Topcon Hyper Pro RTK dGPS system was used to mark resistivity (electrode) and seismic profile (geophones and offend shots) locations with a survey accuracy of +/- 2.5 cm. In some cases, positional accuracy was not adequate due to extensive tree cover, and so a Trimble robotic total station was employed using dGPS established reference stations. All measurements were recorded in Ordnance Survey National Grid coordinates.

3.3 Ground conductivity mapping

An electromagnetic ground conductivity survey involves the transmission of an electromagnetic field into the subsurface and then recording the returning signal via a receiver in the same instrument. Data are acquired on a grid covering the area of interest, and a contoured plan of the variation in ground conductivity response across the site is produced. The presence of conductive materials in the subsurface such as clay, water, mudstone, ash, metal, rebar, leachate, etc. will be evident as regions of high values on the ground conductivity plan. Materials such as coarse-grained sediments, dry zones, and many bedrock types will appear as regions of low values.

3.3.1 *Electromagnetic survey - field activity*

The conductivity data were acquired using a multi-frequency *Geophex GEM-2* instrument (Plate 2), and data were acquired under the control of an EGNOS corrected dGPS (accuracy +/- 0.5m) at a nominal 0.25 m interval along a series of parallel 5 m spaced survey lines. The instrument was primarily configured to investigate depths of up to 3 to 5 m below ground level. The sensor was mounted on a cart and pulled behind an ATV.

Plate 2. *Ground conductivity data collection method. Geophex GEM-2 instrument mounted on a bespoke cart which was pulled across the site using an ATV, under the control of a GPS system (Library photo).*

3.3.2 Electromagnetic survey – data processing

The conductivity data were downloaded from the data logger and compiled using dedicated software *WINGEM-3*. Initial editing was then carried out to remove positional errors and rogue values. The data were then exported as an 'XYZ' file and translated into the OSGB36 Coordinate system using the OSTN02 transformation. The software program *OASIS MONTAJ* was used to compile, edit and manipulate the data to enhance any features of interest. The colour contour plots were then integrated with the base plan information and the resulting plans exported to *CORELDRAW* for final annotation.

3.4 Electrical Resistivity Tomography (ERT)

An ERT survey involves the injection of DC electrical current into the ground at various electrode locations along a profile line. An electrical cross-section of the subsurface is then derived from the recorded data. A diverse range of features such as clay-rich sediments, fracture zones, infilled solution features, bedrock structure and mineralisation can be imaged in cross-section using a resistivity survey. A feature may be targeted using resistivity tomography given sufficient electrical contrast with its surroundings. A description of the field activity is provided below, and some background information on the survey method is found in the Appendix.

3.4.1 ERT survey field activity

A 72-channel *IRIS Syscal* resistivity system (Plate 3) was used to acquire two profiles across the survey area, as shown in Figure 32. The ERT profiles were acquired with an electrode spacing of 3 m using a standard Wenner-Schlumberger array. For both profiles, 'roll-ons' were required to cover the required area of interest. A 'roll-on' simply involves adding one or two cables to the end of the initial 72-channel setup and then selecting the appropriate protocol file from the IRIS resistivity meter to continue data acquisition from the initial setup and into the new cables. A summary of the ERT profiles is given in Table 1.

ERT Profile No.	Fig.	Start (OSGB)		End (OSGB)		Length (m)	Electrode Spacing (m)	~ Depth of penetration (m)
		Easting	Northing	Easting	Northing			
Line 25	34	394673.0	213990.2	394693.1	213779.0	213	3	30
Line 26	35	394775.1	214033.5	394798.1	213768.1	267	3	30

Table 1. *ERT profile summary.*

3.4.2 *ERT survey data processing*

The data were processed using *Res2DInv* software to derive modelled electrical cross-sections of the subsurface. Elevation data were added to the models, using electrode positions surveyed using a TOPCON network RTK GPS. All topographic data were transformed into National Grid (OSGB36) using the OSTN02b transformation; elevations are given in m AOD. The ERT data was then exported into *Surfer 7* where it was gridded and presented as a 2D cross-sections of resistivity. These cross-sections were then exported to *CorelDraw* for final annotation. All resistivity profiles are presented on the same colour scale and are not vertically exaggerated.

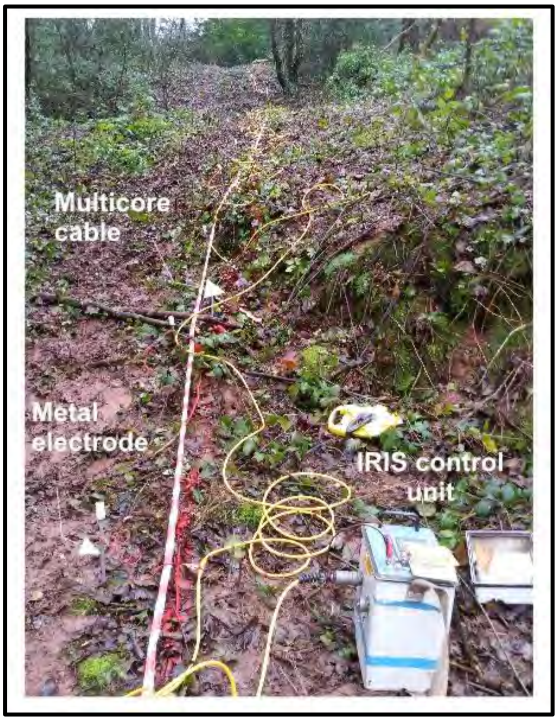

Plate 3. *Resistivity Tomography data collection. A 72 channel IRIS Syscal ERT system used to acquire eleven profiles across the site (Library photo).*

3.5 Seismic survey – P and S-wave refraction

A seismic survey involves generating a shock wave signal at the surface to investigate the geological structure beneath a chosen profile line. A series of vibration sensors (geophones, or hydrophones in water) are deployed along the line and are used to record the travel times of incident seismic signal as it returns from below ground. Features such as rockhead, the water table, made ground, soft sediments and dense tills all have distinct velocity ranges and can be imaged in cross-section using a seismic refraction survey. A description of the field activity is provided below, and some further background information on the survey method is found in the appendices.

3.5.1 Seismic survey field activity: P-wave refraction

P-wave seismic refraction data were acquired along two profile lines using a high precision 72 channel *GEODE* (Plate 4a) seismic system. To target the broad depth range, low frequency (4Hz) geophones were deployed at 2 m intervals providing individual geophone spread lengths of 142 m. For both profiles, several setups were required to achieve full line coverage. The seismic wave was generated by a combination of sledgehammer striking a nylon plate and Seismic Impulse Device (SID) firing 12- and 8-gauge black powder cartridges (Plate 4b). To build up the refraction data set, seismic shots were taken at several positions along the geophone spread (usually every 6-12 geophones) and set distances beyond the geophone spread. For this particular survey, the 'offend' shots were limited by site constraints, but the maximum distance was 100 m. A summary of the seismic profiles is given in Table 2.

Plate 4. *a) Field setup and b) Seismic Impulse Source deployment (Library photo).*

Seismic Profile No.	Fig.	Start (OSGB)		End (OSGB)		Length (m)	Geophone Spacing (m)	~ Depth of penetration (m)
		Easting	Northing	Easting	Northing			
Line 25	34	394693.0	213782.0	394673.0	213988.5	208	2	25
Line 26	35	394793.0	213827.1	394776.1	214019.7	192	2	25

Table 2. *Seismic Profile summary.*

3.5.2 Seismic survey field activity: S-wave refraction (Shear)

S-wave seismic refraction data were also acquired using a 72 channel *GEODE* seismic system. Horizontally mounted geophones were deployed at 2 m intervals producing individual geophone spread lengths of up to 142 m. For both profiles, several setups were required to achieve full line coverage. A weighted S-wave plate struck sideways with a sledgehammer was used as the energy source (Plate 5). At each shot location, the shot plate was aligned perpendicular to the profile line and subsequently struck on both ends to generate two sets of shear wave recordings that have opposite polarity. To build up the refraction data set, seismic shots were taken at several positions along the geophone spread (usually every 6-12 geophones) and set distances beyond the geophone spread.

Plate 5. *S-wave source plate being struck (Library photo).*

3.5.3 Seismic survey data processing: P and S-wave refraction

The data processing was carried out using *PICKWIN* and *PLOTREFA* software. The first stage involved the accurate determination of the first-arrival times of the seismic signal (time from the shot going off to each recording geophone) for every shot record using *PICKWIN*. Time-distance graphs showing the first-arrival times were then generated for each seismic line and analysed using *PLOTREFA* software to determine the number of seismic velocities layers. Modelled depth profiles for the observed seismic velocity layers were produced by a tomographic inversion procedure that was revised iteratively to develop a best-fit model.

The final output of a seismic refraction survey is a velocity model section of the subsurface based on an observed layer sequence. The measured velocities correspond to physical properties such as levels of compaction/saturation in the case of sediments and strength/rippability in the case of bedrock. A transitional velocity model will be considered if distinct layers are not expected, or velocity contrasts between layers are marginal. However, a layered model appears most appropriate to this site. The final sections were exported to *CORELDRAW* for annotation and presentation.

3.6 Seismic survey – MASW

Multichannel Analysis of Surface Waves (MASW) employs 'rolling' surface waves to derive shear velocity. This is achieved through analysis of the dispersion that occurs as surface wave energy propagates through the subsurface and separates into different frequencies travelling at different velocities depending on the stiffness of the sediments and/or rock encountered.

This technique utilises Rayleigh-type surface waves (normally considered noise in seismic refraction/reflection surveys and called "ground roll") recorded by multiple geophones deployed on an even spacing and connected to a common recording device (seismograph), as shown in Plate 6.

As the dispersion of the seismic wave can be dependent on the geology and ground conditions (i.e. variability, terrain, etc.), MASW profiles are usually limited to relatively flat areas or where the ground more homogenous.

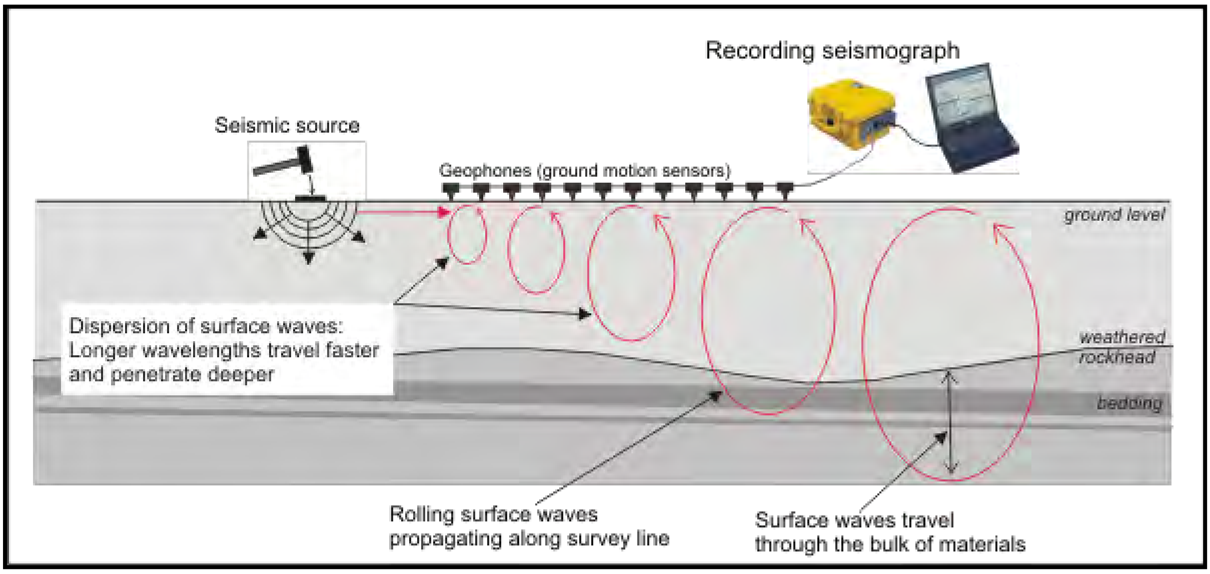

Plate 6. *MASW survey setup.*

3.6.1 Seismic survey field activity: MASW

For this particular survey, the setup is very similar to the refraction setup; however, instead of a discreet number of shot points, shots were acquired at every other geophone position along the profile. In this case, low frequency (4Hz) geophones were set at 2 m intervals, and the data were acquired using the sledgehammer as the source. A one-second record length was used to fully capture the frequency dispersion.

3.6.2 Seismic survey data processing - MASW

Analysis of surface waves recorded on multichannel shot records was carried out using SurfSeis software, which considers the dispersion properties of all types of waves (both body and surface waves) through a wave field transformation method. This directly converts the multichannel record into an image, where a dispersion pattern is recognised, and the necessary dispersion properties are extracted. These dispersion properties are used to generate modal dispersion curves that are subsequently inverted and used to produce the resultant shear-wave velocity (Vs) profile. The final velocity sections are created in SURFER then exported to CorelDraw for annotation and presentation.

4 RESULTS AND DISCUSSION

The results of the geophysical surveys are presented as a series of interpreted colour contour plots and scaled sections in Figures 33 to 35. A general description of the interpretation process is given below, followed by a summary of the findings in Sections 4.5 and 4.6.

4.1 Ground Conductivity

The results are presented as a colour contoured plot of ground conductivity (Figure 33). Following a review of the electromagnetic data; it was decided only to consider the response of the 47,925 MHz frequency channel. A relative increase in conductivity values usually indicates a comparative increase in the clay/ash/water content, which could signify either a lateral change in lithology or a variation in bedrock depth. Extreme fluctuations in conductivity/in-phase values are usually indicative of instrument 'overload' due to high metal content. The interpretation of the conductivity data is based on both published electrical properties of typical sedimentary materials (Plate 7) and when available, correlation with on-site information.

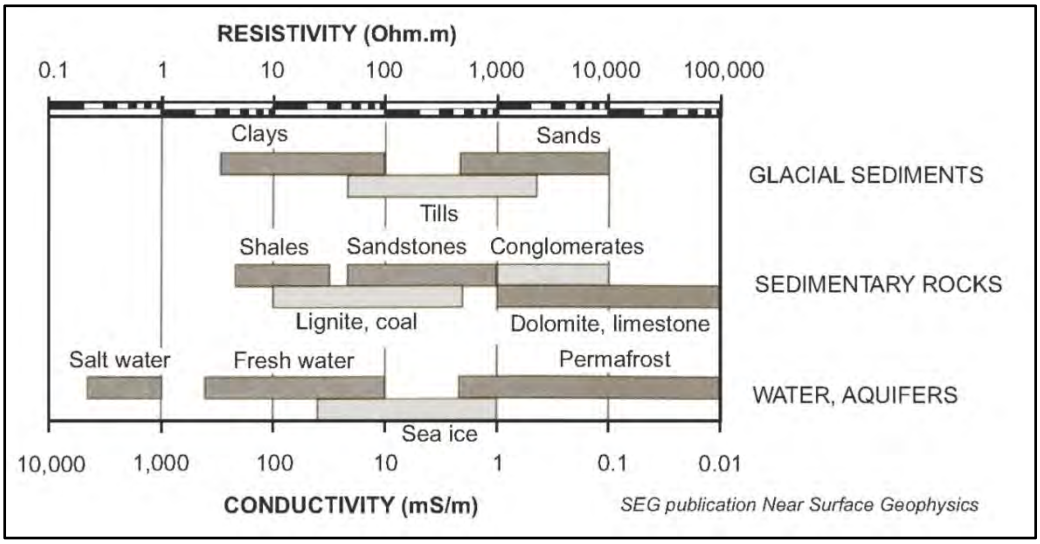

Plate 7. *Conductivity and resistivity values of common materials.*

4.2 Resistivity tomography

The results of the resistivity survey are presented as colour contoured scaled sections of the subsurface showing changes in resistivity, with blue colours representing low values, and red colours representing relatively high resistivity values. The vertical and horizontal axes display elevation and chainage along the profile line, respectively. The interpretation of the modelled resistivity sections is based on both published electrical properties of typical sub-surface materials (Plate 7) and when available, correlation with on-site information or observations. In principle, an increase in resistivity values usually indicates a relative decrease in the clay content or groundwater saturation. However, due to the non-uniqueness of the electrical properties (i.e. different material exhibiting same resistivity values), the final interpretation may be limited and may require addition calibration (i.e. drilling or other supplementary geophysical techniques).

The results of the ERT survey are discussed in the summary discussions, in conjunction with the results of the seismic survey. To assist with the interpretation, the resistivity sections have been overlain with the interpreted seismic velocity boundaries where acquired.

4.3 Seismic Refraction – compressional (P) and shear (S) wave

Interpretation of the refraction sections is based on the widely understood and published velocities of typical sub-surface materials (provided in the appendices). It is beneficial to correlate model sections with on-site information/observations, but at the time of reporting, only limited borehole information was available.

4.3.1 Compressional (P) wave

Analysis of the P-wave refraction data has identified up to five distinct layers of contrasting velocity (V_p), and a typical description of each layer is given below and summarised in Table 3. It is worth noting that the seismic refraction section represents the measured bulk characteristics of the subsurface and in certain cases, it can prove difficult to correlate with point source data (boreholes/trial pits) where the underlying material is variable.

Layer	P-wave velocity	Sediment/Rock Description
P1 (pink)	< 300 m/s (low)	Thin, dry loose surface soils and sediments
P2 (orange)	301 – 800 m/s (low to medium velocity)	Unconsolidated, dry overburden material
P3 (light green)	801 - 1400 m/s (medium velocity)	Compacted, dry overburden material
P4 (green)	1401 - 1900 m/s (medium to high velocity)	Compacted, saturated overburden material or highly weathered bedrock
P5 (dark green)	> 1901 m/s (high velocity)	Weathered to unweathered bedrock

Table 3. *A guide to the composition of the P-wave velocity layers identified.*

Layers P1 has a low velocity that relates to loose, surface soil and uncompacted sands and gravels. Layers P2 and P3 typically reflect a relative increase in consolidation or compaction of the still dry overburden material. Layer P4 can be more difficult to interpret as the overlap in velocities means that it can represent both overburden material (potentially wet, compact material) and weathered/weak/fractured bedrock. The most effective way to differentiate between sediment and rock type material is to consider the corresponding S-wave velocity, as discussed below. Layer P5 represents the highest (and deepest) velocity unit and is likely to reflect a more competent boundary within the bedrock strata.

4.3.2 Shear (S) wave

By carrying out an analysis of the S-wave refraction data, four distinct layers of contrasting velocity (V_s) have been identified and summarised in Table 4. They are characterised by their correlation with standard tables (see appendices).

In general, the shear-wave velocity (V_s) is much more sensitive than the P-wave velocity (V_p), where the ground becomes abruptly stiffer due to increases in rock strength. For this reason, it is possible to use the V_s to distinguish between sediments and ‘rock’ (i.e. cemented) material, which is particularly useful for grading the P-wave layer P4. A further advantage of shear waves is that they are unaffected by the groundwater table.

Layer	S-wave velocity	Sediment/Rock Description
S1	<180 m/s	Soft soils and loose sediments
S2	180 - 360 m/s	Stiff soils/overburden
S3	361 - 760 m/s	Very stiff, compacted overburden or highly weathered bedrock
S4	>761 m/s	Rock

Table 4. *A guide to the composition of the S-wave velocity layers identified.*

When comparing the resulting P-wave and S-wave velocity sections, there is a rough 'rule of thumb' with regards to the ratio of the velocities. For unconsolidated sediment, V_p/V_s is usually between 4.0 to 8.0, while for consolidated rocks, the V_p/V_s ratio can vary between 1.5 to 2.0. Even though these are accepted values, they can vary between sites depending on the geology and ground conditions.

When correlating between the respective P-wave and S-wave refraction boundaries, in some instances there can be discrepancies in observed depth values. This depends on the prevailing geology and can reflect different survey parameters (horizontal/vertical polarised S-waves, spacing, etc.), weathering profile (vertical and horizontal), lithology or bedding structure. It has been noted on some sites that the S-wave refractor appears to correlate with internal bedding units as opposed to the general rock mass.

4.4 MASW

The results of the MASW survey are presented as colour contoured S-wave velocity panels showing changes in velocity (i.e. ground stiffness) below the surface. The seismic signal frequency dispersion required for the MASW technique has yielded reliable results to a depth of up to approximately 20 m bgl. The persistent traffic noise from the A417 and the limited power of a sledgehammer energy source meant lower frequency dispersions (giving an increased depth of investigation) suffered from a high signal to noise ratio and were not suitable for modelling. The MASW sections have been colour scaled from white to red, with red representing the highest velocity modelled.

4.5 Summary Discussion – Ground Conductivity

Features or anomalies of interest have been listed and discussed in Table 5 below.

Zone	Feature	Description
4	F12	Homogenous, resistive area, indicating a decrease of clay and/or water within the overburden, possibly associated with a change of lithology or shallowing of the bedrock.
	F13	Interpreted fault location, although this is marked as being further south. Extremely sharp conductive/resistive boundary marks the transition between more resistive material to the north (e.g. shallow limestone bedrock) and more conductive material to the south (e.g. clay-rich sediments).
	F14	Homogenous, conductive area, indicating an increase of clay and/or water within the overburden, possibly associated with a change of lithology or deepening of the bedrock.
	F15	Banded, resistive features are probably indicative of dipping limestones of the Great Oolite Group (interbedded with more conductive mudstone). They correlate very well with similar features observed along both Profiles 25 and 26.

Table 5. *Features and anomalies of interest as identified by the ground conductivity survey.*

4.6 Summary Discussion – ERT and Seismic Refraction

Features or anomalies of interest have been listed and discussed in Table 6 below.

Profile	Feature	Description
25	F25a	This resistive layer indicates a decrease of clay and/or water within the near-surface sediments (silt or gravel of completely weathered limestone).
	F25b	Abrupt, vertical conductive/resistive boundary is likely to indicate the location of a fault, with limestone from the Great Oolite Group to the north, and dipping mudstone from the Fuller's Earth Formation to the south. The marked fault location is approximately 60 m to the south.
	F25c	There is very good correlation between Layers S4/P5 and the top of the

		interpreted mudstone bedrock. A Layer S4 velocity of 1276m/s indicates the presence of hard, competent rock condition. As with other nearby profiles, the mudstone is of a more conductive nature than the limestone.
	F25d	Broader zone of increased conductivity to the south of the fault indicates an increase of water/clay within the superficial deposits or change in sediment lithology. Corresponding ‘soft’ zones on the MASW section and an increase in Layer S1/S2 thickness also indicates less stiff and possibly more unconsolidated sediments than to the north of the fault.
	F25e	Dipping resistive feature possibly represents a bed of more resistive limestone from the Great Oolite Group.
	F25f	Abrupt boundary between very stiff sediments and much softer material correlates with the interpreted fault location.
	F25g	Deepening of the Layer P5 boundary to the north correlates with the interpreted position of the fault, and may be attributed to the fault, or a variation in lithology or weathering, although in contrast Layer S4, which represents hard competent bedrock appears to be shallowing (Layer P5 could possibly represent a mudstone lithology deepening under the limestone).
	F25h	Deepening of both the Layer S4/P5 boundaries to the south, although this is more pronounced for Layer P5 suggesting a ‘step’ in the bedrock.
26	F26a	This resistive layer indicates a decrease of clay and/or water within the near-surface sediments (silt or gravel of completely weathered limestone).
	F26b	Broader zone of increased conductivity to the south of the fault indicates an increase of water/clay within the superficial deposits or change in sediment lithology. Corresponding ‘soft’ zones on the MASW section and an increase in Layer S1/S2 thickness also indicates less stiff and possibly more unconsolidated sediments than to the north of the fault.
	F26c	Abrupt, vertical conductive/resistive boundary is likely to indicate the location of a fault, with limestone from the Great Oolite Group to the north, and dipping mudstone from the Fuller’s Earth Formation to the south (although Great Oolite Group limestone is shown on the BGS geological mapping). The marked fault location is approximately 70 m to the south.
	F26d	There is very good correlation between Layers S4/P5 and the top of the

		mudstone bedrock. A Layer S4 velocity of 1024 m/s indicates the presence of hard, competent rock condition, although the velocity is lower than observed along Profile 25. As with other nearby profiles, the mudstone is of a more conductive nature than the limestone.
	F26e	Dipping resistive feature possibly represents a bed of more resistive limestone from the Great Oolite Group at, or close to, surface.
	F26f	Abrupt boundary between very stiff sediments and much softer material correlates with the interpreted fault location. The highly variable velocity structure suggests a highly variable rock condition with soft and hard, fractured zones.
	F26g	Very good correlation between Layer P5/S4 bedrock boundaries, with Layer P5 indicating an increase in velocity to the south up to 2713m/s, and possible transition into another bedrock lithology or increase in bedrock condition.

Table 6. *Features and anomalies of interest as identified by the seismic refraction and MASW surveys.*

5 CONCLUSIONS

- The geophysical surveys have provided a non-invasive means for investigating the subsurface with a high degree of 'spatial' coverage using the electromagnetic survey technique, and detailed profile cross-sections of ground composition using resistivity tomography, seismic refraction and MASW.

- The ground conductivity plots have revealed variations in near-surface sediment composition (notably clay content and saturation) and thickness, as well as mapping shallow bedrock. A number of services have also been shown to cross the surveyed areas, as highlighted.

- The modelled resistivity sections were characterised by zones of contrasting resistivity values that reflect lithological (including an increase/decrease in clay content), hydrogeological (e.g. groundwater level, saturated zones), structural (e.g. faults, steeply dipping beds) and weathering variations within the sub-surface.

- The analysis of both the P and S-wave refraction data has identified distinct velocity layers that have provided detailed information to assist with the bulk characterisation of the shallow subsurface and, in particular, the thickness of overburden sediments and depth to weathered and unweathered bedrock. In summary, five distinct layer boundaries have been identified by the P-wave refraction survey, with velocities ranging from <300 m/s (weak, loose sediments) to >1901 m/s (weathered to unweathered bedrock). This has been further characterised by the S-wave refraction survey, which has revealed up to four notable layers of increasing material stiffness from <180 m/s (weak, loose sediments) to >761 m/s (rock). Where layer velocities vary laterally, this may be due to structural changes such as faulting or steeply dipping bedding. Finally, zones of increased rock stiffness and/or deterioration in bedrock condition have been further highlighted by the results of the MASW survey.

- Available borehole data has been included on the cross-sections for direct correlation, and if any additional borehole data becomes available, it may be possible to extend further/refine the interpretation and calibrate the acquired datasets.

Disclaimer

This report represents an opinionated interpretation of the geophysical data. It is intended for guidance with follow-up invasive investigation. Features that do not produce measurable geophysical anomalies or are hidden by other features may remain undetected. Geophysical surveys complement invasive/destructive methods and provide a tool for investigating the subsurface; they do not produce data that can be taken to represent all of the ground conditions found within the surveyed area. Areas that have not been surveyed due to obstructed access or any other reason are excluded from the interpretation.

FIGURES

KEY

- Resistivity/Seismic Profile
- EM 'ground conductivity' survey extents
- Proposed road scheme

See individual line figures for start and end coordinates and profile orientation

KEY TO BGS GEOLOGY MAP

(Taken from the British Geological Survey Geology of Britain viewer, bedrock geology only)

- Lias
- Birdlip Limestone Formation
- Aston Limestone Formation
- Salperton Limestone Formation
- Fullers Earth Formation
- Hampen Formation
- White Limestone Formation
- Great Oolite Group
- Fault (expected location)

Source: Map data ©2020 Google.

Title:
OVERALL LOCATION PLAN (ZONES 1 TO 4)

Project:
A417 CRICKLEY HILL BIRDLIP

TERRADAT down to earth geophysics

Tel: +44 (0) 2920 700127
Web:www.terradat.co.uk
Email: web@terradat.co.uk

Scale:	1:15000 at A3
Drawn by/Ref:	MB/6688/1
Date:	23 JULY 2020

FIGURE 31

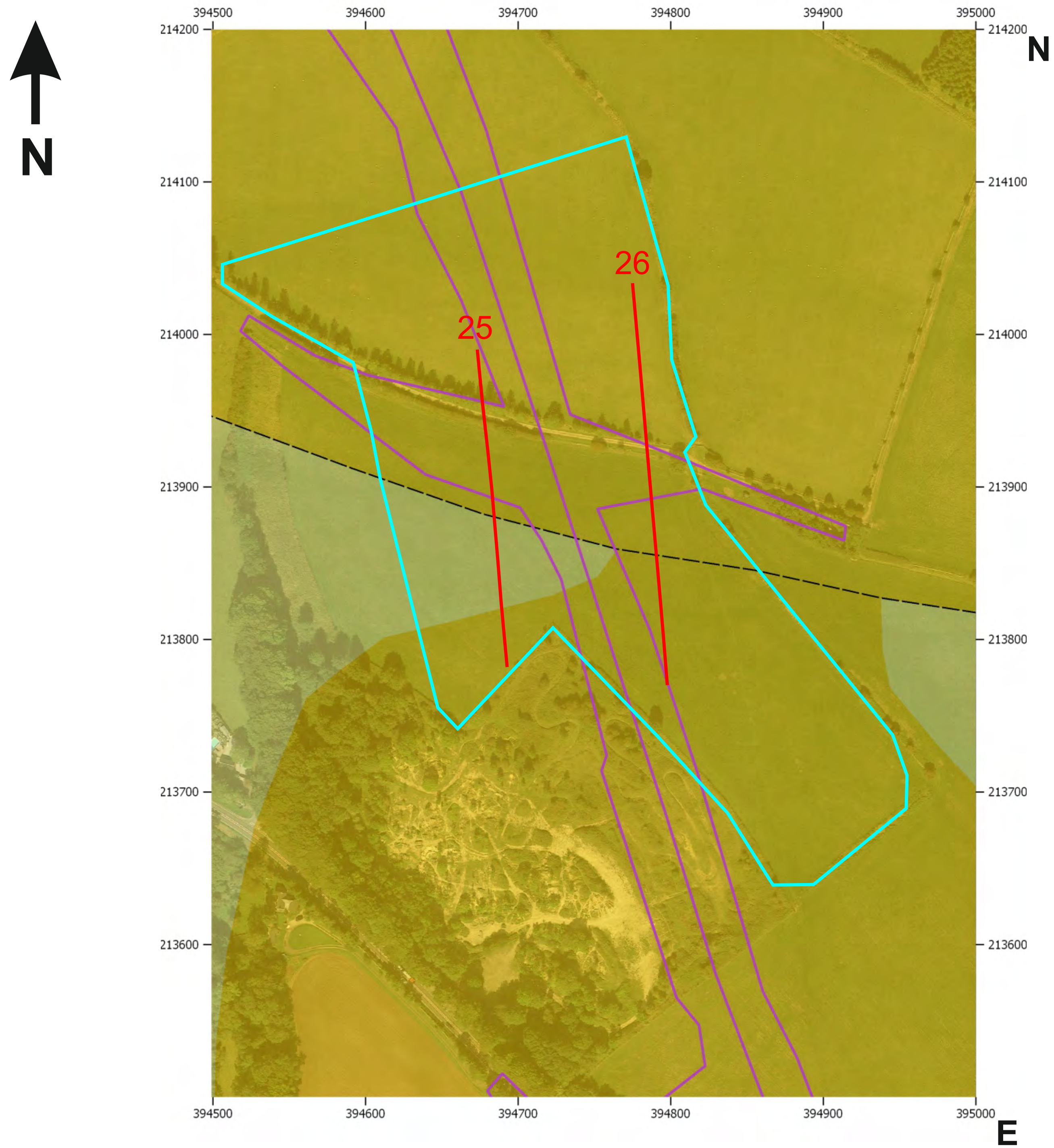

KEY
- Resistivity/Seismic Profile
- EM Survey Extents
- Proposed road scheme
- Borehole/Trial Pit

KEY TO BGS GEOLOGY MAP
(Taken from the British Geological Survey Geology of Britain viewer, bedrock geology only)

- Lias
- Birdlip Limestone Formation
- Aston Limestone Formation
- Salperton Limestone Formation
- Fullers Earth Formation
- Hampen Formation
- White Limestone Formation
- Great Oolite Group
- Fault (expected location)

NOTES
1. See individual line figures for start and end coordinates and profile orientation

Source: Map data ©2020 Google.

Project: **BIRDLIP**

Title: **LOCATION MAP (ZONE 4)**

TERRA DAT down to earth geophysics

Tel: +44 (0) 2920 700127
Web:www.terradat.co.uk
Email: web@terradat.co.uk

Scale: 1:4000 at A4
Drawn by/Ref: MB/6688/32
Date: 09 JULY 2020

FIGURE 32

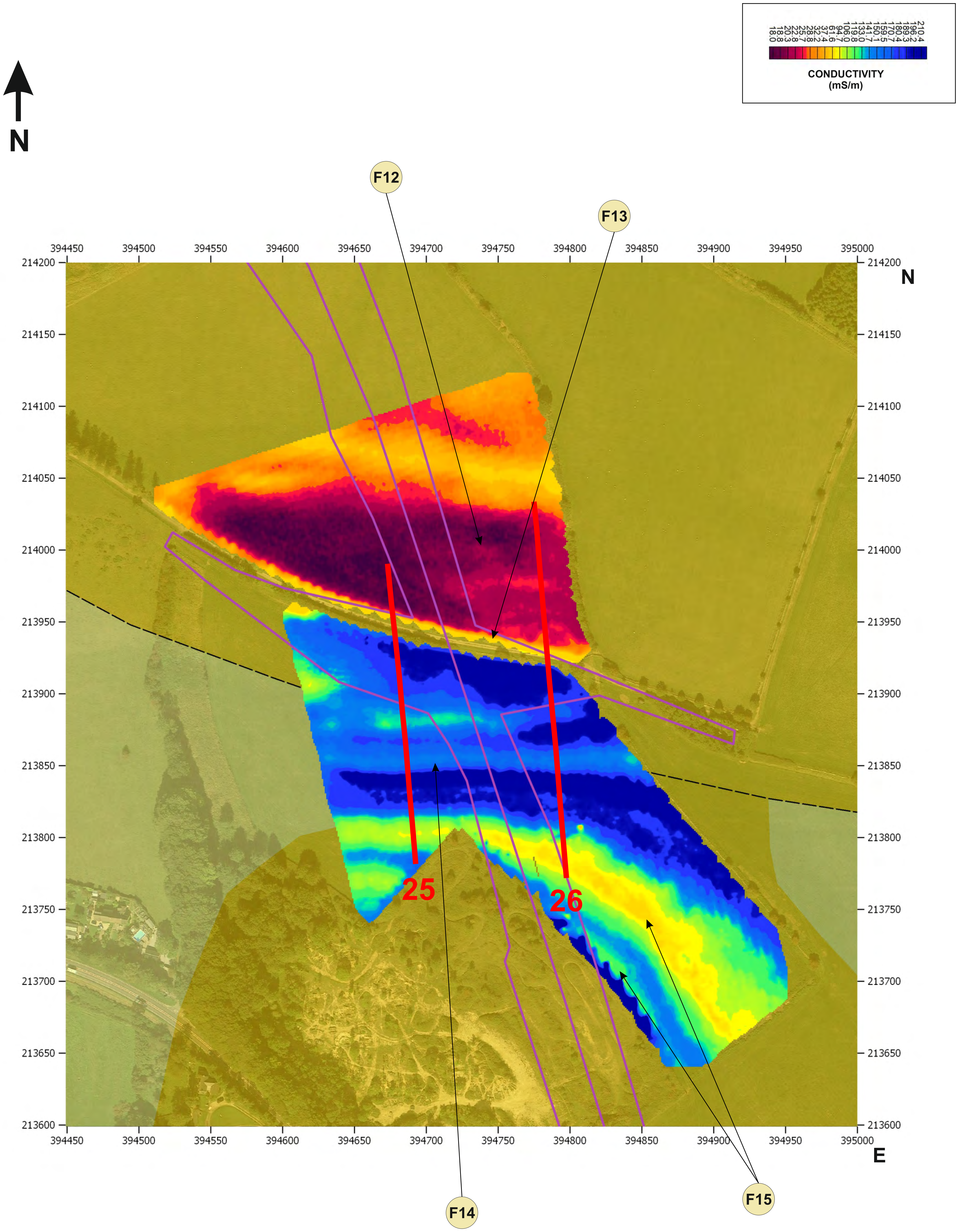

NOTES

1. See individual line figures for start and end coordinates

KEY TO BGS GEOLOGY MAP

(Taken from the British Geological Survey Geology of Britain viewer, bedrock geology)

- Lias
- Birdlip Limestone Formation
- Aston Limestone Formation
- Salperton Limestone Formation
- Fullers Earth Formation
- Hampen Formation
- White Limestone Formation
- Great Oolite Group
- Fault (expected location)

KEY

- Resistivity profile
- Proposed road scheme
- Borehole

Title: **GROUND CONDUCTIVITY (ZONE 4)**

Project: **A417 CRICKLEY HILL BIRDLIP**

TERRADAT
down to earth geophysics

Tel: +44 (0) 2920 700127
Web:www.terradat.co.uk
Email: web@terradat.co.uk

Scale: 1:2500 @ A3
Drawn by/Ref: MB/6688/33
Date: 14 JULY 2020

FIGURE 33

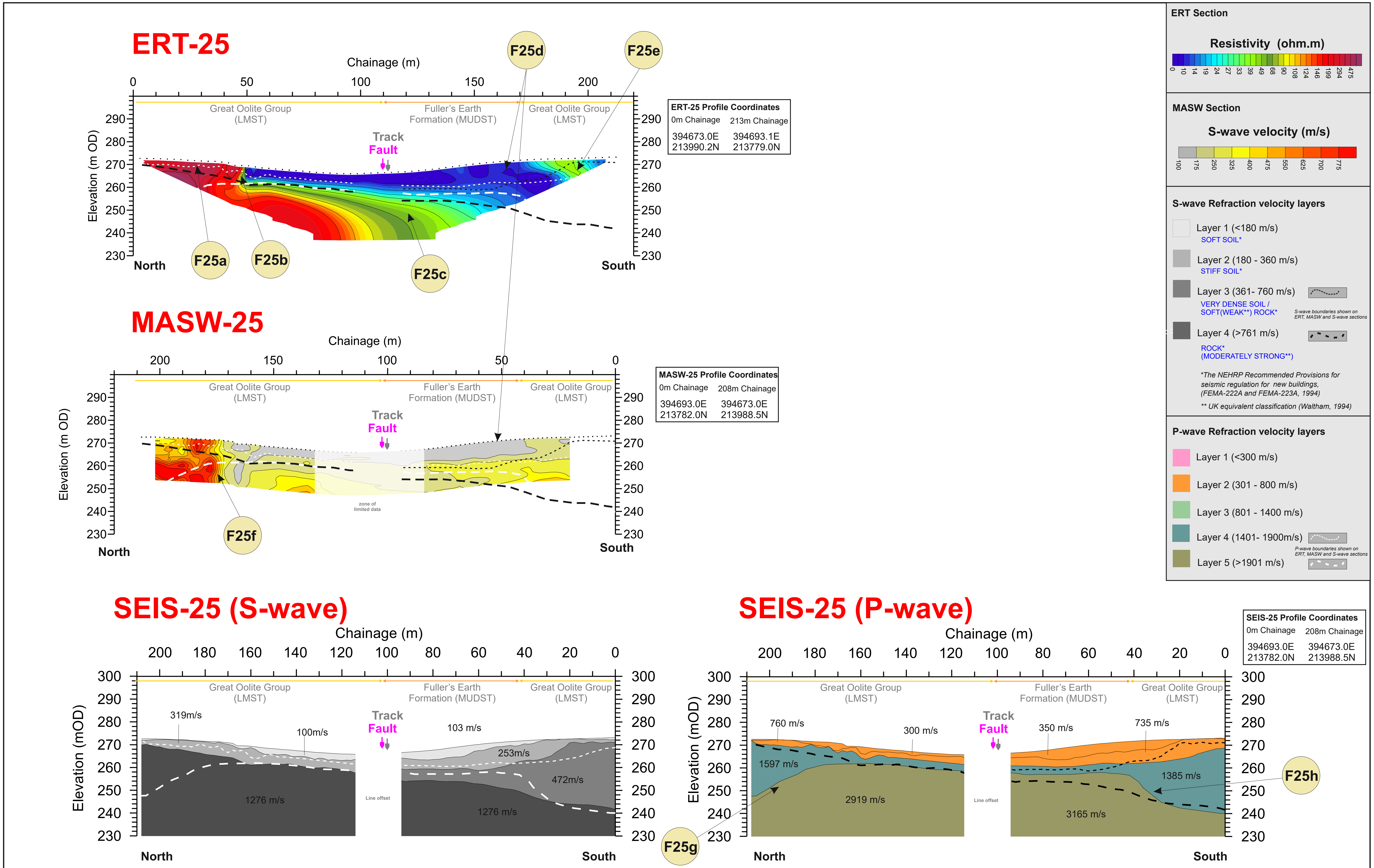

BOREHOLE KEY

Made ground	Sandstone
Clay	Mudstone
Silt	Siltstone
Sand	Limestone
Gravel	Core loss

KEY

Line 1 — Profile intersection

Fault — Reported fault positions

Bedrock geology subcrop

NOTES/OBSERVATIONS

Title: ERT AND SEISMIC PROFILES

Project: A417 CRICKLEY HILL BIRDLIP

TERRA DAT — down to earth geophysics

Tel: +44 (0) 2920 700127
Web:www.terradat.co.uk
Email: web@terradat.co.uk

Scale:	1:1500 at A3
Drawn by/Ref:	JT/6688/34
Date:	14 FEB 2020

FIGURE 34

ERT-26

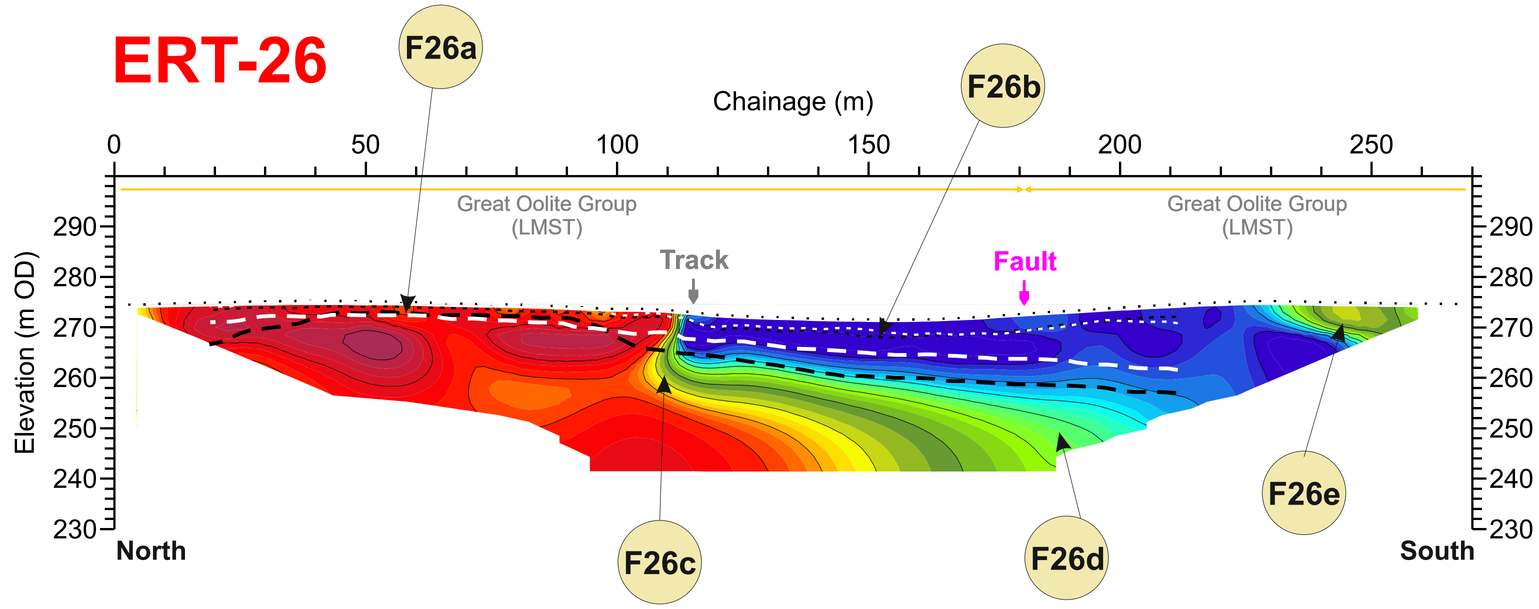

ERT-26 Profile Coordinates

0m Chainage	267m Chainage
394775.1E	394798.1E
214033.5N	213768.1N

MASW-26

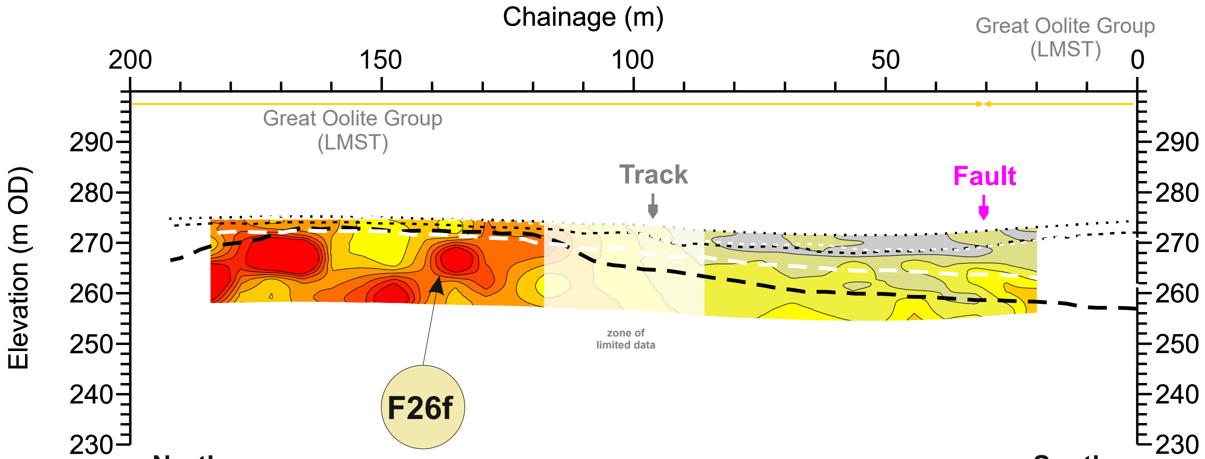

MASW-26 Profile Coordinates

0m Chainage	192m Chainage
394793.0E	394776.1E
213827.1N	214019.7N

SEIS-26 (S-wave)

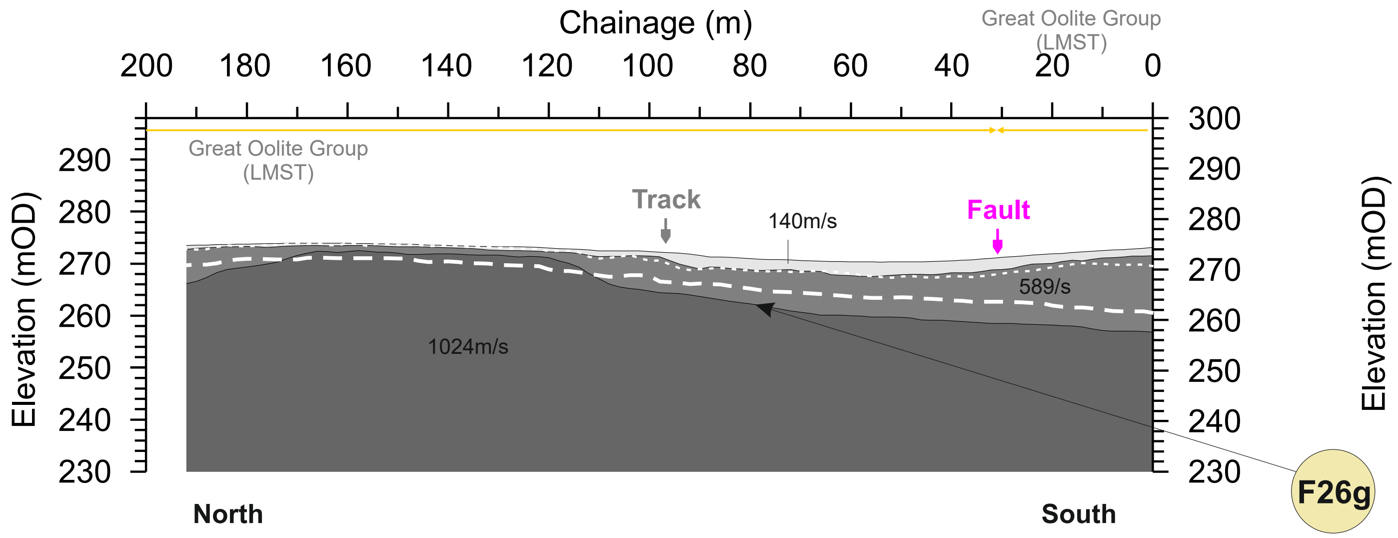

SEIS-26 (P-wave)

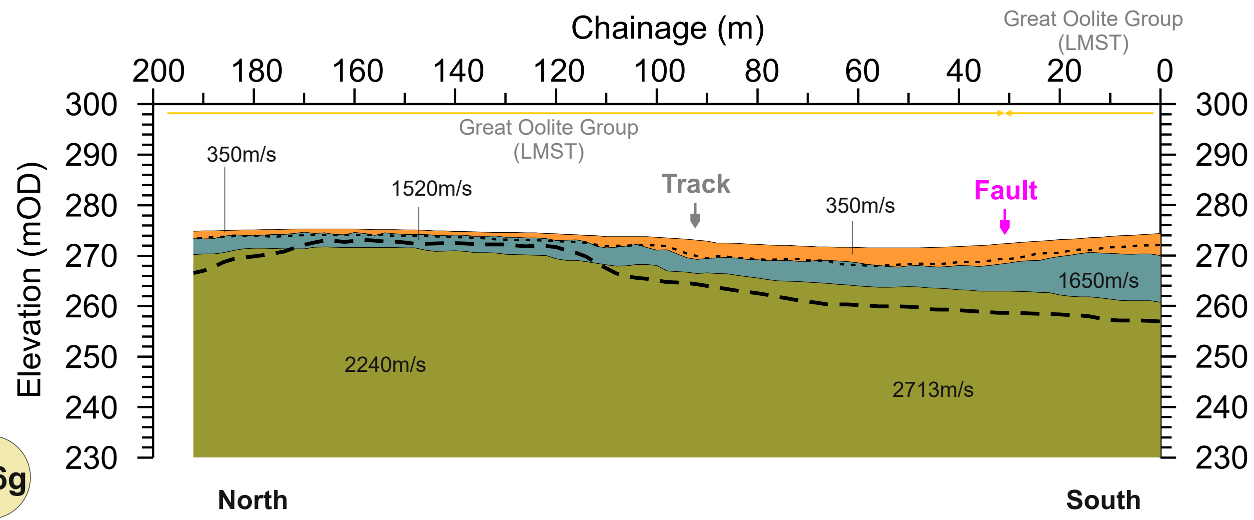

SEIS-26 Profile Coordinates

0m Chainage	192m Chainage
394793.0E	394776.1E
213827.1N	214019.7N

ERT Section

Resistivity (ohm.m)

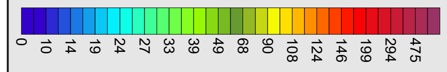

MASW Section

S-wave velocity (m/s)

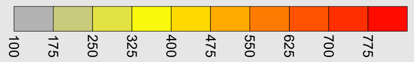

S-wave Refraction velocity layers

- Layer 1 (<180 m/s) SOFT SOIL*
- Layer 2 (180 - 360 m/s) STIFF SOIL*
- Layer 3 (361- 760 m/s) VERY DENSE SOIL / SOFT(WEAK**) ROCK*
- Layer 4 (>761 m/s) ROCK* (MODERATELY STRONG**)

S-wave boundaries shown on ERT, MASW and S-wave sections

*The NEHRP Recommended Provisions for seismic regulation for new buildings, (FEMA-222A and FEMA-223A, 1994)

** UK equivalent classification (Waltham, 1994)

P-wave Refraction velocity layers

- Layer 1 (<300 m/s)
- Layer 2 (301 - 800 m/s)
- Layer 3 (801 - 1400 m/s)
- Layer 4 (1401- 1900m/s)
- Layer 5 (>1901 m/s)

P-wave boundaries shown on ERT, MASW and S-wave sections

BOREHOLE KEY

Made ground	Sandstone
Clay	Mudstone
Silt	Siltstone
Sand	Limestone
Gravel	Core loss

KEY

- Line 1 — Profile intersection
- Fault — Reported fault positions
- Bedrock geology subcrop

NOTES/OBSERVATIONS

Title: ERT AND SEISMIC PROFILES

Project: A417 CRICKLEY HILL BIRDLIP

TERRA DAT — down to earth geophysics

Tel: +44 (0) 2920 700127
Web:www.terradat.co.uk
Email: web@terradat.co.uk

Scale:	1:1500 at A3
Drawn by/Ref:	JT/6688/35
Date:	14 FEB 2020

FIGURE 35

APPENDICES

Appendix - Ground conductivity (EM) survey

A ground conductivity or electromagnetic (EM) survey involves the generation of an EM field at the surface and subsequent measuring of the response as it propagates through the subsurface. The main components of the instrument are a transmitter coil (to generate the primary EM field) and receiver coil (to measure the induced secondary EM field). The amplitude and phase-shift of the secondary field are recorded and are then converted into values for ground conductivity and in-phase component (metal indicator).

The ground conductivity (EM) instruments are either hand carried or mounted/towed behind a quad bike. Readings are usually taken on a regular grid or along selected traverse lines and positional control can be provided by dGPS if there is sufficient satellite coverage.

The selection of the particular EM instrument (EM-38/EM-31/GEM-2) is primarily based on the required penetration depth of the survey. However for most conductivity surveys the GEM-2 has replaced the more conventional EM-31 instrument due to its ability to simultaneously acquire data at different frequencies (i.e. different depth levels) and a greater depth of penetration. At the end of each survey, the survey data is downloaded to a field computer and corrected for instrument, diurnal and positional shifts. Additional editing may be carried out to remove any 'noisy' data values/positions.

The results from the EM survey can be presented as colour contoured plots of conductivity and inphase (metal response) data. In general terms, a relative increase in conductivity values usually indicates a local increase in clay content or water saturation. However, if there is a corresponding increase in the inphase response, the influence of some artificial source is likely (i.e. metal).

EM-38
Single frequency
Exploration depth ~1.5m

EM-31
Single frequency
Exploration depth ~3 to 5m

GEM-2
Multi-frequency
Exploration depth up to 10m

Towed EM-38 with dGPS

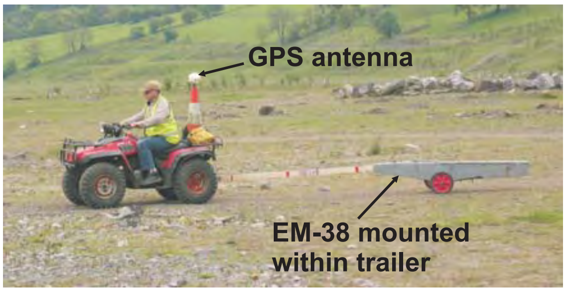

General principle of EM surveying

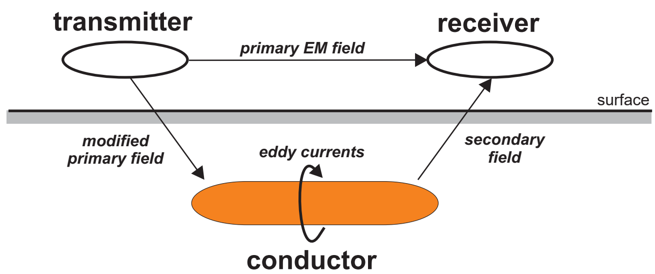

Mounted EM-31 with dGPS

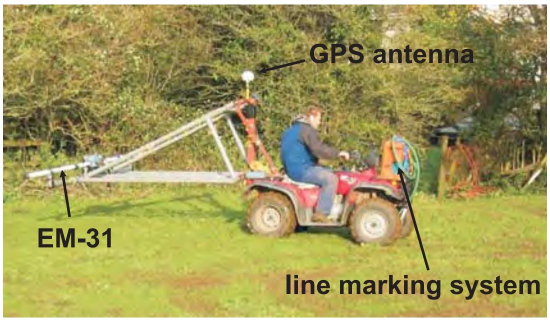

Ground conductivity data plot

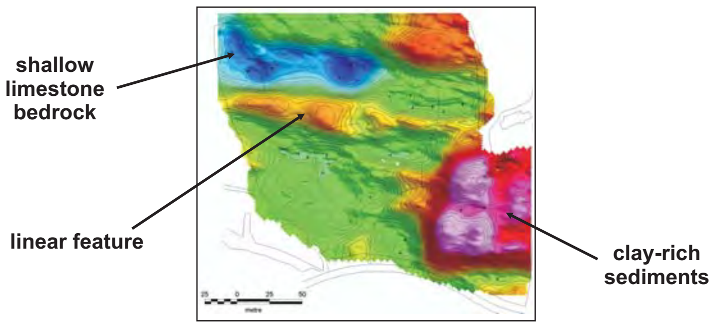

Constraints
Power lines, buildings, metal structures (fences, rebar, vehicles, debris etc.) and buried services can interfere with the electro-magnetic measurements.

Appendix - Resistivity Tomography

The Resistivity technique is a useful method for characterising the sub-surface materials in terms of their electrical properties. Variations in electrical resistivity (or conductivity) typically correlate with variations in lithology, water saturation, fluid conductivity, porosity and permeability, which may be used to map stratigraphic units, geological structure, sinkholes, fractures and groundwater.

The acquisition of resistivity data involves the injection of current into the ground via a pair of electrodes and then the resulting potential field is measured by a corresponding pair of potential electrodes. The field set-up requires the deployment of an array of regularly spaced electrodes, which are connected to a central control unit via multi-core cables. Resistivity data are then recorded via complex combinations of current and potential electrode pairs to build up a pseudo cross-section of apparent resistivity beneath the survey line. The depth of investigation depends on the electrode separation and geometry, with greater electrode separations yielding bulk resistivity measurements from greater depths.

The recorded data are transferred to a PC for processing. In order to derive a cross-sectional model of true ground resistivity, the measured data are subject to a finite-difference inversion process via RES2DINV (ver 5.1) software.

General resistivity principle

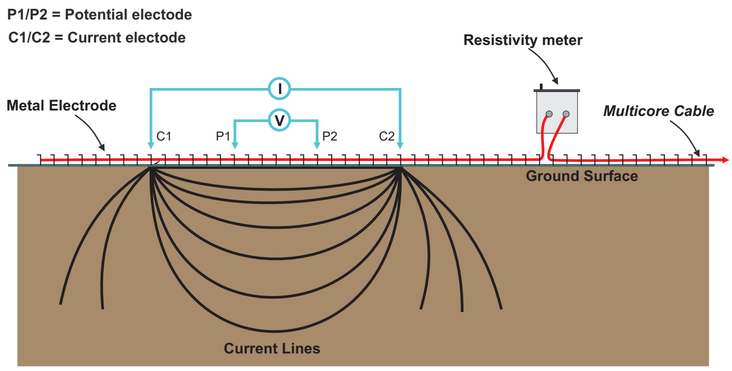

Typical field set-up

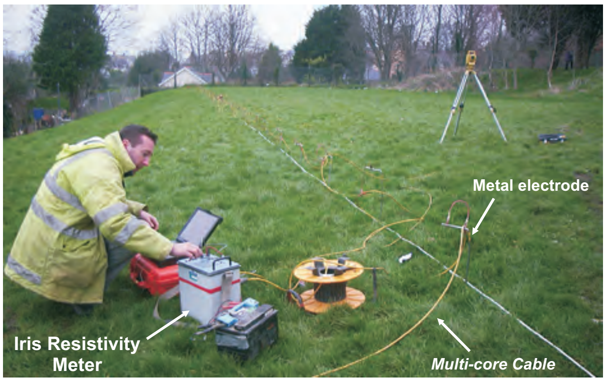

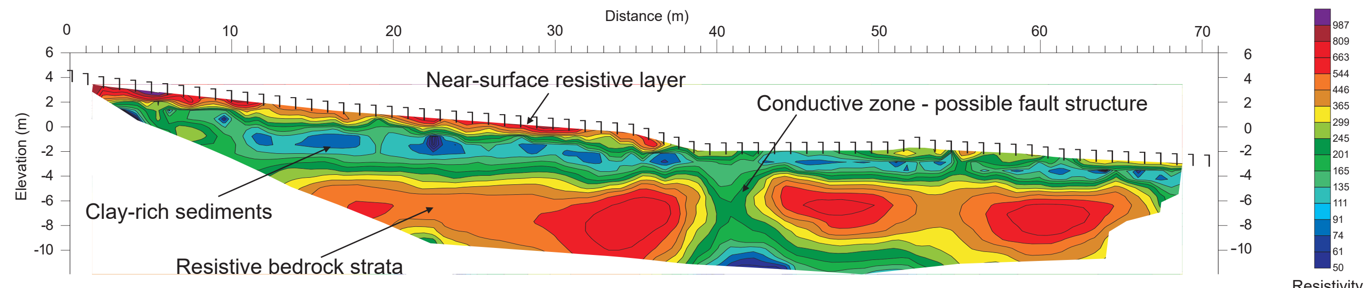

Modelled resistivity section

Data processing is based on an iterative routine involving determination of a two-dimensional (2D) simulated model of the subsurface, which is then compared to the observed data and revised. Convergence between theoretical and observed data is achieved by non-linear least squares optimisation. The extent to which the observed and calculated theoretical models agree is an indication of the validity of the true resistivity model (indicated by the final root-mean-squared (RMS) error).

The true resistivity models are presented as colour contour sections revealing spatial variation in subsurface resistivity. The 2D method of presenting resistivity data is limited where highly irregular or complex geological features are present and a 3D survey maybe required. Geological materials have characteristic resistivity values that enable identification of boundaries between distinct lithologies on resistivity cross-sections. At some sites, however, there are overlaps between the ranges of possible resistivity values for the targeted materials which therefore necessitates use of other geophysical surveys and/or drilling to confirm the nature of identified features.

Constraints:

Readings can be affected by poor electrical contact at the surface. An increased electrode array length is required to locate increased depths of interest therefore the site layout must permit long arrays. Resolution of target features decreases with increased depth of burial.

Appendix - Seismic Refraction Survey

Seismic refraction is a useful method for investigating geological structure and rock properties. The technique involves the observation of a seismic signal that has been refracted between layers of contrasting seismic velocity, i.e., at a geological boundary between a high velocity layer and an overlying lower velocity layer.

Shots are deployed at the surface and recordings made via a linear array of sensors (geophones or hydrophones). Refracted seismic signal travels laterally through the higher velocity layer (refractor) and generates a 'head-wave' that returns to surface. Beyond a certain distance away from the shot, the signal that has been refracted at depth is observed as first-arrival signal at the geophones. Observation of the travel-times of refracted signal from selectively deployed shots enables derivation of the depth profile of the refractor layer. Shots are typically fired at locations at and beyond both ends of the geophone spread and at regular intervals along its length.

The results of the seismic refraction survey are usually presented in the form of seismic velocity boundaries on interpreted cross-sections. Seismic sections represent the measured bulk properties of the subsurface and enable correlation between point source datasets (boreholes/trialpits) where underlying material is variable. Reference to the published seismic velocity tables enables derivation of rippability values.

Typical field set-up

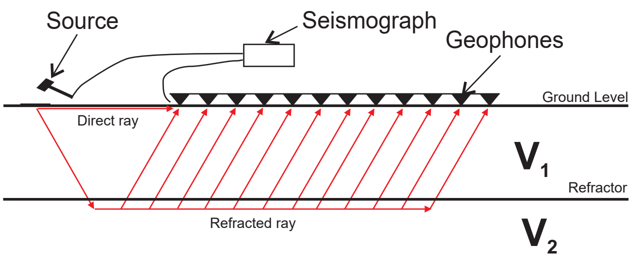

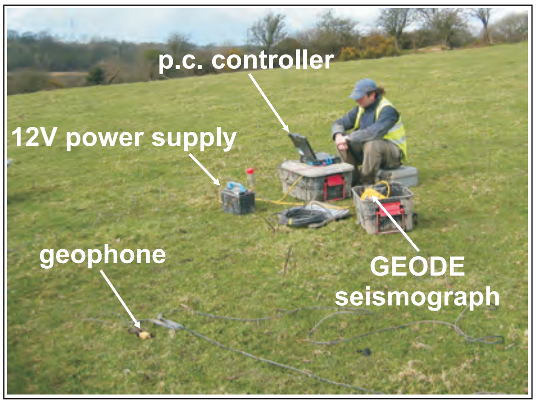

Travel-time curve

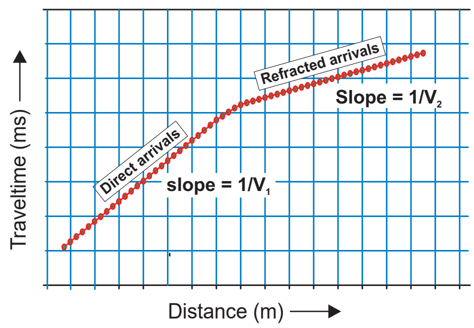

Modelled velocity section

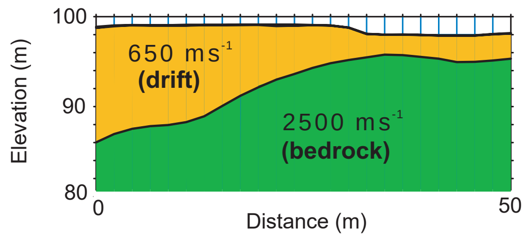

The data processing is carried out using PICKWIN & PLOTREFA (OYO ver2.2) software. The first stage involves accurate determination of the first-arrival times of the seismic signal (time from the hammer blow to each recording hydrophone) for every shot record, using PICKWIN. Time-distance graphs showing the first-arrival times were then generated for each seismic shot record and analysed using PLOTREFA software to determine the number of seismic velocity layers. Modelled depth profiles for the observed seismic velocity layers are produced by a tomographic inversion procedure that is revised iteratively to develop a best fit-model. The final output of a seismic refraction survey is a velocity model section of the subsurface based on an observed layer sequence with measured velocities that correspond to physical properties such as levels of compaction/ saturation in the case of sediments and strength/rippability in the case of bedrock.

Constraints

Layer velocity (density) must increase with depth; true in most instances. Layers must be of sufficient thickness to be detectable. Data collected directly over loose fill (landfills) or in the presence of excessive cultural noise may result in sub-standard results. In places where compact clay-rich tills and/or shallow water overly weak bedrock an S-wave survey may be used to profile rockhead where insufficient velocity contrast may prevent use of a P-wave survey.

Rippability Chart

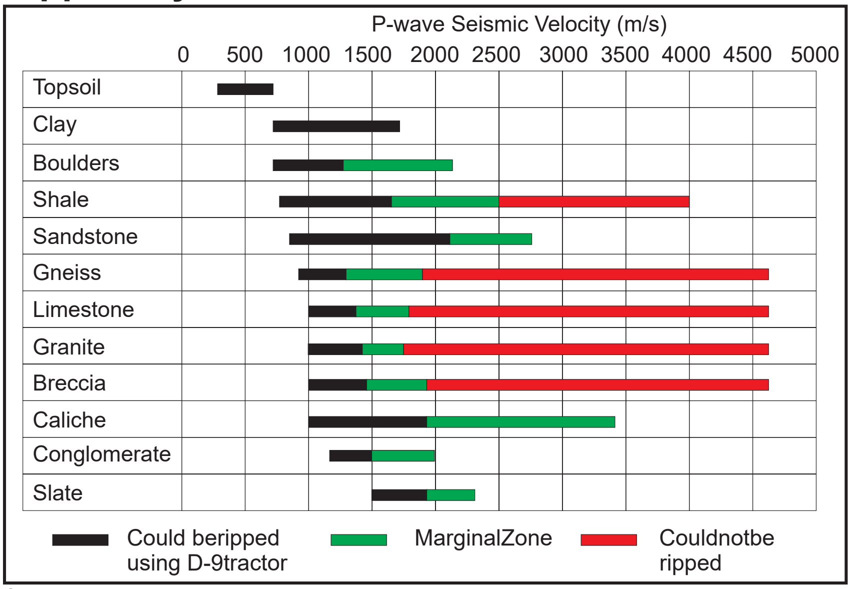

Ground preparation by ripping in open pit mining, Mining Magasine, 122, 458-469. Atkinson, 1970

Compressional P-wave velocity

Unconsolidated materials	***Vp (m/s)***
Sand (dry)	200 - 1000
Sand (water saturated)	1500 - 2000
Clay	1000 - 2500
Glacial till (water saturated)	1500 - 2500
Permafrost	3500 - 4000
Sedimentary rocks	
Sandstones	2000 - 6000
Tertiary sandstones	2000 - 2500
Pennant sandstone (Carboniferous)	4000 - 4500
Cambrian quartzite	5500 - 6000
Limestones	2000 - 6000
Cretaceous chalk	2000 - 2500
Jurassic limestones	3000 - 4000
Carboniferous limestones	5000 - 5500
Dolomites	2500 - 6500
Salt	4500 - 5000
Anhydrate	4500 - 6500
Gypsum	2000 - 3500
Igneous/Metamorphic rocks	
Granite	5500 - 6000
Gabbro	6500 - 7000
Ultramafic rocks	7500 - 8500
Serpentite	5500 - 6500
Other materials	
Steel	6100
Iron	5800
Aluminium	6600
Concrete	3600

An introduction to Geophysical Exploration 3rd Ed.
Kearey, Brooks & Hill: 2002

Diggability Chart

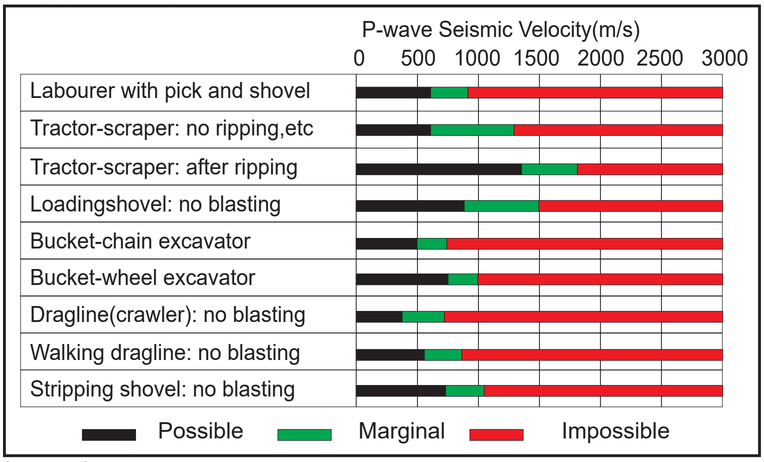

Selection of open pit excavation and loading equipment.
Transactions of the Institute of Mining and Metallurgy, 80, A101-A129, Atkinson 1971

Effect of ground water

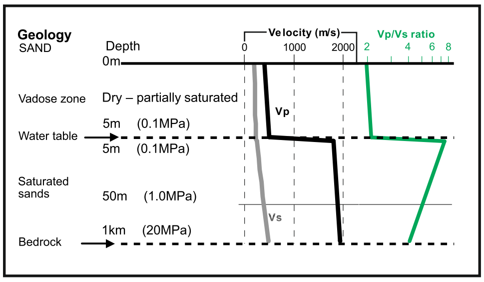

Prasad et al., Measurement of velocities and attenuation in shallow soils,
Near-Surface Geophysics Volume II Case Histories, SEG, Tulsa (2004)

Shear Waves

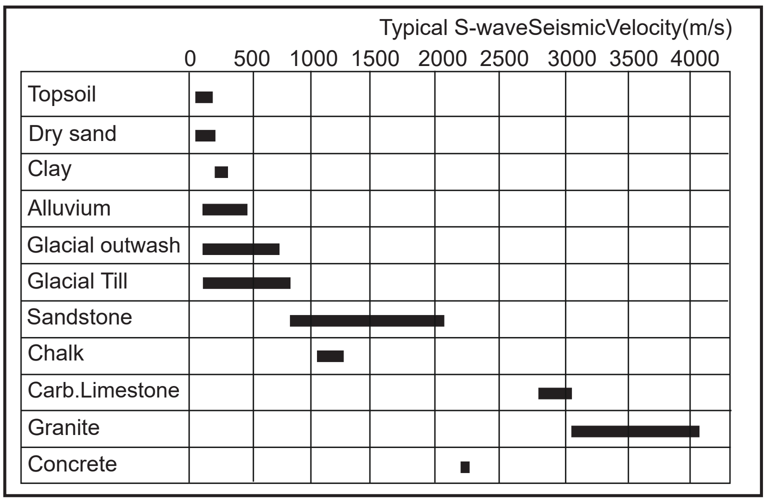

Rock / Soil Description (top 30m)	**S-wave velocity (m/s)**
Hard rock (*strong**)	> 1,500
Rock (*moderately strong**)	760 - 1,500
Very dense soil / soft (*weak**) rock	360 - 760
Stiff soil	180 - 360
Soft soil	<180

The NEHRP Recommended Provisions for seismic regulation for new buildings, (FEMA-222A and FEMA-223A, 1994)

** UK equivalent classification (Waltham, 1994)*

Applied Geophysics, Telford et al, 1990
Shear wave velocity determination of unlithified geologic materials (CUSEC region) Illinois State Geological Survey, Bauer, 2004.
Bauer et al., 2007, Illinois State Geological Survey.
Shear Wave Velocity, Geology and Geotechnical Data of Earth Materials in the Central U.S. Urban Hazard Mapping Areas.
An Introduction to Geophysical Exploration, 3rd Edition, Keary and Brooks, 2002.
Conceptual Overview of Rock and Fluid Factors that Impact Seismic Velocity and Impedance,
Stanford Rock Physics Laboratory, n.d.

PUBLISHED SEISMIC VELOCITY TABLES

APPENDIX B

B3 CONE PENETRATION TESTING

IN SITU
SITE INVESTIGATION

STATIC CONE PENETRATION TEST

FACTUAL REPORT

CLIENT: Geotechnical Engineering Ltd

PROJECT: A417 Missing Link

Project	A417 Missing Link
Project No.	1190295
Client	Geotechnical Engineering Ltd
Address	Centurion House, Olympus Park, Quedgeley, Gloucester, GL2 4NF

Attention: Mr Dave Owen

Dear Mr Owen,

We have pleasure in providing a digital copy of our report and data in AGS format for the above project.

We hope that you are satisfied with the performance of our staff, equipment and reporting on this project. If you should have any queries about any aspect of the works carried out, please do not hesitate to contact us. We look forward to being of service to you in the future.

Yours faithfully,

In Situ Site Investigation Limited

[redacted]

Darren Ward

Director

Report Issue

Issue	Date	Prepared	Sign	Checked	Sign	Approved	Sign
03	06/04/2020	Chloe Wickens	[redacted]	Luisa Dhimitri	[redacted]	Darren Ward	[redacted]

Table of Contents

1.0 INTRODUCTION

In Situ Site Investigation Limited (In Situ) was engaged in a geotechnical site investigation at A417 Missing Link at the request of Geotechnical Engineering Ltd. The site investigation consisted of completing 3 Static Piezocone Penetration Tests (CPTU), and 3 Dissipation Tests to provide information on the soil conditions and derived geotechnical parameters at:

Land package 948,
Witcombe,
Gloucestershire,
GL3 4UF

All test locations were provided by the client. A site map is included in the end of Appendix A of this report (if provided by the client). The tests were stopped when they reached the target depth as per the client's technical specifications or for other technical reasons, as detailed in the *Project Summary Table* in *Appendix A.1* and on each CPTU log included in Appendix B of this report.

The fieldwork was carried out from 9th July 2019 to 10th July 2019 as per the client's request.

The work on site and the final factual reporting have been undertaken in accordance with the international technical standard *BS EN ISO 22475-1:2012*.

2.0 FIELDWORK

2.1 CONE PENETRATION TESTS

The fieldwork activity is summarised in Table 2.1.

Table 2.1 Fieldwork Summary	
CPT Operator/s	Ashley Lelliott
Date Started	9th July 2019
Date Finished	10th July 2019
In Situ S.I. Project Manager	Darren Ward
Main Contractor's Site Manager	Dave Owen

2.1.1 Rig Information

Details of CPTU rig used in this project are shown in Table 2.2. Full data sheet for the rig is presented in *Appendix A.2*.

Table 2.2 Rig Summary	
Rig Name	**Rig Description**
CPT 012	20 Tonne Track Mounted CPT Rig

2.1.2 CPTU Cone

Details of electric CPTU cone (Type TE2) used in this project conforming to the requirements of Application Class 2 of *ISO 22476-1:2012*, are shown in Table 2.3.

Table 2.3 Cone Summary		
Number	**Cross-section area**	**Filter position**
DP15-CFPTxy.71007	15cm^2	u_2
DP15-CFPTxy.70102	15cm^2	u_2

A full datasheet of the cone used is shown in *Appendix A.3*.

The cone's measured parameters are shown in Table 2.4.

Table 2.4 Completed Fieldwork Summary
3 CPTU to a maximum depth of 15.02m. Each test measured Cone Resistance, q_c, Sleeve Friction, f_s, Porewater Pressure in the shoulder position, u_2, Inclination in X and Y axes.
Provision of factual report with estimated soil type, derived geotechnical parameters & AGS data file.

2.1.3 CPTU Cone Calibration

The cone resistance and sleeve friction are recorded by calibrated load cells in the cone. The CPTU load cells and pressure transducers are regularly calibrated in line with *ISO 22476-1:2012* standard by the cone manufacturer. The cone calibration certificate for the cone used at this site are presented in *Appendix A.4*.

2.1.4 CPTU Cone Saturation

The pore water pressure is recorded using a calibrated pressure transducer located in the piezocone. To ensure pore water pressure measurements are not affected by the presence of air in the measuring transducer, a de-airing procedure is carried out prior to each test. The cone and filter are saturated using a glycerine fluid with a viscosity of 10,000 CST.

2.1.5 Test Procedure

The tests are carried out in accordance with the *International Standard for Electrical Cone and Piezocone Penetration Test (ISO 22476-1:2012)*.

The final depths of the tests were determined by either completion to the specified test depth or when the maximal safe capacity of the equipment was reached. A schedule of the tests performed is shown in *Appendix A.1*, which has been compiled from the operators' daily progress reports.

The data is transmitted from the digital CPTU through an umbilical cable that runs through the push rods to the data acquisition system. Results are displayed instantaneously on the computer logging screen. The results are recorded on the computer hard disc.

The rate of penetration is kept constant at 2cm/s ±10% except when penetrating very dense or hard strata. Before each test is carried out zero values are taken of the cone to check if it is within calibration. At the end of each test, zero values are taken again to see if there has been any drift during the test. These values are inspected during the post processing stage. This is a quality check on the data and the testing procedure. Individual test zero values are shown on their corresponding test results in *Appendix B*.

2.1.6 In Situ Pore Pressure (u_0)

The in situ or hydrostatic pore pressure is required for the calculation of several derived parameters included in this report. For this report, the groundwater level is assumed at 2.00 m below ground surface, for calculation purposes. The in situ pore pressure (u_0) values are presented on the pore pressure plot, on *CPT Log 01,* which is included in *Appendix B*.

2.2 POSITIONING

Positioning and surveying of all investigated locations was the responsibility of the client

2.3 DISSIPATION TESTS

As per the client's request 3 dissipation tests were performed at the required depth.
A summary table of the dissipation tests is presented in *Appendix A1*.

The dissipation test is carried out by pausing the penetration at a point when there is excess porewater pressure. This excess pore pressure generated around the cone will then start to dissipate, and the decay of pore pressure with time is recorded. The rate of dissipation depends upon the coefficient of consolidation, which in turn depends on the compressibility and permeability of the soil and on the diameter of the probe. It is common to record the time to reach 50% dissipation, t_{50}. If the equilibrium pore pressure is required, the dissipation test is continued until no further dissipation is observed. This can occur rapidly in sands, but may take many hours in plastic clays. If t_{50} is not reached, due to soils' conditions, t_{40}, t_{30} or t_{20} are calculated. The calculation procedures for dissipation tests are explained in Section 4.16 of this report.

The data recorded from the dissipation tests on site is used to calculate the consolidation characteristics, as shown in Dissipation Test Graphs, *Appendix B*.

3.0 CONE PENETRATION MEASURED PARAMETERS

All measured parameters of tests carried with the CPTU cone are shown in *Appendix B* and all the information about data processing and results are given in sections *3.1*, *3.2* and *3.3*.

3.1 DATA PROCESSING

The measured parameters, cone end resistance, q_c, sleeve friction, f_s, porewater pressure measurements with filter in shoulder position, u_2 and inclination for *x* and *y* axis, I_x, I_y, were recorded for every *10 mm* of penetration keeping a constant speed of *20 mm/s* ± *5 mm/s*, which may slightly change when the cone is penetrating hard strata.

The measured data from the site works is processed and presented using specialised CPT software. The interpretations on the CPTU results were carried out following the recommendations of *Lunne et al. (1997)*, *Robertson (2015)* and *BS EN ISO 22475-1:2012.* Measured parameters, mentioned in *Sections 3.2* and *3.3*, were used to derive all the geotechnical parameters, which are presented in *Chapter 4.0*. The soil behaviour type method used on this report is *Robertson et al. (1986)*, shown in *Figure 3.2*.

3.1.1 Zero Measurements

Before and after each CPTU test, zero measurements are recorded for each channel of the cone. The zero measurements are presented on the logs in *Appendix B*. This is a routine quality check carried out on site.

3.2 MEASURED PARAMETERS

3.2.1 Cone Resistance (q_c)

Cone resistance, q_c, is measured as the total force acting on the cone, divided by the projected area of the cone. The results are presented in *MPa*, on *CPT Log 01*, in *Appendix B*, scale *0-20 MPa* with a minor scale printing on the same graph at *0-4 MPa*.

3.2.2 Sleeve Friction (f_s)

Sleeve friction, f_s, is measured as the total frictional force acting on the friction sleeve divided by its surface area. The results are presented in *kPa*, on *CPT Log 01*, in *Appendix B*, using a scale of *0-500 kPa*.

3.2.3 Porewater pressure (u_2)

The pore pressure, u_2, is measured during the test. If the material is free draining and saturation is maintained it will normally measure hydrostatic pore pressure. In materials that are not free draining, it will record the total pore pressure (hydrostatic plus any excess pore pressures generated) created by the cone penetration through this material.

The filter element can be mounted in one of three positions. For all tests carried out in this project the filter was mounted in the u_2 position (see *Figure 3.1*).

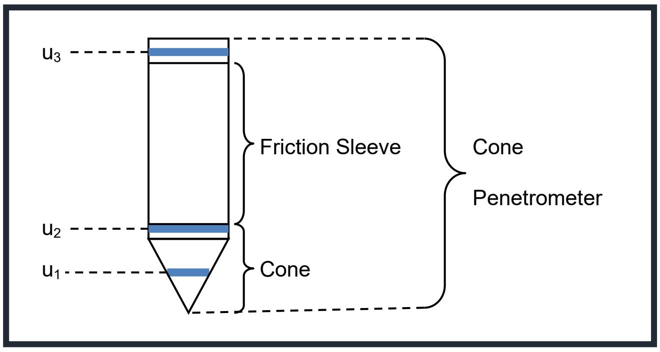

Figure 3.1: *Diagram showing pore pressure filter locations (after Lunne et al., 1997)*

3.2.4 Inclination (I_x, I_y)

The CPT rig was set up to obtain a thrust direction as near as possible to vertical. The CPTU cones have inclinometers incorporated to measure the non-verticality of the test. For test depths less than *15 m*, significant non-verticality is unusual, provided the initial thrust direction is vertical.

3.3 ESTIMATED SOIL BEHAVIOUR TYPE

3.3.1 Friction Ratio (R_f)

The friction ratio, R_f is the ratio between the sleeve friction and the cone resistance (Lunne *et al.,* 1997).

$$Fricton\ Ratio\ (R_f) = \left(\frac{Sleeve\ Friction\ (f_s)}{Cone\ Resistance\ (q_c)}\right) \times 100$$

3.3.2 Estimated Soil Behaviour Type (SBT)

The estimation of soil behaviour type, *SBT*, using measurements of cone resistance and sleeve friction is based upon the variations of the friction ratio and cone resistance. The friction ratio varies depending upon whether the soil is cohesive or granular. The cone resistance varies depending on the strength and densities of the soil.

The interpretation used in this report is *Robertson et al. (1986)*, which is shown in Figure 3.2. The results are presented on *CPT Log 01*, in *Appendix B*.

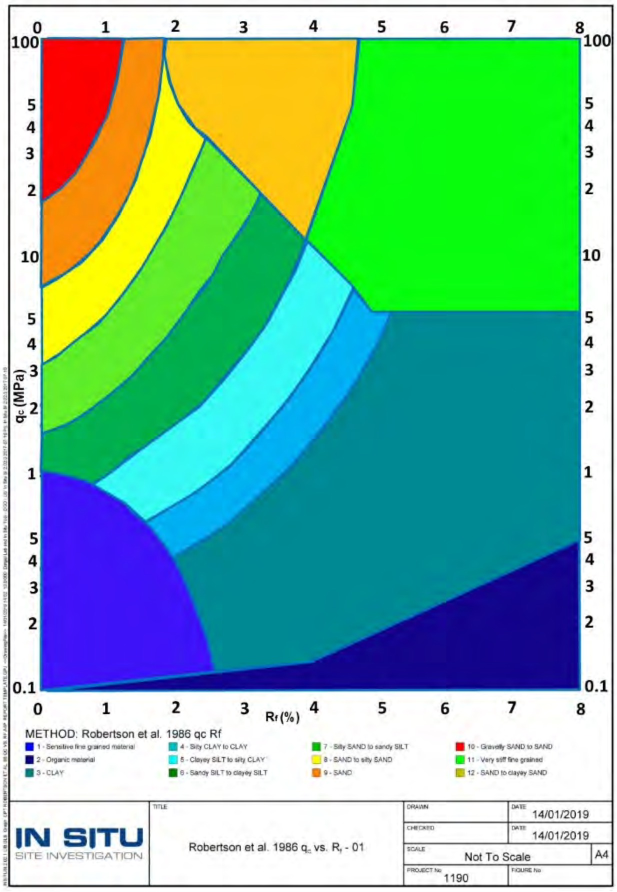

Figure 3.2: *Robertson et al., 1986 soil behaviour type chart.*

3.3.3 Pore Pressure Ratio (B_q)

Pore pressure ratio, B_q is the ratio between the measured pore pressure generated during penetration and the corrected cone resistance minus the total overburden stress.

Pore pressure ratio as defined by *Senneset and Janbu (1985)* is defined as:

$$B_q = \frac{u_2 - u_0}{q_t - \sigma_{vo}}$$

where

- u_2 is pore pressure measured between the cone and the friction sleeve
- u_0 is equilibrium pore pressure
- σ_{vo} is total overburden stress
- q_t is cone resistance corrected for unequal end area effects

3.4 APPLIED CORRECTIONS

3.4.1 Corrected Cone Resistance (q_t)

For each penetration test, the measured cone resistance, q_c, can be corrected for the ‘‘unequal area effect’’ due to the influence of the ambient pore water pressure acting on the cone.

The correction has been applied using the following equation by Lunne et *al.,* 1997:

$$q_t = q_c + [u_2.(1 - \alpha)]$$

where

α	is the cone area ratio

The cone used on this project has a cone area ratio of *0.79*. This value is geometrically measured.

3.4.2 Depth Correction

All tests in the report have been corrected for depth difference caused by inclination. This has been calculated using the method described in *ISO 22476-1:2012*.

To calculate the corrected depth the following formula is used:

$$z = \int_0^l C_{inc} \cdot dl$$

where

z	is penetration depth, in *m*
l	is penetration length, in *m*
C_{inc}	is correction factor for the effect of the inclination of the CPTU relative to the vertical axis.

The equation for calculating the correction factor for the influence of the inclination for a bi-axial inclinometer is:

$$C_{inc} = \frac{1}{\sqrt{(1 + tan^2\beta_1 + tan^2\beta_2}}$$

where

β_1	is the angle between the vertical axis and the projection of the axis of the CPTU on a vertical plane, in degrees
β_2	is the angle between the vertical axis and the projection of the axis of the CPTU on a vertical plane that is perpendicular to the plane of angle β_1, in degrees

4.0 GEOTECHNICAL DERIVED PARAMETERS

A number of empirical correlations can be used to derive geotechnical parameters from CPTU data. This report includes only the parameters which are described in this chapter. The results of all correlations used to obtain the geotechnical derived parameters are presented on *CPT Log 02* and *CPT Log 03* in *Appendix B*.

Please, note that each empirical correlation is derived for a certain type of soil, and may not be appropriate for all the soil types encountered on this project.

4.1 SOIL BEHAVIOUR TYPE INDEX (I_c)

The soil behaviour type index, I_c, was derived by *Jefferies and Davies (1991)*, and was created to simplify the application of CPTU SBT chart shown in *Chapter 3*, *Figure 3.2*. This approach has been modified for use with the *Robertson (1990)* normalised CPT soil classification chart, *Figure 4.1*. The normalised cone parameters Q_t and F_r (for definitions see *Appendix A5* Symbol List) can be combined into one Soil Behaviour Type Index, I_c, *(Lunne et al., 1997)*.

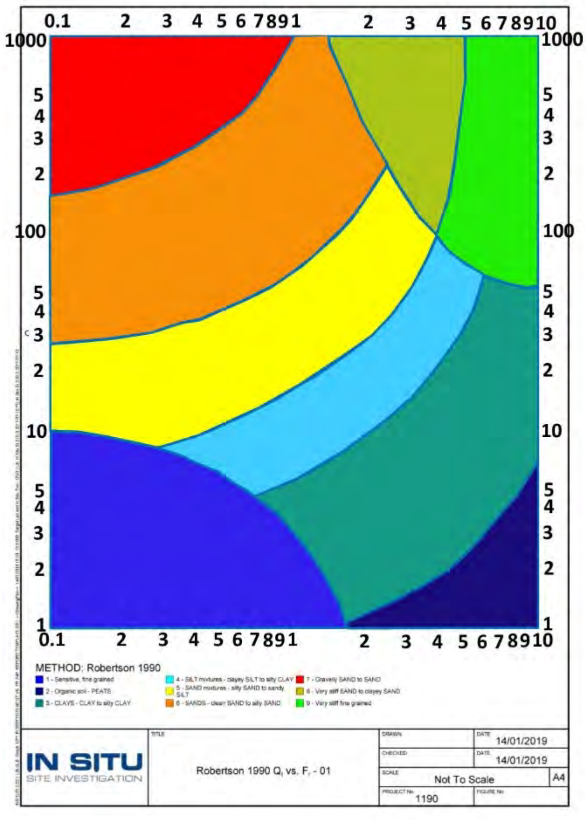

Figure 4.1: *Robertson 1990 soil behaviour type chart.*

The soil behaviour type index, I_c, can then be defined using *Robertson (2010)* formula, given below:

$$I_c = ((3.47 - logQ_t)^2 + (logF_r + 1.22)^2)^{0.5}$$

where

Q_t is the normalized cone resistance which represents the simple normalization with a stress exponent (n) of *1.0*, which applies well to clay-like soils

F_R is the normalized friction ratio, in *%*

The boundaries of soil behaviour type are then given in terms of the index, I_c, presented in *Table 4.1* below.

The soils behaviour type index does not apply to zones *1*, *8* and *9*. The profiles of I_c provide a simple guide to the continuous variation of soil behaviour type in a given soil profile based on CPTU results, with a reliability greater than *80%* compared with soil samples *(Robertson, 2015).*

Zone	Soil Behaviour Type	I_c
1	Sensitive fine grained	N/A
2	Organic Soils – clay	>3.6
3	Clays – silty clay to clay	2.95 – 3.6
4	Silt mixtures – clayey silt to silty clay	2.60 – 2.95
5	Sand mixtures – silty sand to sandy silt	2.05 – 2.6
6	Sands – clean sand to silty sand	1.31 – 2.05
7	Gravelly sand to dense sand	<1.31
8	Very stiff sand to clayey sand*	N/A
9	Very stiff fine grained *	N/A

** Heavily over consolidated or cemented*

Table 4.1: *Normalized CPTU Soil Behaviour Type (SBT_n) Index values, I_c.(Robertson, 2010)*

4.2 N VALUE OF STANDARD PENETRATION TEST (SPT) (N_{60})

The derived *N* value of *SPT, N_{60}*, is strongly and directly related to the cone resistance, q_c.

In this report the N_{60} value is derived using the following correlations, developed by *Robertson and Wride (1998)* and *Jefferies and Davies (1998)*

1) *Robertson & Wride (1998)*

$$N_{60} = \frac{q_c}{8.5 \cdot p_a \left(1 - \frac{I_C}{4.6}\right)}$$

2) *Jefferies and Davies (1993)*

$$N_{60} = \frac{q_c}{0.85 \cdot \left(1 - \frac{I_C}{4.75}\right)}$$

where

q_c is the cone resistance
p_a is the atmospheric pressure equal to *100 kPa*
I_c is the soil behaviour type index calculated as given in *section 4.1*

It is suggested that this method provides a better estimation of the *N* value than the actual *SPT* test, due to its poor repeatability. But in fine grained soil with high sensitivity these methods of estimating N_{60} may overestimate it *(Jefferies and Davies, 1991).*

4.3 RELATIVE DENSITY (D_r)

Relative density, D_r, is an intermediate parameter for coarse grained soils, widely used to describe sand deposits. All the research on deriving the relative density from CPTU tests results are carried out for ***clean predominantly quartz sands***. The studies have shown that CPTU resistance in granular soils is controlled by sand relative density, in situ effective stresses and compressibility. The more compressible sands tend to give lower penetration resistance for a given relative density then less compressible sands.

In this report relative density is calculated using the methods suggested by *Baldi et al., (1986)*, *Jamiolkowski et al., (2001)* and *Kulhawy and Mayne (1990)* as shown in the equations below:

1) Baldi et al., (1986)

$$D_r = \frac{1}{C_2} \cdot ln\left(\frac{q_c \cdot Wehr}{C_1 \cdot (\sigma'_{v0})^{0.55}}\right) \cdot 100$$

where

C_1 is a consolidation coefficient which is *157* for normally consolidated soils and *181* for over consolidated soils

C_2 is a consolidation coefficient which is *2.41* for normally consolidated soils and *2.46* for over consolidated soils

Wehr is a correction coefficient for calcareous soils

2) Jamiolkowski et al., (2001)

$$D_r = 100 \cdot \left[0.268 \cdot ln\left(\frac{q_t/\sigma_{atm}}{\sqrt{\sigma'_{v0}/\sigma_{atm}}}\right) + C_1\right]$$

where

C_1 is a compressibility coefficient which is *-0.675* for average compressible soils, ≤*1.0* for high compressible soils and carbonate or calcareous sands and ≥*-2.0* for low compressible soils

q_t is corrected cone resistance

σ_{atm} is the atmospheric pressure

3) Kulhawy and Mayne, (1990)

$$D_r = \left[\frac{q_{c1}}{305 \cdot C_1 \cdot OCR^{0.18} \cdot \left(1.2 + 0.05 \cdot log(t/100)\right)}\right]^{0.5} \cdot 100$$

where

q_{c1} is the cone resistance corrected for initial vertical effective stress and atmospheric pressure, calculated by the following formula

$$q_{c1} = \frac{q_c}{\sqrt{\sigma'_{v0} \cdot \sigma_{atm}}}$$

where

q_c is the cone resistance in *kPa*
σ'_{v0} is the initial vertical effective stress in *kPa*

C_1 is a compressibility coefficient which is *-0.91* for low compressible sands, *1.0* for medium compressible sands and *1.09* for high compressible sands
t is time in years

4.4 FRICTION ANGLE (φ')

Friction angle, *φ*', is used to express the shear strength of uncemented, coarse grained soils. In this report friction angle is derived by the correlations of *Mayne and Campanella (2005)*, *Robertson and Campanella (1983)* and *Kulhawy and Mayne (1990)*.

1) Mayne and Campanella, (2005)

$$\varphi' = 29.5^0 \cdot B_q^{0.121} \cdot [0.256 + 0.336 \cdot B_q + log Q_t]$$

where

B_q is the pore pressure ratio, calculated as in Session 3.3

Q_t is the normalized cone resistance

2) Robertson and Campanella, (1983)

$$\varphi' = \tan^{-1}\left(0.1 + 0.38 \cdot log\left(\frac{q_t}{\sigma'_{v0}}\right)\right)$$

where

q_c is the cone resistance in *kPa*
σ'_{v0} is the initial vertical effective stress in *kPa*

3) Kulhawy and Mayne, (1990)

$$\varphi' = 17.6^0 + 11.0^0 \cdot log(q_{t1})$$

where

q_{t1} is the corrected cone resistance corrected for initial vertical effective stress and atmospheric pressure, calculated by the following formula

$$q_{t1} = \frac{q_t}{\sqrt{\sigma'_{v0} \cdot \sigma_{atm}}}$$

The method suggested by *Mayne and Campanella (2005)* will not provide reliable results for heavily over consolidated soils, fissured geomaterials and highly cemented or structures clays. This approach gives reliable results when pore pressure is positive and varies $0.1 < B_q < 1.0$. The correlation suggested by *Robertson and Campanella (1983)* estimates the peak friction angle for uncemented, unaged, moderately compressible, predominately quartz sands. For sands of higher compressibility, the method will tend to predict low friction angles. The method suggested by *Kulhawy and Mayne (1990)* is an alternate relationship for clean, rounded, uncemented, quartz sands.

4.5 FINES CONTENT (*FC*)

The fines content, *FC*, in this report is estimated using two different methods, one from *Robertson and Wride (1998)* and the other, *Suzuki et al. (1998)* as presented below:

1) Robertson and Wride (1998)

$$I_C < 1.26: FC = 0$$
$$1.26 \leq I_C \leq 3.5: FC(\%) = 1.75 I_C^{3.25} - 3.7$$
$$3.5 < I_C: \ FC = 100\%$$

2) Suzuki et al. (1998)

$$FC(\%) = 2.8 I_C^{2.6}$$

where

I_c is the soil behaviour type index, calculated as in section 4.1

4.6 UNDRAINED SHEAR STRENGTH (s_u)

Estimation of undrained shear strength, s_u, from CPTU tests using corrected cone resistance is carried out using the following correlation from *Lunne et al. (1981)*:

$$S_u = \frac{(q_t - \sigma_{v0})}{N_{kt}}$$

where

N_{kt} is the empirical cone factor, which varies from *10* (*6* for very soft sensitive fine grained soils) to *20*. In this report 3 values are considered: *15*, *17.5* and *20*. N_{kt} tends to increase with increasing plasticity and decrease with increasing soil sensitivity. It decreases as B_q increases. (*Lunne et al., 1997*)

σ_{vo} = total overburden stress.

This report only presents the undrained shear strength data on soils with soil behaviour type index, I_c values greater than *2.60*.

The value of undrained shear strength, s_u to be used in analysis depends on the design problem. In general, the simple shear in the direction of loading often represents the average undrained strength. For larger, moderate to high risk projects, where high quality field and laboratory data may be available, site specific correlations should be developed based on appropriate and reliable values of s_u.

4.7 SENSITIVITY (S_t)

The sensitivity, S_t of clays is defined as the ratio of undisturbed peak undrained shear strength to totally remoulded undrained shear strength.

In this report S_t is calculated using two correlations developed by *Schmertmann (1978)* and *Mayne (2007)*.

1) Schmertmann (1978)

$$S_t = \frac{s_u}{s_{u(rem)}} = \frac{q_t - \sigma_v}{N_{kt}} \left(\frac{1}{f_s}\right)$$

where

$s_{u(rem)}$ is the remoulded undrained shear strength. It can be assumed equal to the sleeve resistance, f_s.

2) Mayne (2007)

$$S_t = \frac{0.073 \cdot (q_t - \sigma_{v0})}{f_s}$$

For relatively sensitive clays, $S_t > 10$, the value of f_s can be very low and not very accurate, hence the estimate of sensitivity should be used as a guide only.

4.8 SOIL UNIT WEIGHT (γ)

Soil unit weight, γ in this report is calculated by using one method for sands, considered under dry conditions and two methods for clays, considered under saturated conditions. These relationships are developed by *Mayne (2007)* and the equations are presented below:

1) Mayne (2007)

Dry unit weight for sands:

$$\gamma_{dry} = 1.89 \cdot log(q_{t1}) + 11.82$$

Saturated unit weight for clays method 1

$$\gamma_{sat} = 8.32 \cdot log(V_S) - 1.61 \cdot log(z)$$

Saturated unit for clays method 2

$$\gamma_{sat} = 2.60 \cdot log(f_s) + 15 \cdot G_s - 26.5$$

where

q_{t1} is the corrected cone resistance corrected for initial vertical effective stress and atmospheric pressure, calculated by the following formula:

$$q_{t1} = \frac{q_t}{\sqrt{\sigma'_{v0} \cdot \sigma_{atm}}}$$

z is the depth

V_s is the shear wave velocity, calculated as $V_S = 118.8 \cdot log\left(f_s\right) + 18.5$

G_s is the specific gravity of solids, typically between *2.40* and *2.90*

4.9 STATE PARAMETER (ψ)

The state parameter, ψ is defined as the difference between the current void ratio, *e* and the void ratio at critical state e_{cs}, at the same mean effective stress for granular soils.

The problem of evaluating the state parameter from CPTU response is complex and depends on several soil parameters, including shear stiffness, shear strength, compressibility and plastic hardening. (*Jefferies and Been, 2006*)

In this report, the state parameter is calculated based on five methods as follows:

1) Been et al. (1987)

$$\psi = -\frac{ln\left(\frac{Q_p}{k}\right)}{m}$$

and

$$Q_p = \left(\frac{3Q_t}{1+2K_0}\right)$$

where

Q_t is the normalized cone resistance

K_0 is the coefficient of lateral earth pressure

2) Shuttle and Jefferies (1998)

$$\psi = -\frac{ln\left(\frac{Q_p}{k}\right)}{m}$$

where

$$k = \left((3.79+1.12ln(I_r))(1+1.06(M-1.25))(1-0.30(N-0.2))(H/1000)^{0.326}(-1.55(\lambda-0.01))\right)^{1.45}$$

$$m = 1.45(1.04+0.46ln(I_r))(1-0.4(M-1.25))(1-0.30(N-0.2))(H/100)^{0.15}(1-2.21(\lambda-0.01))$$

where

Q_t is the normalised cone resistance

I_r is rigidity index

K_0 is the coefficient of lateral earth pressure

M is critical state ratio

N is dilation parameter

H is plastic hardening modulus;

λ is slope *CSL* line

3) Shuttle and Jefferies (1998)

The state parameter calculated according this third method is similar to state parameter calculated as presented in the second method, except for the rigidity index that is calculated as follows:

$$I_r = I_{r100}\left(\frac{P_a}{\sigma'_{v0}}\right)^{0.5}$$

where

- I_{r100} is rigidity index in reference pressure
- P_a is the reference pressure equal to 100 kPa
- σ'_{v0} is effective vertical overburden stress

4) Plewes (1992)

$$\psi = -\frac{ln\left(\frac{Q_p/(1-B_q)}{k'}\right)}{m'}$$

where

$$k' = M\left(3+\frac{0.85}{\lambda}\right)$$
$$m' = 11.9 - 13.3\lambda$$
$$\lambda = \frac{F_r}{10}$$

where

- Q_t is the normalised cone resistance
- B_q is pore pressure ratio
- K_0 is the coefficient of lateral earth pressure
- F_R is normalised friction ratio
- M is critical state ration

5) Been and Jefferies (1992)

$$\psi = -\frac{ln\left(\frac{Q_p/(1-B_q)}{k'}\right)}{m'}$$

where

$$k' = M\left(3+\frac{0.85}{\lambda}\right)$$
$$m' = 11.9 - 13.3\lambda$$
$$\lambda = \frac{1}{34-10I_C}$$

For high-risk projects a detailed interpretation of CPTU results using laboratory results and numerical modelling can be appropriate (e.g. *Shuttle* and *Cunning*, *2007*), although soil variability can complicate the interpretation procedure. For low risk projects and in the initial screening for high-risk projects there is a need for a simple estimate of soil state.

Plewes et al (1991) provided a mean to estimate soil state using the normalised soil behaviour type, *SBTn* chart suggested by *Jefferies and Davies (1991)*. *Jefferies and Been (2006)* suggested that soils with a state parameter less than *-0.05* are dilative at large strains.

4.10 IN SITU STRESS RATIO (K_0)

There are various estimations to determine in situ stress ratio, K_0, from CPTU in fine grained soils. In this report the methods suggested by *Mayne (2007)* and *Kulhawy and Mayne (1990)* are used, as given below:

1) Mayne (2007)

$$K_0 = (1 - sin\varphi')OCR^{sin\varphi'}$$

$$Max\ K_0 = K_p = \frac{(1 + sin\varphi')}{(1 - sin\varphi')}$$

$$K_0 = 0.192(\frac{q_t}{\sigma_{atm}})^{0.22}(\frac{\sigma_{atm}}{\sigma_{v0}})^{0.22}OCR^{0.27}$$

where

OCR is the overconsolidation ratio, calculated as presented in session *4.12*

2) Kulhawy and Mayne (1990)

$$K_0 = 0.1(\frac{q_t - \sigma_{v0}}{\sigma_{v0}'})$$

These approaches are generally limited to mechanically overconsolidated, fine grained soils. As considerable scatter exits in the database used for these correlations, in moderate to high risk projects further tests should be performed and these correlations must be considered only as a guide.

4.11 OVERCONSOLIDATION RATIO (OCR)

Overconsolidation ratio, *OCR* is defined as the ratio of the maximum past effective consolidation stress and the present effective overburden stress:

$$OCR = \frac{\sigma'_p}{\sigma'_{v0}}$$

This definition is appropriate for mechanically overconsolidated soils, where the only change has been the removal of overburden stress. For cemented and aged soils, the *OCR* may represent the ratio of the yield stress and the present effective overburden stress.

In this report σ'_p is calculated based on six methods as presented below:

1) Mayne (1995)

$$\sigma_p' = 0.33(q_t - \sigma_{v0})$$

2) Chen and Mayne (1996)

$$\sigma_p' = 0.53\Delta u$$

3) Mayne (2005)

$$\sigma_p' = 0.6(q_t - u_2)$$

4) Robertson (2009)

$$\sigma_p' = 0.25(Q_t^{1.25} - \sigma'_{v0})$$

5) Mayne (2005)

$$\sigma_p' = [\frac{0.192\left(\frac{q_t}{\sigma_{atm}}\right)^{0.125}}{(1 - sin\varphi')\left(\frac{\sigma_{v0}'}{\sigma_{atm}}\right)^{0.31}}]^{(\frac{1}{sin\varphi' - 0.27})}\sigma'_{v0}$$

6) Mayne (2007)

$$\sigma_p' = 0.101\sigma_{atm}^{0.102}(G_0)^{0.478}{\sigma'_{v0}}^{0.420}$$

For larger, moderate to high risk projects, where additional high-quality field and laboratory data may be available, site specific correlations should be developed based in consistent and relevant values of *OCR*.

4.12 SMALL STRAIN YOUNG'S MODULUS (E_0)

Deriving small strain undrained Young's modulus, E_0, from CPTU is difficult. There is insufficient data available to make a direct correlation and it is recommended that c_u should be derived, then E_U estimated as a rough order of value from one of the available correlations between E_U and c_u (*Meigh, 1987*).

In this report the small strain Young's modulus is derived as follows:

1) Defined from elastic theory:

$$E_0 = 2(1 + \nu)G_0$$

where

v is the Poisson ratio, equal to *0.2*
G_0 is the small strain shear modulus calculated by the formula given below:

$$G_0 = 1634\left(\frac{q_c}{\sqrt{\sigma'_{v0}}}\right)^{-0.75} q_c$$

2) Calculated based on the degree of loading, q_c, effective stress and reduction factor

$$E_0 = \alpha q_c$$

where

α is calculated from degree of loading, q_c, effective stress and reduction factor, given in *Figure 4.2*

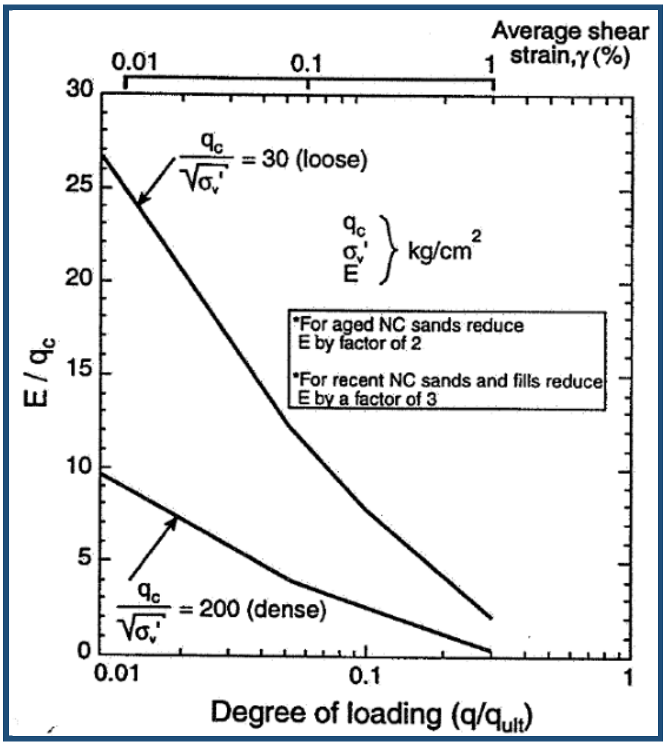

Figure 4.2: *Estimation of equivalent Young's modulus for sand based on degree of loading (Robertson, 1990)*

4.13 CONSTRAINED MODULUS (M)

Constrained Modulus, *M*, can be estimated by CPTU using the following empirical relationship:

$$M = \alpha_M (q_t - \sigma_{v0})$$

where

α_M varies with soil plasticity and natural water content for a wide range of fine-grained soils and organic soils. *Meigh (1987)* suggested that α_M lies in the range of *2 to 8*, whereas *Mayne (2001)* suggested the value of *5*.

Robertson (2001) suggested that α_M varies with Q_t, such that:

When $I_c > 2.2$ (fine grained soils) use: $\alpha_M = Q_t$ when $Q_t < 14$

$\alpha_M = 14$ when $Q_t > 14$

When I_c < *2.2* (coarse grained soils) use: $\alpha_M = 0.0188[10^{(0.55I_c+1.68)}]$

In this report the Constrained Modulus, *M*, is calculated after *Kulhawy and Mayne (1990)* using the equation below:

$$M = 8.25(q_t - \sigma_{v0})$$

Also, an alternative method is included in the results, developed by *Burns and Mayne (2002)* using the following relationship:

$$M = 0.02G_0$$

4.13.1 Equivalent Oedometer Coefficient of Compressibility (mv)

Equivalent oedometer coefficient of compressibility, m_v can be calculated directly by the Constrained Modulus, *M*, as follows:

$$m_v = \frac{1}{M}$$

4.14 SMALL STRAIN SHEAR MODULUS (G_0)

Elastic theory states that the small strain shear modulus, G_0, can be determined from the following equation:

$$G_0 = \rho v_s^2$$

where

- ρ is the mass density of the soil
- v_s is the shear wave velocity

In this report the small strain shear modulus, G_0, will be presented calculated by the two methods shown below, developed by *Rix and Stoke (1992)* and *BE, UB Rix* and *Stoke (1992)*, respectively.

$$G_0 = 1634(\frac{q_c}{\sqrt{\sigma'_{v0}}})^{-0.75} q_c$$

$$G_0 = \frac{\gamma_{bulk}}{g} v_s^2$$

where

- q_c is the net cone tip resistance in kPa
- σ'_{v0} is the effective initial vertical stress in kPa
- γ_{bulk} is the bulk density of the soil
- v_s is the shear wave velocity

This correlation of G_0 is applicable to all soil types.

4.14.1 Mass Density of Soil (ρ)

Mass density of soil, ρ, is defined as:

$$\rho = \frac{\gamma}{g}$$

where

γ is the elastic stiffness of the soils at shear strain less than 10^{-4} %, $\gamma<10^{-4}$ %.

4.15 HYDRAULIC CONDUCTIVITY (k)

An approximate estimate of soil hydraulic conductivity or coefficient of permeability, *k*, can be made from an estimate of soil behaviour type using the CPTU *SBT chart* as presented in the table below:

SBT Zone	SBT	Range of k (m/s)	SBT_n I_c
1	Sensitive fine grained	$3x10^{-10}$ to $3x10^{-8}$	NA
2	Organic soils-clay	$1x10^{-10}$ to $1x10^{-8}$	$I_c>3.60$
3	Clay	$1x10^{-10}$ to $1x10^{-9}$	$2.95<I_c<3.60$
4	Silt Mixture	$3x10^{-9}$ to $1x10^{-7}$	$2.60<I_c<2.95$
5	Sand Mixture	$1x10^{-7}$ to $1x10^{-5}$	$2.05<I_c<2.60$
6	Sand	$1x10^{-5}$ to $1x10^{-3}$	$1.31<I_c<2.05$
7	Dense sand to gravelly sand	$1x10^{-3}$ to 1	$I_c<1.31$
8	*Very dense/ stiff soil	$1x10^{-8}$ to $1x10^{-3}$	NA
9	*Very stiff fine grained soil	$1x10^{-9}$ to $1x10^{-7}$	NA

Table 4.2: *Estimated soils' permeability (k) based on the CPTU SBT chart by Robertson (2009)*

Table 4.2: *Estimated soils' permeability (k) based on the CPTU SBT chart by Robertson (2009)*

**Overconsolidated and/ or cemented*

The average relationship between soils' permeability, *k* and SBT_n I_c, shown in *Table 4.2*, can be represented by the following relationships:

When $1.0 < I_c \leq 3.27$ $\quad k = 10^{(0.952-3.04 I_c)}$

When $3.27 < I_c \leq 4.0$ $\quad k = 10^{(-4.52-1.37 I_c)}$

In this report, the hydraulic conductivity is estimated as a function of soil types from 2 CPTU classification charts, *Robertson et al. (1986)* and *Robertson et al. (1990)*, considering both minimum and maximum values.

The hydraulic conductivity (coefficient of permeability), *k*, values (minimum and maximum), defined after soils' behaviour type by *Robertson et al. (1986)* are presented in *Table 4.3*, below:

SBT Zone	**Soil Behaviour Type (SBT)**	**Range of hydraulic conductivity, *k (m/s)***
1	Sensitive fine grained	$3x10^{-9}$ to $3x10^{-8}$
2	Organic soils	$1x10^{-8}$ to $1x10^{-6}$
3	Clay	$1x10^{-10}$ to $1x10^{-9}$
4	Silty CLAY to CLAY	$3x10^{-9}$ to $1x10^{-8}$
5	Clayey SILT to silty CLAY	$1x10^{-8}$ to $1x10^{-7}$
6	Sandy SILT to clayey SILT	$1x10^{-7}$ to $1x10^{-6}$
7	Silty SAND to sandy SILT	$1x10^{-5}$ to $1x10^{-6}$
8	SAND to silty SAND	$1x10^{-5}$ to $1x10^{-4}$
9	SAND	$1x10^{-4}$ to $1x10^{-3}$
10	Gravelly SAND to SAND	$1x10^{-3}$ to 1
11	Very stiff fine grained	$1x10^{-8}$ to $1x10^{-6}$
12	SAND to clayey SAND	$3x10^{-7}$ to $3x10^{-4}$

Table 4.3: *Estimated soil permeability (k) based on SBT chart by Robertson et al. (1986)*

The hydraulic conductivity (coefficient of permeability), *k* values (min and max), defined after soils' behaviour type by *Robertson et al. (1990)* are presented in *Table 4.4*, below:

SBT Zone	**Soil Behaviour Type (SBT)**	**Range of hydraulic conductivity, *k (m/s)***
1	Sensitive fine grained	$3x10^{-9}$ to $3x10^{-8}$
2	Organic soils	$1x10^{-8}$ to $1x10^{-6}$
3	Clay	$1x10^{-10}$ to $1x10^{-9}$
4	Silt Mixture	$3x10^{-9}$ to $1x10^{-7}$
5	Sand Mixture	$1x10^{-7}$ to $1x10^{-5}$
6	Sand	$1x10^{-5}$ to $1x10^{-3}$
7	Gravelly sands to dense sands	$1x10^{-3}$ to 1
8	Very stiff sand to clayey sand	$1x10^{-8}$ to $1x10^{-6}$
9	Very stiff fine grained	$1x10^{-8}$ to $1x10^{-6}$

Table 4.4: *Estimated soils' permeability (k) based on SBT chart by Robertson et al. (1990).*

4.15.1 Coefficients of permeability (hydraulic conductivity, k_h, k_v)

The horizontal coefficient of permeability can be estimated from the following expression:

$$k_h = \frac{\gamma_w}{2.3\sigma'_{v0}} RR c_h$$

where

RR is the compression ratio in the overconsolidated range. It represents the strain per log cycle of effective stress during recompression and can be determined from laboratory consolidation tests (*$0.5x10^{-2}$ <RR<$2x10^{-2}$* was recommended by *Baligh and Levadoux*).

Robertson et al. (1992a) presented a summary of available data from dissipations and laboratory tests to determined k_h values (Figure 4.3), which can be used as a rough guide to estimate k_h from t_{50}.

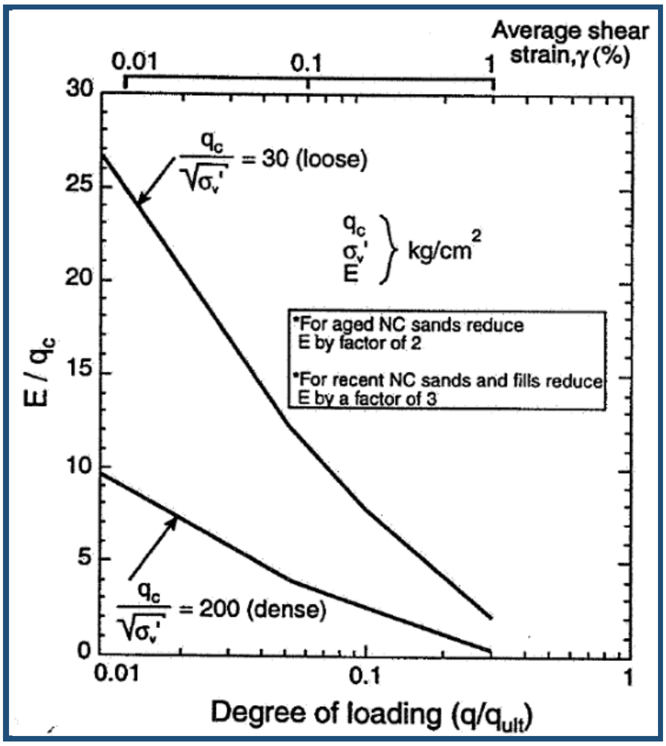

Figure 4.3: *Proposed chart for evaluating k_h from t_{50} for $10cm^2$ piezocones (Robertson et al., 1992a)*

Jamiolkowski et al. (1985) presented Table 4.4 which can be used to estimate k_v from k_h.

Based on the table below, the nature of clay is considered no macrofabric, or only slightly developed macrofabric, essentially homogenous deposits, so the ratio use is k_h/k_v equal to 1.5, unless it is specified otherwise from the clients.

Nature of clay	k_h/k_v
No macrofabric, or only slightly developed macrofabric, essentially homogeneous deposits	1 to 1.5
From fairly well to well developed macrofabric, e.g. sedimentary clays with discontinuous lenses and layers of more permeable material	2 to 4
Varved clays and other deposits containing embedded and more or less continuous permeable layers	3 to 15

Table 4.4: *Range of field values of k_h/k_v for soft clays (from Jamiolkowski et al., 1985).*

Estimation of soil permeability from CPTU and dissipation data is subject to much uncertainty and should be used as a guide only.

4.16 CONSOLIDATION CHARACTERISTICS

All the results of consolidation characteristics calculated using the formulas below are presented in *Dissipation Graphs, Appendix B*.

4.16.1 Rigidity Index (I_R)

The rigidity index, I_R, for fine grained soils is defined using the following formula, developed by *Mayne (2001)*:

$$I_R = \exp\left[\left(\frac{1.5}{M} + 2.925\right)\left(\frac{q_t - \sigma_{v0}}{q_t - u_2}\right) - 2.925\right.$$

where

M is the Cam-Clay constant, slope of the critical state line defined as:

$$M = \frac{6 sin\varphi'}{3 - sin\varphi'}$$

where

φ' is the internal friction angle.

The second method used to define the rigidity index, I_R, for fine grained soils is based on plasticity index and overconsolidation ratio, *OCR* and calculated after the relationship developed by *Keaveny and Mitchell (1986)* as follows:

$$I_R = \frac{\exp\left(0.0435(137 - PI)\right.}{[1 + \ln\{1 + 0.385(OCR - 1)^{3.2}\}]^{0.8}}$$

where

PI is the plasticity index of the soil, equal to 20.

OCR is the overconsolidation ratio of the soil

4.16.2 Coefficients of consolidation (c_h, c_v)

The coefficient of consolidation is interlinked with the hydraulic conductivity through the formula below:

$$c = \frac{kM}{\gamma_w}$$

where

M	is the 1-D constrained modulus relevant to the problem (i.e. unloading, reloading, virgin loading, etc)
γ_w	is the unit weight of water
k	is the hydraulic conductivity

In geotechnical practice it is very difficult to measure *c* and *k*, because due to soil anisotropy *c* and *k* have different values in the horizontal, c_h and k_h and vertical c_v and k_v directions. The relevant design values depend on drainage and loading direction.

The coefficient of consolidation can be estimated by measuring the dissipation or rate of decay of pore pressure with time after a stop in CPTU penetration. The coefficient of consolidation should be interpreted at *50%* dissipation, using the following formula:

$$c = (\frac{T_{50}}{t_{50}})r_0^2$$

where

T_{50}	is theoretical time factor
t_{50}	is measured time for *50%* dissipation
r_0	is penetrometer radius

In soils of very low permeability the time for dissipation can be decreased by using smaller diameter probes. A theoretical solution for these cases is given by *Teh and Houlsby (1991)* and it is compared with data from around the world by *Robertson et al. (1992)*, as shown in *Figure 4.3*.

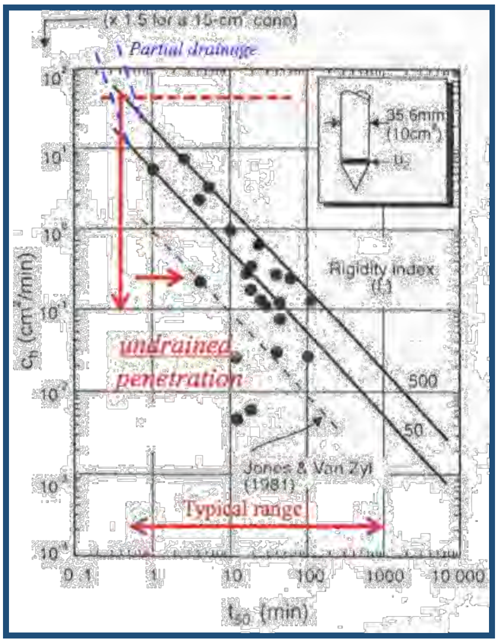

Figure 4.3: *Average laboratory c_h values and CPTU results*
(after Robertson et al. 1992, Teh and Houlsby theory shown as solid lines for I_R = 50 and I_R = 500).

c_h estimation is controlled by soil stress history, sensitivity, anisotropy, rigidity index (relative stiffness), fabric and history. In overconsolidated soils, the pore pressure behind the cone tip can be low or negative, results in dissipation data that can initially rise before decreasing to the equilibrium values. Care is required to ensure the dissipation test to end at the right moment of time, not stopped prematurely after the initial rise.

An approximate estimate of the coefficient of consolidation in the vertical direction can be obtained using the ratios of permeability in the horizontal and vertical directions given in the Section 4.15 on Hydraulic Conductivity, since:

$$c_v = c_h(\frac{k_v}{k_h})$$

Considering that k_h/k_v = 1.25 (from Table 4.4), the ratio c_h/c_v used for calculation purposes in this report is equal to 1.25.

For relative short dissipations, the dissipation results can be plotted on a square-root time scale. The gradient of the initial straight line in m, where:

$$c_h = (\frac{m}{M_T})^2 r^2 I_r^{0.5}$$

where

M_T is *1.15* for u_2 position and *10 cm²* cone (*r=1.78 cm*).

5.0 CPTU RESULTS APPLICATIONS

5.1 SOIL PROFILING AND APPLICATIONS IN GEOTECHNICAL DESIGN

5.1.1 Soil Behaviour Type

The major applications of CPTU are on *soil behaviour type and soil profiling*. Typically, the cone resistance, q_c is high in sands and low in clays, and the friction ratio, $R_f = f_s/q_t$ is low in sands and high in clays. The CPTU cannot be expected to provide accurate predictions of soil type based on *physical characteristics,* e.g. *grain size distribution*, but provides a guide to the *mechanical characteristics*, including: *strength*, *stiffness*, and *compressibility* of the soils, or the *soil behaviour type*, *SBT*.

The most commonly used CPTU soil behaviour type chart, suggested by *Robertson et al. (1986)* uses the basic CPTU measured parameters of cone resistance, q_c and friction ratio, R_f. The chart is global in nature and can provide reasonable predictions of soil behaviour type for CPTU testing. The expected overlap in some zones is modified in the interpretations of this report somewhat based on previous experience or local knowledge of the site.

Since both the penetration resistance and sleeve resistance increase with depth due to the increase in effective overburden stress, the CPTU data requires normalization for overburden stress for very shallow and/or very deep tests. A popular CPTU soil behaviour chart based on normalized CPTU data is firstly proposed by *Robertson (1990)*. The chart identifies general trends in ground response, such as: *increasing soil density*, *OCR*, *age* and *cementation* for granular soils, and *increasing stress history*, *OCR* and *soil sensitivity* for cohesive soils.

A more general normalized CPTU *SBT* chart, using large strain *soil behaviour* descriptions, proposed by *Robertson (2012)* is shown in *Figure 5.1*.

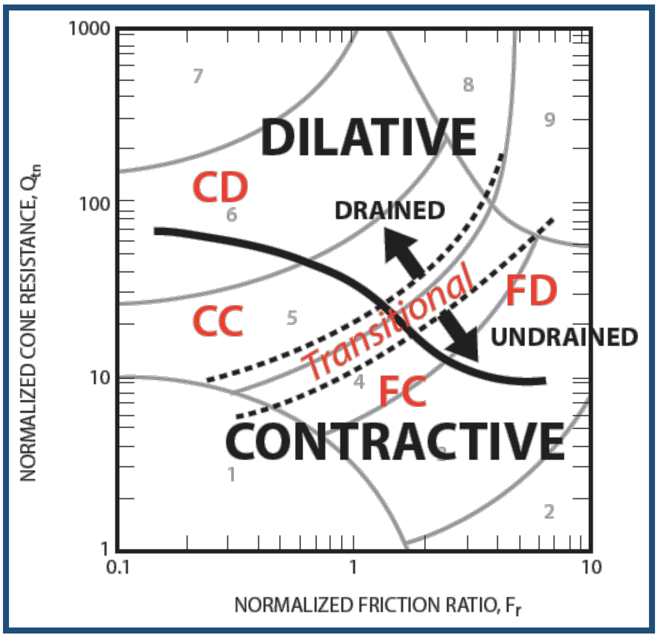

Figure 5.1: Normalized CPTU Soil Behaviour Type (SBT_n) chart, Q_{tn}-F_R using general large strain soil behaviour description (Robertson, 2012).

*

CD	is coarse grained dilative soil-predominately drained CPTU
CC	is coarse grained contractive soil-predominately drained CPTU
FD	is fine grained dilative soil-predominately undrained CPTU
FC	is fine grained contractive soil-predominately undrained CPTU

5.1.2 Soil Profiling

CPTU is an excellent test for soil profiling. The continuous monitoring of pore pressure during the cone penetration improves the soil stratigraphy descriptions. The pore pressure develops in response to the soil type being penetrated in the area where the pore pressure element is located. Soft, firm or stiff clays and contractive silts can show very high pore pressure. Very stiff overconsolidated clays and dilative silts can give very low or negative pore pressures same as very dense silty sands.

The thin layers of sand, or silt in a thick layer of clay, or thin layers of clay or silt in a thick layer of sand are easily distinguished during a CPTU test, which will give a response time sufficiently fast to observe pore pressure changes even in the very thin layers of soils (< *5mm*), depending on the response of soil to the advancing of cone.

The sandy soils tend to produce high cone resistance and low friction ratio, whereas soft clayey soils tend to produce low cone resistance and high friction ratio. Organic soils such as peat tend to have very low cone resistance and very high friction ratio. Soils with high horizontal stresses (*high OCR*) tend to have higher cone resistance and friction ratio.

CPTU is an excellent tool to classify the soils based on their behaviour type, and not based on grain size distribution.

The measurement of sleeve friction, f_s is often less reliable than the measurement of cone resistance, q_c (*Lunne et al., 1986*), but to overpass these problems pore pressure parameter ratio, B_q, and the classification charts based on it.

For more reliability in soil profiling, the soil interpretations in this report are carried out based on three parameters measured on site, cone resistance, sleeve friction and pore pressure and three derived geotechnical parameters soil behaviour type index for all soils, undrained shear strength for cohesive soils and relative density for granular soils.

Generally, soils that fall in zones *8*, *9* and *10* of *Robertson et al. (1986)* chart (*6* and *7* of *Robertson (1990)* chart) represent approximately drained penetration, whereas, soils in zones 1, 2, 3, 4, 5 and 6 of *Robertson et al. (1986)* chart (1, 2, 3 and 4 of *Robertson (1990)* chart) represent approximately undrained penetration. Soils in zones 7, 11 and 12 of *Robertson et al. (1986)* (5, 8 and 9 of *Robertson (1990)* chart) may represent partially drained penetration. The classification is often influenced by changes in *stress history*, *in situ stresses*, *sensitivity*, *stiffness*, *mineralogy*, etc. An advantage of pore pressure measurements during cone penetration is the ability to evaluate drainage conditions more directly. (*Lunne et al., 1997*)

The information about the rate and manner of excess pore pressures during the dissipations significantly helps the accurate classification in the corresponding depths of dissipation tests. In very stiff, overconsolidated clayey soils, the pore pressure behind the cone is very low and sometimes negative of the equilibrium pore pressure, u_0, whereas the pore pressure on the face of the cone is very large due to the large increase in normal stresses created by the cone penetration. When penetration is stopped in overconsolidated clays, pore pressure recorded behind the cone may initially increase before decreasing to the equilibrium pore pressure. The rise is caused by local equalization of the high pore pressure gradient around the cone.

Cone penetration in fine grained soils, such as clays and silts, is generally undrained. Cone penetration tests under undrained conditions generate high pore pressure and this reading is extremely useful, because it affects both cone resistance and sleeve friction measurements. These parameters should be corrected using the measured pore pressure.

CPTU in coarse gained soils, such as sandy or gravelly soils is generally drained. In these conditions there is no excess pore pressure generated as a result of cone penetration. Relative density has been used as the main parameter for description of sandy deposits.

5.1.3 Applications in geotechnical design

CPTU measured parameters are used to derive geotechnical parameters, which are the input in several geotechnical analyses. An alternate approach is to directly apply CPTU results to the geotechnical calculations.

As a guide, *Table 5.1* shows a summary of the applicability of CPTU results for direct design applications. The ratings shown in the table have been assigned based on current experience and represent a qualitative evaluation of the confidence level assessed to each design problem and general soil type. Details of ground conditions and project requirements can influence these ratings.

Type of soil	**Pile Design**	**Bearing Capacity**	**Settlement**	**Compaction Control**	**Liquefaction**
Sand	A-B	A-B	B-C	A-B	A-B
Clay	A-B	A-B	B-C	C-D	A-B
Intermediate Soils	A-B	B-C	B-C	B-C	A-B

***Table 5.1:** Perceived applicability of CPTU for various direct design problems.*

A is high
B is high to moderate
C is moderate
D is moderate to low

6.0 REFERENCES

ASTM D7400-14 (2015), “Standard and ISSMGE TC10 guideline”, by *Butcher, A. P. et al.*

Baldi et al. (1986) / Al-Hamoud and Wehr (2006), “Interpretation of CPTs and CPTUs; 2nd part: drained penetration of sands / Experience of vibrocompaction in calcareous sand of UAE”

Been at al. (1987), “Cone Penetration Test Calibration for Erksak (Beaufort Sea) Sand”, Canadian Geotechnical Journal, 24, 4, pp. 601-610

Been and Jefferies (1992), “Towards Systematic CPT Interpretation”, Proceedings Wroth Memorial Symposium, Thomas Telford, London, pp. 121–134

Boulanger and Idriss (2014), “CPT and SPT Based Liquefaction Triggering Procedures”, Report No. UCD/CGM-14/01, Centre of Geotechnical Modelling, Department of Civil and Environmental Engineering, College of Engineering, University of California at Davis

British Standard BS5930:1999, “Code of practice for site investigations”. BSI, 1999

British Standard BS EN ISO 22475-1:2012

Burns and Mayne (2002), “Analytical Cavity Expansion Critical State Model for Piezocone Dissipation in Fine Grained Soils, Soils and Foundations”, Vol. 42, No. 2, 2002

Houlsby and Teh (1998), “Analysis of the piezocone in clay”. Proceedings of the International Symposium on Penetration Testing, ISOPT-1, Orlando, 2, 777-83, Balkema Pub., Rotterdam

Idriss and Boulanger (2008), “Soil liquefaction during earthquakes”, Earthquake Engineering Research Institute, MNO-12

International Standard for Electrical Cone and Piezocone Penetration Test, ISO 22476-1:2012

International Standard, “Geotechnical Investigation and testing- field testing – part 1: electrical cone and piezocone penetration test”, ISO/ FDIS 22476-1.

Jamiolkowski et al. (2001), Evaluation of relative density in shear strength of sands from cone penetration tests (CPT) and flat dilatometer (DMT), Soil Behaviour and Soft Ground Construction (GSP 119), American Society of Civil Engineers, Reston, Va., 2001, pp. 201-238

Jefferies and Davies (1991), "Soil classification by the cone penetration test": Discussion. Canadian Geotechnical Journal, 28(1), 173-6

Jefferies and Been (2006), "Soil liquefaction: a critical state approach", Taylor and Francis.

Jones and Rust (1995), "Piezocone settlement prediction parameters for embankments on alluvium". Proceedings of the International Symposium on Cone Penetration Testing, CPT '95, Linköping, Sweden, 2, 501-8, Swedish Geotechnical Society

Kulhawy and Mayne (1990) "Manual on estimating soil properties for foundation design". Electric Power Research Institute, EPRI, August, 1990.

Keaveny and Mitchell (1986), "Strength of Fine-Grained Soils Using the Piezocone," Use of In Situ Tests in Geotechnical Engineering (GSP 6), American Society of Civil Engineers, Reston, Va., 1986, pp. 668–699

Lord, Clayton and Mortimore (2002), "Engineering in chalk". Ciria Guide C574.

Lunne and Kleven (1981), "Role of CPT in North Sea foundation engineering". Session at the ASCE National Convention: Cone Penetration Testing and Materials, St. Louis, 76-107, American Society of Engineers (ASCE).

Lunne and Christophersen (1983), "Interpretation of cone penetrometer data for offshore sands". Proceedings of the Offshore Technology conference, Richardson, Texas, Paper No. 4464.

Lunne, Robertson and Powell (1997), "Cone Penetration testing in Geotechnical Practice". Blackie.

Mayne and Rix (1995) / Lune et al. (1997), "Gmax-qc relationships for clays", Geotechnical Testing Journal, ASTM, 16 (1), pp. 54-60/ CPT in Geotechnical Practice (1997)

Mayne (2001), "Stress-Strain-Strength-Flow Parameters from Enhanced In-Situ Tests", International Conference on In-Situ Measurement of Soil Properties and Case Histories, Indonesia, 2001, pp. 27–48

Mayne and Campanella (2005), "National Cooperative Highway Research Program", Synthesis 368 (2007)

Mayne (2007), "National Cooperative Highway Research Program", Synthesis 368 (2007)

Mitchell and Gardner (1975), "In situ measurement of volume change characteristics". Proceedings of the ASCE Specialty Conference on In Situ Measurements of Soil Properties, Raleigh, North Carolina, 2, 279-345, American Society of Engineers (ASCE)

Rix and Stokoe (1992), “Correlation of Initial Tangent Modulus and Cone Resistance”, Proceedings of the International Symposium on Calibration Chamber Testing, Potsdam, New York, 1991, pp. 351-362, Elsevier

Robertson and Campanella (1983) “Interpretation of cone penetrometer test: Part 1: Sand”. Canadian Geotechnical Journal, 20(4), 718-33

Robertson, Campanella, Gillespie and Greig (1986), “Use of piezometer cone data”. Proceedings of the ASCE Specialty Conference In Situ ’86: Use of In Situ Tests in Geotechnical Engineering, Blacksburg, 1263-80, American Society of Engineers (ACE)

Robertson (1990), “Soil classification using the cone penetration test”. Canadian Geotechnical Journal, 27(1), 151

Robertson and Fear (1995), “Liquefaction of sands and its evaluation. IS TOKYO ‘95”. First International Conference on Earthquake Geotechnical Engineering, Keynote Lecture, November, 1995

Robertson and Wride (1998), “Evaluating cyclic liquefaction potential using the cone penetration test”. Can. Geotech. J. Vol. 35

Robertson (2010), “Soil behaviour type from the CPT: an update”, Gregg Drilling and Testing Inc. Signal Hill, California, USA, CPT 10, paper 2-56

Robertson (2015), “Guide to Cone Penetration Testing”, 6th Edition (2015)

Senneset and Janbu (1985), “Shear strength parameters obtained from static cone penetration tests. Strength Testing of Marine Sediments; Laboratory and In Situ Measurements”. Symposium, San Diego, 1984, ASTM Special technical publication, STP 883, 41-54

Senneset, Sandven and Janbu (1989), “The evaluation of soil parameters from piezocone tests”. Transportation Research Record, No. 1235, 24-37

Schmertmann (1978), “Guidelines for cone penetration test, performance and design”, US Federal Highway Administration, Washington, DC, Report, FHWA-TS-78-209, 145

Shuttle and Jefferies (1998), “Dimensionless and unbiased CPT interpretation in sand”, International Journal for Numerical and Analytical Methods in Geomechanics, 22, pp. 351-391.

Suzuki, Tokimatsu, Taya, and Kubota (1995), “Correlation between CPT data and dynamic properties of in situ frozen samples”. Proceedings of the Third International Conference on Recent Advances in Geotechnical Earthquake Engineering and Soil Dynamics, St. Louis, 1, 249-52, University of Missouri Rolla.

APPENDIX A

APPENDIX A1 – Project Summary Sheet

Piezocone Tests Summary Sheet

HOLE ID	Final Depth (m)	Date of Test	Cone Used	Test Remarks
CPT 202	15.02	09/07/2019	DP15-CFPTxy.71007	Test refused on inclination.
CPT 203	7.07	10/07/2019	DP15-CFPTxy.70102	Test refused on tip resistance.
CPT 206	8.91	09/07/2019	DP15-CFPTxy.70102	Test refused on tip resistance.

Dissipation Tests Summary Sheet

HOLE ID	Final Depth (m)	Date of Test	Cone Used	Test Remarks
CPT 202	6.00	09/07/2019	DP15-CFPTxy.71007	Test OK.
CPT 203	4.00	10/07/2019	DP15-CFPTxy.70102	Test OK.
CPT 206	3.00	09/07/2019	DP15-CFPTxy.70102	T50 not reached.

Piezocone Tests Summary Sheet

HOLE ID	Northing	Easting	Elevation
CPT 202	392345.90	215691.00	132.45
CPT 203	392595.10	215609.50	159.70
CPT 206	392355.90	215502.20	179.70

APPENDIX A2 – CPT Rig Datasheet

RIGS

20 TONNE CPT TRACK MOUNTED RIG (CPT012)

CPT012 (Bob) is a 20 Tonne tracked crawler rig. Its relatively high weight serves as a counterweight to provide the required penetrative force when testing. This machine is ideal for soft, boggy sites where access can be tricky. Fitted with three levelling jacks, the crawler can be levelled exactly horizontally and furthermore, it assures its stability during testing. All movements of the rig are driven hydraulically using a remote control thus allowing 100% accuracy over positions.

CPT RIG DETAILS	
DRIVE SYSTEM:	TRACKED RIG
TOTAL WEIGHT:	20 TONNES
CPT RAM THRUST CAPACITY:	20 TONNES
MAXIMUM PENETRATION:	30-40M DEPENDING ON THE GROUND CONDITIONS
PERFORMANCE RATES:	100-150M OF TESTING A DAY, DEPENDING ON ACCESS TO POSITIONS
TYPICAL SITES FOR THIS RIG:	SOFT, BOGGY SITES. THE RIG HAS LOW GROUND BEARING PRESSURE.



CPT RIG DIMENSIONS

IN SITU SITE INVESTIGATION
Penetration House, 13 Vale Road, Battle,
E Sussex, TN33 0HE, United Kingdom

T: +44 (0) 845 862 0566
F: +44 (0) 845 862 0564
E: info@insitusi.com

IN SITU SITE INVESTIGATION INSITUSI.COM

APPENDIX A3 – Cone Datasheet

Geo Point Systems bv

Rijksstraatweg 22F
2171 AL Sassenheim
Tel. : +31 71 301 92 51
Fax : +31 71 301 92 52
E-mail : info@geopoint.nl
ING bank : 68.23.01.396
Postbank : 5226758
BTW nr. : NL806331677B01

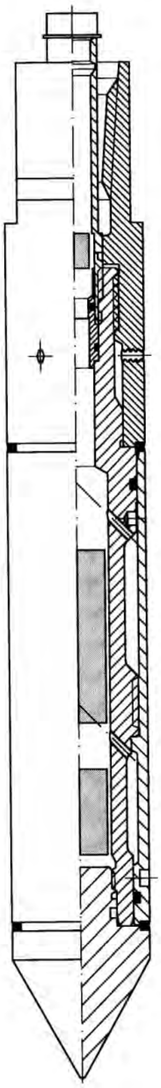

SPECIFICATIONS
S15 SERIES
ELECTRICAL CONES

The electronic subtraction cones have been developed to address the durability problems inherent in other cone designs. The unit consists of a single element temperature compensated strain gauge transducer for measuring both cone resistance and local sleeve friction. This design is therefore more robust than a compression type cone. The cone support electronics package is located directly behind the transducer. The precision strain gauge amplifiers and power supply eliminate the effects of cable resistance on the measurements. A standard subtraction cone is capable of measuring simultaneously the following channels: Tip, Local friction, Pore pressure, Temperature and Inclination.

GENERAL SPECIFICATIONS

Cone Tip Section Area	1,500 mm2
Friction Sleeve Surface	22,500 mm2
Total Length	325 mm
Weight	4200 g
Power Supply	± 15 VDC, 100 mA.
Output	0 – 10 VDC*
Working Temperature	0 - 60˚C
Storage Temperature	- 40 to + 85˚C
Connector	Lemo 10 pins (others on request)

TIP RESISTANCE

Range	100/150* kN
Accuracy	0.25 % FS
Maximum Load	150 % of range
Cone Area Ratio	0.75

LOCAL SLEEVE FRICTION

Range	100/150* kN
Accuracy	0.50 % FS
Maximum Load	150 %
Sleeve Area Ratio	1.0 (EA)

PORE PRESSURE

Range	1/2/5/10* MPa
Accuracy	0.5 % FS
Maximum Load	150 % of range

INCLINATION

Range	25 ˚ (biaxial)
Accuracy	< 2 ˚

All our equipment complies with the ISSMGE, ASTM, DIN and NEN Standards.

**Other output and voltage ranges available on request. Loadcells may be calibrated for lower ranges.*

APPENDIX A4 – Cone Calibration Certificate

WWW.GOUDA-GEO.COM
Down to Earth

Gouda Geo-Equipment B.V.
Satellietbaan 8
2181 MH Hillegom
The Netherlands

Tel. + 31 (0)715.318.475
E-mail: info@gouda-geo.com

Certificate of Calibration

Certificate No. CMI 19.03.2291

Instrument

Instrument Type:	Electrical Subtraction Cone	Calibration Result: Certified	
Manufacturer:	GGE		
Model No.:	DP15 CFPTxy	Date Calibrated:	22-3-2019
Serial No.:	71007	Next Due Date:	22-9-2019

Used Calibration Procedure: GGECP004, ISO22476 — Location: Hillegom (The Netherlands)

Customer

Insitu

Calibration Instruments

Instrument Type: CPT Logger	Instrument Type: CPT Logger	Instrument Type: Load-cell + amplifier
Manufacturere: Gouda Geo Equipment	Manufacturere: Gouda Geo Equipment	Manufacturer: Futek
Model No.: A	Model No.: A	Model No.: LCF500 + CSG110
Serial No.: 3010	Serial No.: 3014	Serial No.: 232191 + 573307
Accuracy: 0.01% + 2 Counts	Accuracy: 0.01% + 2 Counts	Accuracy: 0.060%
Date Calibrated: December, 2018	Date Calibrated: December, 2018	Date Calibrated: November 16, 2018
Next Due Date: Juni, 2019	Next Due Date: Juni, 2019	Next Due Date: November 16, 2019
Calibrated By: Manufacturer	Calibrated By: Manufacturer	Calibrated By: Futek
Traceability: CMI19.03.2274	Traceability: CMI19.03.2275	Traceability: 1811160068

Calibration Conditions

Environmental conditions whilst performing the calibration:

Ambient Temperat	22,4 ºC
Relative Humidity:	36,4 %

Condition of Calibrated Apparatus when Received: Fair

Measurement Parameters

zero value	252 mV	zero value	252 mV
Full scale	4014 @ 150kN	Full scale	4010 @ 150kN

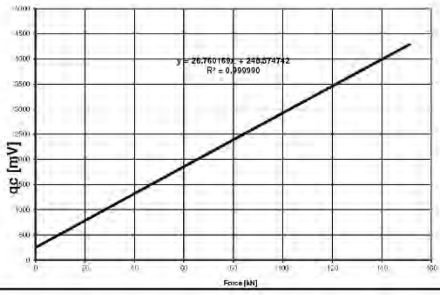

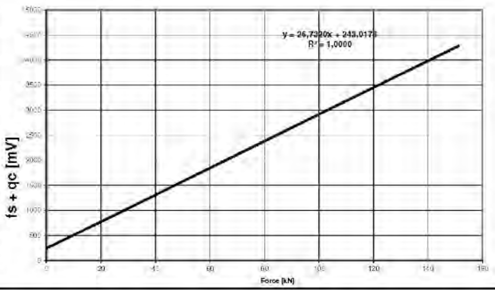

Remarks

Data "As Received" = "As Left" unless otherwise noted. Calibration data for this item was derived from one or more of the following sources: the Nederlands Meetinstituut (NMI) or other national laboratory, a natural physical constant, or a ratio technique. The data is on file at the NMI. This calibration is compliant with Gouda Geo-Equipment's internal quality system, internal calibration procedure and meets the requirements of standard ISO22476.
The Calibration Interval will vary from customer use and different conditions. All calibrations are verified at a moment in time; and confirmed within controlled temperature and humidity specified standards. Gouda Geo-Equipment is not responsible for future calibrations. Improper use of the apparatus (e.g. dropping) may cause loss of calibration.

Calibration performed by:

Ing. Johan van Stijn
(Senior Engineer)

Approved by:

Ir. Rob Hogervorst
(Technical Director)

WWW.GOUDA-GEO.COM
Down to Earth

Gouda Geo-Equipment B.V.
Satellietbaan 8
2181 MH Hillegom
The Netherlands

Tel. + 31 (0)715.318.475
E-mail: info@gouda-geo.com

Certificate of Calibration

Certificate No. CMI 19.02.2244

Instrument

Instrument Type: Electrical Subtraction Cone
Manufacturer: GGE
Model No.: DP15 CFPTxy
Serial No.: 70102

Calibration Result: Certified
Date Calibrated: 22-2-2019
Next Due Date: 22-8-2019

Used Calibration Procedure: GGECP004, ISO22476
Location: Hillegom (The Netherlands)

Customer

In Situ

Calibration Instruments

Instrument Type: Volt/mA Loop Calibrator
Manufacturere: Fluke
Model No.: 715
Serial No.: 9408105
Accuracy: 0.01% + 2 Counts
Date Calibrated: February 27, 2018
Next Due Date: February 27, 2019
Calibrated By: Manufacturer
Traceability: 2040545

Instrument Type: Load-cell + amplifier
Manufacturer: Futek
Model No.: LCF500 + CSG110
Serial No.: 232191 + 573307
Accuracy: 0.060%
Date Calibrated: November 16, 2018
Next Due Date: November 16, 2019
Calibrated By: Futek
Traceability: 1811160068

Calibration Conditions

Environmental conditions whilst performing the calibration:
Ambient Temperat 18,7 ºC
Relative Humidity: 40,3 %

Condition of Calibrated Apparatus when Received: Fair

Measurement Parameters

zero value	250 mV	zero value	251 mV
Full scale	3993 @ 150kN	Full scale	4016 @ 150kN

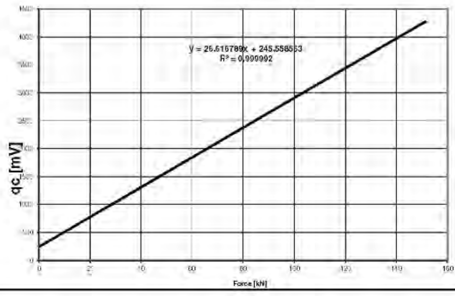

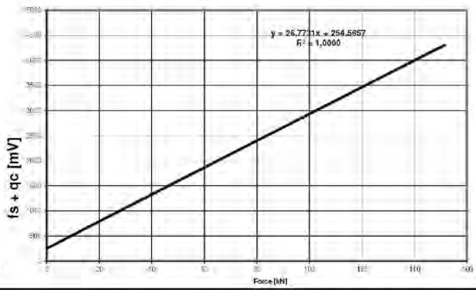

Remarks

Data "As Received" = "As Left" unless otherwise noted. Calibration data for this item was derived from one or more of the following sources: the Nederlands Meetinstituut (NMI) or other national laboratory, a natural physical constant, or a ratio technique. The data is on file at the NMI. This calibration is compliant with Gouda Geo-Equipment's internal quality system, internal calibration procedure and meets the requirements of standard ISO22476.
The Calibration Interval will vary from customer use and different conditions. All calibrations are verified at a moment in time; and confirmed within controlled temperature and humidity specified standards. Gouda Geo-Equipment is not responsible for future calibrations. Improper use of the apparatus (e.g. dropping) may cause loss of calibration.

Calibration performed by:
Ing. Johan van Stijn
(Senior Engineer)

Approved by:
Ir. Rob Hogervorst
(Technical Director)

APPENDIX A5 – Symbol List

English

- a is area ratio of the cone ($= A_n / A_c$)
- A is area
- A_c is projected area of the cone
- A_n is cross sectional area of load cell or shaft
- A_s is area of friction sleeve
- A_{sb} is bottom end area of friction sleeve
- A_{st} is top end area of friction sleeve
- B_q is pore pressure parameter ($= (u_2 - u_0) / (q_t - \sigma_{v0})$)
- c_h is horizontal coefficient of consolidation
- c_v is vertical coefficient of consolidation
- D is diameter
- D_r is relative density ($= \frac{e_{max} - e}{e_{max} - e_{min}} x100\%$)
- e is void ratio
- e_{max} is maximum void ratio
- e_{min} is minimum void ratio
- E is Young's modulus
- f_s is unit sleeve friction resistance
- f_t is sleeve friction corrected for pore pressure effects
- F_s is total force acting on friction sleeve
- F_R is normalized friction ratio ($= f_s / (q_t - \sigma_{v0})$)
- FoS is factor of safety
- FC is fines content
- g is acceleration due to gravity
- G_0 is initial or maximum shear modulus, shear stiffness
- I_c is soil behavior type index
- I_r is rigidity index ($= G / s_u$)
- I_p is plasticity index
- k is coefficient of permeability
- k_h is coefficient of permeability in horizontal direction
- k_v is coefficient of permeability in vertical direction
- K_0 is coefficient of earth pressure at rest ($= \sigma'_{h0} / \sigma'_{v0}$)
- L is length
- m_v is coefficient of volume change
- M is constrained deformation modulus
- M7.5 is earthquake magnitude of 7.5 Richter scale
- N is number of blows of SPT
- N_{60} is SPT energy ratio
- N_k is cone factor
- N_{ke} is cone factor
- N_{kt} is cone factor
- $N_{\Delta u}$ is cone factor
- p_a is reference stress ($= 100\ kPa$)
- q_c is measured cone resistance
- q_e is effective cone resistance ($= q_t - u_2$)
- q_n is net cone resistance ($= q_t - \sigma_{v0}$)
- q_t is corrected cone resistance ($= q_c - (1 - a)u_2$)
- Q_c is total force acting on the cone
- Q_t is normalized cone resistance ($= q_t - \sigma_{v0} / \sigma'_{v0}$)

R_f is friction ratio $(= \left(f_t/q_t\right) x100\%$ or alternatively $= \left(f_t/q_t\right) x100\%)$
s_u is undrained shear strength
s_{ur} is remoulded undrained shear strength
S_t is sensitivity
t is time
t_{50} is time for 50% dissipation of excess pore water pressure
T_{50} is time factor at $U = 50\ \%$
u is pore water pressure
u_0 is in situ pore pressure
u_1 is pore pressure measured on the cone
u_2 is pore pressure measured behind the cone
u_3 is pore pressure measured behind sleeve friction
Δu is excess pore water pressure
U is normalized excess pore pressure
V_s is shear wave velocity
z is depth

Greek

α is constant
α is cone roughness
β is constant
$β_1$ is the angle between the vertical axis and the projection of the axis of the CPTU on a vertical plane, in degrees
$β_2$ is the angle between the vertical axis and the projection of the axis of the CPTU on a vertical plane that is perpendicular to the plane of angle β_1, in degrees
γ is unit weight of soil
$γ_w$ unit weight of water
Δ is change
Δu is excess pore pressure $(= u - u_0)$
μ is Poisson's ratio
ρ is density
ψ is state parameter
σ, σ' is normal stress (total, effective)
$σ_h$, $σ_h$' is horizontal stress (total, effective)
$σ_v$, $σ_v$' is horizontal stress (total, effective)
$σ_{v0}$,$σ_{v0}$' is overburden stress (total, effective)
$τ_{av}$ is average cyclic shear stress
$τ_{cy}$ is cyclic shear stress
φ' is effective friction angle

APPENDIX A6 – Abbreviations

ASTM	American Society for Testing and Materials
CPTU	Cone Penetration Test with Pore Pressure Measurement (Piezocone Test)
CRR	Cyclic Resistance Ratio
CSR	Cyclic Stress Ratio
GWT	Ground Water Table
NC	Normally Consolidated
OC	Over consolidated
OCR	Over consolidation Ratio
PL	Limit Pressure
SDMT	Seismic Dilatometer Marchetti
SPT	Standard Penetration Test
TC	Technical Committee

APPENDIX A7 – Glossary

CPT
Cone Penetration Test.

Cone
The part of the cone penetrometer on which the end bearing is developed.

Cone Penetrometer
The assembly containing the *cone*, *friction sleeve*, any other sensors and measuring systems, as well as the connections to the *push-rods.*

Cone resistance, q_c
The total force acting on the cone, Q_c, divided by the projected area of the cone, A_c. $q_c = Q_c / A_c$

Corrected cone resistance, q_t
The *cone resistance*, q_c corrected for pore water pressure effects.

Corrected sleeve friction, f_t
The *sleeve friction* corrected for pore water pressure effects on the ends of the *friction sleeve*.

Data acquisition system
The system used to measure and record the measurements made by the *cone penetrometer*.

Dissipation Test
A test when the decay of the pore water pressure is monitored during a pause in penetration.

Filter element
The porous element inserted into the cone penetrometer to allow transmission of the pore water pressure to the pore pressure sensor, while maintaining the correct profile of the *cone penetrometer*.

Friction ratio, R_f
The ratio, expressed as a percentage of the *sleeve friction*, f_s, to the *cone resistance*, q_c, both measured at the same depth.

Friction reducer
A local enlargement on the push-rod surface, placed at a distance above the cone penetrometer, and provided to reduce the friction on the *push-rods*.

Friction sleeve
The section of the *cone penetrometer* upon which the *sleeve friction* is measured.

Normalized cone resistance, Q_c or Q_t
The *cone resistance* expressed in a non-dimensional form and taking account of stress changes *in situ*, $Q_c = (q_c - \sigma_{v0}) / \sigma'_{v0}$, or when the *corrected cone resistance* is used $Q_t = (q_t - \sigma_{v0}) / \sigma'_{v0}$. Where σ_{v0} and σ'_{v0} are the total and effective vertical stress respectively.

Net cone resistance, q_n
The *corrected cone resistance* minus the vertical total stress. $q_n = q_t - \sigma_{v0}$

Normalized friction ratio, F_r
The *sleeve friction* normalized by the *net cone resistance*.

Piezocone
A *cone penetrometer* containing a pore pressure sensor.

Pore pressure, *u*
The pore pressure generated during penetration and measured by a pore pressure sensor, u_1 when measured on the cone, u_2 when measured just behind the cone and u_3 when measured just behind the friction sleeve.

Pore pressure ratio, B_q
The *net pore pressure* normalized with respect to the *net cone resistance*.

Push-rods
The thick-walled tubes or rods used for advancing the cone penetrometer.

Rig machine
The equipment which pushes the cone penetrometer and rods into the ground.

Sleeve friction, f_s
The total frictional force acting on the *friction sleeve*, F_s, divided by its *surface area*, A_s. $f_s = F_s / A_s$

APPENDIX A8 – Soils Description Tables

GRANULAR SOILS (Sands and Gravels)

Description	Relative Density D_r (%)	SPT N value, N_{SPT}
Very Loose	0 – 15	0 - 4
Loose	15 – 35	4 - 10
Medium Dense	35 – 65	10 - 30
Dense	65 – 85	30 - 50
Very Dense	>85	>50

COHESIVE SOILS (Clays and Silts)

Term based on measurement	Undrained Shear Strength Classification, s_u (kPa)
Extremely low	<10
Very low	10 - 20
Low	20 - 40
Medium	40 - 75
High	75 - 150
Very high	150 - 300
Extremely high	>300

APPENDIX A9 – Pictures from Site Works

APPENDIX B

Cone Penetration Measured Parameters and Geotechnical Derived Parameters

IN SITU SITE INVESTIGATION Working with: geotechnical

CPT LOG 01

PointID **CPT 202**

CLIENT : Geotechnical Engineering PROJECT : A417 Missing Link LOCATION : Gloucester PROJECT No. : 1190295	EASTING : 392345.9 m NORTHING : 215691.0 m ELEVATION : 132.45 m OD CHECKED BY : LD TERMINATION REASON : Refusal	Remark: Test refused on inclination.	SHEET : 1 OF 2 STATUS : Final TEST DATE : 09/07/2019 PLOT DATE : 06/04/2020 METHOD : ISO 22476-1:2012

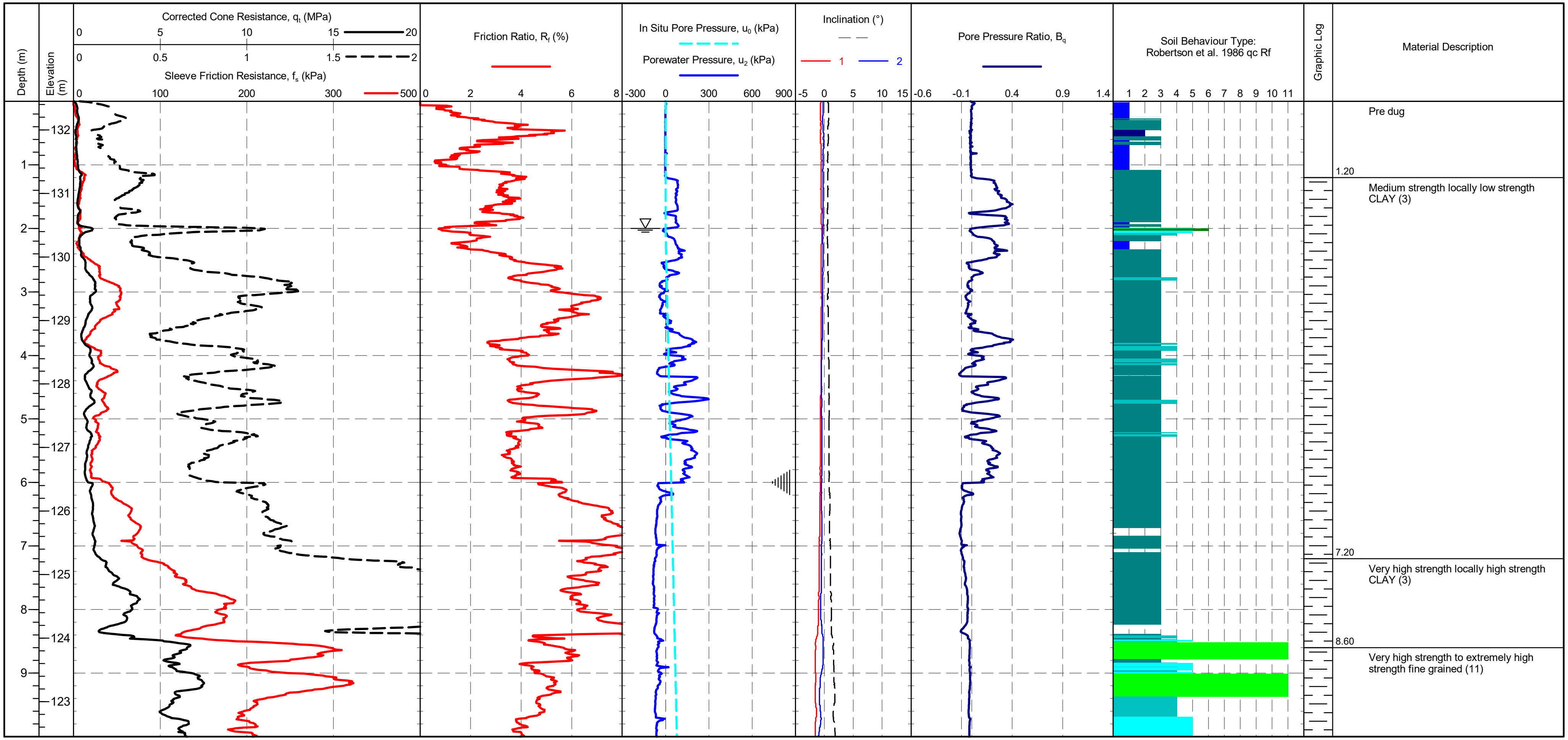

CONE ID	:	DP15-CFPTxy.71007
CONE MODEL	:	DP15-CFPTxy
CONE AREA	:	15cm^2
CONE AREA RATIO	:	0.85
FILTER POSITION	:	u2
FILTER TYPE	:	HDPE

TEST TYPE	:	TE2
APPLICATION CLASS	:	2
RIG	:	CPT 012
OPERATOR	:	AL
FRICTION REDUCER	:	None
WEATHER	:	Overcast & Mild

CPTU ZERO VALUES

Transducer	Pre	Post	Difference
Tip	0.0972 MPa	0.125 MPa	
Sleeve	0.0533 kPa	0.0565 kPa	
Pore Pressure 2	0.0183 kPa	-0.0374 kPa	
X-Y Inclinometer			

METHOD: Robertson et al. 1986 qc Rf

1 - Sensitive fine grained material	5 - Clayey SILT to silty CLAY	9 - SAND
2 - Organic material	6 - Sandy SILT to clayey SILT	10 - Gravelly SAND to SAND
3 - CLAY	7 - Silty SAND to sandy SILT	11 - Very stiff fine grained
4 - Silty CLAY to CLAY	8 - SAND to silty SAND	12 - SAND to clayey SAND

Groundwater Level

Dissipation Test

IN SITU SITE INVESTIGATION Working with: geotechnical

CPT LOG 01

PointID
CPT 202

CLIENT : Geotechnical Engineering PROJECT : A417 Missing Link LOCATION : Gloucester PROJECT No. : 1190295	EASTING : 392345.9 m NORTHING : 215691.0 m ELEVATION : 132.45 m OD CHECKED BY : LD TERMINATION REASON : Refusal	Remark: Test refused on inclination.	SHEET : 2 OF 2 STATUS : Final TEST DATE : 09/07/2019 PLOT DATE : 06/04/2020 METHOD : ISO 22476-1:2012

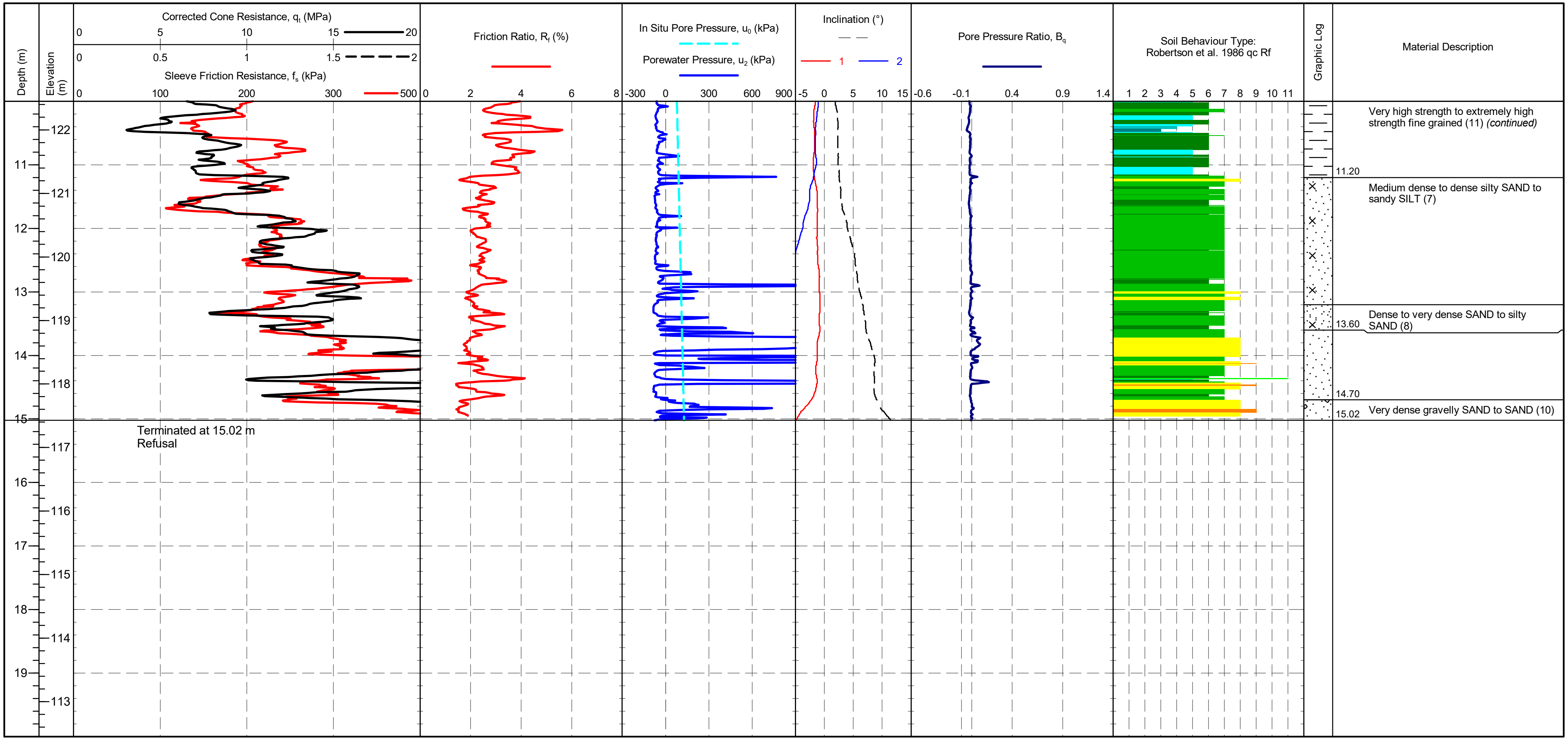

CONE ID : DP15-CFPTxy.71007 CONE MODEL : DP15-CFPTxy CONE AREA : 15cm² CONE AREA RATIO : 0.85 FILTER POSITION : u2 FILTER TYPE : HDPE	TEST TYPE : TE2 APPLICATION CLASS : 2 RIG : CPT 012 OPERATOR : AL FRICTION REDUCER : None WEATHER : Overcast & Mild	CPTU ZERO VALUES	METHOD: Robertson et al. 1986 qc Rf 1 - Sensitive fine grained material 2 - Organic material 3 - CLAY 4 - Silty CLAY to CLAY 5 - Clayey SILT to silty CLAY 6 - Sandy SILT to clayey SILT 7 - Silty SAND to sandy SILT 8 - SAND to silty SAND 9 - SAND 10 - Gravelly SAND to SAND 11 - Very stiff fine grained 12 - SAND to clayey SAND	Groundwater Level Dissipation Test

CPTU ZERO VALUES

Transducer	Pre	Post	Difference
Tip	0.0972 MPa	0.125 MPa	
Sleeve	0.0533 kPa	0.0565 kPa	
Pore Pressure 2	0.0183 kPa	-0.0374 kPa	
X-Y Inclinometer			

CPT LOG 02

IN SITU SITE INVESTIGATION Working with: geotechnical

PointID
CPT 202

CLIENT : Geotechnical Engineering PROJECT : A417 Missing Link LOCATION : Gloucester PROJECT No. : 1190295	EASTING : 392345.9 m NORTHING : 215691.0 m ELEVATION : 132.45 m OD CHECKED BY : LD TERMINATION REASON : Refusal	Remark: Test refused on inclination.	SHEET : 1 OF 2 STATUS : Final TEST DATE : 09/07/2019 PLOT DATE : 06/04/2020 METHOD : ISO 22476-1:2012

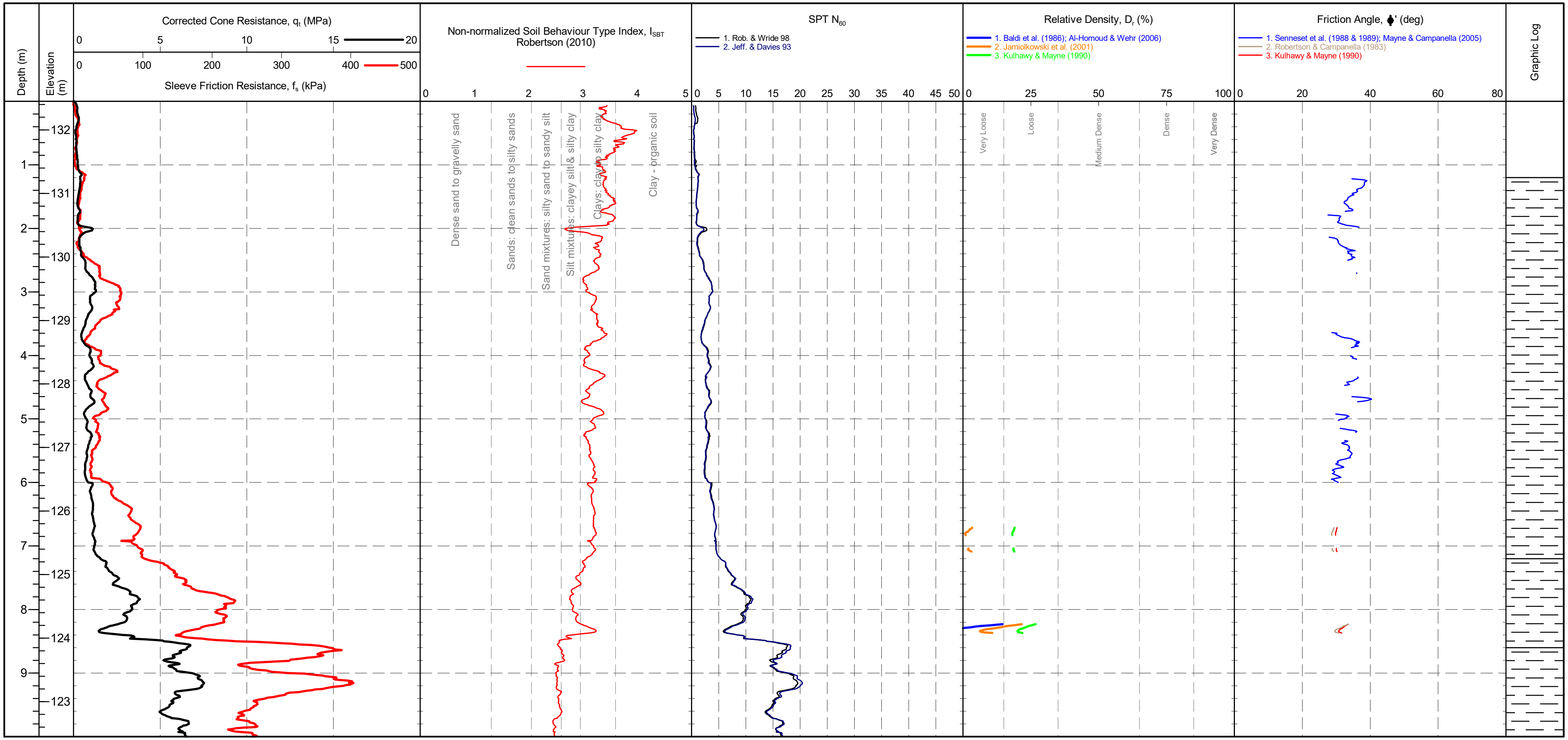

CONE ID	: DP15-CFPTxy.71007
CONE MODEL	: DP15-CFPTxy
CONE AREA	: 15cm^2
CONE AREA RATIO	: 0.85
FILTER POSITION	: u2
FILTER TYPE	: HDPE

TEST TYPE	: TE2
APPLICATION CLASS	: 2
RIG	: CPT 012
OPERATOR	: AL
FRICTION REDUCER	: None
WEATHER	: Overcast & Mild

CPTU ZERO VALUES

Transducer	Pre	Post	Difference
Tip			
Sleeve			
Pore Pressure 2			
X-Y Inclinometer			

GRANULAR SOILS (Sands & Gravels) Robertson et al. 1986 Zones 7-10 and Zone 12

Description	SBT Index, Ic	Description	SPT N value, NSPT	Description	Relative Density Dr (%)
Clays	2.95-3.60	Very Loose	0 - 4	Very Loose	0 - 15
Silt mixtures	2.60-2.95	Loose	4 - 10	Loose	15 - 35
Sand mixtures	2.05-2.60	Medium Dense	10 - 30	Medium Dense	35 - 65
Sands	1.31-2.05	Dense	30 - 50	Dense	65 - 85
Gravelly sand	<1.31	Very Dense	>50	Very Dense	>85

Groundwater Level

Dissipation Test

CPT LOG 02

IN SITU SITE INVESTIGATION — Working with: geotechnical

PointID
CPT 202

CLIENT : Geotechnical Engineering	EASTING : 392345.9 m	Remark:	SHEET : 2 OF 2
PROJECT : A417 Missing Link	NORTHING : 215691.0 m	Test refused on inclination.	STATUS : Final
LOCATION : Gloucester	ELEVATION : 132.45 m OD		TEST DATE : 09/07/2019
PROJECT No. : 1190295	CHECKED BY : LD		PLOT DATE : 06/04/2020
	TERMINATION REASON : Refusal		METHOD : ISO 22476-1:2012

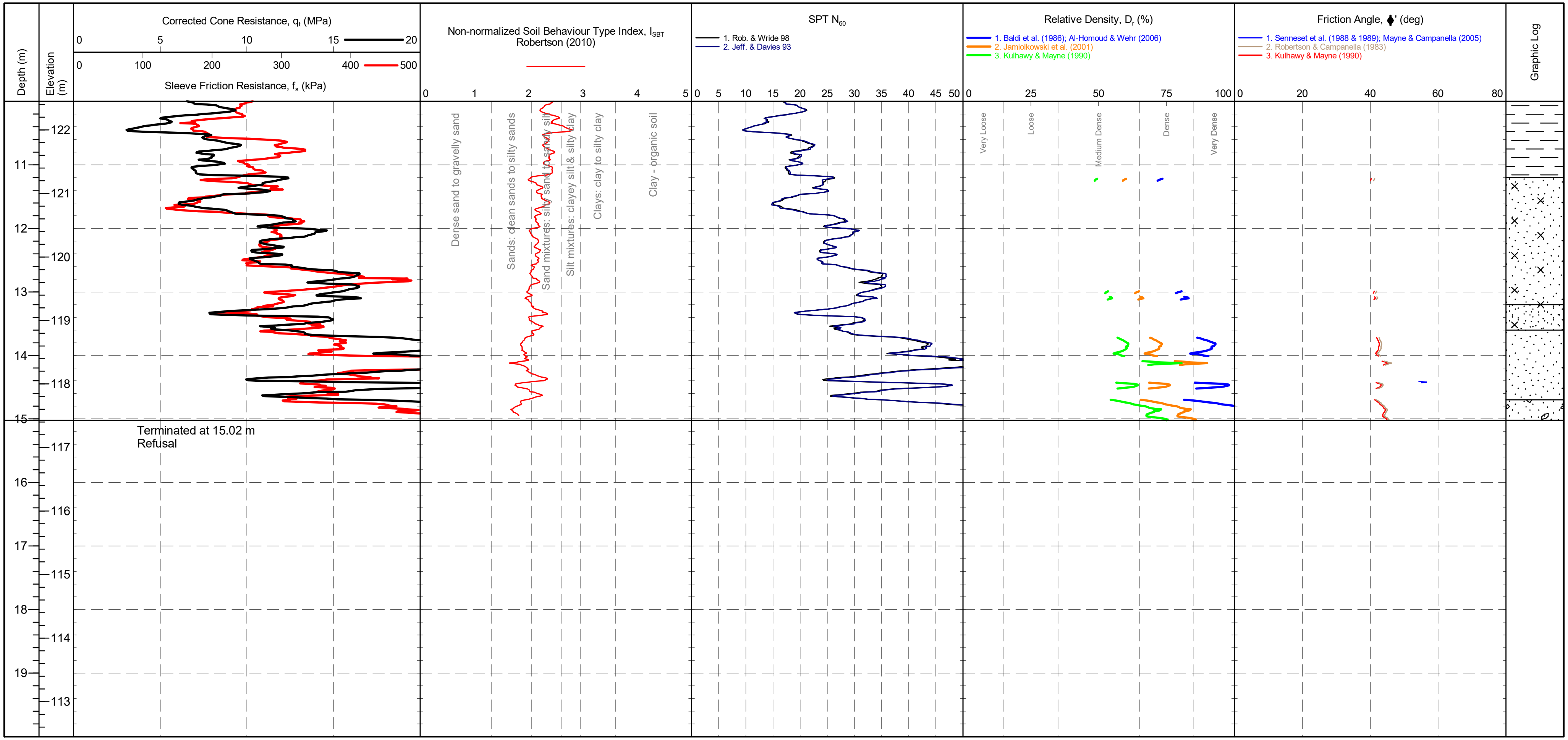

CONE ID : DP15-CFPTxy.71007	TEST TYPE : TE2		
CONE MODEL : DP15-CFPTxy	APPLICATION CLASS : 2		
CONE AREA : 15cm^2	RIG : CPT 012		
CONE AREA RATIO : 0.85	OPERATOR : AL		
FILTER POSITION : u2	FRICTION REDUCER : None		
FILTER TYPE : HDPE	WEATHER : Overcast & Mild		

CPTU ZERO VALUES

Transducer	Pre	Post	Difference
Tip			
Sleeve			
Pore Pressure 2			
X-Y Inclinometer			

GRANULAR SOILS (Sands & Gravels) Robertson et al. 1986 Zones 7-10 and Zone 12

Description	SBT Index, Ic	Description	SPT N value, NSPT	Description	Relative Density Dr (%)
Clays	2.95-3.60	Very Loose	0 - 4	Very Loose	0 - 15
Silt mixtures	2.60-2.95	Loose	4 - 10	Loose	15 - 35
Sand mixtures	2.05-2.60	Medium Dense	10 - 30	Medium Dense	35 - 65
Sands	1.31-2.05	Dense	30 - 50	Dense	65 - 85
Gravelly sand	<1.31	Very Dense	>50	Very Dense	>85

Groundwater Level

Dissipation Test

IN SITU SITE INVESTIGATION Working with: geotechnical

CPT LOG 03

PointID

CPT 202

CLIENT	: Geotechnical Engineering
PROJECT	: A417 Missing Link
LOCATION	: Gloucester
PROJECT No.	: 1190295
EASTING	: 392345.9 m
NORTHING	: 215691.0 m
ELEVATION	: 132.45 m OD
CHECKED BY	: LD
TERMINATION REASON	: Refusal
SHEET	: 1 OF 2
STATUS	: Final
TEST DATE	: 09/07/2019
PLOT DATE	: 06/04/2020
METHOD	: ISO 22476-1:2012

Remark:
Test refused on inclination.

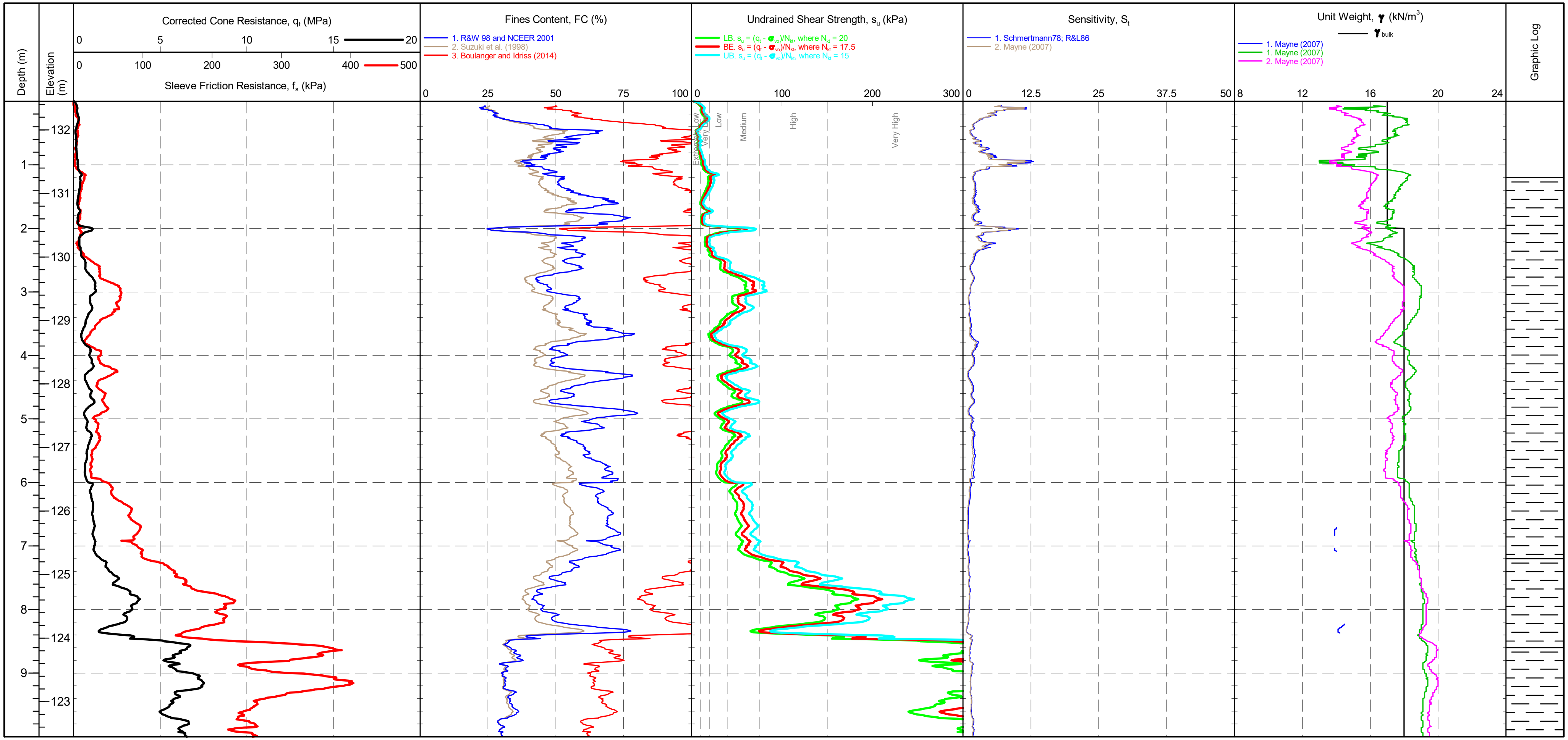

CONE ID	: DP15-CFPTxy.71007
CONE MODEL	: DP15-CFPTxy
CONE AREA	: 15cm^2
CONE AREA RATIO	: 0.85
FILTER POSITION	: u2
FILTER TYPE	: HDPE

TEST TYPE	: TE2
APPLICATION CLASS	: 2
RIG	: CPT 012
OPERATOR	: AL
FRICTION REDUCER	: None
WEATHER	: Overcast & Mild

CPTU ZERO VALUES

Transducer	Pre	Post	Difference
Tip			
Sleeve			
Pore Pressure 2			
X-Y Inclinometer			

COHESIVE SOILS (Clays & Silts) Robertson et al. 1986 Zones 1-6 and Zone 11

Term based on measurement	su (kPa)	Term based on measurement	su (kPa)
Extremely low strength	<10	Medium strength	40-75
Very low strength	10-20	High strength	75-150
Low strength	20-40	Very high strength	150-300
		Extremely high strength	>300

Groundwater Level

Dissipation Test

CPT LOG 03

IN SITU SITE INVESTIGATION — Working with: geotechnical

PointID
CPT 202

CLIENT : Geotechnical Engineering PROJECT : A417 Missing Link LOCATION : Gloucester PROJECT No. : 1190295	EASTING : 392345.9 m NORTHING : 215691.0 m ELEVATION : 132.45 m OD CHECKED BY : LD TERMINATION REASON : Refusal	Remark: Test refused on inclination.	SHEET : 2 OF 2 STATUS : Final TEST DATE : 09/07/2019 PLOT DATE : 06/04/2020 METHOD : ISO 22476-1:2012

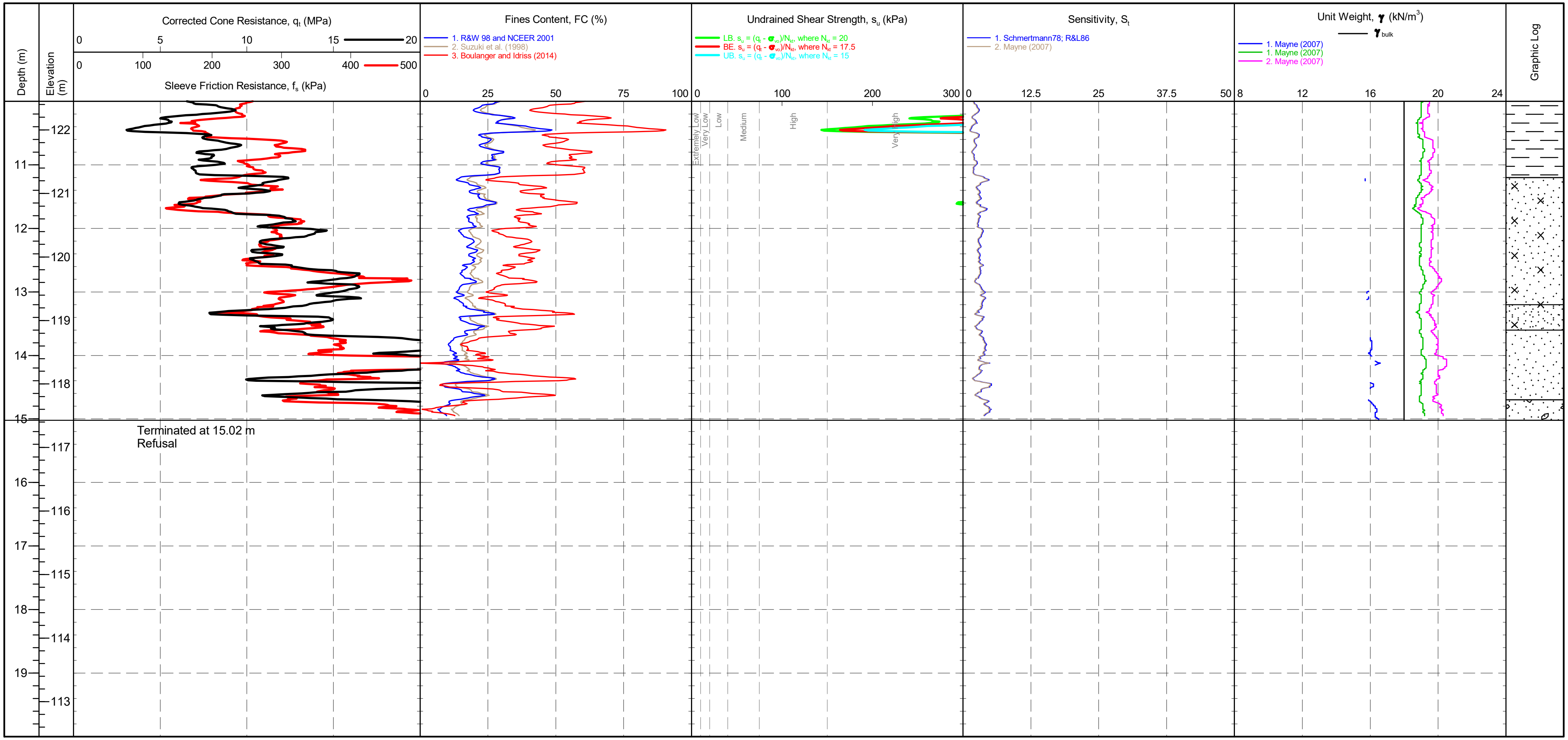

CONE ID	: DP15-CFPTxy.71007	TEST TYPE	: TE2
CONE MODEL	: DP15-CFPTxy	APPLICATION CLASS	: 2
CONE AREA	: 15cm^2	RIG	: CPT 012
CONE AREA RATIO	: 0.85	OPERATOR	: AL
FILTER POSITION	: u2	FRICTION REDUCER	: None
FILTER TYPE	: HDPE	WEATHER	: Overcast & Mild

CPTU ZERO VALUES

Transducer	Pre	Post	Difference
Tip			
Sleeve			
Pore Pressure 2			
X-Y Inclinometer			

COHESIVE SOILS (Clays & Silts) Robertson et al. 1986 Zones 1-6 and Zone 11

Term based on measurement	su (kPa)	Term based on measurement	su (kPa)
Extremely low strength	<10	Medium strength	40-75
Very low strength	10-20	High strength	75-150
Low strength	20-40	Very high strength	150-300
		Extremely high strength	>300

Groundwater Level

Dissipation Test

IN SITU SITE INVESTIGATION Working with: geotechnical

CPT LOG 04

PointID: **CPT 202**

CLIENT	: Geotechnical Engineering
PROJECT	: A417 Missing Link
LOCATION	: Gloucester
PROJECT No.	: 1190295

EASTING	: 392345.9 m
NORTHING	: 215691.0 m
ELEVATION	: 132.45 m OD
CHECKED BY	: LD
TERMINATION REASON	: Refusal

Remark:
Test refused on inclination.

SHEET	: 1 OF 2
STATUS	: Final
TEST DATE	: 09/07/2019
PLOT DATE	: 06/04/2020
METHOD	: ISO 22476-1:2012

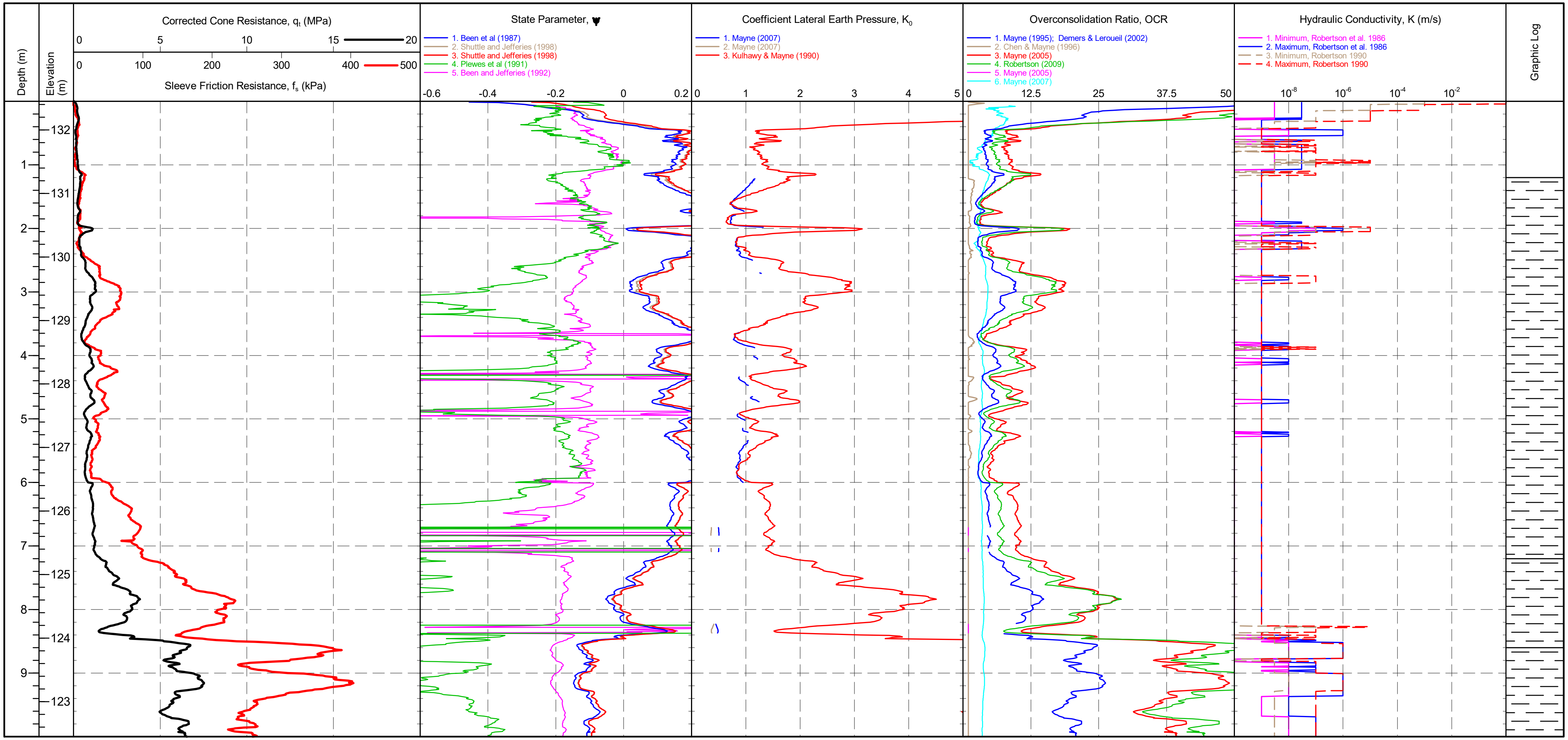

CONE ID	: DP15-CFPTxy.71007
CONE MODEL	: DP15-CFPTxy
CONE AREA	: 15cm²
CONE AREA RATIO	: 0.85
FILTER POSITION	: u2
FILTER TYPE	: HDPE

TEST TYPE	: TE2
APPLICATION CLASS	: 2
RIG	: CPT 012
OPERATOR	: AL
FRICTION REDUCER	: None
WEATHER	: Overcast & Mild

CPTU ZERO VALUES

Transducer	Pre	Post	Difference
Tip			
Sleeve			
Pore Pressure 2			
X-Y Inclinometer			

Groundwater Level

Dissipation Test

CPT LOG 04

IN SITU SITE INVESTIGATION Working with: geotechnical

PointID **CPT 202**

CLIENT	: Geotechnical Engineering
PROJECT	: A417 Missing Link
LOCATION	: Gloucester
PROJECT No.	: 1190295

EASTING	: 392345.9 m
NORTHING	: 215691.0 m
ELEVATION	: 132.45 m OD
CHECKED BY	: LD
TERMINATION REASON	: Refusal

Remark:
Test refused on inclination.

SHEET	: 2 OF 2
STATUS	: Final
TEST DATE	: 09/07/2019
PLOT DATE	: 06/04/2020
METHOD	: ISO 22476-1:2012

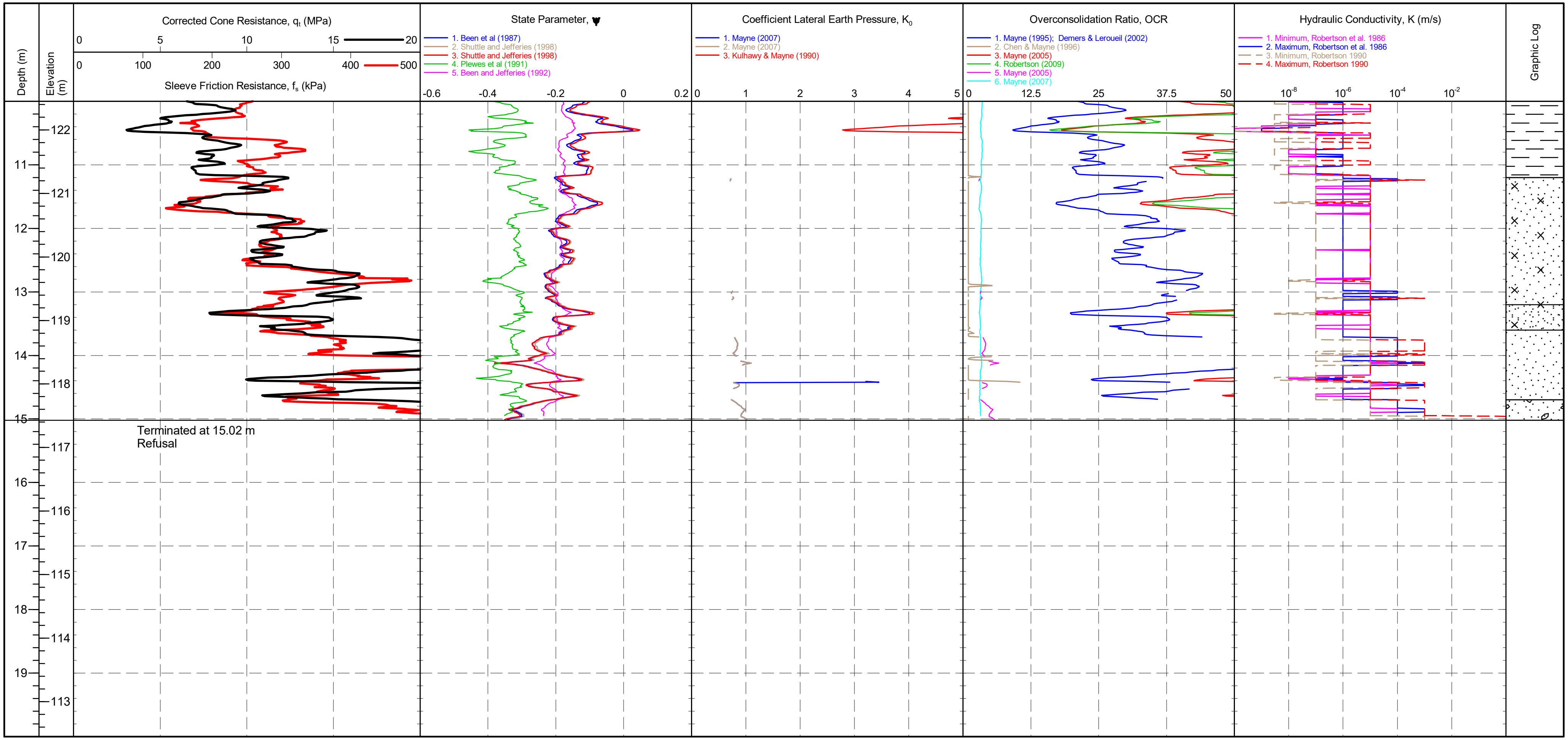

CONE ID	: DP15-CFPTxy.71007
CONE MODEL	: DP15-CFPTxy
CONE AREA	: 15cm²
CONE AREA RATIO	: 0.85
FILTER POSITION	: u2
FILTER TYPE	: HDPE

TEST TYPE	: TE2
APPLICATION CLASS	: 2
RIG	: CPT 012
OPERATOR	: AL
FRICTION REDUCER	: None
WEATHER	: Overcast & Mild

CPTU ZERO VALUES

Transducer	Pre	Post	Difference
Tip			
Sleeve			
Pore Pressure 2			
X-Y Inclinometer			

Groundwater Level

Dissipation Test

IN SITU SITE INVESTIGATION Working with: geotechnical

CPT LOG 05

PointID
CPT 202

CLIENT : Geotechnical Engineering PROJECT : A417 Missing Link LOCATION : Gloucester PROJECT No. : 1190295	EASTING : 392345.9 m NORTHING : 215691.0 m ELEVATION : 132.45 m OD CHECKED BY : LD TERMINATION REASON : Refusal	Remark: Test refused on inclination.	SHEET : 1 OF 2 STATUS : Final TEST DATE : 09/07/2019 PLOT DATE : 06/04/2020 METHOD : ISO 22476-1:2012

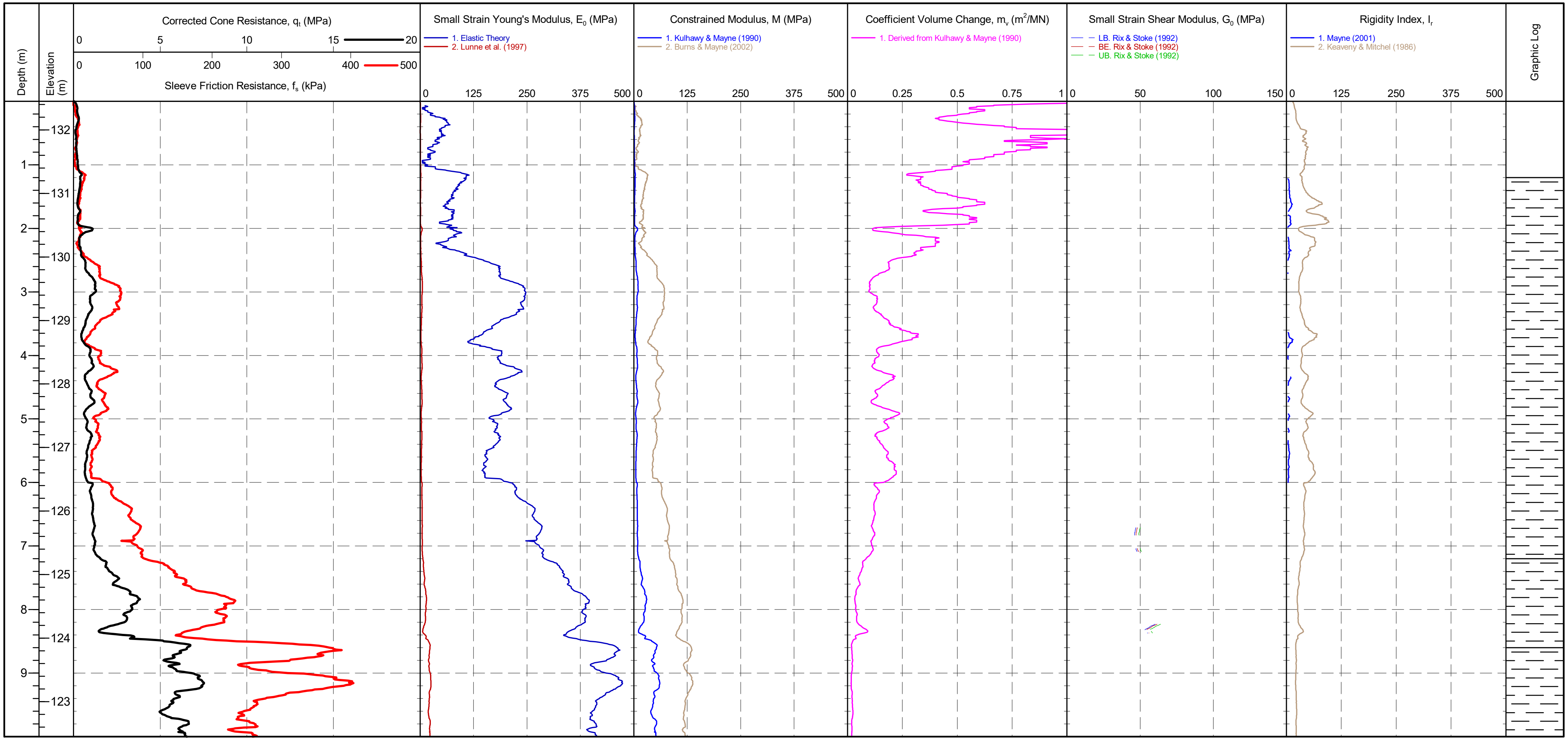

CONE ID	: DP15-CFPTxy.71007	TEST TYPE	: TE2	CPTU ZERO VALUES		
CONE MODEL	: DP15-CFPTxy	APPLICATION CLASS	: 2	Transducer	Pre	Post
CONE AREA	: 15cm^2	RIG	: CPT 012	Tip		
CONE AREA RATIO	: 0.85	OPERATOR	: AL	Sleeve		
FILTER POSITION	: u2	FRICTION REDUCER	: None	Pore Pressure 2		
FILTER TYPE	: HDPE	WEATHER	: Overcast & Mild	X-Y Inclinometer		

Difference

Groundwater Level

Dissipation Test

IN SITU SITE INVESTIGATION Working with: geotechnical

CPT LOG 05

PointID
CPT 202

CLIENT	: Geotechnical Engineering
PROJECT	: A417 Missing Link
LOCATION	: Gloucester
PROJECT No.	: 1190295

EASTING	: 392345.9 m
NORTHING	: 215691.0 m
ELEVATION	: 132.45 m OD
CHECKED BY	: LD
TERMINATION REASON	: Refusal

Remark:
Test refused on inclination.

SHEET	: 2 OF 2
STATUS	: Final
TEST DATE	: 09/07/2019
PLOT DATE	: 06/04/2020
METHOD	: ISO 22476-1:2012

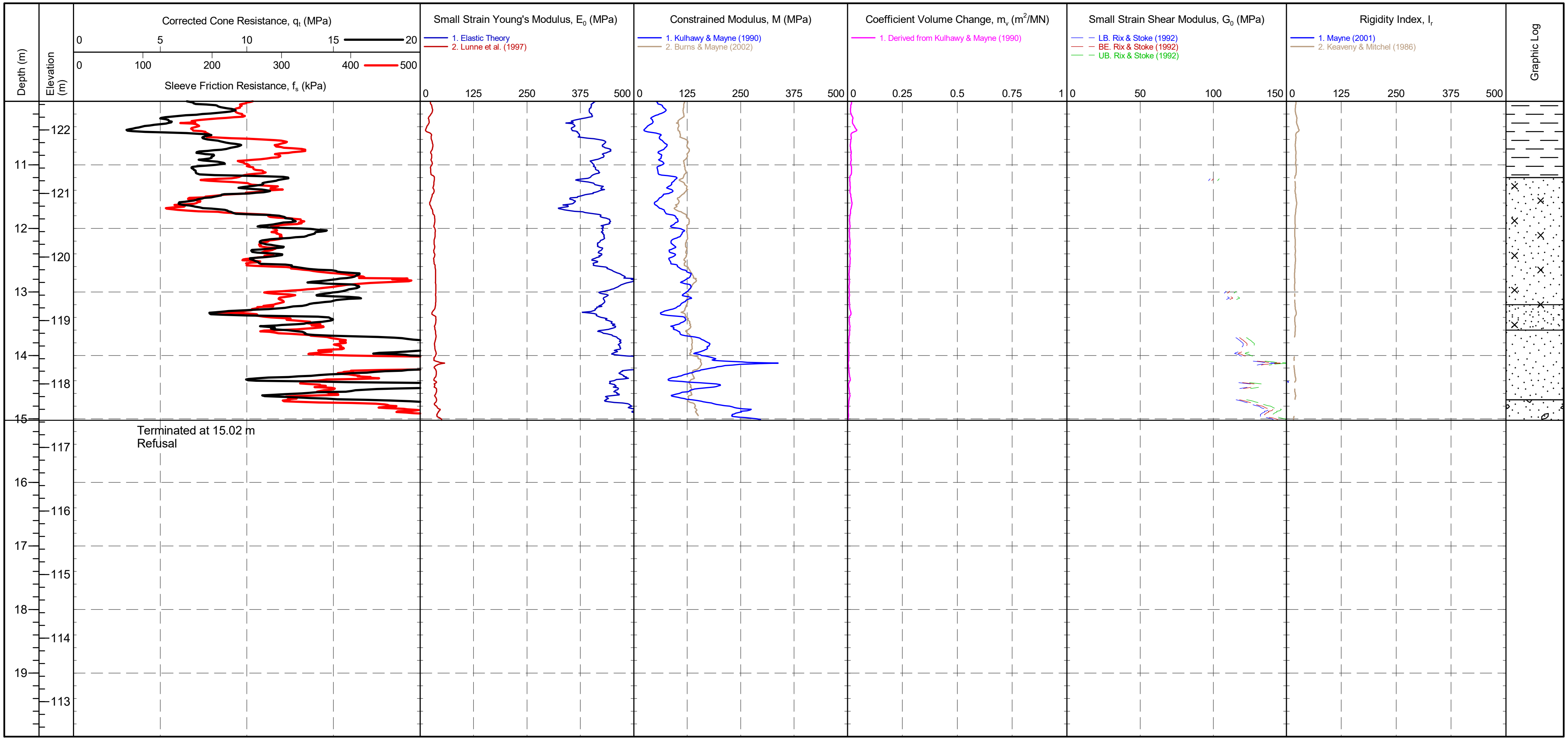

CONE ID	: DP15-CFPTxy.71007
CONE MODEL	: DP15-CFPTxy
CONE AREA	: 15cm^2
CONE AREA RATIO	: 0.85
FILTER POSITION	: u2
FILTER TYPE	: HDPE

TEST TYPE	: TE2
APPLICATION CLASS	: 2
RIG	: CPT 012
OPERATOR	: AL
FRICTION REDUCER	: None
WEATHER	: Overcast & Mild

CPTU ZERO VALUES

Transducer	Pre	Post	Difference
Tip			
Sleeve			
Pore Pressure 2			
X-Y Inclinometer			

Groundwater Level

Dissipation Test

IN SITU
SITE INVESTIGATION

Working with: geotechnical

DISSIPATION TEST

Test ID
CPT 202 - 6.00 m

CLIENT	: Geotechnical Engineering	AREA	: A417 MISSING LINK	SHEET	: 1 OF 1
ENGINEER	:	EASTING	: 392345.9 m	STATUS	: Final
PROJECT	: A417 Missing Link	NORTHING	: 215691.0 m	DATE	: 09/07/19
LOCATION	: Gloucester	COORD. SYS.	:		
PROJECT No.	: 1190295	ELEVATION	: 132.45 m		

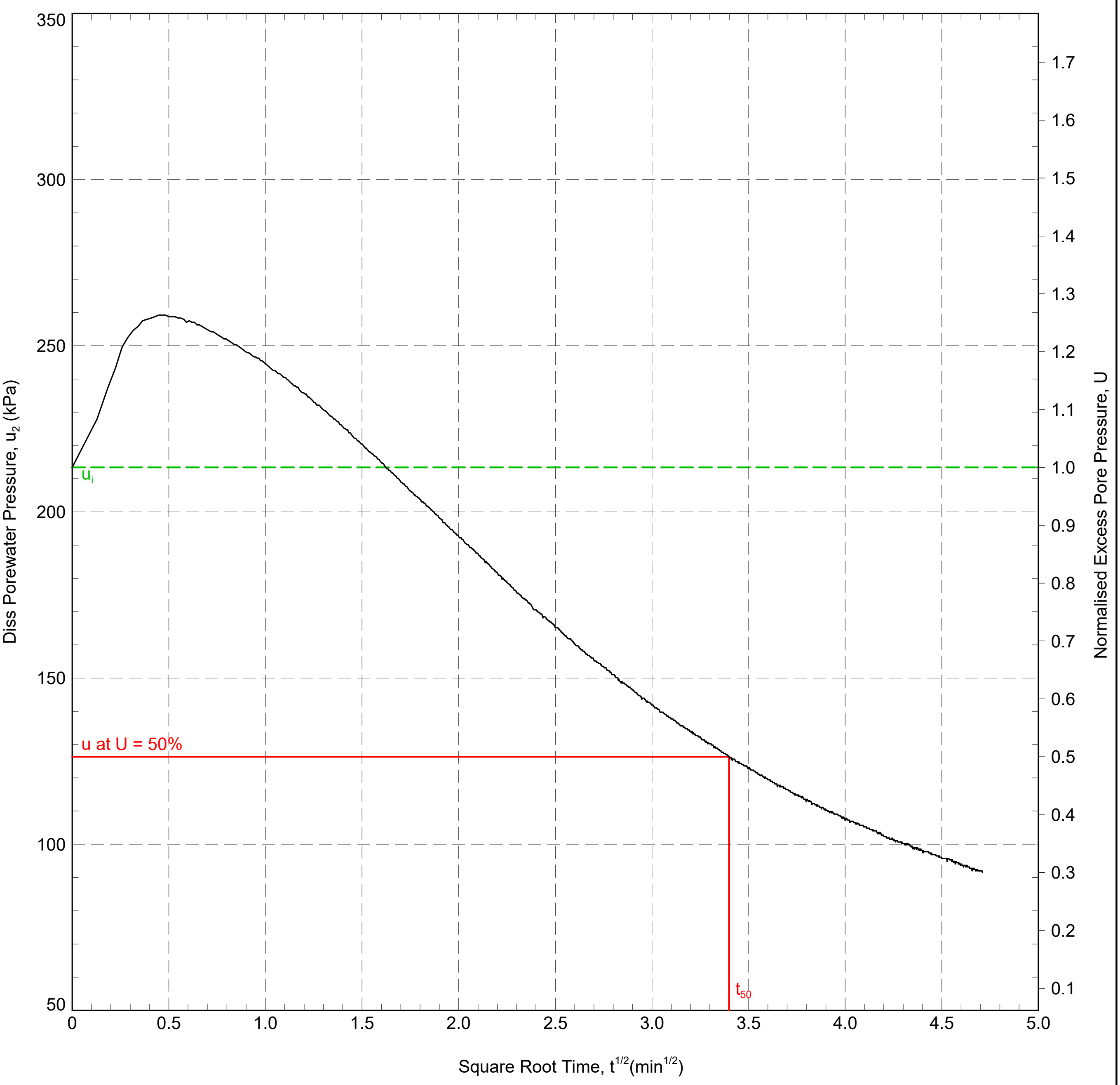

In Situ Pore Pressure, u_0:	39.2 kPa	Rigidity Index, I_r:	50
Initial Pore Pressure, u_i:	213.4 kPa	Horizontal Coefficient of Consolidation, c_h:	4.17×10^1 m^2/yr
Final Pore Pressure:	91.5 kPa	Ratio c_h/c_v:	1.25
Degree of Dissipation:	50%	Vertical Coefficient of Consolidation, c_v:	3.33×10^1 m^2/yr
Dissipation Pressure:	126.3 kPa		
Time for 50% Dissipation, t_{50}:	11.56 min		

RIG	: CPT 012	ANALYSED BY : LD	DATE: 29/07/2019	REMARK
CONE TYPE	: DP15-CFPTxy	CHECKED BY : LD	DATE: 29/07/2019	Test OK.
CONE ID	: DP15-CFPTxy.71007	APPROVED BY : DW	DATE: 29/07/2019	
OPERATOR	: AL			

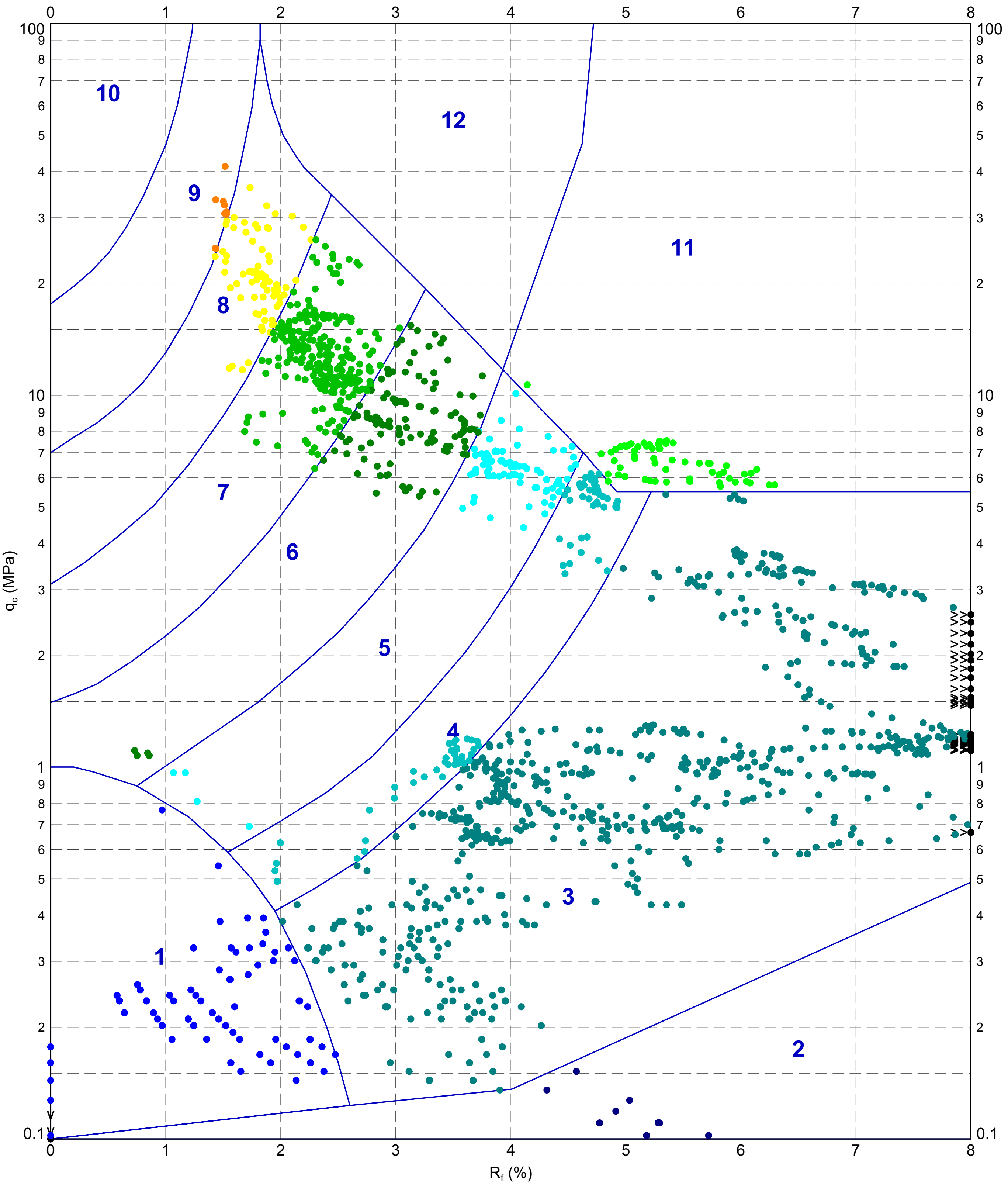

METHOD: Robertson et al. 1986 qc Rf

1 - Sensitive fine grained material	4 - Silty CLAY to CLAY	7 - Silty SAND to sandy SILT	10 - Gravelly SAND to SAND
2 - Organic material	5 - Clayey SILT to silty CLAY	8 - SAND to silty SAND	11 - Very stiff fine grained
3 - CLAY	6 - Sandy SILT to clayey SILT	9 - SAND	12 - SAND to clayey SAND

IN SITU
SITE INVESTIGATION

TITLE	DRAWN	DATE
Geotechnical Engineering Gloucester A417 Missing Link Robertson et al. 1986 q_c vs. R_f - CPT 202		06/04/2020
	CHECKED	DATE 06/04/2020
	SCALE Not To Scale	A4
	PROJECT No 1190295	FIGURE No

CPT LOG 01

IN SITU SITE INVESTIGATION Working with: geotechnical

PointID
CPT 203

CLIENT : Geotechnical Engineering PROJECT : A417 Missing Link LOCATION : Gloucester PROJECT No. : 1190295	EASTING : 392595.1 m NORTHING : 215609.5 m ELEVATION : 159.70 m OD CHECKED BY : LD TERMINATION REASON : Refusal	Remark: Test refused on tip resistance.	SHEET : 1 OF 1 STATUS : Final TEST DATE : 10/07/2019 PLOT DATE : 06/04/2020 METHOD : ISO 22476-1:2012

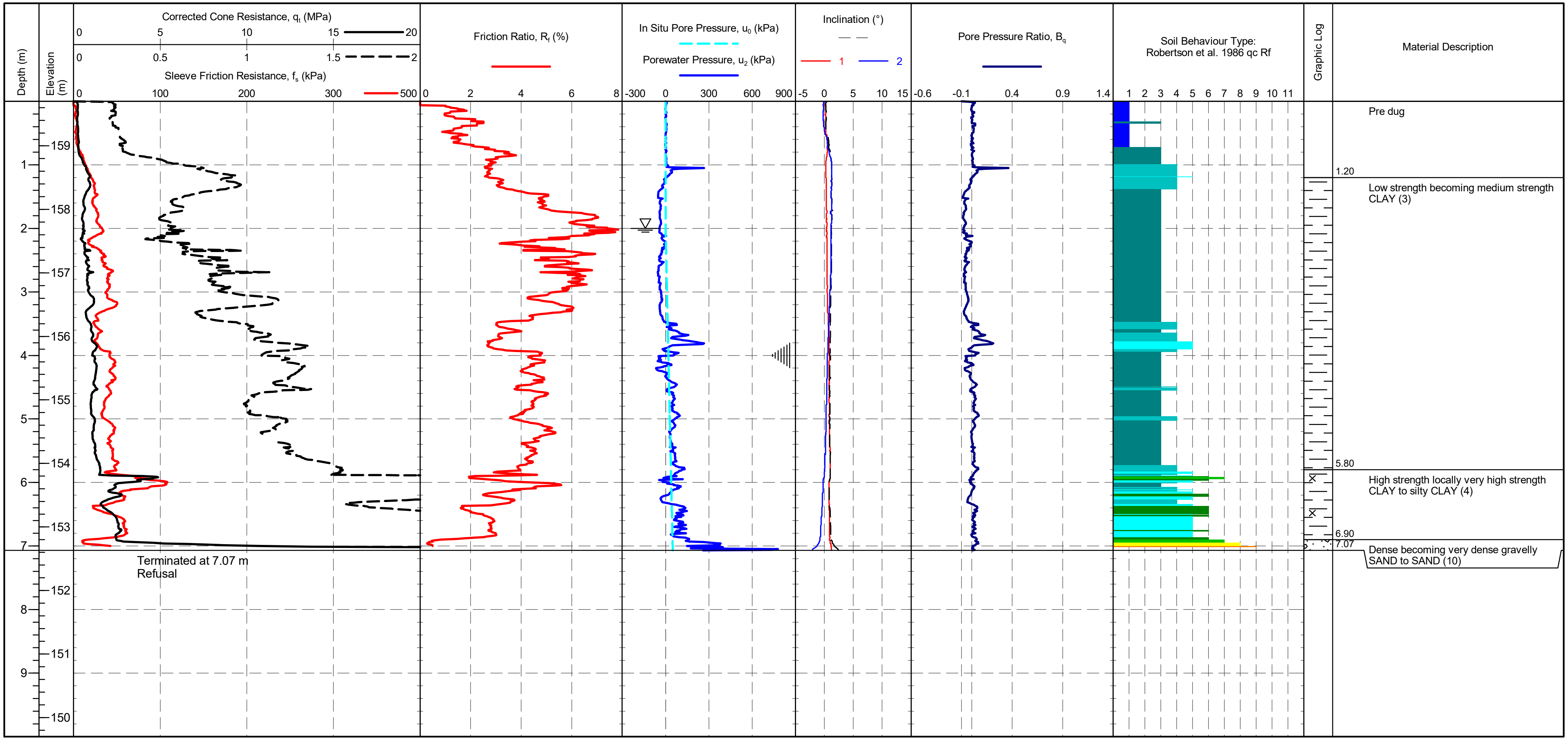

CONE ID	: DP15-CFPTxy.70102	TEST TYPE	: TE2		
CONE MODEL	: DP15-CFPTxy	APPLICATION CLASS	: 2		
CONE AREA	: 15cm^2	RIG	: CPT 012		
CONE AREA RATIO	: 0.85	OPERATOR	: AL		
FILTER POSITION	: u2	FRICTION REDUCER	: None		
FILTER TYPE	: HDPE	WEATHER	: Overcast & Mild		

CPTU ZERO VALUES

Transducer	Pre	Post	Difference
Tip	-0.0417 MPa	-0.0109 MPa	
Sleeve	0.00476 kPa	-0.000166 kPa	
Pore Pressure 2	-0.00445 kPa	-0.00728 kPa	
X-Y Inclinometer			

METHOD: Robertson et al. 1986 qc Rf

- 1 - Sensitive fine grained material
- 2 - Organic material
- 3 - CLAY
- 4 - Silty CLAY to CLAY
- 5 - Clayey SILT to silty CLAY
- 6 - Sandy SILT to clayey SILT
- 7 - Silty SAND to sandy SILT
- 8 - SAND to silty SAND
- 9 - SAND
- 10 - Gravelly SAND to SAND
- 11 - Very stiff fine grained
- 12 - SAND to clayey SAND

Groundwater Level

Dissipation Test

IN SITU SITE INVESTIGATION Working with: geotechnical

CPT LOG 02

PointID

CPT 203

CLIENT : Geotechnical Engineering
PROJECT : A417 Missing Link
LOCATION : Gloucester
PROJECT No. : 1190295

EASTING : 392595.1 m
NORTHING : 215609.5 m
ELEVATION : 159.70 m OD
CHECKED BY : LD
TERMINATION REASON : Refusal

Remark:
Test refused on tip resistance.

SHEET : 1 OF 1
STATUS : Final
TEST DATE : 10/07/2019
PLOT DATE : 06/04/2020
METHOD : ISO 22476-1:2012

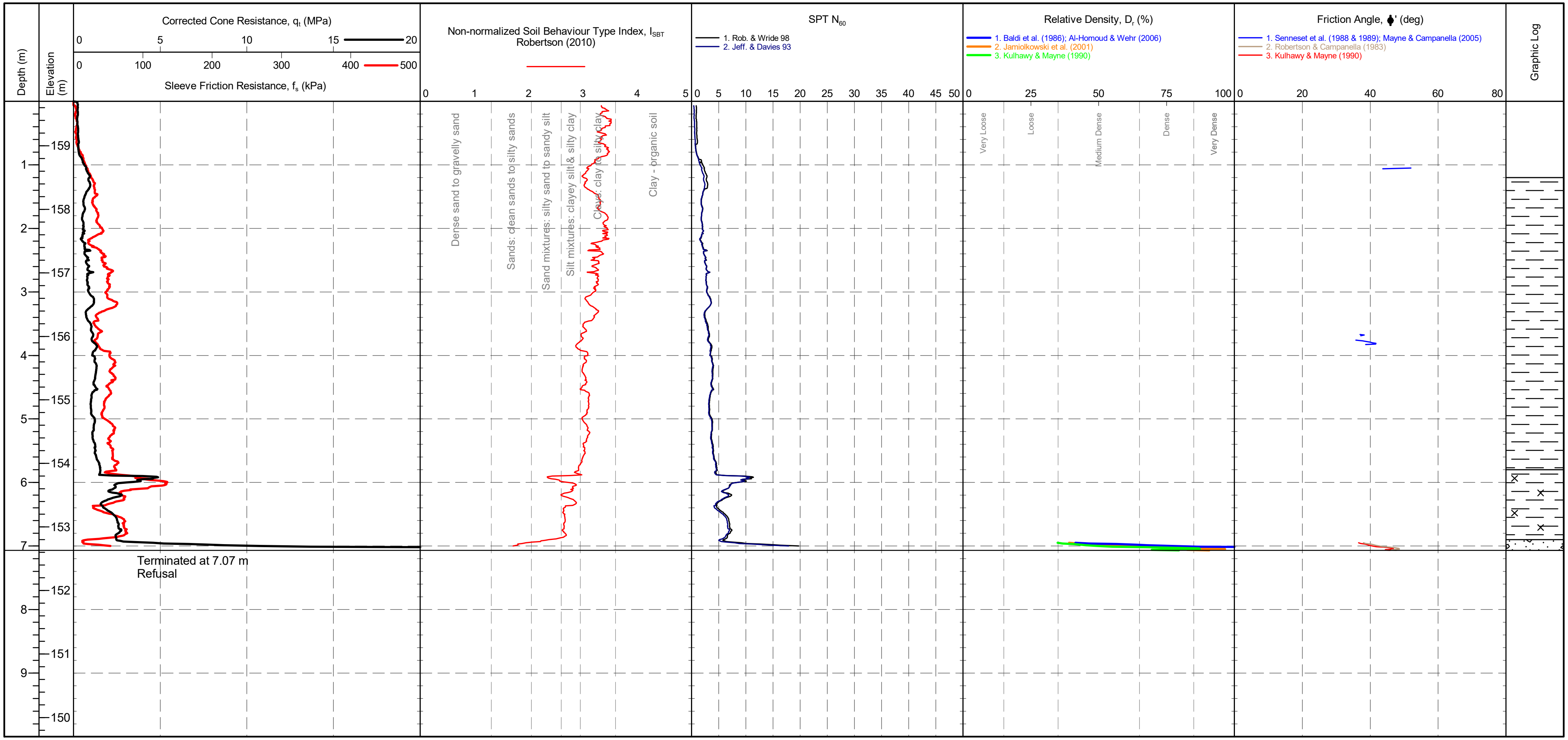

CONE ID : DP15-CFPTxy.70102
CONE MODEL : DP15-CFPTxy
CONE AREA : 15cm²
CONE AREA RATIO : 0.85
FILTER POSITION : u2
FILTER TYPE : HDPE

TEST TYPE : TE2
APPLICATION CLASS : 2
RIG : CPT 012
OPERATOR : AL
FRICTION REDUCER : None
WEATHER : Overcast & Mild

CPTU ZERO VALUES

Transducer	Pre	Post	Difference
Tip			
Sleeve			
Pore Pressure 2			
X-Y Inclinometer			

GRANULAR SOILS (Sands & Gravels) Robertson et al. 1986 Zones 7-10 and Zone 12

Description	SBT Index, Ic	Description	SPT N value, NSPT	Description	Relative Density Dr (%)
Clays	2.95-3.60	Very Loose	0 - 4	Very Loose	0 - 15
Silt mixtures	2.60-2.95	Loose	4 - 10	Loose	15 - 35
Sand mixtures	2.05-2.60	Medium Dense	10 - 30	Medium Dense	35 - 65
Sands	1.31-2.05	Dense	30 - 50	Dense	65 - 85
Gravelly sand	<1.31	Very Dense	>50	Very Dense	>85

Groundwater Level
Dissipation Test

IN SITU SITE INVESTIGATION Working with: geotechnical

CPT LOG 03

PointID
CPT 203

CLIENT : Geotechnical Engineering PROJECT : A417 Missing Link LOCATION : Gloucester PROJECT No. : 1190295	EASTING : 392595.1 m NORTHING : 215609.5 m ELEVATION : 159.70 m OD CHECKED BY : LD TERMINATION REASON : Refusal	Remark: Test refused on tip resistance.	SHEET : 1 OF 1 STATUS : Final TEST DATE : 10/07/2019 PLOT DATE : 06/04/2020 METHOD : ISO 22476-1:2012

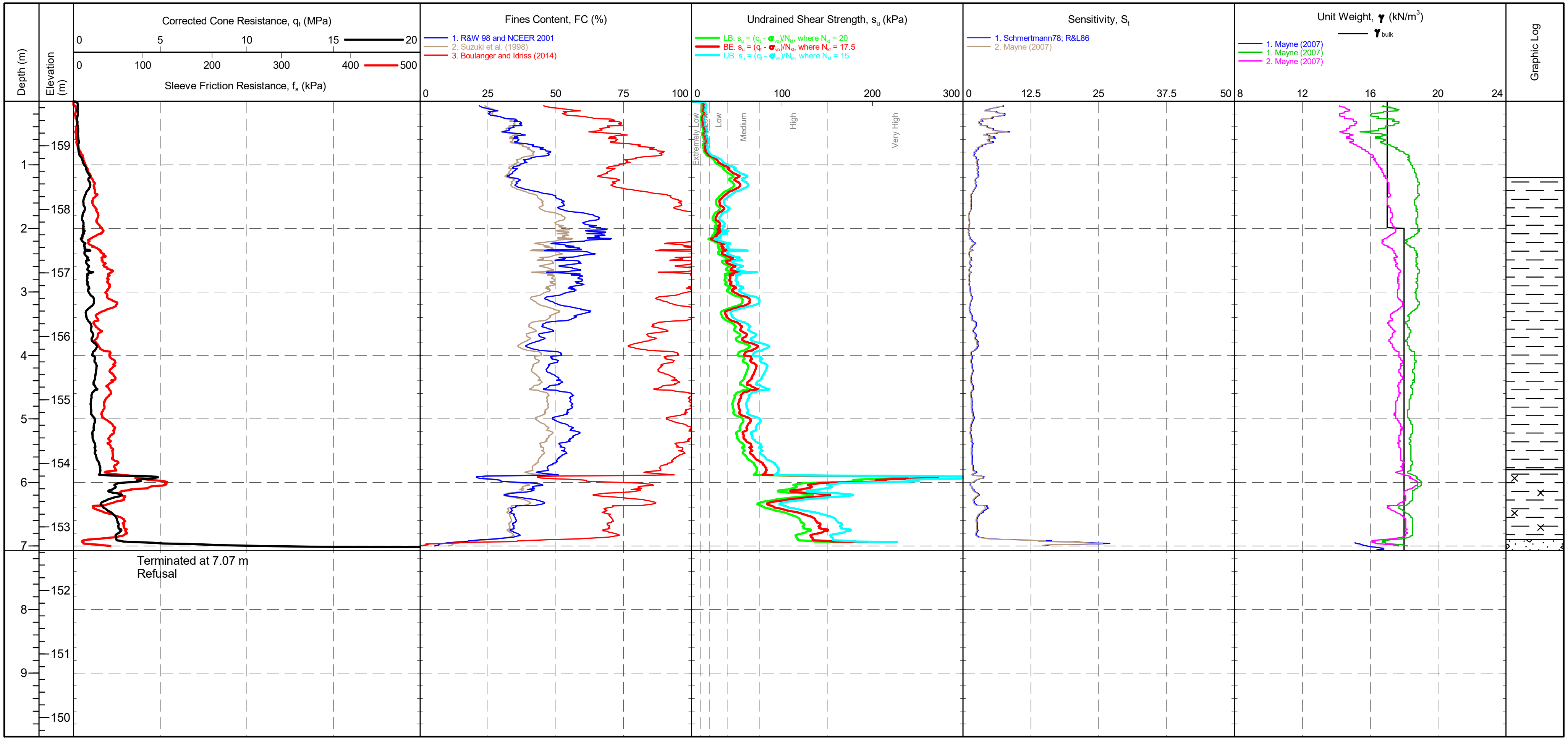

CONE ID	: DP15-CFPTxy.70102	TEST TYPE	: TE2		
CONE MODEL	: DP15-CFPTxy	APPLICATION CLASS	: 2		
CONE AREA	: 15cm^2	RIG	: CPT 012		
CONE AREA RATIO	: 0.85	OPERATOR	: AL		
FILTER POSITION	: u2	FRICTION REDUCER	: None		
FILTER TYPE	: HDPE	WEATHER	: Overcast & Mild		

CPTU ZERO VALUES

Transducer	Pre	Post	Difference
Tip			
Sleeve			
Pore Pressure 2			
X-Y Inclinometer			

COHESIVE SOILS (Clays & Silts) Robertson et al. 1986 Zones 1-6 and Zone 11

Term based on measurement	su (kPa)	Term based on measurement	su (kPa)
Extremely low strength	<10	Medium strength	40-75
Very low strength	10-20	High strength	75-150
Low strength	20-40	Very high strength	150-300
		Extremely high strength	>300

Groundwater Level

Dissipation Test

IN SITU SITE INVESTIGATION Working with: geotechnical

CPT LOG 04

PointID
CPT 203

CLIENT	: Geotechnical Engineering
PROJECT	: A417 Missing Link
LOCATION	: Gloucester
PROJECT No.	: 1190295

EASTING	: 392595.1 m
NORTHING	: 215609.5 m
ELEVATION	: 159.70 m OD
CHECKED BY	: LD
TERMINATION REASON	: Refusal

Remark:
Test refused on tip resistance.

SHEET	: 1 OF 1
STATUS	: Final
TEST DATE	: 10/07/2019
PLOT DATE	: 06/04/2020
METHOD	: ISO 22476-1:2012

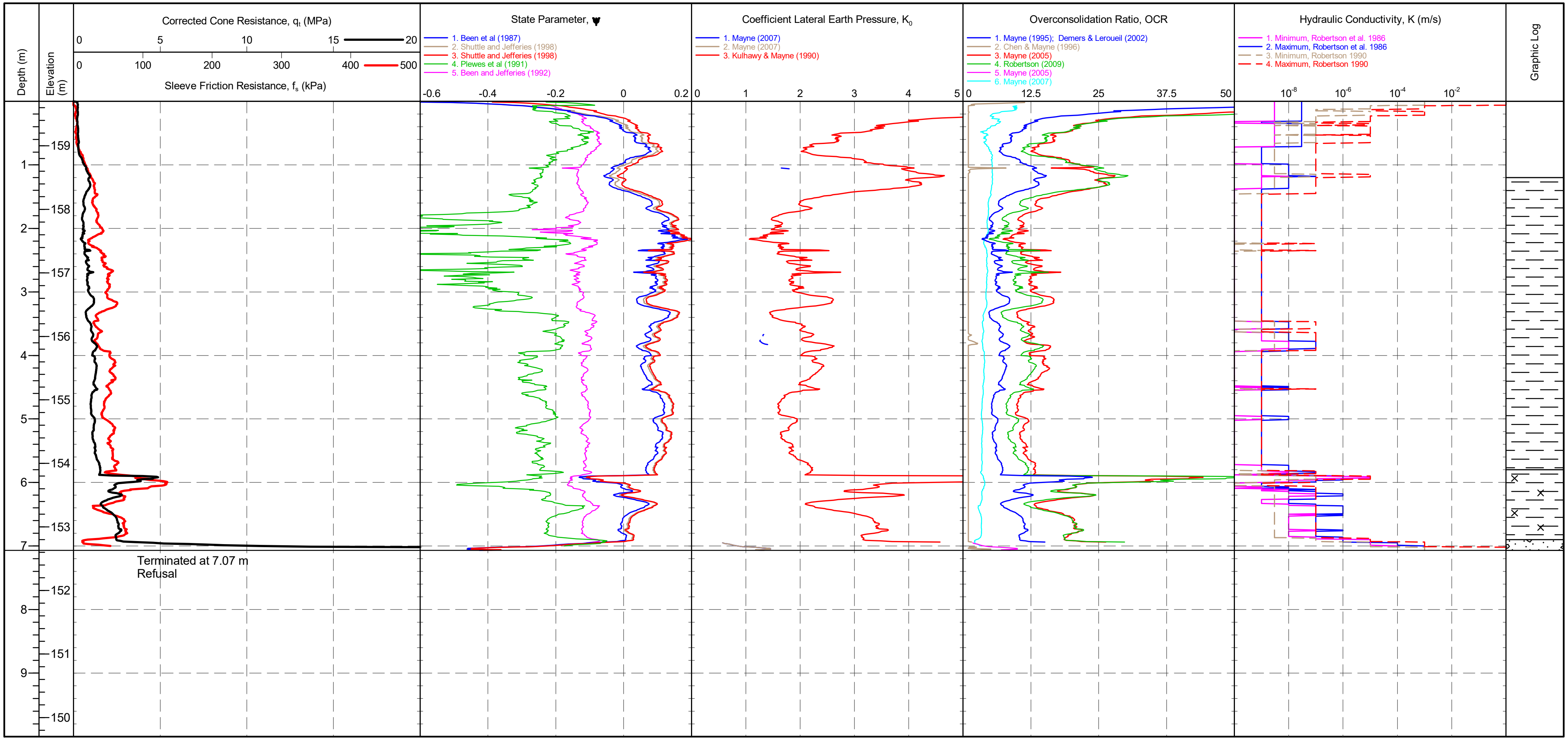

CONE ID	: DP15-CFPTxy.70102
CONE MODEL	: DP15-CFPTxy
CONE AREA	: 15cm²
CONE AREA RATIO	: 0.85
FILTER POSITION	: u2
FILTER TYPE	: HDPE

TEST TYPE	: TE2
APPLICATION CLASS	: 2
RIG	: CPT 012
OPERATOR	: AL
FRICTION REDUCER	: None
WEATHER	: Overcast & Mild

CPTU ZERO VALUES

Transducer	Pre	Post	Difference
Tip			
Sleeve			
Pore Pressure 2			
X-Y Inclinometer			

Groundwater Level
Dissipation Test

IN SITU
SITE INVESTIGATION
Working with: geotechnical

CPT LOG 05

PointID
CPT 203

CLIENT : Geotechnical Engineering PROJECT : A417 Missing Link LOCATION : Gloucester PROJECT No. : 1190295	EASTING : 392595.1 m NORTHING : 215609.5 m ELEVATION : 159.70 m OD CHECKED BY : LD TERMINATION REASON : Refusal	Remark: Test refused on tip resistance.	SHEET : 1 OF 1 STATUS : Final TEST DATE : 10/07/2019 PLOT DATE : 06/04/2020 METHOD : ISO 22476-1:2012

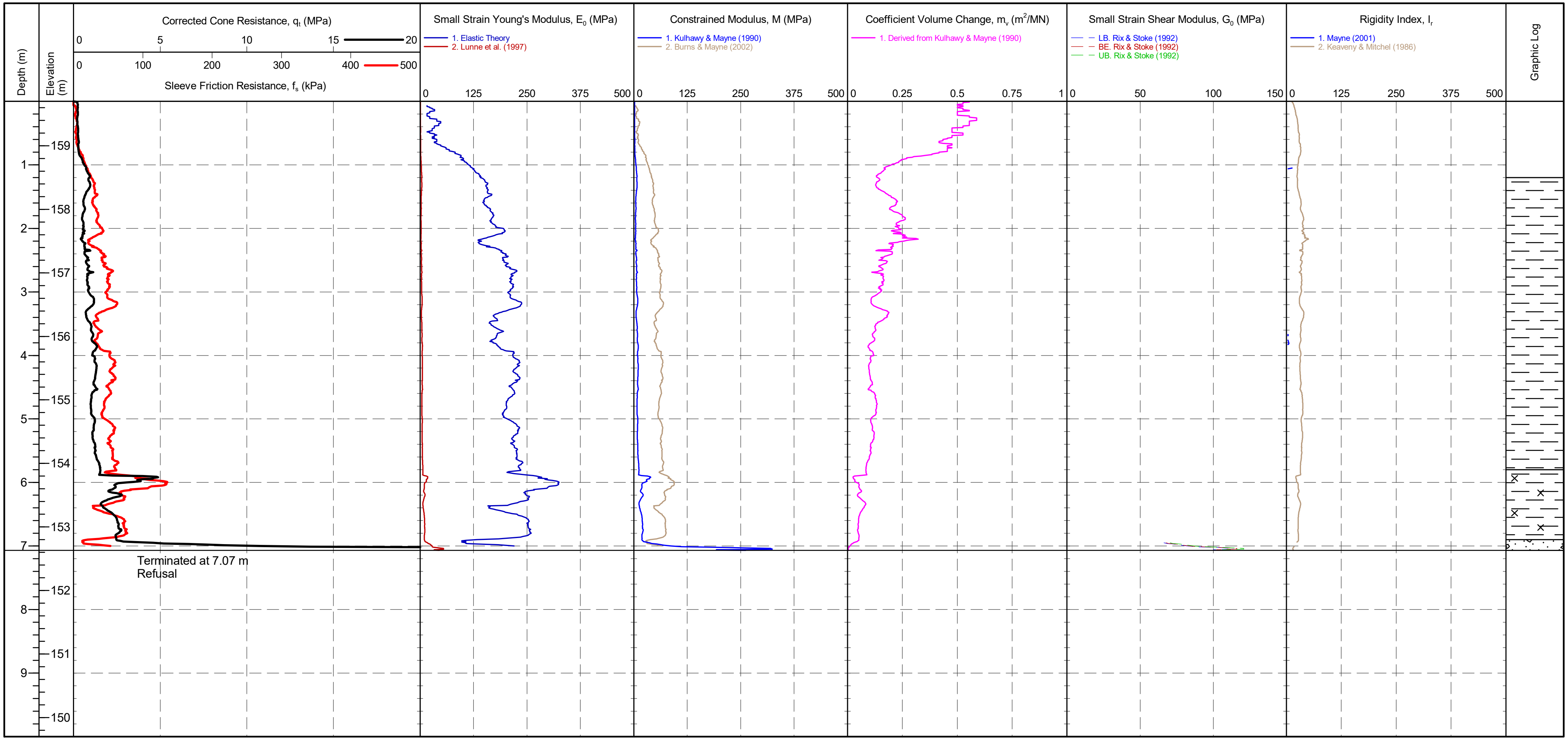

CONE ID : DP15-CFPTxy.70102 CONE MODEL : DP15-CFPTxy CONE AREA : 15cm^2 CONE AREA RATIO : 0.85 FILTER POSITION : u2 FILTER TYPE : HDPE	TEST TYPE : TE2 APPLICATION CLASS : 2 RIG : CPT 012 OPERATOR : AL FRICTION REDUCER : None WEATHER : Overcast & Mild	CPTU ZERO VALUES Transducer / Pre / Post / Difference Tip Sleeve Pore Pressure 2 X-Y Inclinometer

Groundwater Level
Dissipation Test

DISSIPATION TEST

IN SITU SITE INVESTIGATION

Working with: geotechnical

Test ID

CPT 203 - 4.00 m

CLIENT : Geotechnical Engineering	AREA : A417 MISSING LINK	SHEET : 1 OF 1
ENGINEER :	EASTING : 392595.1 m	STATUS : Final
PROJECT : A417 Missing Link	NORTHING : 215609.5 m	DATE : 10/07/19
LOCATION : Gloucester	COORD. SYS.:	
PROJECT No. : 1190295	ELEVATION : 159.70 m	

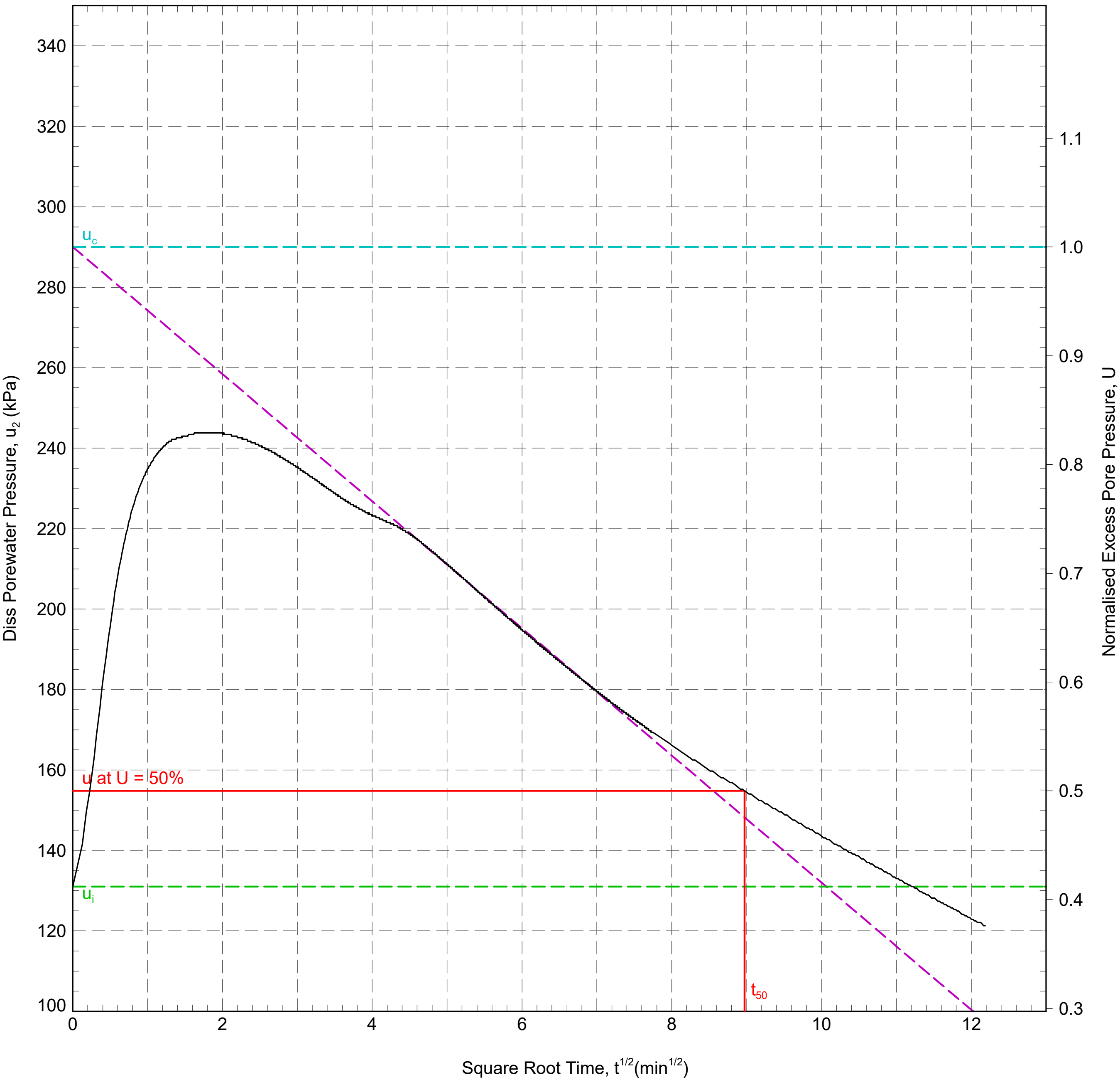

In Situ Pore Pressure, u_0:	19.6 kPa	Rigidity Index, I_r:	100
Initial Pore Pressure, u_i:	131.0 kPa	Horizontal Coefficient of Consolidation, c_h:	$8.46x10^0$ m^2/yr
Final Pore Pressure:	121.3 kPa	Ratio c_h/c_v:	1.25
Back Extrapolated Pore Pressure, u_c:	290 kPa	Vertical Coefficient of Consolidation, c_v:	$6.77x10^0$ m^2/yr
Degree of Dissipation:	50%		
Dissipation Pressure:	154.8 kPa		
Time for 50% Dissipation, t_{50}:	80.52 min		

RIG : CPT 012	ANALYSED BY : LD	DATE: 29/07/2019	REMARK
CONE TYPE : DP15-CFPTxy	CHECKED BY : LD	DATE: 29/07/2019	Test OK.
CONE ID : DP15-CFPTxy.70102	APPROVED BY : DW	DATE: 29/07/2019	
OPERATOR : AL			

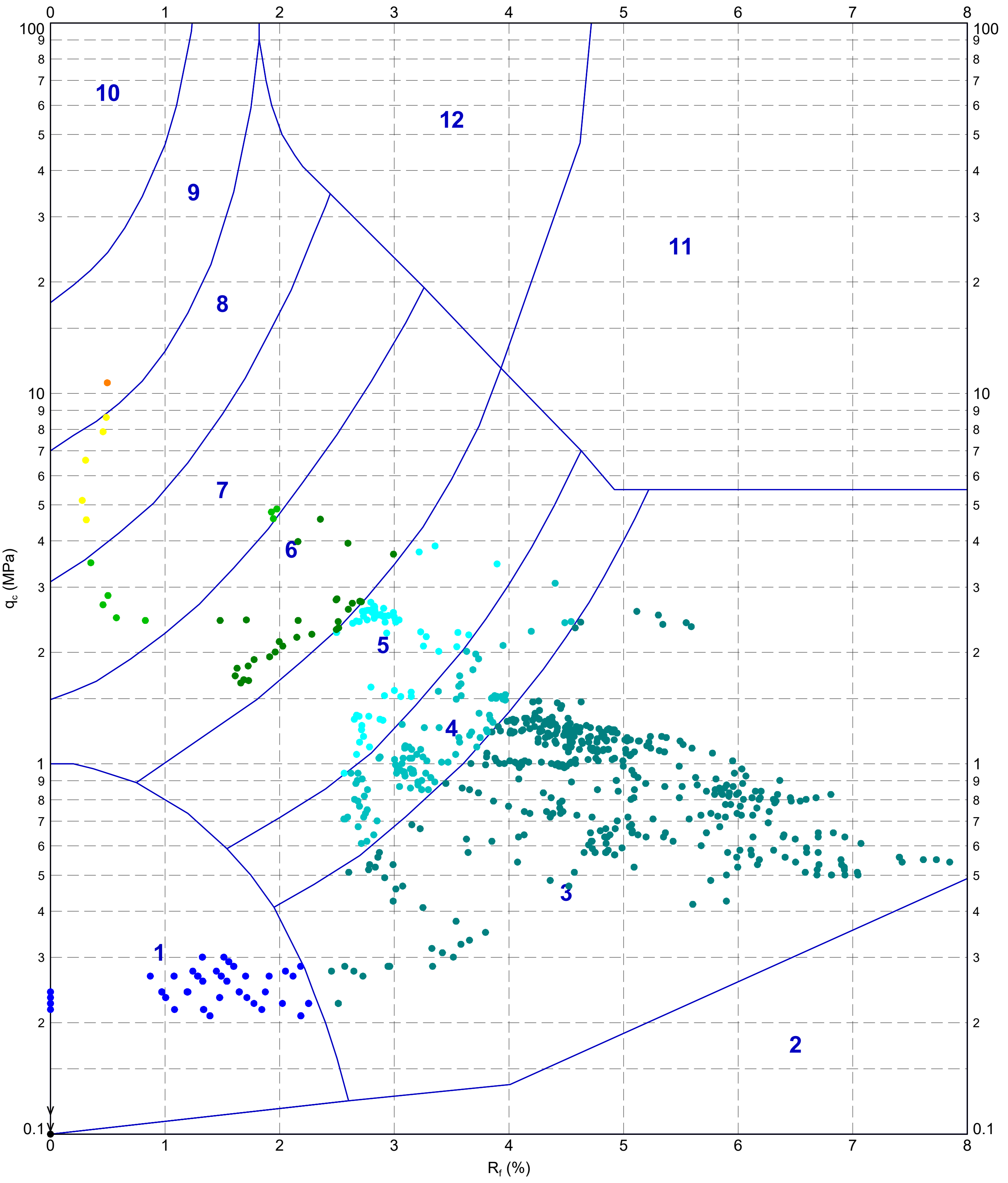

METHOD: Robertson et al. 1986 qc Rf

- 1 - Sensitive fine grained material
- 2 - Organic material
- 3 - CLAY
- 4 - Silty CLAY to CLAY
- 5 - Clayey SILT to silty CLAY
- 6 - Sandy SILT to clayey SILT
- 7 - Silty SAND to sandy SILT
- 8 - SAND to silty SAND
- 9 - SAND
- 10 - Gravelly SAND to SAND
- 11 - Very stiff fine grained
- 12 - SAND to clayey SAND

IN SITU
SITE INVESTIGATION

TITLE	DRAWN	DATE 06/04/2020
Geotechnical Engineering Gloucester A417 Missing Link Robertson et al. 1986 q_c vs. R_f - CPT 203	CHECKED	DATE 06/04/2020
	SCALE Not To Scale	A4
	PROJECT No 1190295	FIGURE No

IN SITU SITE INVESTIGATION Working with: geotechnical

CPT LOG 01

PointID

CPT 206

CLIENT : Geotechnical Engineering
PROJECT : A417 Missing Link
LOCATION : Gloucester
PROJECT No. : 1190295

EASTING : 392355.9 m
NORTHING : 215502.2 m
ELEVATION : 179.70 m OD
CHECKED BY : LD
TERMINATION REASON : Refusal

Remark:
Test refused on tip resistance.

SHEET : 1 OF 1
STATUS : Final
TEST DATE :
PLOT DATE : 06/04/2020
METHOD : ISO 22476-1:2012

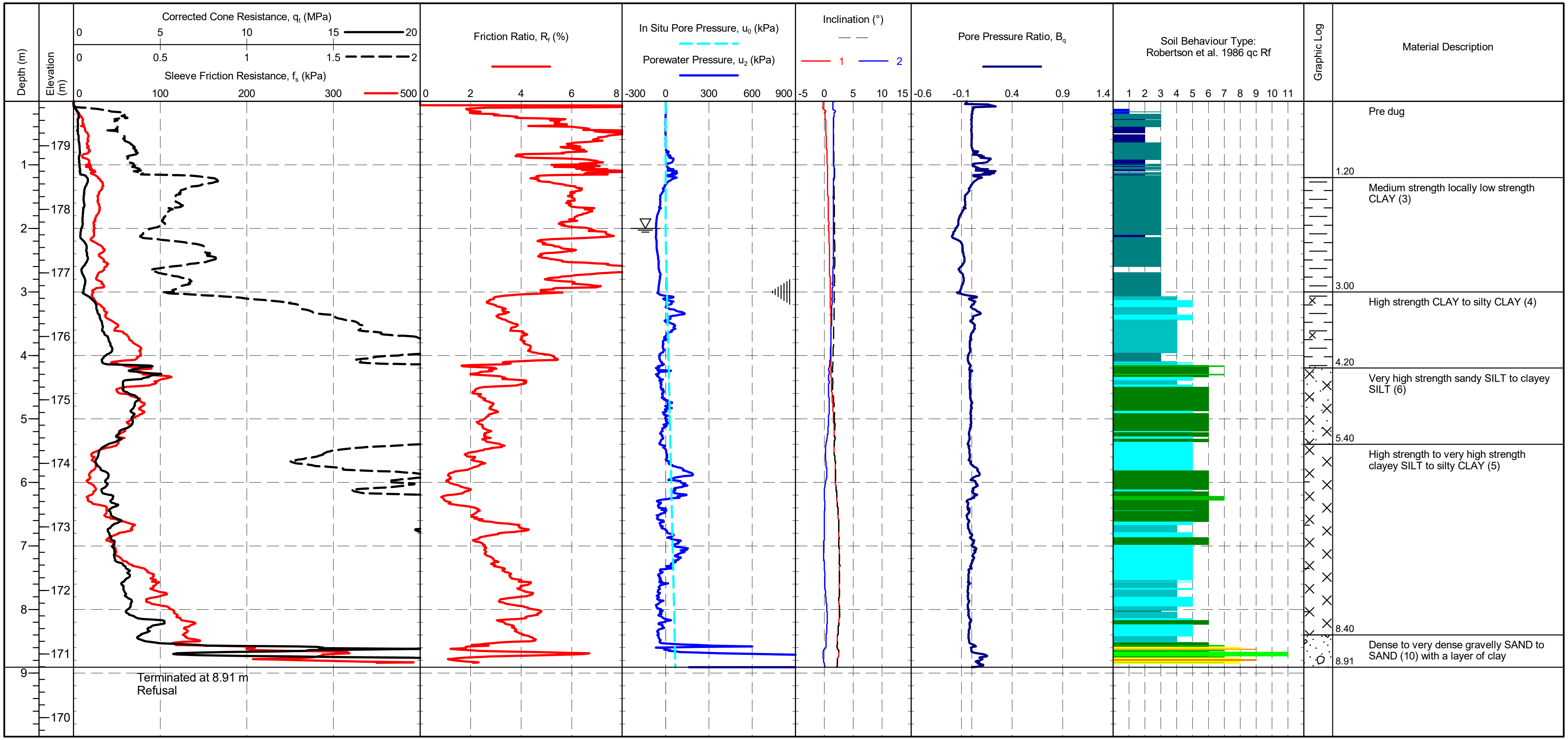

CONE ID	:	DP15-CFPTxy.70102
CONE MODEL	:	DP15-CFPTxy
CONE AREA	:	15cm²
CONE AREA RATIO	:	0.85
FILTER POSITION	:	u2
FILTER TYPE	:	HDPE

TEST TYPE	:	TE2
APPLICATION CLASS	:	2
RIG	:	CPT 012
OPERATOR	:	AL
FRICTION REDUCER	:	None
WEATHER	:	Overcast & Mild

CPTU ZERO VALUES

Transducer	Pre	Post	Difference
Tip			
Sleeve			
Pore Pressure 2			
X-Y Inclinometer			

METHOD: Robertson et al. 1986 qc Rf

1 - Sensitive fine grained material
2 - Organic material
3 - CLAY
4 - Silty CLAY to CLAY
5 - Clayey SILT to silty CLAY
6 - Sandy SILT to clayey SILT
7 - Silty SAND to sandy SILT
8 - SAND to silty SAND
9 - SAND
10 - Gravelly SAND to SAND
11 - Very stiff fine grained
12 - SAND to clayey SAND

Groundwater Level

Dissipation Test

CPT LOG 02

IN SITU SITE INVESTIGATION Working with: geotechnical

PointID
CPT 206

CLIENT : Geotechnical Engineering	EASTING : 392355.9 m	Remark:	SHEET : 1 OF 1
PROJECT : A417 Missing Link	NORTHING : 215502.2 m	Test refused on tip resistance.	STATUS : Final
LOCATION : Gloucester	ELEVATION : 179.70 m OD		TEST DATE :
PROJECT No. : 1190295	CHECKED BY : LD		PLOT DATE : 06/04/2020
	TERMINATION REASON : Refusal		METHOD : ISO 22476-1:2012

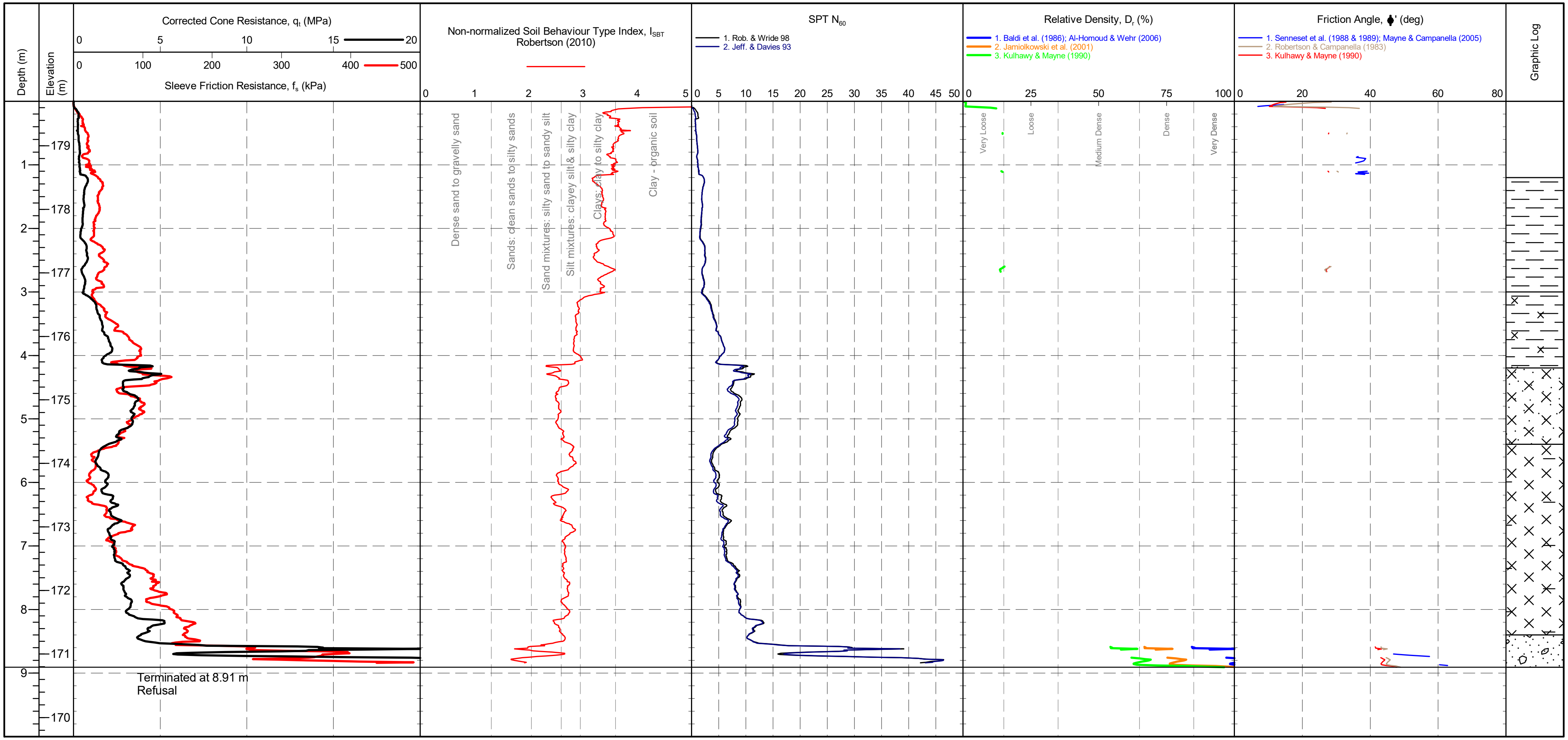

CONE ID	: DP15-CFPTxy.70102	TEST TYPE	: TE2
CONE MODEL	: DP15-CFPTxy	APPLICATION CLASS	: 2
CONE AREA	: 15cm^2	RIG	: CPT 012
CONE AREA RATIO	: 0.85	OPERATOR	: AL
FILTER POSITION	: u2	FRICTION REDUCER	: None
FILTER TYPE	: HDPE	WEATHER	: Overcast & Mild

CPTU ZERO VALUES

Transducer	Pre	Post	Difference
Tip			
Sleeve			
Pore Pressure 2			
X-Y Inclinometer			

GRANULAR SOILS (Sands & Gravels) Robertson et al. 1986 Zones 7-10 and Zone 12

Description	SBT Index, Ic	Description	SPT N value, NSPT	Description	Relative Density Dr (%)
Clays	2.95-3.60	Very Loose	0 - 4	Very Loose	0 - 15
Silt mixtures	2.60-2.95	Loose	4 - 10	Loose	15 - 35
Sand mixtures	2.05-2.60	Medium Dense	10 - 30	Medium Dense	35 - 65
Sands	1.31-2.05	Dense	30 - 50	Dense	65 - 85
Gravelly sand	<1.31	Very Dense	>50	Very Dense	>85

Groundwater Level

Dissipation Test

IN SITU SITE INVESTIGATION   Working with: geotechnical

CPT LOG 03

PointID
CPT 206

CLIENT : Geotechnical Engineering PROJECT : A417 Missing Link LOCATION : Gloucester PROJECT No. : 1190295	EASTING : 392355.9 m NORTHING : 215502.2 m ELEVATION : 179.70 m OD CHECKED BY : LD TERMINATION REASON : Refusal	Remark: Test refused on tip resistance.	SHEET : 1 OF 1 STATUS : Final TEST DATE : PLOT DATE : 06/04/2020 METHOD : ISO 22476-1:2012

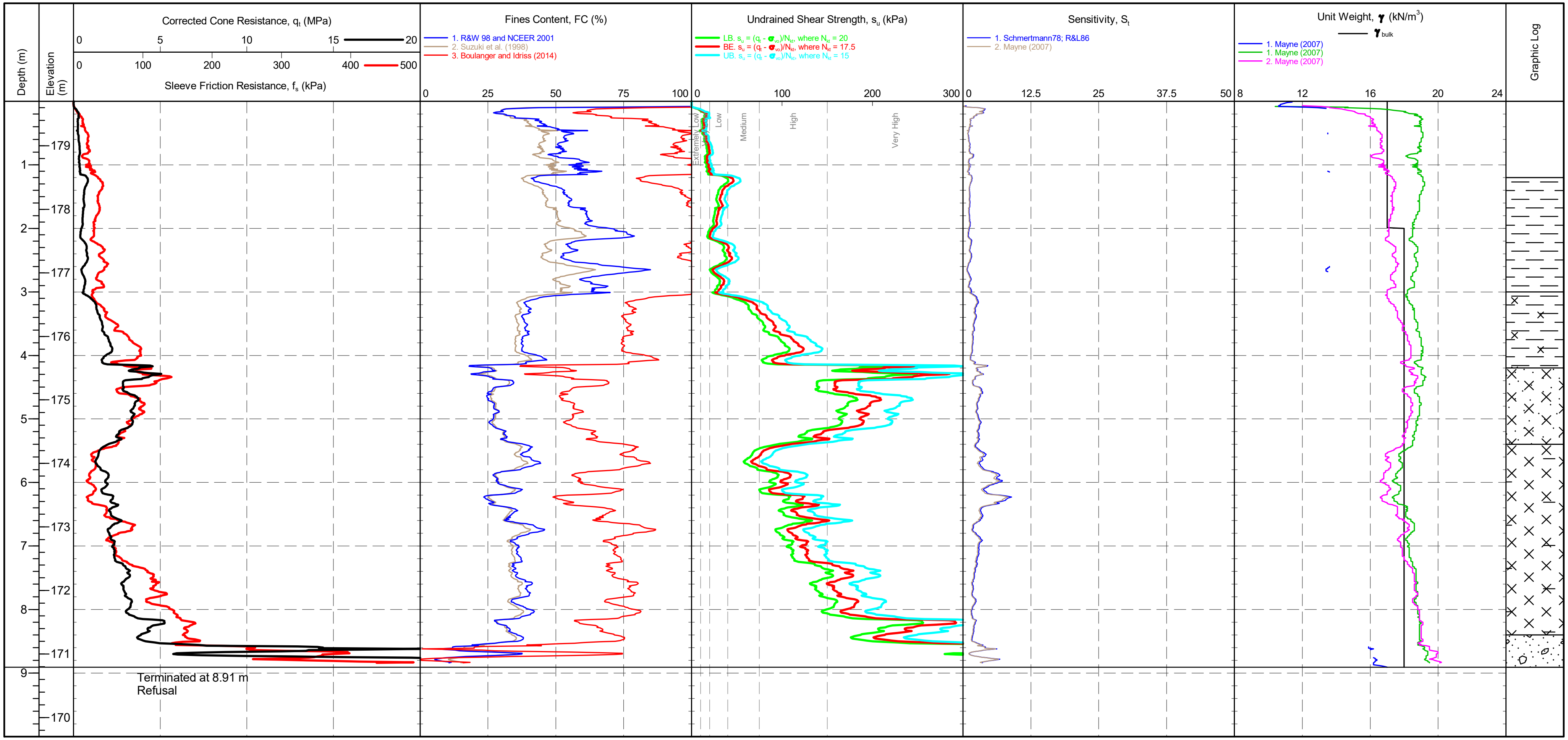

CONE ID	: DP15-CFPTxy.70102	TEST TYPE	: TE2
CONE MODEL	: DP15-CFPTxy	APPLICATION CLASS	: 2
CONE AREA	: 15cm²	RIG	: CPT 012
CONE AREA RATIO	: 0.85	OPERATOR	: AL
FILTER POSITION	: u2	FRICTION REDUCER	: None
FILTER TYPE	: HDPE	WEATHER	: Overcast & Mild

CPTU ZERO VALUES

Transducer	Pre	Post	Difference
Tip			
Sleeve			
Pore Pressure 2			
X-Y Inclinometer			

COHESIVE SOILS (Clays & Silts) Robertson et al. 1986 Zones 1-6 and Zone 11

Term based on measurement	su (kPa)	Term based on measurement	su (kPa)
Extremely low strength	<10	Medium strength	40-75
Very low strength	10-20	High strength	75-150
Low strength	20-40	Very high strength	150-300
		Extremely high strength	>300

Groundwater Level

Dissipation Test

IN SITU SITE INVESTIGATION Working with: geotechnical

CPT LOG 04

PointID

CPT 206

CLIENT : Geotechnical Engineering	EASTING : 392355.9 m	Remark:	SHEET : 1 OF 1
PROJECT : A417 Missing Link	NORTHING : 215502.2 m	Test refused on tip resistance.	STATUS : Final
LOCATION : Gloucester	ELEVATION : 179.70 m OD		TEST DATE :
PROJECT No. : 1190295	CHECKED BY : LD		PLOT DATE : 06/04/2020
	TERMINATION REASON : Refusal		METHOD : ISO 22476-1:2012

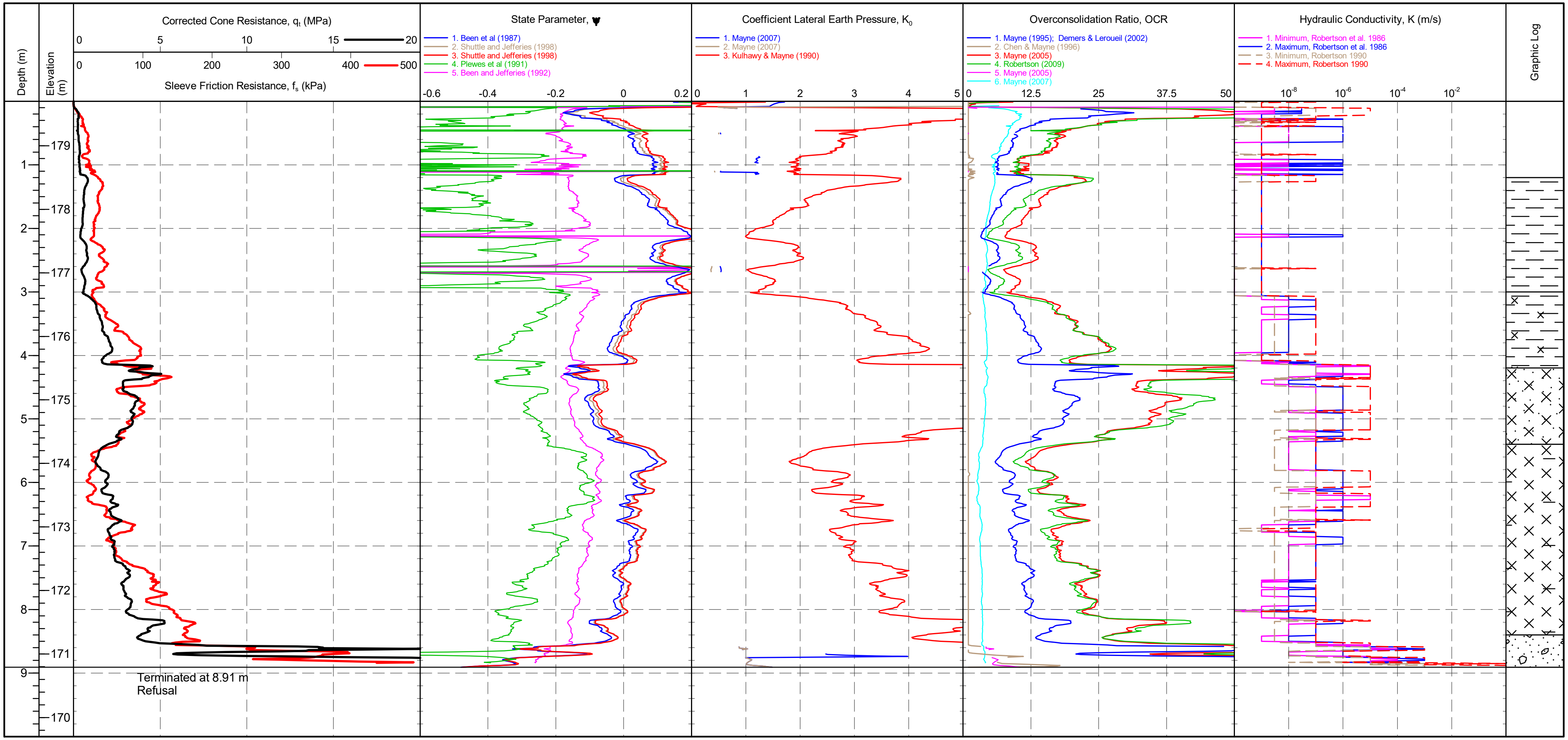

CONE ID : DP15-CFPTxy.70102	TEST TYPE : TE2	
CONE MODEL : DP15-CFPTxy	APPLICATION CLASS : 2	
CONE AREA : 15cm²	RIG : CPT 012	
CONE AREA RATIO : 0.85	OPERATOR : AL	
FILTER POSITION : u2	FRICTION REDUCER : None	
FILTER TYPE : HDPE	WEATHER : Overcast & Mild	

CPTU ZERO VALUES

Transducer	Pre	Post	Difference
Tip			
Sleeve			
Pore Pressure 2			
X-Y Inclinometer			

Groundwater Level

Dissipation Test

CPT LOG 05

IN SITU SITE INVESTIGATION Working with: geotechnical

PointID
CPT 206

CLIENT : Geotechnical Engineering PROJECT : A417 Missing Link LOCATION : Gloucester PROJECT No. : 1190295	EASTING : 392355.9 m NORTHING : 215502.2 m ELEVATION : 179.70 m OD CHECKED BY : LD TERMINATION REASON : Refusal	Remark: Test refused on tip resistance.	SHEET : 1 OF 1 STATUS : Final TEST DATE : PLOT DATE : 06/04/2020 METHOD : ISO 22476-1:2012

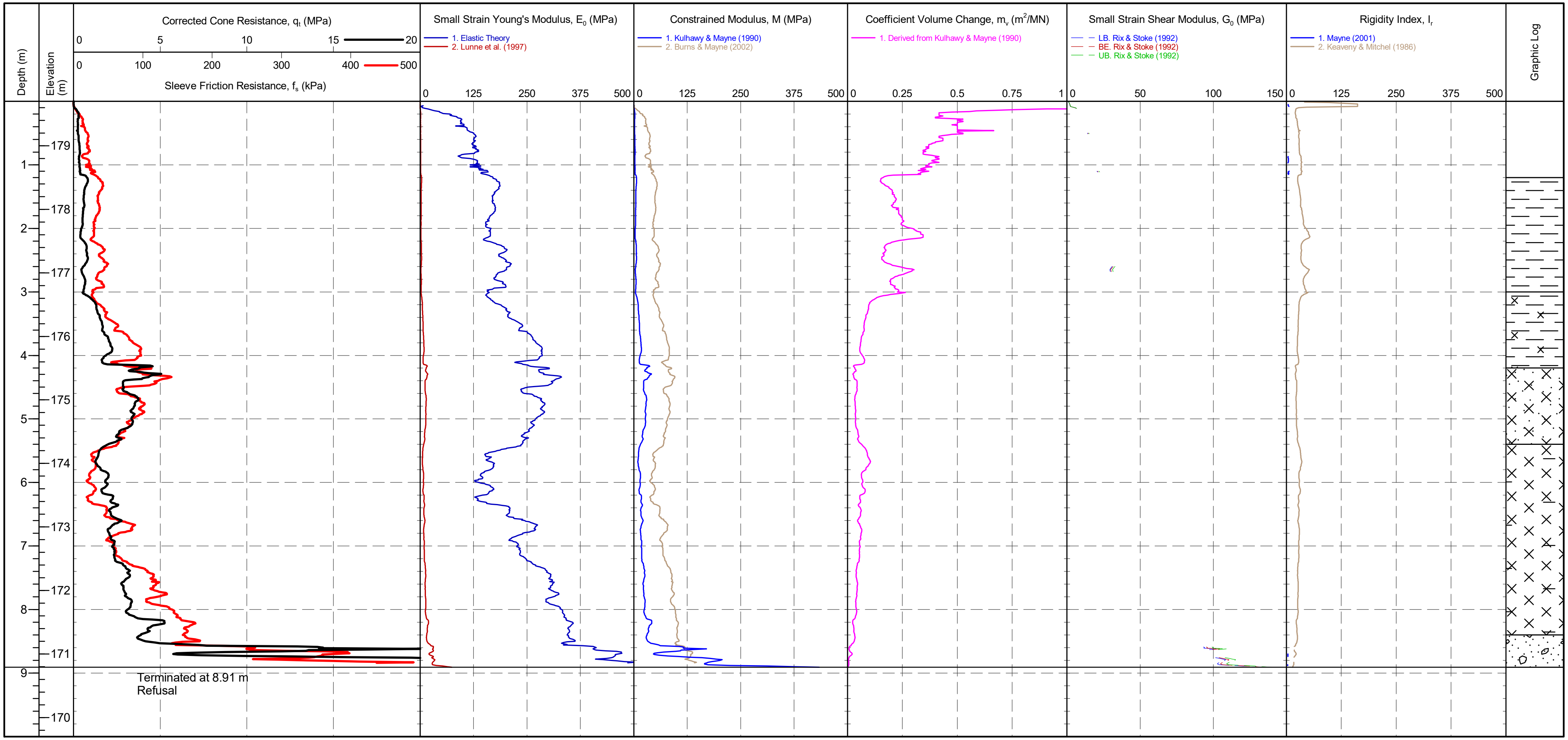

CONE ID : DP15-CFPTxy.70102 CONE MODEL : DP15-CFPTxy CONE AREA : 15cm^2 CONE AREA RATIO : 0.85 FILTER POSITION : u2 FILTER TYPE : HDPE	TEST TYPE : TE2 APPLICATION CLASS : 2 RIG : CPT 012 OPERATOR : AL FRICTION REDUCER : None WEATHER : Overcast & Mild	Groundwater Level Dissipation Test

CPTU ZERO VALUES

Transducer	Pre	Post	Difference
Tip			
Sleeve			
Pore Pressure 2			
X-Y Inclinometer			

DISSIPATION TEST

IN SITU SITE INVESTIGATION

Working with: geotechnical

Test ID
CPT 206 - 3.00 m

CLIENT : Geotechnical Engineering	AREA : A417 MISSING LINK	SHEET : 1 OF 1
ENGINEER :	EASTING : 392355.9 m	STATUS : Final
PROJECT : A417 Missing Link	NORTHING : 215502.2 m	DATE : 09/07/19
LOCATION : Gloucester	COORD. SYS.:	
PROJECT No. : 1190295	ELEVATION : 179.70 m	

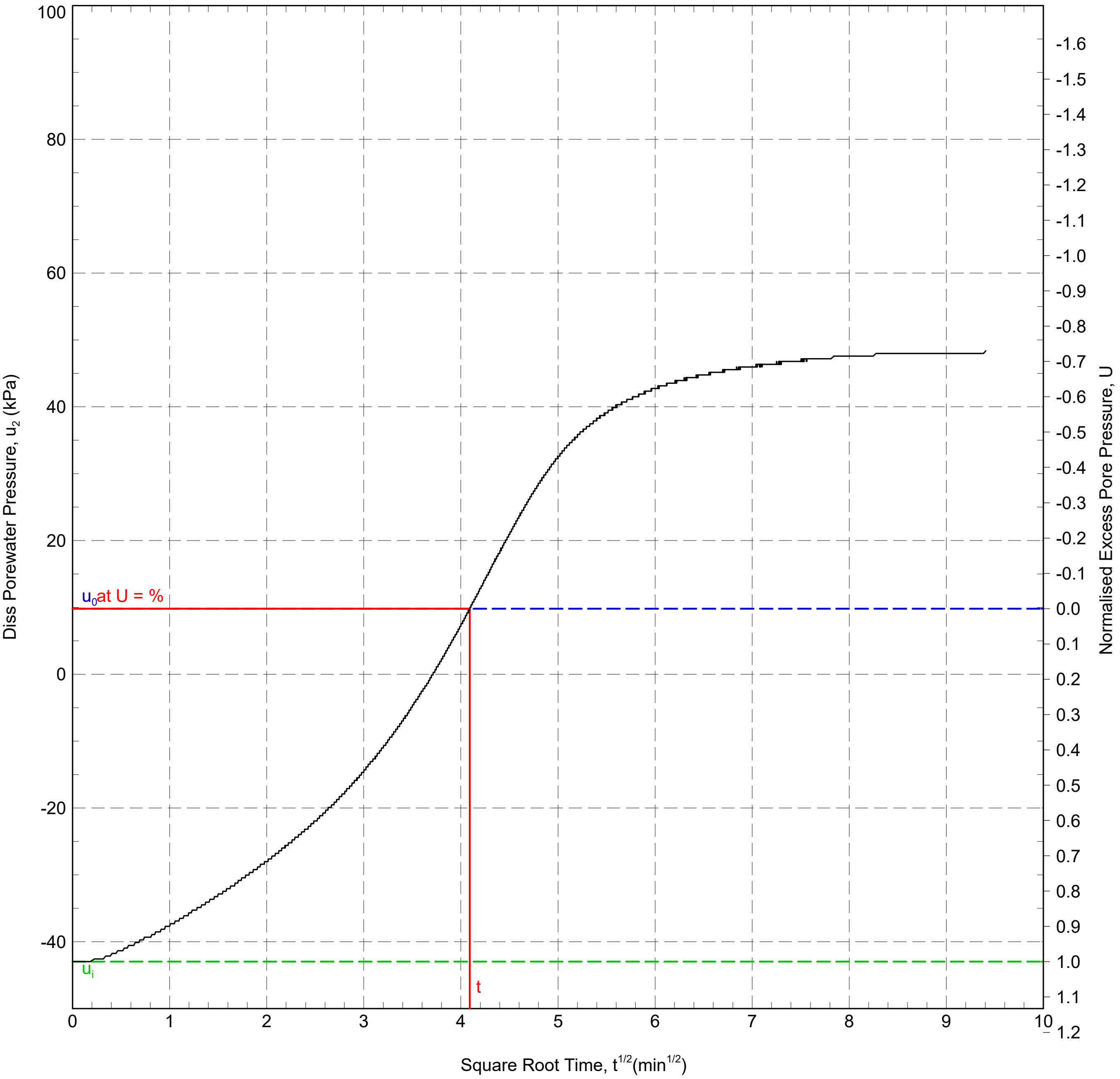

In Situ Pore Pressure, u_0:	9.8 kPa	Rigidity Index, I_r:	100
Initial Pore Pressure, u_i:	-43.0 kPa	Ratio c_h/c_v:	1.25
Final Pore Pressure:	48.4 kPa		
Dissipation Pressure:	9.8 kPa		
Time for % Dissipation, t:	16.74 min		

RIG : CPT 012	ANALYSED BY : LD	DATE: 29/07/2019
CONE TYPE : DP15-CFPTxy	CHECKED BY : LD	DATE: 29/07/2019
CONE ID : DP15-CFPTxy.70102	APPROVED BY : DW	DATE: 29/07/2019
OPERATOR : AL		

REMARK

T50 not reached.

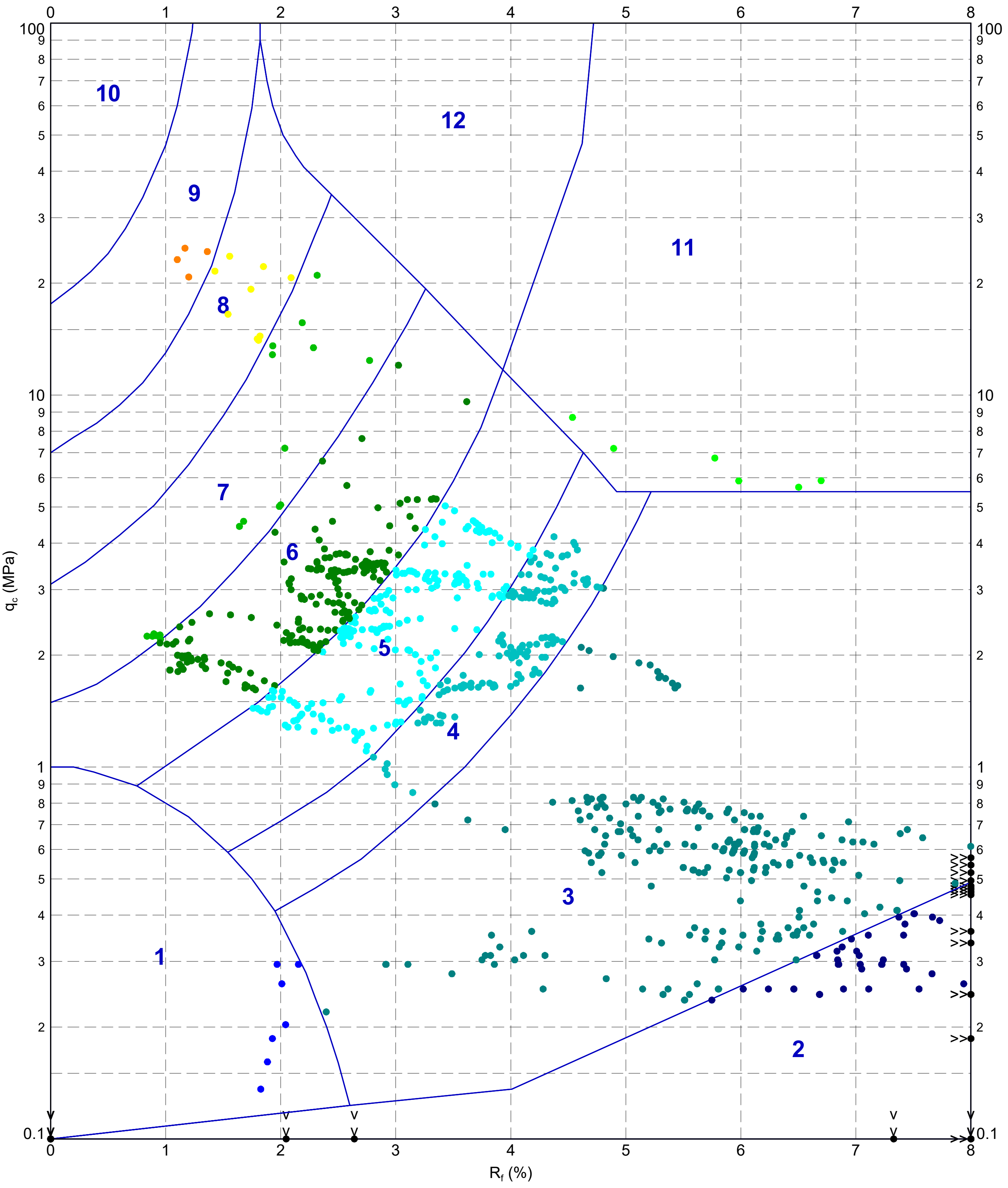

METHOD: Robertson et al. 1986 qc Rf

1 - Sensitive fine grained material	4 - Silty CLAY to CLAY	7 - Silty SAND to sandy SILT	10 - Gravelly SAND to SAND
2 - Organic material	5 - Clayey SILT to silty CLAY	8 - SAND to silty SAND	11 - Very stiff fine grained
3 - CLAY	6 - Sandy SILT to clayey SILT	9 - SAND	12 - SAND to clayey SAND

IN SITU
SITE INVESTIGATION

TITLE: Geotechnical Engineering Gloucester A417 Missing Link Robertson et al. 1986 q_c vs. R_f - CPT 206	DRAWN	DATE 06/04/2020	
	CHECKED	DATE 06/04/2020	
	SCALE Not To Scale		A4
	PROJECT No 1190295	FIGURE No	

IN SITU SITE INVESTIGATION

Unit 23 Hastings Innovation
Centre,
Highfield Drive
St. Leonards on Sea, East Sussex,
TN38 9UH, U.K.

Company No.: 6339499
VAT No.: 922 3561 41

LANKELMA Limited
Cold Harbour Barn, Cold Harbour Lane, Iden
East Sussex, TN31 7UT
T: +44 (0)1797 280050
E: info@lankelma.com
www.lankelma.com

A417 GLOUCESTERSHIRE

SOIL INVESTIGATION

CPT REPORT

Cone penetration test
Geotechnical data interpretation

Project ref.: P-107175-1




PROJECT:	A417 Gloucestershire

CLIENT:	Geotechnical Engineering

FIELDWORK

CPT rig(s)	1.3-tonne mini-crawler CPT unit (UK19)
Date fieldwork started	29th April 2019
Date fieldwork completed	29th April 2019
Lankelma's representative	Emma Stickland
Client's representative	David Owen

REPORT

Status	Revision	Action	Date	Name
Final	00	**Completed**	09/05/19	Chris Player
		Checked	10/05/19	Emma Stickland
		Approved	10/05/19	Joseph Hobbs

CONTENTS

SUMMARY TABLES

APPENDICES

1 INTRODUCTION

At the request of Geotechnical Engineering, a soils investigation was carried out on project *A417 Gloucestershire*.

Site location (in the general region of):

Barrow Wake Viewpoint
Birdlip, Gloucestershire
GL4 8JY

2 DISCLAIMER

The investigation information, raw data and interpretations provided in this report are for the sole benefit of the Client identified at the front of the report.

Lankelma has exercised reasonable skill, care and diligence in the fieldwork and preparation of this report. This report has been completed based on information available to Lankelma at the time of preparation. The measurement and interpreted data in this report do not constitute recommendations for design purposes. An appropriately qualified person must review and interpret the data given in this report, together with any assumptions we have made that affect the data, before using the data for design or recommendation.

Lankelma accepts no responsibility for the accuracy or appropriateness of any assumptions, derived soil parameters, soil descriptions or soil unit boundaries contained in this report.

3 COMPLETED WORKS

- 3 nr. cone penetration tests (CPTu) with piezo measurement; and
- Factual report plus additional geotechnical data interpretation.

The *Summary Tables* section contains tabulated summaries of the works completed together with analysis results where necessary.

4 FIELDWORK GENERAL

Fieldwork was performed with a 1.3-tonne mini-crawler CPT unit (UK19) equipped with a 12-tonne capacity hydraulic ram set.

The Client was responsible for the positioning and re-survey of all investigative locations.

The target depth for the investigation was 35 m below ground level. Table 1 details the final test depths and reasons for test termination (r*efusal factor). W*here penetration refusal was encountered the termination depth was advised to, and agreed with, the Client's on-site representative.

5 CONE PENETRATION TESTING

Cone penetration testing was carried out in general accordance with BS ISO 22476-1:2012.

Penetrometer measurements included cone tip resistance, friction sleeve resistance and dynamic pore water pressure sampled at a 10 mm resolution.

The penetrometer was calibrated in accordance with BS8422:2003 and ASTM E74-13a. The management of calibration records is in accordance with ISO 10012. Copies of all calibration certificates for the cones used are presented in Appendix A. Penetrometer details and calibration certificates are reported in Table 1 and Appendix A respectively.

The piezometer filter element was in the u_2 position and was vacuum saturated. The pore pressure system was saturated with de-aired 10000 cSt silicone oil.

5.1 CPT DATA REDUCTION AND PRESENTATION

The CPT results are presented in Appendix B. The corrected cone resistance (q_t), local side friction (f_s), dynamic pore water pressure (u_2), friction ratio (R_f) and inclination are all presented against depth and elevation in accordance with recommendations of the BS ISO 22476-1:2012. CPT data and the associated derived geotechnical parameters are included in the AGS 3.1 and 4.0 data files provided.

The cone tip resistance and sleeve force measurements were converted to pressures using the nominal dimensions of the penetrometer.

For piezocone tests the corrected tip resistance was calculated according to the formula:

$$q_t = q_c + u_2 \times (1 - a)$$

Where a is the 'area ratio' and (1- a) is the proportion of cross-sectional area between the cone tip and cone body where pore pressures (positive or negative) can act to add or subtract from the total external axial force on the tip. The difference between measured and corrected values is largest in low strength soils with large excess pore pressures. The relationship between measured resistance, excess pressure and correction difference is described by the curves in the following chart for alpha factor of 0.8:

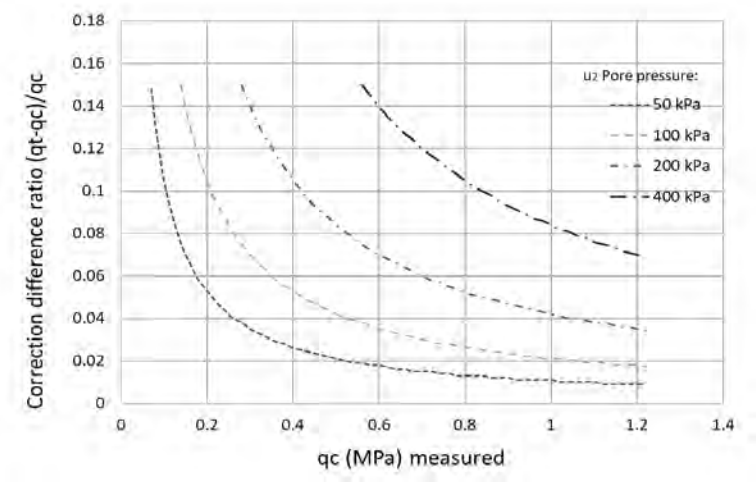

Figure 5-1 corrected tip resistance fraction with measured tip resistance

Penetration length readings were corrected for inclination and sleeve readings were depth corrected for the dimensional offset between cone tip and sleeve during post processing. An additional shift of -80 mm was applied to the sleeve to account for tip failure zone offset (see 'CPT Interpretation Notes'). 'Rod spikes', artefacts of the pause for push rod addition, were filtered from the cone tip and sleeve data.

The raw (or corrected) data are presented in Appendix B.

Geotechnical parameters appropriate for drained and undrained cone penetration conditions were derived for corresponding drained and undrained derived soil behaviour types (SBTs) respectively, however, to account for uncertainty in the SBT correlation with drainage behaviour, all parameters were derived over a range of transitional soils within the range $2.4 < Ic < 2.7$ (see section 6.3).

In general, the engineering parameters derived are intended for non-cemented predominantly silicate soils.

5.2 IN-SITU STRESS CONDITIONS

The in-situ total and effective stress state was calculated based on an assumed total unit weight of 17 kN/m^3 above the principal phreatic surface and 18 kN/m^3 below.

The depth of the principal phreatic surface, or groundwater table, was taken as equal to the groundwater level(s) provided by the Client.

Note: The term phreatic surface is used here, however when it is based on piezocone measurements it is assumed that the piezometric level (under hydrostatic conditions) and groundwater table coincide. The phreatic or piezometric surface reported is only intended to provide information about the assumed pore pressure distribution for calculation of relevant derived parameters from the CPT and may not represent the true position of the groundwater table or perched water bodies. Complex groundwater pressure distributions, if they are observed from the measurements, will be applied to relevant derived parameters.

5.3 SOIL BEHAVIOUR TYPE

The soil behaviour type (SBT) was interpreted using the Robertson (1990) classification system based on the normalised cone resistance (Qt) and normalised friction sleeve resistance (Fr) for silicate soils.

While the classification based on normalised parameters is considered more accurate, particularly at depths exceeding 15-20 m, the classification is often significantly in error (artificially granular/drained) at very shallow depth (< 1-3 m). The error at shallow depth is associated with the potentially large difference between the estimated vertical effective stress (applied in normalisation) and the unknown horizontal stress influencing penetration resistance.

Robertson (2010) proposed a non-normalised version of the 1990 chart which uses dimensionless cone resistance (q_c/Pa) and friction ratio, Rf. The classification according to this chart can be more reliable at shallow depth and has been plotted as an approximate SBT index (discussed below) for comparison to the normalised classification.

The SBT chart is provided in Appendix A – *General Information,* titled 'CPT Soil Behaviour Type Chart'.

It should be noted that the SBT classification provides the general soil 'type' which typically provides a similar CPT measurement range of q_c and f_s. Correspondingly, it will also show biased towards the soil fraction that dominates the mechanical behaviour. While the repeatability and behavioural bias of the SBT is usually beneficial, the classification is not always an appropriate substitute for classification based on grain-size distribution.

The results are presented on the plots of Appendix C – *Standard interpretation results (set 1)*.

5.4 SOIL BEHAVIOUR TYPE INDEX - I_C

The main trend in soil behaviour type (SBT) variation can be expressed a continuous index, I_C, proposed by Robertson and Wride (1998) based on a similar index proposed by Jefferies and Davies (1993). The index provides a continuous profile of SBT variation with depth for end-user analysis of soil units and variation within units.

The equivalent non-normalised version, as proposed by Robertson (2010), is provided for comparison.

The basis of I_c and its approximation of the original chart classification zones may be seen from Appendix A figure 'CPT Soil Behaviour Type Chart'. The method does not identify zones 1 (*sensitive fine grained)* and zones 8 & 9 (*overconsolidated or cemented*).

Normalised SBT index I_C (Robertson and Wride, 1998)***:***

$$I_c = [(3.47 - \log Q_t)^2 + (log F_r + 1.22)^2]^{0.5}$$

Non-normalised SBT index I_C (Robertson, 2010)***:***

$$I_c = \left[\left(3.47 - \log\left(\frac{q_c}{\sigma_{atm}}\right)\right)^2 + (logR_f + 1.22)^2\right]^{0.5}$$

(See glossary of terms and symbols Appendix A)

The results are presented on the plots of Appendix C – *Standard interpretation results (set 1)*.

5.5 RELATIVE DENSITY

The relative density of sands was calculated based on an empirical relationship proposed by Jamiolkowski *et al.* (2001) based on a large database of undisturbed frozen samples and calibration chamber tests. The expected accuracy may be evaluated from the figures presented below.

$$D_r = 100\left[0.268 \cdot \ln\left(\frac{q_t/\sigma_{atm}}{\sqrt{\sigma_{vo}'/\sigma_{atm}}}\right) - k\right]$$

(See glossary of terms and symbols appendix A – *General information*)

k = Compressibility dependant constant can be taken as -0.675 for medium compressibility (applied value in our interpretation), <= 1 for high compressibility and >= 2 for compressible sands.

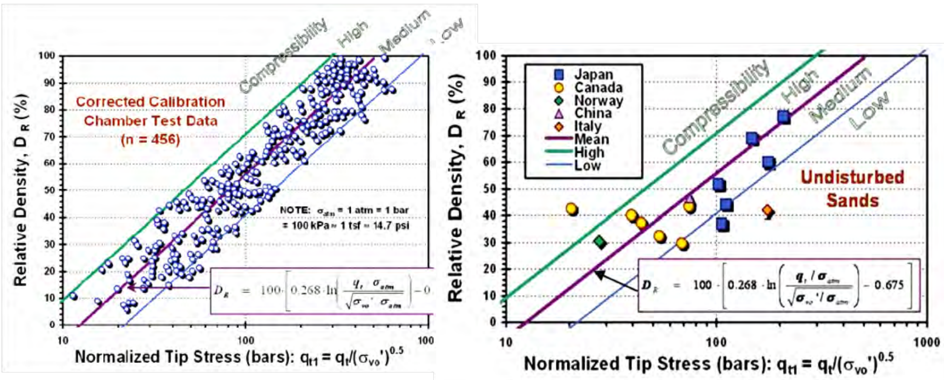

Figure 5-2 Relative density with normalised tip stress and sand compressibility from calibration chamber tests (left) and undisturbed frozen samples (right). Jamiolkowski *et al.* (2001). Reproduced from Mayne (2007).

The results are presented on the plots of Appendix D – *Standard interpretation results (set 2)*.

5.6 UNDRAINED SHEAR STRENGTH

The undrained shear strength s_u is usually estimated as a factor of net cone tip resistance (Lunne *et al*, 1981):

$$s_u = \frac{q_c - \sigma_{v0}}{N_k}$$

where N_k is an empirical cone factor which varies with soil type, stress history, structure/fabric, plasticity and the mode of shearing.

(See glossary of terms and symbols appendix A – *General information*)

Mayne and Peuchen (2018) performed and evaluation of 407 high-quality triaxial compression tests against net tip resistance and proposed N_{kt} factors with regression analysis details for five categories of clays shown in Table 1.

Table 1 Summary of CAUC s_u versus q_{net} for clays. Reproduced from Mayne and Peuchen (2018).

Clay Group	Number of sites	No. Data	Correlation Coefficient r_2	Factor N_{kt}	Mean Pore Pressure Parameter B_q
Offshore NC-LOC	17	115	0.98	12.32	0.51
Onshore NC-LOC	30	191	0.867	12	0.53
Sensitive NC-LOC	5	43	0.507	10.33	0.84
OC Intact	5	36	0.862	13.57	0.49
OC Fissured	5	22	0.393	22.47	-0.01
All clays	62	407	0.923	13.33	0.55

Alternatively, a variable N_{kt} factor can be estimated for the profile as a function of the pore pressure parameter B_q, applicable for B_q values of > -0.01. The following equation proposed by Mayne and Peuchen is based on the same database evaluation:

$$N_{kt} = 10.5 - 4.6 \cdot \ln(B_q + 0.1)$$

Where the pore pressure parameter B_q is the ratio of excess pore pressure to net tip resistance:

$$B_q = \frac{u_2 - u_0}{q_t - \sigma_{v0}}$$

The N_{kt} estimate has a standard error of 2.4 N_k and correlation coefficient of 0.645.

The estimate based on B_q is presented as 's_u5' on the parameter plots and is only suitable for tests that have a high-quality pore pressure data, often indicated by a positive, repeatable and dynamic response. For tests that have a reliable pore pressure response throughout, the evaluation on a point by point basis is warranted. For projects with variable response quality and with possible piezo desaturation (for example in the unsaturated zone or by dilation/cavitation) it is preferable to identify zones with reliable pore pressure response for representative soils and select a characteristic value of B_q for evaluation of N_{kt}. Lankelma are not always in view of the effort that has been made in preparation of the test location to maintain saturation of the piezo sensor.

Note: N_{kt} (with subscript 't') indicates a N_k factor that has been established using the corrected tip resistance q_t. N_{kt} can be applied to the uncorrected tip resistance q_c (non-piezocone tests) but results in a slightly lower estimate of s_u depending on the correction magnitude (q_c - q_t) in lower strength soils.

Undrained shear strengths corresponding to selected values of N_k are presented on the plots of Appendix C – *Standard interpretation results (set 1). 's_u3'* on the logs (N_k = 15) has been included as a reference for comparison to traditional arbitrary N_k values of 15 and 20.

5.7 OVERCONSOLIDATION RATIO

The preconsolidation stress σ_p' was calculated based on the method proposed by Mayne et al (2009):

$$\sigma_p' = k \cdot (q_t - \sigma_{vo})^{m'}$$

$$OCR = \sigma_p'/\sigma'_{v0}'$$

(See glossary of terms and symbols Appendix A)

Mayne *et al* found that the trend with mean grain size followed a power law through the addition of exponent m' and that its value can be estimated by relation to soil behaviour type index I_c:

$$m' = 1 - \frac{0.28}{1 + \frac{I_c}{2.65}^{25}}$$

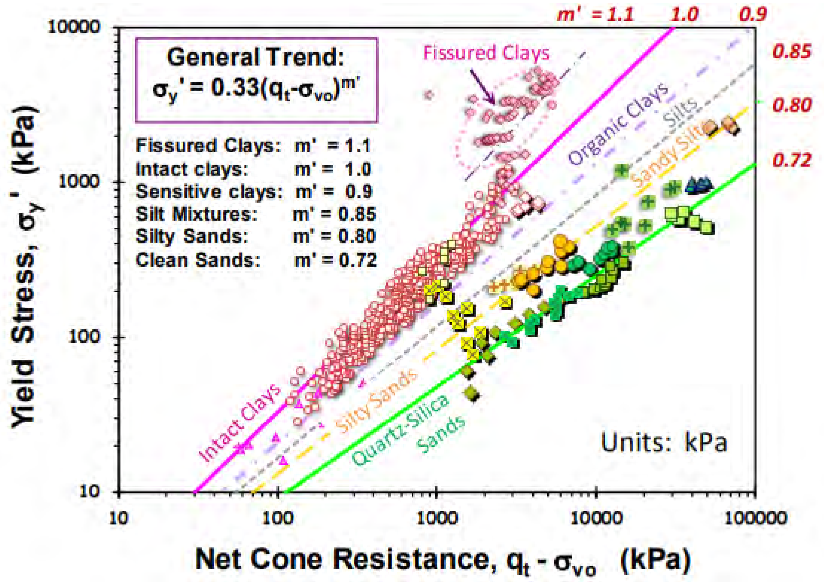

Figure 5-3 Preconsolidation stress with net cone resistance power law, reproduced from Mayne (2014).

An additional σ_p' and OCR was calculated for m' = 1.1 to reflect the upper trend for over consolidated fissured clays not captured by the soil behaviour type index I_c

5.8 SPT N60 VALUES

Equivalent SPT N60 values, defined as the non-normalised SPT blow count over a 30 cm interval, were derived for two correlations and are presented together in the results section for comparison.

Method 1 - Lunne *et al.* (1997)

$$N_{60} = \frac{q_t}{8.5 \cdot \sigma_{atm} \cdot \left(1 - \frac{I_c}{4.6}\right)}$$

Method 2 - Robertson (2012)

$$\frac{\left(\frac{q_t}{p_a}\right)}{N_{60}} = 10^{(1.268 - 0.2817 I_c)}$$

(See glossary of terms and symbols Appendix A)

The correlations are intended for clays, silts and sands and not for carbonates or cemented geo-materials.

The results are presented in Appendix D – *Standard interpretation results (set 2).*

5.9 FRICTION ANGLE

Sands

The peak friction angle of granular materials was calculated using the Kulhawy and Mayne (1990) method and is an empirical relationship as a function of stress normalised cone tip resistance. The relationship is based on a calibration chamber database from 24 sands of varying mineralogy. The relationship has the form:

$$\phi' = 17.6 + 11.0 \cdot \log(q_{t1})$$

Where:

ϕ' = Peak friction angle (degrees)

q_{t1} = stress normalised cone resistance =

$$\left(\frac{q_t}{\sigma_{atm}}\right) / \left(\frac{\sigma_{v0}'}{\sigma_{atm}}\right)^{0.5}$$

The presence of compressible minerals tends to reduce tip resistance resulting in lower estimate of friction angle, while very coarse (sand) or larger grain size tends to increase tip resistance resulting in higher estimate.

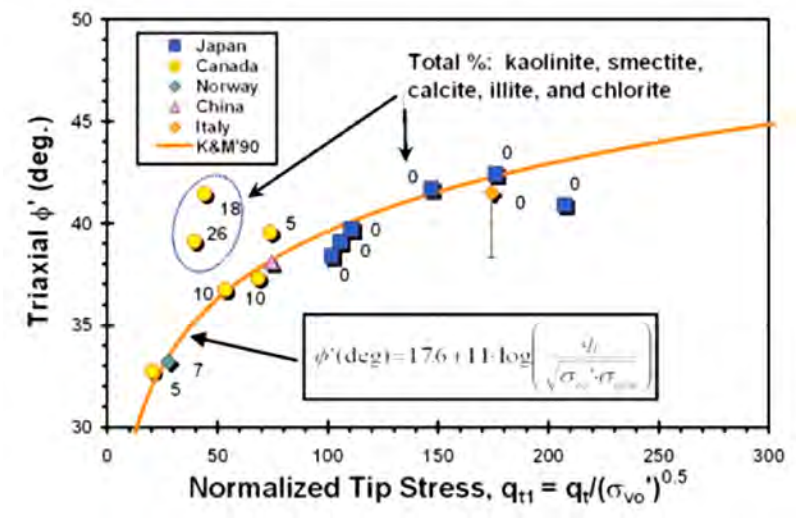

Figure 5-4 Peak triaxial friction angle from undisturbed sands with normalised cone resistance.

Fine grained soils

The effective friction angle for fine grained soils was calculated based on the Senneset *et al.* (1988, 1989) method by applying the approximate closed form solution by Mayne & Campanella (2005) as a direct function of the pore pressure parameter Bq and normalised tip resistance Q. The method is applicable where $0.1 < B_q < 1.0$ and $20° < \phi' < 45°$ and generally appropriate for non-cemented NC-LOC soils.

$$\phi' = 29.5° \, B_q^{0.121} [0.256 + 0.336 \, B_q + \log Q]$$

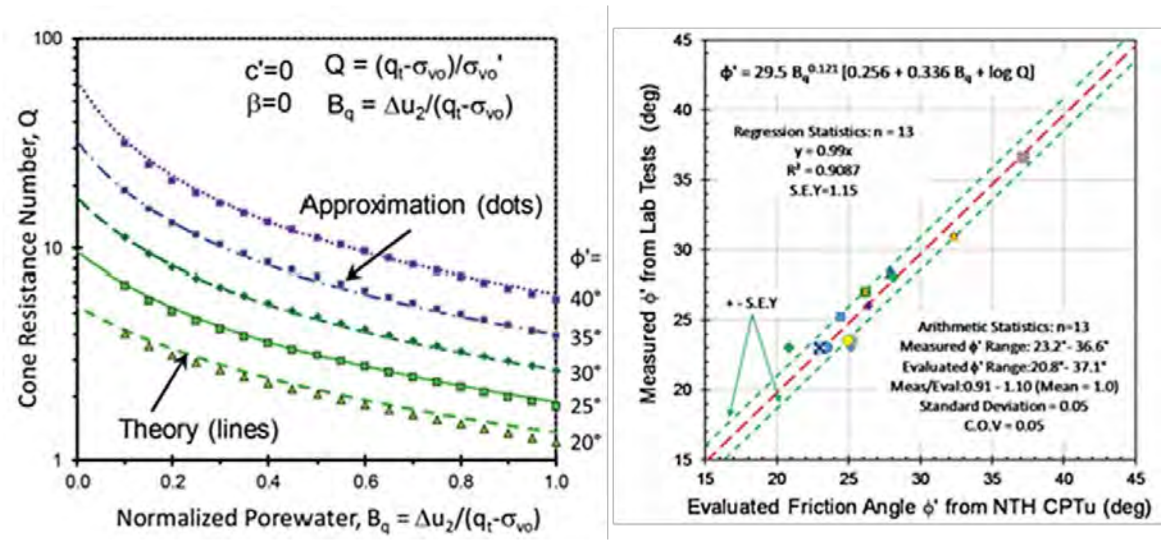

Figure 5-5 [Left] Theoretical curves with function approximation (dots) overlay [Right] calibration data from geotechnical centrifuge tests for a variety of soils. Redrawn from Ouyang & Mayne (2018).

The results are presented in Appendix D – *Standard interpretation results (set 2).*

5.10 COEFFICIENT OF VOLUME CHANGE

Coefficient of volume change (m_v) defined as the inverse of the constrained modulus (M), is evaluated for all soil types using the constrained modulus method proposed by Mayne (2006) cited in Mayne (2007) applicable to the present state of vertical effective stress up to the pre-consolidation stress.

$$m_v = \frac{1}{M}$$

Where:

$$M = \alpha \cdot (q_t - \sigma_v)$$

$$\alpha = 5$$

An alpha factor of 8.25 reported by Kulhawy & Mayne (1990) for fine grained soils appears to provide a better fit through the data for intact non-organic clays, reducing to around 1 to 2 for organic plastic clays.

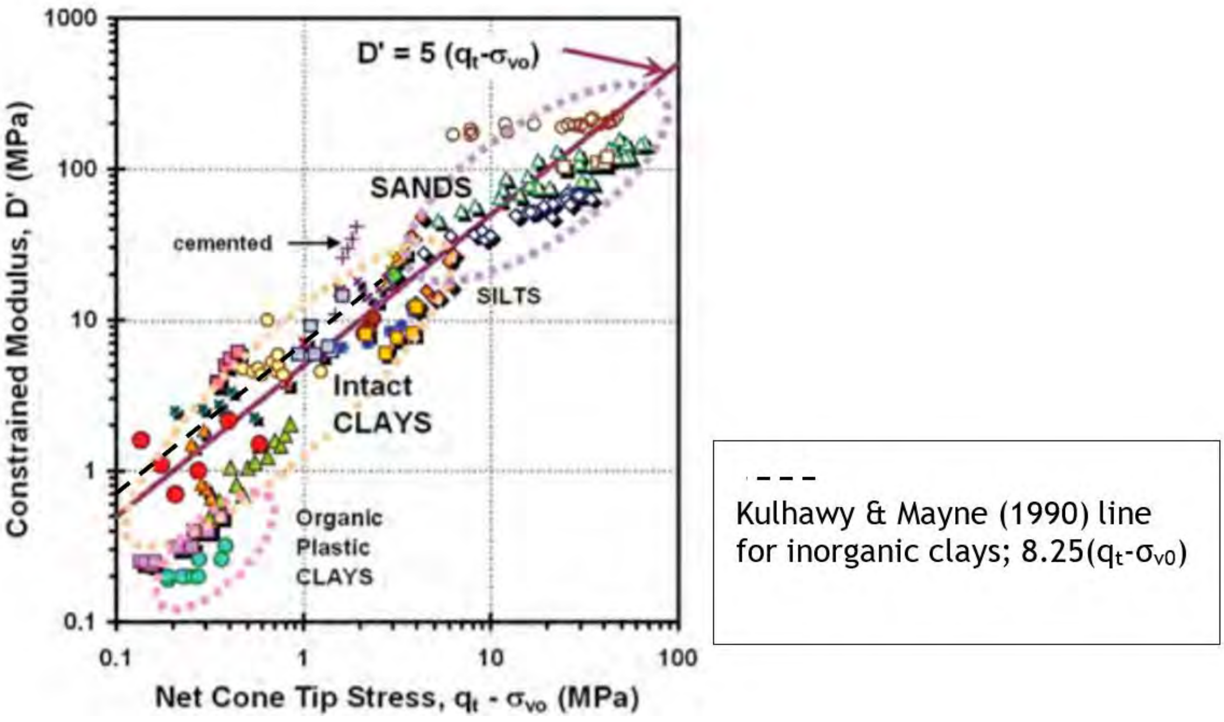

Figure 5-6 Constrained modulus of Mayne (2006). Annotated/redrawn from NCHRP Synthesis 368 (2007).

The results are presented on the plots of Appendix C – *Standard interpretation results (set 1)*.

5.11 YOUNG'S MODULUS

The Young's Modulus at 25% mobilised shear strength (FOS = 4) was calculated according to the method proposed by Robertson (2009):

$$E' = \alpha(q_t - \sigma_v)$$

Where:

$$\alpha = 0.015(10^{0.55\boldsymbol{Ic}+1.68})$$

(See glossary of terms and symbols Appendix A)

The method described by Robertson may be adapted to estimate E' for loading at different percentages of yield stress.

The results are presented in Appendix D – *Standard interpretation results (set 2)*.

5.12 CPT INTERPRETATION NOTES

Provided below is a non-exhaustive set of notes on interpretation of the acquired CPT data with reference to examples within the dataset where appropriate.

DRAINED AND UNDRAINED SOIL BEHAVIOUR

Geotechnical parameters appropriate for drained and undrained cone penetration conditions are derived for drained and undrained soil behaviour types (SBTs) respectively, however, to help mitigate the uncertainty in the SBT correlation with drainage behaviour, all parameters are derived over the Soil Behaviour Type range 2.4 < *Ic* < 2.7. For partially drained conditions, error will be introduced within derived parameters.

Piezocone dynamic pore pressure and dissipation tests may be used to identify drainage conditions. Dissipation t_{50} values exceeding 50 seconds indicate undrained penetration behaviour based on findings of Kim *et al.,* 2010.

In partially drained materials the friction sleeve resistance may rise significantly immediately following a pause in penetration due to consolidation and increased effective stress on the friction sleeve.

DYNAMIC PORE PRESSURE DATA (CPTu)

While the piezo system is saturated before use, testing through unsaturated soils may result in some degree of desaturation leading to a less accurate and more 'sluggish' pore pressure response. Desaturation can also occur during penetration due to suction during dilative shear at the cone shoulder. Dissipation tests that are undertaken following desaturation are likely to have a more pronounced initial rise and some degree of error will be present in the analysis.

If the system becomes desaturated it may or may not re-saturate at higher excess pressures later in the test. The pore pressure response in saturated contractive soils normally have a dynamic 'peaky' appearance.

The tip resistance in lower strength contractive soils without pore pressure measurement in the u2 position is likely to be significantly lower than the equivalent corrected tip resistance depending on the magnitude of pore pressure acting in the gap between cone tip and cone body.

CONE TIP AND SLEEVE OFFSET

The accuracy of the SBT over thin layers and at layer boundaries is sensitive to offset error in the friction ratio often seen as sharp spikes or drops at boundaries. The friction ratio is often inaccurate in heavily disturbed soils with a 'blocky' macro fabric.

For this investigation a friction sleeve depth offset correction of -80mm was applied together with a 5-point moving average on the friction ratio to minimise the influence of this effect.

CONE TYPE

The reference cone type has a 10 cm^2 projected cone tip area and 150 cm^2 friction sleeve area, however it is common to use the larger 15 cm^2 cone with 225 cm^2 friction sleeve area for improved sensitivity and penetration depth potential. Use of the 15 cm^2 cone will produce more pronounced transitions zones and thin layer effects (larger zone of influence and failure zone).

TRANSITION ZONES AND THIN LAYER EFFECTS

During penetration at the boundary between soils of contrasting stiffness, a transition zone is often evident prior to mobilisation of the true soil stiffness. These should be cautiously ignored in assessment of soil behaviour type and parameter evaluation. Where the stiff layer is thin (<~0.75 m) mobilised resistance may be significantly less than that of an equivalent thick layer. The effect for thin low stiffness layers is less significant. Procedures for thin-layer effect correction are provided by Robertson and Wride (1998). In choosing characteristic values of the cone tip and its derived parameters, large scale peaks are likely to be more representative of the material than layer averages.

GRAVELS

The presence of gravel or larger clasts in a soil is often characterised by short peaks in the CPT tip and sleeve readings, possibly with associate inclinometer 'shake' and/or sharp reductions in pore water readings due to dilation effects. Frequent gravels in soft or loose soils may generate erroneous friction ratio values. Where gravels are matrix supported the tip and sleeve peaks may be ignored or filtered in choosing characteristic values for bulk behaviour.

6 REFERENCES

ASTM E74-13a (2013), Standard Practice of Calibration of Force-Measuring Instruments for Verifying the Force Indication of Testing Machines, ASTM International, West Conshohocken, PA.

British Standards Institution (2003) BS 8422:2003, Force measurement – Strain gauge load cell systems – Calibration method. London: British Standards Institution.

Houlsby, G.T. and Teh, C.I. (1988) "Analysis of the Piezocone in Clay". Proceedings of the International Symposium on Penetration Testing (ISOPT-1), Orlando, Vol. 2, pp. 777-783. Balkema Pub., Rotterdam.

ISO 10012:2003 Measurement management systems - Requirements for measurement processes and measuring equipment. New Delhi: Bureau of Indian Standards (2003).

ISO 22476-1:2012 Geotechnical investigation and testing - Field testing - Part 1: Electrical cone and piezocone penetration test. New Delhi: Bureau of Indian Standards (2012).

ISSMGE, 1999. International reference test procedure for the cone penetrometer test CPT and the cone penetration test CPTU, Report of ISSMGE TC16 on Ground Property Characterisation for in situ Testing, In *Proceedings of the 12th European conference on Soil Mechanics and Geotechnical Engineering* 3:2195-222 (1999).

Jamiolkowski, M., LoPresti, D.C.F., and Manassero, M. (2001) "Evaluation of Relative Density and Shear Strength of Sands from Cone Penetration Test and Flat Dilatometer Test". Soil Behaviour and Soft Ground Construction (GSP119), American Society of Civil Engineers, pp. 201-238. Reston, Va. 2001

Jefferies, M.G. and Davies M.P. (1993)," Use of CPTu to estimate equivalent SPT N60", Geotechnical Testing Journal, 16(4), pp. 458-467.

Kim, K., Prezzi, M., Salgado, R., and Lee, W. (2008) "Effect of Penetration Rate on Cone Penetration Resistance in Saturated Clayey Soils", Journal of Geotech. Geoenviron. Eng., Vol. 134(8), pp. 1142-1153.

Kulhawy, F.H. and Mayne, P.W. (1990) "Manual on Estimating Soil Properties for Foundation Design". Report EPRI EL-6800 Research Project 1493-6, Electric Power Research Institute, Palo Alto, CA, pp. 306.

Ladd, C.C. and DeGroot, D.J. (2003) "Recommended Practice for Soft Ground Site Characterization: Arthur Casagrande Lecture". Soil & Rock America 2003 (Proceedings. 12th Pan American Conference on Soil Mechanics and Geotechnical Engineering, Boston, MA). Verlag Glückauf, Essen, Germany. pp. 3–57.

Lunne, T., Robertson, P.K. and Powell, J.J.M. (1997) "Cone Penetration Testing in Geotechnical Practice" Blackie Academic, New York 1997.

Lunne, T. and Kleven, A. (1981) "Role of CPT in North Sea Foundation Engineering". Session at the ASCE National Convention: Cone Penetration Testing and Materials. pp. 76-107. American Society of Engineers (ASCE).

Mayne, P.W. and Campanella, R.G. (2005) "Versatile Site Characterisation by Seismic Piezocone". Proceedings of the 16th International Conference on Soil Mechanics and Geotechnical Engineering, Vol. 2. Millpress, Rotterdam, The Netherlands 2005. pp 721-724.

Mayne, P.W. and Peuchen J. (2018), "Evaluation of CPTU Nkt cone factor for undrained strength of clays". Proceedings of the 4th International Symposium on Cone Penetration Testing (CPT'18), 21-22 June 2018, Delft, The Netherlands. CRC Press. pp. 423-429.

Mayne, P.W. (2007) "Cone Penetration Testing – A Synthesis of Highway Practice". NCHRP Synthesis 368, Transportation Research Board, Washington, D.C.

Mayne, P.W. (2014). KN2: "Interpretation of geotechnical parameters from seismic piezocone tests". Proceedings of the 3rd International Symposium on Cone Penetration Testing (CPT'14), June 2014, ISSMGE Technical Committee TC 102, Edited by P.K. Robertson and K.I. Cabal: pp. 47-73.

Parez, L. and Fauriel, R. (1988). "Le piézocône. Améliorations apportées à la reconnaissance de sols". Revue Française de Géotech, Vol. 33, 13-27.

Robertson, P.K. (2009). Cited in "Guide to Cone Penetration Testing - 6th edition (2015)", pp. 58, Gregg Drilling & Testing, Inc.

Robertson, P.K. (2009). Interpretation of cone penetration tests – a unified approach. Canadian Geotechnical Journal, 46, p. 1337–1355.

Robertson, P.K. (2010) "Soil Behaviour Type from the CPT: an update". 2nd International Symposium on Cone Penetration Testing. Huntingdon Beach, CA, USA.

Robertson, P.K. (2012). Interpretation of in-situ tests – some insights, Proc. 4th Int. Conf. on Geotechnical & Geophysical Site Characterization, ISC'4, Brazil, 1.

Robertson, P.K (2014) "Estimating in-situ soil permeability from CPT & CPTu". Proceedings of the 3rd International Symposium on Cone Penetration Testing (CPT'14), June, 2014, ISSMGE Technical Committee TC 102.

Senneset, K., R. Sandven, and N. Janbu (1989), "Evaluation of Soil Parameters from Piezocone Tests," Transportation Research Record 1235, Transportation Research Board, National Research Council, Washington D.C, pp. 24-37.

Sully, J.P., Robertson, P.K., Campanella, R.G. and Woeller, D.J. (1999) "An approach to evaluation of field CPTU dissipation data in overconsolidated fine-grained soils". Canadian Geotechnical Journal. Vol. 36, pp. 369-381.

SUMMARY TABLES

Table 1 CPT test summary

Test ID	Final depth (mBGL)	Cone ID {C=Cone tip; F=Friction Sleeve; I= Inclination; P = Piezo; S=Subtraction cone; 15/10 = cone projected area (cm2))}	CPT rig	Pre-drilled / inspection pit (m)	Casing depth (m)	Refusal factor	Dissipations	Seismic cone	Samples	Easting	Northing	Elevation (m)	Date of test	Remarks
CPT204	8.40	S10-CFIP.673	UK19			Total reaction force							29/04/2019	
CPT205	2.32	S10-CFIP.673	UK19			Inclination							29/04/2019	
CPT205A	11.28	S10-CFIP.673	UK19			Total reaction force							29/04/2019	

CPT test plots are presented in Appendices B, C & D

APPENDIX A GENERAL INFORMATION

LIST OF FIGURES

LANKELMA — CALIBRATION CERTIFICATE

Geopoint-S10-100kN-5MPa

Cone Serial Number: S10.CFIIP-673

REFERENCE INSTRUMENTS:	CONE END RESISTANCE	SLEEVE FRICTION	PORE WATER PRESSURE
ID	51998	51998	4009509
TYPE	AM DSCC-100kN	AM DSCC-100kN	Druck DPI 104
UNCERTAINTY (±%)	0.01	0.01	0.05
Nominal pressure (MPa,MPa,MPa)	50.00	3.33	2.00
Maximum pressure (MPa,MPa,MPa)	100.00	6.67	5.00
Area (cm²)	10	150	N/A
Sensitivity (mV/MPa)	75.11	1136.92	1905.55
Calibration file scaling factor:			
Nominal cal force (kN, kN, BAR)	50	50	20
Calibration number (mV)	3755	3790	3811
Zero point (mV)	270	386	399
Sensitivity (mV/kN, mV/kN, mV/BAR)	75.108	75.795	190.555
Inclination factors (mV)	X -20°= 633, 0°= 2647, 20°= 4566 / Y -20°= 229, 0°= 2396, 20°= 4364		
Measured alpha factor:	0.70		
Uncertainty (%):			
Reproducibility	0.09	0.06	0.02
Linearity	0.14	0.07	0.16
Hysteresis	0.09	0.03	0.12
Combined expanded (k=2)	0.33	0.51	0.35
Application class	1	1	1

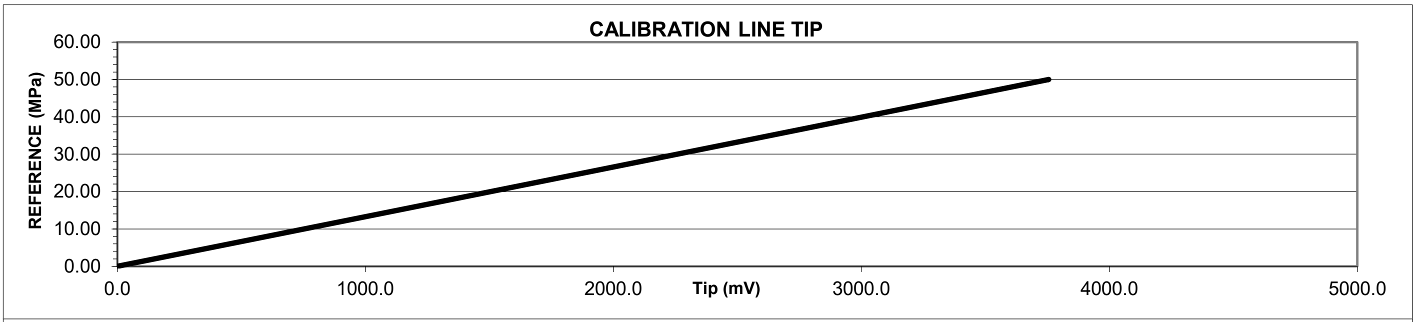

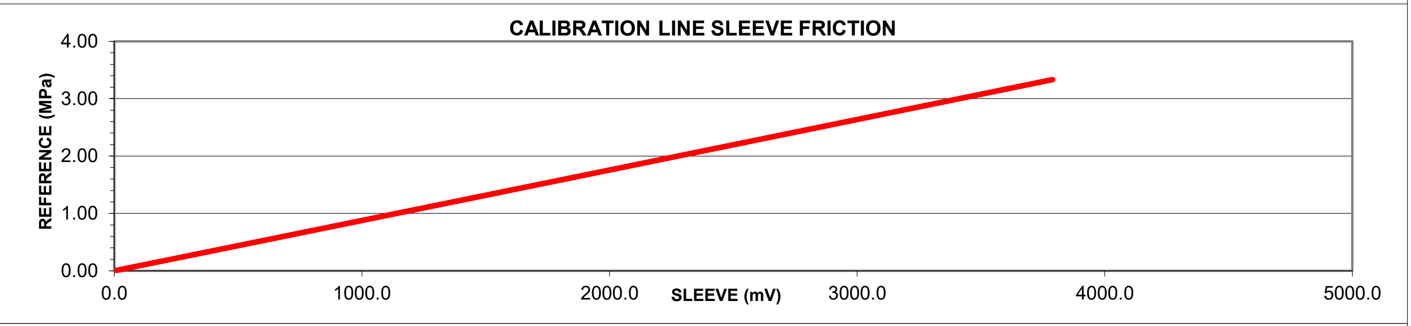

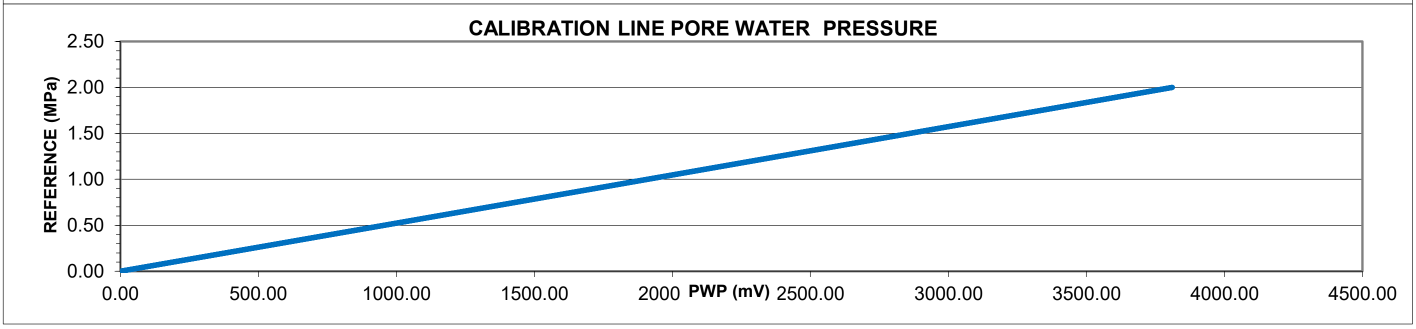

Instrument:	**S10-100kN**	**Location:**	**Lankelma Calibration Laboratory**
Serial Number:	**S10.CFIIP-673**	**Temperature(° C)**	**18.6**
Manufacturer:	**Geopoint**	**Calibration Engineer**	**ed f. white**
Date of calibration:	**05/04/2019**	**Calibration Expiry**	**04/07/2019**

Calibration signed and dated by:	**Calibration checked and dated by:**
[redacted]	[redacted]

UK19
MINI CRAWLER RIG

Ideal for sites with challenging access, this rig has previously been utilised in London's residences. The rubber tracks provide the rig with a low bearing pressure making it suitable for soft terrain whilst causing minimal tracking damage.

The mini-crawler has 4 ground anchors (0.5 m in length) which screw into the ground to give a reaction force.

The mini crawler is suitable for projects on rivers, canals, flood and sea defenses/embankments and other sites where access is difficult for conventional rigs.

Performance Rates

Up to 50 m of standard CPTu testing can be executed in a day (dependent on site conditions and access).

Applications

- Specialist testing
  - Seismic
  - Pressuremeter
  - Magnetometer
  - Video cone
- Installations
  - VWP
  - Piezometer
  - Inclinometer
- Sampling
  - MOSTAP
  - Shelby

TECHNICAL DETAILS

Rig Weight	1.3 T
Length	2.75 m
Width	0.75 m
Minimum Travel Height	1.5 m
Minimum Working Height	2.5 m
Maximum Operating Ram Capacity	12 T
Maximum Travelling Speed	2.6 – 4.0 km/h
Track Material	Rubber
Track Length	1.15 m
Track Width	0.18 m
Footprint Of Tracks	1.15 x 0.75 m
Maximum Ground Bearing Pressure	Tracking / Pushing – 27 kPa
Maximum Testing Gradient	Flat (No Self-Levelling)
Noise Output at 2 m	Testing – 76 dBA
Noise Output at 5 m	Testing – 62 dBA
Clamp Arrangement	36 Ball Clamp
Ram Stroke	0.70 m

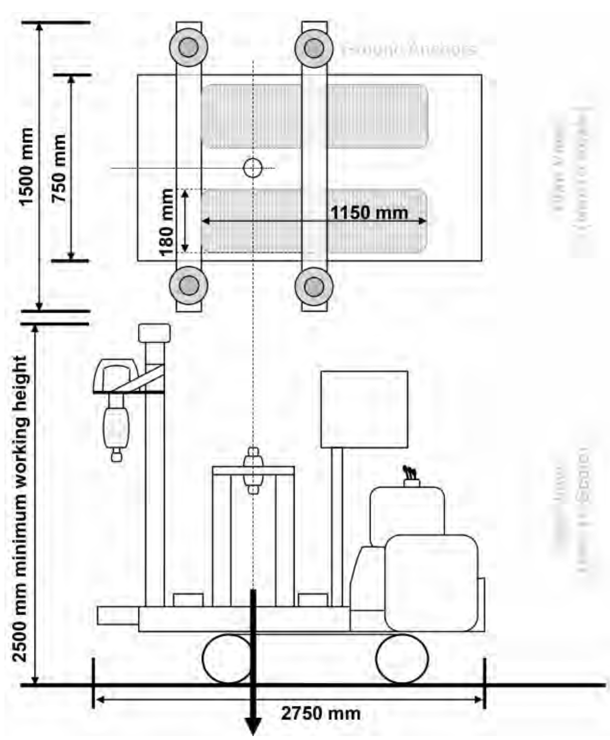

www.lankelma.com

Tel: **+44 (0)1797 280050** Fax: **+44 (0)1797 280195** Email: **info@lankelma.com**

Lankelma Limited, Cold Harbour Barn, Cold Harbour Lane, Iden, East Sussex. TN31 7UT

CPT SOIL BEHAVIOUR TYPE CHART

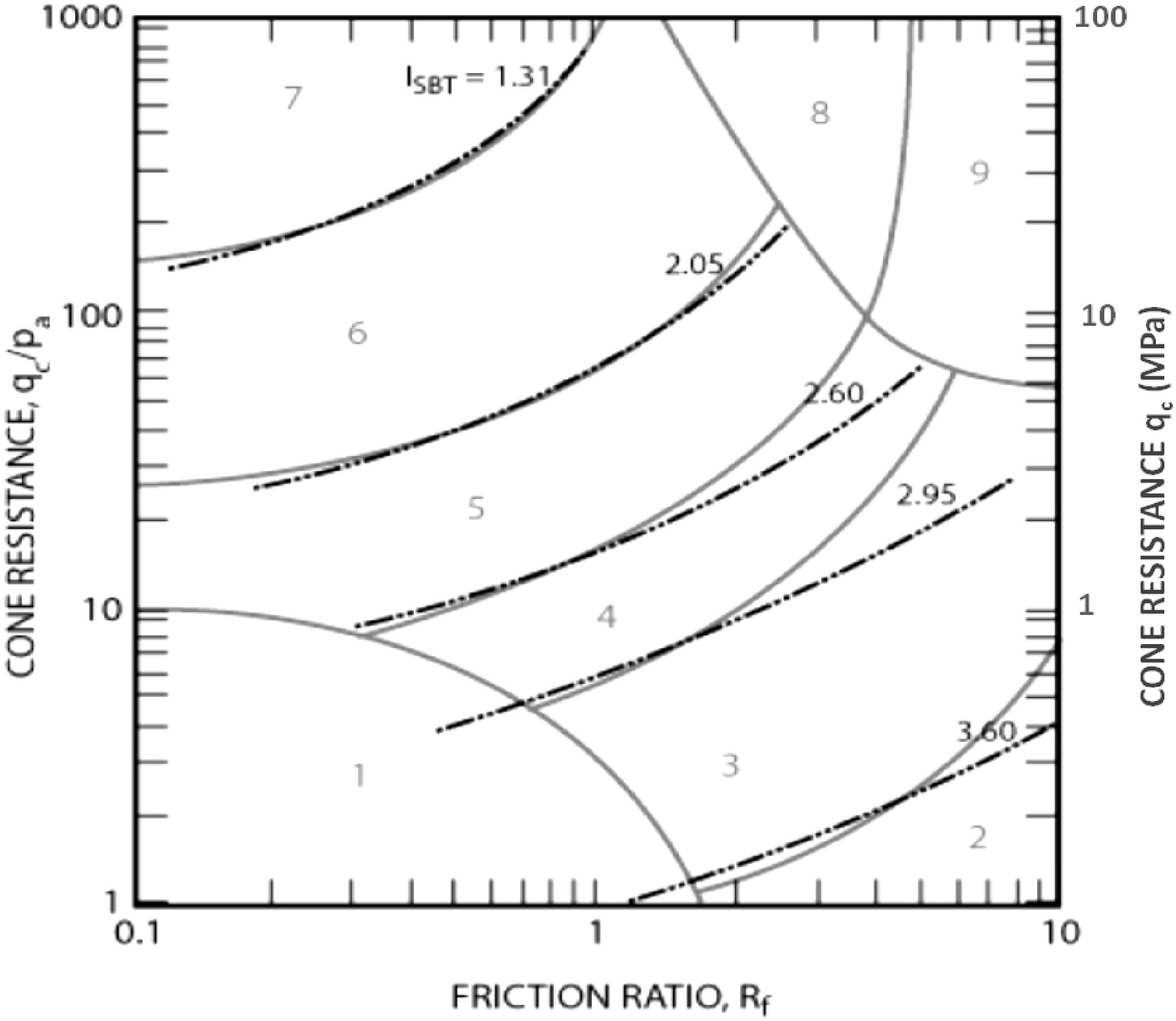

Non-normalised SBT chart by Robertson *et al.* (2010) based on dimensionless cone resistance (qc/Pa) and friction ration, Rf, showing contours of *Ic* index. The chart is also applicable to normalised tip/sleeve values Q_t and F_r.

Zone	Soil Behaviour Type (SBT)		
1	Sensitive fine-grained	6	Sands: clean sand to sandy silt
2	Clay – organic soil	7	Dense sand to gravelly sand
3	Clays: Clay to silty clay	8	Stiff sand to clayey sand*
4	Silt mixtures: clayey silt to silty clay	9	Stiff fine grained*
5	Sand mixtures: Silty sand to sandy silt	*Overconsolidated or cemented*	

GLOSSARY OF CPT TERMS AND SYMBOLS

SYMBOLS

q_c :- **Cone resistance.** The total force acting on the cone Q_c, divided by the projected area of the cone, A_c; **(q_c=Q_c/A_c)**.

q_t :- **Corrected cone resistance.** The cone resistance q_c corrected for unequal pore water pressure effects on the cone face and shoulder.

f_s :- **Friction sleeve resistance.** The total frictional force acting on the friction sleeve, F_s, divided by its surface area, A_s.**f_s= F_s/A_s**.

R_f :- **Friction ratio** The ratio, expressed as a percentage, of the sleeve friction, f_s, to the cone resistance, q_c, both measured at the same depth; **[R_f= (f_s/q_c) · 100].**

$q_{t\text{-}net}$:- **Not cone resistance** (Method 1) **= (q_c – σ_v)**

Q_t :- **Normalised cone resistance** (Method 1) **= (q_c – σ_v)/σ'_v**

q_{t1}:- **Normalised cone resistance** (Method 2) **= (q_t)/(σ'_v)$^{0.5}$**

F_r:- **Normalised friction sleeve resistance = f_s /(q_c- σ_v)**

σ_v:- **Total overburden stress**

σ'_v:- **Effective overburden stress**

σ_{atm}, or, P_a:- **Reference atmospheric stress = 100kPa**

I_c:- **Soil Behaviour Type Index**

B_q :- **Pore pressure ratio.** The net pore pressure normalized with respect to the net cone resistance. = **(u_2 – u_0)/(q_t -σ_v)**

TERMS

Cone (or 'tip'): - The conical tip section of the cone penetrometer.

Friction sleeve: - The section of the cone penetrometer upon which the sleeve friction is measured, located behind the cone tip.

Piezocone: - A cone penetrometer with a pore pressure measurement system.

Dynamic pore pressure: - The pore pressure generated during penetration and measured by a pore pressure sensor. u_1 when measured on the conical tip face, u_2 when measured just behind the conical tip.

APPENDIX B CONE PENETRATION TEST RESULTS

RAW DATA PLOTS

LIST OF FIGURES:

LANKELMA

Project: A417 GLOUCESTERSHIRE
Client: GEOTECHNICAL ENGINEERING

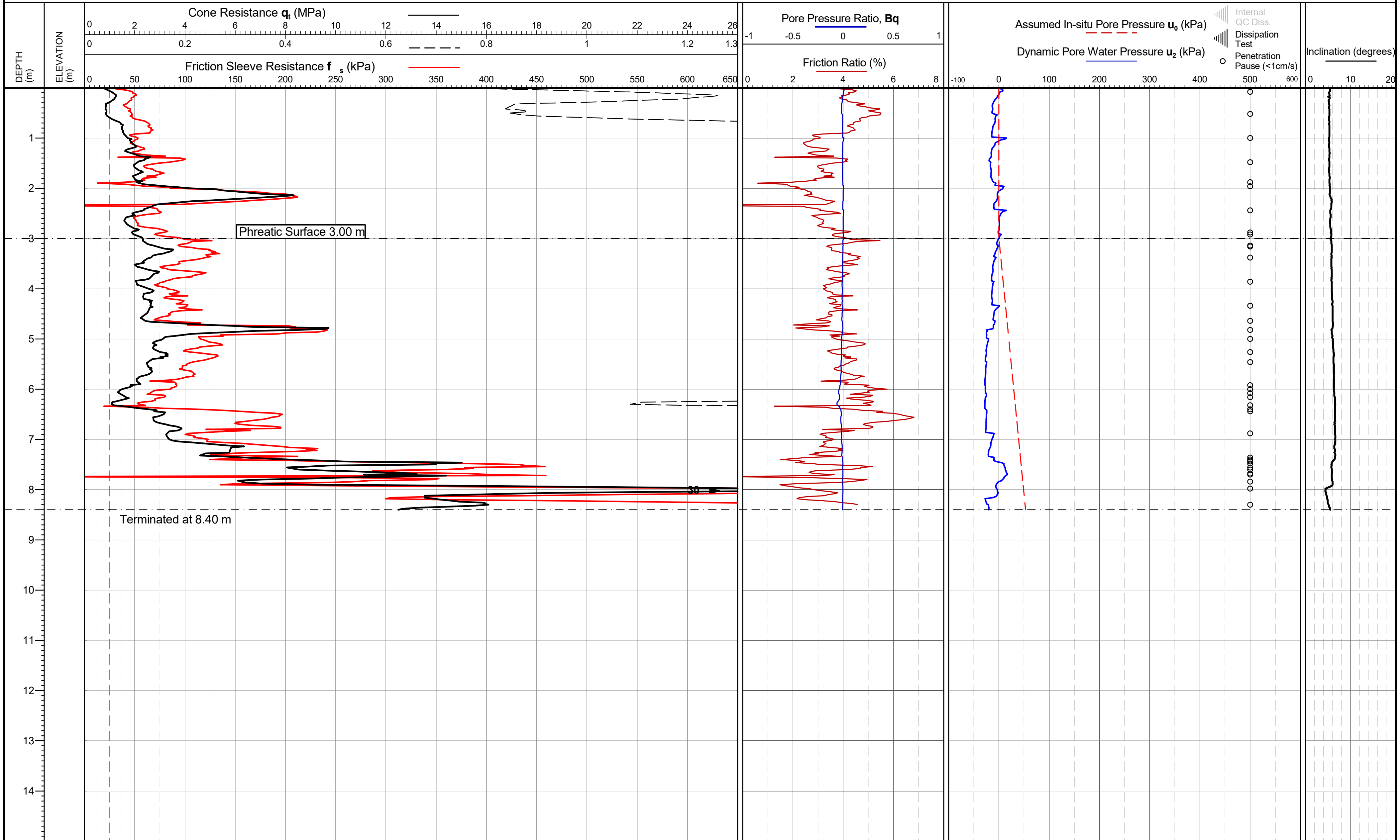

Cone area (mm2):1000
Cone ID: S10-CFIP.673
Operator: Gerard Balp
Rig Used: UK19
Date of test: 29/04/2019 12:12:00

Location: Gloucestershire, UK

Coordinates: ,

Elevation:

Remarks:
*Phreatic surface origin: Default site value from arbitrary value

Termination Remark: Total reaction force

Date of plot:
30-04-19

Lankelma Project Ref:
P-107175-1

Checked by:
Chris Player

TEST ID: CPT204

LANKELMA

Project: A417 GLOUCESTERSHIRE

Client: GEOTECHNICAL ENGINEERING

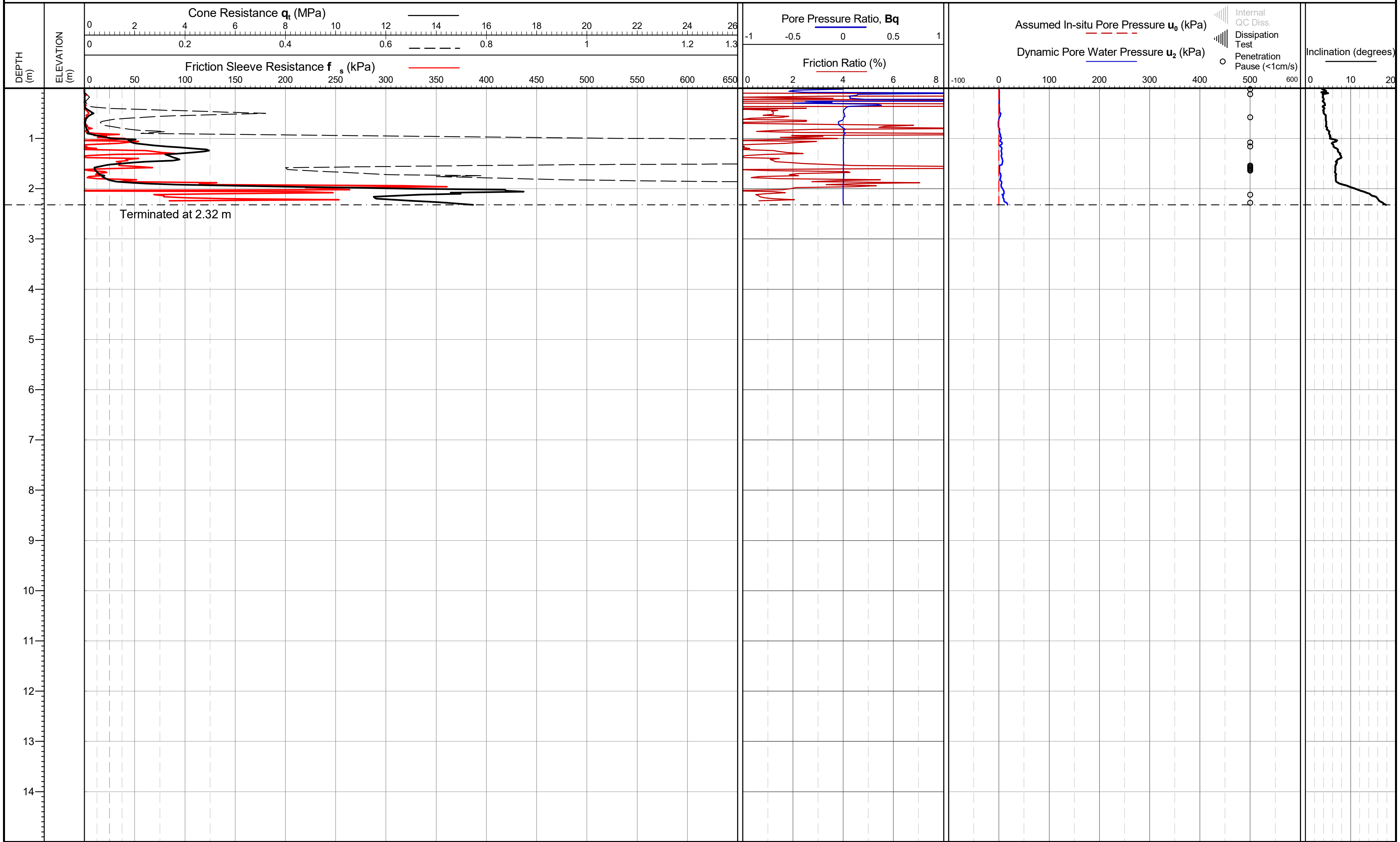

Cone area (mm2):1000 Cone ID: S10-CFIP.673 Operator: Gerard Balp Rig Used: UK19 Date of test: 29/04/2019 15:12:00	Location: Gloucestershire, UK Coordinates: , Elevation:	Remarks: *Phreatic surface origin: Default site value from arbitrary value Termination Remark: Inclination	Date of plot: 30-04-19 Lankelma Project Ref: P-107175-1 Checked by: Chris Player	**TEST ID: CPT205** Page 1 of 1

LANKELMA

Project: A417 GLOUCESTERSHIRE

Client: GEOTECHNICAL ENGINEERING

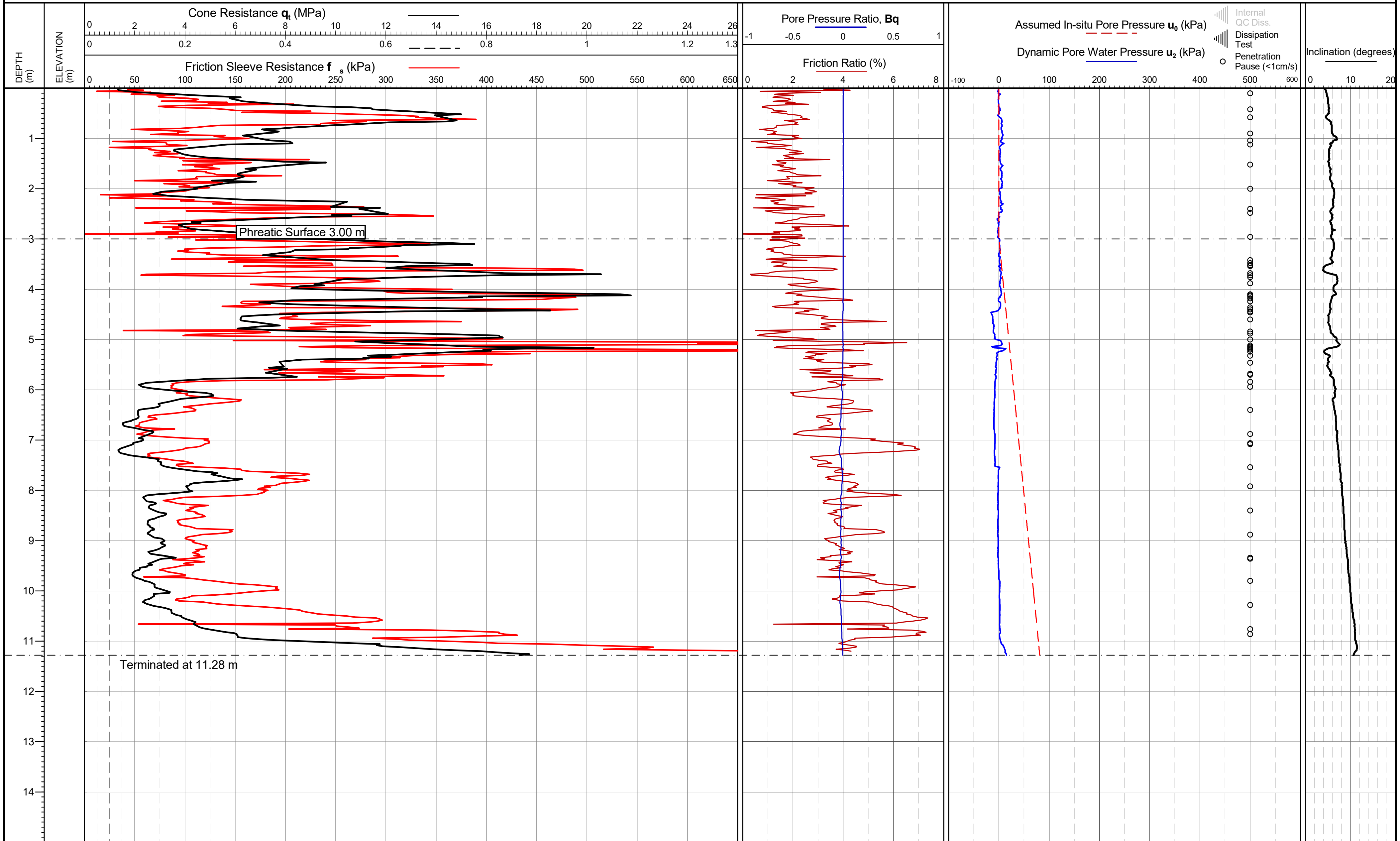

Cone area (mm2):1000 Cone ID: S10-CFIP.673 Operator: Gerard Balp Rig Used: UK19 Date of test: 29/04/2019 15:22:00	Location: Gloucestershire, UK Coordinates: , Elevation:	Remarks: *Phreatic surface origin: Default site value from arbitrary value Termination Remark: Total reaction force	Date of plot: 30-04-19 Checked by: Chris Player	Lankelma Project Ref: P-107175-1	**TEST ID: CPT205A** Page 1 of 1

APPENDIX C STANDARD INTERPRETATION RESULTS - SET 1

UNDRAINED SHEAR STRENGTH
COEFFICIENT OF VOLUME CHANGE
OVERCONSOLIDATION RATIO
SOIL BEHAVIOUR TYPE (SBT) DESCRIPTIONS

LIST OF FIGURES:

LANKELMA

Project: A417 GLOUCESTERSHIRE
Client: GEOTECHNICAL ENGINEERING

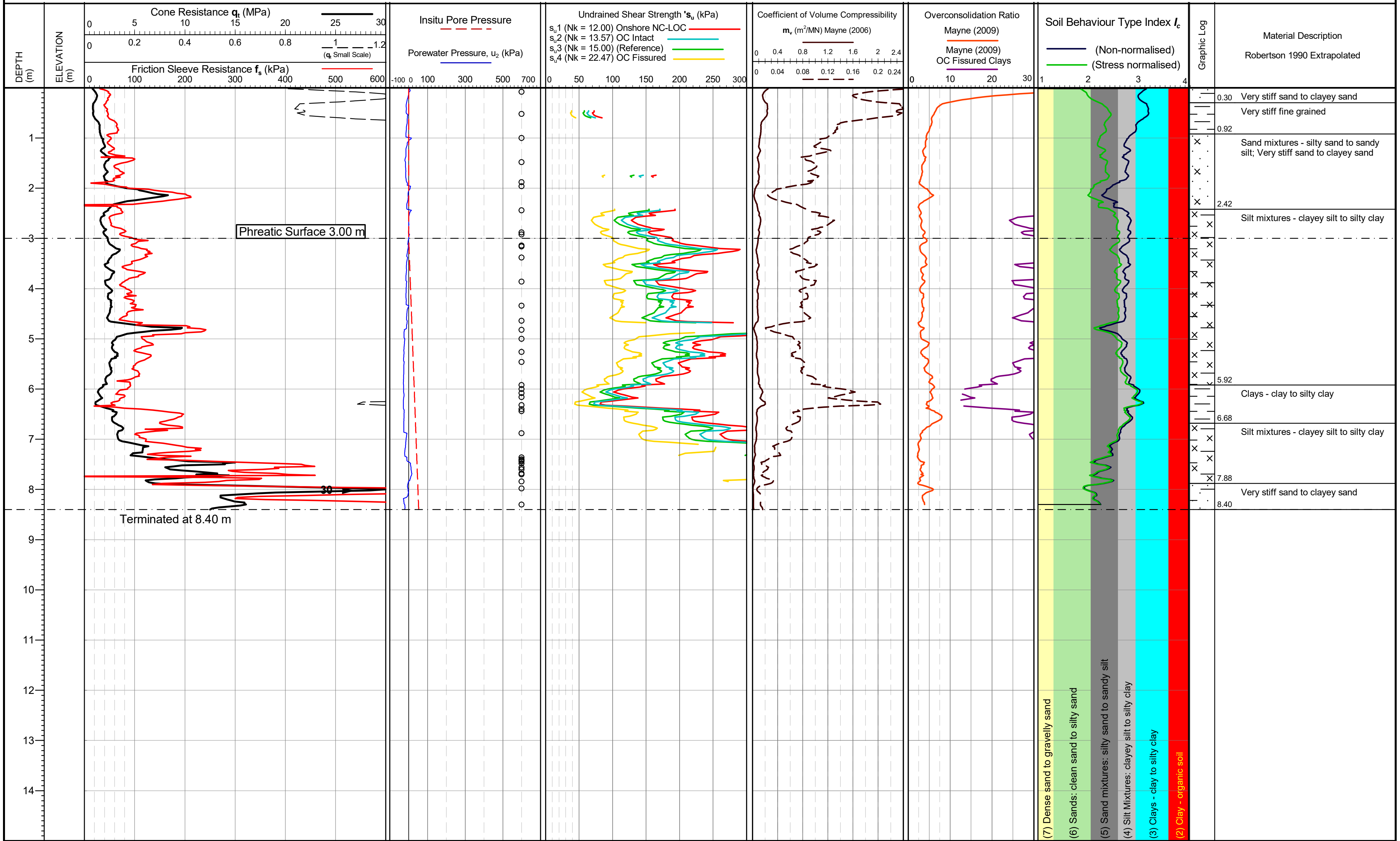

Cone area (mm2):1000 ConeID: S10-CFIP.673 Operator: Gerard Balp Rig Used: UK19 Date of test: 29/04/2019 12:12:00	Location: Gloucestershire, UK Coordinates: , Elevation:	Remarks: *Phreatic surface origin: Default site value from arbitrary value Termination Remark: Total reaction force	Internal QA Diss. Dissipation Test Penetration Pause (<1cm/s)	Both drained and undrained parameters are calculated for mixed SBTs = Ic 2.40-2.70. See report section 'Drained and Undrained Behaviour' for discussion. See report section 'Interpretive Data' for methods and discussion of parameter evaluation.	Date of plot: 30-04-19 Checked by: Chris Player	Lankelma Project Ref: P-107175-1	**TEST ID: CPT204** Page 1 of 1

LANKELMA

Project: A417 GLOUCESTERSHIRE

Client: GEOTECHNICAL ENGINEERING

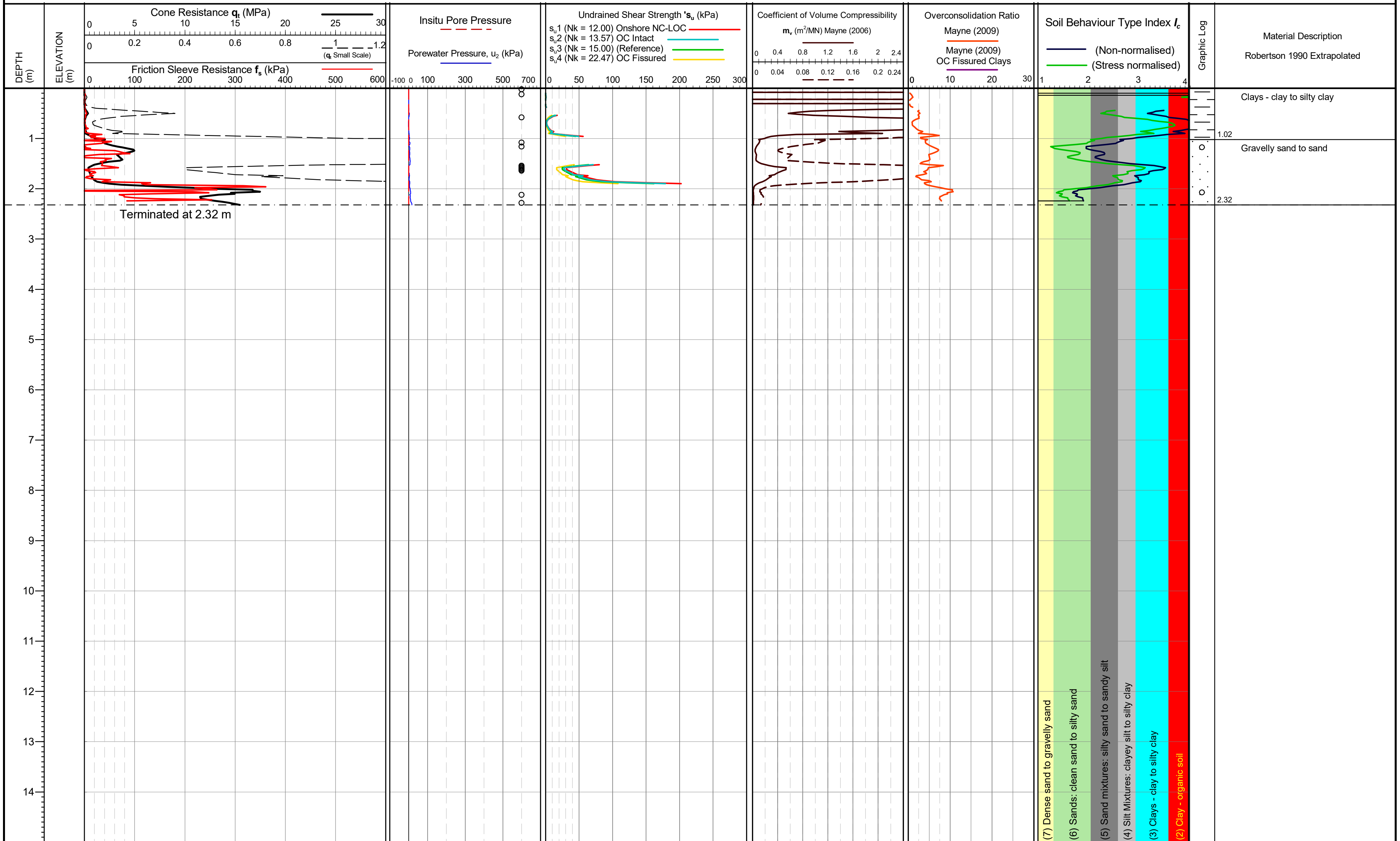

Cone area (mm2):1000
ConeID: S10-CFIP.673
Operator: Gerard Balp
Rig Used: UK19
Date of test: 29/04/2019 15:12:00

Location: Gloucestershire, UK

Coordinates: ,

Elevation:

Remarks: *Phreatic surface origin: Default site value from arbitrary value

Termination Remark:
Inclination

Internal QA Diss.
Dissipation Test
Penetration Pause (<1cm/s)

Both drained and undrained parameters are calculated for mixed SBTs = Ic 2.40-2.70. See report section 'Drained and Undrained Behaviour' for discussion.

See report section 'Interpretive Data' for methods and discussion of parameter evaluation.

Date of plot: 30-04-19

Checked by: Chris Player

Lankelma Project Ref: P-107175-1

TEST ID: CPT205

Page 1 of 1

Project: A417 GLOUCESTERSHIRE

Client: GEOTECHNICAL ENGINEERING

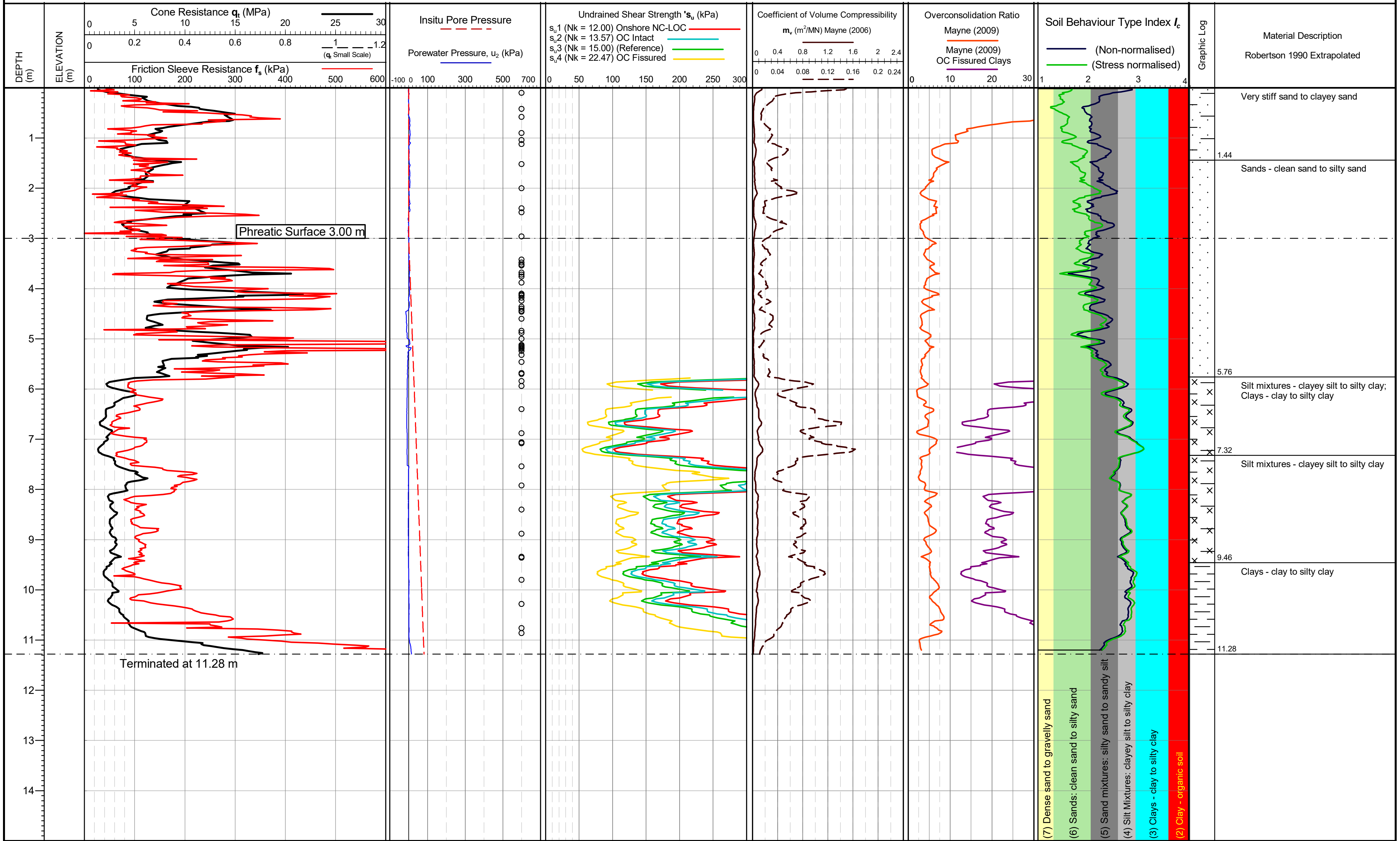

Cone area (mm2):1000 ConeID: S10-CFIP.673 Operator: Gerard Balp Rig Used: UK19 Date of test: 29/04/2019 15:22:00	Location: Gloucestershire, UK Coordinates: , Elevation:	Remarks: *Phreatic surface origin: Default site value from arbitrary value Termination Remark: Total reaction force	Internal QA Diss. Dissipation Test Penetration Pause (<1cm/s)	Both drained and undrained parameters are calculated for mixed SBTs = Ic 2.40-2.70. See report section 'Drained and Undrained Behaviour' for discussion. See report section 'Interpretive Data' for methods and discussion of parameter evaluation.	Date of plot: 30-04-19 Checked by: Chris Player	Lankelma Project Ref: P-107175-1

TEST ID: CPT205A

Page 1 of 1

APPENDIX D STANDARD INTERPRETATION RESULTS - SET 2

EQUIVALENT SPT N60
PEAK FRICTION ANGLE
RELATIVE DENSITY
YOUNG'S MODULUS

LIST OF FIGURES:

LANKELMA

Project: A417 GLOUCESTERSHIRE

Client: GEOTECHNICAL ENGINEERING

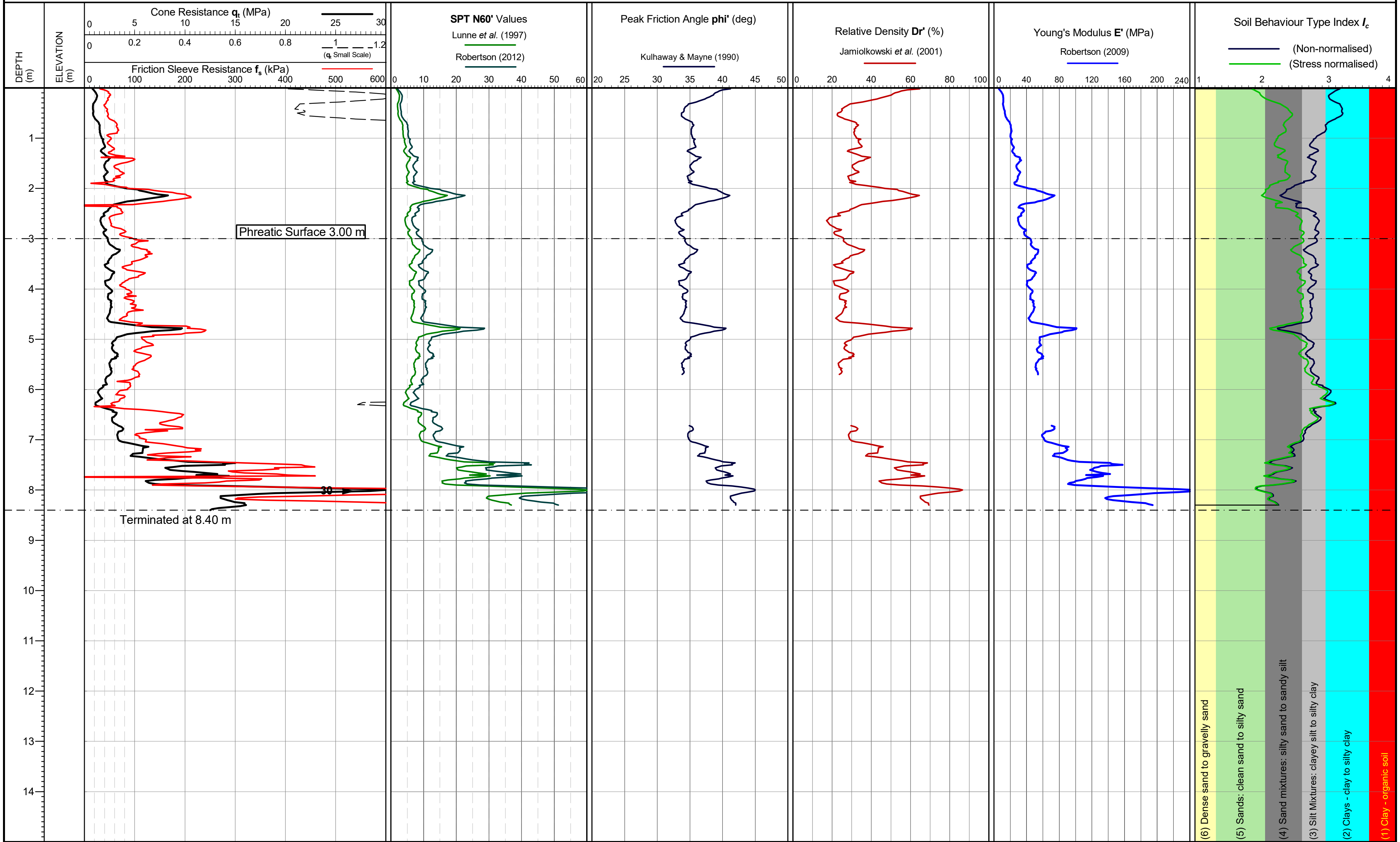

Cone area (mm2):1000
Cone ID: S10-CFIP.673
Operator: Gerard Balp
Date of test: 29/04/2019 12:12:00

Location: Gloucestershire, UK
Coordinates: ,
Elevation:
Coordinate system:

Both drained and undrained parameters are calculated for mixed SBTs = Ic 2.40-2.70. See report section 'Drained and Undrained Behaviour' for discussion.
See report section 'Interpretive Data' for methods and discussion of parameter evaluation.

Date of plot: 30-04-19
Checked by: Chris Player

Lankelma Project Ref: P-107175-1

TEST ID: CPT204

Page 1 of 1

LANKELMA

Project: A417 GLOUCESTERSHIRE
Client: GEOTECHNICAL ENGINEERING

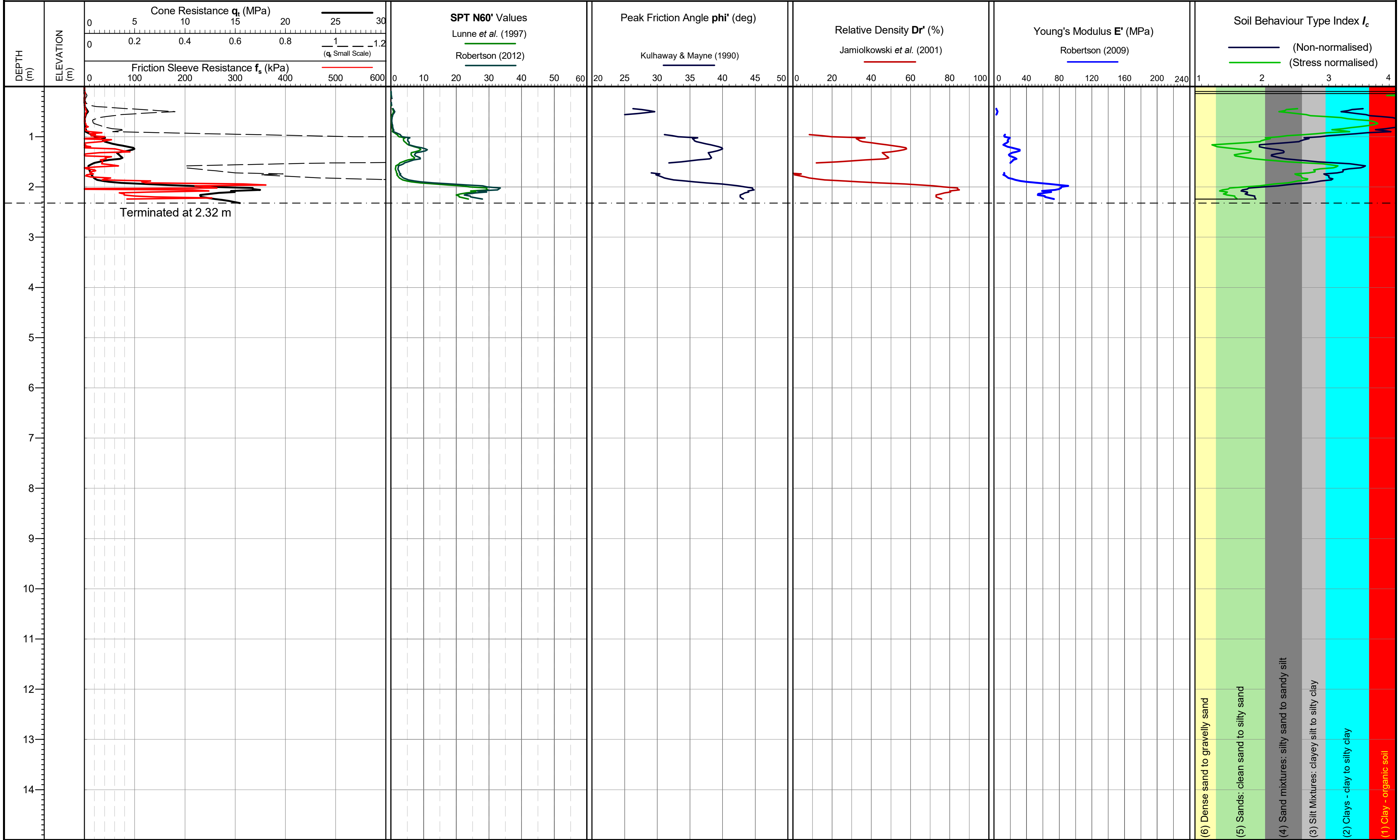

Cone area (mm2):1000
Cone ID: S10-CFIP.673
Operator: Gerard Balp
Date of test: 29/04/2019 15:12:00

Location: Gloucestershire, UK
Coordinates: ,
Elevation:
Coordinate system:

Both drained and undrained parameters are calculated for mixed SBTs = Ic 2.40-2.70. See report section 'Drained and Undrained Behaviour' for discussion.
See report section 'Interpretive Data' for methods and discussion of parameter evaluation.

Date of plot: 30-04-19

Lankelma Project Ref: P-107175-1

Checked by: Chris Player

TEST ID: CPT205

LANKELMA

Project: A417 GLOUCESTERSHIRE

Client: GEOTECHNICAL ENGINEERING

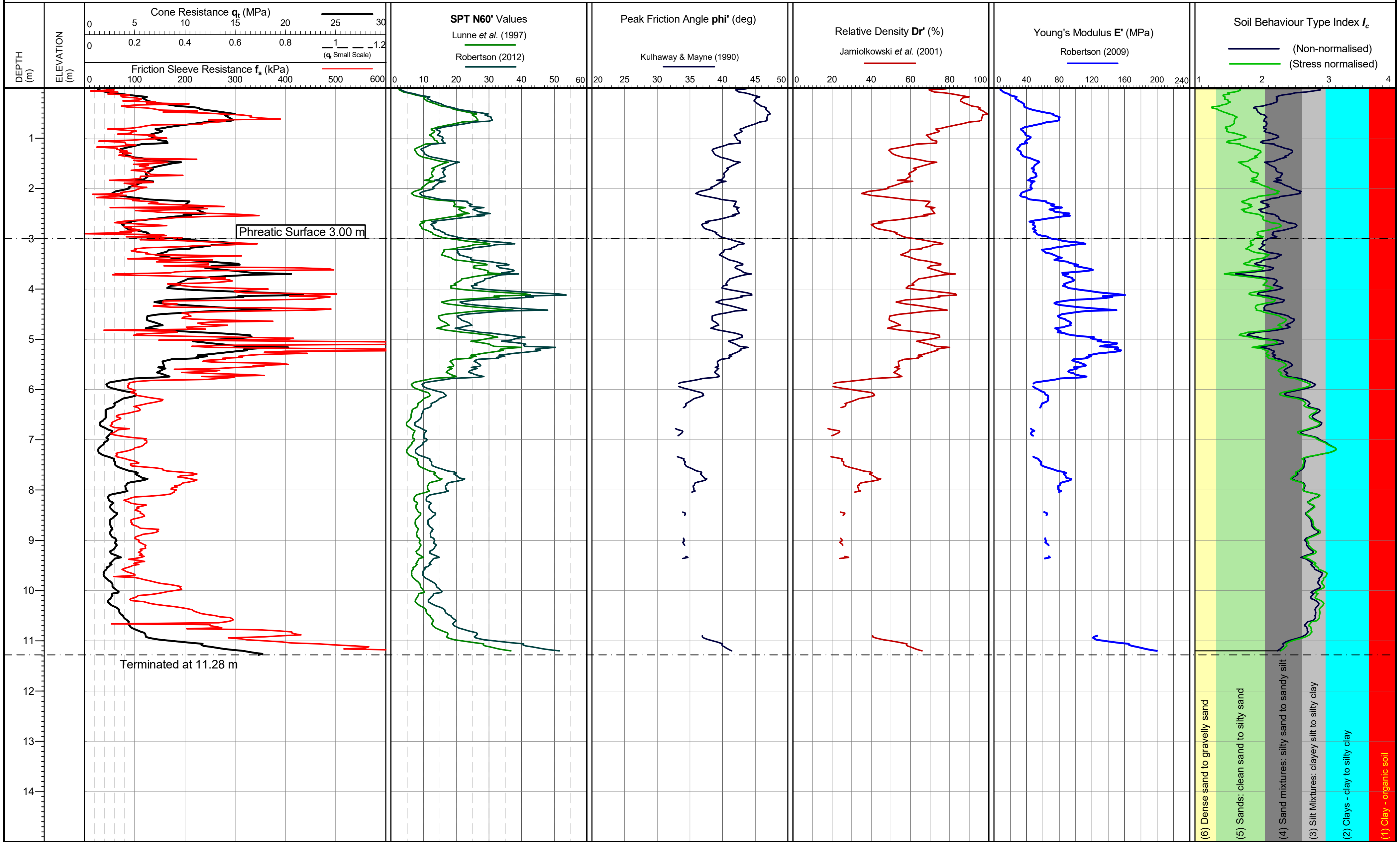

Cone area (mm2):1000
Cone ID: S10-CFIP.673
Operator: Gerard Balp
Date of test: 29/04/2019 15:22:00

Location: Gloucestershire, UK
Coordinates: ,
Elevation:
Coordinate system:

Both drained and undrained parameters are calculated for mixed SBTs = Ic 2.40-2.70. See report section 'Drained and Undrained Behaviour' for discussion.

See report section 'Interpretive Data' for methods and discussion of parameter evaluation.

Date of plot: 30-04-19

Lankelma Project Ref: P-107175-1

Checked by: Chris Player

TEST ID: CPT205A

APPENDIX C

PHOTOGRAPHS

Borehole: DSRC110 Box 1 1.10-3.20m

Borehole: DSRC110 Box 2 3.20-6.20m

Borehole: DSRC110 Box 3 6.20-9.20m

Borehole: DSRC110 Box 4 9.20-12.20m

Borehole: DSRC110 Box 5 12.20-15.20m

Borehole: DSRC110 Box 6 15.20-18.20m

Borehole: DSRC110 Box 7 18.20-21.20m

Borehole: DSRC110 Box 8 21.20-24.20m

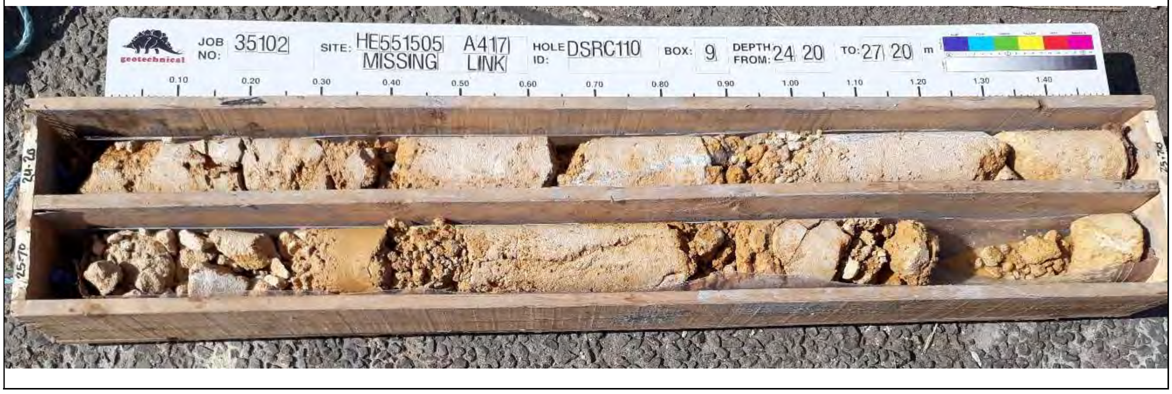

Borehole: DSRC110 Box 9 24.20-27.20m

Borehole: DSRC110 Box 10 27.20-30.20m

Borehole: DSRC110 Box 11 30.20-33.20m

Borehole: DSRC110 Box 12 33.20-36.20m

Borehole: DSRC110 Box 13 36.20-39.20m

Borehole: DSRC110 Box 14 39.20-42.20m

Borehole: DSRC110 Box 15 42.20-45.20m

Borehole: DSRC110 Box 16 45.20-48.20m

Borehole: DSRC110 Box 17 48.20-51.20m

Borehole: DSRC110 Box 18 51.20-54.20m

Borehole: DSRC110 Box 19 54.20-57.20m

Borehole: DSRC110 Box 20 57.20-60.20m

Borehole: DSRC302 Box 1 1.20-3.70m

Borehole: DSRC302 Box 2 3.70-6.70m

Borehole: DSRC302 Box 3 6.70-9.70m

Borehole: DSRC302 Box 4 9.70-12.70m

Borehole: DSRC302 Box 5 12.70-15.70m

Borehole: DSRC302 Box 6 15.70-18.70m

Borehole: DSRC302 Box 7 18.70-21.70m

Borehole: DSRC302 Box 8 21.70-24.70m

Borehole: DSRC302 Box 9 24.70-27.70m

Borehole: DSRC302 Box 10 27.70-30.70m

Borehole: DSRC302 Box 11 30.70-33.70m

Borehole: DSRC302 Box 12 33.70-35.20m

Borehole: DSRC303 Box 1 1.20-3.50m

Borehole: DSRC303 Box 2 3.50-6.50m

Borehole: DSRC303 Box 3 6.50-9.50m

Borehole: DSRC303 Box 4 9.50-12.50m

Borehole: DSRC303 Box 5 12.50-15.50m

Borehole: DSRC303 Box 6 15.50-18.50m

Borehole: DSRC303 Box 7 18.50-21.50m

Borehole: DSRC303 Box 8 21.50-24.50m

Borehole: DSRC303 Box 9 24.50-27.50m

Borehole: DSRC303 Box 10 27.50-30.50m

Borehole: DSRC303 Box 11 30.50-33.50m

Borehole: DSRC303 Box 12 33.50-36.50m

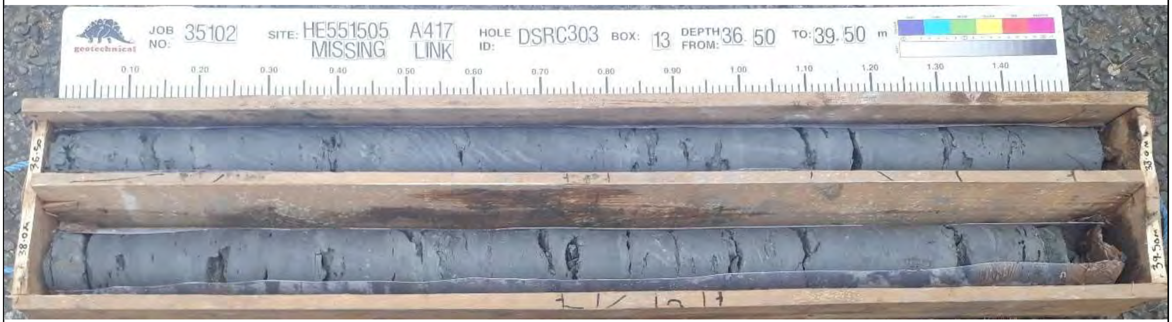

Borehole: DSRC303 Box 13 36.50-39.50m

Borehole: DSRC303 Box 14 39.50-41.00m

Borehole: RC508 Box 1 1.20-4.20m

Borehole: RC508 Box 2 4.20-7.20m

Borehole: RC508 Box 3 7.20-10.20m

Borehole: RC508 Box 4 10.20-13.20m

Borehole: RC508 Box 5 13.20-17.70m

Borehole: RC508 Box 6 17.70-20.70m

Borehole: RC508 Box 7 20.70-23.70m

Borehole: RC508 Box 8 23.70-26.70m

Borehole: RC508 Box 9 26.70-29.70m

Borehole: RC508 Box 10 29.70-32.70m

Borehole: RC508 Box 11 32.70-35.70m

Borehole: RC508 Box 12 35.70-38.70m

Borehole: RC508 Box 13 38.70-41.70m

Borehole: RC509 Box 1 1.20-4.20m

Borehole: RC509 Box 2 4.20-7.20m

Borehole: RC509 Box 3 7.20-10.20m

Borehole: RC509 Box 4 10.20-13.20m

Borehole: RC509 Box 5 13.20-16.20m

Borehole: RC509 Box 6 16.20-19.20m

Borehole: RC509 Box 7 19.20-22.20m

Borehole: RC509 Box 8 22.20-25.20m

Borehole: RC509 Box 9 25.20-28.20m

Borehole: RC509 Box 10 28.20-31.20m

Borehole: RC509 Box 11 31.20-34.20m

Borehole: RC509 Box 12 34.20-37.20m

Borehole: RC509 Box 13 37.20-40.20m

Borehole: RC509 Box 14 40.20-43.20m

Borehole: RC509 Box 15 43.20-46.20m

Borehole: RC509 Box 16 46.20-49.20m

Borehole: CP105 Box 1 1.20-4.00m

Borehole: CP105 Box 2 4.00-7.50m

Borehole: CP105 Box 3 7.50-10.50m

Borehole: CP105 Box 4 10.50-13.50m

Borehole: CP105 Box 5 13.50-16.50m

Borehole: CP105 Box 6 16.50-19.50m

Borehole: CP105 Box 7 19.50-22.50m

Borehole: CP105 Box 8 22.50-25.50m

Borehole: CP105 Box 9 25.50-28.50m

Borehole: CP105 Box 10 28.50-30.00m

Borehole: CP106 Box 1 1.20-4.00m

Borehole: CP106 Box 2 4.00-7.00m

Borehole: CP106 Box 3 7.00-10.00m

Borehole: CP106 Box 4 10.00-13.00m

Borehole: CP106 Box 5 13.00-17.50m

Borehole: CP106 Box 6 17.50-20.50m

Borehole: CP106 Box 7 20.50-23.50m

Borehole: CP106 Box 8 23.50-26.50m

Borehole: CP106 Box 9 26.50-29.50m

Borehole: CP106 Box 10 29.50-32.50m

Borehole: CP106 Box 11 32.50-35.50m

Borehole: CP206 Box 1 1.20-4.00m

Borehole: CP206 Box 2 4.00-7.00m

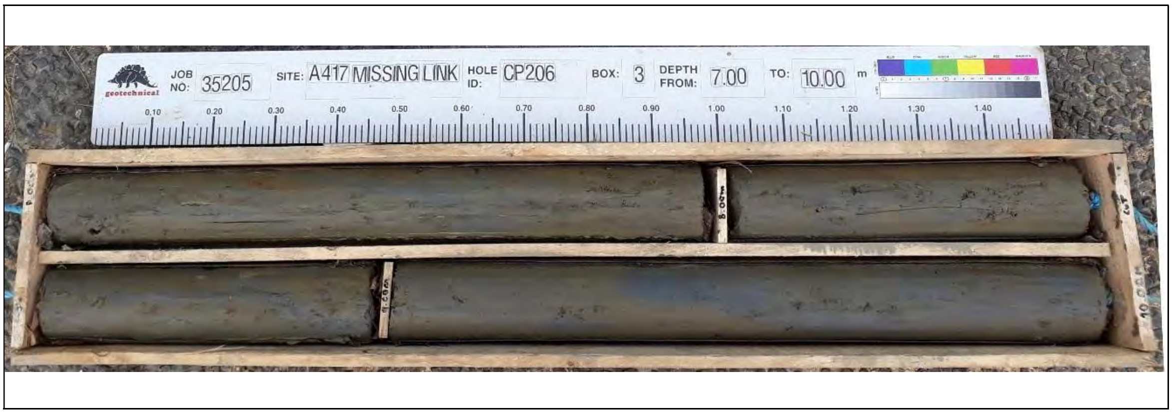

Borehole: CP206 Box 3 7.00-10.00m

Borehole: CP206 Box 4 10.00-12.00m

Borehole: CP206 Box 5 12.00-15.20m

Borehole: CP206 Box 6 15.20-18.20m

Borehole: CP206 Box 7 18.20-19.70m

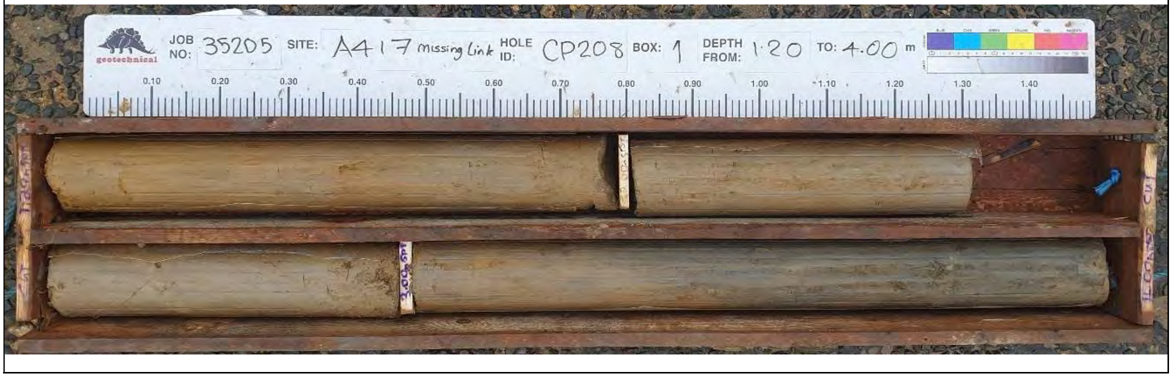

Borehole: CP208 Box 1 1.20-4.00m

Borehole: CP208 Box 2 4.00-7.00m

Borehole: CP208 Box 3 7.00-10.00m

Borehole: CP208 Box 4 10.00-13.00m

Borehole: CP208 Box 5 13.00-16.00m

Borehole: CP208 Box 6 16.00-19.00m

Borehole: CP208 Box 7 19.00-22.00m

Borehole: CP208 Box 8 22.00-25.00m

Borehole: CP209 Box 1 1.90-4.50m

Borehole: CP209 Box 2 4.50-7.50m

Borehole: CP209 Box 3 7.50-10.50m

Borehole: CP209 Box 4 10.50-13.50m

Borehole: CP209 Box 5 13.50-16.50m

Borehole: CP209 Box 6 16.50-19.50m

Borehole: CP209 Box 7 19.50-22.50m

Borehole: CP209 Box 8 22.50-25.50m

Borehole: CP209 Box 9 25.50-28.50m

Borehole: CP209 Box 10 28.50-31.50m

Borehole: CP209 Box 11 31.50-34.00m

Borehole: CP209 Box 12 34.00-35.00m

Borehole: CP212 Box 1 1.20-3.70m

Borehole: CP212 Box 2 3.70-6.70m

Borehole: CP212 Box 3 6.70-9.20m

Borehole: CP212 Box 4 9.20-12.70m

Borehole: CP212 Box 5 12.70-16.20m

Borehole: CP212 Box 6 16.20-18.50m

Borehole: CP212 Box 7 18.50-21.50m

Borehole: CP212 Box 8 21.50-24.50m

Borehole: CP216 Box 1 1.20-4.20m

Borehole: CP216 Box 2 4.20-7.20m

Borehole: CP216 Box 3 7.20-9.10m

Borehole: CP216 Box 4 9.10-12.10m

Borehole: CP216 Box 5 12.10-15.10m

Borehole: CP216 Box 6 15.10-18.10m

Borehole: CP216 Box 7 18.10-21.10m

Borehole: CP216 Box 8 21.10-24.10m

Borehole: CP216 Box 9 24.10-25.60m

Borehole: CP223 Box 1 1.20-4.00m

Borehole: CP223 Box 2 4.00-5.00m

Borehole: CP223 Box 3 5.00-7.50m

Borehole: CP223 Box 4 7.50-10.50m

Borehole: CP223 Box 5 10.50-13.50m

Borehole: CP223 Box 6 13.50-16.50m

Borehole: CP223 Box 7 16.50-19.50m

Borehole: CP223 Box 8 19.50-22.50m

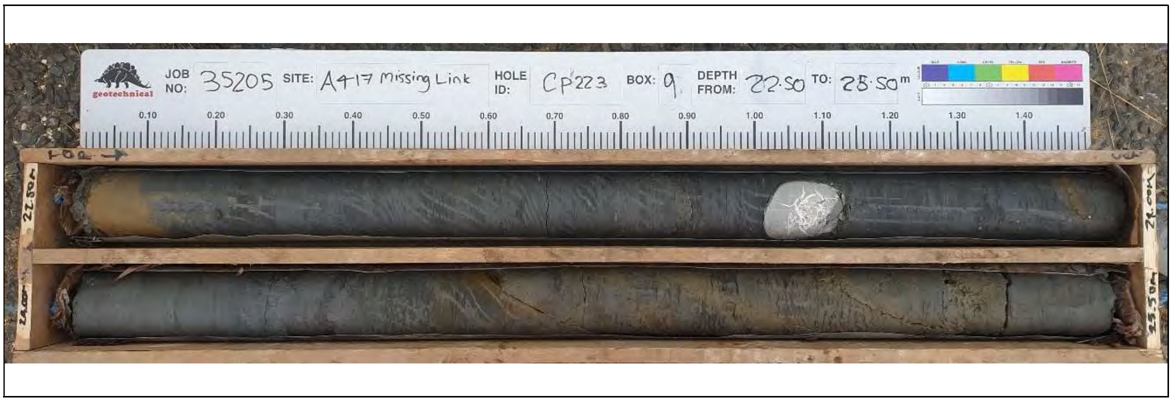

Borehole: CP223 Box 9 22.50-25.50m

Borehole: CP230 Box 1 1.20-4.00m

Borehole: CP230 Box 2 4.00-7.50m

Borehole: CP230 Box 3 7.50-10.50m

Borehole: CP230 Box 4 10.50-13.50m

Borehole: CP230 Box 5 13.50-16.50m

Borehole: CP230 Box 6 16.50-19.50m

Borehole: CP230 Box 7 19.50-22.50m

Borehole: CP230 Box 8 22.50-24.60m

Borehole: CP230 Box 9 24.60-27.50m

Borehole: CP230 Box 10 27.50-30.50m

Borehole: CP230 Box 11 30.50-33.50m

Borehole: CP230 Box 12 33.50-35.00m

Borehole: DSRC107 Box 1 1.20-4.20m

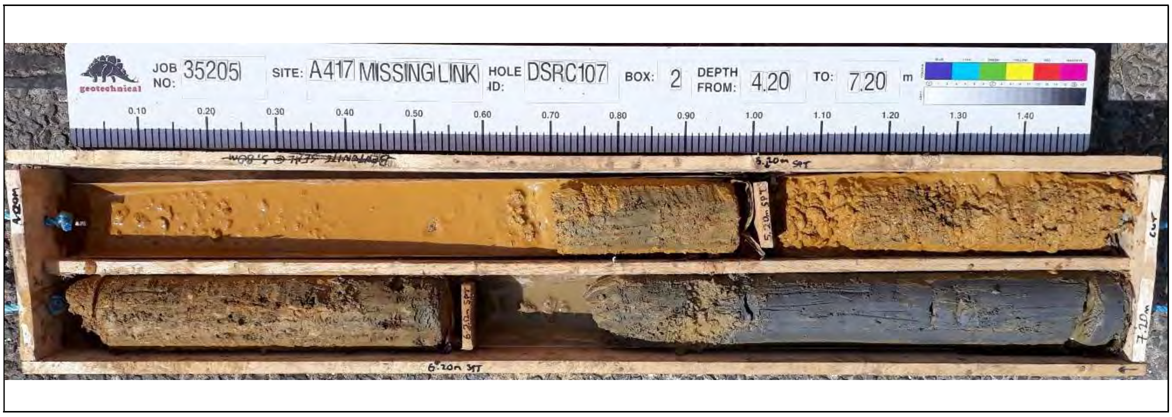

Borehole: DSRC107 Box 2 4.20-7.20m

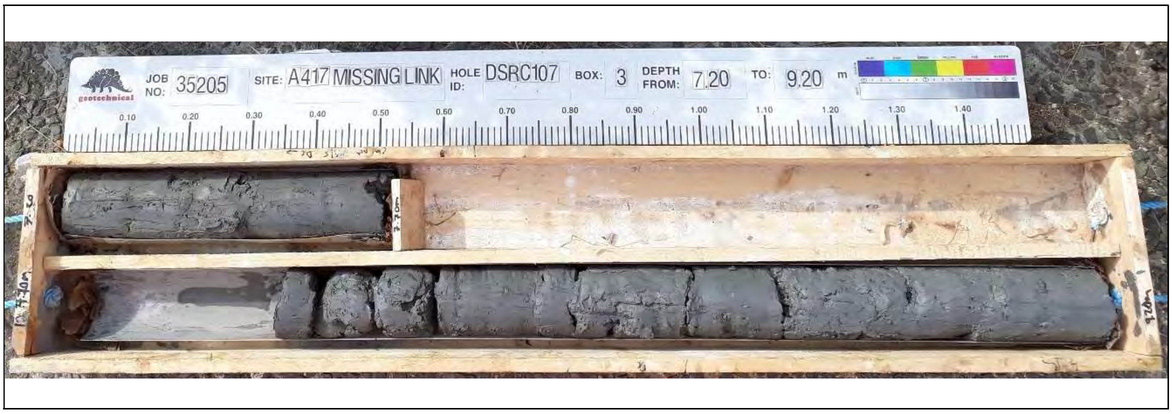

Borehole: DSRC107 Box 3 7.20-9.20m

Borehole: DSRC107 Box 4 9.20-12.20m

Borehole: DSRC107 Box 5 12.20-15.20m

Borehole: DSRC107 Box 6 15.20-18.20m

Borehole: DSRC107 Box 7 18.20-21.20m

Borehole: DSRC107 Box 8 21.20-24.20m

Borehole: DSRC107 Box 9 24.20-27.20m

Borehole: DSRC107 Box 10 27.20-30.20m

Borehole: DSRC108 Box 1 1.20-4.20m

Borehole: DSRC108 Box 2 4.20-7.00m

Borehole: DSRC108 Box 3 7.00-9.00m

Borehole: DSRC108 Box 4 9.00-12.00m

Borehole: DSRC108 Box 5 12.00-15.00m

Borehole: DSRC108 Box 6 15.00-18.00m

Borehole: DSRC108 Box 7 18.00-21.00m

Borehole: DSRC108 Box 8 21.00-24.00m

Borehole: DSRC108 Box 9 24.00-27.00m

Borehole: DSRC108 Box 10 27.00-30.00m

Borehole: DSRC108 Box 11 30.00-33.00m

Borehole: DSRC108 Box 12 33.00-36.00m

Borehole: DSRC108 Box 13 36.00-39.00m

Borehole: DSRC108 Box 14 39.00-42.00m

Borehole: DSRC108 Box 15 42.00-45.00m

Borehole: DSRC108 Box 16 45.00-48.00m

Borehole: DSRC108 Box 17 48.00-49.50m

Borehole: DSRC207 Box 1 1.20-4.20m

Borehole: DSRC207 Box 2 4.20-10.50m

Borehole: DSRC207 Box 3 10.50-13.50m

Borehole: DSRC207 Box 4 13.50-16.50m

Borehole: DSRC207 Box 5 16.50-19.50m

Borehole: DSRC207 Box 6 19.50-22.50m

Borehole: DSRC207 Box 7 22.50-25.50m

Borehole: DSRC207 Box 8 25.50-28.50m

Borehole: DSRC207 Box 9 28.50-31.50m

Borehole: DSRC207 Box 10 31.50-34.50m

Borehole: DSRC207 Box 11 34.50-37.50m

Borehole: DSRC207 Box 12 37.50-40.50m

Borehole: DSRC224 Box 1 1.20-4.20m

Borehole: DSRC224 Box 2 4.20-7.20m

Borehole: DSRC224 Box 3 7.20-10.00m

Borehole: DSRC224 Box 4 10.00-13.00m

Borehole: DSRC224 Box 5 13.00-16.00m

Borehole: DSRC224 Box 6 16.00-19.00m

Borehole: DSRC224 Box 7 19.00-22.00m

Borehole: DSRC224 Box 8 22.00-25.00m

Borehole: DSRC224 Box 9 25.00-28.00m

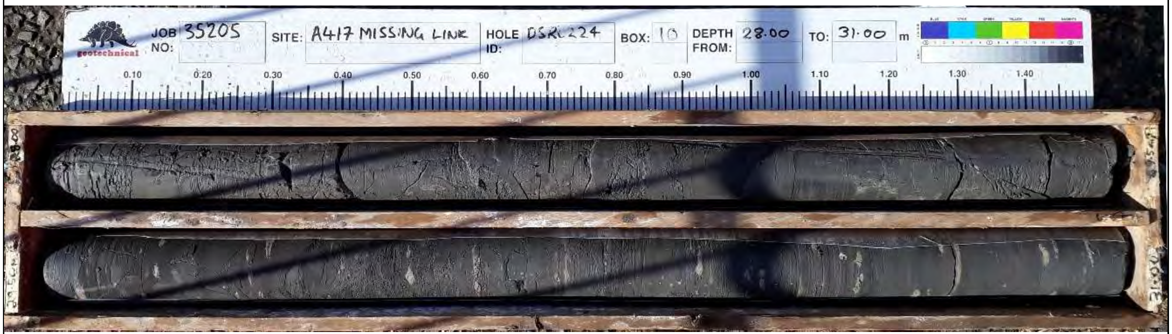

Borehole: DSRC224 Box 10 28.00-31.00m

Borehole: DSRC224 Box 11 31.00-34.00m

Borehole: DSRC224 Box 12 34.00-37.00m

Borehole: DSRC224 Box 13 37.00-40.00m

Borehole: DSRC224 Box 14 40.00-43.00m

Borehole: DSRC224 Box 15 43.00-46.00m

Borehole: DSRC224 Box 16 46.00-49.00m

Borehole: DSRC224 Box 17 49.00-52.00m

Borehole: DSRC224 Box 18 42.00-55.00m

Borehole: DSRC224 Box 19 55.00-58.00m

Borehole: DSRC224 Box 20 58.00-61.00m

Borehole: DSRC224 Box 21 61.00-64.00m

Borehole: DSRC224 Box 22 64.00-67.00m

Borehole: DSRC224 Box 23 67.00-70.00m

Borehole: DSRC224 Box 24 70.00-73.00m

Borehole: DSRC224 Box 25 73.00-76.00m

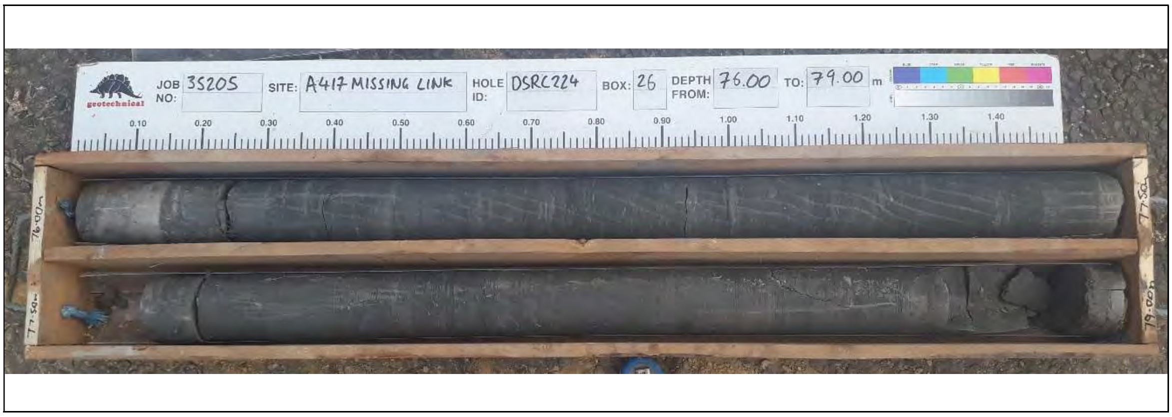

Borehole: DSRC224 Box 26 76.00-79.00m

Borehole: DSRC224 Box 27 79.00-80.50m

Borehole: CP102 Inspection pit

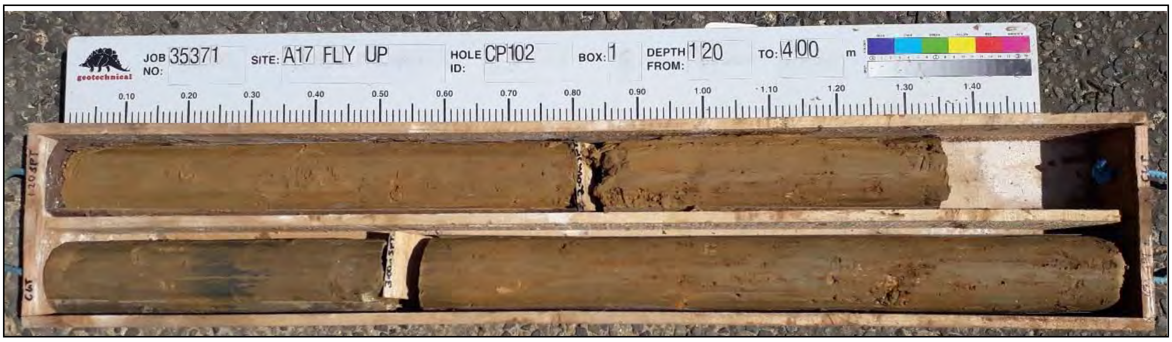

Borehole: CP102 Box 1: 1.20-4.00m

Borehole: CP102 Box 2: 4.00-7.00m

Borehole: CP102 Box 3: 7.00-10.00m

Borehole: CP102 Box 4: 10.00-13.00m

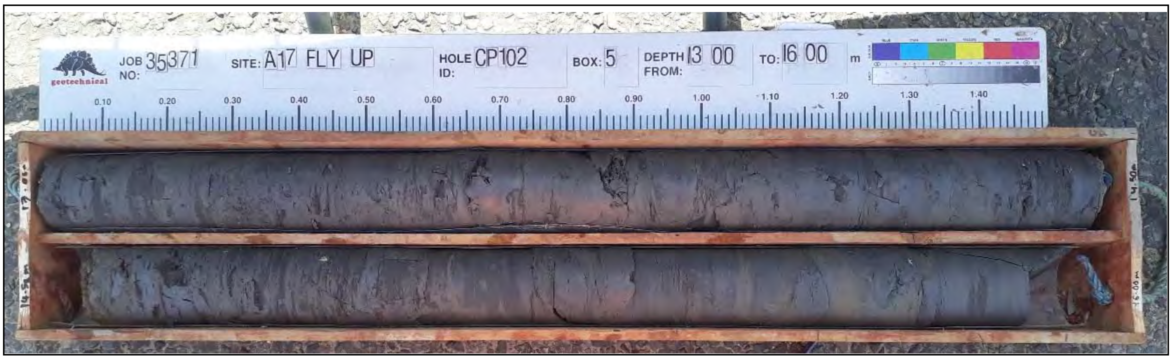

Borehole: CP102 Box 5: 13.00-16.00m

Borehole: CP102 Box 6: 16.00-19.00m

Borehole: CP102 Box 7: 19.00-20.00m

Borehole: CP104 Inspection pit

Borehole: CP104A Inspection pit